Acta Zoologica

Academiae Scientiarum Hungaricae

VOLUME 44 - NUMBER 1–2 - 1998

HUNGARIAN NATURAL HISTORY MUSEUM, BUDAPEST

ACTA ZOOLOGICA
ACADEMIAE SCIENTIARUM HUNGARICAE

AN INTERNATIONAL JOURNAL OF
ANIMAL TAXONOMY AND ECOLOGY

Acta Zoologica Academiae Scientiarum Hungaricae is published quarterly from February 1994 (other issues in May, August and November) by the Hungarian Natural History Museum and the Biological Section of the Hungarian Academy of Sciences with the financial support of the Hungarian Academy of Sciences.

For detailed information (contents, journal status, instructions for authors, subscription, and from Volume 40 onward title, author, authors' addresses, abstract, keywords and a searchable taxon index) please visit our website at

http://actazool.nhmus.hu/

Acta Zoologica Academiae Scientiarum Hungaricae 44 (1–2), pp. 1–6, 1998

INTRODUCTION TO THE SYMPOSIUM: PUTTING THE MORPHOMETRIC SYNTHESIS TO WORK

KLINGENBERG, C. P.[1] and F. L. BOOKSTEIN[2]

[1] *Department of Zoology, Duke University, Durham, North Carolina 27708–0325, U.S.A.*
[2] *Institute of Gerontology, University of Michigan, Ann Arbor, Michigan 48109–2007, U.S.A.*

The discipline of morphometrics looks back on a history of about a century. Especially in the last two decades, it has undergone tremendous change described by some authors as a revolution (ROHLF & MARCUS 1993). In this short time, numerous methodological approaches have been developed by researchers in various fields, especially evolutionary biology, physical anthropology, paleontology, and systematics. Some of these methods have been consolidated into the morphometric synthesis, of which BOOKSTEIN (1998) gives a detailed account. This consolidation, mainly in the past few years, has been every bit as remarkable as the momentous change preceding it. Now that the synthesis is established, the emphasis can shift to the application of morphometrics in various biological disciplines. This is the principal focus of the symposium proceedings in this issue of *Acta Zoologica Academiae Scientiarum Hungaricae*.

The essay by BOOKSTEIN (1998) compares the various methodological approaches in morphometrics. While the paper compares the different approaches in an historical perspective, it is much more than just recounting the sequence of how the invention of new methods rendered older ones obsolete. A surprising result of the morphometric synthesis is that some (but not all) methods that we perceived as competitors a short time ago are now complementary parts within the larger framework of the synthesis. Therefore, this re-evaluation from a "post-synthesis" viewpoint serves two purposes: to readers unfamiliar with morphometric methodology, it offers an introduction to the development of ideas in the field, whereas even seasoned morphometricians should find new insights on how familiar techniques relate to each other.

As morphometricians shift their attention from methodology to application, careful attention to acquisition of data becomes ever more important. The papers by REIG (1998) and by ARNQVIST and MÅRTENSSON (1998) discuss the problem of measurement error. REIG (1998) investigates the importance of measurement error relative to differences within and between populations and species. His paper also illustrates a way to deal with specimens missing one or more landmarks (for an alternative approach, see YAROCH 1996). The paper by ARNQVIST and MÅRTENSSON (1998) reviews various sources of random and systematic error in morphometric measurements, and uses a simple data set to demonstrate

repeatability as a relative measure of error. The example presented is limited to a demonstration of the technique because repeatabilities are computed for principal component scores (which are only meaningful for the particular specimens in the sample). Actual analyses will apply the methodology to other statistics, like loadings (coefficients) for principal components or interpretable scores such as canonical variates (in the context of multigroup comparisons). Despite its simplicity, however, the analysis does illustrate a general point: repeatability is low for principal components that account for small portions of variance, indicating that extra attention to measurement error is necessary whenever subtle features of variation are of interest. The paper by MARCUS (1998) also briefly discusses measurement error, including the differences between measurements made by different observers.

How serious is measurement error for "real-life" morphometric studies? The answer depends on the context. Studies of variation among different species or across ontogenetic stages will often find a sufficiently large amount of shape variation that the noise introduced by measurement error will have little effect on the results. Studies of intraspecific variation within a particular growth stage, however, will be much more vulnerable because they are aimed at more subtle shape variation. For example, fluctuating asymmetry is a field where the true variation is often not much more than the precision of the measurements. Thus, as asymmetry studies begin to use the methods of geometric morphometrics (BOOKSTEIN 1991 pp. 267 ff., AUFFRAY *et al.* 1996, SMITH *et al.* 1997, ARNQVIST *et al.* 1997, KLINGENBERG & MCINTYRE 1998, KLINGENBERG *et al.* 1998), repeat measurements will be imperative, just as they are for the conventional measurements of interlandmark distances (PALMER 1994).

Allometry is another topic that is equally relevant in the framework of the morphometric synthesis as it has been in more traditional morphometric methods (e.g. BOOKSTEIN 1989, KLINGENBERG 1996, 1998). The paper by BAYLAC and PENIN (1998) uses the traditional analyses of interlandmark distances and the methods of geometric morphometrics to study static allometry in the wings of the fly *Drosophila simulans*. This study system is particularly interesting because so much is known about the development and genetics of the closely related *Drosophila melanogaster*. BAYLAC and PENIN (1998) use this source of information to ask whether developmentally distinct compartments of the wing are also different in terms of their morphometric variation, and to interpret the findings of their analyses.

For the most part, morphometric approaches have been used in evolutionary biology. The article by MARCUS (1998) gives a detailed account of evolutionary changes in fossils of a bovid species that lived on the island of Mallorca in the Pleistocene and early Holocene. This species has a number of morphological features in its skull and jaws that make it truly remarkable. MARCUS discusses his

morphometric studies of these and other features in the light of functional and ecological considerations.

Whereas the paper by MARCUS (1998) concerns the evolution over time in what was presumably a single evolutionary lineage, CORTI *et al.* (1998) focus on a group of related species of rodents that currently inhabit different areas in the northern part of South America. CORTI *et al.* (1998) relate morphometric variation to a dendrogram derived from genetic differences among these populations. They used an averaging method for mapping of morphometric variables onto the dendrogram (ROHLF 1997), which is similar to the parsimony methods routinely used in comparative studies of quantitative traits (HARVEY & PAGEL 1991, MADDISON & MADDISON 1992; for discussion in the context of morphometrics, see KLINGENBERG & EKAU 1996). Recently, methods for maximum-likelihood estimation of ancestral trait values have been introduced (e.g. SCHLUTER *et al.* 1997); this approach, based on an explicit model of evolutionary change (e.g. random walks; BOOKSTEIN 1988), will provide the opportunity to integrate morphometrics, evolutionary quantitative genetics, and phylogenetic analysis. While we see promise in this endeavour to map morphometric variation onto a known phylogeny (which will also provide measures of uncertainty for estimates of ancestral morphology), we are pessimistic about attempts to do the reverse, i.e., to estimate phylogenies from morphometric data.

The papers by LOY and CAPANNA (1998) and by RÁCZ and DEMETER (1998) deal with character displacement in related species of moles and shrews, respectively. They are thus concerned with the interactions within and between populations, and with the relationships of populations to their environment. In addition to documenting character displacement, these contributions also underscore that morphometrics has long been, and continues to be, a powerful method for delimiting species, and is thus an indispensable tool in alpha taxonomy.

The application of morphometric approaches is not limited to basic science. For instance, the primary example in the essay by BOOKSTEIN (1998) is from medicine. As another example from applied science, RINDERER (1998) gives a review of the long-term program to identify Africanized honey bees, and its implementation in a regulatory context. This program, based on samples from thousands of bee colonies, is certainly one of the largest morphometric projects ever realized. Because the methods need to be applied in the context of quarantine measures, it is important that the methods are fast, perform reliably under varied circumstances, and can be used by personnel with little previous experience. Moreover, cost is an additional consideration for such a program. RINDERER reports that the morphometric approach compares favorably to alternatives like biochemical and molecular methods with regard to all these criteria.

Altogether, the contributions in this issue encompass most of the range of topics to which morphometric methods have been applied. Where do we go from

here? BOOKSTEIN (1998) lists a number of further developments in methodology that will add to the flexibility available in the morphometric synthesis. But we also expect a substantial expansion in the range of questions addressed with morphometric methods. Morphometrics has been used mostly in evolutionary biology, but the quantitative analysis of morphology is relevant not only within this field. We see many promising opportunities for morphometric analyses in a number of other disciplines, especially in developmental biology. There has been a recent synthesis of evolutionary and developmental biology (e.g. RAFF 1996), which has mostly been a merger of the experimental methodology of developmental biology with a phylogenetic framework of evolution. Using morphometric methods in developmental contexts not only contributes to the unification of developmental and evolutionary biology, but it can yield entirely new results concerning developmental mechanisms. For instance, studies using geometric morphometrics found that the wings of the honey bee (SMITH *et al.* 1997) and of three species of flies including *Drosophila melanogaster* (KLINGENBERG *et al.* 1998) consistently show directional asymmetry between left and right body sides. This implies that a left-right axis must be involved in wing development, which establishes the difference between the two body sides. However, developmental biologists have not yet found a left-right axis in any insect, despite the vast research on specification of body axes in *Drosophila*, which led some authors to conclude that a left-right axis does not exist in insects (e.g. RAFF 1996, pp. 80 f., 302 f.). The morphometric studies clearly established that it does exist (for detailed discussion, see KLINGENBERG *et al.* 1998). We expect that morphometric methods will lead more discoveries of morphological patterns that have direct implications for fields such as development and physiology, and therefore can pinpoint new questions for experimental research.

BOOKSTEIN (1998) ends his article with a general reflection on the origin of quantitative methodology in the sciences. He concludes that it is most effective to use general principles of applied mathematics as the basis for new methodology. The morphometric synthesis is an excellent example of this approach. The next challenge is to integrate these methods into the various disciplines that apply morphometrics, in order to create a unified framework for the quantitative study of morphology. The contributions in this issue are testimony to the fact that this second stage of the synthesis is well underway.

* * *

Acknowledgements – The articles in this issue originated from presentations at the symposium "Morphometrics and Evolution" (organizers: C. P. KLINGENBERG and F. L. BOOKSTEIN) held at the Fifth International Congress of Systematic and Evolutionary Biology (Budapest, August 17–24, 1996), and at the symposium "Insect Morphometrics" (organizers: C. P. KLINGENBERG and M. ZIMMERMANN), held at the XX. International Congress of Entomology (Florence, August 25–31,

1996). We thank the symposium participants for their stimulating contributions, and the congress organizers for providing excellent venues for the symposia.

REFERENCES

ARNQVIST, G. & T. MÅRTENSSON (1998) Measurement error in geometric morphometrics: empirical strategies to assess and reduce its impact on measures of shape. *Acta zool. hung.* **44**: 73–96.

ARNQVIST, G., R. THORNHILL & L. ROWE (1997) Evolution of animal genitalia: morphological correlates of fitness components in a water strider. *J. Evol. Biol.* **10**: 613–640.

AUFFRAY, J-C., P. ALIBERT, S. RENAUD, A. ORTH, & F. BONHOMME (1996) Fluctuating asymmetry in Mus musculus subspecific hybridization. Pp. 275–283. *In* L. F. MARCUS *et al.* (eds): *Advances in Morphometrics*. Plenum Press, New York.

BAYLAC, M. & X. PENIN (1998) Wing static allometry in Drosophila simulans males (Diptera, Drosophilidae) and its relationships with developmental compartments. *Acta zool. hung.* **44**: 97–112.

BOOKSTEIN, F. L. (1988) Random walk and the biometrics of morphological characters. *Evol. Biol.* **23**: 369–398.

BOOKSTEIN, F. L. (1989) "Size and shape": a comment of semantics. *Syst. Zool.* **38**: 173–180.

BOOKSTEIN, F. L. (1991) *Morphometric Tools for Landmark Data: Geometry and Biology*. Cambridge University Press, Cambridge, 435 pp.

BOOKSTEIN, F. L. (1998) A hundred years of morphometrics. *Acta zool. hung.* **44**: 7–59.

CORTI, M., AGUILERA, M. & E. CAPANNA (1998) Phylogeny and size and shape changes in the skull of the South American rodent Proechimys. *Acta zool. hung.* **44**: 139–150.

HARVEY, P. H. & M. D. PAGEL (1991) *The Comparative Method in Evolutionary Biology*. Oxford University Press, Oxford, 239 pp.

KLINGENBERG, C. P. (1996) Multivariate allometry. Pp. 23–49. *In* L. F. MARCUS *et al.* (eds): *Advances in Morphometrics*. Plenum Press, New York.

KLINGENBERG, C. P. (1998) Heterochrony and allometry: the analysis of evolutionary change in ontogeny. *Biol. Rev.* **73**: 79–123.

KLINGENBERG, C. P. & W. EKAU (1996) A combined morphometric and phylogenetic analysis of an ecomorphological trend: pelagization in Antarctic fishes (Perciformes: Nototheniidae). *Biol. J. Linn. Soc.* **59**: 143–177.

KLINGENBERG, C. P. & G. S. MCINTYRE (1998) Geometric morphometrics of developmental instability: analyzing patterns of fluctuating asymmetry with Procrustes methods. *Evolution* (in press)

KLINGENBERG, C. P., G. S. MCINTYRE & S. D. ZAKLAN (1998) Left-right asymmetry of fly wings and the evolution of body axes. *Proc. R. Soc. Lond. B Biol. Sci.* **265**: 1255–1259.

LOY, A. & E. CAPANNA (1998) A parapatric contact area between two species of moles: character displacement investigated through the geometric morphometrics of skull. *Acta zool. hung.* **44**: 151–164.

MADDISON, W. P. & D. R. MADDISON (1992) *MacClade: Analysis of Phylogeny and Character Evolution*. Sinauer Associates, Sunderland, MA.

MARCUS, L. F. (1998) Variation in selected skeletal elements of the fossil remains of Myotragus balearicus, a Pleistocene bovid from Mallorca. *Acta zool. hung.* **44**: 113–137.

PALMER, A. R. (1994) Fluctuating asymmetry analyses: a primer. Pp. 335–364. *In* T. A. MARKOW (ed.): *Developmental Instability: Its Origins and Evolutionary Implications*. Kluwer, Dordrecht, The Netherlands.

RAFF, R. A. (1996) *The Shape of Life: Genes, development, and the Evolution of Animal Form.* The Univ. Chicago Press, Chicago, 520 pp.

RÁCZ, G. & A. DEMETER (1998) Character displacement in mandible shape and size in two species of water shrews (Neomys, Mammalia: Insectivora). *Acta zool. hung.* **44**: 165–175.

REIG, S. (1998) 3D digitizing precision and sources of error in the geometric analysis of weasel skulls. *Acta zool. hung.* **44**: 61–72.

RINDERER, T. E. (1998) The identification of Africanized honey bees: an assessment of morphometric, biochemical, and molecular approaches. *Acta zool. hung.* **44**: 177–194.

ROHLF, F. J. (1997) *TpsTree.* Dept. Ecology and Evolution, State Univ. New York at Stony Brook.

ROHLF, F. J. & MARCUS, L. F. (1993) A revolution in morphometrics. *Tr. & Ecol. Evol.* **8**: 129–132.

SCHLUTER, D., T. PRICE, A. MOOERS & D. LUDWIG (1997) Likelihood of ancestors in adaptive radiation. *Evolution* **51**: 1699–1711.

SMITH, D. R., B. J. CRESPI & F. L. BOOKSTEIN (1997) Fluctuating asymmetry in the honey bee, Apis mellifera: effects of ploidy and hybridization. *J. Evol. Biol.* **10**: 551–574.

YAROCH, L. A. (1996) Shape analysis using the thin-plate spline: Neanderthal cranial shape as an example. *Yearb. Phys. Anthropol.* **39**: 43–89.

Acta Zoologica Academiae Scientiarum Hungaricae 44 (1–2), pp. 7–59, 1998

A HUNDRED YEARS OF MORPHOMETRICS*

F. L. BOOKSTEIN

Institute of Gerontology, The University of Michigan
Ann Arbor, Michigan 48109, U.S.A.
E-mail: fred@brainmap.med.umich.edu

This paper recounts the development of methods for quantifying, summarizing, and contrasting the spatial relationships of biologically corresponding loci across samples of specimens: the history of morphometrics in the broadest technical sense. In its contemporary version, this toolkit fuses two once-disparate scientific methodologies (BOOKSTEIN 1993). The older of the two, the elaboration of diagrams that convey geometrical differences among biological forms to the viewing eye, has been with us (as the art of caricature) since the Renaissance. The junior partner, comprising the strategies of multivariate statistical analysis for optimal summaries of multiple empirical measurements, began to emerge around 1900 in the hands of the biometrician KARL PEARSON. This lecture reviews the main themes of their successful combination over the present century.

Earliest to appear was multivariate morphometrics, the analysis of variables arising from operations with rulers and protractors by standardized matrix manipulations that ignore the geometry of their original measurement (e.g., which distance measures share endpoints, which ratios share denominators). Several familiar methods for dealing with the allometric model – dependence of shape on size when size was not explicitly measured – come under this heading. Another specialized multivariate analysis deals with biological outlines without landmarks, for which the dimensionality of the signal might be arbitrarily high but its content of usable information likely limited. Beyond these stratagems of limited power, the melding of these two traditions into a true Synthesis (which will be referred to with a capital S in this article) arose first in applications to *landmark data,* configurations of discrete punctate loci deemed homologous across the forms of a data set. In the middle 1980's, many of us, working independently for the most part, realized that in this special case geometrical tactics (such as superposition of coordinate systems) and visualizations (such as deformation grids) arise that are unprecedented in standard versions of multivariate analysis. In practice, there is a good deal more information in these data sets than what is conveyed by their covariance structures. The requisite modifications of multivariate methods that preserve this information are now substantially complete. Develop-

* Symposium presentation, 5th International Congress of Systematic and Evolutionary Biology, 1996, Budapest

ments still in progress extend these formalisms further to encompass outline data, displacement fields, and extended images or surface representations.

The basic argument of this paper is set out all at once in the immediately following Table, which sorts our literature into seven general themes corresponding to the paper's seven main sections. It is easiest to enumerate them via the associated formal data sources: mixed quantitative features, interpoint distances, outlines, landmark configurations, curving form with homology information, images with homology information, and "others." For each of these, the Table lists apposite quantitative manipulations (to the extent they have been standardized), diagrammatic styles associated with data explorations or findings, key elements of the jargon (see also SLICE *et al.* 1996), typical scientific contexts, and a selection of explanatory presentations or instructive exemplars. The succeeding text is mainly gloss upon the Table, section by section, elaborating upon the summary judgments there, incorporating historical notes and figured examples, and musing upon false starts, ironies, or analogous methodologies whose relation to the core formalisms of the synthesis is not yet clear. The Synthesis of which we are so proud is the subject of an extensive overview in Sections 4 and 5.

1. "MULTIVARIATE MORPHOMETRICS"

At the core of modern applied statistics lies the highly linearized toolkit of applied multivariate analysis: covariance-based manipulation of multiple measurements via the vector space of their linear combinations. Examples of these methods include principal components, multivariate analysis of variance and covariance, canonical correlations, and factor analysis. The accumulation of methods of this class in the first half of the twentieth century induced a style of quantitative analysis of form, row 1 of the Table, that used to be called "multivariate morphometrics" (BLACKITH & REYMENT 1971); it is now typically called "traditional morphometrics" instead. Multivariate morphometrics treats a fairly general data structure: variables that arrive as measured extents (lengths, areas, volumes) or shape features (angles, ratios) without further formal (geometrical) justification. The most recent technique incorporated in this part of the toolkit – the part that pays no attention to where variables come from – is the machinery of biplots, singular-value decomposition of data matrices. Their algebra unites principal components with principal coordinates and thus formalizes relationships that had hitherto been understood only intuitively (see MARCUS 1993).

The principal scientific contexts for this work, classification and ordination, typify old-style systematics, and perhaps also contemporary ecology, more than evolutionary or developmental biology. In keeping with that context of serendipi-

tous accrual of differentia, practitioners of these methods have no methodology for the origin of the variables subject to analysis. As a result, the only geometry that appears pertains to the linear vector space in which the statistical maneuvers are couched. The geometry of traditional morphometrics, in other words, is the linear geometry of covariance structures, not the geometry of the organism. Furthermore, as variables are subject to no requirement of coherence – short distances, diameters and widths, areas, ratios, angles all mixed together – the analysis has to be independent of the scaling of the variables separately. In practice, this enforces the study of correlation matrices, not covariances. "Phenetic distance", if it appears at all, is derived from the measured variables by some sum-of-squares maneuver rather than from any computation involving Euclidean distances between points of similar organisms similarly placed. Likewise, all graphics pertain to these vectors or to specimens' scores in the dual vector space, rather than to familiar creatural shapes in the original pictures. "Morphospace" is the linear vector space of these scores, not any more informed mathematical construction, and "morphotypes" are sample forms lying in interesting spots in that space, rather than constructed forms optimally depicting interesting features such as group centers or variability.

A typical investigation in this traditional morphometric form would begin with a single diagram showing distances and angles measured and then proceed to a collection of tables and scatterplots. The tables are either correlation matrices or orthogonal sets of principal or canonical vectors that describe within-group or between-group covariance matrices and their relationships. The scatterplots, usually with enhancements such as group-specific symbols or hulls, show the correspondence (or no) of the measured data to various intuitive models of clustering, adjacency, or orthogenesis.

Examples come readily to hand throughout the literature of morphometrics, right up through the present day. BLACKITH and REYMENT (1971) is a survey of the field dating from the high-water mark of its credibility. Almost immediately afterward, certainly by the time I was writing my doctoral dissertation (BOOKSTEIN 1978), growing acknowledgement of its alienation from the actual pictorial context of the creatures ostensibly under study led to a great adaptive radiation of geometrical innovations, culminating in the synthesis (Secs 4–5) that is the core of the field a generation further on. MARCUS (1990), written in the light of hindsight, is a fine review of the strengths of this school, including excellent examples of the associated diagrams for provenance of variables and ordination of forms. OXNARD's compilations of theoretically informed analyses (e.g., 1973, 1984) likewise show the expert style of arguing from these displays, here in a context that combines systematics with biomechanics. The "traditional" toolkit cannot properly be pushed any farther than examples like these.

Table 1. The main sequence of modern morphometric methods

	Data, source	Manipulations	Graphics	Key words and phrases	Scientific uses, notes	References, examples
1.	Mixed size and shape measures Any other quantitative features	Univariate analyses Clustering "Multivariate morphometrics" Singular-value decomposition	Scatterplots Biplots Post-hoc morphotypes	Phenetic distance Morphospace	Classification ordination Homology is by fiat Roster of variables is arbitrary	BLACKITH & REYMENT 1971 MARCUS 1990 OXNARD 1984
2.	Interpoint distances	Multivariate statistics of log covariance matrices	Scatterplots Trusses with loadings	General size Geometric shape (= ratio shape) Allometric shape	Classification Factor explanations	PEARSON 1935 WRIGHT 1968 BOOKSTEIN 1985 BOOKSTEIN 1989
3.	Outlines	Orthogonal decompositions of function spaces (e.g. Fourier)	Scatters Principal shapes	Eigenshapes	Subsumed in SII Many arbitrary homologies possible	BOOKSTEIN 1991 LOHMANN 1990 FERSON 1985
4.	Landmark locations	**The Synthesis:** Procrustes averaging Procrustes fits Multivariate statistics in Kendall tangent space Visualizations in the original coordinate system Goodall's F-test and its permutation version	Procrustes scatters Derived scatters Deformations Predicted forms Salient new variables Interchangeability of vectors with grids	Similarity group Shape space Shape coordinates Centroid Size Procrustes distance Thin-plate spline Bending energy Principal, partial, relative warps Uniform component	Localization Prediction Rigorous multivariate testing of geometric hypotheses No arbitrariness of statistics; landmark selection, homology still unformalized *The major collective achievement of the last decade*	BOOKSTEIN 1991 GOODALL 1991 BOOKSTEIN 1996*a*, 1997*a* MARCUS 1996 DRYDEN 1998
	along with: exogenous variables, e.g., geography or behavior	Partial Least Squares	Singular warps	SVD of cross-covariance structure		BOOKSTEIN 1991, 1997*d* TABACHNICK unpubl.

Table continued

5.	Curves/surfaces, perhaps with landmarks	**Synthesis, Phase II [SII]:** as above, along with mapping curves onto curves by relaxation	Procrustes scatters Derived scatters Deformations Curve bundles	Spline relaxation Semilandmarks	Generalized notion of homology for landmarks together with curves	Bookstein 1997*b, c* Bookstein 1998*a*
6.	Images with landmarks or curves Solid medical images	Isosurface curvature, ridge extraction Unwarping, SII	Average pictures Image differences and covariances Singular images	Vertical vs. horizontal comparisons Image normalization Ridge curves	Increase in statistical power Localization of change	Bookstein 1997*a* Bookstein 1998*b* Cutting 1995 Buckley 1998
7.	Others, not yet integrated					
	Displacement fields, time-lapse photos, etc.	Kinematics, continuum mechanics, partial differential equations	Vector fields Tensor fields Rigid motion, gait, linkages	Strain tensors Other real energy terms and integrals	In biomechanics: rare but elegant In image analysis: work in progress	Bookstein 1978 Avery 1933 Dagognet 1992 Jacobson 1976
	"Morphometry" (photomicrographs)	Stereology Mathematical morphology Size and shape indices, textures, fractal properties, etc.	none standard	A great many, some very specialized	"Same part" is only notion of homology Very broadly applicable	Stoyan 1995

The fundamental limitations of these approaches, which came to our attention only as the successor techniques were being invented, are averred to in the second-last column of the Table. They involve mainly the absence of criteria for integrity of data sets: criteria for when variable quantities can properly be considered homologous, and criteria for appropriate diversity, redundancy, and exhaustiveness of the rosters displayed. From these lacunae follow the arbitrariness of any notion of interspecimen "distance" emerging from data sets like these, lists of variables typically deriving from merely qualitative experience with taxonomic keys, and likewise the inappropriateness of reifying (interpreting) principal components (save possibly the first, in allometric modeling: see next Section). In particular, these rosters of variables never embodied any formalism of the information available in whole specimens or their photographs. Indeed, as BLACKITH said in 1965, such a "morphometrics" was a branch of taxonomy per se (in the sense of 1965), not amenable to richer modes of biological explanation. But this did not block its applications in richer contexts, for instance paleobiology or historical geology (REYMENT 1991, REYMENT & JÖRESKOG 1993), until better techniques came along. Those improvements required a sharpening of the focus within the domain of "all quantitative variates" to concentrate on data representations specific to morphometrics per se.

2. MODELS FOR SIZE MEASURES

Row 2 of the Table is concerned with a modest but potent restriction on the roster of variables that led to considerable improvements in the explanatory power of the ensuing statistical analyses. By the 1920's, SEWALL WRIGHT had extended the algebra of correlation structures to models of linear causation – path models and path-analytic factor models – that permanently fused the biometric methods of PEARSON to the explanatory styles emerging from the genetic approaches to evolution and development. WRIGHT's models allowed the interpretation of specific coefficients of the vector-space approach as referring to biologically real causes or effects. When this approach was applied to variables restricted to measured distances *only,* without the admixture of areas, shape variables, or other differently scaling quantities, there immediately emerged the first great explanatory morphometric method: the *allometric model* developed in the 1960's. When multivariate analysis is carried out on covariances of log-distances, every coefficient has a coherent empirical interpretation: a standardized rate or ratio of factor effects on length. When the distances are taken, furthermore, in a systematic pattern over the organism (as in the method of trusses, BOOKSTEIN *et al.* 1985), the resulting analysis can be used (though with difficulty; it is easier if landmarks are available) to provide *predicted forms*, not just

predicted measures. For the first time, statistical analyses could be visualized back in the picture plane or space of the organism.

While in most applications these methods are superseded by the tools of the Synthesis, the advance they represent over the earlier state of our toolkit is nevertheless substantial. By allometric modeling or the generalizations that WRIGHT had already suggested, the explanatory role of "size" in developmental or evolutionary studies could be identified with a computed vector of "loadings" (implied regression coefficients) that pertained to discrete structural or functional aspects of the form being measured. In this way, "general size" could serve in cogent biometric explanations without itself having been measured. Although it was WRIGHT who first understood this fruitful explanatory conflation of "general size" in its statistical and its biological senses, the special power of its application to suites of variables all in units of length emerged only in the 1960's (see JOLICOEUR 1963). With pure suites of size measures, the coefficients of the first principal component conveyed information about all possible Huxleyan relative growth rates at the same time.

Shortly afterward, spurred by this reification of one sense of "size", BURNABY (1966) and others noticed, very helpfully, that it was inconsistent with another sense of the same term. MOSIMANN immediately formalized the distinction in his theorem of 1970 that in any such data set at most one size measure (in linear models, exactly one) is matched to an explanatory notion of size-free shape in the statistical domain. To every other size variable corresponds a notion of allometric size instead. In the context of the Synthesis this theorem leads directly to Centroid Size as the preferred size measure; see below. This interplay of vectors with two divergent varieties of biological explanation is reviewed concisely in BOOKSTEIN (1989).

The core of these methods has been extensively commented on in earlier publications by myself and my colleagues (BOOKSTEIN *et al.* 1985), and their relation to the classic explanatory styles of evolutionary and developmental biology thoroughly explored. This part of the toolkit offers useful versions of WRIGHT's path analysis for explaining effects of processes over separate parts of the organism and for statistical dissection of multiple effects (size, gender, cline) on the same form. For a good contemporary review, see KLINGENBERG (1996). Here I would like to dwell instead on a pioneering article, recently come to my attention, that shows its application to the earlier style of investigation, the systematic spirit, in a most unexpected context.

PEARSON and MORANT (1935) report a forensic morphometric investigation that centers upon a single severely weathered dried head from the seventeenth century. The history of this object is fascinating, although macabre. The body of OLIVER CROMWELL was buried, disinterred, hanged, and beheaded, in that order. For about thirty years after that, his head was mounted on a pike at the

south end of Westminster Hall, *pour encourager les autres*. At some time thereafter it was lost to general view. A century later, a skull accompanied by a claim that it was the skull of CROMWELL, as picked up by a "sentinel on guard at Westminster" after it fell off its pole during a thunderstorm, turned up in the possession of a family named WILKINSON. It is this specific object that concerned our authors. The WILKINSON skull was "that of a person who has been embalmed and decapitated after embalmment, and ... exposed long enough on an iron spike fastened to an oak pole for the pole to rot and the worms to penetrate pole and head." What can one say about the claim that it is CROMWELL's?

The very British eccentricity of this question conceals its methodological importance. To supply an answer, it became necessary for PEARSON to construct a version of his extant multivariate toolkit that exploited the full information content of data from solid objects in the space of his workroom. He inspected all the extant death masks of CROMWELL, the single life mask, and all the busts, and upon each located a variety of useful points: the deepest point of the nasal bridge, external orbital corners, diameter of mouth, height of lipline, "subnasal point", tip of chin, interpupillary, and, most cleverly, the center of CROMWELL's prominent wart over the right eyebrow. (The WILKINSON head sported a wart socket at a very similar location.) These configurations were archived first as sets of interlandmark distances (inasmuch as electronic digitizers had not yet been invented) and subsequently as one series of size-standardized ratios (the busts were originally to diverse scales). Upon the resulting quantities one could then carry out a sturdy statistical inference regarding a hypothesis of identity.

The issue is whether the WILKINSON skull, as measured in the twentieth century, matches this compendium of quantities as averaged over the various representations from three centuries before, each first painstakingly adjusted for factors known to have intervened on the living CROMWELL, such as aging, or on the postmortem head, such as desiccation. An example of that match, between the skull and the life mask, is reproduced here as my Fig. 1.

The procedure on which PEARSON lit remains in the modern toolkit: the representation of all the specimens in terms of scaled distances. (Here he missed a bet. The two-point shape coordinates that his mentor FRANCIS GALTON introduced in 1907 – see Fig. 8 below – is a procedure mathematically equivalent to the *next* stage of the synthesis, the construction of variables free of geometric size in a statistically exhaustive way, but we didn't know about this until the 1980's. The theorem, but not the historical aperçu, appears in BOOKSTEIN 1986.) PEARSON's analysis is summarized in the table I've incorporated in Fig. 1. The finding, which PEARSON interprets as a "moral certainty" that the WILKINSON head is CROMWELL's, inheres in the agreement between the two lines of scaled distances (one the WILKINSON's, one a CROMWELL average) in the table. Notice that the entries in this table are vectors of shape descriptors *sensu stricto,* exactly the ma-

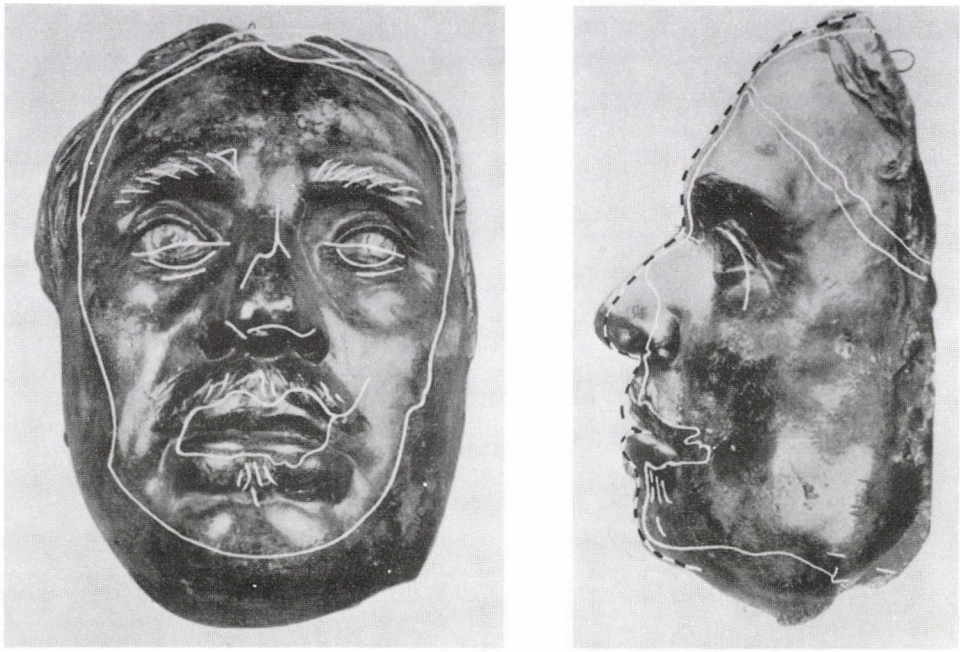

Characters	External Ocular Distance	External Orbital Distance	Length of Mouth	Nasion to Lip-line	Nasion to Wart Centre	Nasion to Gnathion	Nasion to lowest point of "beardlet" root	Nasion to Subnasal Point	Wart Centre to Right External Lid-meet	Wart Centre to Right External Orbital Margin
Mean Masks and Busts	98·7	113·75	58·9	75·2	28·05	122·3	95·9	53·8	48·9	52·4
Wilkinson Head	96·6	112·3	59·5	76·2	27·2	117·7	98·8	53·3	49·3	51·1

Characters	Wart Centre to Left External Lid-meet	Wart Centre to Left External Orbital Margin	Glabella to Subnasal Point	Glabella to Lip-line	Glabella to lowest point of "beardlet" root	Glabella to Gnathion	Subnasal Point to lowest point of "beardlet" root	Breadth of Nose, without alae	Interpupillary Distance
Mean Masks and Busts	74·9	81·2	71·9	96·65	121·9	139·6	48·25	32·2	73·35
Wilkinson Head	74·4	81·3	71·7	98·1	125·8	135·7	48·4	32·0	70·7

Fig. 1. Unusual example of analysis of interlandmark distances. Top: Superposition of the unique surviving life mask of CROMWELL over salient features of the WILKINSON head. Bottom: Vector of shape features for the WILKINSON head compared to the mean of the same vectors for the extant masks and busts of CROMWELL, corrected (from PEARSON and MORANT 1935, Plate LXXXVIII and Table II)

terial of MOSIMANN's theorems and mine. Had PEARSON gone on to supplement this splendid analysis with a distribution theory for such comparisons of vectors, instead of merely asserting their identity, he would have invented the entire core of contemporary morphometrics in 1935, and I would be out of a job.

I should not conclude this section without mentioning an intentional anachronism, a method developed in the 1990's that nevertheless ignores all the advances in analysis of landmark data since those just reviewed. The technique of "Euclidean Distance Matrix Analysis," LELE and RICHTSMEIER (1991), investigates shape differences between two groups of landmark configurations by recourse to one omnibus permutation test that relies mainly on standard errors of between-group ratios of mean pairwise landmark distances. (It is thus, in a sense, the obverse of the method PEARSON needed to show identity.) Neither this original method nor any later variant offers any of the other maneuvers of the traditional toolkit (principal components analysis, canonical variates, regressions of shape on continuous causes or effects), nor do they incorporate any of the recent advances within the Synthesis that afford much greater power for statistical inference in most applications and that allow the explicit analysis of shape variation right alongside inferences about group differences.

3. OUTLINES WITHOUT HOMOLOGY

As recently as 1984, another data structure was considered to be potentially as powerful as the scheme of interpoint distances: the analysis of continuously curving outlines, row 3 of the Table. In the apparent absence of information about "biological" correspondence, these analyses proceeded by methods borrowed not from biometric statistical analysis but from orthogonal functional analysis, an older technique central to nineteenth-century mathematical physics but also crucial to signal processing and other modern applied information technologies. At a Woods Hole workshop in 1984, equal time was afforded to the distance-based methods and to the curve-decomposition methods. (A third day, intended to lay the groundwork for a synthesis, proved frustrating; see Sec. 5 below.) At that time, a new technique, eigenshape analysis, had just been introduced by G. P. LOHMANN and P. SCHWEITZER. They hoped that it would supply for outline data what the existing multivariate toolkit was already supplying for distance data: optimal analysis of the information about variation they bear.

Eigenshape analysis attempted to supply an *empirical* orthogonal basis for a space of variation of shape, in contrast to the *geometrically* orthogonal bases – Fourier analysis, Legendre polynomials – that had hitherto been customary in this field. (Geometric orthogonal functions, a generalization of orthogonal rotations, are sets products of which integrate to zero over some domain; empirical ortho-

gonal functions, a generalization of principal components, are sets having covariance zero over some sample.) Representations of outlines as functions of different domains and ranges (curvature, radius, tangent angle), all submitted to the "standard" decompositions (e.g., Fourier series for closed circuits, or Legendre polynomials for widths along an axis), resulted in remarkably different ordinations; LOHMANN and SCHWEITZER wanted to cut through this confusion with a new standardization. They took advantage of an untraditional modification of multivariate geometry in which vectors are restricted to a sphere. A sample mean then emerges as a first principal component of a data scatter out of the center of the sphere. What we normally think of as a first principal component of variation emerges as the second principal component around the center of the sphere, and so on. When shape features are extracted in this way, every component looks itself like a shape, not like a change of shape. The full set of principal components, not only those representing variation but also the mean form itself, might then be called *principal shapes* or *eigenshapes*. This stratagem continues to be convenient in many applications. It supplies, for instance, an alternative (KENT 1994) to the linearized algorithm (ROHLF 1993) for computing relative warps, Section 4, and likewise underlies the Procrustes approach to the analysis of landmark-poor outlines in SAMPSON *et al.* (1996).

The Woods Hole meeting led to no synthesis between the landmark-based and the outline-based approaches. We know now, in hindsight (cf. ROHLF 1990), that the problem that challenged LOHMANN and SCHWEITZER originated not in competition between bases for a space of functions – empirical orthogonal components are invariant against orthogonal changes of basis, anyway – but instead in irreconcilable differences among models for morphological distance between curves. Analysis of curves in which "distance" was integral squared Euclidean distance between points at corresponding proportions of arc-length from a starting landmark would all give the same ordinations. The simplest basis in which to carry out this analysis does not seem to refer to distances at all, but instead parametrizes point locations by borrowing from computer graphics the so-called *elliptic Fourier* basis. Analysis of a "distance" based on radii as a function of angle out of some centroid necessarily gives a different sample ordination, regardless of the basis in which those radii are expressed; analysis of curvature, yet another basis. The original eigenshape method relied on yet a fourth distance measure, a variant of the rotation of tangent angle in which deviation from a circle was normalized out ("shape amplitude") before proceeding with the otherwise standard statistical computations. (This idiosyncratic decision unfortunately precludes all intuitive understanding of subsequent steps in the procedure.)

More fundamentally, there was, and remains, no a-priori method for adjudicating the competition among these "natural" correspondences between points of different outlines or "natural" distances between curves so labelled. Some of the

choices available are sketched in Fig. 2; an example using elliptic Fourier analysis (Euclidean sum of squares) at equal fractions of arc-length from an optimal starting point is shown in Fig. 3. Only last year has an approach from a wholly different direction indicated a possible resolution of these difficulties, and that only in the case of Euclidean distance. The same Procrustes approach (Sec. 4) that generates natural ordinations of shape space for landmarks extends, when combined with the bending-energy formalism embedded in the thin-plate spline, to supply a very similar statistical machinery for unlabeled outlines. We will return to this possibility in Section 5.

4. THE MORPHOMETRIC SYNTHESIS

Over the last decade there has been a remarkable convergence of several disciplines in one shared core of techniques, a **morphometric synthesis**, for the

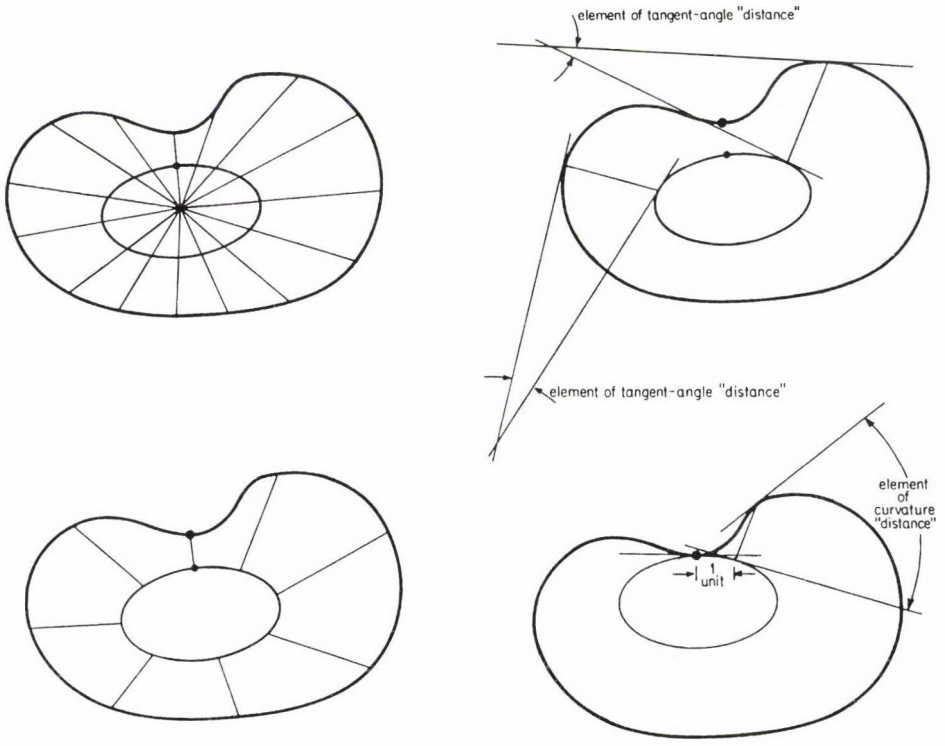

Fig. 2. Any a-priori choice of distance measure between unhomologized outlines is driven by an arbitrary assignment of correspondence. Left, two different versions of homology for a one-landmark outline. Above, radial out of a center; below, linear in arc-length from a single landmark. Right, two additional measures of morphological distance for a homology driven by arc-length. From BOOKSTEIN (1990)

handling of landmark configurations and associated biological shape information as data.

The speed of this development caught most of us by surprise. The first announcement of the mathematical foundation (the Riemannian geometry of Kendall's shape space) came only in KENDALL 1984, via a long and difficult exposition making no reference at all to biological or medical concerns. The initial publication of what is now taken to be the obvious associated multivariate statistical method (BOOKSTEIN 1986) made no reference to this fundamental geometry except in one sentence of a contributed discussion. For describing and decomposing group differences, BOOKSTEIN (1989) combined that multivariate statistical praxis for shape with the thin-plate spline, a technique borrowed from interpolation theory, still without acknowledgement of the geometric foundation. My full-

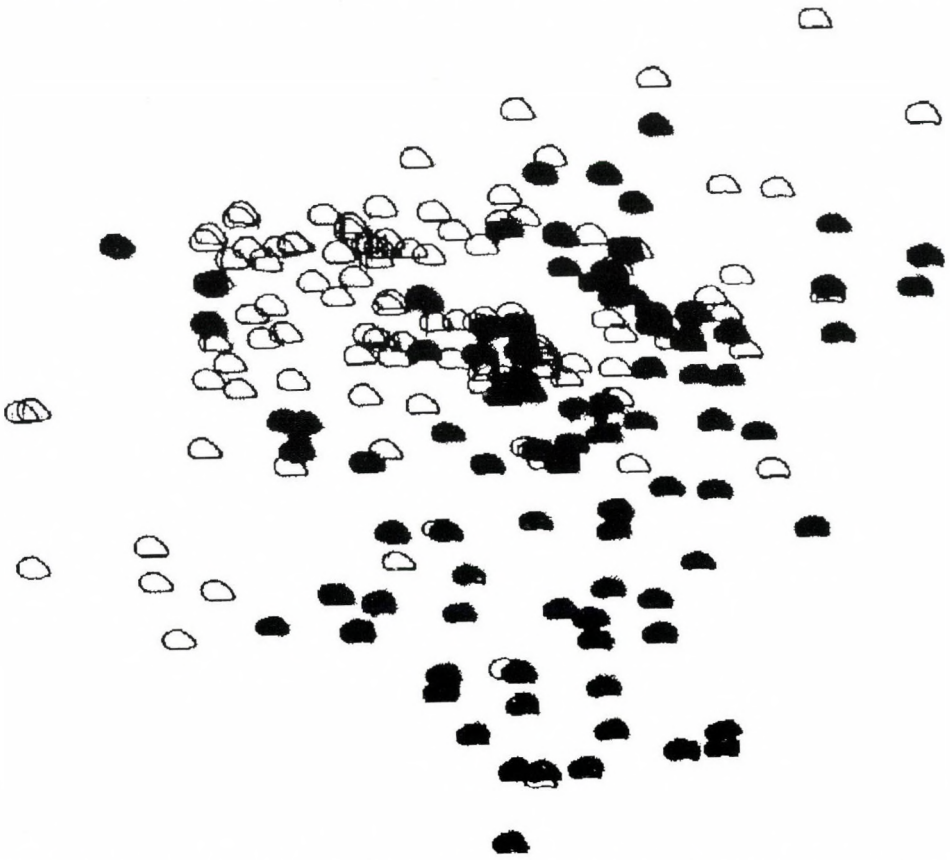

Fig. 3. Two-dimensional ordination of mussel outlines, using the elliptic Fourier basis for homology linear in arc-length from computed starting points. Axes here are the first and second sample principal components of elliptic Fourier coefficients. The shaded outlines have a genetic marker for phosphoglucomutase or glucosephosphate isomerase, and grow more slowly than the wild type. From FERSON and ROHLF 1985, courtesy of F. J. ROHLF

length monograph, BOOKSTEIN 1991, continued to overlook the geometric roots of the relation between the spline and the statistics. We did not understand until the mid-1990's why the splines were so effective for the visualization of statistical effects on shape: it owes to the elementary fact that the eigenfunctions of the spline are orthonormal in the Procrustes geometry of shape. This observation did not appear in the technical literature until 1995 and is only now being disseminated beyond the narrow collegium of interested statisticians (cf. BOOKSTEIN 1996*a, b*, 1997*c*). The following exposition is adapted from BOOKSTEIN (1997*a*).

In ordinary language, the *shape* of an object is described by words or quantities that do not vary when the object is moved, rotated, enlarged, or reduced. The translations, rotations, and changes of scale we thereby ignore constitute the *similarity group* of transformations of the plane. When the "objects" are landmark sets, it turns out to be useful to say that their shape simply *is* the set of all point sets that "have the same shape." That is, we formally define *the* shape of a set of points as the *equivalence class* of that point set, within the collection of all point sets of the same cardinality, under the operation of the similarity group.

The space of these equivalence classes becomes a metric space as soon as we specify a distance measure between any two of them. Were it not for that complication of the similarity group, the obvious formula would involve the usual Pythagorean sum of squared distances between corresponding landmarks. It proves reasonable to define the squared distance between two shapes (that is, two equivalence classes) as the *minimum* of these sums of squares over representatives of the equivalence classes – over the operation of the group of similarities that shape is supposed to ignore. Informally, the squared shape distance between one landmark set A and another landmark set B is the minimum of summed squared Euclidean distances between the landmarks of A and the corresponding landmarks in point sets C as C ranges over the whole set of shapes equivalent to B. For this definition to make sense, we have to fix the scale of A. The mathematics of all this is most tractable (KENDALL 1984) only when the sum of squares of the points of A around their center-of-gravity is constrained to be exactly 1.

The steps in this computation follow down the rows of Fig. 4. At the top are two quadrilaterals of landmarks presumed to arise from real images. Connect each landmark to the centroid of its own form and, for each form, rescale the sum of squares of the distances shown to unity (second row). The scaling parameter, square root of the summed squared distances between the landmarks and their centroid, is usually called Centroid Size. Then (third row) translate one of the forms so that its centroid directly overlies the centroid of the other form. Finally, identify the rotation (third row right) that minimizes the sum of squares of the residual distances between matched landmarks. The squared Procrustes distance between the forms (fourth row) is (to a very good approximation) the sum of squares of those residuals at this minimum: total area of the circles, divided by π.

In two dimensions, the approximation is represented by a simple formula using complex numbers (BOOKSTEIN 1991). While this approach seems quite arbitrary, it is in fact the only way to proceed that seems mathematically natural (KENDALL 1984).

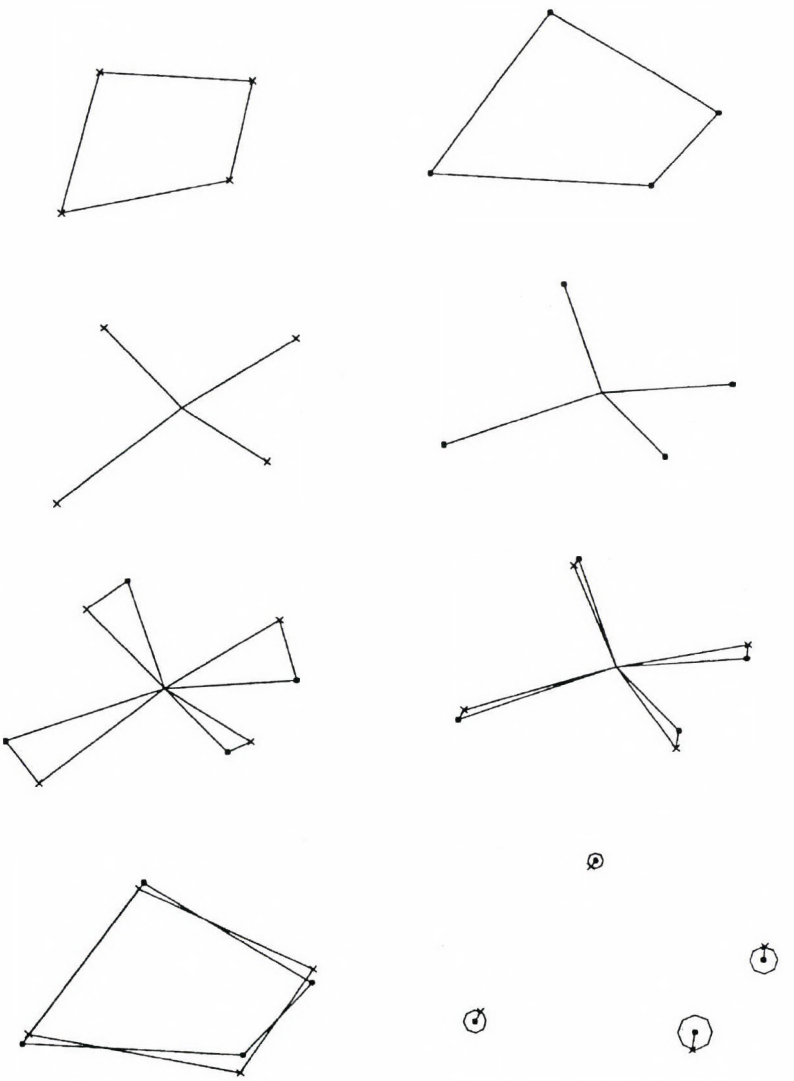

Fig. 4. The Procrustes superposition for a pair of forms. Upper row: Two forms of four homologous landmarks. Middle row: Each form is rescaled so that the sum of squares of the distances to the centroid of its four landmarks is 1. This is the sum of squares of the four lines shown. Third row: The centroids are superposed, and then one form is rotated over the other so that the sum of squared distances between corresponding landmarks is a minimum. Fourth row: With the construction lines erased, the squared Procrustes distance between the pair of forms is that sum of squared distances. It is proportional to the total area of the circles drawn at lower right

Not all problems of landmark configuration are problems of shape. If our scientific problem includes aspects of size, the similarity group is too large – the appropriate group to normalize out might be the smaller group of rigid motions (Euclidean isometries) only. In applications of the morphometric synthesis to studies like those, the scaling parameter of the passage to KENDALL's space (Centroid Size, normalized between row 1 and row 2 of Fig. 2) is not restored but archived as an ordinary scalar variable. It is appended to any data base of shape coordinates (see below) to complete the archive of the original coordinate information modulo the isometry group.

Fig. 5. Procrustes averaging and Procrustes shape coordinates. Top row: four forms of four landmarks. Middle row: Procrustes fit of each (X's) to an arbitrary starting guess (dots: the first form). Bottom left: the next estimate of the average (dots) is the average of the fitted locations from the previous step. Bottom right: a second round of fits and averages changes it hardly at all – the algorithm seems to have converged already. Procrustes shape coordinates (again, X's) are the locations of the landmarks after the fitting step upon the average shape (dots) at the convergence of the algorithm. These actually represent the orthogonal projection of the sample onto the tangent space to KENDALL's shape manifold at the shape represented by the dots on the left (see text)

The average of an ordinary list of numbers is their sum divided by their count. This can't work for shapes because we lack an addition operator for these beasts. Instead we exploit a different characterization of that ordinary average: the *least-squares fit* to those numbers, the quantity about which they have the least sum of squared differences. From a distance between shapes, then, we inherit *this* notion of average shape directly.

In practice, this *Procrustes average shape* is more often computed by the iterative approach sketched in Fig. 5. The algorithm is an alternation between fitting to a tentative average and averaging of the fitted locations landmark by landmark. As in this toy example, beginning from any shape in the sample, typically the algorithm converges to sufficient accuracy by the second iteration.

At the left in Fig. 6 is an exemplar of a ten-landmark scheme from midsagittal magnetic resonance (MR) images of the adult human brain. The main example for the rest of this section deals with a data set of 28 of these configurations, 14 from normal adults and 14 from adults with schizophrenia. (That this is a psychiatric study, rather than an evolutionary or developmental one, owes to the principal source of my funding.) In the course of computing the sample average (Fig. 6, center), each individual shape is superimposed over the average using the similarity transformation that made the sum-of-squares around the average a minimum for that particular case. There results the diagram at the right in the figure.

The dual characterization of this maneuver – average alongside the individual forms that have been Procrustes-fitted to it – is the crux of its utility. The collection of superpositions, far from being merely a step in the algorithm of Fig. 5, is the most useful representation for export to applied multivariate statistical packages in most applications. The set of shapes construed as equivalence classes in this wise actually make up a Riemannian manifold, the **Kendall shape manifold**, with Procrustes distance as metric. The manifold is of dimension $2k$–4: $2k$ original Cartesian coordinates, decremented by the four degrees of freedom (two for translation, one for rotation, one for scale) of the similarity group of the plane. For instance, when $k = 3$ (triangles of landmarks), $2k$–4 = 2, so this manifold is an ordinary surface that turns out to have the geometry of a globe: the *spherical blackboard* of shapes of triangles under the Procrustes metric (see, for example, BOOKSTEIN 1991, Fig. 5.6.1).

The tangent space to this manifold is likewise of dimension $2k$–4 at every point. We will attend only to one of those tangent spaces, the one that is tangent at the sample average shape. The construction that concludes Fig. 5 or 6 is the *normal projection* of each shape of our sample onto the tangent space to that manifold at that average. The projection preserves the metric "in the small" – in the vicinity of the sample average – meaning that for each pair of specimens, the summed squared distance between the representatives of the cases in Fig. 5 or 6

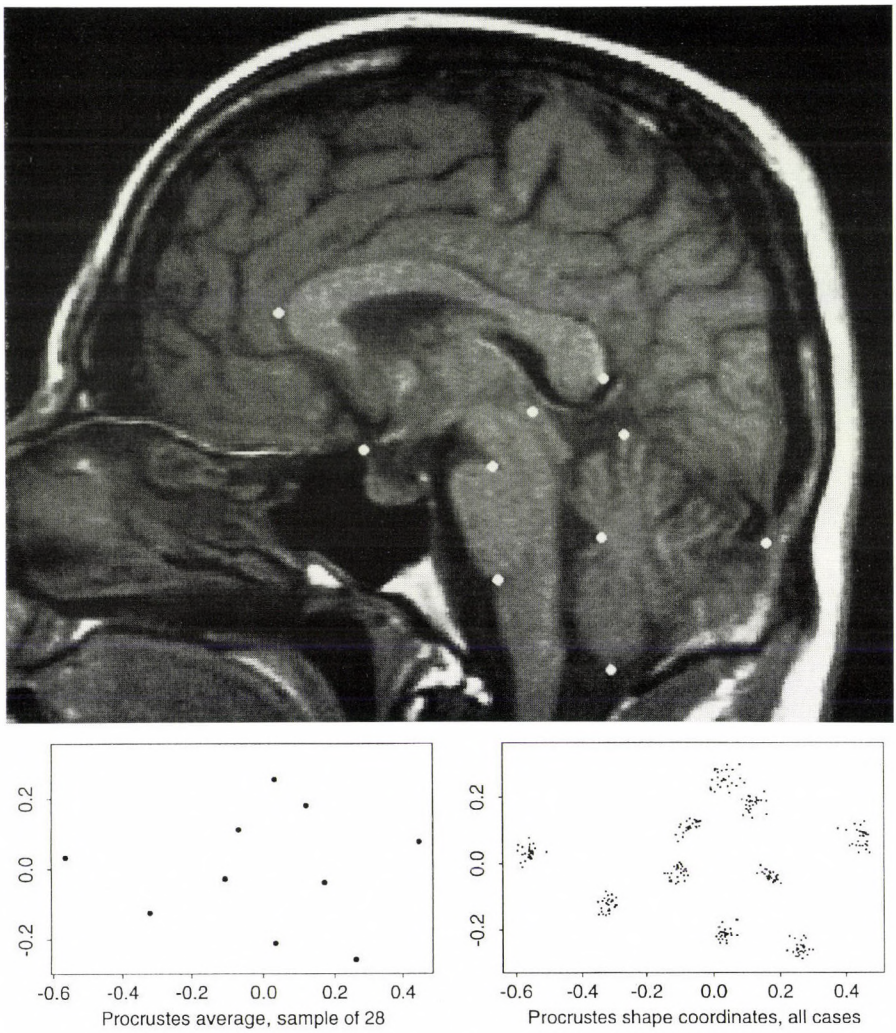

Fig. 6. Procrustes analysis of the midsagittal MR data set. Top: One midsagittal brain image, with its ten landmarks indicated. Landmarks, bottom to top: bottom of cerebellum, bottom of pons at medulla, tentorium at dura, obex of fourth ventricle, top of pons, optic chiasm, top of cerebellum, superior colliculus, splenium of corpus callosum, genu of corpus callosum (see DEQUARDO *et al.* 1996). Bottom, left: Procrustes average of these ten landmarks for 28 cases. Bottom, right: Procrustes shape coordinates: optimal fit of each separate landmark configuration to the common average. The diagram is scaled to sum-of-squares 1 around (0,0); both axes are in units of Procrustes distance per se. The landmark-specific scatters are remarkably well-behaved. This is not an artifact of the method, but an empirical finding about brains. The total variance of these ten scatters about their own centroids, which comes to .0074, is equal to the mean squared Procrustes distance of these 28 landmark configurations from their grand mean shape. This *total Procrustes variance* of the data set will be partitioned in various ways in the course of the analyses to follow. In the rightmost two frames, orientation is with principal moments horizontal and vertical, for simplicity in the formulas for the uniform component further down

is very nearly equal to the Procrustes shape distance that would be computed were they considered as a single pair. The k coordinate pairs of that figure actually serve as a set of $2k$ redundant coordinates for this $(2k–4)$–dimensional tangent space. They are the most natural set of **shape coordinates**. All other useful sets (for instance, the two-point shape coordinates shown in Fig. 8, or the partial warps in Fig. 12) will turn out to be linear combinations of this original set.

The mean squared Procrustes distance from the 28 shapes of this sample to their grand mean (Fig. 6 center) is .0074. This is also the sum of ten mean squared distances, one for each of the little scatters at the right, of the dots from their own centroids scatter by scatter. The statistical analyses to follow partition this mean square in several different ways. The test of group mean difference to follow shortly pulls out a piece of special interest, the mean-squared group difference, and checks to see how large it is with respect to the remainder. Fig. 10 partitions the .0074 total into the empirical principal components of variability. Finally, Fig. 12 is concerned with a partition of the same .0074 by a-priori geometric components of variation at a hierarchy of spatial scales.

An alternate way of construing tangent spaces provides the conceptual link to the next theme of the synthesis. The same tangent space to a Riemannian manifold that one initially intuits as a higher-dimensional plane touching a curving hypersurface, rather as a sphere rests on the ground, can be construed instead as the space of all linear germs of scalar functions along curves through a point of the manifold. To the statistician, these functions are just what we mean by **shape variables.** That is, the tangent space construction of Fig. 5 provides the setting for all possible linearized multivariate analyses of the information in the shapes of the landmark configurations. The Procrustes-fit shape coordinates are one *basis* for the space of such variables, but a redundant one: they are four more than necessary ($2k$ instead of $2k–4$). Eventually we will rotate them into a full-rank basis of $2k–4$ new variables, the *partial warps*, that are orthonormal in the underlying Procrustes geometry; see Fig. 12 below.

For shapes that are concentrated in a small region of the full shape space (as any industrial part, or any within-species sample of the shape of an organ like a brain or heart or pelvis is likely to be), one can carry out most of the ordinary maneuvers of multivariate statistical analysis – tests of group differences, correlations of shape with causes or effects, diagonalization of the sample covariance matrix with respect to Procrustes distance – directly in terms of this Procrustes-fit basis, even though it is redundant. Techniques like multiple regression or MANOVA that require matrix inversion are handled by deletion of any two of the k vectors of fit.

Multivariate sample averaging, for instance, is a fine statistical technique that can go forward using bases like this one. At the left in Fig. 7 is shown a pair of averages for subsets of the 28 cases: one for the fourteen patients actually di-

agnosed schizophrenic, the other for the fourteen age- and sex-matched normals. Here this contrast is computed as a vector in the tangent space to KENDALL's manifold and visualized by way of k separate (but not orthogonal) projections onto k planes within that tangent space.

There is a way to render that same vector in the tangent plane as one coherent graphical construction: a deformation grid. Imagine one of the averages, say, that for the normals (the dots), put down on ordinary square graph paper. Deform the paper so that the dots now fall directly over the *other* set of points, the triangles. The right panel in Fig. 7 shows one plausible representation of what happens to the grid.

Naturally it matters what deformation one uses. The morphometric synthesis emphasizes one particular choice, the *thin-plate spline*, that minimizes yet another calculus of squares. In this context, we are minimizing the summed squared second derivatives (integrated over the whole plane) of the map in the figure. Interpreted as the summed squared deviations of the shapes of the little

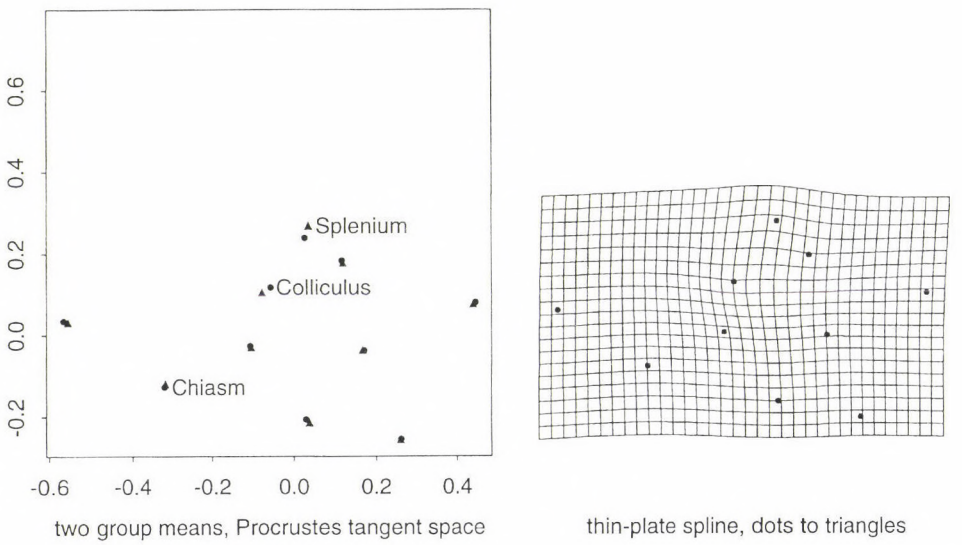

Fig. 7. Statistics and visualizations in the tangent space to KENDALL's manifold. (left) The simplest example of statistical analysis in the tangent space: Average shapes for the two subgroups making up our original sample. Triangles, schizophrenics; dots, normals. The most striking discrepancy is at upper center. The squared Procrustes distance between these group means is .0020; the squared distance of either mean from the grand mean, .0005, is one piece of the usual analysis of variance of the total Procrustes variance of .0074 (see text). (right) The thin-plate spline is an interpolation function from one point set to another having the minimum variation (over the whole plane) of affine derivative. In the Synthesis, it serves to visualize vectors in the tangent space. The grid here, the spline from the dots to the triangles at left, directly leads the eye to a local characterization of the shape difference under study. In other applications an equally obvious signal may appear at much larger scale

squares from the shapes of their neighbors, it becomes a measure of local information in the mapping.

The formulas for this spline are useful, and astonishingly simple. Let U be the function $U(r) = r^2 \log r$, and let $P_i = (x_i, y_i)$, $i=1,\ldots, k$, be k points in the plane. Writing $U_{ij} = U(P_i - P_j)$, build up matrices

$$K = \begin{pmatrix} 0 & U_{12} & \ldots & U_{1k} \\ U_{21} & 0 & \ldots & U_{2k} \\ . & . & . & . \\ . & . & . & . \\ . & . & . & . \\ U_{k1} & U_{k2} & \ldots & 0 \end{pmatrix}, \quad Q = \begin{pmatrix} 1 & x_1 & y_1 \\ 1 & x_2 & y_2 \\ . & . & . \\ . & . & . \\ . & . & . \\ 1 & x_k & y_k \end{pmatrix},$$

and

$$L = \begin{pmatrix} K & Q \\ Q^t & O \end{pmatrix}, \ (k+3)\times(k+3)$$

where O *is a* 3×3 matrix of zeros. Write $H = (h_1 \ldots h_k \ 0\,0\,0)^t$ and set $W = (w_1 \ldots w_k \, a_0 \, a_x \, a_y)^t = L^{-1} H$. Then the thin-plate spline $f(P)$ having heights (values) h_i at points $P_i = (x_i, y_i)$, $i=1, \ldots, k$, is the function

$$f(P) = \sum_{i=1}^{k} w_i U(P - P_i) + a_0 + a_x x + a_y y .$$

This function $f(P)$ has three crucial properties:

1. $f(P_i) = h_i$, all i: f interpolates the heights h_i at the landmarks P_i.

2. The function f has minimum **bending energy** of all functions that interpolate the heights h_i in that way: the minimum of

$$\int\int_{\mathbf{R}^2} \left(\frac{\partial^2 f}{\partial x^2}\right)^2 + 2\left(\frac{\partial^2 f}{\partial x \, \partial y}\right)^2 + \left(\frac{\partial^2 f}{\partial y^2}\right)^2$$

where the integral is taken over the entire picture plane. This quantity is often called the *integral quadratic variation.*

3. The value of this bending energy is

$$\frac{1}{8\pi} W^t K W = \frac{1}{8\pi} W^t \cdot H = \frac{1}{8\pi} H_k^t L_k^{-1} H_k ,$$

where L_k^{-1}, the *bending energy matrix*, is the $k \times k$ upper left submatrix of L^{-1}, and H_k is the initial k-vector of H, the vector of k heights.

In the application to two-dimensional landmark data, we compute two of these splined surfaces, one (f_x) in which the vector H of heights is loaded with the x-coordinate of the landmarks in a second form, another (f_y) for the y-coordinate. Then the first of these spline functions supplies the interpolated x-coordinate of the map we seek, and the second the interpolated y-coordinate. The resulting map

$(f_x(P), f_y(P))$ is now a deformation of one picture plane onto the other which maps landmarks onto their homologues and has the minimum bending energy of any such interpolant.

The quadratic form L_k^{-1} joins two others, the Procrustes metric (now the sum of squared shape coordinate differences) and the empirical covariance matrix of the Procrustes coordinates, to make up the geometrical substrate of the Synthesis. Morphometrics is unusual among branches of modern applied statistics in the centrality of this set of three quadratic forms rather than the usual two (identity matrix and covariance matrix only).

The spline is not claimed to be a realistic model for the correspondence of images between their landmarks. It is, rather, a visualization of directions in the tangent space to the shape manifold defined solely by the shapes of the landmark configurations. What is crucial about the spline is that its coefficients W are linear in the coordinates of the landmark shapes after projection, for instance, the coordinates of the points in the right-hand panel in Fig. 7.

It is often of interest to state the probability of a particular shape finding on a so-called "null hypothesis" setting out a probabilistic structure of uninteresting variability around a signal that is invariable – the same shape all the time. For the simple two-group design here, there is a standard statistic owing to GOODALL 1991, that often serves to reassure anxious collaborators, reviewers and editors. GOODALL's statistic, which pertains equivalently to either of the presentations paired in Fig. 7, is based in the ratio

$$R = \frac{\| \bar{P}_1 - \bar{P}_2 \|^2}{\sum_{\text{cases}} \| P_{\text{case}} - \bar{P}_i \|^2} .$$

Here $\bar{P}_1$ and $\bar{P}_2$ are the group average shapes in the common (pooled) Procrustes registration, and $\| \cdot \|^2$ is squared Procrustes distance. In words, this is the ratio of squared Procrustes distance between group means (sum of squares of the distances between dots and triangles at the left in Fig. 7) to the total of the squared Procrustes distances from each specimen to its group mean (sum of the squares of the distances of the points at the right in Fig. 6 from their group- and landmark-specific centroids). In the data set here, the numerator – the squared Procrustes distance between the group average shapes – is .00197, and the denominator – summed squared Procrustes distance around those group means – is .192, for a ratio R of .0103. This is one version of the usual analysis of variance: The mean-squared group residual per case is .192/28=.0069, and the difference between .0069 and the full Procrustes mean square of .0074 is the mean squared distance of either group mean from the grand mean, which is one-quarter of .0020, or .0005. These values, neither unusually large nor unusually small in magnitude, are typical of findings in applications like this one.

Let N_1, N_2 be the sample sizes of the two groups. Under the assumption that all forms vary around a single average shape by circular Gaussian noise of the same small variance at every landmark, GOODALL showed that, approximately,

$$\frac{N_1 + N_2 - 2}{{N_1}^{-1} + {N_2}^{-1}} \; R \;\sim\; F_{2k-4,\,(2k-4)(N_1+N_2-2)} \;,$$

the statistician's standard tabulated -distribution. The symbol "~" is read here as "is distributed as." In the data set here, the test statistic is $\frac{14+14-2}{14^{-1}+14^{-1}} \frac{.0020}{.192} = 1.87$, tested as an F on 16 and 16×26 degrees of freedom; it is significant at $p = .021$. (Under the same assumptions, Centroid Size is uncorrelated with the entire space of shape features; this observation leads to a convenient omnibus test for allometry [BOOKSTEIN 1991].)

GOODALL's formulation is quite powerful. It combines information about shape variation in all directions of Procrustes space into one single test, because under the assumptions specified that distribution is actually spherically symmetric. Such an assumption sounds "too good to be true" for real data sets. Nevertheless, it is surprisingly realistic in many applications that lack "factors" (systematic effects on shape) that stretch out the covariance structure within groups in predictable ways, factors such as developmental stage or symmetry. Verification of these assumptions is a somewhat delicate matter. In the example of the MRI landmarks here, the assumption is supported by noticing that the scatters in Fig. 6 are not far from circular and of commensurate variance and the scatters in Fig. 12 below are likewise – these are sets of sections of a distribution that, under the null hypothesis, ought to have perfect spherical symmetry in the KENDALL tangent space – and that the eigenvalues printed on Fig. 10 don't fall too fast.

In practice, however, we need not worry overmuch about that verification (just as well, since often even "pure digitizing error" is far from circularly distributed). In accord with the computational turn in modern statistical practice, it is usually just as effective to evaluate this ratio by a permutation test that makes hardly any assumptions. For this computation, the observed value of the ratio R is calibrated against the cumulative distribution of analogous ratios computed after group is assigned by (hundreds or even thousands of) random permutations of group assignment rather than according to the true group (actual diagnosis) case by case. The probability associated with this significance test is then the actual tail-probability of the observed ratio within that cumulative distribution. (Think of this as simulating the correct distribution of the ratio R to get the degrees of freedom for a more appropriate approximating F.) Since the sum of squares of all the shapes around the grand Procrustes mean is a constant, it is sufficient to compute the permutation distribution of the numerator alone, the quantity analogous to .00197 here. After 500 permutations, the probability of finding a squared Pro-

crustes distance between mean shapes of random nonoverlapping 14-specimen subgroups to be greater than .00197 is the same 2% we had already estimated by GOODALL's F. For more on permutation tests, see GOOD 1994. Note that this testing protocol, along with GOODALL's original, applies whether or not there are more cases (n) than variables for analysis ($2k$–4 or so). The punctilious may wish to report permutation p's only up to sampling variation, which is Poisson for small tails like these. That value of 2% is really $10 \pm \sqrt{10}$ out of 500, or, going out 2 s.e.'s either way, "1% to 3%."

For group comparisons and for correlations of shape with exogenous variables, though not for the study of shape variability within homogeneous populations, recourse to the Procrustes basis just reviewed is unnecessary. Among the other bases for this same KENDALL tangent space, all of which can be derived from the Procrustes basis by linear transformation, there is one that antedates the Procrustes basis by several decades: the **two-point shape coordinates** originally devised by FRANCIS GALTON in 1907 and rediscovered (without attribution) in BOOKSTEIN 1986. As laid out in Fig. 8, these consist of a "Procrustes superposition" on just two of the landmarks rather than the whole set. For two landmarks, that "least-squares fit" is simply the superposition on both endpoints simultaneously. By convention, one landmark is set to (0,0) and the other to (1,0); the resulting shape coordinates are, in complex notation,

$$\frac{z_j - z_1}{z_2 - z_1}, j = 3, \ldots, k.$$

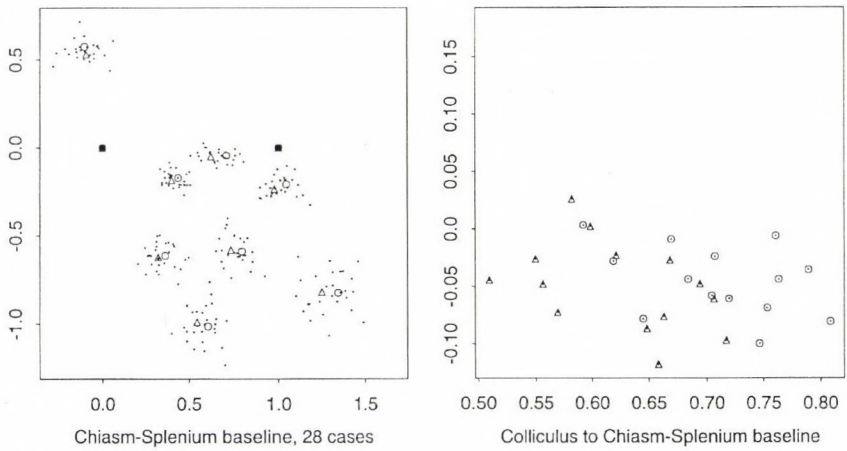

Fig. 8. Two-point shape coordinates. Left: the scatter of shape coordinates (eight triangles per form) to a Chiasm-Splenium baseline (see Fig. 6). Group mean shapes are indicated by larger symbols inside the scatters. Right: enlargement of scatter at Colliculus from the preceding frame. Circles, normal subgroup; triangles, schizophrenic subgroup. The extent of group separation here is no surprise, as this coordinate pair was chosen by study of the deformation grid in Fig. 7 in order to capture the group difference as well as possible in a simple ratio.

Each of these k–2 coordinate pairs is the shape of one "triangle" on the fixed pair of landmarks as baseline. These total $2k$–4 coordinates, just as they should.

Effects noticed first by inspection of grids can often be reported cogently, reduced to discriminant functions, contemplated to generate scientific hypotheses, etc., by careful construction of a set of these triangles. Except for three-landmark data sets, the two-point shape coordinates ought not to be tested pair by pair for "significance" – they are selected instead to be the most informative about the scientific signal under study – but they certainly ease the task of interpretation. Inspection of the grid in Fig. 7 suggests a baseline along the segment from Chiasm to Splenium, a transect showing great inhomogeneity of change between the group means. The left panel of Fig. 8 shows the corresponding "substitute Procrustes fit" to the endpoints of this segment, Chiasm and Splenium (see Fig. 6). It is clearly inferior to that in Fig. 6. But a magnification of the scatter of Colliculus in this registration, at right, shows a group difference that is significant separately (by ordinary normal-model Hotelling's T^2) at $p \sim .003$. Multiplied by the appropriate factor of 8 (we picked it out of eight triangles, after all), this p nicely matches the actual significance level of 2% that was computed without any a posteriori selection by the permutation test. We can thus classify cases about as well by thresholding the ratio of distances

$$\frac{\text{Colliculus} - \text{Chiasm}}{\text{Colliculus} - \text{Splenium}}$$

as by any other combination of shape coordinates based in these landmark configurations. Multivariate regressions on shape and canonical analyses can go forward using these coordinates, but not principal components analysis or Partial Least Squares, as these techniques require the reference metric that two-point shape coordinates lack.

The same Procrustes geometry that optimally handles the four (in 3D, seven) nuisance parameters of the similarity group (translation, rotation, scale) extends directly to the additional two parameters, no longer nuisances, specifying forms that derive from the sample average landmark configuration by uniform transformations (simple shears). These forms lie on an ordinary (two-dimensional) plane through the average shape in the tangent construction for shape space. This construction is geometrical, not statistical: the plane is determined solely by the average shape, not by the nature of variation around it. Every specimen has a *uniform coordinate pair* derived from Procrustes-orthogonal projection onto this subspace, and also a Procrustes-orthogonal *residual* from that projection, which is the geometrically unique *nonuniform part* of shape variation. The Pythagorean decomposition applies: squared Procrustes distance equals squared uniform distance plus squared nonuniform distance, and the two parts can be averaged, tested, eigenanalyzed, and correlated separately.

Let the Procrustes mean form (Fig. 6 center), oriented with principal axes horizontal and vertical (as it is here), have coordinates $(x_1,y_1),(x_2,y_2),\ldots,(x_k,y_k)$, and let $\alpha = \Sigma\, x_i^2$ and $\gamma = \Sigma\, y_i^2$ be the principal moments along those axes. Then the elements of this uniform coordinate pair may be taken as dot products of the Procrustes fit coordinates (Fig. 6, right), treated as a $2k$-vector of real numbers, with the vectors Un_1 and Un_2 where

$$\lambda\, U\, n_1{}^t = ((\alpha\, y_1 , \gamma\, x_1) , (\alpha\, y_2 , \gamma\, x_2) , \ldots , (\alpha\, y_k , \gamma\, x_k))$$

$$\lambda U\, n_2{}^t = ((-\gamma\, x_1 , \alpha\, y_1) , (-\gamma\, x_2 , \alpha\, y_2) , \ldots , (-\gamma\, x_k , \alpha\, y_k)).$$

Here λ is a factor $\sqrt{\alpha\gamma}$ that scales the vectors Un to have unit Procrustes length. The first of the vectors corresponds to Cartesian shears aligned with the x-axis, the second to Cartesian dilations along the y-axis. Notice that these formulas are closed – for two-dimensional data, the Procrustes uniform term is evaluated from the Procrustes shape coordinates without iteration. Any two-vector of scores on this component can be converted to an orthogonal pair of principal strains by the angle-bisecting algorithm of BOOKSTEIN (1991); the anisotropy of the transformation is (approximately) the length of that score vector, divided by λ.

For the data set here, there is one pair of scores for each case, scattered with group coded in the left frame of Fig. 9. The total Procrustes variance (sum of squares here) is .0014, less than 20% of the total shape variation. In other examples (e.g., postnatal growth of the rat skull, BOOKSTEIN 1996*a*), the uniform term

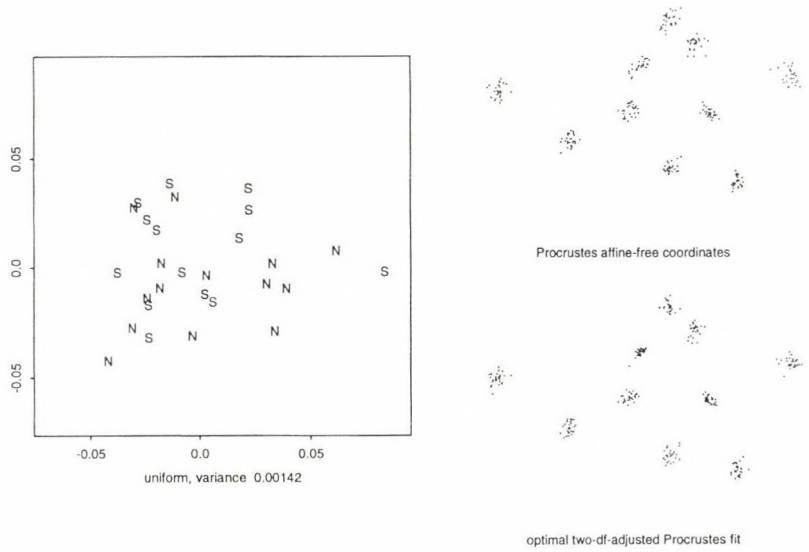

Fig. 9. The uniform component for the ten-point schizophrenia data. Left: Sample scatter for 28 forms in two groups. Right, top: Nonaffine variation, Procrustes variance .0060. Right, bottom: Residual after partialling out the first two relative warps (see next figure), Procrustes variance .0047

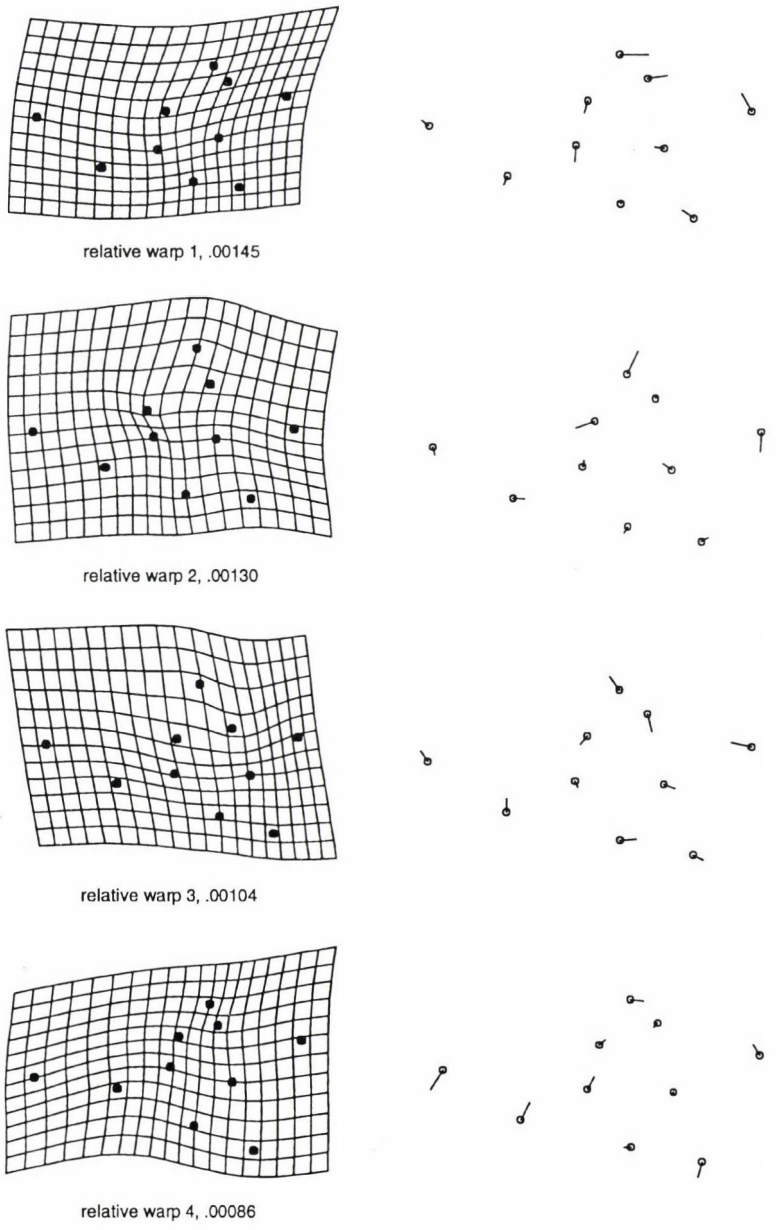

Fig. 10. Relative warps (empirical principal components in shape space) of the full Procrustes shape scatter. Top two rows: first and second. Lower two rows: third and fourth. Each is shown both as a thin-plate spline and as a pattern of displacements in Procrustes space. Each warp is drawn at Procrustes length equal to its sample range as a deformation or displacement of the sample average form. Each warp is labelled with its eigenvalue, the sample Procrustes variance it accounts for. Notice that the second component is very localized and strongly resembles the group difference in Fig. 7. Of the total Procrustes variance of .0074, 63% is in these four dimensions

can account for 50% or more of the shape variation. In such cases, it is worth standardizing separately prior to the search for nonaffine (localized) signals. The center panel here shows the variation remaining after this uniform term is partialled out – the *nonaffine variation* of the data set. The panel at right will be explained in a moment.

Group difference is one grand theme of applied multivariate analysis; the other is within-group ordination. As the uniform component does not explain much of the shape variation in this actual sample, to what features might we turn instead? Because the Procrustes metric is retained alongside the sample covariance structure, there is an exact analogue of principal components analysis for Procrustes-registered shapes: a set of empirical orthogonal components of shape that account for as much shape variation as possible (in the Procrustes metric) for a given number of components. They are computed straightforwardly as ordinary principal components of the Procrustes shape coordinates (Fig. 6 right) in their own $2k$-dimensional space. (The principal component extraction must be "unstandardized" – the shape coordinates must be left in the original Procrustes metric of that figure, and the principal components software must use the covariance, not the correlation, matrix.) In BOOKSTEIN (1991) I named these components *relative warps* for a reason that no longer seems particularly cogent; nevertheless, the name has stuck (e.g., ROHLF 1993).* As Fig. 10 shows, for the data set at hand the first two of these components are *not* particularly aligned with the uniform part of the transformation. There is thus no good reason for any standardization (of this particular data set, anyway) to begin there. As it happens, the second relative warp is closely aligned with the shape difference between our two groups of cases: the excess variance in which we were interested all along. Were the figure extended to all 16 panels, the eigenvalues printed panel by panel would partition the total Procrustes mean square of .0074 that we have already encountered. Relative warps supply the optimal lower-dimensional linear reconstructions of empirical shape data vectors just as principal components do in any other application. In this Procrustes context, furthermore, they are identical to principal-coordinates analysis of the original pairwise Procrustes distances.

This was the *empirical* orthogonal basis for shape variation (recall Section 3). The morphometric synthesis includes a *geometric* orthogonal basis as well. For our ten-point brain example, it is shown in Fig. 11: the eigenvectors of the bending-energy quadratic form L_k^{-1} of the spline formalism. Drawn as splined surfaces in this style, they are called *principal warps*. Like the uniform component, they depend only upon the sample average form, not any aspect of its variability. When projected onto both the *x- and y*-axes of the Procrustes shape

* These relative warps are the standard set in which a parameter α representing the relative weight of smaller-scale phenomena is set to zero. The use of the technique for other values of α is discussed in BOOKSTEIN 1996*b*.

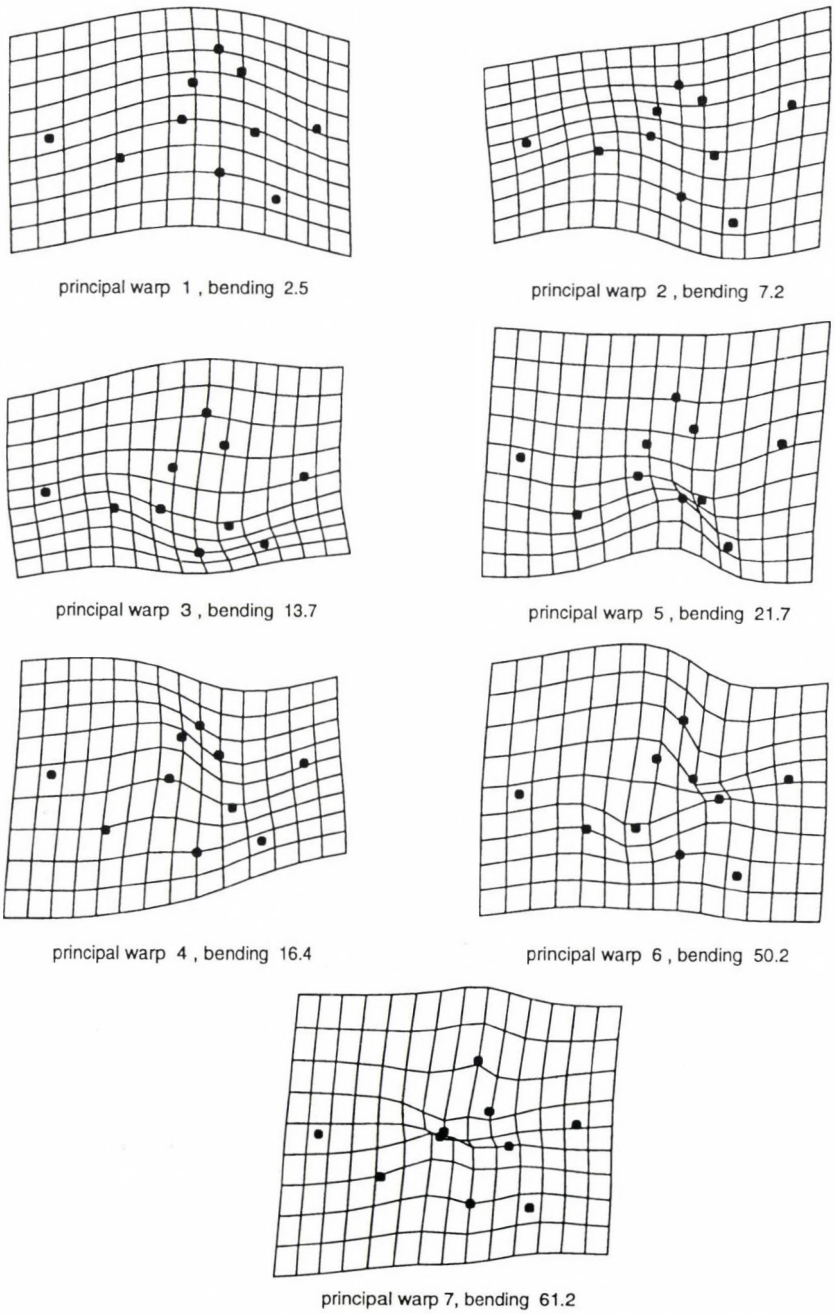

Fig. 11. The seven principal warps of the sample average shape (Fig. 6, bottom, left): eigenfunctions of the bending-energy quadratic form, drawn at Procrustes length 0.16, to be read as splined surfaces. Augmented by the uniform component, this basis provides a Procrustes-orthogonal rotation of the redundant 20-dimensional basis at right in Fig. 6 into its 16 nontrivial dimensions

space, and supplemented by the uniform term just reviewed, they are an orthogonal rotation of the original Procrustes shape coordinates, Fig. 6 (right), into a basis of the correct rank, $2k$–4.

The bending energy of each of these normal modes serves as a useful index of its localization in the geometry of the original image plane. It is these features, far more than, say, polynomials of progressively higher order (SNEATH 1967), that constitute the natural extension of the a-priori geometric basis beyond the uniform term. For the ten-landmark average shape here, the next two natural parameters are the x- and y-projections of the surface at upper left in Fig. 11, and the next two after those are the projections of the surface to its right. The resulting set of scores is set out all together in Fig. 12, where the uniform component from Fig. 9 is duplicated at upper left because it represents the eigenspace of eigenvalue 0 – no bending – and thus completes the series.

This basis of principal warps for the KENDALL tangent plane is the only a-priori orthonormal set that has yet been presented for scrutiny in the morphometric literature. Both principal components analyses and Partial Least Squares can exploit this basis, as well as multiple regression on shape and multivariate analysis of its variance, and Procrustes distance remains the sum of squared shape coordinates. The new set of shape coordinates in Fig. 12 are called *partial warp scores*; in general they will not be uncorrelated. The rotation they represent of the original Procrustes basis continues to depend only on the mean form, and so supports reasonably objective inquiries into the scale(s) of shape phenomena. Each partial warp has a variance as summed over its two dimensions of scatter. These eight values (printed under the scatterplots), like the two other decompositions I have reviewed earlier, total .0074, the total Procrustes variance of the data set. (But the sort order here is the underlying bending energy, not sample variance accounted for.) In the present data set, the first four partial warps account for only 40% of the sample variation, vs. 63% for the same number of relative warps.

While relative warps summarize sample variability in the usual canonical way, the formulation of partial warps pays no attention to variation. They are instead a delicate function of the mean shape quite sensitive to details of the spacing of landmark points (which is a subjective decision of the scientist, not a property of the organism). Geometrically, partial warp formulas express the relative eigenanalysis of Procrustes distance with respect to bending energy, and thus, while surely a descriptive convenience, stand at considerable remove from biological reality. They could be reified as biological (rather than statistical) variates only if those two quadratic forms are *each* biologically meaningful, which is not likely to be the case in any evolutionary or developmental context. It is relative warps, not partial warps, that supply the morphometric equivalent of "characters." Moreover, any analysis of shape that requires one specific choice of basis, such as the abuse of partial warps by FINK *et al.* (1995), is morphometric

nonsense. All valid morphometric methods must yield reports, like the grid in Fig. 7, that are invariant against rotations of the basis for linearized description of shape (see also ROHLF 1998).

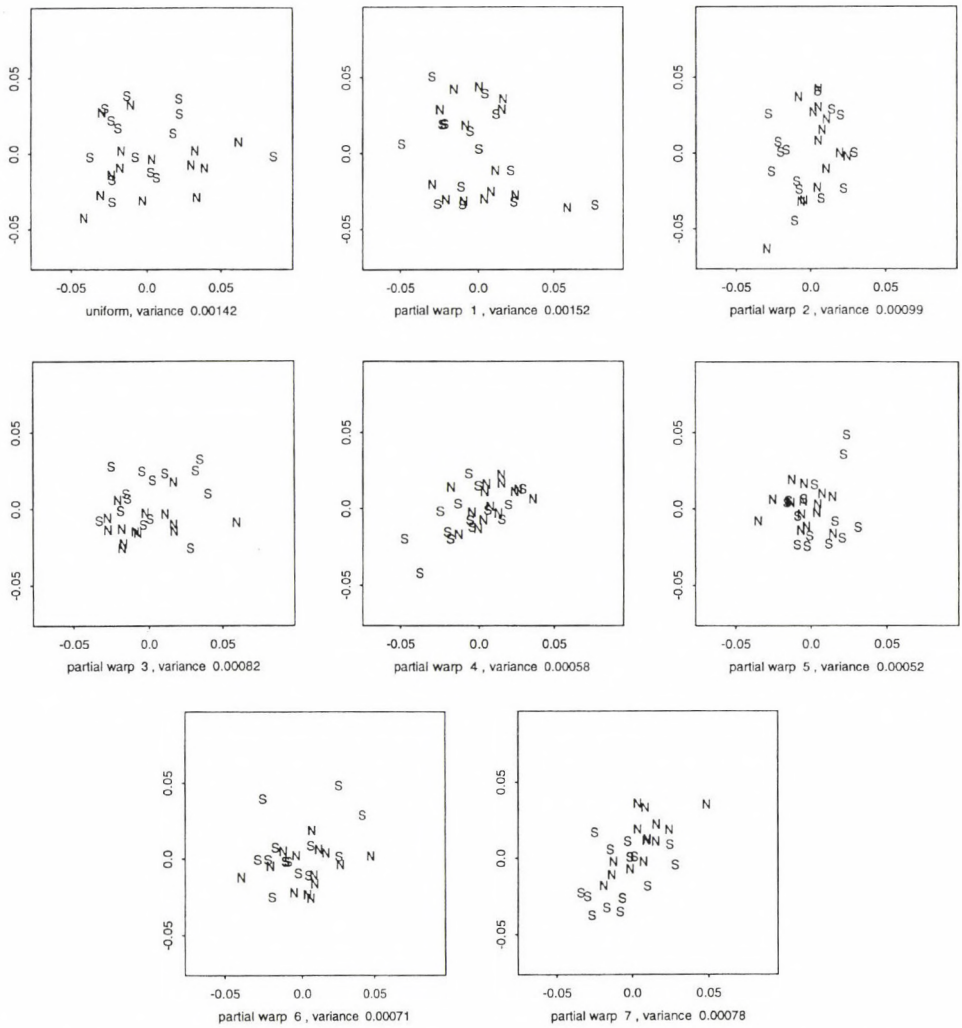

Fig. 12. Decomposition of sample variation by partial warps (projections onto the orthonormal basis of Fig. 11), together with the uniform component (upper left). Of the total shape variance of .0074, less than 20% is uniform, and about the same fraction is aligned with the largest-scale nonlinear bending (Fig. 11, upper left). N, normals; S, schizophrenics. All frames are commensurate in the Procrustes metric. The separation of N's and S's is largest in the panel at lower right, corresponding to the most focused dimension of warping. Axes are in the same units as Fig. 6 or 9

All this machinery goes over to the context of three-dimensional data without substantial changes. Here are two more examples, again dealing with the neuromorphometrics of schizophrenia, that exemplify these extensions.

COPPOLA and colleagues (1998) digitized 21 landmarks on left and right parasagittal planes (planes symmetrically positioned near the midsagittal plane on opposite sides) in a sample of twenty male schizophrenics and age-matched normals from a data resource at NIMH. Fig. 13 shows the difference between the diagnostic groups on left and right sides separately. It is concentrated in two regions: that at upper right in the grids, where landmarks are alas noisy and variable, and that at upper left, where they are fortunately quite precise. In this latter region (the prefrontal gyrus), the contrast between these two grids – that is, the difference in asymmetry per se between normals and syndromals – is significant beyond the .0001 level by permutation test (which takes quite a while to compute). A useful representation of the within-group scatters, at right in the figure, shows the difference between left and right quadrilaterals (landmarks of anterior/inferior cingulate gyrus and genu of corpus callosum) as displacements from the grand bilateral mean.

In BUCKLEY *et al.* (1998), PETER BUCKLEY and DAVID DEAN of Case Western Reserve University report on group differences in the positions of 38 landmarks manually located upon automatically extracted ridge curves (see Sec. 6) in 10 normal males and 10 schizophrenics. There is a substantial mean difference between normals and syndromals in the form of the lateral ventricle, represented here by three characteristic points that more or less circle the notch of the lateral horn somewhat proximally. At left, Fig. 14 shows a fivefold magnification of this effect (i.e. a transformation using five times the shift component of the coefficient vector W of the spline equations) as it affects one single plane through the original solid form, and the right panel is one display of the resulting group separation (two shape coordinates for the hexahedron of three paired landmarks involved). This separation is statistically significant past the .00001 level by ordinary univariate statistical tests: there really *is* a localized group difference here.

By now my readers must be desperately anxious to return to their familiar contexts of evolutionary or developmental biology. Examples of such applications of these techniques fill the pages of MARCUS *et al.* (1996). See, for instance, the contributions there by VAN DAM, WALKER, JOHNSON and BUDD, LOY *et al.*, or BAYLAC and DAUFRESNE. Analyses in this spirit are appearing with increasing frequency in the peer-reviewed literature as well.

This sturdy and resourceful toolkit of interrelated statistical and graphical methods for landmarks subsumes and supersedes a great many techniques put forward earlier for partial aspects of this shared task. The original method of Cartesian grids (THOMPSON 1917) was one such candidate method, as was the exten-

sion by HUXLEY to growth gradients. To these graphics, however, never corresponded a statistical method, multivariate or otherwise; I have reviewed their infelicities in BOOKSTEIN (1978). In the Synthesis here, multivariate statistical ana-

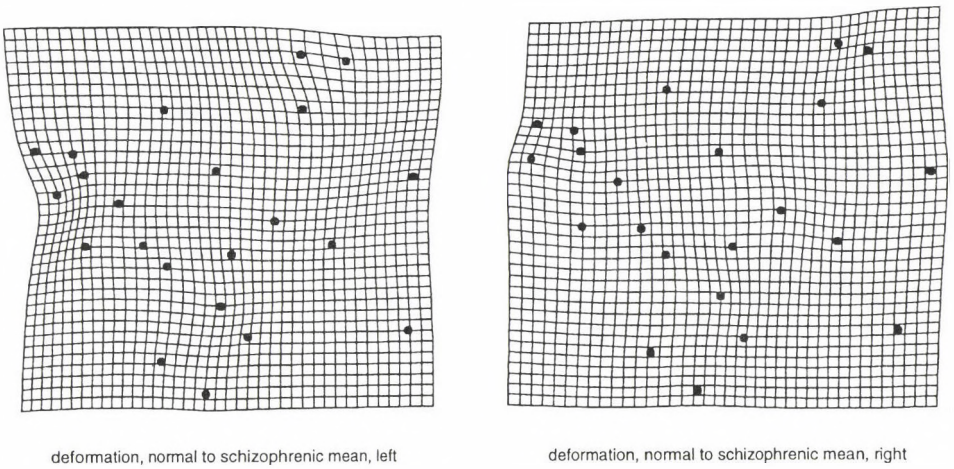

Fig. 13. Analysis of parasagittal asymmetry from COPPOLA *et al.* (1998). Top: Thin-plate splines for group mean difference (normal to schizophrenic), separately for planes about 3 mm lateral to the midline left and right. Bottom: Scatterplot of the most contrasting region of these grids (about ten o'clock), showing the enormous discriminatory power of information on left-right asymmetry for this simple quadrilateral of landmarks

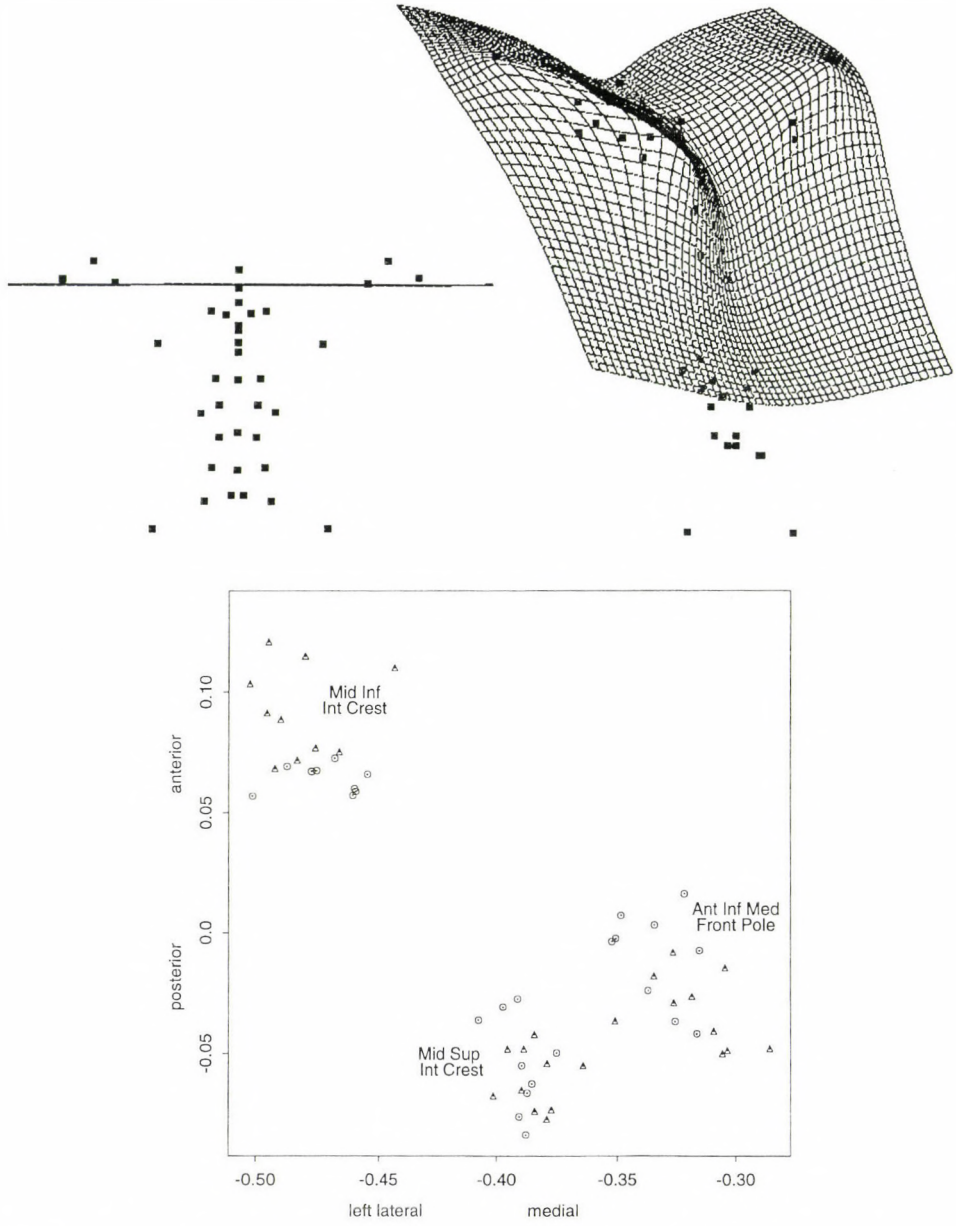

Fig. 14. Analysis of symmetrized cerebral ventricles, from BUCKLEY *et al.* (1998). Top: From a three-dimensional thin-plate spline on 38 landmarks, one plane through the necks of both lateral ventricles, and its image after eightfold magnification of the actual group difference. The figure is in two different coordinate systems: the plane is viewed edge-on at the left, to show how it cuts the ventricular horns, and, after deformation, in perspective at the right. Bottom: Group separation in the shape of the prism formed by these three landmarks on the two sides of the ventricle, coronal projection. Note the nearly perfect separation at the anterior lateral landmark

lysis comes first, and diagrams of "deformation" actually correspond to vectors back in the tangent structure attached to shape space. In other, less satisfactory approaches to analysis of landmark locations, deformation grids are the primary datum, and statistical analysis attempts to "keep up" by ad-hoc testing of extracted features. This reversal of what we now believe to be the correct relationship of diagrams to statistics characterizes my original attempt at a grid-based morphometric method (BOOKSTEIN 1978), the method of biorthogonal grids, as well as several other approaches that, in general, lose considerable amounts of statistical power by comparison with the inferential machinery of the Synthesis. For instance, the general class of tensor analyses, which includes both the biorthogonal grid approach and also Finite Element Scaling Analysis, applies to small regions of an interpolation a statistical method that, construed correctly, pertains only to estimates of the uniform component (as presented above) over extended sets of landmarks. This critique has been published before, in BOOKSTEIN (1991), and will not be repeated here. Similarly, the method of trusses, which attempted to capture the multivariate statistics of shape variation via a series of quadrilaterals (for plane data), is subsumed under the analysis of landmark locations, even for the allometric model that was its primary intended application (see, again, BOOKSTEIN 1991).

While the Morphometric Synthesis per se deals only with data about forms, the presence of the underlying Procrustes metric, with its a-priori notion of orthogonality, encourages the practicing multivariate analysis to augment the usual toolkit of matrix techniques with one additional strategy, the singular-value decomposition of cross-covariance matrices, known, for unconvincing but indubitably historical reasons, as Partial Least Squares (BOOKSTEIN 1991, MCINTOSH *et al.* 1996). In the language of biplots (MARCUS 1993), PLS is a biplot of a cross-covariance matrix, not of the more usual raw data matrix. In many studies a landmark data set is to explain or to be explained by one or more blocks of simultaneous predictors or consequences: another landmark set, perhaps, a vector of ecological indices, or a vector of measures of function. In these applications, classical techniques like regression or canonical correlations should be replaced by a maneuver that permits interpretation of coefficients of the resulting canonical vectors as *saliences* independently pertinent to the dimensions of shape space, one by one, while still optimizing a very useful explanatory quantity (covariance, rather than explained variance or correlation). Like principal components analysis, furthermore, PLS findings are independent of any rotation of basis for shape space: Procrustes residuals, partial warp scores, relative warp scores all give the same analyses.

Like all other vectors in shape space, the canonical vectors from a Partial Least Squares analysis can be drawn as deformations. The corresponding singular vectors, then, are called *singular warps*. Fig. 15 shows an unpublished

example from a study by Elena TABACHNICK of the relation between variations of landmark shape in two different views (apertural and spiral) of a planktonic foraminiferan, *Globorotalia truncatulinoides*. Another example of landmark–landmark analysis can be found in BOOKSTEIN 1997*d*. For an ecophenotypic example that shows the corresponding scores but not the singular warps, see CORTI *et al.* 1996.

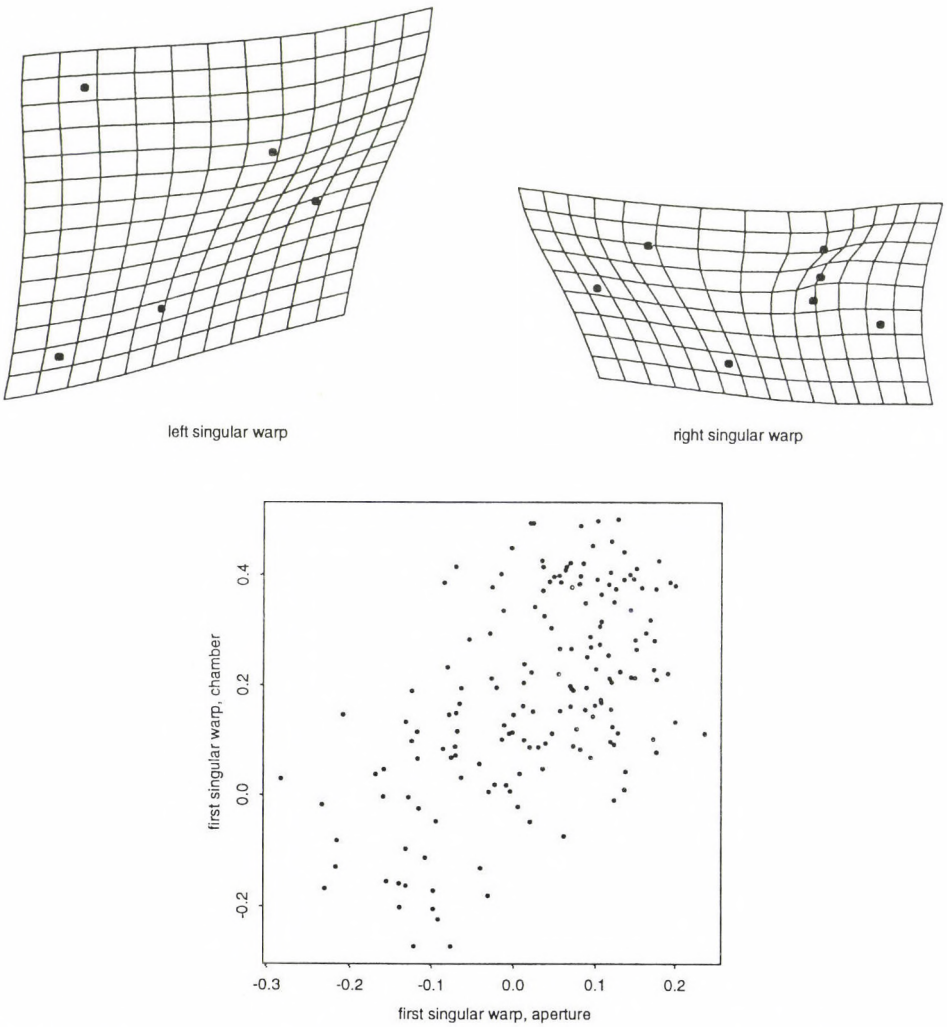

Fig. 15. Example of a Partial Least Squares analysis: singular warps and latent variable scores for landmarks from two views of *Globorotalia truncatulinoides*. The left landmark set is from a lateral view aligned with the aperture; the right set, from the chamber outline. The scatter at bottom shows the correlation of the best-covarying pair of projections of Procrustes unit length. From TABACHNICK and BOOKSTEIN 1998

5. INFORMATION FROM CURVING FORM

Landmark locations are image features, but as a set they constitute a stringent abstraction of the information from that biological image. There is considerably more to be learned about shape and shape variation from parts of boundaries between landmarks: curves in two dimensions, curves or surfaces in three. A joint modification of the two main methods of the synthesis, Procrustes projections and the thin-plate spline, seems to handle this extended class of data with striking effectiveness. The spline serves to relax claims of point-correspondence along the smooth manifolds upon which homologues are actually bound. The Procrustes procedures continue to apply to construct useful statistical spaces, to diagram interesting dimensions of those spaces, and to provide optimal detection and statistical assessment of scientifically important differences. The material here is explained in more detail in BOOKSTEIN 1997*b*, but was already hinted at in an appendix to BOOKSTEIN 1991.

The classical thin-plate spline computes the interpolant of one set of landmarks $X_1 \ldots X_k$ onto another set $Y_1 \ldots Y_k$ that minimizes integral quadratic variation. Collect these coordinates as the vector $Y \equiv (Y_x \mid Y_y) = (Y_{1x},\ldots,Y_{kx}, Y_{1y},\ldots,Y_{ky})$. The minimand for the spline turned out to be the quadratic form $Y_x{}^t L_k{}^{-1} Y_x + Y_y{}^t L_k{}^{-1} Y_y$, where $L_k{}^{-1}$ is the familiar bending-energy matrix.

We modify this setup for the problem of splining curves of unknown homology as follows. Let there be a "nominal set" of landmarks $Y_1{}^0,\ldots, Y_k{}^0$ again collected coordinatewise as the vector $Y^0 = Y_{1x}^0,\ldots, Y_{kx}^0, Y_{1y}^0,\ldots, Y_{ky}^0$). We seek the spline of one set of landmarks $X_1 \ldots X_k$ onto another set of landmarks $Y_1 \ldots Y_k$ of which a sublist $Y_{i_1} \ldots Y_{i_m}$ are free to slide away from those nominal positions $Y_{i_j}{}^0$ along directions $u_j = (u_{jx}, u_{jy})$ that are usually taken as observed tangent vectors to the outline under consideration. To minimize the bending energy $Y_x{}^t L_k{}^{-1} Y_x + Y_y{}^t L_k{}^{-1} Y_y$ as the landmarks Y_{i_j} of the sublist range over lines $Y_{i_j}{}^0 + t_j u_j$, collect the parameters $t_1,\ldots,t_m$ in a vector T and the directional constraints $u_1,\ldots,u_m$ in a matrix of $2k$ rows by m columns in which the (i_j,j)-th entry is u_{jx} and the $(k+i_j,j)$-th entry is u_{jy}, otherwise zeroes. The task is now to minimize the form

$$Y^t \begin{pmatrix} L_k^{-1} & 0 \\ 0 & L_k^{-1} \end{pmatrix} Y \equiv Y^t \mathbf{L_k^{-1}} Y$$

over the hyperplane $Y = Y^0 + UT$. The solution to this familiar *generalized* or *weighted least squares* problem is achieved for parameter vector

$$T = -(U^t \mathbf{L}_k^{-1} U)^{-1} U^t \mathbf{L}_k^{-1} Y^0.$$

A similar setup (involving more complicated notation) applies to relax points upon approximate tangent planes to empirical surfaces and to various special cases (multiple curves, landmarks bound to others in rigid linkages, landmarks

restricted to curves in space), and the whole suite of computations is sometimes iterated for greater accuracy (meaning that once the points Y_j are "slipped", each is projected back onto the original outline curve and a new tangent direction u_j computed). We believe, though we have not yet formally proved it, that the alternation of these relaxations with the standard Procrustes averaging scheme (Fig. 5) will converge to useful representations of the sample average shape and variation around it in all of these extended settings.

Wherever an outline is adequately sampled, the general effect of the splined smoothing is to attenuate the components of bending around the sample mean that have higher bending energy – the more localized components – in favor of those of lower bending energy, right up through the affine term (of zero bending energy). At every point, however, the relaxation is authorized in only one direction, the direction of the tangent to the (average) curve. Thus the splined relaxation strongly suppresses small-scale variations of spacing along the curve in favor of coordinated shifts at larger scale; but displacements perpendicular to the curve remain unaffected, and changes near corners are compromised.

The data set in Fig. 16 is typical of the intended applications for which this hybrid technique may prove suitable. The original images are single parasagittal slices selected from a different set of clinical MR brain scans, 12 doctors and 13 schizophrenic patients. From a larger data scheme I have extracted only the outline of the *corpus callosum* (a bundle of nerve tracts connecting the left and right cerebral hemispheres). It proved convenient to digitize it as a polygon of 26 vertices in one form; the technique here propagates that count of points to all the

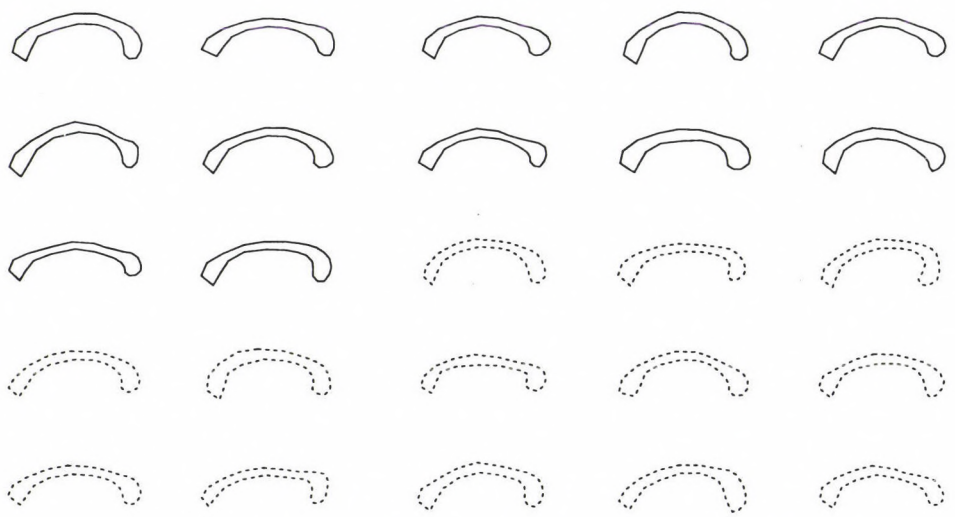

Fig. 16. A typical data set for analysis of outline 26-semilandmark polygons for 25 callosal outlines from thick midsagittal MR images. Solid lines, normals; dotted lines, schizophrenics

other forms of the data set as well as to the average. It is this data set (already fairly extensively processed, of course), 25 polygons of 26 vertices, that is displayed in Fig. 17 after relaxation to its own average. At convergence of the alternation of the two algorithms, Procrustes averaging and splined relaxing, each of the 26 vertices is the splined transform of the same point of the Procrustes average outline. The loci that result have no anatomical identifiers but remain "corresponding" points in a sense satisfactory for subsequent morphometric interpretation: each derives from the spline-based slipping onto its own outline of the full configuration of the sample average. Here we will call them **semilandmarks.** The Procrustes step incorporates a scatter of fitted values, Fig. 17 upper left, in the usual way.

The thin-plate spline can sharpen the visual impact of shifts like these. At lower center in Fig. 17 is the transformation from the normal average to the schizophrenic average (the two curves of the middle panel), magnified threefold. Two features are visually obvious: compression of genu (bulb at the far left) and upward-rightward translation of the isthmus at right center. The grid suggests that isthmus is dragged by "forces" in its vicinity. The enlargement of the bulb of splenium, at the right (posterior) end of the form, is clearly directional, combining vertical extension with horizontal compression; by contrast, the change in genu, far left, is more nearly isotropic.

The omnibus GOODALL F-test as tabulated does not apply to slipped data, owing to the enormous spatial autocorrelation of landmark positions induced by the relaxation. (The same is true in applications to symmetric data.) The corrected (permutation) version supplies a p-value of .25 only, which is not promising. But we know that the spline is inattentive to affine transformations – in the application to curves like these, for which the centering of the arch is arbitrary, it is quite reasonable to consider the uniform component of the data variation separately, then partial it out. There is no group difference in this component, but the residuals show a scatter that is remarkably more focused, at lower left in Fig. 17. The same permutation test that supplied a p of 25% for the full data scatter yields a tail-probability of 1.2% (12/1000) for the null in the nonaffine subspace of this same data set. That is, the two mean shapes in question, the doctors' and the patients', differ in nonaffine shape at about the 1.2% significance level. The most popular competing technique, which compares areas of "sectors" of this arch, is not powerful enough to demonstrate any difference between these mean shapes. More detailed investigation (BOOKSTEIN 1997*a*) shows that the shape of the lower border of isthmus affords a discrimination between the groups with a signal-to-noise ratio of 1.75, sufficient for a classification with only three errors. A frame from that analysis completes Fig. 17 here.

Another modification of the main toolkit that is sometimes useful for application to curves is the restriction of Procrustes distance to the direction normal to

Fig. 17. Analysis of the data in Fig. 16 by Procrustes and spline methods from this toolkit. (upper left) Procrustes shape coordinates after relaxation to the grand mean. (upper center) Mean shapes by group (solid line, normals; dashed line, schizophrenics); note shift at isthmus (underside of right-hand arch). (upper right) Uniform component, no group difference. (lower left) Procrustes scatter after partialling out the uniform component. In this subspace, the two groups of shapes are statistically significantly different at the 1.2% level by the permutation version of GOODALL's omnibus test. (lower center) Thin-plate spline for three times the difference of means by diagnosis. Notice the substantial displacement of isthmus. (lower right) Recomputation of Procrustes scatter restricted to a small region of isthmus. The separation at the most shifted landmark is almost perfect; it accounts for the significance of the contrast as a whole

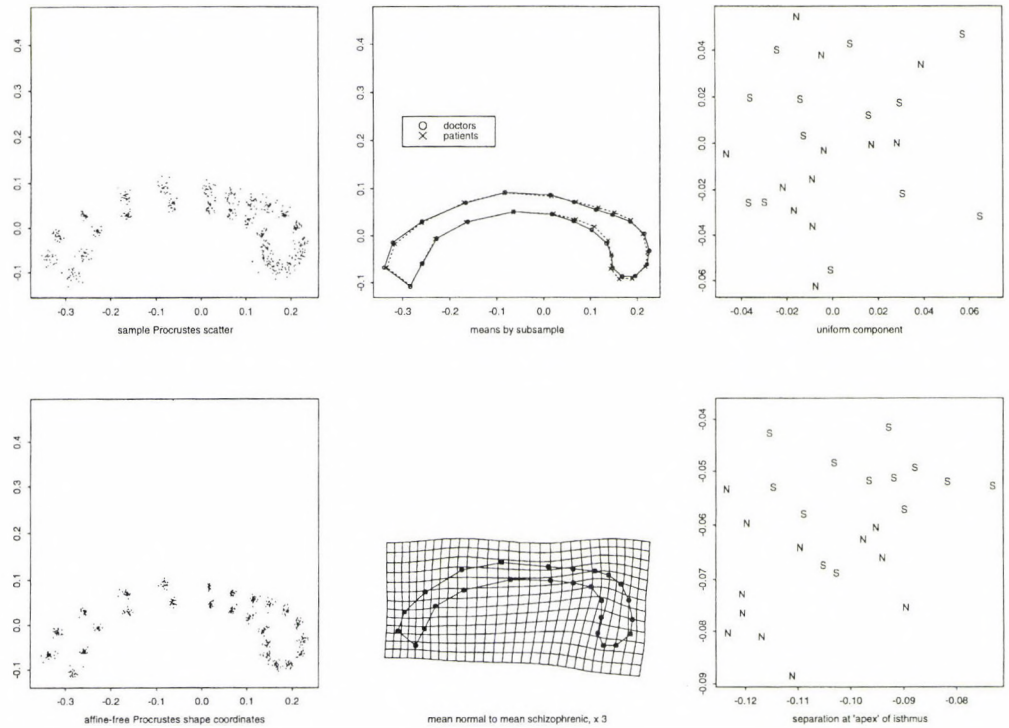

the mean curve (see BOOKSTEIN 1998*a*). All analyses of this class are adequately robust against variations in the count of semilandmarks and also, within reason, against unevenness in their spacing.

In my view, the combination of splines and Procrustes statistics here supersedes the analyses reviewed in Section 3 whenever the claim of pointwise homology among a data set of outlines is at all plausible. The question raised at that 1984 Woods Hole meeting has finally been settled: for typical data sets of organismal form, the Synthesis for landmarks engulfs the corresponding unhomologized analysis for closed outlines virtually whole. (For a gentle presentation of an implicitly dissenting view, see O'HIGGINS 1997.) The new treatment of the problem of homology no longer presumes any particular functional representation for the single outline, but is couched instead within the original comparative biological context, the investigation of a sample of forms. The correspondence sought for curves is, in a useful sense, the "most landmark-like" possible given the information available (which may include true landmarks either on or off the curves in question). The operationalization of homology afforded by the spline-slip tactics is the matching among all the curves of a data set that (1) guarantees a coherent relationship between the sample of curves and their joint average, as explained in the course of defining semilandmarks above, and (2) minimizes the overall bending (equivalent to spatial localization of variation) of the resulting data set. For example, if curves have landmark points given by stable local features of curving – Type II landmarks in the sense of BOOKSTEIN 1991 – the spline, which is typically quite concerned with mismatches of curvature, will map them appropriately: it sends Type II landmarks very nearly atop their homologues whether or not they had been explicitly located beforehand. It thus replaces all the a-priori approaches to homology, Fig. 2, by a single a-posteriori variant relying only on the usual two quadratic forms, Procrustes distance and bending energy.

The cost of commitment to these two formalisms in the course of a statistical description is the looseness of their connection to morphogenetic or selectional theories, which, of course, typically do not reference either Procrustes distance or localization of morphogenetic fields in the course of their formulation. (Perhaps presently they will.) Of course, none of the other alternatives in Fig. 2 have any biotheoretical basis either. Worse, they cannot even be relied on to match such clearly homologous shape features as happen to be present. While every attempt to assign homology pointwise along curves is necessarily arbitrary, in other words, the present approach adds no further arbitrariness to the combination of Procrustes distance and the spline formalism that has proved so fruitful in application to landmark data sets. We have thereby reduced the case of outlines to the simpler case of landmark-based methods. This constitutes a considerable advance.

In contrast, a different earlier attempt at a multivariate statistical method for outlines attempted a rigorously form-based homology function. In the method of *medial axes* (BOOKSTEIN *et al.* 1985, BOOKSTEIN 1991), constructions such as that in Fig. 17 are replaced by shape-specific geometric instructions that take the lobation of the form into account – its organization is modelled as expressing processes of "evolution" (here, a foreign term from partial differential equations) out of an originally undifferentiated circle or sphere. In certain applications, e.g. BLUM and NAGEL (1978), TABACHNICK and BOOKSTEIN (1988), or STRANEY (1990), these features prove topologically reliable over most forms of a data set, leading to ordinations midway in their power between the outline analyses of Sec. 3 and the semilandmark analyses of the present section. But Nature seems not to delight in populations for which the topology of these decompositions is sufficiently reliable for subsequent covariance-driven statistical investigation. In my view, the new methodology here supersedes the promise of the medial-axis methods as well.

The mixed Procrustes-spline toolkit also supersedes an earlier suggestion of mine for incorporation of outline information, the method of *edgels* (BOOKSTEIN 1994). In that method, information about homology along curves was imported into the landmark context by pairing of real landmarks with others "infinitesimally close" that bore information about tangent direction there. These auxiliary points, but not the actual landmarks, were allowed to slip along outlines. There resulted a rigorous separation between the landmark-based information and the edge-based information (BOOKSTEIN 1995) that, in retrospect, seems to have nothing much to do with the reality of how landmarks are selected. Such a separation was never necessary – the same computer program that fits edgels to data also fits outlines without landmarks according to the present formalism – but we did not realize until last year how much more powerful the symmetrical treatment of all coordinates is for subsequent statistical analysis.

6. IMAGES (USUALLY MEDICAL) WITH HOMOLOGY INFORMATION

The thin-plate spline applies to unwarp a data set of images to the average landmark configuration. Introduced in 1990, the splined unwarping uses the *inverse* of the thin-plate spline interpolant from sample mean landmark shape to each specimen of the sample. Image by image, pixel values are pulled back to the coordinate system of the mean landmark configuration, where they may be subjected to various further manipulations.

The import of the morphometric synthesis for medical image analysis follows mainly from the scientific power of these straightforward geometric maneu-

vers. The $2k$-vector of landmark shape from Fig. 6 behaves just like any other classic vector-valued **biometric covariate**, a list of associated values after correction for which effects on the primary datum (in this context, effect of diagnosis on the gray levels of the normalized image) can be estimated more precisely. In view of its relatively low dimension (low, that is, relative to the count of pixels or voxels), such a landmark-driven unwarping is more appropriately considered a relabeling of the pixels or voxels than any form of image processing per se. In a convenient metaphor, the image analysis afforded by landmarks casts findings from a *vertical* domain of gray levels "above" particular locations, levels to be treated by averages or eigenanalyses, into a *horizontal* domain having far more powerfully focused quantitative tactics. Of course, the real morphometric adjustment is *not* by any sort of linear regression machinery – the analogy with analysis of covariance goes only so far. For a much more technical discussion of the relation between this conceptual "rotation" and conventional tactics of image analysis, see BOOKSTEIN 1998*c*.

The context in which the morphometric synthesis is applicable to medical image analysis is thus not the consideration of images one at a time, as as for segmentation, or even two at a time, as in the more recent methods of deformable-template analysis, but their consideration in whole stacks of samples, for the extraction of patterns, typologies, forecasts, or scientific understanding. Such an approach to shape information in images presumes from the outset that that information is ultimately to be combined with other information outside the image – taxonomic labels, geographic location, ecological context – toward the formulation or testing of quantitative biological hypotheses.

Example. As part of the pilot study for a much larger investigation of brain anomalies and behavior in fetal alcohol syndromes (see BOOKSTEIN 1998*a, b*), ANN STREISSGUTH and colleagues at the University of Washington gathered ten landmark locations and nineteen callosal semilandmarks on the barest scrap of a data set: four adults with Fetal Alcohol Syndrome (alcohol exposure during gestation accompanied by a characteristic pattern of facial anomalies), four with Fetal Alcohol Effects (alcohol exposure during gestation but *not* the complete set of facial stigmata), and four normals. Semilandmarks were slipped in the course of digitization rather than by the averaging algorithm of the previous section; this will make no difference for subsequent visualizations. The unwarped averaged images for the four FAS versus the eight others, Fig. 18, look strikingly different. In the underlying Procrustes representation of the morphometric data, the FAS group differ from the pool of the others according to the grid shown in two versions in Fig. 19. The impression of thinning throughout most regions of the corpus callosum is very strong in the second of these presentations. The corresponding scatter of features, lower row in the figure, indicates a perfect separation of the four FAS cases from the FAE cases as well as the four normals at both ex-

tremes of the callosum, along the isthmus and also near the rostrum. The ordinary p-value of either of those separations is .004, and the isthmus finding need not be corrected for multiple comparisons, as the literature of FAS already richly calls one's attention to cases of callosal agenesis, in whole or in part, known from stillbirth data. The implications of this single finding for the whole domain of alcohol embryopathy are potentially enormous. From images taken of *adult* cases, using diagnoses established in childhood, we have managed to generate evidence for a mechanism – the correlation of the facial defect and the callosal defect on embryogenic grounds – that must date back to the very earliest moment of cortical development. I consider this excellent example to be a prototype for the role of morphometrics in evolutionary developmental biology more generally, whenever it attains a sufficient level of maturity to begin wrestling with the images that are, after all, the ultimate raw data.

To make it as obvious as in Fig. 19 that there is signal in a data set so ridiculously small as this required strenuous exploitation of all the tools already reviewed: slipping of the spline along curves, Procrustes averaging, adjustment of the uniform component out of the analysis, and extrapolation of the spline. The same tools are available for application to any other data set as part of the standard toolkit.

The "three-dimensional" example of Fig. 13 was really a pair of two-dimensional examples. A true three-dimensional analysis, such as in Fig. 14, requires strenuous effort at preliminary stages if it is to proceed using punctate

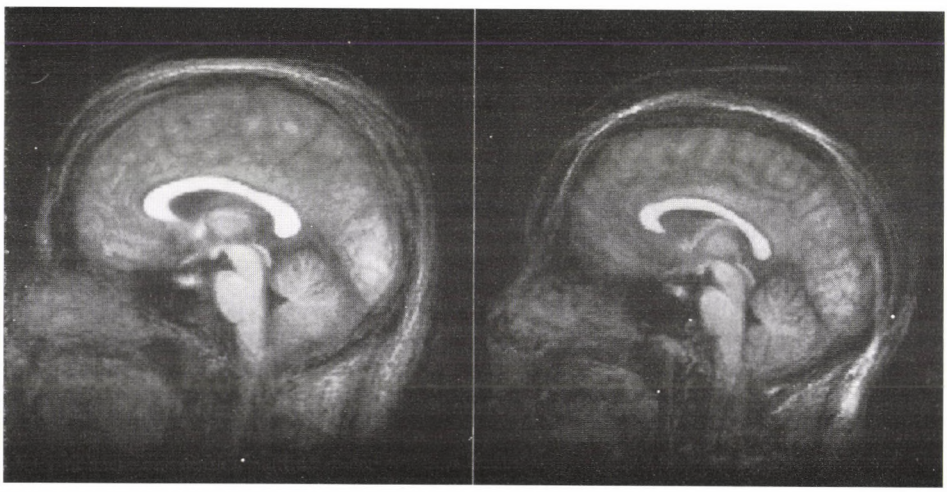

Fig. 18. Example of the extension of the Synthesis to the full content of images: unwarped averaged images for four cases of Fetal Alcohol Syndrome (right) and eight others (left). Landmarks and semilandmarks are distributed as in the next figure: ten points plus an outline of the entire callosum in this plane. Except at tentorium, there are no landmarks on the outer margin of the cortex

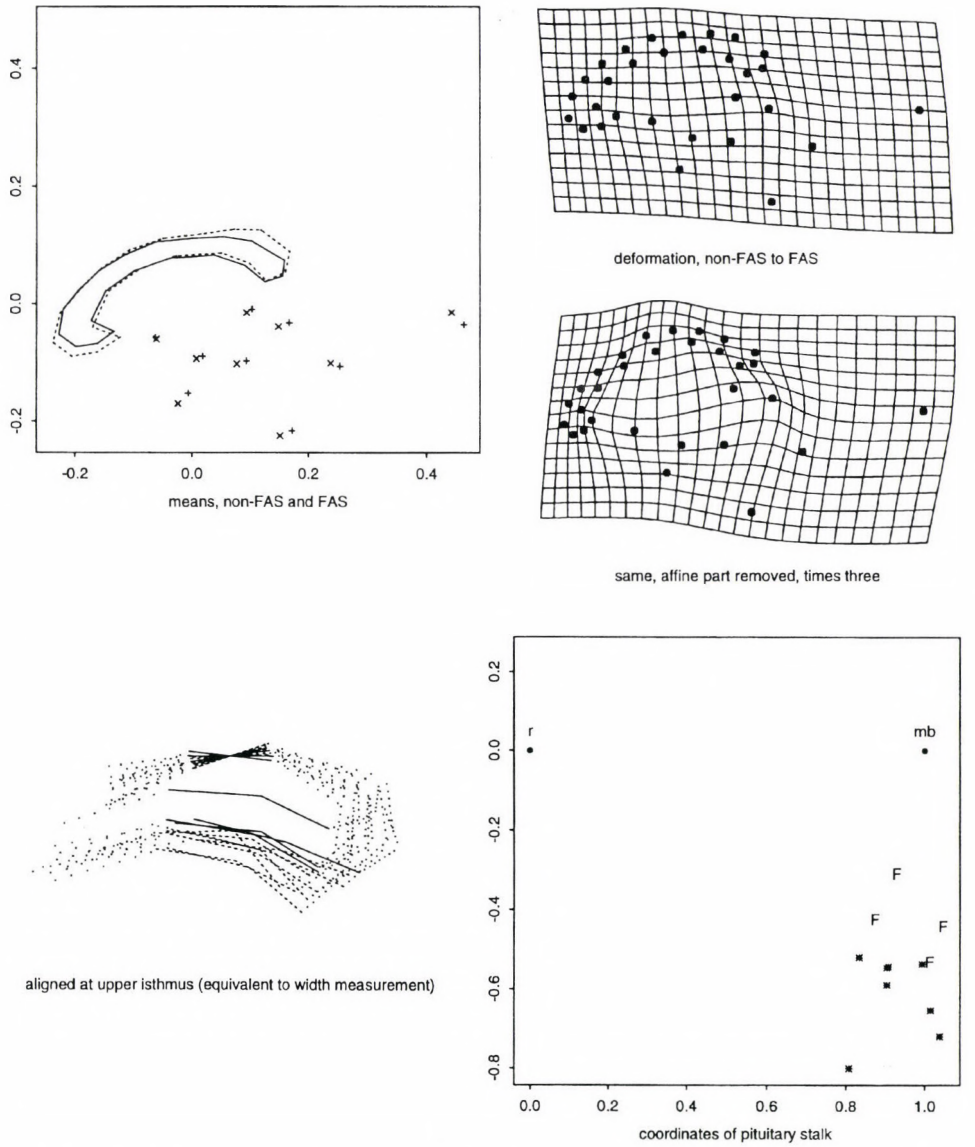

Fig. 19. Morphometrics underlying the images in the preceding figure. Upper left: Procrustes means for the full data configuration for the two groups. Dashed line and ×, non-FAS subgroup; solid line and +, FAS subgroup. Upper right: Thin-plate spline deformation grid, non-FAS to FAS. Right center: The same, times three, after the uniform component is removed. Lower left: Superposition on isthmian width corresponds to a perfect group separation. Solid lines, FAS cases. Lower right: The same for a two-point shape coordinate (infundibulum to a rostrum-mamillary baseline) representing hypoplasia at rostrum. r, rostrum; mb, mamillary body; F, the four fetal alcohol cases

landmark locations only. The extension of the toolkit of the Synthesis to curves, Sec. 5, arrived just in time for a promising new data source that considerably simplifies the analysis of three-dimensional images: the device of *ridge curves* (cf. KOENDERINK 1990, or CUTTING *et al.* 1995). A ridge curve, informally speaking, is a curving locus on a surface, like the edge of a table or the corner of the human mandible, at which the surface is most sharply curved in one direction. Where structures in images have relatively sharp boundaries, these curves can be extracted automatically from data sets by computations that deal with the surface in implicit form (THIRION & GOURDON 1995), and which is which can be identified appropriately by eye and, very soon, by algorithm. The slipping-spline technique applies to them directly as raw data in three dimensions; also, the extrema of curvature along these curves supply punctate landmarks that usually suit the analyses of Section 4. The data for Fig. 14 actually come from ridge curves in this fashion.

7. OTHER APPROACHES

The previous section concluded my overview of the Morphometric Synthesis in its present state. Most of the techniques that have ever been put forward for analysis of spatial locations of corresponding parts of organisms find their places within it as special cases or as partial analyses of geometrical information that we now know how to handle more extensively. Yet there are many other types of quantitative morphological data than those driven by the geometry of images in this wise. The Table concludes with a sketch of two that are particularly well-developed: analysis of spatial displacement fields, and analyses of photomicrographic textures. Both are based in extensive mathematical foundations that diverge from the covariance-driven coordinate algebra here.

The study of displacement fields dates back to the earliest days of scientific photography (you may be familiar with the work of EADWEARD MUYBRIDGE in this regard; but he followed on work of ETIENNE-JULES MAREY beginning even earlier, in the 1860's). Much clever work early in this century went into techniques for getting organisms (especially, plants) to draw their own developmental histories or locomotive processes in this regard: see, for instance, AVERY 1933, DAGOGNET 1992, or the review in BOOKSTEIN 1978. Other competing sources include the classic study of material displacements by the methods of continuum mechanics (stress and strain tensors). In all these applications, there is no immediate need for either of the main quadratic forms of the Synthesis, Procrustes distance or bending energy: instead, a real physical energy (kinetic or strain, depending on the scientific context) takes precedence, whether or not it is conveniently quadratic in the data.

Nevertheless, when studies of this sort arrive at a consideration of whole samples of forms, and in particular when they turn to the task of summarizing observed variations, the most apposite formalisms tend to be those of this Synthesis rather than anything developed specifically in those fields of origin. Studies of variations of strain tensors in structural geology, for instance, cannot do any better than the treatment of the uniform term in this Synthesis (or the version for large deformations, BOOKSTEIN 1991), although the diagrams may be different. In particular, techniques from computer vision or biomedical image analysis that culminate in *simulations* of deformation, such as models of form-change via displacement fields applied to an "atlas", are subject to all of the critical tools reviewed above.

A typical investigation of this sort, such as the brain mapping techniques reviewed in TOGA (1998), uses extensive and difficult mathematical machinery to arrive at computed correspondences between parts of homologous organs in different organisms. This identification obtained, one is then tempted to scrutinize the variability of locations of "the same" points of a template or an average, perhaps to identify regions of greatest "abnormality" case by case. But at this juncture it is necessary to shift from the picture plane of those "fiducial" locations to the machinery of shape descriptors reviewed here, the appropriate protocol for extracting descriptors of shape difference that characterize particular empirical contrasts. The maneuvers of Fig. 8 or 17 are then quite generally applicable. The signal features that announce and then localize shape difference exist in the space of linear combinations of these displacements, not the picture plane itself; to identify their visible manifestations in two dimensions requires the tools of the Synthesis. For the application to localization of expansion or contraction, for example, see BOOKSTEIN 1998*d*. Because the notion of homology is held in common between the displacement methods and the new morphometrics, information about *variation* of real displacement representations comes under the methods of the Synthesis regardless of the provenance of the signals. In the corresponding statistical analyses, real physical energetics serve as a sort of boundary condition.

Rigid linkages, for instance, can be studied by these methods when rigidity is incorporated as a (sometimes linearizable) constraint (BOOKSTEIN 1991). As an experiment in this context, I have made a videotape (BOOKSTEIN 1997*e*) in which a thin-plate spline grid reënacts five minutes of gesture by a professional dancer as recorded by the positions of 21 landmarks (ankles, knees, shoulders, ears, etc.) digitized from ordinary videotape. After the image of the dancer is erased – indeed, with the locations of the landmarks themselves erased – the corresponding 6000-frame animation of splined grids can nevertheless be seen clearly to be executing the same dance. The spline machinery thus captures one useful species of "meaning" (in this case, a humanistic one) of sequences of

forms regardless of the processes by which those sequences are actually produced in space.

In contrast, methods of a second large class outside the synthesis seem to me likely to remain unarticulated with morphometrics indefinitely. These are the methods of "morphometry" and stereology. Both study biologically based spatial patterns by techniques informed almost wholly by probability theory rather than multivariate statistical method; stereology specializes in the problem of reconstructing three-dimensional properties from the statistics of one- or two-dimensional sections. Neither has any analogue for the notion of a "multivariate observation." Rather, each separate feature is one single set-valued datum, a patch of image or a polygon relating a point to its neighbors. STOYAN *et al.* (1995), a good review of current techniques, cites in turn a huge range of the earlier literature. At root, the notion of homology here has little in common with either the landmark version of Section 4 or the extensions in later sections. Instead it is a far more intuitive, qualitative translation of the underlying etymology of the word, referring to parts (in arbitrary number) that for one reason or another come to have "the same name." The concerns of stereology are fundamentally issues of counting and integrating, not of describing spatial position, its variation and its covariances, which is the special concern of the Synthesis here.

CONCLUDING REMARK

This has been a "Whig history," a retelling of past events as a series inevitably culminating in the currently (perhaps transiently) dominant point of view. One can imagine many other narratives of the history of multivariate analysis in biology, most of which would not be as cheerful as this one, and also many other surveys of the origins and destinations of image-based information in the biological sciences (cf. GLASBEY and HORGAN 1995, which overlaps with the present review only insofar as parts of each are concerned with outline form).

Yet the developments reported here, taken as a whole, represent one of the principal successes of applied statistics in the late twentieth century. Beginning from a general set of multivariate tools that applied as much to economics, say, or political science as to biology, a core formalism has been erected that imported from far afield two quite specialized tactics (Procrustes distance and the thin-plate spline) ingeniously apposite to the explanatory problems at hand (incorporation of information about the average shape right alongside the representation of variations) and yet, because they are quadratic forms, articulating very nicely with that pre-existing matrix machinery. Certain aspects of the resulting praxis are odd – the centrality of three quadratic forms rather than the usual two, for instance, making possible three different simultaneous diagonalizations – but other

aspects, such as principal components analysis, appear unchanged in computation, however contextualized the subsequent interpretation.

The resulting toolkit can be conveyed in the usual notations of applied statistics. The special concerns it encodes, which are the additional structures required for these biological and biomedical applications, thus emerge in concise and fully manipulable form. By this means a surprisingly broad range of application domains, from biomechanics through psychiatry to evolutionary history, all benefit from a common core of shared methodological expertise. Contemporary morphometrics is the finest available tool for the efficient analysis of all the spatial information about homology in biological images. At the same time, in a quite different context it serves as one of the finest current examples of how useful quantitative methodologies are developed: as the syncretic accumulations of insights into the formalisms of quantities, driven by continual and often brusque criticism of prior art. BLACKITH was wrong when he declared morphometrics to be a branch of systematics. Quantitative methods are not the property of particular quantitative sciences, and the best quantitative methods hardly ever emerge as expressions of particular quantitative theories. Instead, in the overwhelming majority of cases, quantitative methods exist as branches of applied mathematics. The best of these methods (and I think the morphometric synthesis counts as one of these) share far more of their spirit with problems of quantitative analysis in other scientific fields than with qualitative analyses of the fields (here, medicine and evolutionary and developmental biology) to which they apply.

* * *

Acknowledgement – Earlier versions of this paper were presented at the Fifth International Congress of Systematic and Evolutionary Biology, Budapest, August 1996, and the 20th International Conference of Entomology in Florence a week later. I have benefited by commentary from LES MARCUS, JIM ROHLF, and CHRIS KLINGENBERG. Preparation of those lectures and this paper was supported in part by USPHS grants DA–09009 and GM–37251 to the author. The first of these is jointly underwritten by the National Institute on Drug Abuse, the National Institute on Aging, and the National Institute of Mental Health as part of NIH's Human Brain Project. Edgewarp, a workstation-based package for digitizing and unwarped averaging of medical images, is available by FTP from ftp://brainmap.med.umich.edu/pub/edgewarp. Statistical graphics for this paper were computed in Splus, a commercial statistical package for workstations. Equivalent software for most of the specifically statistical manipulations here is available from JIM ROHLF's morphometric bulletin board at Stony Brook, http://life.bio.sunysb.edu/morph/morph.html, where the schizophrenia data of Figs 6 through 12 are also publicly archived. (This paper makes use of 10 of the 13 points in that data set.) I am grateful to JOHN DEQUARDO, DAVID DEAN, MICHAEL MYSLOBODSKY, and ANN STREISSGUTH for access to the data analysed in all these examples, and to JIM ROHLF for a usable copy of Fig. 3.

REFERENCES

AVERY, G. S. (1933) Structure and development of the tobacco leaf. *Am. J. Bot.* **20:** 565–592.

BAYLAC, M. & T. DAUFRESNE (1996) Wing venation variability in Monarthropalpus (Diptera, Cecidomyiidae) and the quaternary coevolution of box (Buxus sempervirens L.) and its midge. Pp. 285–301. *In* MARCUS, L. F. *et al.* (eds): *Advances in Morphometrics.* NATO ASI Series A: Life Sciences, Vol. 284. Plenum Press, New York.

BLACKITH, R. E. (1965) Morphometrics. Pp. 225–249. *In* WATERMAN, T. & H. MOROWITZ (eds): *Theoretical and Mathematical Biology.* Blaisdell, New York.

BLACKITH, R. E. & R. A. REYMENT. (1971) *Multivariate Morphometrics.* Academic Press, New York, 412 pp.

BLUM, H. & R. NAGEL (1978) Shape description using weighted symmetric axis features. *Pattern Recognition* **10:** 167–180.

BOOKSTEIN, F. L. (1978) *The Measurement of Biological Shape and Shape Change.* Lecture Notes in Biomathematics, Vol. 24. Springer-Verlag, New York.

BOOKSTEIN, F. L. (1986) Size and shape spaces for landmark data in two dimensions. (With Discussion and Rejoinder.) *Statistical Science* **1:** 181–242.

BOOKSTEIN, F. L. (1989) "Size and shape": a comment on semantics. *Systematic Zoology* **38:** 173–180.

BOOKSTEIN, F. L. (1990) Overview of morphometrics: geometry and biology. Pp. 61–74. *In* ROHLF F. J. & F. BOOKSTEIN (eds): *Proc. Michigan Morphometrics Workshop.* Univ. Michigan Museums.

BOOKSTEIN, F. L. (1991) *Morphometric Tools for Landmark Data.* Cambridge University Press, New York, 435 pp.

BOOKSTEIN, F. L. (1993) A brief history of the morphometric synthesis. Pp. 15–40. *In* MARCUS, L. F. *et al.* (eds): *Contributions to Morphometrics.* Monografias, Museo Nacional de Ciencias Naturales, Consejo Superior de Investigaciones Cientificas, Madrid.

BOOKSTEIN, F. L. (1994) Landmarks, edges, morphometrics, and the brain atlas problem. Pp. 107–119. *In* THATCHER, R. *et al.* (eds): *Functional Neuroimaging: Technical Foundations.* Academic Press, San Diego, CA.

BOOKSTEIN, F. L. (1995) The Morphometric Synthesis for landmarks and edge-elements in images. *Terra Nova* **7:** 393–407.

BOOKSTEIN, F. L. (1996*a*) Biometrics, biomathematics, and the morphometric synthesis. *Bull. Math. Biology* **58:** 313–365.

BOOKSTEIN, F. L. (1996*b*) Combining the tools of geometric morphometrics. Pp. 131–151. *In* MARCUS, L. F. *et al.* (eds): *Advances in Morphometrics.* NATO ASI Series A: Life Sciences, Vol. 284. Plenum Pres, New York.

BOOKSTEIN, F. L. (1997*a*) Biometrics and brain maps: the promise of the Morphometric Synthesis. Pp. 203–254. *In* KOSLOW & M. HUERTA (eds): *Neuroinformatics: An Overview of the Human Brain Project. Progress in Neuroinformatics,* vol. 1. Lawrence Erlbaum, Hillsdale, NJ.

BOOKSTEIN, F. L. (1997*b*) Landmark methods for forms without landmarks: Localizing group differences in outline shape. *Medical Image Analysis* **1:** 225–243.

BOOKSTEIN, F. L. (1997*c*) Shape and the information in medical images: a decade of the morphometric synthesis. *Computer Vision and Image Understanding* **66:** 97–118.

BOOKSTEIN, F. L. (1997*d*) Analyzing shape data from multiple sources: The role of the bending energy matrix. Pp. 106–115. *In* MARDIA, K. V., GILL, C. A. & I. L. DRYDEN (eds): *Proc. Art and Science of Bayesian Image Analysis.* Leeds Univ. Press, Leeds, UK.

BOOKSTEIN, F. L. (1997*e*) The dancing grid for *Seven Enigmas.* Videotape for a dance concert. Univ. Michigan.

BOOKSTEIN, F. L. (1998*a*) Morphometrics for callosal shape studies. *In* ZAIDEL, E. & M. IACOBONI (eds): *Proc. NATO ASI on the Corpus Callosum.* [in print]

BOOKSTEIN, F. L. (1998*b*) Measures and caricatures of facial form. [MS].

BOOKSTEIN, F. L. (1998*c*) Linear methods for nonlinear maps: Procrustes fits, thin-plate splines, and the biometric analysis of shape variability. Pp. 157–182. *In* TOGA, A. (ed.): *Brain Warping.* Academic Press, San Diego, CA.

BOOKSTEIN, F. L. (1998*d*) Singularities and the features of deformation grids. Pp. 46–55. *In* VEMURI, B. (ed.): *Proc. Workshop on Biomedical Image Analyis.* IEEE Press, Los Altos, CA.

BOOKSTEIN, F. L., B. CHERNOFF, R. ELDER, J. HUMPHRIES, G. SMITH & R. STRAUSS (1985) *Morphometrics in Evolutionary Biology. The Geometry of Size and Shape Change, with Examples from Fishes.* Acad. Nat. Sci. Philadelphia, 277 pp.

BUCKLEY, P. F., D. DEAN, F. BOOKSTEIN, L. FRIEDMAN, D. KWON, J. LEWIN, J. KAMATH & C. LYS (1998) Three-dimensional MR-based morphometrics and ventricular dysmorphology in schizophrenia. *Biological Psychiatry,* [in press].

BURNABY, T. P. (1966) Growth-invariant discriminant functions and generalized distances. *Biometrics* **22:** 96–110.

COPPOLA, R., F. BOOKSTEIN, M. MYSLOBODSKY & D. WEINBERGER (1998) Landmark-driven averaging of parasagittal magnetic resonance images in patients with schizophrenia. [MS]

CORTI, M., C. FADDA, S. SIMSON & E. NEVO (1996) Size and shape variation in the mandible of the fossorial rodent Spalax ehrenbergi. Pp. 303–320. *In* MARCUS, L. F. *et al.* (eds): *Advances in Morphometrics.* NATO ASI Series A: Life Sciences, Vol. 284. Plenum Press, New York.

CUTTING, C., D. DEAN, F. BOOKSTEIN, B. HADDAD, D. KHORRAMABADI, F. ZONNEFELD & J. MCCARTHY (1995) A three-dimensional smooth surface analysis of untreated Crouzon's disease in the adult. *J. Craniofacial Surgery* **6:** 444–453.

DAGOGNET, F. (1992) *Etienne-Jules Marey: A Passion for the Trace.* Zone Books, New York, 204 pp.

DAM, J. VON (1996) Stephanodonty in fossil murids: A landmark-based morphometric approach. Pp. 449–461. *In* MARCUS, L. F. *et al.* (eds): *Advances in Morphometrics.* NATO ASI Series A: Life Sciences, Vol. 284. Plenum Press, New York.

DEQUARDO, J. R., F. BOOKSTEIN, W. D. K. GREEN, J. BRUMBERG & R. TANDON (1996) Spatial relationships of neuroanatomic landmarks in schizophrenia. *Psychiatry Research: Neuroimaging* **67:** 81–95.

DRYDEN, I. L. & K. V. MARDIA (1998) *Statistical Shape Analysis.* Wiley, New York, 363 pp.

FERSON, S., F. J. ROHLF & R. KOEHN (1985) Measuring shape variation of two-dimensional outlines. *Systematic Zoology* **34:** 59–68.

FINK, W. L., M. L. ZELDITCH & D. L. SWIDERSKI (1995) Morphometrics, homology, and phylogenetics: quantified characters as synapomorphies. *Systematic Biology* **44:** 179–189.

GLASBEY, C. & G. W. HORGAN (1995) *Image Analysis for the Biological Sciences.* John Wiley, Chichester, 218 pp.

GOOD, P. (1994) *Permutation Tests.* Springer Verlag, New York, 226 pp.

GOODALL, C. R. (1991) Procrustes methods in the statistical analysis of shape. *J. Royal Stat. Soc.* **53:** 285–339.

JACOBSON, A. G. & R. GORDON (1976) Changes in the shape of the developing vertebrate nervous system analyzed experimentally, mathematically, and by computer simulation. *J. Experimental Zool.* **197:** 191–246.

JOHNSON, K. G. & A. F. BUDD (1996) Three-dimensional landmark techniques for the recognition of reef coral species. Pp. 345–353. *In* MARCUS, L. F. *et al.* (eds): *Advances in Morphometrics.* NATO ASI Series A: Life Sciences, Vol. 284. Plenum Press, New York.

JOLICOEUR, P. (1963) The multivariate generalization of the allometry equation. *Biometrics* **19:** 497–499.

KENDALL, D. G. (1984) Shape-manifolds, procrustean metrics, and complex projective spaces. *Bull. London Math. Soc.* **16:** 81–121.

KENT, J. T. (1994) The complex Bingham distribution and shape analysis. *J. Royal Stat. Soc.* **B56:** 285–299.

KLINGENBERG, C. P. (1996) Multivariate allometry. Pp. 23–49. *In* MARCUS, L. F. *et al.* (eds): *Advances in Morphometrics.* NATO ASI Series A: Life Sciences, Vol. 284. Plenum Press, New York.

KOENDERINK, J. (1990) *Solid Shape.* The MIT Press, Cambridge, 699 pp.

LELE, S. & J. RICHTSMEIER (1991) Euclidean distance matrix analysis: A coordinate-free approach for comparing biological shapes using landmark data. *Am. J. Physical Anthropology* **86:** 415–428.

LOHMANN, G. P. & P. SCHWEITZER (1990) On eigenshape analysis. Pp. 147–166. *In* ROHLF, F. J. & F. L. BOOKSTEIN (eds): *Proc. Michigan Morphometrics Workshop.* Univ. Michigan Museums, Ann Arbor, Michigan.

LOY, A., S. CATSUDELLA & M. CORTI (1996) Shape changes during the growth of the sea bass, Dicentrarchus labrax (Teleostea: Perciformes), in relation to different rearing conditions. Pp. 399–405. *In* MARCUS, L. F. *et al.* (eds): *Advances in Morphometrics.* NATO ASI Series A: Life Sciences, Vol. 284. Plenum Press, New York.

MARCUS, L. F. (1990) Traditional morphometrics. Pp. 77–122. *In* ROHLF, F. J. & F. L. BOOKSTEIN (eds): *Proc. Michigan Morphometrics Workshop.* Univ. Michigan Museums, Ann Arbor, Michigan.

MARCUS, L. F. (1993) Some aspects of multivariate statistics for morphometrics. Pp. 95–130. *In* MARCUS, L. F. *et al.* (eds): *Contributions to Morphometrics.* Monografias, Museo Nacional de Ciencias Naturales, Consejo Superior de Investigaciones Cientificas, Madrid.

MARCUS, L. F., M. CORTI, A. LOY, G. NAYLOR & D. SLICE (eds) (1996) *Advances in Morphometrics.* NATO ASI Series A: Life Sciences, Volume 284. Plenum Press, New York, 587 pp.

MCINTOSH, A. R., F. BOOKSTEIN, J. HAXBY & C. GRADY (1996) Multivariate analysis of functional brain images using Partial Least Squares. *NeuroImage* **3:** 143–157.

MOSIMANN, J. E. (1970) Size allometry: size and shape variables with characterizations of the lognormal and generalized gamma distributions. *J. Am. Stat. Assoc.* **65:** 930–945.

O'HIGGINS, P. (1997) Methodological issues in the description of form. Pp. 74–105. *In* LESTREL, P. (ed.): *Fourier Descriptors and their Applications in Biology.* The University Press, Cambridge.

OXNARD, C. E. (1973) *Form and Pattern in Human Evolution.* The University of Chicago Press, Chicago, 218 pp.

OXNARD, C. E. (1984) *The Order of Man.* Yale University Press, New Haven, 366 pp.

PEARSON, K. & G. M. MORANT (1935) The portraiture of Oliver Cromwell with special reference to the Wilkinson head. *Biometrika* **26**(4): 1–106.

REYMENT, R. A. (1991) *Multidimensional Palaeobiology.* Pergamon Press, London, 377 pp.

REYMENT, R. A. & K. G. JÖRESKOG (1993) *Applied Factor Analysis in the Natural Sciences.* The University Press, Cambridge, 371 pp.

ROHLF, F. J. (1990) Fitting curves to outlines. Pp. 167–177. *In* ROHLF, F. J. & F. L. BOOKSTEIN (eds): *Proc. Michigan Morphometrics Workshop.* Univ. Michigan Museums, Ann Arbor, Michigan.

ROHLF, F. J. (1993) Relative warp analysis and an example of its application to mosquito wings. Pp. 131–159. *In* MARCUS, L. F. *et al.* (eds): *Contributions to Morphometrics.* Monografias, Museo Nacional de Ciencias Naturales, Consejo Superior de Investigaciones Cientificas, Madrid.

ROHLF, F. J. (1998) On applications of geometric morphometrics to studies of ontogeny and phylogeny. *Systematic Biology* **41:** 147–158.

SAMPSON, P. D., F. BOOKSTEIN, F. SHEEHAN & E. BOLSON (1996) Eigenshape analysis of left ventricular outlines from contrast ventriculograms. Pp. 211–233. *In* MARCUS, L. F. *et al.* (eds): *Advances in Morphometrics.* NATO ASI Series A: Life Sciences, Vol. 284. Plenum Press, New York.

SLICE, D., F. BOOKSTEIN, L. MARCUS, L. & F. J. ROHLF (1996) A glossary for geometric morphometrics. Pp. 531–551. *In* MARCUS, L. F. *et al.* (eds): *Advances in Morphometrics.* NATO ASI Series A: Life Sciences, Vol. 284. Plenum Press, New York. [Also available electronically as http://life.bio.sunysb.edu/morph/gloss1.html]

SNEATH, P. H. A. (1967) Trend-surface analysis of transformation grids. *J. Zool.* **151:** 65–122.

STOYAN, D., W. KENDALL & J. MECKE (1995) *Stochastic Geometry and its Applications,* 2nd ed. John Wiley, New York, 436 pp.

STRANEY, D. (1990) Median axis methods in morphometrics. Pp. 179–200. *In* ROHLF, F. J. & F. BOOKSTEIN (eds): *Proc. Michigan Morphometrics Workshop.* Univ. Michigan Museums.

TABACHNICK, E. & F. L. BOOKSTEIN (1990) The structure of individual variation in Miocene Globorotalia, DSDP Site 593. *Evolution* **44:** 416–434.

TABACHNICK, E. & F. BOOKSTEIN (1998) Work in progress.

THIRION, J.-P. & A. GOURDON (1995) Computing the differential characteristics of isointensity surfaces. *Computer Vision and Image Understanding* **61:** 190–202.

THOMPSON, D'A. W. (1961) *On Growth and Form.* BONNER, J. T. (ed.), Cambridge University Press, New York, 346 pp.

TOGA, A. W. (ed.) (1998) *Brain Warping.* Academic Press, [In press].

WALKER, J. A. (1996) Principal components of body shape variation within an endemic radiation of threespine stickleback. Pp. 321–334. *In* MARCUS, L. F. *et al.* (eds): *Advances in Morphometrics.* NATO ASI Series A: Life Sciences, Vol. 284. Plenum Press, New York.

WRIGHT, S. (1968) *Evolution and the Genetics of Populations. Vol. 1, Genetic and Biometric Foundations.* The University of Chicago Press, Chicago, 456 pp.

Contributions to a MANUAL OF PALAEARCTIC DIPTERA

edited by L. PAPP and B. DARVAS

Volume 2
Nematocera and Lower Brachycera

In the bulky volumes of the "*Contributions to a Manual of Palaearctic Diptera*" morphological, physiological, genetical, ecological and economic up-to-date knowledge of dipterous species (midges and flies), which have significant importance in genetics as model organisms, in plant cultivation as pests or beneficial parasitoids, in animal husbandry and human health as vectors of serious illnesses and which are important for ecosystem function, are treated. Morphological keys (with excellent figures) for adults and larvae, which help readers with identification of dipterous pests and parasitoids are provided, while readers in field of applied dipterology will find suitable environmentally friendly methods against pests or biological control methods, among others. Time table of series: 1997 – Volume 2, 1998 Volume 3 (Higher Brachycera), 1999 – Volume 1 (General and Applied Dipterology) and Appendix Volume.

The 2nd volume contains 38 dipterous family chapters by 23 specialists from 12 countries. with 1895 figures on 258 plates.

November 30, 1997, 592 pages
ISBN 963 04 8836 1 (Series)
ISBN 963 04 8837 x (Volume 2)
Foundation for the Publicity of the Hungarian Science
Publisher: Science Herald, Budapest

Order should be sent to

E. w. Classey Ltd.
Natural History Publisher & Bookseller
Oxford House, 6 Marlborough Street, Faringdon
Oxon SN7 7JP, UK
Facsimile: (44)-1367 244800
E-mail: bugbooks@classey.demõn.co.uk

Acta Zoologica Academiae Scientiarum Hungaricae 44 (1–2), pp. 61–72, 1998

3D DIGITIZING PRECISION AND SOURCES OF ERROR IN THE GEOMETRIC ANALYSIS OF WEASEL SKULLS*

S. REIG

Museo Nacional de Ciencias Naturales, CSIC
José Gutiérrez Abascal 2, Madrid 28006, Spain
Mustela@Pinar1.csic.es

A collection of 112 weasel skulls was used to investigate various sources of error involved in the morphometric analysis of 3D landmark data, using a Polhemus 3Space digitizer. Average precision in the location of 38 landmarks in three repeated digitizations was 0.303 mm, ranging from 0.204 to 0.542 mm. The Generalized Least Squares fit performed for alignment seems to have little impact on the estimation of digitizing error, absolute deviations being always below 0.01 mm. Merging dorsal and ventral configurations into a complete reconstruction of the skull adds an error ranging from 0.002 to 0.257 mm, which may represent up to a 55.5% increase in digitizing error. Estimation of missing coordinates by multiple regression produced an increase in error ranging from 0.215 to 1.016 mm. Relative to population variability, the amount of digitizing error could represent more than 50% of landmark dispersion when the lowest level of variation (between populations of the same species) was considered. Despite digitizing error, statistical analysis of morphological differences within or between groups showed a good degree of resolution. However, the magnitude of the error shown by some of the landmarks might be too large for some studies of within population or within individual variability.

Key words: geometric morphometrics, 3D digitizing error, missing data

INTRODUCTION

Topics related to measurement error have attracted a great deal of attention by workers interested in the use of geometric morphometric techniques, mainly because of the wide variety of systems available for data collection (MARCUS *et al.* 1996). Estimation of measurement error becomes a critical issue when the amount of variabity being considered is very low, like in studies of within population variation, asymmetry, etc (HUTCHINSON & CHEVERUD 1995, ARNQVIST & MÅRTENSSON 1998).

Data capturing using two-dimensional (2D) systems can be assisted with optical and software enhancements to facilitate the digitizing process. In contrast, most three-dimensional (3D) digitizing systems are based on a direct contact with the study object and its size is an important limitation for the accuracy of data

* Symposium presentation, 5th International Congress of Systematic and Evolutionary Biology, 1996, Budapest

collection. The size of the weasel skulls used in this paper, only around 45 mm of maximum length are probably near the lower limit for the Polhemus 3D Space digitizing system (DEAN 1996).

In addition to their small size, weasels pose yet another difficulty for geometric morphometrics: its rather bare and plain skull morphology, which lacks many of the morphological features that are frequently used in other mammals to define landmarks, like bone sutures, foramina and conspicuous bone processes (Fig. 1). For this reason, unfortunately most of the landmarks selected in this study are derived from standard points used in traditional morphometric studies of carnivores and mammalian species in general. Those points have been selected to provide information about variation in the main dimensions of the skull, and therefore their homology lies in the definition of the dimension described (e.g., maximum width or length) rather than in the description of the points used. Because of its restricted homology and ambiguous definition, this category of landmarks, classified as "type 3" by BOOKSTEIN (1991) is the least recommended in geometric morphometrics.

Thus, the unfavorable attributes of weasel skulls for data collection in 3D systems explored in this paper may somehow serve as an indication of the limitations imposed by poor circumstances in a geometric analysis. The data presented here will help to set the expectations of digitizing error in other studies carried out under better circumstances. Digitizing error using the same device as in this paper (Polhemus 3D Space) has been thoroughly studied in Anthropology studies (HILDEBOLT & VANNIER 1988, CORNER *et al.* 1992) focusing on the precision of the device to record interlandmark distances. However, instead of interlandmark distances, this study is directed towards the collection of configurations of landmark data to be used with the newest methods available in geometric morphometrics (ROHLF & MARCUS 1993). Thus, the main focus of the study will be the precision of landmark location in 3D space.

The sources of error studied included digitizing precision, effect of the alignment fit on the estimation of digitizing error, reconstruction of complete skulls from separate dorsal and ventral configurations, and estimation of missing coordinates by multiple regression.

MATERIALS AND METHODS

The skulls used in the study included 46 *Mustela erminea* and 66 *M. frenata* that belong to the collections of the US National Museum of Natural History (Smithsonian Institution), Washington D.C. and the American Museum of Natural History, New York. These weasel specimens were collected in the North Central and Eastern United States. To simulate a common scenario in systematic studies, the total sample of skulls included four factors of variation: species, population, sex, and individual variation. In *M. frenata*, the skulls were from two areas, Eastern and Western range of the subspecies *M. f. noveboracensis*, which should have low geographic variation between them

(HALL 1951). The sample of *M. erminea* included specimens form two subspecies *M. e. bangsi* and *M. e. cicognanii* (HALL 1951). Only adult skulls, older than one year, were selected. Age was determined using relative age criteria based on obliteration of sutures, date of capture, tooth wear and bone texture (HALL 1951).

Digitizing procedure

Landmarks were digitized directly on each skull, using a Polhemus 3Space digitizer (Polhemus, Inc.) (DEAN 1996). This system has a sensor in a stylus point that is placed directly on the skull landmark and records and stores *x y z* coordinates in a server PC. A total of 38 landmarks (22 ventral, 16 dorsal) were recorded on each skull following the scheme of Fig. 1. To measure digitizing precision, a series of 15 *M. frenata* skulls of the same sex and from the same region were digitized three times. Six of these 15 skulls were digitized three times each while the skull was fixed all the time to the digitizing platform, eliminating the need for alignment prior to computing the error. Analysis of this data set of 6 skulls with and without alignment was used to test the additional component of error introduced by the alignment of the three repeated configurations by Generalized Least Squares "GLS" (SLICE 1994). Skulls were fixed to the digitizing platform using plasticine and special care was taken to guard against involuntary motion of the skull during the digitizing process.

Estimation of error

Instead of using the traditional approach of finding repeatability estimates (YEZERINAC *et al.* 1992) I choose to focus on the variation of landmark location in 3D space, which was compared to the location of other repeats, the expected mean, etc. The analysis was therefore based on each landmark's position, rather than on its *x y z* variables separately. The error estimated in this way depicts digitizing precision; it is the deviation of replicate measures from the average of all replicates.

Thus, digitizing error for each landmark was computed as the average distance from the three repeats to the mean (center) of the three. This is slightly different from the root-mean-square construction of the same variation that would be standard in analysis of variance (cf. BOOKSTEIN 1991), but the rank order of different landmarks can be expected to be mostly unaffected.

Combining dorsal and ventral configurations for each skull

For each skull, dorsal and ventral landmarks were digitized separately, because it was not possible to fix the skull to the digitizing tablet in a way that allowed easy access to the entire skull with the Polhemus' stylus.

Reconstruction of the whole 3D skull configuration upon the dorsal and ventral sets (collected in two separate runs) was made using three common points: 1V, 17V, 18V, and their dorsal equivalents: 1D, 15D, 16D (Fig. 1), which were collected in both dorsal and ventral positions. These landmarks were chosen because they had no missing data and showed low digitizing error. Dorsal and ventral sides were put together by performing a GLS Procrustes fit (GLS option in GRF-ND, SLICE 1994) using only the coordinates of these three common points. For this purpose, the dorsal and ventral sets of the same skull were each input into GRF–ND (SLICE 1994) as if they were a pair of specimens on which the corresponding set of ventral or dorsal landmarks, respectively, were missing. After a fit that preserved the size of the configurations (GLS + BACKSCALE commands of GRF–ND) was performed using only the three alignment points, a complete specimen was assembled from the dorsal and ventral adjusted sets by eliminating the landmarks missing for each side. The accuracy of this reconstruction was assessed by means of seven landmarks (1V, 8V, 9V, 17V, 18V, 6D, 8D, Fig. 1) that were digitized on both ventral and dorsal sides of the skull. Reconstruction error was then computed as half the distance between dorsal and ventral versions of those landmarks.

Estimation of missing data

Five specimens had some missing values that were estimated by stepwise regression of the remaining variables available in each case. The analysis was performed using the BMDP-AM program (DIXON 1993). This program computes the initial correlation matrix by maximum likelihood for the whole data set and then creates a specific multiple regression model for each case with the variables available. The output of BMDP-AM includes a data set in which the missing data is filled with the estimated values from the regression analysis.

To estimate the accuracy of the predictions using this method, a test data set was produced with *M. frenata* skulls, including one of the series of 15 skulls repeated in which *x y z* values of four landmarks (5V, 12V, 17V, 19V, Figure 1) were deleted. Thus, missing data for those 15 skulls was estimated from the whole matrix of ventral configurations of 52 male skulls of *M. frenata*. Assuming that the best estimate of the true position for each landmark is the average of the three repeats, estimation error was computed as the distance from each regression-estimated point to the mean. Net error due to the estimation process was then assessed as the difference between the estimated bias distance and the digitizing error.

Computations were made using BMDP–7 (DIXON 1993) and SAS 6.3 (SAS Institute Inc. 1989) packages. Geometric analysis and data manipulation were done using GRF-ND (SLICE 1994) and SAS.

RESULTS

Digitizing precision

Mean digitizing error for the whole set of 38 landmarks was 0.303 mm (Table 1), ranging from a minimum of 0.204 to a maximum of 0.542 (Table 1). Landmarks showing the largest error were the two points that define the maximum zygomatic width in traditional morphometrics, 8V and 9V (Fig. 1), which were the only ones showing maximum error larger than 1 mm (Table 1). With a few exceptions, most landmarks showed a digitizing error close to 0.3 mm or below (Table 1). Highest digitizing precision was shown by landmarks more precisely defined like 20V, 7V, 11D, and 12D (Fig. 1). Variability of digitizing error among skulls seems to be associated with precision of the landmarks since it was larger for landmarks with largest digitizing error (Table 1). In terms of RMS (root mean square of the distance from each repeat to the mean of the three) mean error for the 38 landmarks was 0.318 mm.

Influence of the Procrustes fit

The GLS fit performed for alignment of the set of 15 skulls seem to have very little impact on the estimation of digitizing error. Using the set of 6 skulls for which error could be estimated without prior fitting, absolute deviations caused by the fit were always below 0.1 mm (Table 1). The net effect of the GLS fit on the whole configuration of repeated landmarks should be zero, because the alignment error is balanced between landmarks. Taking into account the sign of the alignment error for each landmark, the overall mean deviation for the whole

Table 1. Average difference (av. diff.) from mean values (in mm) in the 34 landmarks shown in Fig. 1. In brackets, sample size for each analysis. GLS fit av. diff. shows the change in values of digitizing error estimated after a GLS fit (av. diff. values refer to 6 skulls only, for which digitizing error values are not shown). Percentages (%) show differences relative to the mean digitizing av. diff. Error from missing data estimation show in brackets R^2 coefficients of the regression models used in the prediction of *x, y, z* coordinates of each landmark. See the text for more details

Land-	Digitizing av. diff. (15)			GLS fit (6)		Miss. est. (15)		Reconstr. (112)	
mark	Max.	Mean	SD	av. diff.	%	av. diff.	%	av. diff.	%
1D	0.422	0.229	0.085	–0.038	–18.0				
2D	0.452	0.335	0.099	+0.028	10.2				
3D	0.611	0.261	0.124	–0.046	–18.9				
4D	0.349	0.232	0.063	–0.026	–12.1				
5D	0.513	0.256	0.094	–0.082	–24.6				
6D	0.489	0.317	0.098	+0.003	1.3			+0.137	43.2
7D	0.424	0.269	0.099	+0.039	23.9				
8D	0.514	0.328	0.087	+0.041	14.1			+0.099	30.2
9D	0.642	0.383	0.146	–0.009	–2.4				
10D	0.579	0.395	0.099	+0.064	18.3				
11D	0.409	0.221	0.071	–0.038	–16.9				
12D	0.396	0.236	0.078	–0.079	–26.2				
13D	0.875	0.490	0.207	–0.078	–17.4				
14D	0.578	0.356	0.133	+0.033	13.4				
15D	0.465	0.318	0.091	+0.091	41.7				
16D	0.490	0.346	0.074	+0.079	29.3				
1V	0.379	0.230	0.075	-0.084	–30.5			+0.205	89.1
2V	0.386	0.248	0.079	–0.040	–14.6				
3V	0.325	0.228	0.066	–0.071	–23.1				
4V	0.412	0.245	0.108	–0.017	–8.1				
5V	0.498	0.298	0.093	+0.068	31.5	+0.388	130.2		
6V	0.491	0.299	0.107	+0.025	9.5	*(0.923, 0.835, 0.592)*			
7V	0.374	0.221	0.076	+0.005	3.0				
8V	1.779	0.511	0.368	+0.031	8.7			+0.179	39.5
9V	1.182	0.542	0.309	+0.018	4.1			+0.257	55.5
10V	0.405	0.283	0.080	+0.070	44.0				
11V	0.391	0.251	0.093	+0.001	0.4				
12V	0.939	0.403	0.187	+0.036	12.0	+1.016	252.1		
13V	0.575	0.360	0.126	–0.082	–19.5	*(0.741, 0.664, 0.511)*			
14V	0.404	0.300	0.079	–0.074	–19.4				
15V	0.582	0.296	0.138	–0.060	–22.8				
16V	0.354	0.227	0.063	–0.015	–6.9				
17V	0.525	0.318	0.095	+0.049	19.6	+0.215	67.6	+0.002	0.6
18V	0.435	0.306	0.086	+0.058	33.1	*(0.966, 0.638, 0.700)*		+0.125	40.1
19V	0.510	0.252	0.116	+0.058	32.0	+0.277	109.9		
20V	0.345	0.204	0.064	+0.042	32.3	*(0.939, 0.615, 0.500)*			
21V	0.376	0.254	0.067	+0.048	28.7				
22V	0.699	0.266	0.159	+0.056	38.1				

set of skull landmarks was almost null (0.003 mm) as expected. However, despite this overall balance, when considered individually, some of the landmarks showed values 35% larger than the error estimated without the fit (e.g., 10V, 15D, 22V, Table 1).

Since only 6 skulls were available for this test, values shown in Table 1 correspond to deviations from the error estimated for those 6 skulls (not shown in the table), instead of the error estimated for the whole set of 15 repetitions. This was done only to increase the accuracy of the estimation. Error values were very similar for the 6 or 15 skull data sets.

Estimation of missing data

In the four landmarks tested, coordinates estimated by multiple regression were off the expected location (the center of the three repeats) more than the average digitizing error estimated for each landmark. The increase in location error ranged from 0.215 mm in 17V to 1.016 mm in 12V (Table 1).

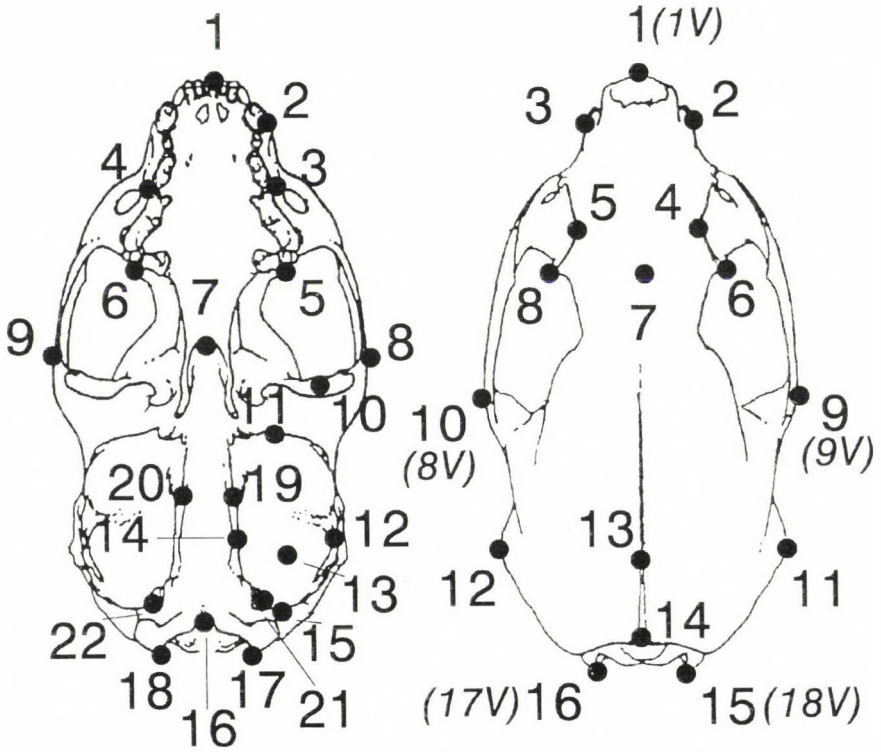

Fig. 1. Dorsal and ventral view of a weasel skull showing the location of the 16 dorsal and 22 ventral landmarks used. Landmarks of the dorsal side are referred to as 1D,..., 16D in the text, and so on for the ventral set. In brackets, landmarks collected in both dorsal and ventral digitalization

Combining dorsal and ventral configurations for each skull

The amount of error added by merging dorsal and ventral configurations into a complete reconstruction of the whole skull was tested in 7 landmarks that were digitized on the ventral and dorsal digitizing runs. The mean location error added to the digitizing precision of each of those seven landmark pairs ranged from 0.002mm (17V) to 0.257mm (9V). This added error may represent up to 55.5% of the digitizing error of landmark 9V (Table 1). Increasing the number of landmarks shared in dorsal and ventral digitizing runs should improve the reconstruction because the GLS fit would include more points. In this study, I purposely used only three, not all, shared landmarks to allow estimation of error due to the reconstruction.

A Generalized Resistant Fit (GRF) instead of a GLS fit might be thought to improve the reconstruction. However, no significant differences in precision between the two methods were observed, reconstruction errors being slightly larger using the GRF fit.

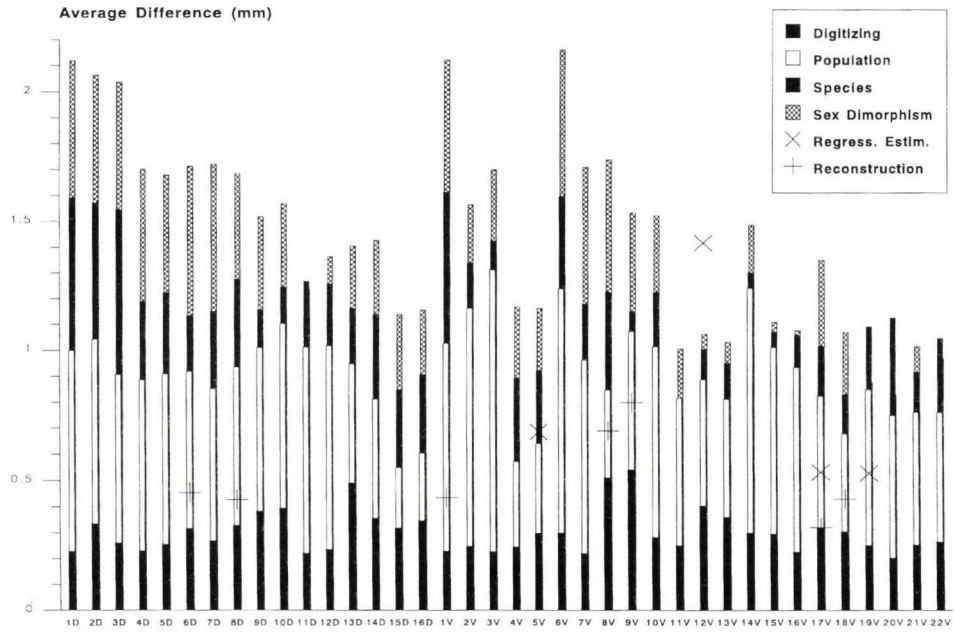

Fig. 2. Histogram bar showing the digitizing error, in terms of average difference, for each landmark, matched with the mean spatial dispersion (average deviation from the mean) of the landmarks when the data matrix included various factors of variation. Population: male skulls of *M. frenata* the same region (n=21). Species: two male samples of *M. frenata* (n=21) and *M. erminea* (n=23). Sex dimorphism: males (n=31) and females (n=10) from a single population of *M. frenata*. Error from reconstruction of the skull using the dorsal and ventral configurations, and from the estimation of missing coordinates by multiple regression are also marked for some of the landmarks

Digitizing error and population variability

A rough estimate of the magnitude of the digitizing error relative to population variability was obtained by comparing digitizing error with the average landmark deviation, or dispersion from the mean, when the data set included one or more groups of species or populations (PANKAKOSKI *et al.* 1987). This method was used because a variance partitioning procedure could not be done with the data since the 15 repeated skulls were from a single population group. When the lowest factor of variation was considered (same species, sex, population) the relative magnitude of digitizing error becomes important for some of the landmarks (Fig. 2). In landmarks 13D, 15D, 16D, 8V, and 9V, digitizing error was near 50% of the average landmark dispersion within a single population of *M. frenata* or *M. erminea* (Fig. 2). Considering a higher factor of variation like sexual dimorphism or between species, the digitizing error becomes much less important (Fig. 2).

To explore the effect of digitizing error in the analysis of population differences, a canonical variate analysis was performed using only the coordinates

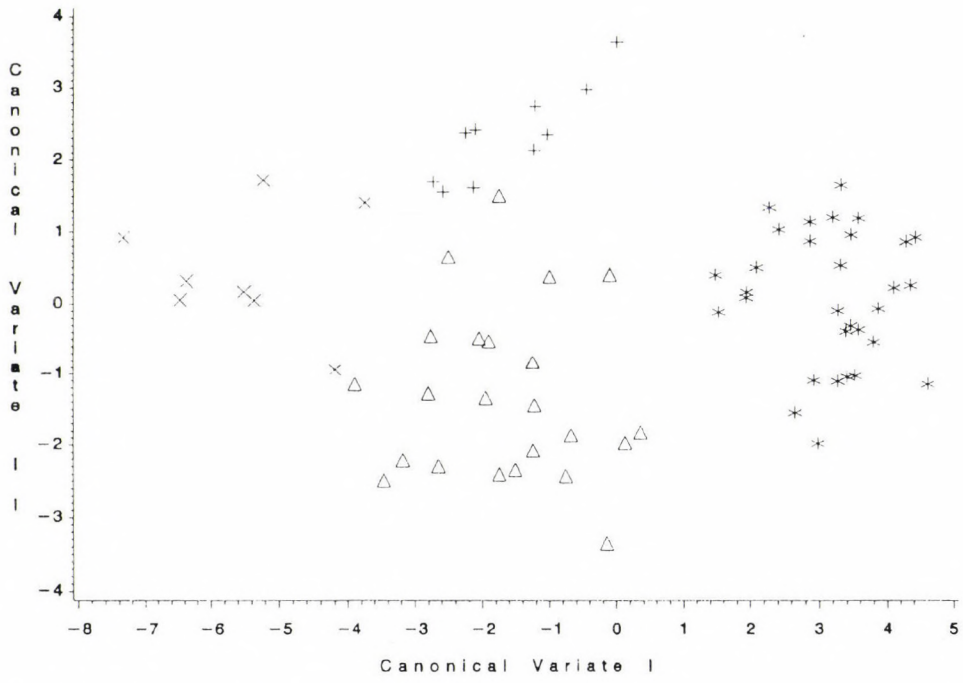

Fig. 3. Bivariate plot of the 2 first Canonical variates performed using landmarks 13D, 12V, 8V, and 9V. (+): *M. frenata* females (n=10) (*): *M. frenata* males (n=31) ; (X): *M. erminea* females (n=8); (triangle): *M. erminea* males (n=23)

of four landmarks (13D, 12V, 8V, 9V) showing largest digitizing error, worst missing estimation, etc. The analysis used GLS residuals for those four landmarks in a data set that included 4 groups: males and females from the two weasel species. The basic results suggest that the information from those landmarks is good enough to allow a fairly good separation of the four groups (Fig. 3). Thus, the use of geometric morphometric techniques in this small species seems fully feasible, despite using landmarks containing a large amount of error from various sources: digitizing error, combining of ventral and dorsal views, and estimation of missing coordinates.

DISCUSSION

Despite the difficulties involved with weasel skulls mentioned in the introduction, the average RMS precision of 0.318 mm observed for the 38 landmarks seems reasonable, considering that maximum resolution of the device reported by Polhemus' manufacturer is 0.152 mm. Other studies using the same device have measured digitizing precision in the estimation of interlandmark distances (HILDEBOLT & VANNIER 1988, CORNER *et al.* 1992) have reported an average RMS close to 0.4 mm. Estimation of precision for interlandmark distances measured with calipers (REIG 1996) gives lower RMS values than for landmark position in this study. For instance, RMS of the distance between landmarks 8V and 9V was 0.121 mm (REIG 1996), whereas digitizing error of those landmarks was near 0.5 mm (Table 1). However, because direction of landmark location error can be along or perpendicular to interlandmark distances, values of digitizing error might not be equivalent. These discrepancies in the error inherent to different instruments illustrate the expectation that points outlining maximum distances are easier to find using calipers than digitizing pointers.

The first lesson to learn from the variety of landmarks studied is that those showing largest digitizing error were of type '3' in BOOKSTEIN's (1991) classification, defined as extreme points representing maximum length, width or height like 8V, 9V, 9D, 10D, and 13D. Landmarks showing the highest precision were those corresponding to BOOKSTEIN's (1991) type '1' points, defined upon explicit anatomical points like foramina, teeth, and intersection of sutures, like 20V, 1D, and 3V (Fig. 1, Table 1). Within the type '3' landmarks, the more precise were points defined upon extreme points of apophyses or bone processes like landmarks 10V and 11V, 7V, and 16V (Fig. 1, Table 1). Thus, the main recommendation from this study is to avoid the use of type '3' landmarks (BOOKSTEIN 1991) or try to use landmarks defined at the edge of bone features that help placing the stylus in the right position.

Another indication of the unsuitability of landmarks 8V and 9V is the lack of correspondence of the results obtained with their equivalent points taken on the dorsal side: 9D and 10D (Fig. 1). Digitizing error was consistently lower when landmarks were located in dorsal position, and also the bias resulting from reconstruction of the whole skull was largest for these landmarks (Table 1). This suggests that somehow the way these two landmarks are seen or defined in the dorsal view changes in the ventral side. Other landmarks common to both sides of the skull (1V, 17V, 18V) show a good consensus between dorsal and ventral results (Table 1). On the other hand, the low amount of error involved in the reconstruction of the skull using its dorsal and ventral configurations is encouraging because the problem of incomplete digitization often occurs in mammals.

In addition to the nature of each landmark, there was considerable individual variation among skulls in digitizing error. This was more evident in landmarks with large digitizing error like 8V and 9V, showing a CV among skulls of 72 and 57% respectively (Table 1). Thus, it seems important to consider among individual variation of digitizing error for complete studies of measurement error (CORNER *et al.* 1992, YEZERINAC *et al.* 1992). Estimates of digitizing error based on repeated digitizations of a single individual may therefore compromise the results for some landmarks, especially if particularly good specimens are chosen for the study.

Estimation of digitizing error for a series of landmarks depends slightly on whether repeated digitizing is done without fixing the skull to the digitizing tablet and therefore requiring the alignment of configurations (CORNER *et al.* 1992). Though the net difference caused by the geometric alignment is negligible when all the landmarks are considered, the difference can be up to 40% for particular landmarks after the alignment (Table 1). This problem extends further, considering the different criteria that can be used to align configurations.

For the problem of missing data, multiple regression methods might offer an alternative for landmark data (SLICE 1996, and references therein). Though stepwise procedures have been recommended to find best predictive models in multiple regression (DIXON 1992, JAMES & MCCULLOCH 1990) the method might not be suitable for landmark data (BOOKSTEIN, pers. comm.). In two out of the four landmarks studied, the error added was of similar magnitude to digitizing error (Table 1). However, estimation of landmark 12V differed from the expected value by almost 3 times its digitizing error (Table 1). Thus, despite the large number of variables available, estimation of landmarks showing large digitizing error like 5V and 12V was not very reliable. The results may have been even worse for the dorsal side, because of a smaller number of variables available. The number of variables (landmark coordinates) entered in each regression equation ranged from 2 to 9. Adding more variables into the regression equations (by lowering the minimum *F-to enter* value at each step) produced an overall in-

crease in R^2 values. However, in spite of a larger R^2, the error added by the estimation increased.

Relative to population variability, the amount of digitizing error could represent more than 50% of landmark dispersion when the lowest level of variation (between populations of the same species) is considered (Fig. 2). In most landmarks, the amount of digitizing error was around 30% of interpopulation dispersion (Fig. 2). Other studies with small mammals have reported values of measurement error up to 45.4% of interpoulation variability using caliper measurements (PANKAKOSKI *et al.* 1987). Despite this proportion of digitizing error was high for some of the landmarks, its influence on the statistical analysis of interpopuation and interspecific segregation seems low, at least regarding the possibilities of analysis in geometric morphometrics. Even a data set in which landmarks had a considerable amount of error showed a good degree of resolution in the distinction of groups in the Canonical Variate analysis performed (Fig. 3). These results are encouraging considering that the small size of weasels is probably near the acceptable limit to work with the Polhemus 3D.

On the other hand, for morphometric analysis of within-population variation, in which the ranges of shape change measured are much smaller, the errors reported here associated with some landmarks or arising from data manipulations might pose serious limitations (see ARNQVIST & MÅRTENSSON, this volume).

* * *

Acknowledgments – Use of the Polhemus 3Space at the AMNH was made possible thanks to L. MARCUS and E. DELSON, whereas R. CHAPMAN kindly facilitated the use of the same device at the National Museum of Natural History, Smithsonian Institution. Assistance from the curatorial staff of those two institutions to use their collections is very much appreciated. Special thanks to L. MARCUS and J. SHAPIRO for their kind hospitality while visiting New York City. I'm indebted to the staff of the Biology Department of the California State University at Bakersfield, for their kind help and hospitality while I was preparing this manuscript. An early version of this paper benefited from comments by G. ARNQVIST, F. BOOKSTEIN and C. KLINGENBERG. Their help is very much appreciated.

REFERENCES

ARNQVIST, G. & MÅRTENSSON, T. (1998) Measurement error in geometric morphometrics: Empirical strategies to assess and reduce its impact on measures of shape. *Acta zool. hung.* **44**(1–2): 73–96.

BOOKSTEIN, F. L. (1991) *Morphometric tools for landmark data: geometry and biology*. Cambridge Univ. Press, New York, 435 pp.

CORNER, B. D., S. LELE & RICHTSMEIER, J. T. (1992) Measuring precision of three–dimensional landmark data. *J. Quant. Anthrop.* **3:** 347–359.

DEAN, D. (1996) Three-dimensional data capture and visualization. Pp. 53–72. *In* MARCUS *et al.* (eds): *Advances in Morphometrics*. NATO ASI Series A: Life Sciences. Vol. 284. Plenum Press, New York.

DIXON, W. J. (ed.) (1992) BMDP Statistical software. Univ. California Press, Berkeley, California.

HALL, E. R. (1951) American weasels. Univ. Kansas Publications No. 4, Lawrence, KS.

HILDEBOLT, C. F. & VANNIER, M. W. (1988) Three–dimensional measurement accuracy of skull surface landmarks. *Am. J. Ph. Anthrop.* **76:** 497–503.

HUTCHINSON, D. W. & CHEVERUD, J. M. (1995) Fluctuating asymmetry in Tamarin (Saguinus) cranial morphology: intra– and interspecific comparisons between taxa with varying levels of genetic heterozygosity. *J. Heredity* **86:** 280–288.

JAMES, F. C. & MCCULLOCH, C. E. (1990) Multivariate analysis in ecology and systematics: panacea or Pandora's box? *Ann. Rev. Ecol. Syst.* **21:** 129–166.

MARCUS, L. F., M. CORTI, A. LOY, G. J. P. NAYLOR & SLICE, D. E. (eds): (1996) *Advances in Morphometrics*. NATO ASI Series A: Life Sciences, Vol. 284. Plenum Press, New York, 587 pp.

PANKAKOSKI, E., VAISANEN, R. A. & NURMI, K. (1987) Variability of muskrat skulls: measurement error, environmental modification and size allometry. *Syst. Biol.* **36:** 35–51.

REIG, S. (1996). Correspondence between interlandmark distances and caliper measurements. Pp. 371–387. *In* MARCUS *et al.* (eds): *Advances in Morphometrics*. NATO ASI Series A: Life Sciences, Vol. 284. Plenum Press, New York.

RICHTSMEIER, J. T., CHEVERUD, J. M. & LELE, S. (1992) Advances in anthropological morphometrics. *Ann. Rev. Anthrop.* **21:** 283–305.

ROHLF, F. J. & MARCUS, L. F. (1993) A revolution in morphometrics. *TREE* **8:** 129–132.

SAS INSTITUTE INC. (1989) SAS user's guide statistics. Version 6.3. ed. Cary, North Carolina, SAS Institute Inc.

SLICE, D. E. (1994) GRF-ND. Generalized rotational fitting of n-dimensional landmark data. Computer program distributed by author (Revision of 11–1–94). Stony Brook, New York.

SLICE, D. E. (1996). Three-dimensional generalized resistant fitting and the comparison of least-squares and resistant-fit residuals. Pp. 201–208. *In* MARCUS *et al.* (eds): *Advances in Morphometrics*. NATO ASI Series A: Life Sciences, Vol. 284. Plenum Press, New York.

YEZERINAC, S. M., LOUGHEED, S. C. & HANDFORD, P. (1992) Measurement error and morphometric studies: statistical power and observer experience. *Syst. Biol.* **41:** 471–482.

Acta Zoologica Academiae Scientiarum Hungaricae 44 (1–2), pp. 73–96, 1998

MEASUREMENT ERROR IN GEOMETRIC MORPHOMETRICS: EMPIRICAL STRATEGIES TO ASSESS AND REDUCE ITS IMPACT ON MEASURES OF SHAPE*

ARNQVIST, G.** and T. MÅRTENSSON

Department of Animal Ecology, University of Umeå
S-901 87 Umeå Sweden
E-mail: Goran.Arnqvist@animecol.umu.se

Random measurement error is ubiquitous in morphometric data, and it can cause serious statistical problems. We stress that measurement error is a potential problem primarily when true phenotypic variation in shape is relatively small, such as in studies of intraspecific variation in shape. A model for the partitioning of measurement error in landmark based morphometrics is presented. The impact of measurement error can be reduced in a number of ways, depending on the methods used to collect, process and analyse data, and we give some practical advice. We also recommend that repeated measures of all individuals are taken routinely in morphometric studies where measurement error may be a potential problem. This enables both a quantification, by estimating repeatabilities from analyses of variance, and a reduction, by averaging repeated measures, of the relative impact of measurement error. We perform an analysis of shape variation in a uniform sample of young perch (*Perca fluviatilis*), solely aimed at illustrating how different components of measurement error can be quantified, and demonstrate (a) that estimates of repeatability will only be informative of the error components that are actually repeated in each repeated measure, (b) that the relative impact of different components of measurement error can be partitioned and assessed by planned hierarchical repeated measurement protocols followed by nested analyses of variance, (c) that measurement error is unevenly distributed among different shape variables and (d) that the relative magnitude of ME in a given shape variable can be reduced to an estimable extent by averaging several repeated measures.

Key words: shape analysis, repeatability, repeated measures, measurement error, *Perca fluviatilis*

INTRODUCTION

Whenever a value is assigned to a physical quantity, it is associated with uncertainty to some extent; an initially unknown magnitude of measurement error (henceforth, ME) is ubiquitous (FULLER 1987, RABINOVICH 1995). Recent developments in the methodology of data acquisition in morphometrics has led to an increasing level of sophistication of our technical equipment (FINK 1990, MACLEOD 1990, MARCUS *et al.* 1996). However, every biometric measure, no mat-

* Symposium presentation, 5th International Congress of Systematic and Evolutionary Biology, 1996, Budapest

** Corresponding author

ter how sophisticated and/or accurate our methods are, will be associated with ME. It is thus important to understand the effects that ME has on our data and our analyses. In order to do so, we need a framework to classify different sources of potential ME as well as strategies to "cope" with such error. These are the main objectives of the current contribution.

Measurement error is defined as the deviation of the result of a measurement from the true value of the measured quantity. There are two main types of ME; random and systematic (RABINOVICH 1995). The effect of random ME is an increase in the variance of the estimated parameters, by introducing error which is randomly distributed with regards to the true value of the measured quantity. Systematic ME, in contrast, will cause systematic bias in the magnitude of the estimate, by introducing error which is non-randomly (i. e., systematically) distributed with regards to the true value of the measured quantity. Most statistical models of parameter estimation and statistical inference incorporate ME (at least in the dependent variable) that is purely random, and many of the methods used to evaluate geometric morphometric data assume isotropic normal errors in landmark locations (GOODALL & MARDIA 1993, MARDIA & DRYDEN 1994, BOOKSTEIN 1996*a*).

Systematic and random ME entail quite different and distinct problems for the empirical investigators. First, the data that we are analysing for a given specimen will only be an approximation of the true data. This will be a potential problem if systematic ME is present, since systematic deviations from the true values essentially mean that we then analysing shapes that are systematically false approximations of the true underlying shape (see for example Fig. 2). While there are sometimes methods for quantifying and compensating for systematic ME (RABINOVICH 1995), these are often case specific and complex. Second, random variations in the magnitude of error across specimens generates problems when statistical inferences are made (see below). Since systematic ME will occur only if the particular methods or instruments used for gathering data are flawed, while random ME is ubiquitous and often a potential problem, we focus strictly on the more general problem of random ME here. It is important to remember, however, that presence of systematic ME will violated the assumption of isotropic normal errors and may lead to deviations from multivariate normality in the tangent space (BOOKSTEIN 1991 1996*a*, GOODALL & MARDIA 1993, MARDIA & DRYDEN 1994, KENT & MARDIA 1997).

WHY, AND WHEN, IS MEASUREMENT ERROR A PROBLEM?

In a world of error-free measurements, all our data would be true. Unfortunately, our data are always contaminated with ME, and there is no reason to be-

lieve *a priori* that geometric morphometrics generally suffer less from problems with ME than does traditional morphometrics. Two classes of problems can arise from ME. The first, and most general, problem with ME is that it increases our measure of total phenotypic variance in shape, by introducing a component of residual "noise" to our data. Since statistical models are typically based on the relationship between "explainable" and "residual" variation in morphology (ME is a component of the latter), ME dilutes trends and patterns in data by increasing residual variance. Hence, while ME in morphometric data does not necessarily violate any assumptions of statistical models, it is a potentially very serious problem for the practitioner since it reduces the statistical power of our analyses by increasing the type II error rate (i. e., our inability to reject false null hypotheses) (FRANCIS & MATLIN 1986, COHEN 1988, BAILEY & BYRNES 1990, LEE 1990, YEZERINAC *et al.* 1992). The degree to which investigators need to worry about ME in this respect, will be inversely related to the relative magnitude of true between-individual variance in shape in the sample. Thus, comparative studies of shape variation in different species (or higher order taxa) or ontogenetic stages rarely suffer from serious problems with ME. In contrast, in studies where more subtle morphological variation in shape within species, or even populations, is being analysed, ME can be a serious problem. Since the development of the morphometric synthesis now has reached a mature stage (BOOKSTEIN 1996*a*, MARCUS *et al.* 1996) and since ecological morphology is currently receiving an increasing amount of attention (WAINWRIGHT & REILLY 1994), we anticipate that the amount of applications of the latter kind will increase. Thus, it is of great importance that we acknowledge ME, and create a framework for coping with problems caused by it (HIMES 1989, MARKS *et al.* 1989, BAILEY and BYRNES 1990, LOUGHEED *et al.* 1991, YEZERINAC *et al.* 1992).

Secondly, statistical models commonly make two critical assumptions with regards to ME, that may be violated more often than we would wish (FLEISS & SHROUT 1977). (a) It is generally assumed that the magnitude of a variable of interest and the error with which is measured are uncorrelated. The most classical violation of this assumption includes the commonly observed covariance between the true size of a trait and ME (PANKAKOSKI 1987, YEZERINAC *et al.* 1992). This kind of association has been shown, e. g., to generate artifactual relationships between within- and among-population variation across traits (see ROHLF *et al.* 1983) and to generate apparent patterns of decreasing variance in traits during ontogeny as individuals grow larger (see LEE 1990). (b) It is also generally assumed that, when more than one variable is measured, the errors across variables are uncorrelated. Violations of this assumption may be common when there are systematic components of ME involved, for example when more than one person is involved in recording data (LEE 1990, YEZERINAC *et al.* 1992, EASON *et al.* 1996). When the errors across variables are correlated, it will gener-

ally be impossible to determine the extent to which an observed relationship between two variables reflects associations between the true scores and the extent to which it reflects associations between the errors (FLEISS & SHROUT 1977). Violation of this assumption has been shown to generate serious problems in multivariate procedures, such as discriminant analysis (JAMISON & ZEGURA 1974, FRANCIS & MATTLIN 1986, LEE 1982, 1990).

THE ORIGIN OF MEASUREMENT ERROR IN LANDMARK DATA – IDENTIFYING AND CLASSIFYING SOURCES OF ERROR

In order to develop strategies to deal with ME, we first need to identify its sources. A general partitioning of the components of total ME (ζ) is

$$\zeta = \zeta_m + \zeta_i + \zeta_p \qquad [1]$$

where ζ_m is methodological error, ζ_i is instrumental error and ζ_p is personal error (RABINOVICH 1995). A variety of methods and instruments can be employed to capture morphometric data, and the sources of error will of course vary with the methods (see below). We focus below primarily on landmark data, i. e. two- or three-dimensional co-ordinates of specific points on a biological specimen, since this is the most common type of data in geometric morphometrics (BOOKSTEIN 1991, 1996*a*). For such data, the primary origin of error is erroneous locations of landmarks, but this error will then secondarily cascade through the subsequent geometric and statistical analyses to result in ME in shape variables.

The accuracy and precision of recorded data will in theory depend partly on which methods are being used to gather landmark data. In order to recognise this, we first need to identify the sources of error in greater detail than the general partitioning above. Such a systematic functional partitioning of principal sources of ME in landmark data is proposed in Fig. 1, and will be commented on below.

1. Virtually all morphometric data are gathered from specimens that are prepared in one way or the other. What we call error due to specimen preparation occurs as result of slight variations in the way different specimens are prepared for data gathering. Examples of "preparations" include preservation of specimens, skeletonization, histological preparations, dyeing techniques and various forms of presentation/mounting strategies. The latter includes distortions in the "state" in which specimens are represented (e. g., the degree of compression, expansion or flexure), which may be a big source of error in specimens with soft tissue (LEE 1982, CARPENTER 1996).

2. Structures which are truly three dimensional are often reduced to two dimensions in landmark based studies, by two dimensional views of, or cuts through, specimens. In such cases, dimensionality reduction error will arise as a

result of lack of perfect orthogonality between the major axes of the specimen (x,y) to that of the dimension which is being reduced (z), i. e. any variation across specimens in the orientation (alignment) when data is captured. A second, and independent, form of dimensionality reduction error (which is systematic and will

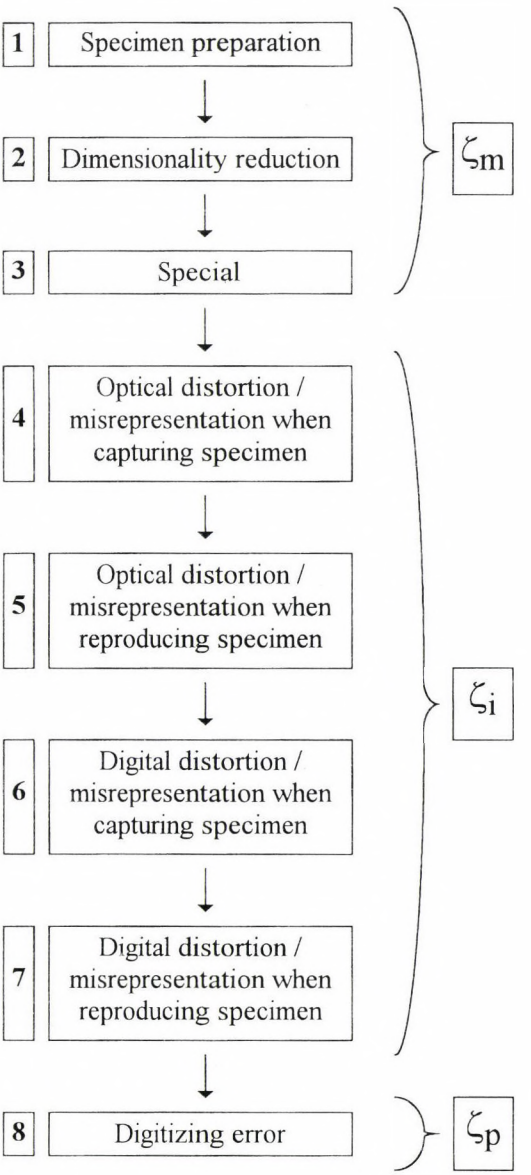

Fig. 1. A sequential partitioning of the main components of measurement error in landmark based morphometrics. ζ_m denotes methodological error, ζ_i instrumental error and ζ_p personal error. See text for descriptions of each of the components

thus not be treated further here) always occurs when whole specimens are viewed through a camera or microscope, by registration of false x,y co-ordinates of landmarks due to differences in their true location in the reduced z dimension (Fig. 2) (see BOOKSTEIN 1991, ROTH 1993, for discussions of dimensionality reduction). Dimensionality reduction error does not occur when three dimensional landmark points are collected directly (ROTH 1993, DEAN 1996).

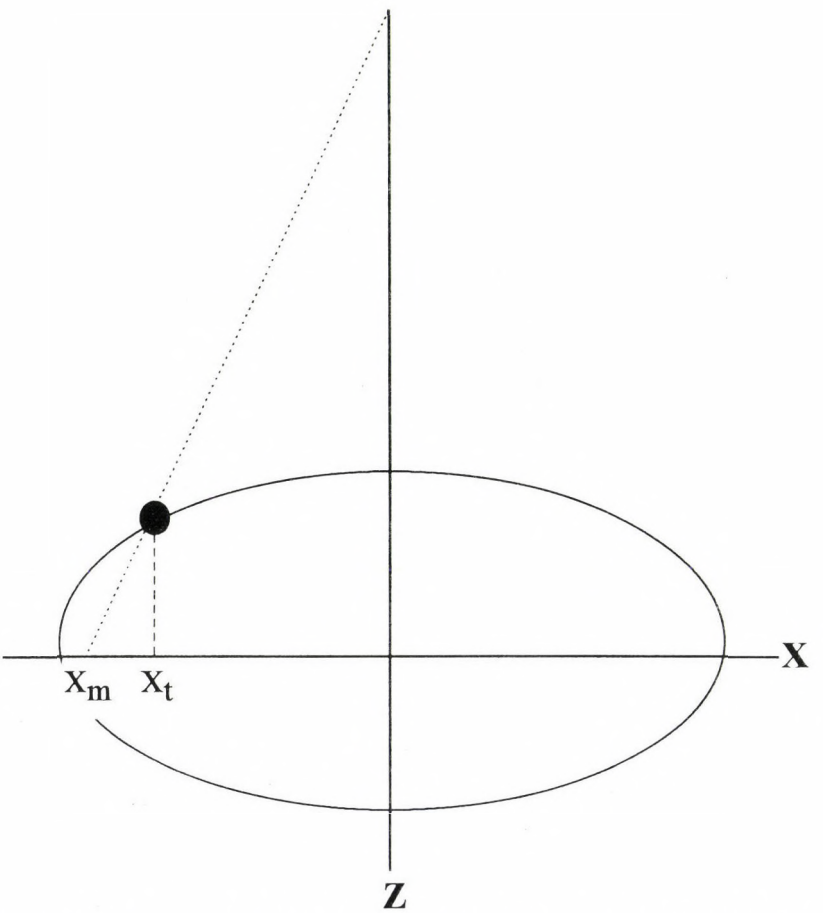

Fig. 2. An illustration of a systematic measurement error in landmark data. This particular type of error arises as a result of dimensionality reduction, when three-dimensional objects are viewed from a single point (camera or microscope). In the illustrated case, a landmark situated on the surface of an oval shaped specimen is being measured. The error equals the difference between the landmark's true and measured location in the x-dimension ($\vartheta = x_t - x_m$). This type of error in landmark location will be systematic, and will occur whenever the true three dimensional location of a landmark is not in the two dimensional plane in which it is projected, unless it is located exactly along the z-axis (i. e., whenever $z \neq 0$; provided that $x,y \neq 0,0$)

3. When special methodological routines are employed to attain or prepare data prior to analysis, this may introduce special methodological error. An example of such a routine, which may introduce considerable error, is when parts of specimens are recorded separately and then merged into complete landmark configurations prior to analysis (see REIG 1998).

4. Landmark data are typically acquired from images of specimens that have been captured in some way. What we call error due to optical distortion/misrepresentation when capturing specimens occurs as a result of imperfections of the optical system (lenses) used when an image of the specimen is being captured and transformed into an analysable form. Examples include distortions due to the characteristics of the lenses in microscope and camera systems (when specimens are viewed directly, or are being transferred to a photographic film or a plane in a video camera).

5. Images of specimens are often being reproduced prior to data acquisition. Error due to optical distortion/misrepresentation when reproducing specimens occurs when already captured images of specimens are being reproduced, and result from imperfections in the optical systems used (photo enlargers and slide projectors). Examples include enlargements of images when transferred from small photographic images (i. e. negatives or colour slides) to larger ones (photographic prints or slide projections) prior to data recording.

6. When a specimen is captured and transformed into digital form, error due to digital distortion/misrepresentation will occur. These types of errors are often complex, resulting from a series of potential imperfections in the digital system used, and they can be considerable (ARNQVIST, unpubl). Examples includes various properties of digital framegrabbers and scanners, but also the more problematic and general sources of error due to image distortion resulting from non-square pixels and the various algorithms used to compensate for this (see MACLEOD 1990). In general, digitising tablets suffer less from this component or error compared to other digital techniques (FINK 1990).

7. To acquire landmarks from digital images, they are reproduced on video monitors or computer screens. Digital distortion/misrepresentation when reproducing specimens occurs as a result of imperfections in the system employed in reproducing the digital data to a visual form (MACLEOD 1990), but also from various manipulations aimed at "enhancing" the reproduced images whenever such software options are used (see ROHLF 1990).

8. When the relative position of landmarks are localised and their co-ordinates are recorded, digitising error will occur as a result of imperfect and/or inconsistent localisation of landmarks. The magnitude of this personal component of error will vary greatly depending on, for example, the type of landmark (FRANCIS & MATLIN 1986, BOOKSTEIN 1991, LOUGHEED *et al.* 1991, DEMETER *et al.* 1996, REIG 1998), the accuracy of the equipment (DEAN 1996), the

quality/resolution of the image/projection and the personal characteristics of the investigator. The sequential and additive input of different components of ME can be illustrated by the following example. Numbers refers to components of error. An investigator wishes to assess potential shape differences due to habitat occupation in a fish species. Samples of fish are taken in the pelagic and benthic zones of a local lake. First, each fish is placed on a flat board in a certain position (1). A picture of each fish is taken (4) from a right angle to the board with a camera mounted on a tripod (2). Photographic prints are produced from the negatives (5), and these are then transformed into digital format by means of a digital scanner (6). Each picture is then reproduced and "enhanced" on a computer screen (7), and landmarks are entered with a pointing device (8). In this case, total ME will equal the sum of all seven components of error.

MINIMISING THE IMPACT OF MEASUREMENT ERROR

Due to its negative effects on statistical evaluations of morphometric data, the impact of ME should, of course, be minimised. There are several things that should be kept in mind in order to do so.

(A) The route between the actual specimen itself and the data should in principle be made as "short" as possible. Landmark data can be gathered in several ways (see ROHLF & BOOKSTEIN 1990, MARCUS *et al.* 1996), the most common being: (a) landmarks located on the specimen itself, by placing the specimen directly on a digitising tablet, (b) landmarks located on a projection of the specimen, by projecting the specimen onto a digitising tablet through a camera lucida, (c) landmarks located on a projection of the specimen, by placing/projecting a photographic reproduction of the specimen (print or slide) onto a digitising tablet, (d) landmarks located on a digital image of the specimen, by capturing a digital representation of the specimen itself through a video-camera or other digital instrument and projecting this onto a video screen, (e) landmarks located on a digital image of the specimen, by capturing a digital representation of a photographic reproduction of the specimen through a video-camera, scanner or other digital instrument and projecting this onto a computer screen. Since the total amount of ME in data is related to the number of methodological steps involved (Fig. 1), steps should be avoided if possible. One important conclusion of this is that there might actually be a positive relationship between the technical sophistication of the methods of data collection and the relative amount of ME present! For example, given that everything else is equal, method (a) above is strongly preferable over method (e).

(B) Methods of specimen preparation, presentation and digitising should be very thoroughly standardised across specimens. Error due to specimen prepara-

tion is often a major source of ME (LEE 1982, CARPENTER 1996, and example below), so the importance of standardisation in this stage cannot be overestimated. Important implications are also that one and the same person should do all the specimen preparations as well as the actual digitising, and that the same equipment and instruments should be used throughout the data collection process within single studies (cf., LEE 1990, YEZERINAC *et al.* 1992, EASON *et al.* 1996).

(C) It has been suggested that certain instruments are more prone to error than others. For example, FINK (1990) recommended that optical slide projectors not be used to project slides of specimens, since these in general have lower optical quality than do other optical instruments. Similarly, digitising tablets in general suffer less from digital distortion/misrepresentation and have higher precision than do visual digital systems (i. e., image analysis systems) (MACLEOD 1990). Thus, the choice of methodology will affect the amount of error present. The instrumental components of measurement error can be assessed, and sometimes partly compensated for, by careful calibration of the equipment. This can be done by, for example, measuring a distance of precisely known length in varied positions and locations (MACLEOD 1990, BECERRA 1993, BECERRA *et al.* 1996, DEMETER *et al.* 1996).

(D) The amount of optical and digital distortion/misrepresentation error that burden data to some extent depends on the quality *per se* of the instruments and equipment used. Thus, the instruments and hardware used to gather data should be chosen carefully. This may be especially true for various digital components, such as different framegrabbers, scanners and digitising tablets which may vary a lot in quality, precision, accuracy and suitability for quantitative morphometrics (FINK 1990, MACLEOD 1990, ROHLF 1990, BECERRA *et al.* 1993, KOHN *et al.* 1995, DEAN 1996, GARCÍA-VALDECASAS 1996). Apart from problems with distortion/misrepresentation, the accuracy and resolution of both capturing equipment (e. g., digitising tablets) and reproducing equipment (e. g., computer monitors) will affect the amount of error present in data.

(E) Using reduced data sets can sometimes decrease the relative amount of error. The impact of ME in a study will depend on the amount of true variation in shape relative to that due to ME. It may sometimes be desirable to use only a restricted subset of all the landmarks collected for the final analysis and statistical evaluation, even if this potentially compromises the information content of a given data set. Choosing which landmarks to use will, however, often be a tedious task. For example, while landmarks located closely together may potentially give valuable information of small scaled and localisable true shape variation, they will also tend to duplicate information of more large scaled true shape variation and hence be redundant to some extent. Information on the absolute precision of landmark locations (ROTH 1993, REIG 1998) can be of great help in choosing landmarks, as can various superimposition methods (ROHLF & SLICE

1990, SLICE 1996) and multivariate techniques (RUSAKOV 1996) aimed at finding regions of independent variation in data.

(F) The most general, and often a very effective, way to reduce the amount of ME in geometric morphometrics is to take repeated measures of each specimen, and then base subsequent statistical inferences on the average shape scores for each individual (HIMES 1989, BAILEY & BYRNES 1990, RABINOVICH 1995) (see below for a discussion of the number of repeated measures that should be taken for each individual specimen). Access to repeated measures also enables assessments of the absolute and relative magnitudes of measurement error (see below).

ASSESSING THE IMPACT OF MEASUREMENT ERROR: TAKING REPEATED MEASURES

Despite its potentially very serious impact, ME has very rarely been explicitly dealt with in morphometric studies (BAILEY & BYRNES 1990). Since there are now established strategies with which to assess and reduce ME, the general awareness of the problem will hopefully increase. It is not possible to assess the amount of ME in a single measure of a single specimen. In contrast, whenever repeated measures (≥ 2) of each of a series of specimens are available, it is possible to assess the magnitude of ME. When taking repeated measures, one should make a great effort to repeat all, or at least as many as possible, of the methodological steps involved in data gathering (i. e., start from "scratch" with each repeated measurement). The importance of this has not previously been recognised (cf., SLICE 1993*a*, DEMETER *et al.* 1996, but see LEE 1982).

Sometimes this can not be done, as in cases when specimens are irreversibly prepared (e. g., skeletonizations, histological preparations) or when only a single reproduction of each specimen is available. It is important to realise that assessments of ME in such cases will not reflect total ME: it will only embody the components of error (Fig. 1) that are in fact repeated across repeated measurements, and will hence reflect only the minimum amount of error present (see example below).

Depending on circumstances, thus, repeated measures will be informative of different components of error (RABINOVICH 1995). The *reproducibility* of measurements reflects the closeness of results of measurements performed under different conditions, with different methods and with different equipment. The reproducibility indicates the magnitude of both random and systematic ME, and is important when systematic errors are suspected to influence the results (LEE 1990, YEZERINAC *et al.* 1992, DEMETER *et al.* 1996, EASON *et al.* 1996). The *repeatability* of measurements reflects the closeness of results of measurements

performed under identical conditions, with the same methods and with the same equipment. The repeatability is informative primarily of the amount of random error present in data (but see below), and is thus the focus of this section. There are two alternative, though not mutually exclusive, ways of assessing ME.

Absolute measures of measurement error

The most common method used so far to assess ME in geometric morphometrics is to calculate absolute accuracy or precision. This is expressed either as an average distance from the mean, or a measure of dispersion such as the standard deviation, among a set of repeated measures of a linear distance or a particular landmark location (e. g., BECERRA *et al.* 1993, LOY *et al.* 1993, DEAN 1996, DEMETER *et al.* 1996, REIG 1998). These measures (e. g., the root mean square – RMS) are absolute in the sense that they can be expressed in an absolute metric unit (e. g., mm), and can be very valuable and appropriate (a) when different data acquisition techniques, or equipment, are compared or (b) when selecting which subset of landmarks, or distances, to include in morphometric analysis (BAILEY & BYRNES 1990, ROTH 1993, REIG 1998, but see KOHN *et al.* 1995).

As mentioned above, the statistical problems generated by ME in empirical morphometrics are related to the amount of true variance in the variables of interest. Because of this, absolute measures of ME are often inadequate to asses the impact of ME in a given study, and investigators are typically left to subjectively deem absolute ME as being either "problematic" or "negligible" (e. g., LOY *et al.* 1993). Most would intuitively agree, for example, that an instrument with an accuracy of 0. 5 mm root mean square (RMS) would be perfectly relevant for a comparative study of cranial shape among primates, and equally inadequate for a study of intraspecific variation of cranial shape in a small rodent species (DEAN 1996). But would this instrument be adequate for a comparison of the cranial shape of two closely related species of eagles? This problem is overcome by the use of relative measures of ME, since they provide quantitative measures of the relative magnitude of ME in shape variables for specific data sets.

Relative measures of measurement error

Several authors have stressed that a meaningful measure of the impact of ME in morphometric studies must relate the amount of ME in a variable to true variation among individuals in the sample (HAGGARD 1958, FLEISS & SHROUT 1977, PALMER & STROBECK 1986, SCHLUTER & SMITH 1986, HIMES 1989, MARKS *et al.* 1989, BAILEY & BYRNES 1990, LEE 1990, LOUGHEED *et al.* 1991, YEZERINAC *et al.* 1992, KOHN *et al.* 1995). This is done by simply performing a model II one-way analysis of variance on repeated measures from each of a series of individuals, with individual as a categorical factor. From such an ana-

lysis, we attain a ratio R of the variance due to differences among individuals to the total variance:

$$R = S^2_A / (S^2_W + S^2_A) \quad [2]$$

where S^2_A is the among-individuals variance component and S^2_W is the within-individuals variance component. Variance components are calculated from the analysis of variance table as:

$$S^2_W = MS_{within} \quad [3]$$

and

$$S^2_A = (MS_{among} - MS_{within}) / n \quad [4]$$

where n is the number of repeated measures per individual (≥ 2) (see LESSELS & BOAG 1987, for cases where the number of repeated measures varies between individuals). This variance ratio has formally been given the somewhat misleading term "intraclass correlation coefficient", since it equals the Pearson correlation coefficient in the simplest case where only two repeated measures have been taken (SOKAL & ROHLF 1995). It has a long history as a measure of ME in the anthropometric literature (e. g., HAGGARD 1958, LORD & NOVICK 1968, FLEISS & SHROUT 1977) as well as in quantitative genetics (FALCONER 1960, BECKER 1984, FALCONER & MACKAY 1996), and has more recently been "rediscovered" as a measure of the impact of ME in morphometrics (BAILEY & BYRNES 1990, LOUGHEED *et al.* 1991, YEZERINAC *et al.* 1992). The variance ratio has been termed reliability in the first, repeatability in the second, and %ME in the third discipline. We suggest that the term repeatability is maintained for the use of R in morphometrics, to agree with its frequent use in other domains of evolutionary biology.

The most attractive characteristic of the repeatability is that it, in contrast to absolute measures, directly relates the magnitude of ME in a particular variable to the magnitude of true morphological variation. Repeatability parameterises the proportion of variance due to true variation between individuals, and ranges between 0 and 1; in the former case all variance is attributable to variance within individuals (i. e., 100% ME), and in the latter all variance is found between individuals (i. e., 0% ME). For the empiricist interested in statistical inferences, it is thus a direct and adequate measure of the relative impact of ME for a given variable in a specific sample.

As mentioned above, the relative magnitude of ME in a given variable decreases when multiple scores of each individual is averaged. The relationship between number of repeated measures per individual, n, and the repeatability after averaging the n measures, R_n, is

$$R_n = \frac{n\,R}{1 + (n - 1)\,R} \quad [5]$$

where R is the estimated repeatability of single measures (eq. [2] above) (FLEISS & SHROUT 1977, HIMES 1989, ARNOLD 1994, FALCONER & MACKAY 1996). In general, the lower the repeatability is of a variable, the more can be gained by averaging repeated measures (Fig. 3). The number of repeated measures necessary to achieve a desired level of repeatability after averaging is given by

$$n = \frac{R_n (1 - R)}{R (1 - R_n)} \qquad [6]$$

These relationships are derived from the Spearman-Brown prophesy formula (FLEISS & SHROUT 1977, HIMES 1989), and can be very helpful when deciding how many repeated measures one should take from each individual.

A STRATEGY TO COPE WITH MEASUREMENT ERROR IN GEOMETRIC MORPHOMETRICS

It is important to stress, again, that the problem with ME in empirical studies is a relative one. In some cases, the relative impact of ME can be safely

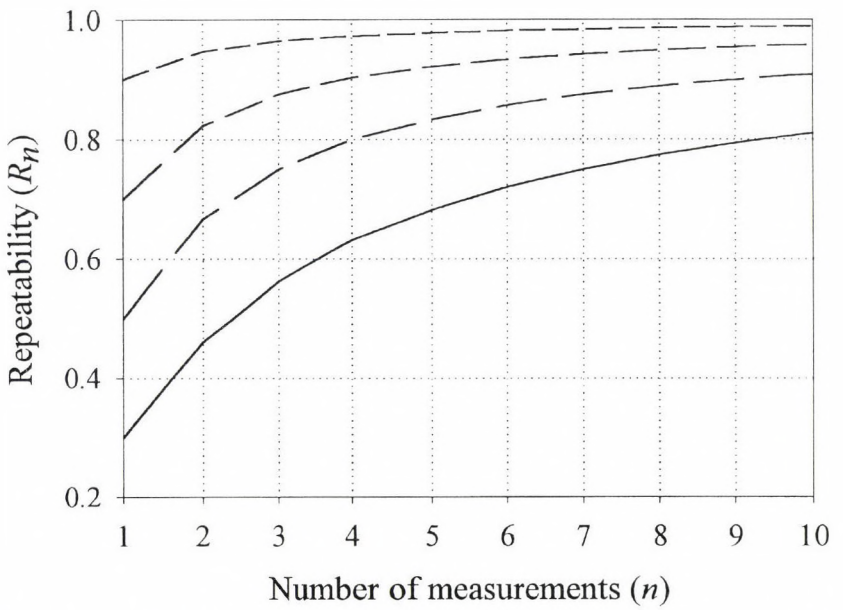

Fig. 3. Estimates of the repeatability that results from averaging several repeated measures (R_n) as a function of the number of repeated measures taken on each individual, for four different values of single measure repeatability (R = 0.3, 0.5, 0.7 and 0.9) (see eq. [5]). This illustrates that the relative proportion of true between-individual variation in a variable can be dramatically increased by averaging several repeated measures

assumed *a priori* to be very low, such as when the method of data acquisition is known to be very accurate and the magnitude of true between-individual variation in shape is known to be very large. However, in cases where this can not be safely assumed, such as in many studies of intraspecific variation, the quality of a study increases significantly when repeated measures are taken (BAILEY & BYRNES 1990). As mentioned above, the benefits of taking repeated measures are two-fold. First, it enables assessments of the relative magnitude of ME in various variables in the sample, by making the estimation of repeatabilities possible (eq. [2]). Second, it increases the statistical power (COHEN 1988), by decreasing the impact of ME to an estimable degree (eq. [5]) when averages of repeated measures for each individual are used for inferential statistical evaluation.

If possible, we recommend that repeated measures are taken routinely for all individuals in the sample, but repeated measures of a subset of all individuals included at least enables estimation of repeatabilities. With regards to the number of repeated measures that should be taken on each individual, we refer to equation [6]. It should be mentioned, however, that it is rarely worth while taking more than four repeated measures (HIMES 1989, FALCONER & MACKAY 1996), unless single measure repeatability is very low (Fig. 3) or one is interested in a further partitioning of ME (see below). If the total number of measurements is logistically constrained, for example if each measure is "costly", a trade-off between the number of individuals measured and the number of repeated measures per individual may occur. BAILEY & BYRNES (1990) gives some valuable guidelines as to how such trade-offs are optimised. In general, increasing the number of individuals measured (if possible), rather than the number of measures per individuals, will often be the preferred strategy.

When repeated measures of individuals (multiple repeated landmark configurations per individual) are present one can either (1) use average landmark co-ordinates (e. g., means produced by GLS) for each individual for all further analytical purposes, or one can (2) use all repeated measures of all individuals in the morphometric analysis and then calculate repeatability of the shape variables. In the latter case, subsequent statistical inferences (e. g., various tests of shape differences between groups) can then be based on average shape (e. g., mean partial warp or relative warp score) for each specimen. While the former strategy does increase the quality of the data, we suggest that the latter strategy is most useful for morphometric analyses (see also the example below). The primary advantage of method (2) over (1) is a higher biological and statistical direct relevance of the repeatability estimates. While it may be possible in theory to understand how ME in single landmarks affects the relative magnitude of ME in certain multivariate shape variables (see GOODALL & MARDIA 1993, MARDIA & DRYDEN 1994, DRYDEN *et al.* 1997, KENT & MARDIA 1997, and references therein), the link between the precision or repeatability of a given landmark loca-

tion and the repeatability of multivariate shape variables is typically very obscure for the empiricist. For example, it is not easy to assess and compare the relative impact of ME in a set of multivariate shape variables given that we have information of the precision of the landmark locations on which the analysis is based. In contrast, method (2) generates direct estimates of the relative impact of ME for various components of shape space, by providing repeatability estimates of the multivariate shape variables. This is very important for two reasons. First, statistical inferences in morphometric studies are typically based on shape variables rather than landmark locations *per se*. Second, biological inferences are made by visualising multivariate shape components. We believe that it is critical to assess the impact of ME in a given study by evaluating the variables on which we base our inferences. For example, the relative magnitude of ME in different multivariate shape variables typically vary tremendously, sometimes in non-intuitive ways (LOUGHEED *et al.* 1991, ARNQVIST *et al.* 1997, ARNQVIST & THORNHILL 1998, and below). If the investigator is to make inferences (statistical and biological) of differences in shape between groups of individuals, information on the relative magnitudes of ME in the shape variables in the sample is key. This also allows exclusion of shape dimensions gravely affected by ME from further analysis, and can hence decrease the impact of ME in the study as a whole (BAILEY & BYRNES 1990).

In some cases, one may be interested in partitioning the variance in a given variable beyond the within- and between-individual components discussed so far (cf. eq. [2]). This will be the case, for example, if one wishes to assess the relative magnitude of different components of ME in relation to between-individual variation. This can be made by a strategically planned hierarchical repeated measures protocol, where repetition is done on several different levels that correspond to different sources of error (see Fig. 4). This type of measurement protocol requires a slightly more complex analytical design; it is analysed by extracting variance components from nested analyses of variance (SOKAL & ROHLF 1995), where each level of replication is nested in the ones above (see KOHN *et al.* 1995, and below for examples, and SLICE 1993*a*, for an analogous case). With this design, total ME can be divided into its components.

Finally, one topic that is worth special attention is the measurement of asymmetry, especially fluctuating asymmetry, in bilateral symmetrical traits. This is an area where geometric morphometrics can potentially be a very valuable tool (see AUFFRAY *et al.* 1996, ARNQVIST *et al.* 1997, SMITH *et al.* 1997). In these cases, it is absolutely critical to estimate the relative impact of ME (e. g., repeatability) in ones measures of asymmetry in shape, since ME alone will produce apparent fluctuating asymmetry (see, for example, PALMER & STROBECK 1986, 1997, SWADDLE *et al.* 1994, FIELD *et al.* 1995, HUTCHISON & CHEVERUD 1995, MERILÄ & BJÖRKLUND 1995, BJÖRKLUND & MERILÄ 1997, RABITSCH 1997).

Fig. 4. An example of a hierarchical repeated measures protocol. In this example, each of the levels 2 and 3 are repeated twice and level 4 three times. Each individual is, hence, measured twelve times, and each of the levels 2 – 4 correspond to a certain component of measurement error. For example, level 2 may represent specimen preparation, level 3 specimen capture and reproduction, and level 4 the different measures. Relative measurement error could then be partitioned into components due to methodological, instrumental, and personal (digitising) measurement error, respectively

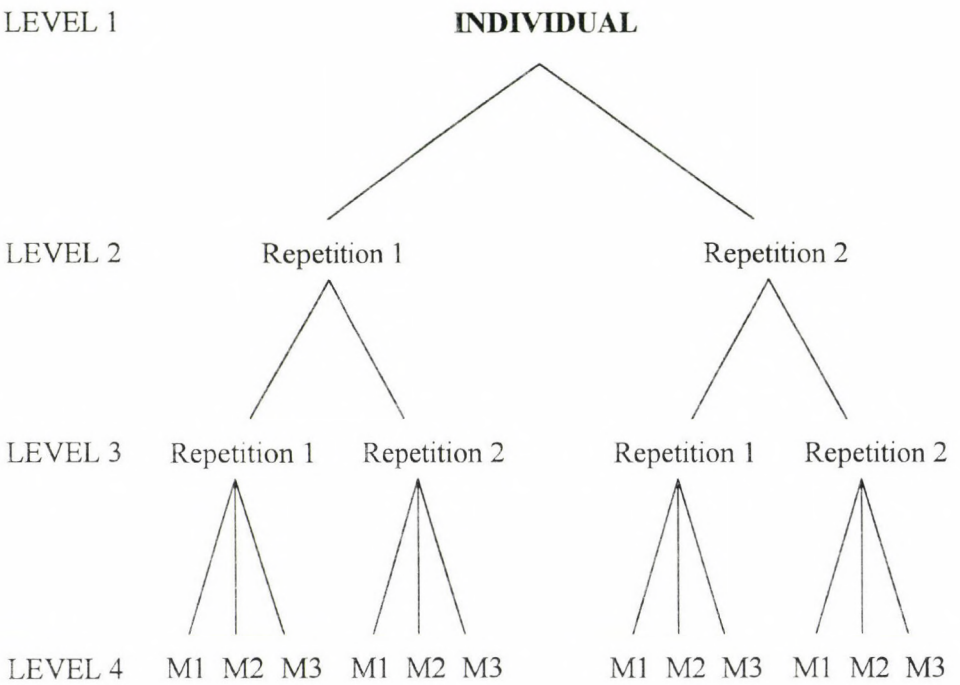

To discuss the merits of various methods of assessing the relative magnitude of ME in measures of fluctuating asymmetry is beyond the scope of the current presentation, but it seems that a mixed model analysis of variance approach is the preferred method (see PALMER & STROBECK 1986, MERILÄ & BJÖRKLUND 1995, for details).

AN EXAMPLE: QUANTIFYING MEASUREMENT ERROR OF SHAPE IN YOUNG PERCH

To illustrate some of the points made in the current contribution, we here present an analysis of the impact of ME in measures of shape variation in young fish (perch). We wish to stress that the purpose of this analysis is not a biological one, but exclusively confined to methodological issues relating to ME. We illus-

trate four things: 1) that estimates of repeatabilities depend on the error components that are actually repeated for each measure, 2) that the impact of different components of ME can be assessed by hierarchical repeated measurements and analyses, 3) that the relative magnitude of ME in a variable can be reduced by averaging several repeated measures, and 4) that ME is unevenly distributed among different multivariate shape variables.

Materials and methods

For the purposes of this study, a number of young of the year (0+) perch (Perciformes; *Perca fluviatilis*) were collected by means of electrofishing, in a lake situated in northern Sweden (Åmsele, Västerbotten). Twenty of these individuals (3.5–4.5 cm total body length) were fresh frozen, and later thawed and subjected to morphometric analysis. Landmarks were collected by viewing the fish directly in a dissecting microscope (Leica® MZ8), and projecting the image through a camera lucida onto a digitising tablet (Summasketch® III). In total, 21 landmarks were collected for each repeated measure of each fish (see Fig. 5) by means of DS-DIGIT (SLICE 1994). We collected the repeated measures from each individual fish, in the following way. Each fish was positioned (presented) under the microscope, and three repeated measures were entered for the presentation without altering the position of the fish. The fish was then removed from the microscope stage. This whole procedure was repeated three times for each individual. Hence, this protocol yielded nine repeated "landmark maps" for each individual fish, hierarchically repeated as three repeated measures in each of three repeated presentations (3×3) (cf., Fig. 4).

Morphometric analysis

All sets of landmarks (N = 180) for all individuals were translated, scaled and rotated by generalised least-squares Procrustes fit using the GLS option in GRF-ND (SLICE 1993*b*), retaining the centroid size as a measure of size variation in the sample. The uniform components of shape space were then analysed according to BOOKSTEIN (1996*c*). Finally, the non-uniform sub-space of shape was analysed with a thin-plate spline relative warp analysis ($\alpha = 0$), using TPSRW (ROHLF 1993). For each repeated measure, 23 variables were retained for analysis; standardised scores of the first 20 relative warps, the two uniform components and the centroid size (see Table 1). For each variable we performed a nested analysis of variance, from which we extracted variance component estimates (see SOKAL & ROHLF 1995) corresponding to differences (1) among individuals, (2) among presentations within individuals and (3) among repeated measures within presentations and individuals. These will correspond to variance due to (1) true differences between individuals, (2) methodological and instrumental error (varying across presentations) and (3) personal error, respectively. We also calculated explicit repeatabilities from one-way analysis of variance (see eq. [2]

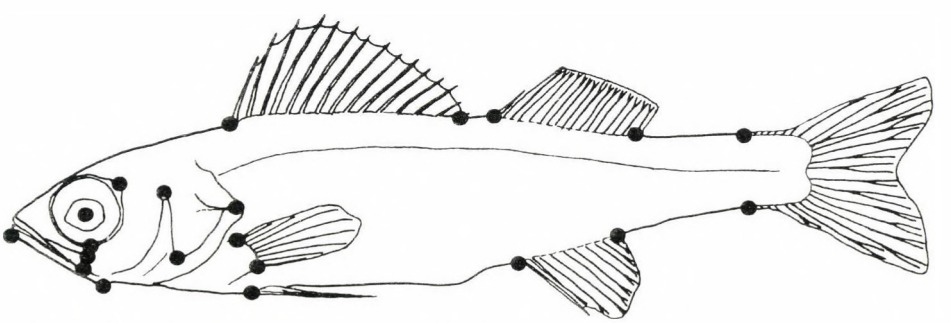

Fig. 5. Locations of landmarks used in the perch data set

above) for all variables in two different ways. First, a subset of only three repeated measures for each individual fish, all from one and the same presentation (the first one), was used to estimate repeatability (R_1) thus including only personal error. Second, all nine repeated measures from all three different presentations for each individual was used to estimate repeatability (R_2), thus including both methodological, instrumental and personal error. In addition, we estimated the repeatability that would result from averaging the nine repeated measures, R_n, as

$$R_n = \frac{9\,R_2}{1 + 8\,R_2} \qquad [7]$$

where R_2 represent the estimate mentioned above (cf., eq. [5]).

RESULTS AND DISCUSSION

We found our measure of size (centroid size) to be considerably less affected by ME than our multivariate measures of shape (Table 1), an expected pattern that should be very general (see also LOUGHEED *et al.* 1991, ARNQVIST & THORNHILL 1998). The proportion of measurement error ranged between approximately 15–30% for the uniform shape components, 10–40% for relative warps #1–10, and 35–80% for relative warps #11–20 (see R_2 in Table 1). One should bear in mind, however, that these figures are inflated relative to most "real" data sets. In this analysis, we were deliberately trying to keep between-individual variation in shape low (we used only a limited number of similar-sized individuals that were collected at the same locality and at the same occasion), in order to elevate the overall relative impact of ME.

As mentioned above, it is sometimes impossible to repeat all the methodological steps in one's repeated measures. Examples of such steps are when skeletal parts have been skeletonised, histological preparations have been made, each specimen is only available as a single photographic/digital reproduction, or when specimens have been preserved in preservatives (LEE 1982, CARPENTER 1996). In all these cases, the specimens are prepared once and for all, and the method is irreversible and hence unrepeatable. In these cases, the repeatabilities will reflect primarily personal error (ζ_p), and depending on circumstances possibly certain components of instrumental error (ζ_i). However, since the methodological error (ζ_m) is often a major component of ME, the estimated repeatabilities will represent highly inflated estimates of the quality of ones data in such samples. Our analyses illustrate this in two ways. First, the repeatabilities of all shape scores were considerably higher when only personal error was accounted for (cf. R_1 versus R_2 in Table 1). Second, variance due to personal error was in average about half that due to methodological and instrumental error (cf. 2nd versus 3rd variance component in Table 1). The major source of methodological error in our case was undoubtedly slight variations in the exact positioning of the fish across

Table 1. Estimates of repeatability for a series of morphometric variables in the perch data set. Given are also scaled variance component estimates for each trait, expressed in percent of the total variance. These three components estimate true phenotypic variance, variance due to methodological and instrumental error ($\zeta_m + \zeta_i$) and variance due to personal error (ζ_p), respectively. Numbers within brackets represent percentage of variance in shape explained by each relative warp. See text for further explanation

Variable		Repeatabilities			Variance components		
		R_1[a]	R_2[b]	R_n[c]	(1)	(2)	(3)
					among: Individuals	Presentations	Measures
					within:	Individuals	Presentations
Centroid size		1.00	1.00	1.00	99.4	0.5	0.1
Uniform comp. 1		0.93	0.77	0.97	71.1	23.5	5.4
Uniform comp. 2		0.97	0.86	0.98	82.4	14.8	2.7
Relative warp 1	(30.6)	0.99	0.86	0.98	81.2	18.3	0.5
Relative warp 2	(16.4)	0.98	0.88	0.98	84.4	12.9	2.6
Relative warp 3	(10.7)	0.97	0.81	0.97	75.5	22.0	2.6
Relative warp 4	(8.1)	0.94	0.77	0.97	70.7	24.5	4.8
Relative warp 5	(6.9)	0.90	0.81	0.97	77.0	15.7	7.3
Relative warp 6	(4.5)	0.93	0.77	0.97	72.3	20.6	7.1
Relative warp 7	(4.0)	0.89	0.82	0.98	79.0	12.3	8.7
Relative warp 8	(2.5)	0.90	0.86	0.98	85.2	5.6	9.2
Relative warp 9	(2.3)	0.87	0.59	0.93	48.9	40.8	10.3
Relative warp 10	(1.9)	0.85	0.63	0.94	54.3	33.3	12.5
Relative warp 11	(1.6)	0.86	0.56	0.92	48.1	34.9	17.0
Relative warp 12	(1.4)	0.80	0.65	0.94	58.3	27.2	14.6
Relative warp 13	(1.2)	0.82	0.66	0.95	62.5	17.0	20.5
Relative warp 14	(0.9)	0.79	0.41	0.86	27.6	50.2	22.2
Relative warp 15	(0.8)	0.61	0.39	0.85	27.0	53.5	19.5
Relative warp 16	(0.7)	0.70	0.19	0.67	5.4	51.8	42.9
Relative warp 17	(0.7)	0.59	0.40	0.86	28.9	41.4	29.6
Relative warp 18	(0.6)	0.58	0.40	0.86	30.6	42.5	26.9
Relative warp 19	(0.5)	0.60	0.22	0.72	11.0	43.2	45.8
Relative warp 20	(0.5)	0.66	0.21	0.70	3.8	62.3	34.0

presentations. Thus, our results illustrates the key importance of repeating all, or at least as many as possible, of the steps involved in the data gathering procedure. If this is not done, the investigator must be aware that repeatabilities only give an upper bound of the true "quality" of the data. This is often unsatisfactory, espe-

cially since the relative impact of different components of error is not necessarily correlated across different shape variables (see below).

Our methodological exercise demonstrates how the relative impact of ME in different shape variables can be partitioned, quantified and understood by a strategically planned hierarchical repeated measures protocol, followed by nested analyses of variance. With our design, the variance component that is due to differences among individuals corresponds to the repeatability of ones shape measures (correlation coefficient between variance component 1 and R_2 in Table 1, $r = 0.998$). In empirical studies, where the purpose is to make biological and statistical inferences, further levels can of course be added to such nested models (see SLICE 1993*a*, KOHN *et al.* 1995), including effect factors. In our case, for example, fish could have been sampled from different lakes, adding a variance component due to differences among lakes (variance among individuals would then be nested within a random lake factor). There is much to be gained by this type of analysis, since the potential for biological insight increases significantly by including ME in our statistical models (information on the relative magnitude of ME in different components of shape are available) rather than disregarding any variance that is due to error.

This type of analysis also allows for statistical inferences to be based on average shape of each individual, which increases the statistical power of ones tests (reduces the type II statistical error rate; COHEN 1988). Our repeatabilities were in many cases dramatically improved when averaging the nine repeated measures, especially for variables with low repeatabilities (cf. R_2 versus R_n in Table 1). The overall relative proportion of ME decreased from almost 40% to less than 10% (average for all 22 shape variables). Basing further statistical analysis (for example, tests of differences between groups) on average shape of each individual would thus greatly improve the quality of the analysis.

Our variance component analysis generated two further insights, with regards to the relative impact of ME in different components of shape space. First, and most importantly, the relative impact of ME generally increased with order among relative warps (Spearman rank correlations [r_S] between relative warp order and variance components 1–3; -0.88, 0.78 and 0.98 respectively, $P < 0.001$ in all cases). This pattern is expected since principal component analysis tend to selectively recover true structure from early axes, hence leaving later axes with relatively larger proportions of ME (GAUCH 1982, LOUGHEED *et al.* 1991). This was obvious in our example, where higher order relative warps were not only severely affected by ME but also explained a very low proportion of variance in shape (Table 1). Thus, there are several reasons for why principal components, in this case relative warps, should be interpreted with an increasing amount of caution with their order. Second, within this general trend, the relative impact of different components of ME was remarkably unevenly distributed among different

shape variables (see also LOUGHEED *et al.* 1991). Detailed information of this kind is especially helpful when interpreting negative findings, since some multivariate shape variables can parameterize shape variation that is to a large extent due to ME (e. g., relative warps 16, 19 and 20 in Table 1; see also CARPENTER 1996). Further, though the relative magnitudes of ME due to personal error on the one hand and methodological and instrumental error on the other were positively correlated (Spearman rank correlation [r_s] between variance components 1 and 2, 0.75, $P < 0.001$), it varied considerably among different shape variables (e. g., compare variance components 2 and 3 for relative warps 1 vs 8 and 9 vs 19).

In conclusion, we hope that our contribution has shown that there are several reasons for increasing our awareness of the impact of ME in geometric morphometrics. We do not in any way dispute the tremendous potential of the tools of the morphometric synthesis (ROHLF & MARCUS 1993, BOOKSTEIN 1996*a*, *b*, MARCUS *et al.* 1996), and hence do not wish to discourage anyone from using these methods. On the contrary, we hope to have shown that explicitly acknowledging the existence of ME is key in geometric morphometrics, and that including quantifications of the impact of ME such as those demonstrated here will lead to much more powerful and insightful applications.

* * *

Acknowledgements – We thank F. J. BOOKSTEIN, C. KLINGENBERG, S. REIG & P. WATSON for critical comments on previous versions of this paper; J. ROHLF & D. SLICE for providing the excellent software that made this study possible; P. BYSTRÖM & E. WESTMAN for providing the fish; and P. WATSON for originally acquainting us with geometric morphometrics. This study was made possible by financial support from The Swedish Natural Science Research Council.

REFERENCES

ARNOLD, S. J. (1994) Multivariate inheritance and evolution: a review of concepts. Pp. 17–48. *In* BOAKE (ed.): *Quantitative genetic studies of behavioral evolution.* The Univ. Chicago Press, Chicago.

ARNQVIST, G. & THORNHILL, R. (1998) Evolution of animal genitalia: patterns of phenotypic and genotypic variation and condition dependence of genital and non-genital morphology in a water strider. *Genetical Res.* [in press].

ARNQVIST, G., THORNHILL, R. & ROWE, L. (1997) Evolution of animal genitalia: morphological correlates of fitness components in a water strider. *J. Evol. Biol.* **10**: 613–640.

AUFFRAY, J.-C., ALIBERT, P., RENAUD, S., ORTH, A. & BONHOMME, F. (1996) Fluctuating asymmetry in Mus musculus subspecific hybridization: traditional and Procrustes comparative approach. Pp. 275–284. *In* MARCUS *et al.* (eds): *Advances in Morphometrics.* NATO ASI Series A: Life Sciences, Vol. 284, Plenum Press, New York.

BAILEY, R. C. & BYRNES, J. (1990) A new, old method for assessing measurement error in both univariate and multivariate morphometric studies. *Syst. Zool.* **39**: 124–130.

BECERRA, J. M. (1996) Imagina – a direct tool for image analysis in systematics. Pp. 83–89. *In* MARCUS *et al.* (eds): *Advances in Morphometrics.* NATO ASI Series A: Life Sciences, Vol. 284, Plenum Press, New York.

BECERRA, J. M., BELLO, E. & GARCÍA-VALDECASAS, A. (1993) Building your own machine image system for morphometric analysis: a user point of view. Pp. 65–92. *In* MARCUS *et al.* (eds): *Contributions to morphometrics.* Monografías del Museo Nacional de Ciencias Naturales 8, Madrid.

BECKER, W. A. (1984) *A manual of quantitative genetics.* Academic Enterprises, Pullman, Washington, 130 pp.

BJÖRKLUND, M. & MERILÄ, J. (1997) Why some measures of fluctuating asymmetry are so sensitive to measurement error. *Ann. Zool. Fenn.* **34**: 133–137.

BOOKSTEIN, F. L. (1991) *Morphometric tools for landmark data.* Cambridge Univ. Press, Cambridge, New York, 435 pp.

BOOKSTEIN, F. L. (1996*a*) Biometrics, biomathematics and the morphometric synthesis. *Bull. Math. Biol.* **58**: 313–365.

BOOKSTEIN, F. L. (1996*b*) Combining the tools of geometric morphometrics. Pp. 131–152. *In* MARCUS *et al.* (eds): *Advances in Morphometrics.* NATO ASI Series A: Life Sciences Vol. 284, Plenum Press, New York.

BOOKSTEIN, F. L. (1996*c*) Standard formula for the uniform shape component in landmark data. Pp. 153–168. *In* MARCUS *et al.* (eds): *Advances in Morphometrics.* NATO ASI Series A: Life Sciences Vol. 284, Plenum Press, New York.

CARPENTER, K. E. (1996) Morphometric pattern and feeding mode in emperor fishes (Lethrinidae, Perciformes). Pp. 479–488. *In* MARCUS *et al. (eds): Advances in Morphometrics.* NATO ASI Series A: Life Sciences Vol. 284, Plenum Press, New York.

COHEN, J. (1988) *Statistical power analysis for the behavioral sciences.* Lawrence Erlbaum Ass., Hillsdale, 567 pp.

DEAN, D. (1996) Three-dimensional data capture and visualization. Pp. 53–70. *In* MARCUS *et al.* (eds): *Advances in Morphometrics.* NATO ASI Series A: Life Sciences Vol. 284, Plenum Press, New York.

DEMETER, A., VÁMOSI, J., PEREGOVITS, L. & TOPÁL, G. (1996) An image-capture and data-collection system for morphometric analysis. Pp. 91–102. *In* MARCUS *et al.* (eds): *Advances in Morphometrics.* NATO ASI Series A: Life Sciences Vol. 284, Plenum Press, New York.

DRYDEN, I. L., FAGHIHI, M. R. & TAYLOR, C. C. (1997) Procrustes shape analysis of planar point subsets. *J. Roy. Statist. Soc.* **59**: 353–374.

EASON, T. H., SMITH, B. H. & PELTON, M. R. (1996) Researcher variation in collection of morphometrics on black bears. *Wildl. Soc. Bull.* **24**: 485–489.

FALCONER, D. S. (1960) *Introduction to quantitative genetics*, 1st ed., Oliver and Boyd, London, 365 pp.

FALCONER, D. S. & MACKAY, T. F. C. (1996) *Introduction to quantitative genetics*, 4th ed. Longman, Harlow, 464 pp.

FIELD, S. J., SPIERS, M., HERSHKOVITZ, I. & LIVSHITS, G. (1995) Reliability of reliability coefficients in the estimation of asymmetry. *Am. J. Phy. Anthrop.* **96**: 83–87.

FINK, W. (1990) Data aquisition in systematic biology. Pp. 9–20. *In* ROHLF & BOOKSTEIN (eds): *Proc. Michigan Morphometrics Workshop.* Special Publ. 2, Univ. Michigan Museum of Zoology, Ann Arbor. 380 pp.

FLEISS, J. L. & SHROUT, P. E. (1977) The effects of measurement errors on some multivariate procedures. *Am. J. Public Health* **67**: 1188–1191.

FRANCIS, R. I. C. C. & MATLIN R. H. (1986) A possible pitfall in the morphometric application of discriminant analysis: measurement bias. *Marine Biol.* **93**: 311–313.

FULLER, W. A. (1987) *Measurement error models.* John Wiley, New York, 440 pp.

GARCÍA-VALDECASAS, A. (1996) Two-dimensional imaging: an update. Pp. 71–82. *In* MARCUS *et al.* (eds): *Advances in Morphometrics.* NATO ASI Series A: Life Sciences Vol. 284, Plenum Press, New York.

GAUCH, H. G. (1982) Noise reduction by eigenvector ordinations. *Ecology* **63**: 1643–1649.

GOODALL, C. R. & MARDIA, K. V. (1993) Multivariate aspects of shape theory. *Ann. Stat.* **21**: 848–866.

HAGGARD, E. A. (1958) *Intraclass correlation and the analysis of variance.* Dryden Press, New York, 171 pp.

HIMES, J. H. (1989) Reliability of anthropometric methods and replicate measurements. *Am. J. Phy. Anthrop.* **79**: 77–80.

HUTCHISON, D. W. & CHEVERUD, J. M. (1995) Fluctuating asymmetry in tamarin (Saguinus) cranial morphology – intraspecific and interspecific comparisons between taxa with varying levels of genetic heterozygosity. *J. Hered.* **86**: 280–288.

JAMISON, P. L. & ZEGURA, S. L. (1974) A univariate and multivariate examination of measurement error in anthropometry. *Am. J. Phy. Anthrop.* **40**: 197–204.

KENT, J. T. & MARDIA, K. V. (1997) Consistency of Procrustes estimators. *J. R. Statist. Soc.* **59**: 281–290.

KOHN, L. A. P., CHEVERUD, J. M., BHATIA, G., COMMEAN, P., SMITH, K. & VANNIER, M. W. (1995) Anthropometric optical surface imaging system repeatability, precision, and validation. *Ann. Plast. Surg.* **34**: 362–371.

LEE, J. C. (1982) Accuracy and precision in anuran morphometrics: artifacts of preservation. *Syst. Zool.* **31**: 266–281.

LEE, J. C. (1990) Sources of extraneous variation in the study of meristic characters: the effects of size and inter-observer variability. *Syst. Zool.* **39**: 31–39.

LESSELS, C. M. & BOAG, P. T. (1987) Unrepeatable repeatabilities: a common mistake. *Auk* **104**: 116–121.

LORD, F. M. & NOVICK, M. R. (1968) *Statistical theories of mental test scores.* Addison-Wesley, Reading, 568 pp.

LOUGHEED, S. C., ARNOLD, T. W. & BAILEY, R. C. (1991) Measurement error of external and skeletal variables in birds and its effect on principal components. *Auk* **108**: 432–436.

LOY, A., CORTI, M. & MARCUS, L. F. (1993) Landmark data: size and shape analysis in systematics – a case study on old world Talpidae (Mammalia, Insectivora). Pp. 215–240. *In* MARCUS *et al.* (eds): *Contributions to morphometrics.* Monografías del Museo Nacional de Ciencias Naturales 8, Madrid.

MACLEOD, N. (1990) Digital images and automated image analysis systems. Pp. 21–36. *In* ROHLF, F. J. & BOOKSTEIN, F. L. (eds): *Proceedings of the Michigan Morphometrics Workshop.* Special Publ. 2, University of Michigan Museum of Zoology, Ann Arbor.

MARCUS, L. F., CORTI, M., LOY, A., NAYLOR, G. J. P. & SLICE D. E. (1996) *Advances in Morphometrics.* NATO ASI Series A: Life Sciences Vol. 284, Plenum Press, New York, 587 pp.

MARDIA, K. V. & DRYDEN, I. L. (1994) Shape averages and their bias. *Adv. Appl. Prob.* **26**: 334–340.

MARKS, G. C., HABICHT, J.-P. & MUELLER, W. H. (1989) Reliability, dependability, and precision of anthropometric measurements. *Am. J. Epidemiol.* **130**: 578–587.

MERILÄ, J. & BJÖRKLUND, M. (1995) Fluctuating asymmetry and measurement error. *Syst. Biol.* **44**: 97–101.

PALMER, A. R. & STROBECK, C. (1986) Fluctuating asymmetry: measurement, analysis and pattern. *Ann. Rev. Ecol. Syst.* **17**: 391–421.

PALMER, A. R. & STROBECK, C. (1997) Fluctuating asymmetry and developmental stability: heritability of observable variation vs. heritability of inferred cause. *J. Evol. Biol.* **10**: 39–49.

PANKAKOSKI, E., VÄISÄNEN, R. A. & NURMI, K. (1987) Variability of muskrat skulls: measurement error, environmental modification and size allometry. *Syst. Zool.* **36**: 35–51.

RABINOVICH, S. R. (1995) *Measurement errors: theory and practice*. American Institute of Physics, New York, 279 pp.

RABITSCH, W. B. (1997) Levels of asymmetry in Formica pratensis Retz (Hymenoptera, Insecta) from a chronic metal-contaminated site. *Env. Toxicol. Chem.* **16**: 1433–1440.

REIG, S. (1998) 3D digitizing precision and sources of error in the geometric analysis of weasel skulls. *Acta zool. hung.* **44**(1–2): 61–72.

ROHLF, F. J. (1990) An overview of image processing and analysis techniques for morphometrics. Pp. 37–60. *In* ROHLF, F. J. & BOOKSTEIN, F. L. (eds): *Proc. Michigan Morphometrics Workshop*. Special Publ. 2, Univ. Michigan Museum of Zoology, Ann Arbor.

ROHLF, F. J. (1993) *TPSRW: thin-plate spline relative warp analysis*. Dept. Ecology and Evolution, State University of New York, Stony Brook, New York.

ROHLF, F. J. & BOOKSTEIN, F. L. (1990) *Proc. Michigan Morphometrics Workshop*. Special Publ. 2, University of Michigan Museum of Zoology, Ann Arbor, 380 pp.

ROHLF, F. J., GILMARTIN, A. J. & HART, G. (1983) The Kluge-Kerfoot phenomenon – a statistical artefact. *Evolution* **37**: 180–202.

ROHLF, F. J. & MARCUS, L. F. (1993) A revolution in morphometrics. *Trends Ecol. & Evol.* **8**: 129–132.

ROHLF, F. J. & SLICE, D. E. (1990) Extensions of the Procrustes method for the optimal superimposition of landmarks. *Syst. Zool.* **39**: 40–59.

ROTH, V. L. (1993) On three-dimensional morphometrics, and on the identification of landmark points. Pp. 41–61. *In* MARCUS *et al.* (eds): *Contributions to morphometrics*. Monografías del Museo Nacional de Ciencias Naturales 8, Madrid.

RUSAKOV, D. A. (1996) Dimension reduction and selection of landmarks: a Monte Carlo experiment. Pp. 201–208. *In* MARCUS *et al.* (eds): *Advances in Morphometrics*. NATO ASI Series A: Life Sciences Vol. 284, Plenum Press, New York.

SCHLUTER, D. & SMITH, J. N. M. (1986) Genetic and phenotypic correlations in a natural population of song sparrows. *Biol. J. Linn. Soc.* **29**: 23–36.

SLICE, D. E. (1993*a*) The fractal analysis of shape. Pp. 161–190. *In* MARCUS *et al.* (eds): *Contributions to morphometrics*. Monografías del Museo Nacional de Ciencias Naturales 8, Madrid.

SLICE, D. E. (1993*b*) *GRF-ND: generalized rotational fitting of n-dimensional landmark data*. Dept. Ecology and Evolution, State University of New York, Stony Brook, New York.

SLICE, D. E. (1994) *DS-DIGIT: basic digitizing software*. Dept. Ecology and Evolution, State University of New York, Stony Brook, New York.

SLICE, D. E. (1996) Three-dimensional generalized resistant fitting and the comparison of least-squares and resistant-fit residuals. Pp. 179–199. *In* MARCUS *et al.* (eds): *Advances in Morphometrics*. NATO ASI Series A: Life Sciences Vol. 284. Plenum Press, New York.

SMITH, D. R., CRESPI, B. J. & BOOKSTEIN, F. L. (1997) Fluctuating asymmetry in the honey bee, Apis mellifera: effects of ploidy and hybridization. *J. Evol. Biol.* **10**: 551–574.

SOKAL, R. R. & ROHLF, F. J. (1995) *Biometry*, 3rd ed. Freeman & Co., San Francisco, 887 pp.

SWADDLE, J. P., WITTER, M. S. & CUTHILL, I. C. (1994) The analysis of fluctuating asymmetry. *Anim. Behav.* **48**: 986–989.

WAINWRIGHT, P. C. & REILLY, S. M. (1994) *Ecological morphology: integrative organismal biology*. The Univ. of Chicago Press, Chicago, 367 pp.

YEZERINAC, S. M., LOUGHEED, S. C. & HANDFORD, P. (1992) Measurement error and morphometric studies: statistical power and observer experience. *Syst. Biol.* **41**: 471–482.

Acta Zoologica Academiae Scientiarum Hungaricae 44 (1–2), pp. 97–112, 1998

WING STATIC ALLOMETRY IN DROSOPHILA SIMULANS MALES (DIPTERA, DROSOPHILIDAE) AND ITS RELATIONSHIPS WITH DEVELOPMENTAL COMPARTMENTS*

M. BAYLAC** and X. PENIN

Muséum national d'Histoire Naturelle, Groupe de travail Morphométrie et Analyse de formes, Laboratoire d'Entomologie (EP90)
45, rue Buffon F–75005 Paris, France
E-mail: baylac@mnhn.fr

Static allometric patterns of the wing of *Drosophila simulans* males were estimated by multivariate regression of GLS procrustes residuals on the log of centroid-size, by thin-plate splines regression visualisations, and by multivariate allometry of inter-landmark distances. The allometric shape component equals 6% of the total shape variance. Allometric patterns involve mainly the distal and central parts of the wing. They correspond to a relative contraction of the distal part of the wing, from the posterior cross-veins to the apex. The proximal region of the wing undergoes the lowest allometric transformations. Relationships between allometry and developmental compartments were investigated for uniform transformations. Uniform allometric patterns are significant only for the anterior wing compartment. Principal axes are congruent with known directional patterns of cells clones and landmarks. On the whole, and whatever the compartments are, allometric changes appear basically of the non-uniform type.

Key words: static allometry, multivariate allometry, Procrustes superimposition, developmental compartments, uniform transformations

INTRODUCTION

Since its beginning, geometric morphometrics has been largely concerned by the description of allometric shape changes in various taxa: Foraminifera (MACLEOD & KITCHELL 1990), Fishes (WALKER 1993, LOY *et al.* 1996), Salamanders (REILLY 1990), cotton rat (ZELDITCH *et al.* 1992), rat (BOOKSTEIN 1991, WALKER 1993), Monkeys and Apes (BOOKSTEIN 1978, PENIN & BAYLAC 1995), and Hominoids (BACON & BAYLAC 1995). The direct visualisation of the allometric shape changes of an integrated biological structure, is a major advance in comparison with uni- or multivariate allometry, for which allometric changes had to be deduced from the simple examination of a list of slopes or of PCA coefficients.

* Symposium presentation, 5th International Congress of Systematic and Evolutionary Biology, 1996, Budapest

** To whom correspondence should be addressed.

Rather surprisingly, allometric patterns in *Drosophila*, one of the few universal biological models, have never been extensively described or analysed. This is particularly true for the wings which are frequently used in evolutionary, genetics, and developmental genetic studies (WEBER 1990, 1992, COWLEY *et al.* 1986, WADDINGTON 1940, GARCIA-BELLIDO & DE CELIS 1992). Most of the descriptions and quantitative genetic analyses relied upon selected distances and ratios. Many studies focused on single wing measurements (i.e. wing length) or ratios without taking into account allometric changes of the wing as a whole.

The present study deals with the description of allometric patterns in the wing of males of *Drosophila simulans*. They are described using two approaches, a multivariate allometric one (KLINGENBERG 1996) and a geometric one using Procrustes superimpositions and Thin Plate Splines visualisations (ROHLF & SLICE 1990, BOOKSTEIN 1991, 1996*a, b*), in order to facilitate the comparison with related studies which used distances, or distance ratios.

Analyses of evolutionary shape changes in the wing of Diptera have clearly demonstrated the existence of directional components (ROHLF & SLICE 1990, BAYLAC 1993, BAYLAC & DAUFRESNE 1996). Many displacements may be described as sliding along one vein of the loci at which other veins branch off. Such oriented shape changes are also found during wing morphogenesis. For instance, cellular clones in vein mutants run preferentially along the proximo-distal axis and along longitudinal veins, as indicated by the overall elongated shape of polyclones (GARCIA-BELLIDO 1977, GARCIA-BELLIDO & DE CELIS 1992, GARCIA-BELLIDO *et al.* 1994). At a higher level, differential expression of changes in vein positions, either in relation to temperature selection experiments (CAVICCHI *et al.* 1985), or to geographic divergence (IMASHEVA *et al.* 1995), have been related to developmental compartments. Wing compartments (GARCIA-BELLIDO *et al.* 1973, LAWRENCE 1992) appear at an early stage in the imaginal discs. Each compartmental subdivision results into two independent developmental genetic units, whose boundaries define mutually orthogonal axes of symmetry, one antero-posterior, one dorso-ventral, and one proximo-distal (GARCIA-BELLIDO & DE CELIS, *ibid*).

One of the major interests of geometric morphometrics is the investigation of shape transformations in terms of geometric scales. Uniform transformations are the simplest of the global transformations which can account for simple directional events. The present study attempts to link allometric changes to basic developmental processes using this simple geometric scale decomposition. Beside the now usual analysis of Procrustes linearized uniform terms, we followed BOOKSTEIN's (1996*b*) suggestion to analyse uniform shape changes using a tensor representation: the principal axes. Principal axes, or principal directions, or biorthogonal directions, define two orthogonal directions along which ratios of changes are respectively maximised and minimised (BOOKSTEIN 1991, chapter

6). Substantial alignment of principal axes with directional wing components, as well as significant interactions of allometry with compartment subdivisions, would be a good argument for their role at a late stage of wing differentiation.

MATERIAL AND METHODS

Material

Seventy six male adults of *Drosophila simulans* were randomly selected from a mass culture reared at 19°C. All the flies belonged to the SiIII mitochondrial cytotype (BABA-ASSA & SOLIGNAC 1988). Adults were preserved in 95° alcohol until being measured. Right wings were cut at their base and temporarily slide mounted in lactic acid. Images of the preparations were taken using a Leitz Periplan microscope at ×10 magnification and a video camera connected to an AT-OFG video frame grabber. The definition was 768×512 pixels (columns × lines). The coordinates of fourteen landmarks (Fig. 1) were recorded using the MeasurementTV software (UPDEGRAFF 1990). Each wing was measured 3 times and the results were averaged. Allometric patterns were analysed by means of multivariate allometry (KLINGENBERG 1996) and by geometric morphometrics after Procrustes superimposition (BOOKSTEIN 1991, 1996*a*, ROHLF 1996).

Multivariate allometry

The 91 log-transformed inter-landmark distances were calculated from landmark locations. The covariance matrix of these distances was subjected to a PCA, as examplified in BOOKSTEIN 1991. Bootstrapped 95% confidence intervals and means (MARCUS 1990, KLINGENBERG 1996) of the PCA coefficients were calculated using 1000 replicates. With 91 distances, isometry is defined by a vector whose elements are all equal to 0.1048. (JOLICOEUR 1963). Based on the confidence intervals (CI), three classes were distinguished corresponding to negative allometry (CI < 0.1048), isometry (CI including 0.1048), and positive allometry (CI > 0.1048).

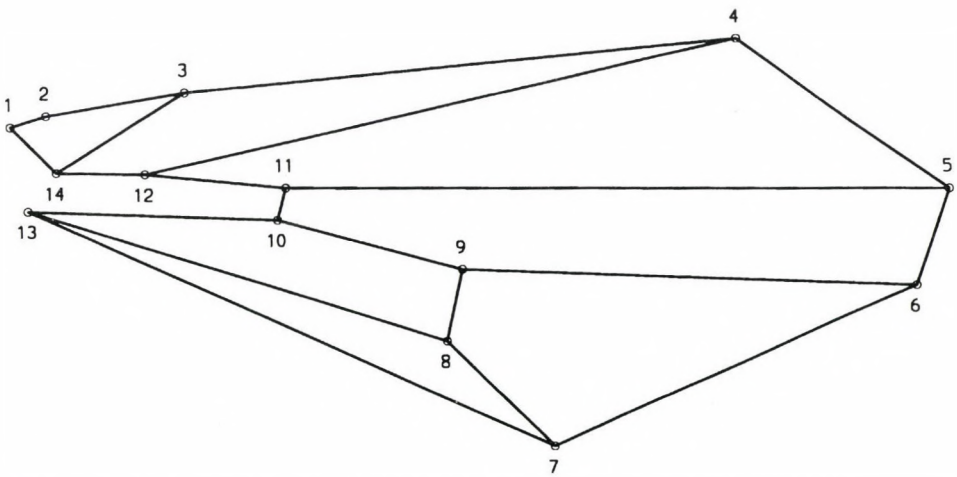

Fig. 1. Landmark locations, simplified outline and venation of a *D. simulans* right wing

Geometric allometry

The raw dataset was superimposed using generalised least-square (GLS) Procrustes fit (ROHLF & SLICE 1990, GOODALL 1991, 1995). Size was defined as the Log of centroid size (BOOKSTEIN 1991). Allometry was tested for selected subregions of the wing, which correspond to subsets of adjacent landmarks. In that case, Procrustes residuals and centroid sizes were calculated using the corresponding subsets of coordinates. The statistical significance of allometry was tested by multiple correlation (MOSIMANN & JAMES 1979, BOOKSTEIN 1996*a*) using all the residuals minus four (BOOKSTEIN 1996*a*). Polynomial regressions were used in order to test for a possible non linear allometry (WALKER 1993). Since quadratic and cubic regression never significatively improved the fits, simple linear regressions were used throughout this study. Allometric shape changes were calculated by multivariate regression (MARDIA *et al.* 1979, BOOKSTEIN 1996*a*). For the visualisation of the allometric shape changes, two sets of predicted landmark locations were calculated, one for a minimum size value, and one for a maximum one. The actual magnification is indicated in the figure legends. Thin plate-splines grids display the allometric patterns for large wings only.

Analyses were done for the whole wing and for the four main developmental compartments separately. Compartments limits were those defined by GARCIA-BELLIDO *et al.* 1973: proximal compartment (landmarks 1 to 3 and 12 to 14) and distal one (landmarks 4 to 11), anterior compartment (landmarks 1 to 5, 11, 12 and 14) and posterior (landmarks 6 to 10 and 13). The boundary between proximal and distal compartments, which could correspond to the basal separation of wing from notum and pleural regions (GARCIA-BELLIDO & DE CELIS 1992), is not apparently as well defined as it is for the halteres (GARCIA-BELLIDO 1975). We followed WEBER (1992) and considered the basal landmarks 1 to 3 + 12 to belong to the wing. The dorso-ventral compartments were not analysed. They are almost impossible to trace. Their limit cannot be localised, either on the wing membrane or on the veins which are of mixed origin, either dorsal or ventral (GARCIA-BELLIDO 1975).

The importance of uniform transformations in allometry was assessed by regressing the linear uniform parameters (BOOKSTEIN 1996*b*) on size. Uniform parameters, U1 and U2, were calculated using the linearized Procrustes formula (BOOKSTEIN 1996*b*). Patterns of uniform relationships between adjacent compartments were analysed by partial-least-square analyses: a singular value decomposition of the cross-covariance matrix (BOOKSTEIN 1991, latent variables, pp. 39 and following) of uniform parameters, provides a pair of linear combinations of the compartments, which have the greatest covariance. Both sets of coefficients are constrained to a sum to square equal to 1, which means unit Procrustes length for these vectors. They have the advantage, over canonical correlation coefficients, to be interpretable as proportional to covariances with the latent variables of the other block (BOOKSTEIN *ibid.*).

Within compartment allometric tests were done using uniform parameters and centroid size, estimated on the landmarks belonging to each compartment. The principal axes of the within-compartment uniform allometric component were calculated following the geometrical construction (BOOKSTEIN 1991, chapter 6; see also enclosed Fig. 4c and 5c), and using the univariate regression slopes of U1 and U2 as directional shape changes. References for directional changes in the wing were chosen as the directions of longitudinal veins and the proximo-distal axis (see introduction). The latter aligns satisfactorily with the horizontal axis of the mean procrustes configuration after rotation on its main axes. Angles between these references directions and principal axes were calculated. However, no statistical testing of angles was undertaken since the reference directions are not defined with precision: within a compartment longitudinal veins are not running parallel, and the directional component of polyclones has not yet been analysed in details. Most calculations were done using MATLAB for Windows v. 4.2. The TPSRegr program (version 1.10, ROHLF 1997) was used in order to visualise the deformations as grids. Statistical analyses were done using MATLAB and SAS for Windows (v. 6.10).

RESULTS

Multivariate allometry

The percentage of variance explained by the first PCA axis of the covariance matrix of distances reached 67.5%. This axis was the only one correlated with the Log of centroid size ($r = 0.498$, $p = 0.001$, df = 74, $R^2 = 0.248$). Despite this relatively low percentage of explained variance, the first PCA axis carried all of the size and allometric patterns, a result which is frequently – although not automatically – encountered (see SPRENT 1972).

Distances undergoing negative allometry, positive allometry or isometry were plotted separately on the mean wing configuration (Figs 2a to 2c). The allometric changes may be described as a longitudinal relative shortening of the wing. This may be seen in the overall reduction of all the subparallel distances between left and right extreme landmarks (5 and 6, and landmarks located to the left of the 8 and 9 ones). Allometry implied also an overall contraction of the distal wing extremity (negative allometry of all distances between landmarks 4 to 7, see Table 1). Most of the changes were longitudinal, with only three transversal ones: a distal compression of the 4–7 distance and an increase of the 8–9 and 2–13 distances. Changes involving the landmark 12, as well as most changes in the basal part (landmarks 1 to 3 and 12 to 14) appeared not significantly different from isometry (Table 1).

Geometric allometry

Whole wing. The multiple correlation of size on GLS residuals was highly significant (Table 2, first line). The percentage of Procrustes variance explained by size equalled 5.7%. Tests for allometry (Table 2) showed isometry to be restricted to the six basal landmarks 1 to 3, and 12 to 14. Nevertheless, the combinations of the landmarks 1, 2 and 14 with either the landmark 3 or 13 were statistically significant, while the combination of the landmarks 1 to 3 + 13 and 14 was isometric (Table 2). These results suggest that the growth of the base of the wing is probably not fully isometric. But, the allometric patterns are of limited amplitude and given the size of the sample, the statistical power of the tests are not great enough. In the basal part region allometry could correspond to both an anterior elongation and to an enlargement of the antero-posterior width. Such a conclusion did not hold with the multivariate study (Fig. 2 and Table 1), a difference which highlights the greater power of geometric morphometrics (see BOOKSTEIN 1991).

Allometric changes are depicted on Fig. 3 (*a* and *b*). If on the whole, they appear congruent with those deduced from multivariate results, small scale patterns are better delineated. The relative enlargement of the basal width, as well as the transversal and longitudinal compression of the distal part of the wing (land-

Fig. 2. Multivariate allometry of inter-landmark distances. Negative allometric (A), isometric (B), and positive allometric inter-landmark distances (C) are plotted in bold onto the inter-landmark mesh (dotted lines)

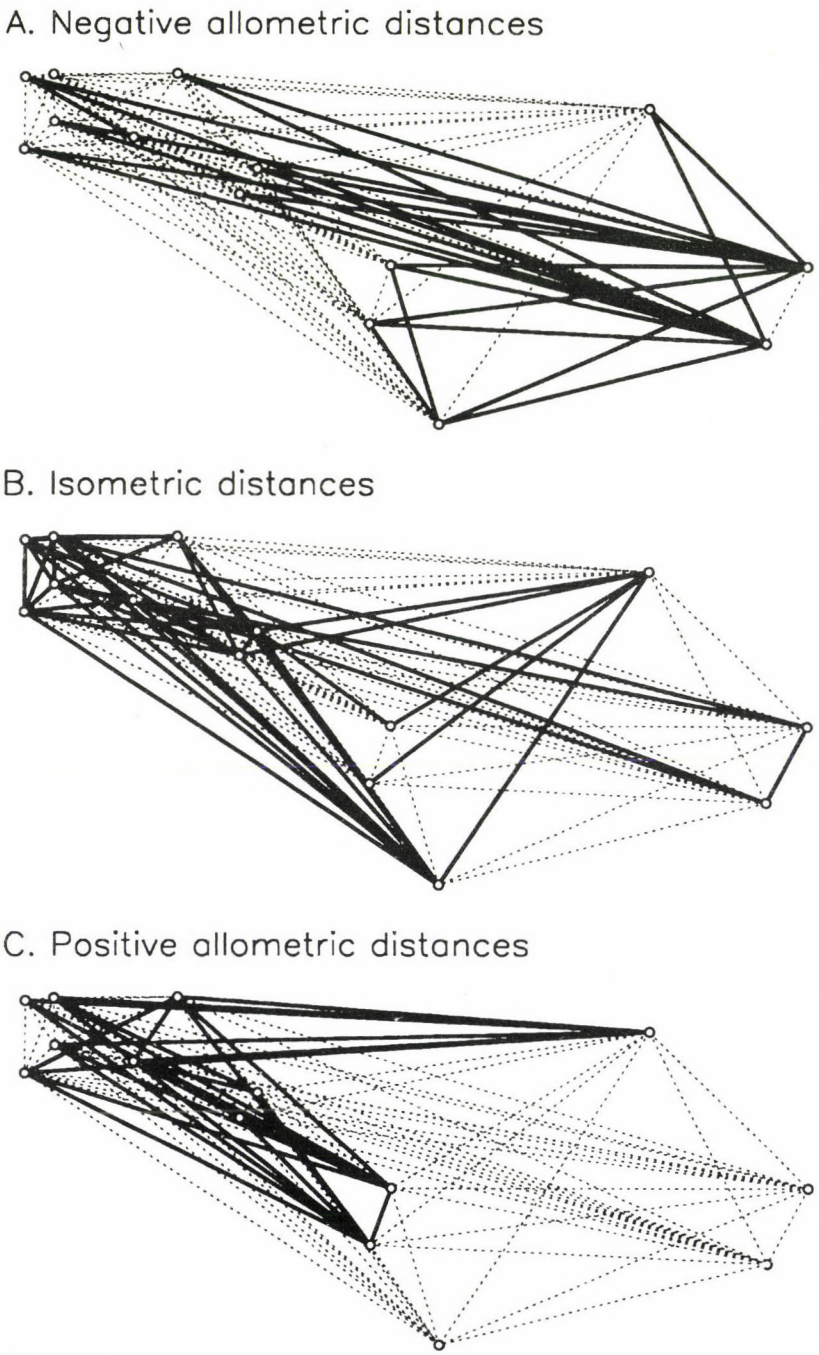

maks 4 to 7) are clearly retrieved, and illustrated by these pictures. The spline (Fig. 3*b*) suggest a regular bending of the distal part which was impossible to observe, either with the multivariate approach or with the Procrustes one. The orientation of the posterior cross-vein (landmarks 8 and 9) remain quite constant. The two landmarks which define this vein seem to be equally implied in the allometric patterns. A similar conclusion holds for the anterior cross-vein.

The multiple regression of the uniform parameters on size was not significant, with $R^2 = 0.0604$, $F(2/73) = 2.347$, $p = 0.103$. The direction defined by the

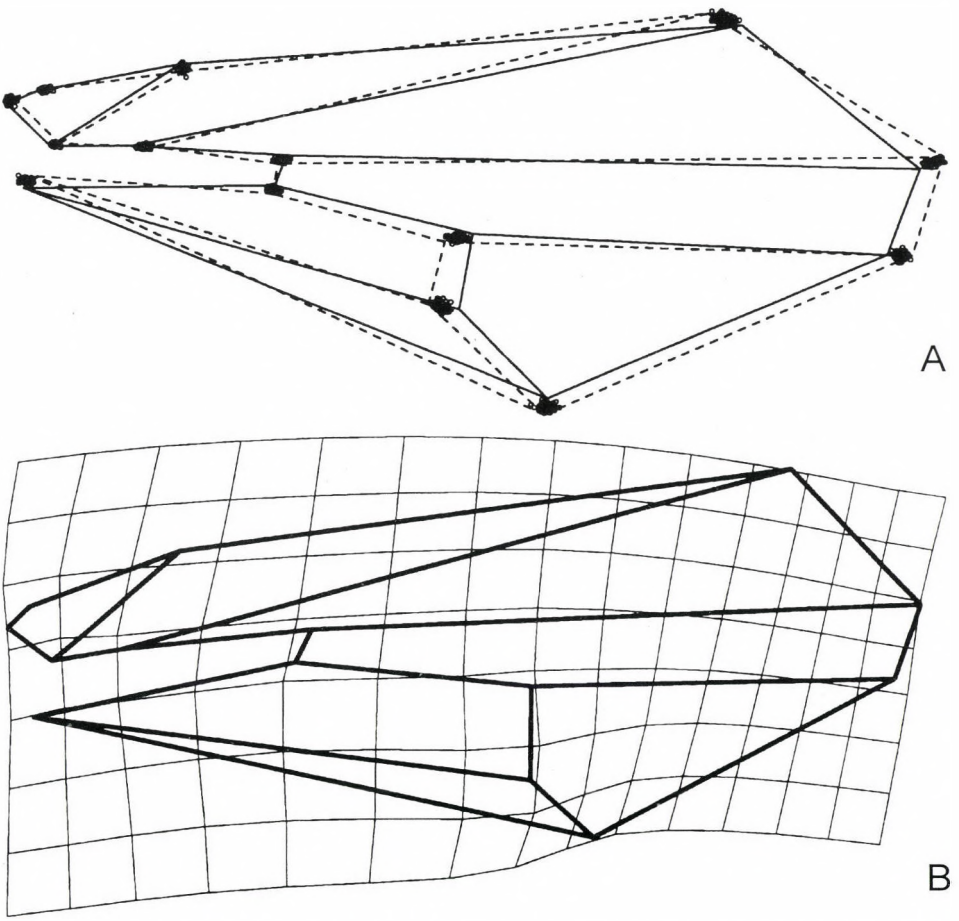

Fig. 3. Geometric allometry. A = Predicted allometric shifts, calculated using Procrustes residuals. Doted lines correspond to small wings, solid line to large ones (actual range ×3). Dots correspond to individual locations after a generalized least-squares superimposition. B = Thin-plate spline visualisation of allometric shape changes for large wings (uniform + non-uniform transformations, ×8.5)

Table 1. Multivariate allometry (PCA of the covariance matrix of the 91 inter-landmark distances): sorted bootstrapped weights, standard errors (s), 0.025 and 0.975 percentiles. Weights (and associated parameters) which are significantly different from isometry are in bold. Isometry = 0.1048. Bootstraps used 1000 replications

dist	weights	s	0.025	0.975	dist	weights	s	0.025	0.975
7–8	**0.0478**	**0.0004867**	**0.0197**	**0.0803**	4–11	0.1051	0.0001605	0.0944	0.1147
4–5	**0.0603**	**0.0003936**	**0.0371**	**0.0862**	10–13	0.1070	0.0003544	0.0842	0.1292
4–6	**0.0691**	**0.0003172**	**0.0511**	**0.0895**	2–14	0.1072	0.0003404	0.0870	0.1292
6–9	**0.0726**	**0.0002286**	**0.0566**	**0.0859**	4–10	0.1074	0.0001641	0.0968	0.1172
5–9	**0.0738**	**0.0002244**	**0.0587**	**0.0868**	3–10	0.1078	0.0003115	0.0902	0.1273
6–8	**0.0744**	**0.0001968**	**0.0613**	**0.0860**	2–10	0.1087	0.0002088	0.0955	0.1216
5–8	**0.0772**	**0.0001888**	**0.0642**	**0.0885**	1–4	0.1098	0.0001138	0.1024	0.1163
12–14	0.0773	0.0004521	0.0483	0.1051	10–14	0.1098	0.0002733	0.0933	0.1262
7–9	**0.0781**	**0.0003181**	**0.0608**	**0.0999**	4–13	0.1099	0.0001478	0.1005	0.1182
1–12	**0.0787**	**0.0003364**	**0.0566**	**0.0993**	1–11	0.1100	0.0002130	0.0964	0.1230
5–6	0.0787	0.0005268	0.0484	0.1138	4–14	0.1110	0.0001093	0.1033	0.1172
1–2	0.0788	0.0008564	0.0176	0.1264	2–4	0.1119	0.0001257	0.1038	0.1189
6–7	**0.0824**	**0.0002061**	**0.0681**	**0.0935**	3–4	0.1119	0.0001425	0.1031	0.1208
5–7	**0.0828**	**0.0001828**	**0.0701**	**0.0930**	2–3	0.1129	0.0002900	0.0953	0.1321
1–14	0.0848	0.0003584	0.0610	0.1063	**1–9**	**0.1131**	**0.0001165**	**0.1057**	**0.1207**
12–13	0.0854	0.0005836	0.0490	0.1204	3–14	0.1136	0.0002405	0.0986	0.1289
6–11	**0.0869**	**0.0001188**	**0.0792**	**0.0943**	**1–8**	**0.1139**	**0.0001151**	**0.1068**	**0.1206**
2–12	0.0870	0.0003635	0.0644	0.1104	3–13	0.1145	0.0002009	0.1010	0.1270
5–11	**0.0870**	**0.0001248**	**0.0794**	**0.0948**	11–13	0.1147	0.0003170	0.0947	0.1345
6–10	**0.0891**	**0.0001299**	**0.0806**	**0.0965**	8–13	0.1149	0.0001529	0.1045	0.1240
5–10	**0.0892**	**0.0001309**	**0.0807**	**0.0974**	9–13	0.1152	0.0001562	0.1047	0.1242
7–11	0.0924	0.0002118	0.0800	0.1067	**4–12**	**0.1155**	**0.0001259**	**0.1069**	**0.1224**
4–9	0.0930	0.0001923	0.0806	0.1050	2–11	0.1159	0.0002038	0.1027	0.1284
3–6	**0.0936**	**0.0000929**	**0.0872**	**0.0989**	**2–9**	**0.1168**	**0.0001187**	**0.1093**	**0.1246**
3–5	**0.0937**	**0.0001016**	**0.0867**	**0.0995**	3–11	0.1174	0.0003179	0.0980	0.1372
6–13	**0.0939**	**0.0001169**	**0.0859**	**0.1005**	**2–8**	**0.1177**	**0.0001167**	**0.1106**	**0.1254**
1–6	**0.0943**	**0.0000740**	**0.0893**	**0.0983**	**9–14**	**0.1177**	**0.0001341**	**0.1093**	**0.1261**
5–13	**0.0944**	**0.0001108**	**0.0869**	**0.1004**	11–14	0.1177	0.0002369	0.1018	0.1320
1–5	**0.0947**	**0.0000772**	**0.0893**	**0.0992**	9–11	0.1182	0.0003719	0.0952	0.1410
4–7	**0.0947**	**0.0001444**	**0.0862**	**0.1040**	10–11	0.1182	0.0005695	0.0821	0.1535
6–14	**0.0948**	**0.0000802**	**0.0890**	**0.0991**	**8–14**	**0.1183**	**0.0001304**	**0.1102**	**0.1263**
7–10	0.0949	0.0002420	0.0810	0.1112	**3–9**	**0.1185**	**0.0001962**	**0.1070**	**0.1303**
5–14	**0.0951**	**0.0000805**	**0.0892**	**0.0995**	1–13	0.1191	0.0005240	0.0892	0.1535

Table 1 (continued)

dist	weights	s	0.025	0.975	dist	weights	s	0.025	0.975
2–6	**0.0956**	**0.0000791**	**0.0901**	**0.0999**	**3–8**	**0.1208**	**0.0002020**	**0.1090**	**0.1336**
2–5	**0.0959**	**0.0000835**	**0.0903**	**0.1007**	8–11	0.1230	0.0003236	0.1037	0.1433
6–12	**0.0970**	**0.0001020**	**0.0902**	**0.1026**	**2–13**	**0.1246**	**0.0003027**	**0.1062**	**0.1433**
5–12	**0.0972**	**0.0001039**	**0.0901**	**0.1034**	13–14	0.1260	0.0006237	0.0848	0.1629
7–13	0.0974	0.0001568	0.0867	0.1062	9–10	0.1270	0.0003927	0.1038	0.1533
1–7	**0.0979**	**0.0000790**	**0.0929**	**0.1030**	**8–12**	**0.1283**	**0.0002026**	**0.1152**	**0.1403**
3–7	0.0990	0.0001265	0.0909	0.1067	**9–12**	**0.1283**	**0.0002129**	**0.1138**	**0.1414**
4–8	0.0993	0.0001349	0.0913	0.1079	10–12	0.1291	0.0003807	0.1048	0.1517
7–14	0.0996	0.0000919	0.0943	0.1057	**8–10**	**0.1298**	**0.0003604**	**0.1088**	**0.1525**
2–7	0.1002	0.0001054	0.0943	0.1074	3–12	0.1319	0.0005679	0.0949	0.1670
7–12	0.1031	0.0001200	0.0964	0.1109	**11–12**	**0.1435**	**0.0003308**	**0.1193**	**0.1634**
1–10	0.1035	0.0002363	0.0884	0.1175	**8–9**	**0.1470**	**0.0004979**	**0.1177**	**0.1776**
1–3	0.1051	0.0002263	0.0894	0.1185	–	–	–	–	–

regression coefficients (-0.005 -0.0305) was almost parallel to the antero-posterior axis, a direction which does not clearly align with known directional components of allometry or variability of the wing.

Developmental compartments and allometry

All compartments but the proximal one (but see the observations in the preceding paragraph) were implied in the allometric patterns, since multiple regression tests of the corresponding Procrustes residuals on size were significant at the 0.05 level (Table 2, four last lines).

Table 2. Multiple correlation tests for isometry of Procrustes residuals on the natural logarithm of centroid size. Global test (first line), tests for the basal wing region, and tests for the four main developmental compartments. * $p < 0.05$; ** $p < 0.01$; *** $p < 0.001$

Landmarks	R^2	df1/df2	F	Wing regions or compartments
1 to 14	0.5708	24 / 51	2.826***	whole wing
1 + 2 + 14	0.0208	2 / 73	0.779	basal region
1 + 2 + 14+ 3	0.1279	4 / 71	2.633*	basal region
1 + 2 + 14 + 12	0.0680	4 / 71	1.294	basal region
1 + 2 + 14+ 13	0.1305	4 / 71	2.793*	basal region
1 to 3 + 12 to 14	0.1336	8 / 67	1.308	proximal compartment
4 to 11	0.2885	12 / 63	2.125*	distal compartment
1 to 5 + 11 + 12 + 14	0.3992	12 / 63	3.488***	anterior compartment
6 to 10 + 13	0.2850	8 / 67	3.339**	posterior compartment

The percentage of Procrustes variance explained by size per landmark amounted respectively to 8.7% for the anterior, and 7% for the posterior compartment. The allometric patterns for the posterior compartment (Fig. 5*A*) were on the whole strongly similar to those deduced from the whole wing grid (Fig. 3*b*). The differences were more pronounced in the case of the anterior compartment with a higher uniform shear (Fig. 4*a*). These observations justified a deeper analysis of the uniform part for these two compartments.

Within-compartment allometry and uniform shape changes

Within compartment, multiple correlation tests of the uniform parameters on size were significant for the anterior one only ($R^2 = 0.1037$, $F(1/74) = 4.2232$,

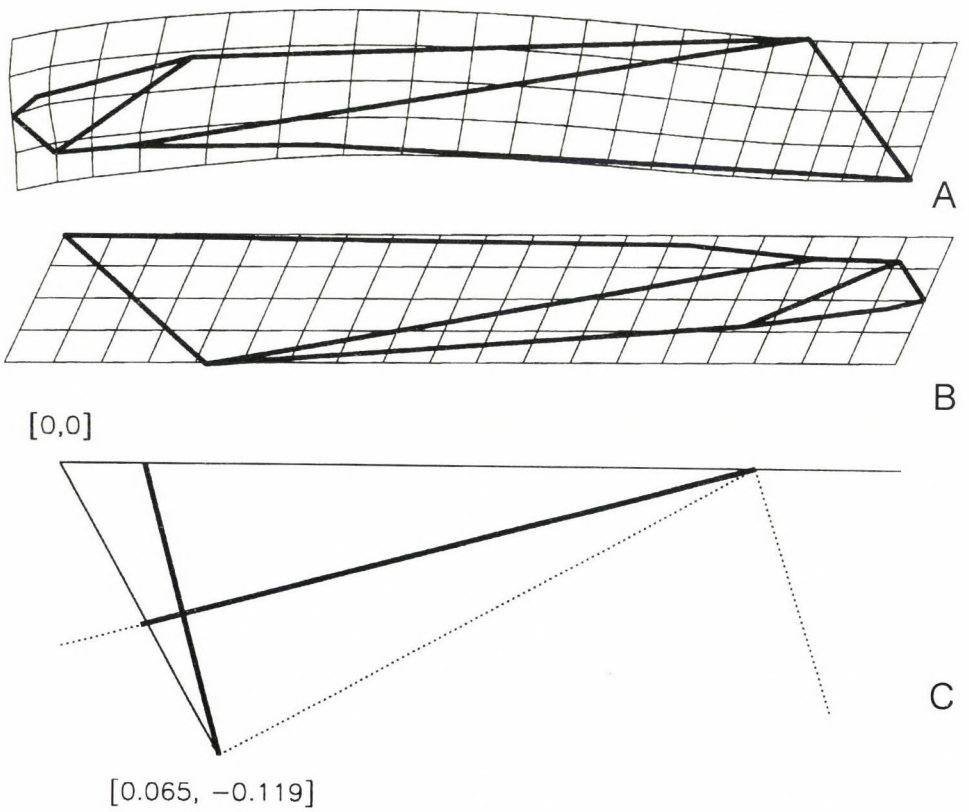

Fig. 4. Anterior compartment and allometry. A = Allometric shifts for large wings, displayed as a thin plate spline grid, ×8. B = Ditto, uniform component alone, ×8. C = Geometric construction of the principal axes (tensors). Fine solid lines correspond to the horizontal reference (base) and to the shift vector (lower). Constructed lines(dotted) correspond to the projection of the shift vector onto the base and to the two bisectors of the angles between the projection and the base. The principal axes (solid bold lines), inscribed into the triangle, are parallel to these bisectors

p = 0.0184). For the proximal and the distal compartments the shift vectors defined by the regressions were almost collinear, making an angle of only 5°. Their respective components [0.36, -0.24] and [0.21; -0.17] pointed towards the apex and the posterior part of the wing. This direction corresponds to a basal extension of the wing. it appears dominated, for the distal compartment, by the directional trends of the posterior one (see next paragraphs).

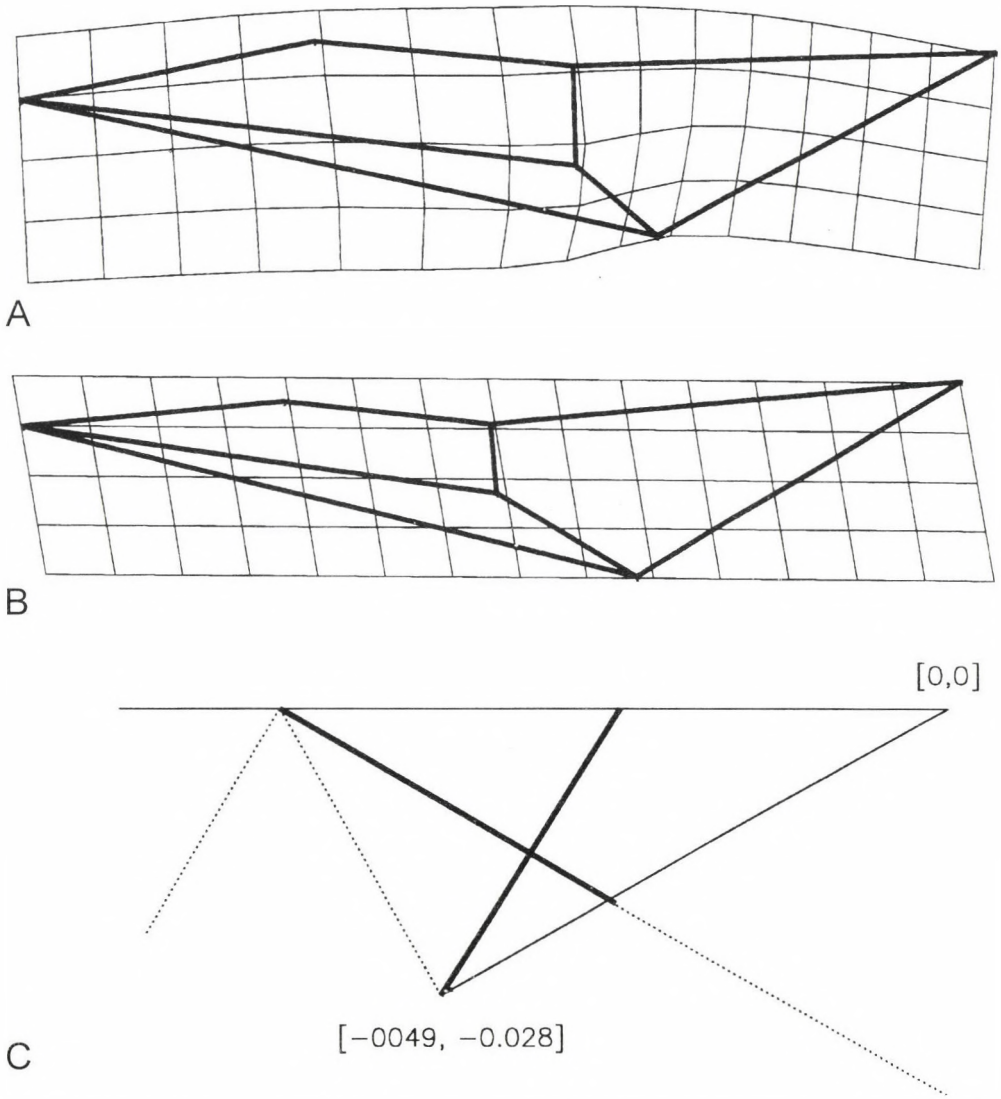

Fig. 5. Posterior compartment and allometry. A = Allometric shifts for large wings, displayed as a thin plate spline grid, ×7. B = Ditto, uniform component alone, ×7. C = Geometric construction of the principal axes (tensors). See legend Fig. 4 for the construction

For the anterior compartment, the direction of the uniform shape change was proportional to [0.065, -0.120]. Geometrically (Fig. 4*b*), the uniform transformation corresponded to a transversal compression and a shear, which may be described as a distal shift of the anterior landmarks (1 to 4), and a basal shift of the most posterior ones (5, 11, 12, 14). The principal axis pointed upwards and distally (Fig. 4*c*). Its angle with the reference axis was 14°, and appeared therefore reasonably well aligned with the directions of the anterior longitudinal veins. The anisotropy, calculated as the square of the length of the uniform vector, equalled 1.36.

For the posterior compartment, the direction of shift was proportional to [-0.049, -0.028], and corresponded to a basal and posterior shift. Geometrically (Fig. 5*b*), this transformation may be described as a shear, which is the reverse of the anterior compartment shear. The principal axis pointed downward and distally (Fig. 5*c*), with a lower anisotropy equal to 0.56. With an estimated angle of 30° with the horizontal reference, the principal direction was also satisfactorily aligned with the longitudinal veins of that compartment.

Relationships between anterior and posterior compartments

The partial-least-squares analysis of uniform parameters for the anterior and posterior compartments provided two axes whose covariances were 0.000149 and 0.00000295. The amount of explained cross-covariance by the first set of vectors reached 96.2%. The corresponding vectors were respectively [0.996, 0.092] for the anterior and [0.965, -0.261] for the posterior compartment. Their directions were roughly aligned with the respective horizontal reference axes (the angles equalled 5° for the anterior and 15° for the posterior compartment). Although congruent with those of the principal axes, these angles are smaller. The non-allometric variability appears therefore more canalised along the proximo-distal axis than the allometric one.

DISCUSSION

Allometric patterns are highly congruent whatever the approaches used here. As one might expect, those deduced from geometric morphometrics are more easily understandood and interpretable. The amount of allometry is particularly low. This result could be related in part to the stability of the rearing conditions in both temperature and food availability. On the whole, allometric shape changes in the male wing of *D. simulans* appear concentrated in the distal part. They deal mainly with landmarks 4 to 9, and can be described as a relative contraction of the region delimited by these 6 landmarks, together with a posterior

bending. By contrast most changes in the basal region (landmarks 1 to 3, 13 and 14) appear isometric or with small scale allometric patterns.

Developmental compartments, appear unequally related to allometric changes. Landmarks belonging to the proximal compartment undergo the smallest allometric displacements. WEBER (1992) demonstrated that this region is fully active and responds to directional selection. His experiments, which used regions less than 100 cells across, included the proximal part with landmarks 1, 2, 3, 12 and 14. It is already known for a long time, that cells in this region are more densely packed (WADDINGTON 1940, GARCIA-BELLIDO 1975). This could be one of the explanations to the limited allometric changes into this wing region. It is interesting to notice that in our results the uniform allometric directions are equivalent in the basal and in the distal part of the anterior compartment. This could be an indication that, at least for allometry, the proximo-distal subdivision into compartments is less relevant than the antero-posterior one. The existence of proximal and distal compartments was apparently only postulated in the wing, whereas it was demonstrated in the halteres (GARCIA-BELLIDO 1975). No major wing mutations affecting the proximal compartment have been reported (WADDINGTON 1940, DIAZ-BENJUMEA & GARCIA-BELLIDO 1990.

For the anterior and posterior compartments, the uniform transformations correspond to two reversed shears, a result which could be interpreted as an overgrowth of the central part of the wing. Both principal directions are congruent with directional references, cellular clones orientation and major longitudinal veins, with an upward shift in the anterior and a downward shift in the posterior compartment. Nevertheless the anterior compartment appears more sensitive to allometric uniform transformations, although the fraction of the allometric changes they explain is very small. The general conclusion is that the anterior compartment appears at the same time, less variable, and more allometrically structured, both in terms of uniform and non-uniform shape changes.

The allometric shape changes of the anterior cross-vein, which is of mixed origin, are interesting to trace. This vein is rooted into the anterior compartment by the landmark 11 and by the landmark 10 into the posterior one, with a dorsal anterior part, and a ventral posterior one (GARCIA-BELLIDO 1977). Allometrically this vein behave apparently as a single unit, both landmarks being subjected to roughly identical allometric changes. Possible explanations are that cross-veins are formed after the longitudinal veins (WADDINGTON 1940, GARCIA-BELLIDO & DE CELIS 1992), and that part of the genes which are involved in their morphogenesis are different. It is now well established that known cross-vein mutations do not affect longitudinal veins (DIAZ-BENJUMEA & GARCIA-BELLIDO 1990).

Interestingly, the patterns of variability and allometry we describe, appear very similar to those involved in the temperature selection experiments of

CAVIC- CHI *et al.* (1985), and in the geographic variability (IMASHEVA *et al.* 1995). In all cases, the shape changes may be described as a relative contraction of the distal part and a widening of the posterior region of the wing. In both cases too, the posterior compartment appears more variable and less canalised than the anterior one. This points out that a large part of the shape transformations induced by temperature selection, or geographic divergence, could be related to allometry, although these hypotheses remain to be tested.

Our results suggest that allometric shape changes have probably complex determinisms. Only a fraction of it appear related to overall directional processes, either preferential orientations of cellular clones, and/or veins interactions. The allometric transformations appear compartment-dependent, both for their directions and modules. Nevertheless, most of the allometric transformations appear non-uniform, and the cellular mechanisms by which they are driven still have to be investigated.

While many aspects of the present analyses and interpretations are preliminary and tentative, they point out the relevance of developmental pathways in morphological analyses and comparisons, even at such a fine scale. This is clearly demonstrated by the geometric congruence between calculated and biological directions, which are higher at the compartment level, than at the wing level, and for the total deformations or for the simple uniform shape changes. These results demonstrate the importance of the geometric morphometric tools in their investigation, which provide at the same time, a deeper insight into the geometry of the underlying biological processes, and more statistical power.

* * *

Acknowledgements – Thanks to the editors for constructive comments, and to L. MARCUS and J. ROHLF for helpful discussions. F. L. BOOKSTEIN provided very useful suggestions and help regarding principal axes and PLS. Thanks to D. VAUTRIN and S. MAZEAU (CNRS PGE, Gif/Yvette) who reared the flies and to Sylvain Charlat who carefully digitised the landmarks. This paper is a contribution from the «Groupe de travail Morphométrie et Analyse de formes» of the Paris Muséum which is granted by a «Contrat Pluriformations» of the «Ministre de l'enseignement supérieur et de la Recherche» (1992–1996 and 1996–1998).

REFERENCES

BABA-ASSA, F., SOLIGNAC, M., DENNEBOUY, N. & DAVID, J. R. (1988) Mitochondrial variability in Drosophila simulans: quasi absence of polymorphism within each of the three cytoplasmic races. *Heredity* **61**: 419–426.

BACON, A. M. & BAYLAC, M. (1995) Landmark analysis of distal femoral epiphysis of modern and fossil Primates with particular emphasis on Australopithecus afarensis (AL 129–1 and AL 333–4). *C. R. Acad. Sci., Paris* **321**: 553–560.

BAYLAC, M. & DAUFRESNE, T. (1996) Wing venation variability in Monarthropalpus buxi (Diptera, Cecidomyiidae) and the quaternary coevolution of Box (Buxus sempervirens L.) and its midge: a geometrical morphometric analysis. Pp. 285–302. *In* MARCUS, L. F., CORTI, M., LOY, A., NAYLOR, G. & SLICE, D. E. (eds): *Advances in Morphometrics* NATO-ASI No. 284, Plenum Press.

BOOKSTEIN, F. L. (1978) The Measurement of Biological Shape and Shape Change. *Lectures Notes in Biomathematics 24*. Springer-Verlag, Berlin, 191 pp.

BOOKSTEIN, F. L. (1991) *Morphometric tools for landmark data: Geometry and Biology*. Cambridge Univ. Press, New York, 435 pp.

BOOKSTEIN, F. L. (1996*a*) Combining the Tools of Geometric Morphometrics. Pp. 131–152. *In* MARCUS, L. F., CORTI, M., LOY, A., NAYLOR, G. & SLICE, D. E. (eds): *Advances in Morphometrics* NATO-ASI No. 284, Plenum Press.

BOOKSTEIN, F. L. (1996*b*) A standard formula for the uniform shape component in landmark data. Pp. 153–168. *In* MARCUS, L. F., CORTI, M., LOY, A., NAYLOR, G. & SLICE, D.E. (eds): *Advances in Morphometrics*. NATO-ASI No. 284, Plenum Press.

CAVICCHI, S., GUERRA, D., GIORGI, G. & PEZZOLI, C. (1985) Temperature-related divergence in experimental populations of Drosophila melanogaster. I. Genetic and developmental basis of wing size and shape variation. *Genetics* **109**: 665–689.

COWLEY, D. E., ATCHLEY, W. R. & RUTLEDGE, J. J. (1986) Quantitative genetics of Drosophila melanogaster. I. Sexual dimorphism in genetic parameters for wing traits. *Genetics* **114**: 549–566.

DIAZ-BENJUMEA, F. J. & GARCIA-BELLIDO, A. (1990) Genetic analysis of the wing pattern of Drosophila. *Roux's Arch. Dev. Biol.* **198**: 336–354.

GARCIA-BELLIDO, A. (1977) Inductive mechanisms in the process of wing vein formation in Drosophila. *Wilhelm Roux's Archives* **182**: 93–103.

GARCIA-BELLIDO, A. & DE CELIS, J. F. (1992) Developmental genetics of the venation pattern of Drosophila. *Ann. Rev. Genet.* **26**: 277–304.

GARCIA-BELLIDO, A., RIPOLL, P. & MORATA, G. (1973) Developmental compartimentalization of the wing disk of Drosophila. *Nature* **245**: 251–253.

GARCIA-BELLIDO, A., CORTES, F. & MILAN, M. (1994) Cell interactions in the control of size in Drosophila wings. *Proc. Natl. Acad. Sci. USA* **91**: 10222–10226.

GOODALL, C. R. (1991) Procrustes methods in the statistical analysis of shape (with discussion and rejoinder). *J. R. Stat. Soc.* **53**: 285–339.

GOODALL, C. R. (1995) Procrustes methods in the statistical analysis of shape revisited. Pp. 18–33. *In* MARDIA, K. V. & C. A. GILL (eds): *Proceedings in current issues in statistical analysis of shape*. Leeds Univ. Press.

IMASHEVA, A. G., BULBLI, O. A., LAZEBNY, O. E. & ZHIVOTOVSKY, L. A. (1995) Geographic differentiation in wing shape in Drosophila melanogaster. *Genetica* **96**: 303–306.

JOLICOEUR, P. (1963) The multivariate generalization of the allometry equation. *Biometrics* **19**: 497–499.

KLINGENBERG, C. P. (1996) Multivariate allometry. Pp. 23–49. *In* MARCUS, L. F., CORTI, M., LOY, A., NAYLOR, G. & SLICE, D. E. (eds): *Advances in Morphometrics* NATO-ASI No. 284, PlenumPress.

LAWRENCE, P. E. (1992) *The making of a fly. The genetics of animal design*. Blackwell Sci. Press.

LOY, A., CATAUDELLA, S. & CORTI, M. (1996) Shape changes during the growth of the Sea Bass, Dicentrarchus labrax (Teleostea: Perciformes), in relation to different rearing conditions: an application of Thin-Plate Spline Regression Analysis. Pp. 399–406. *In* MARCUS, L. F., CORTI, M., LOY, A., NAYLOR, G. & SLICE, D. E. (eds): *Advances in Morphometrics* NATO-ASI No. 284, Plenum Press.

MARCUS, L. F. (1990) Traditional Morphometrics. *In* ROHLF, F. J & BOOKSTEIN, F. L. (eds): *Proceedings of the Michigan Morphometrics Workshop.* Univ. Michigan Museum of Zoology Spec. Publ. **2:** 77–122.

MARDIA, K. V., KENT, J. T. & BIBBY, J. M. (1979) *Multivariate Analysis.* Academic Press, London, 518 pp.

MOSIMANN, J. E. & JAMES, F. C. (1979) New statistical methods for allometry with application to Florida Red-winged Blackbirds. *Evolution* **33**: 444–459.

PENIN, X. & BAYLAC, M. (1995) Analysis of the skull shape changes in Apes, using 3D procrustes superimposition. Pp. 208–210. *In* MARDIA, K. V. & GILL, C. A. (eds): *Proc. Current Issues in Statistical Analysis of Shape*, Leeds Univ. Press.

REILLY, S. M. (1990) Comparative ontogeny of cranial shape in Salamenders using resistant fit theta rho analysis. *In* ROHLF, F. J. & BOOKSTEIN, F. L. (eds): *Proc. Michigan Morphometrics Workshop.* Univ. Michigan Museum of Zoology Special Publ. **2:** 311–321.

ROHLF, F. J. (1996) Morphometric spaces, shape components and the effects of linear transformations. Pp. 117–130. *In* MARCUS, L. F., CORTI, M., LOY, A., NAYLOR, G. & SLICE, D. E. (eds): *Advances in Morphometrics.* NATO-ASI No. 284, Plenum Press.

ROHLF, F. J. (1997) TPSREGR for Windows version 1.10. Department of Ecology and Evolution, State University of New York, Stony Brook, NY 11794–5245. (Available by ftp from life.Bio.SUNYSB.edu/MORPHMET).

ROHLF, F. J. & SLICE, D. (1990) Extensions of the Procrustes methods for the optimal superimposition of landmarks. *Syst. Zool.* **39**: 40–59.

SPRENT, P. (1972) The mathematics of size and shape. *Biometrics* **28**: 23–38.

UPDEGRAFF, G. (1990) MeasurementTV, version 1.3. Data Crunch 304 avenida Adobe, Dan Clemente, CA 92672, USA.

WADDINGTON, C. H. (1940) The genetic control of wing development in Drosophila. *J. Genet.* **41**: 75–139.

WALKER, J. A. (1993) Allometry of threespine stickleback body form using landmark based morphometrics. *In* MARCUS, L. F., BELLO, E. & GARCIA-VALDECASAS, A. (eds): *Contributions to Morphometrics.* Monografias del Museo Nacional de Ciencias Naturales **8**: 192–214.

WEBER, K. E. (1990) Selection on wing allometry in Drosophila melanogaster. *Genetics* **126**: 975–989.

WEBER, K. E. (1992) How small are the smallest selectable domains of form? *Genetics* **130**: 345–353.

ZELDITCH, M. L., BOOKSTEIN, F. L. & LUNDRIGAN, B. L. (1992) Ontogeny of integrated skull growth in the cotton rat Sigmodon fulviventer. *Evolution* **46**: 1164–1180.

Acta Zoologica Academiae Scientiarum Hungaricae 44 (1–2), pp. 113–137, 1998

VARIATION IN SELECTED SKELETAL ELEMENTS OF THE FOSSIL REMAINS OF MYOTRAGUS BALEARICUS, A PLEISTOCENE BOVID FROM MALLORCA*

L. F. MARCUS

Department of Biology, Queens College of the City University of New York and Department of Invertebrates, American Museum of Natural History
E-mail: lamqc@cunyvm.cuny.edu

Three dimensional landmark morphometrics for skulls, mandibles, and metacarpals were used to examine variation in the island Pleistocene bovid *Myotragus balearicus* from three cave sites in Mallorca. Traditional caliper distances were studied for earlier data collected on metatarsals of the same species from only one cave. Missing data is a major problem for fossil skulls, and mandibles and a large number of specimens and landmarks were ignored to have a full data set for multivariate analysis of a restricted sample of specimens. More compact bones like metacarpals have fewer problems. The specimens are highly variable with most coefficients of variation larger than 7 even for samples presumably from one time level in one cave. This study corroborates HAMILTON's (1984) finding that the lower levels in the cave have larger individuals and documents a significant difference over a range of about 11000 years in size of metacarpals from Son Muleta cave. The animal became smaller in the early Holocene before becoming extinct. The other two caves, Cova del Moro and Son Maiol, have different mean sizes, the former similar to the upper level at Son Muleta, while the latter is similar to the lower level. Patterns of variation and the problem of recognizing sexes in these samples are discussed.

Key words: geometric morphometrics, Bovidae, multivariate analysis, three dimensional data, Pleistocene

INTRODUCTION

Shape and size of selected skeletal elements of *Myotragus balearicus* will be described and compared from three Upper Pleistocene samples and one early Holocene cave sample from Mallorca. One of the caves, Son Muleta was clearly stratified and some bones in the strata have been radiocarbon dated. Two Muleta samples of metacarpals differing in age by about 11000 years are compared to each other, and to samples from two other caves, Cova del Moro and Son Maiol. However, at Son Muleta, the strata are sloping and the bones collected according to 50 centimeter intervals from a common 0 level (0 cm) in 1 meter square lettered sectors, so that precise association of dated strata to specific sectors and depths is problematic for some samples.

* Symposium presentation, 5th International Congress of Systematic and Evolutionary Biology, 1996, Budapest

Background

The Balearic Islands of the Western Mediterranean represent a rare opportunity for studying island evolution over the last several million years. Cave deposits preserve large samples of endemic mammalian and other vertebrate fossils from the Upper Pleistocene up into the Holocene. Lower Pleistocene, Pliocene and earlier epochs are represented by rarer deposits. Most collecting localities are not well dated, but a few are – and there is a great potential for additional large samples from both Mallorca and Menorca.

Mallorca (approx. 80 × 65 km) and Menorca (45 × 25 km) can be seen one from the other, and are separated by a shallow strait, less than 75 meters deep (Carta Batimètrica de les Balears. Edit Conselleria d'Agricultura i Conselleria d'Obres Públiques, Govern Balear: A. ALCOVER, pers. comm.). The islands are dominantly marine limestones. However, there is a terrestrial vertebrate fossil record from deposits representing various epochs from the Oligocene to the Pleistocene. The earlier fauna is distinct from the Neogene one – and the late Pleistocene deposits record the latest, now extinct, species of only three terrestrial mammalian lineages: a bizarre miniature extinct caprine – *Myotragus balearicus*; a dormouse *Hypnomys morpheus* larger than its mainland relatives; and a shrew *Nesiotites hidalgo*, also much larger than relatives on the mainland. This is a common pattern – small mammals were larger, and large ones smaller in island environments.

Mallorca has a mountainous karst topography, with sheer cliffs on the north coast, and lesser ranges on the south-east corner. The mountains contain a plethora of caves (TRIAS *et al.* 1989 and ENCINAS 1997). However, more than half of the island is relatively flat and devoted to agriculture.

Myotragus – a member of the family Bovidae, is currently placed *incertae sedis* in the subfamily Caprinae (MCKENNA & BELL 1997), which contains the domestic goats and sheep, mountain goats and sheep, goral, tahr, chamois, ibexes, and musk oxes. Its tribal affinities to genera within the subfamily are contentious (GENTRY 1992). *Myotragus* is the shortest (shoulder height) member of the Caprinae known, but its body weight has been estimated to be as much as 60 kg (KÖHLER 1993). There are a number of other fossil caprines from the Mediterranean basin, and one from Sardinia, *Nesogoral melonii* has been claimed to be the sister taxon of *Myotragus* (GLIOZZI & MALATESTA 1980). Six species of *Myotragus* have been named from the Balearics, and four are interpreted as representing stages in evolution of some of the derived features of the Pleistocene *Myotragus balearicus* (SONDAAR *et al.* 1995). The earliest may be a middle Pliocene extinct collateral, and one species appears to be endemic to Menorca during the lower Pleistocene (*op. cit.*).

Myotragus balearicus is bizarre. A unique character for the species is the presence of only one open rooted ever growing chisel-shaped rodent-like incisor

in each mandible, with the loss of lower canines and other incisors (Fig. 1) (ANDREWS 1915). The usual complement for the family is all three incisors and a canine present on each side. All Bovidae have only a horny pad covering the tip of the pre-maxillae, and lack upper incisors and canines. Other mammals with such ever-growing single lower incisors, a commonly evolved trait in many orders, have a matching pair of ever-growing incisors in the upper jaw (GREGORY 1951, MOELLER 1974).

Other special characters for the skull are forward looking orbits. *Myotragus balearicus* could not see far to the side-and rear when looking straight on (Figs 2*c* and 4*a*). *Myotragus balearicus* is convergent with Primates in this regard. Associated with the forward looking eyes, is a very large temporal fossa with an extensive area for origin of jaw muscles on the skull accompanied by a reduced premolar dentition (loss of P^2 and P_3, and reduced P^3–P^4) and enlarged M^3 and M_3 (MOYA-SOLA & PONS 1981).

In the post-cranial skeleton some of the most derived characters are found in the distal foot elements. The metapodials, and phalanges are extremely short – shorter absolutely and proportionally than for any other member of the family (Fig. 3 – the much larger *Budorcas* has similarly proportioned metacarpals, GUERIN 1965). In addition there is fusion of the distal tarsal elements – navicular, cuboid and cuneiforms – with already fused metatarsals, in a large proportion of individuals. The phalanges are also relatively broad and short (ANDREWS 1915, LEINDERS 1979, KÖHLER 1993).

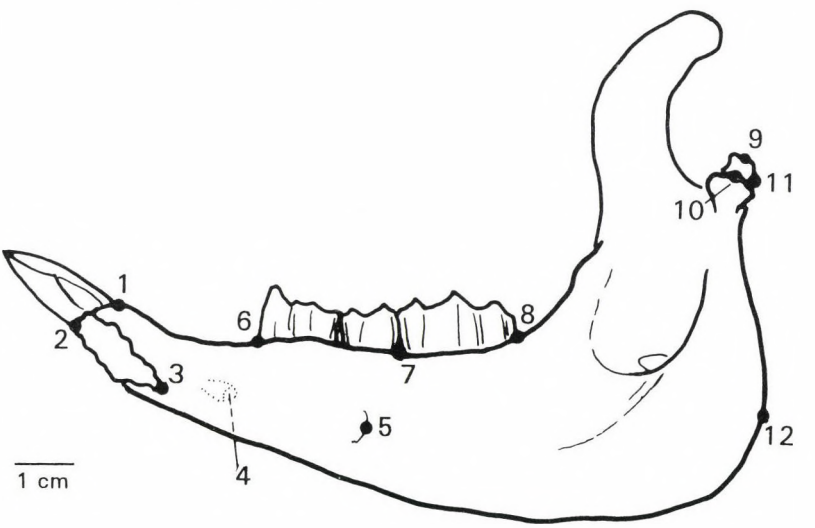

Fig. 1. Lingual view of right mandible of *Myotragus balearicus*, with 12 numbered landmarks indicated. Note that landmark 4 (indicated by a dashed line) is on the labial side of the jaw. Figure simplified from ANDREWS (1915, Plate 19)

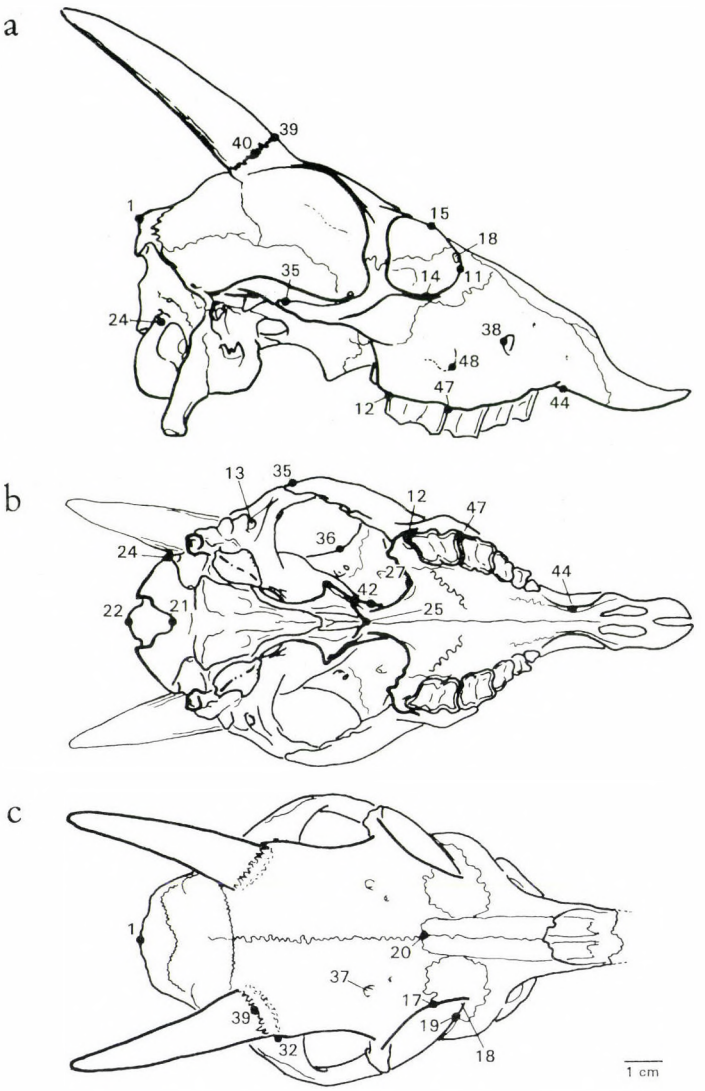

Fig. 2. Landmarks on the skull. Composite figures, largely modified from those of ANDREWS (1915, plates 19 and 20). Specimens from Son Muleta and Cova del Moro were used as well to reconstruct some parts. The 48 landmarks are indicated by a • on the skull. Only the landmarks on the mid-saggital plane and right side are shown. Missing numbers less than 48 are for left side landmarks (see Fig. 5). (**a**) Right side of skull. (**b**) Ventral view of skull. (**c**) Dorsal view of partial skull. 1 – Opisthocranion; 11 – anterior orbit; 12 – rear of M^3; 13 – post-glenoid foramen; 14 – lower-orbit; 15 – superior orbit; 16 – anterior-superior orbit (not shown); 17 – superior lachrymal; 18 – lachrymal foramen; 19 – inferior lachrymal; 20 – nasion; 21 – anterior foramen magnum; 22 – posterior foramen magnum; 24 – right occipital condyle; 25 – posterior edge palate; 27 – palatal inlet; 35 – maxillary zygoma; 36 – center superorbital ridge; 37 – supra-orbital foramen; 38 – rear infra-orbital foramen; 39 - anterior horn; 40 – lateral horn; 42 – palatal bridge; 44 – diastemal ridge; 47 – labial alveolar margin between M^{2-3}; 48 – facial tubercle

There are 83 localities for *Myotragus balearicus* shown in ALCOVER *et al.* (1981, Fig. 6.39) and their number continues to increase. A very new cave site includes coprolites and hair associated with abundant skeletal materials of *Myotragus balearicus* (ENCINAS & ALCOVER 1997). Most collections are from fissure fills, extant caves, or earlier eroded caves. There are some alluvial deposits with *Myotragus balearicus* as well. Caves are excellent accumulators – serving as

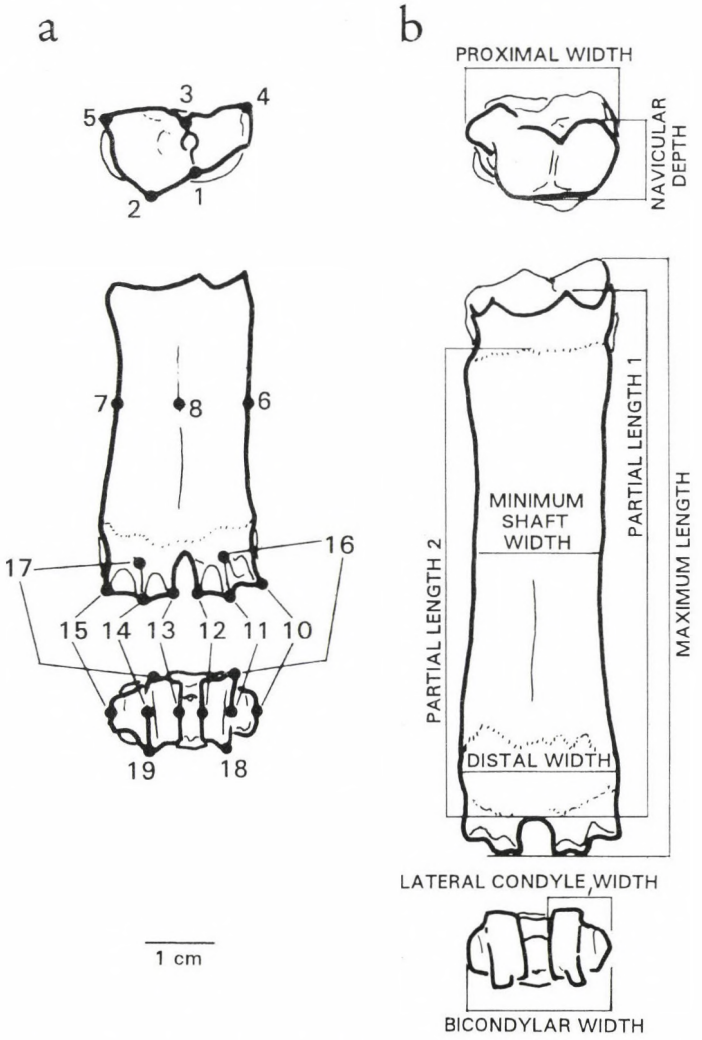

Fig. 3. Metacarpal and metatarsal of *Myotragus balearicus* modified and simplified from ANDREWS (1915, Plate 21). (**a**) Landmarks numbered on a right metacarpal. Landmark 9 is on the opposite side from 7. (**b**) Linear measurements are shown for a left metatarsal. Note proximal fusion of metatarsals with cuneiforms and navicular cuboid at dotted line. Key to abbreviations given in Table 2

natural traps when animals entered, and sometimes fell in shafts, where they died from injuries or starvation.

Caves are such a common source, that some authors have suggested that *Myotragus balearicus* was a troglobyte (ANGEL 1966 and KURTÉN 1968). Most elements of the skeletons are preserved, but only rarely are completely articulated skeletons found. Material may be so abundant that skeletons are completely intermixed in small volumes of a cave. For later caves – less than 40000 years old– carbon 14 dating is available for the organic components of the fossil bone. Some older deposits have been dated using magnetostratigraphy. There is strong evidence that *Myotragus balearicus* played an important role in the economy of man when he arrived on the islands about 6500 years ago. BURLEIGH & CLUTTON-BROCK (1980) and WALDREN (1982) suggest that man may have managed *Myotragus balearicus*. Extinction followed within about 2000 years (BURLEIGH & CLUTTON-BROCK 1980).

MATERIAL AND METHODS

Three large cave samples from different parts of Mallorca were made available to me for study. These are the same cave deposits discussed in the ecological analysis of HAMILTON (1984). She analyzed population structure and sexual dimorphism in *Myotragus balearicus*. The largest collection is from Son Muleta cave, discovered and excavated by the American archeologist William Waldren, near the village of Deià above the northern coast of the island (WALDREN 1982). This is a vast collection including an estimated 200,000 *Myotragus* bones. The cave entrance is at present small, and was presumed so during times of accumulation. The main collections first accumulated in vertical shafts or in lateral passages off these, which apparently served as death traps for the animals. Fossil remains filled most of the 6 or so meters that Waldren excavated. Notes were kept and localities put on the bones using lettered sectors and depth to the nearest 50 centimeters. Approximately 27 radiocarbon dates are available on various levels and parts of the cave, some from *Myotragus* bones. Only one or two completely articulated skeletons were found and additional partial associations of limbs, vertebrae and skull and jaws were collected. However, the collection consists mostly of disarticulated and sometimes broken bones representing all skeletal elements. Ages at death for individuals range from possibly fetal to old adults with highly worn teeth. Waldren invited me to study this collection and I have visited Deià three times to measure and study parts of the collection. Small collections from Son Muleta have been donated to museums in the United States, including the American Museum of Natural History, the Smithsonian Institution, the Carnegie Museum, and the Field Museum.

The radiocarbon dates available for the Son Muleta *Myotragus* containing deposit range from roughly 6000 BP to 32000 BP. Dates are available for different lettered sectors of the cave and different numbered excavation strata. The strata numbers begin at 1 in any one sector at the top of the deposit down to the highest numbers for the bottom of that sector (WALDREN 1982). However, the letters and numbers inscribed on the bones themselves or on associated labels refer to sector letter and depth in centimeters from a base level of 0 for that sector. Contiguous sectors are designated by the same stratum numbers (not depths), but many strata are inclined and not necessarily horizontal, as they were defined by breaks in sedimentation, and so the same stratum may be at different depths in different sectors. Strata in sectors that were not closely connected were independently numbered from top to bottom. Therefore, it requires extrapolation and careful reading of WALDREN (1982) and study of his cave diagrams to extrapolate a tentative date to a sector or stra-

tum (and its depth range) when it was not dated. A measured sample of metacarpals labeled CD150, from sectors C & D at a depth of 150 cms below the 0 cm datum, were interpreted as coming from stratum 7 for these sectors based on the legend scale for the published vertical sections. The nearest dated specimens for this stratum are in the O sector at 150 cms from the datum, and the dates are between 7135±80 and 8570±350 before the present (BP) (KBN 640c, and UCLA 1704c, pers. comm., WALDREN 1982). The other measured sample of metacarpals, all labeled Z400 (coming from sector Z and 400 centimeters below the 0 datum), are interpreted as being from stratum 3 in sector Z, for which a date of 18980±200 BP is available (a Z 400 bone was dated as UCLA1704e, pers. comm., WALDREN 1982). Another date from a bone at Z 350 is 14465±315 (SI 645, STUCKENRATH and MIELKE 1972). It is therefore suggested that these CD 150 and Z 400 samples are separated in time by at most 10 to 12,000 years. As an alternative approach to dating specimens, HAMILTON (1984) divided the collection into 5 levels irrespective of sector. The first 4 levels represent 100 cm. increments, while her level 5 represented all specimens below 401 cms. In her interpretation then CD150 is from her level 2 assigned a rough date of 2000 to 10000 BP; and Z400 represents level 4 from 15000 to 20000 BP. Our assessments thus agree very roughly. Using her figures, as little as 5000 years to as much as 16000 years could separate the levels.

Cova del Moro is on the other side of the island, on the southern coast at the base of a 6 m cliff, and the entrance is about 6 m above sea level (see Fig. 6.39 in ALCOVER *et al.* 1981 and Fig. 1 in HAMILTON 1984). This area has little topography except the cliffs near the sea. I have visited this cave. Miquel Trias, Francesc Mir and Lluis Roca discovered this cave and obtained samples of *Myotragus* (ALCOVER pers. comm.). Students of PAUL SONDAAR, a collaborator on this project, excavated further materials from this site and these were also available for study. New excavations have been recently undertaken by Antonio Alcover of the CSIC and University of Balearics. Excavations continue and some of the very recently collected material is included in this study.

Son Maiol is purported to be an older deposit, and a small collection from that cave was made available by ALCOVER for study. Collections include specimens made by a team directed by Sondaar, and another by Joan Pons (ALCOVER pers. comm.). The location of Son Maiol is shown on the map of localities for *Nesiotites* (Fig. 6.61 in ALCOVER *et al.* 1981) and in HAMILTON (1984, Fig. 1); and is close to the main city, Palma, on Mallorca. I have also visited this cave.

I have concentrated on the collections in Deià and measured mostly Son Muleta specimens. In the summer of 1995 PAUL SONDAAR, SANTIAGO REIG, and I were able to measure additional specimens from Cova del Moro and Son Maiol. A cast of the skull and jaws of *M. batei* was also measured.

Sondaar has had several masters students do theses on aspects of the Son Muleta collection (e.g. SPOOR 1988*a, b*). These were univariate and bivariate studies of the more abundant appendicular skeletal elements. SPOOR (1988*a, b*) published analyses on proportions and variation of limb bones for this and other collections.

On my first visit I took linear measurements on 324 metatarsals using digital calipers, recording to the nearest 0.01 mm, with as many as 136 specimens coming from one sector, X at the 200 cm. level; where fossils were extremely dense. I chose metatarsals as they are usually complete, and may be sexually dimorphic. However, in *Myotragus balearicus* the frequent fusion of the distal tarsal bones with the proximal end of the metatarsals makes it difficult to find a comparable single length measurement for all specimens. One can use the line of fusion between the cuneiforms and metatarsals to measure the length of the metatarsals proper. See Fig. 3 and Table 2 for distances measured.

In the summer of 1995, with a portable 3Draw Polhemus (DEAN 1996), I collected three dimensional (3D) landmark coordinates (x, y, and z recorded to the nearest 0.1 mm) on skulls, lower jaws, and metacarpals. Data was collected from 35 skulls, 75 lower jaws, and 154 metacarpals. Many of the skull measurements were repeated to evaluate precision. Santiago Reig kindly helped me set up the measurement protocol for the skulls; and together we measured and remeasured a number of skulls.

Specimen data and coordinates were collected in an IBM clone personal notebook computer. The protocol is discussed briefly here and in greater detail in MARCUS (1995). Lotus 123 was automatically opened with the cursor in the first cell. A lists of landmarks was copied from a template,

and specimen location data and comments were entered by hand. Then for each press of a hand held switch, the position of the stylus point on the fossil was automatically entered into the spread sheet, as x, y, and z into the three cells of a spreadsheet row. The cursor automatically positioned itself on the first cell of the next row for the next point. One file per specimen was used for skull data; while data for several jaws or metacarpals were collected in a file together with side, stratigraphic level, and sector or locality.

In order to evaluate repeatability (both REIG and I, or my repeated measurements), two sets of measurements were collected on skulls in adjacent sets of columns B to D and E to G respectively. Lotus 123 column H was used to calculate the Euclidean distance between replications. We retained differences of less than 1.0 mm, and discussed larger differences, or in some cases re-entered a point. The tip of the Polhemus stylus is 0.5 mm in diameter (very much like a fine mechanical pencil lead), and the shaft just below about 1.0 mm in diameter. Our procedure did not produce a controlled repeatability measurement study, but it did give us direct and immediate feed-back on how close the repeated landmark points were in millimeters.

On the skull, we measured landmarks on the dorsal, lateral, ventral, anterior and posterior surfaces. 100 landmarks were defined, 8 on the saggital plane and 46 on each side. Frequently one side was damaged and no one specimen was complete. A minimum of 55 landmarks were collected on partial skulls, with up to a maximum of 92 on two of the most complete skulls. However, each of these was missing different landmarks. The anteriormost 5 landmarks were only present on a few skulls; and only one had the tips of premaxillae in place. Only 6 out of the 100 defined landmarks were present on all 35 skulls.

GRF-ND (SLICE 1996) was used at every stage of the data collection and analysis including options Generalized Least Squares (GLS) and Generalized Affine Least Squares (GALS) for least squares alignment. Shape coordinates (option SC) were used to orient the specimens where required. A major use of GRF-ND was to correct data when points were collected out of order. This showed up clearly using the labeling option (L) when the landmarks points were plotted – displaying the vectors relative to the reference and then looking at each specimen in turn (option I), after they had been aligned by generalized least squares (GLS). Errors were obvious as very long vectors pointing from or to the wrong landmark. Points out of order could be corrected in the original spreadsheet or in GRF-ND input data files by exchanging rows in an editor.

GRF-ND worked well even when considerable missing data were present. However, multivariate statistical analysis requires that a complete set of measurements is available. This can be accomplished by discarding data, or by estimating the missing data – using for example the EM algorithm (LITTLE & RUBIN 1987), but this was not attempted in this preliminary study as there was too much missing data. As a first step in filling in the missing coordinates, points missing on one side were reflected across the mid-saggital plane to the other side in SAS. Next, I chose to discard data for the most incomplete skulls and least represented landmarks. This left me with 20 skulls and 48 landmarks for the 3D data set – still including both sides. See Fig. 2 which identifies most of the 48 numbered landmarks.

Landmarks included all three kinds according to BOOKSTEIN's (1990) classification. About half were extrema of one sort or another, a very few represented intersections of sutures; or sutures crossing ridges, and 7 were located at edges of foramina.

The angle of the eyes to the frontal plane was estimated by measuring the angle from the anterior to posterior point of the orbit in a plane parallel to the plane through the posterior glenoid, and the most anterior points on the orbits. The data was subset in SAS to the relevant orbital coordinates (including the inferior and superior points as well), and glenoid points – 5 on each side, together with computed midsagittal points. Skulls were oriented with the midsagital anterior orbit point at 0,0,0, the mid glenoid point 1,0,0, and the left anterior orbit point at x, y, 0 using option SC (Shape Coordinates) in GRF-ND (SLICE 1996). The frontal angle for one side was computed, using SAS, as the arc tangent of the distance from the anterior to posterior orbital points in the lateral y direction divided by their distance in the anterior-posterior x direction. The vertical eye angle for one side was computed as the arc tangent of the lateral y distance from the superior to inferior orbital points, divided by the vertical or z distance between the two points. The angles were added from

the two sides or doubled if only one was present. Only 26 of the skulls had enough data to compute one or both of these angles.

For the 75 adult mandibles. 51 had all 12 landmarks available (see Fig. 1). Of these, 35 were from Son Muleta, 9 from Moro, and 6 from Maiol. A cast of the mandible of *Myotragus batei*, a presumably ancestral species, to *Myotragus balearicus*, was included as well for comparison. One of the less complete mandibles from Cova del Moro, from the pre-human level (ALCOVER pers. comm.), had very extreme wear and a very small incisor (see below). Localities could be compared, but there was not enough data to divide the sample according to stratigraphy. Different wear stages were represented in the data – but all were adult with fully or almost fully erupted dentition – showing some wear on the M_3.

For the metacarpals I recorded 19 landmarks on a sample of 154 right and left metacarpals (Fig. 3). Five landmarks were located on extrema or intersections of proximal articulating surface ridges with the surfaces of the shaft; four were selected to reflect the midshaft anterior-posterior and lateral diameters; and the remaining 10 were all extrema of the two distal condyles. All specimens were complete and adult so there was no missing data (Fig. 3*a*). The sample consisted of 73 bones from Son Muleta – 45 from an upper level interpreted as coming from 7000–9000 years BP; and 28 from a lower level interpreted as near 19000 years BP. Sixty five specimens came from Cova del Moro, and the remaining 16 specimens were from Son Maiol.

RESULTS AND DISCUSSION

Polhemus and human error

A careful analysis of a large piece of mm paper exceeding the active area of the 3Draw and digitized at each 2 cm intersection gave a standard deviation of less than 0.30 mm – very close to the 0.25 mm the manufacturers suggested repeatability in terms of mean squared error. A study of error by CORNER *et al.* (1992) for an earlier model, the Polhemus 3Space, of a fixed object recorded 20 times by each of two experimenters, gave a median standard deviation of 0.248 mm, with a range of 0.143 to 0.451 mm.

An analysis of 2320 differences between SANTIAGO REIG and me or my repeated analysis, trimmed of large extremes (generated by missing points) gave a mean not siginficantly different from 0.0 and a standard deviation for x, y, and z near 0.5 mm. This variation, as expected, was larger than for the piece of graph paper.

Skulls

Eye angles for the 26 skulls in the frontal plane and vertical plane are shown in Figs 4*a* and 4*b* respectively. The 24 frontal angles varied from 66° to 97° with a mean ± standard error of the mean of 81°±1.7°. The vertical angles ranged from 53° to 82° with a mean of 69°±1.5°. The mean angles for the three caves are not significantly different. Angles were computed for 17 skulls from Muleta, 5 from Moro and 4 from Maiol.

For an overall analysis, the skull sample was small, and the 48 landmarks were represented only on 20 specimens – 13 from Muleta, 6 from Moro and 1

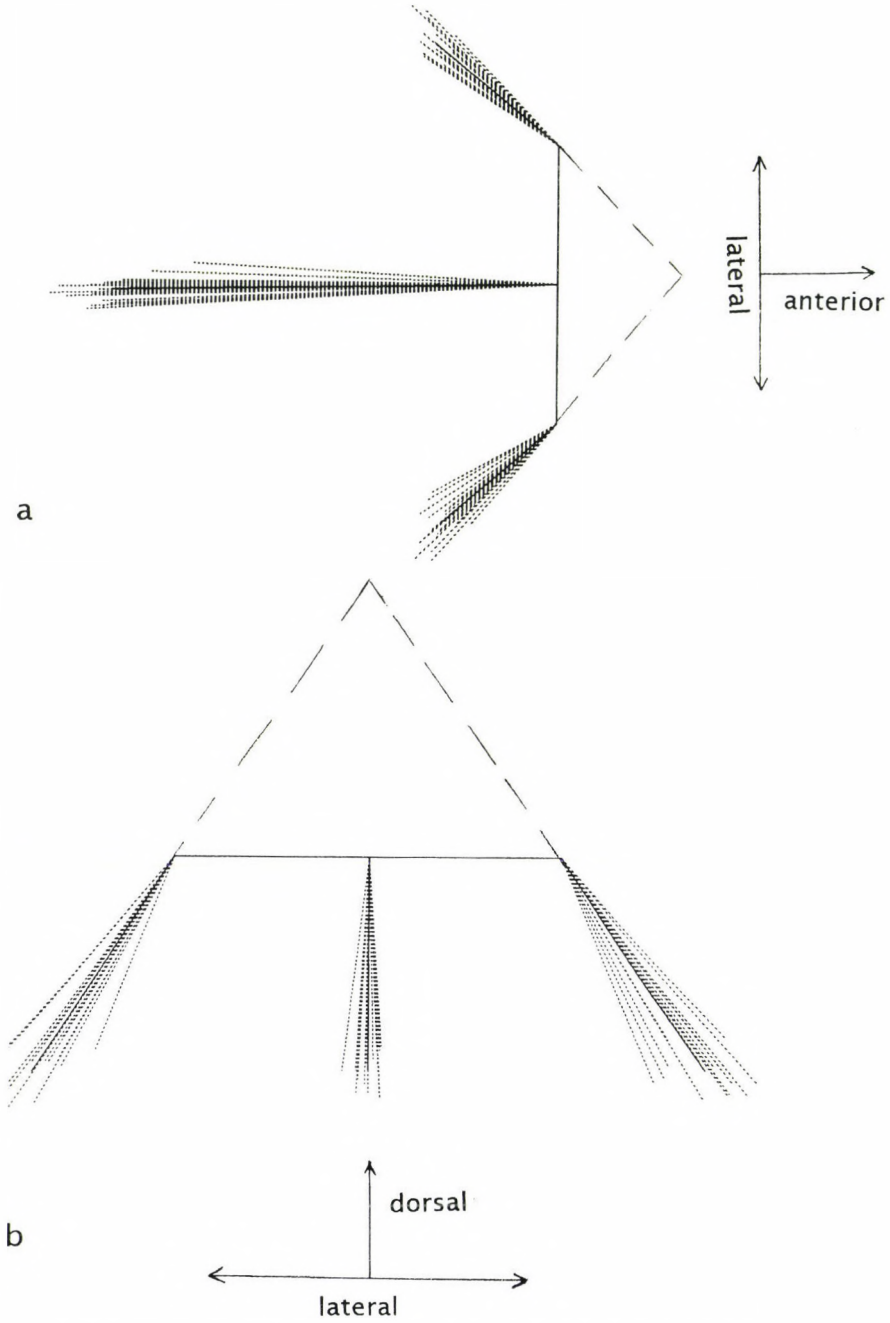

Fig. 4. Variation in eye angles. (**a**) Frontal angle in plane of mid-point of anterior orbits and glenoid. Anterior is to right. (**b**) Vertical angle from perpendicular to same plane from inferior to superior point of orbits. Dorsal is up

from Maiol. The residual sum of squares for the GLS fit for 48 landmarks for the skulls not including *M. batei* was 0.0779 and that after GALS was 0.0691, so that the affine component accounted for less than 10% of the variation in shape. If the GOODALL model is correct, i.e. independent spherical variation at all landmarks then the statistic:

$$\frac{(SS_{GLS} - SS_{GALS})/5}{SS_{GALS}/(3p - 12)}$$

is approximately an F with 5*(n-1) and (n-1)*(3p-12) degrees of freedom, where n= number of specimens; and p = number of landmarks (SLICE, pers. comm.). BOOKSTEIN (pers. comm.) pointed out that since the same left and right landmarks from the skull were used and there are interpretable relative warps, then the number of effective landmarks are certainly fewer than (3p–12) for the denominator. He suggested estimating the effective number of landmarks by fitting a chi-square distribution to the squared Procrustes distances using the method of moments. Effective degrees of freedom, edf = 2*(mean of squared Procrustes distance)^2/(variance of squared Procrustes distance) over all specimens (see DEAN *et al.* 1996 for details). The affine effective degrees of freedom are estimated in a similar way using the unform sums of squares, as the difference between the Procrustes distances from a generalized least squares fit, and affine fit for each specimen (results from GRF-ND). The effective degrees of freedom were 3.79 for the affine, and 24.68 for the squared Procrustes distances. For the 20 skulls and 48 landmarks the adjusted F = (0.0779–0.0691) ± (24.68–3.79)/ /(0.0691 ± 3.79) = 0.70 with 3.79 ± 19 = 72.01 and 20.89 ± 19 = 396.91 degrees of freedom. Thus the amount of shape variation in the uniform subspace is not significant.

The eigenvectors of the residuals for both GLS and GALS provided local shape differences that reinforced observations from examination of the skulls. The first principal component is dominated by the position of the 3rd molar that is a function of the age of the individual, as the teeth wear, because the rear teeth move forward. The second component is dominated by a widening of the zygomatic arches so that among the skulls from Son Muleta it was seen that some were more rounded, while others had aversus a more narrower tapered skull when viewed from above. This pattern showed up nicely in the animation option (A) of GRF-ND (Fig. 5). Other patterns were subtler, and await larger samples for further study.

Mandibles

The overall pattern of variability for the landmarks is shown in Fig. 6*b*. Note the large variability in the position of the boss (landmark 5) representing the posterior lingual end of the bony capsule for the base of the incisor; anterior and posterior ends of M_3 (landmarks 7 and 8 respectively); and the rear end of the

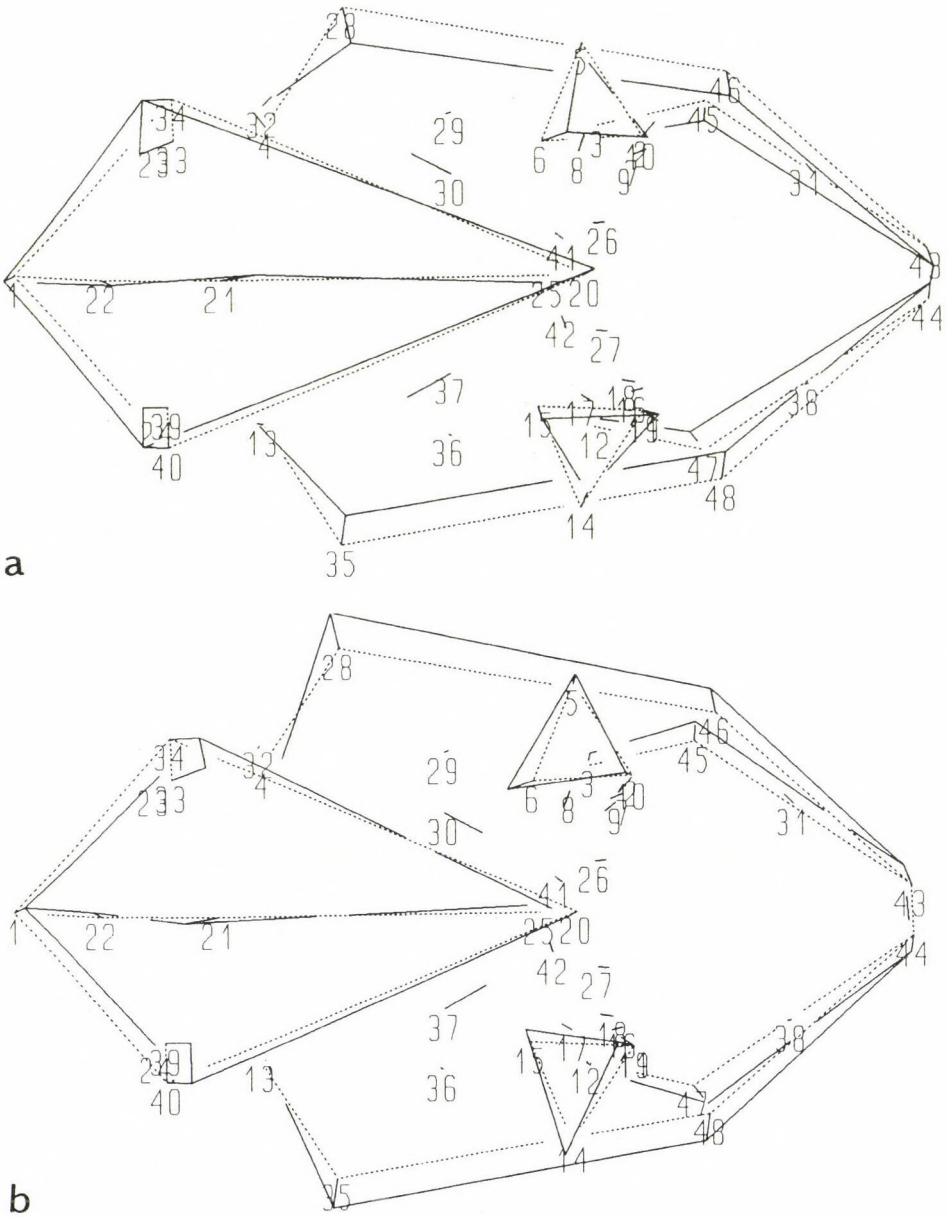

Fig. 5. Plot from GRF-ND of exaggerated extremes of principal component 2 showing exaggerated shapes of skulls. Reference specimen is dotted line in each case. (a) Solid is narrower end of PC 2. (b) Solid is wider end of PC-2. Refer to Fig. 1 for Landmarks. Some guide points are 43 and 44 are respectively left and right diastemal ridge; 1 is the rear of the skull; and 28 and 35 are on the zygomatic arches near the maximal width. The triangles are defined by three orbital landmarks. Nasion is at 20 and the right lateral horn base is at 40.

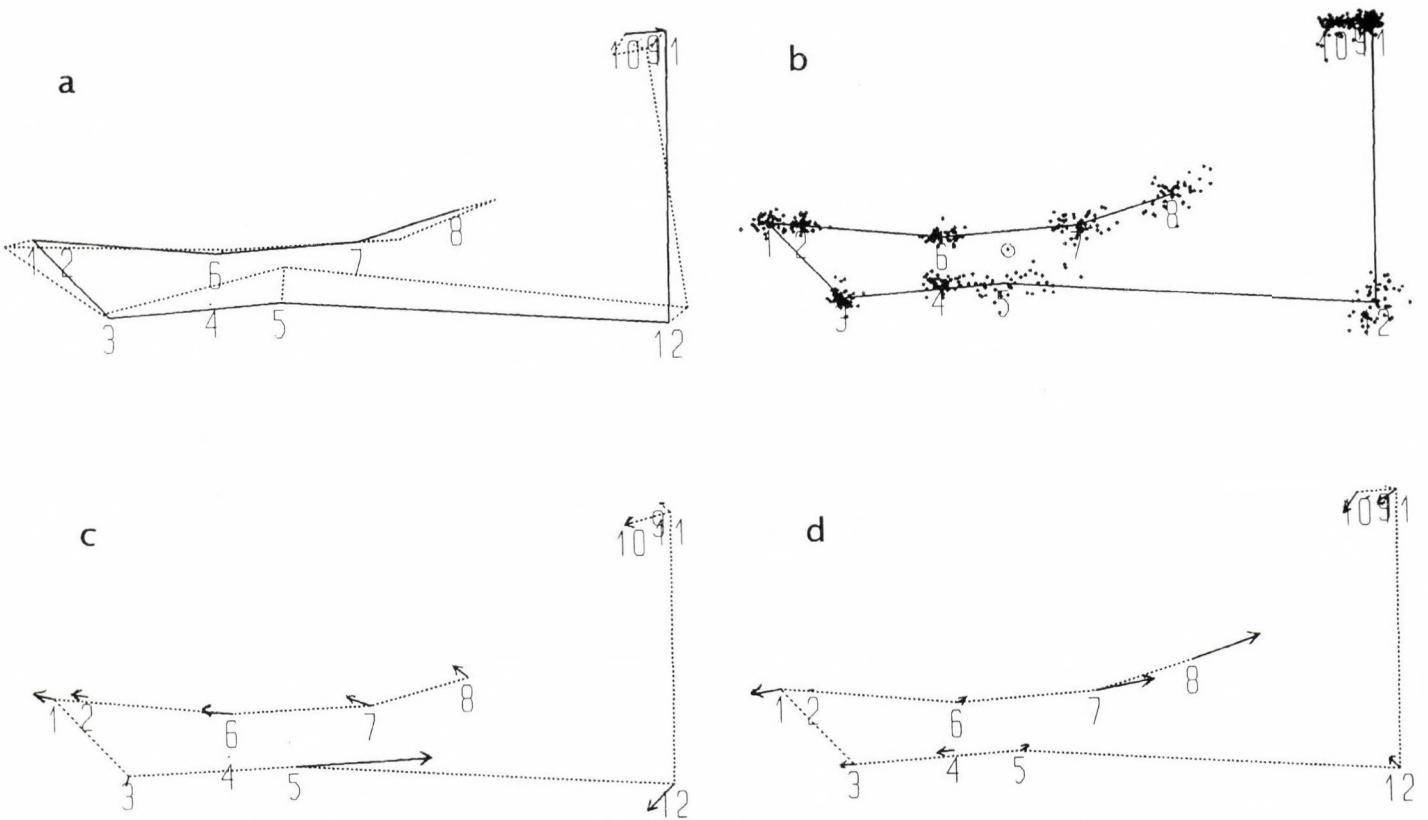

Fig. 6. (**a**). *M. batei* (dotted line) compared to typical *M. balearicus* (solid line) from Muleta. (**b**). Scatter for 51 specimens with all 12 landmarks. (**c**) PC 1 right vectors, emphasizing position of root of incisor (landmark 5). (**d**) PC 2 vectors emphasizing position of third molar relative to rear of jaw. Landmarks 7 and 8 are anterior and posterior ends of M_3 (see Fig. 1)

Table 1. Stem and leaf diagrams for each locality for widths of lower first incisors in jaws. Stem in millimeters and leaves in 0.1 mm. *M. batei* indicated as well, though it has two adult incisors present. Sample statistics are given as well

	Myotragus balearicus			*Myotragus batei*
	Muleta	Moro	Maiol	
Stem	Leaf	Leaf	Leaf	Leaf
10	555		6	
10	24	3	2	
9	677	79	6	
9	1334	4	3	
8	6778888999			
8	001222234444	0	2	
7	5555678999	9	5	
7	002334	34	00	
6	5	5	7	
6	0	12		
5				
5				2
4		7		
n	52	13	9	1
Mean	8.4	7.8	8.5	5.2
Std. dev.	1.03	1.69	1.40	
CV	12.26	21.62	16.40	

mandible (landmark 12). *M. batei* landmarks are shown in Fig. 6*a* and this mandible has a distinctive shape. Its M_3 is positioned quite posteriorly associated with its retention of P_2 and P_3 and consequent longer tooth row, and it is the most extreme vertical point (circled) for landmark 5 in Fig. 6*b* reflecting the lack of a permanently growing incisor. M_3 is little worn on this specimen and it is not fully erupted.

The Moro mandibles were significantly smaller on the average as measured by centroid size; but no striking shape similarities were found for that locality except for the highly worn specimen with a very narrow incisor. *M. batei* showed the most extreme position on a plot of the uniform components, U1 against U2, so that it shows affine differences from *M. balearicus* as well (for a two-dimensional subset of coordinates).

The first PC for GLS residuals showed, not surprisingly, a great deal of variabilty in the incisor boss on the inner mandibular surface (Fig. 6*c*). This picture was almost identical in a two-dimensional (2D) subset of data for relative

Table 2. Variability of metatarsal measurements from Muleta

Measurement (mm)	Total sample				Sector X – depth 200 cms			
	n	Mean	Std. Dev.	CV	n	Mean	Std. Dev.	CV
Maximum length (ML)	190	79.5	6.71	8.45	73	79.2	6.90	8.71
Partial length1 (PL1)	198	67.9	6.14	9.05	76	67.3	6.32	9.38
Partial length2 (PL2)	291	57.9	5.44	9.40	123	57.9	5.46	9.44
Bicondylar width (BCW)	279	23.2	1.46	6.30	114	23.1	1.40	6.05
Distal width (DW)	308	23.9	1.94	8.09	124	23.8	1.77	7.45
Minimum shaft width (SW)	327	18.3	1.42	7.76	133	18.3	1.30	7.10
Proximal width (PW)	318	21.0	1.68	8.02	130	20.7	1.52	7.33
Navicular depth (ND)	215	22.1	1.67	7.55	81	22.0	1.68	7.66
Width lateral condyle (LCW)	271	13.2	1.00	7.56	109	13.1	0.95	7.27

warp 1 (using ROHLF 1996). The second PC is dominated by the position of the third molar (Fig. 6*d*). This feature also shows up in the 2nd relative warp for a 2D subset of the data. Both features, and especially the latter are associated with the age of the individual. As the teeth wear down, they all shorten, and this appears as a shortening of the entire series with a forward repositioning of the third molar. Therefore the distance from the rear of that molar to the rear of the jaw increases; while the diastema between the incisor and premolars is more stable (the distance from landmark 2 to 6).

A traditional analysis of measurements derived from the landmarks, and some taken with calipers showed excessive variability in all characters. Length of the M_3 was the least variable with a coefficient of variation of 5 estimated as 100 * mean / standard deviation (SOKAL & ROHLF 1969) (for 7 specimens from Maiol) to 10.3 (12 specimens from Moro). Length of this tooth estimated from landmarks was larger and more variable than the caliper measurements.

The highly worn specimen alluded to above from Moro has an incisor width of 4.7 mm much smaller than the next largest one (Table 1). This width is narrower than that for *M. batei*, but the latter has two incisors present, and retains a small deciduous incisor. However, one isolated ever-growing incisor from Son Muleta has almost identical width to that of the small Moro individual. The incisor widths have an unusual degree of variation (coeffcients of variation between 12.26 to 21.62 for the three caves). Stem and leaf charts for the incisor widths are given in Table 1. This variability needs further investigation. We could not show any association of incisor width and age category of a jaw, based on wear. If the incisor tapers very slowly, and wears very fast, perhaps this effect is not detectable. There were no significant differences with sector and depth in incisor width and M_3 length at Son Muleta.

Variability of metatarsals

Metatarsals were fused with tarsal elements or not, and the sample of 324 specimens from Muleta was available from many sectors and depths. All coefficients of variation, in Table 2 but one are greater than 7 which is large for a homogeneous sample of caprine metapodials (BOSOLD 1968). Both *Capra ibex* and *Rupicapra rupicapra* show sexual dimorphism (BOSOLD 1968) in this bone. In *Rupricapra* the differences are between 0.6 and 1.5 standard deviations, assumed to be the same for the two sexes (23 females and 18 males); while in *Capra ibex* most differences exceed 2 standard deviations, and some reach 3. This is for samples of 12 females and 23 males. Eleven of 12 coefficients of variation for comparable characters within a sex are less than 5 for *Rupicapra*; while for the 12 coefficients of variation of *Capra ibex* 4 are less than 5 and 2 are greater than 7. It should be noted that BOSOLD (1968) only gave means, minima, and maxima. Standard deviations used here were estimated using a factor from SNEDECOR and COCHRAN (1967, Table 2.4.1) as a function of sample size, and assuming normality.

There are sizable samples from some Muleta cave sectors within 50 centimeter depth ranges. The largest sample measured had 136 specimens from sector X at a depth of 200 cms; and there were 7 or more from several other small regions of the cave. Only a couple of such samples were significantly different, and none taking into consideration Bonferroni corrections. Unfortunately, large size samples were not measured from the same sectors as for the metacarpal samples discussed below. A larger series reported in HAMILTON (1984), however, shows differences in length and width for the upper and lower levels, though details of the measurement procedure are not given.

Metacarpals

This is the bone for which I had the most locality and level information. The 154 specimens were from four distinct populations: 65 from Cova del Moro; 45 from an Upper level of Son Muleta (all labeled as coming from Sector CD at a depth of 150 cm.) which by inference is 7000–9000 years BP (carbon date extrapolated from a near by sector and depth); 28 from the lower level (all labeled as coming from Sector Z at a depth of 400 cm) – bone dated at near 19000 years

Table 3. Variability of centroid size in mm for metacarpals from cave localities

Cave	n	Mean	Min.	Max.	Std. Dev.	CV
Moro	65	88.6	68.8	102.2	8.4	9.48
U. Muleta	45	94.4	78.5	111.4	6.7	7.09
L. Muleta	28	104.3	89.0	122.1	8.5	8.15
Maiol	16	109.0	98.1	120.9	5.7	5.20

BP; and 16 from Son Maiol. The variation of all 154 specimens at each landmark is shown in Fig. 7*a* after a Generalized Least Squares (GLS) fit that removes the affect of size (measured as Centroid Size SLICE *et al.* 1996).

There is a significant difference (one way Analysis of Variance) in centroid-size among these four samples (Table 3). The Son Maiol and Lower Level of Muleta are not significantly different; and the Upper Level and Moro are not significantly different (Bonferroni adjusted). Size differences are shown in the superimposed output of forms from GRF-ND of the sample means using the undocumented command BACKSCALE in GRF-ND, that restores the original size

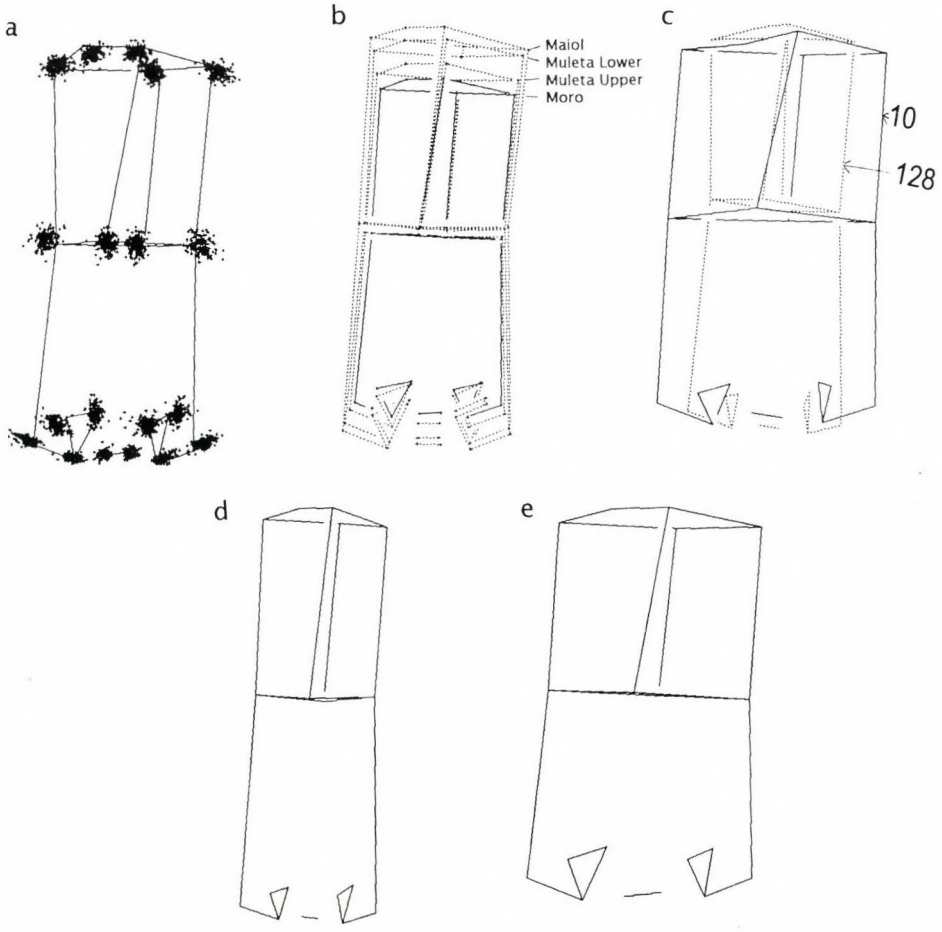

Fig. 7. (**a**) Variation of all 154 metacarpals in 3D from GRF-ND after GLS – compare to Fig. 3 for orientation. (**b**). Differences in size (and shape) for the 4 samples. (**c**) Extreme specimens number 10 (solid line from Cova del Moro) and 128 (dotted line from lower level Son Muleta) after GLS fit in GRF-ND. (**d**) PC1 left or narrow extreme for residuals from GLS. (e) PC2 right or wider extreme for residuals from GLS. Compare **d** and **e**, to cartoons of actual specimens in **c**.

(Fig. 7*b*). The coefficients of variation for centroid size are large – though there is no comparable information for this statistic for metacarpals of living artiodactyls. I would expect that the coefficient of variation for centroid size would behave similarly to that for linear dimensions as it has the same units, here mm, as a linear dimension. Almost all derived distances from landmarks show a similar pattern of sizes for the 4 sub-samples (see HAMILTON 1984 for a different comparison of levels for length and width of metacarpals, though details of measurement are not given). However, centroid size separates these samples better than any other derived linear character (Euclidean distance between landmarks) tested. The affine component is (0.4394–.2996) = 0.1398 and accounts for about a third of the GLS sum of squares (0.4394). In this case using, the same procedure as for skulls, the effective numbers of degrees of freedom are 9.75 for the squared Procrustes distances, and 1.55 for the affine sums of squares. The adjusted F = 2.47 with 237.15 and 1254.6 degrees of freedom for the 154 metacarpals which is highly significant. Affine variation is very important for this skeletal element, and affine degrees of freedom, between 1 and 2, may reflect the single dimension of length–width compression and stretching.

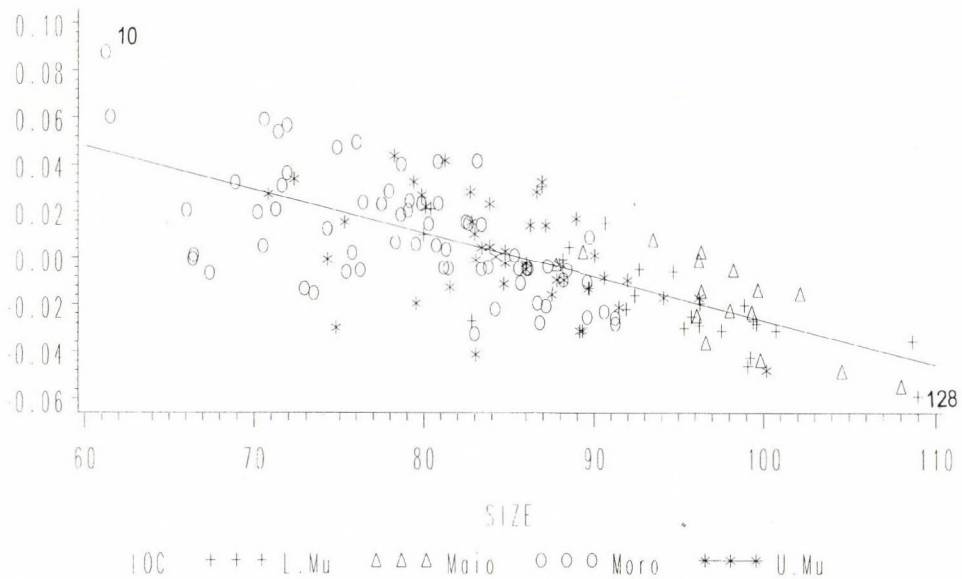

Fig. 8. Plot of Uniform Y against centroid size, with localities indicated. Specimens 10 and 128 are also indicated (see legend for Fig. 7c).

Fig. 9. Plot of canonical variate scores for 45 principal components from GALS residuals for metacarpals. Specimens 10 and 128 are indicated

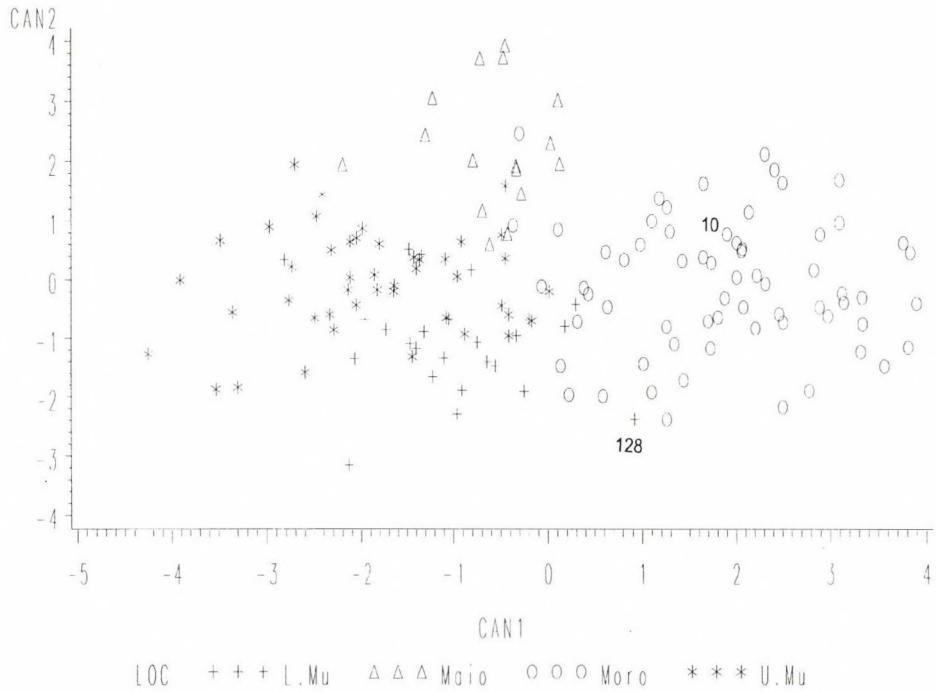

Both a principal components of the GLS residuals and the relative warps including the uniform components, or just U2 alone (the data was reduced to two dimensions and 10 landmarks for the relative warps comparison), show a strong affine difference among the metacarpals and this corresponds to a lateral widening of the bone over its length. This is true for all localities. Figure 8 shows U2 plotted against centroid size. An analysis of covariance on locality differences in U2 with centroid size as the covariate, gives similar slopes for all four samples; and U2 adjusted for centroid size is not significantly different among localities. Therefore, the metacarpals with the smallest centroid size are from Cova del Moro and are relatively the widest, while the largest are from San Maiol and the lower level at Son Muleta and are relatively the narrowest. This is depicted in Fig. 7*c* (all 19 3D coordinates used and specimens at same centroid size) where connections among landmarks for a small specimen from Moro, and a large one from Lower Muleta are shown. Figs 7*d* and 7*e* show the range of shapes using the principal components feature of GLS to show extreme possible shapes for the first principal component and give very similar extremes to 7*c* for the two actual specimens.

There are more subtle differences in the orientation of the condyles, and the facets of the proximal end of the metacarpal; as well as some torsion that shows up in subsequent principal components, though these have not been analyzed in detail. A discriminant analysis of the three dimensional data as principal components of residuals from GALS, adjusting for fitting by discarding the last 12 components (BOOKSTEIN 1996), shows significant differences in shape among some of the cave samples. However, the two Muleta samples show the smallest Mahalanobis D^2 which is still significant at the 0.05 level. Thus the non-affine shape of the Muleta samples are more similar, but still significantly different. The only non-significant difference is between Lower Muleta and Son Maiol. Figure 9 is a plot of the canonical variate scores from this analysis that shows little overlap for Moro and Upper Muleta. Interestingly using the residuals from GLS instead of GALS does not improve the discrimination very much if at all. All the significant differences in non-affine shape are very subtle and difficult to account for in the specimens themselves.

CONCLUSIONS

All measurements whether caliper distances, distances derived from landmarks or centroid size show excessive variability – the coefficient of variation may run from 6 to 14 even for samples controlled for stratum level, and thus presumably time. Many caprines are sexually dimorphic in the lengths and widths of the metapodials – and perhaps some careful comparison with large samples of relatives will be informative. However, some species are more dimorphic than others (BOSOLD 1968), and large samples are not available for many species. *Myotragus* is very distinctive, and different from other caprines in many features so that it will be difficult to know which single species to use as a standard of comparison. Sexual dimorphism was not accounted for here. We may note on the average for two equal samples with equal standard deviations of 5, means of 95 for one and 105 for the other – with CV's of 5.26 and 4.76 respectively – both CV's about 5 (a modal value for the *Rupicapra* data), the separation of sexes by 2 standard deviations in a mixed sex sample increases the CV to 7.1 from a homogeneous one with a CV of 5 for each sex. A difference of 3 standard deviations between the sexes, observed in some of the *Capra ibex* dimensions, would give a CV of about 9.4 for a mixed sample containing both sexes. It takes a difference larger than 2 standard deviations before separate modes are seen in frequency distribution plots of mixed sex samples for very large samples.

HAMILTON (1984) reported sexual dimorphism for Muleta and Cova del Moro, and estimates the sex ratio. She based this on skulls, pelves, and the axis and atlas vertebrae – however, details are not given. She claims that the majority

of skulls at Son Muleta are male, and are distinctly larger, while the sexes are more nearly equal in proportion at Cova Del Moro. WALDREN (1982) had claimed that bone filled sinuses- and solid horn cores suggested males – and proposed a male butting model – but did not consider the horn sheath which might have been at least 50% longer or more than the core, using the Goral as a model with the most similar horn core. Relatives with relatively straight horns of this type (the goral, serow, and mountain goats for example) tend to stab or slash rather than butt, though little is known of their aggressive behavior (NOWAK 1991). HAMILTON (1984) has discussed some possible reasons for the high proportion of males she reported at Son Muleta. I was unable to sex any of the specimens measured and am not able to adjust for this possible source of variation.

From the material measured and summarized here, it was not possible to recognize more than one "species". The excessive variability likely has components due to sexual dimorphism and stratigraphic mixing in addition to other unknown causes such as sampling bias of the death assemblages as representatives of the living populations. causes in addition to so far undetected sexual dimorphism. The change in size of metacarpals documented for an estimated 9–11000 year or less difference in sample ages – about 10% diminution in size – shows that rapid change occurred. Differences in proportions of sexes in the two samples could account for part of this difference – but the sexes and sex ratio would have to be very different among these samples. Stratigraphic mixing would decrease the magnitude of this change, on the other hand. This time period extends is from the height of the last glaciation part way into the Holocene. Samples from narrower stratigraphic ranges, and documented by dating, are required to estimate the actual range of morphologic variation at any one time in Mallorca or Menorca. Most samples from caves or other fossil deposits will have increased variability due to mixed sampling of populations through time when the species is changing rapidly.

The complex of Menorca-Mallorca as an island system had a greatly increased area during the glacial stages when sea level was lower, and was more like the present during interglacials with the islands well separated. A remixing of the populations of *Myotragus balearicus* during each ice age on a much-extended area could lead to greater variation.

The lore concerning the adaptation and evolution of *Myotragus balearicus* has included several hypotheses that need to be tested more thoroughly. One suggestion is that *M. balearicus* evolved to its small size rapidly on arrival in Mallorca and Menorca (MOYA-SOLA & PONS 1982). We neither know its nearest living or fossil relative nor exactly when it got to the Balearics. Messinian arrival has been postulated (ALCOVER *et al.* 1981) and is most consistent with other data together with the idea that *Myotragus* on the average became smaller through time. The data presented here on metacarpals shows that the populations could

have changed size – relatively rapidly, perhaps sometimes getting larger, and sometimes smaller. It is worthy of note that the earliest species recorded *Myotragus pepgonellae* has comparable sized metacarpals to *M. balearicus* (ALCOVER *et al.* 1981).

The earliest relatively well documented species, *M. pepgonellae* (currently interpreted as probably not a direct ancestor of the lineage leading to *M. balearicus* SONDAAR *et al.* 1995) has a larger skull and jaws, but intermediate forms such as *M. batei* (not fully mature) fall at the small end of the size range for *M. balearicus*. Two intriguing, possibly very early ulna-radii, below the deposits containing *M. pepgonellae* (MOYA-SOLA & PONS 1982) are still larger than another identified for that species (PONS 1990). There is no direct evidence for the shortened feet evolving on the islands, as the earliest species with foot elements preserved has relatively short feet.

There is a very good morphotype record for stages in evolution of the dental changes, some with age control based on paleomagnetic dating—so that the loss of lateral incisors, loss of anterior premolars, and evolution of the evergrowing lower central incisor are well documented. The movement of the eyes to more forward-looking positions is less well documented, but seems associated with the loss of canines and incisors, and development of large temporal fossae.

Some of the peculiar adaptations have perhaps been facilitated by a lack of mammal predators where for example loss of running speed would not be important (LEINDERS 1979). There are no fossils of potential mammalian predators on the islands in the Pleistocene, but some large birds of prey – the golden eagle, *Aquila chrysaetos* – are recorded and might be important (SONDAAR *et al.* 1995). MARCUS and SARMIENTO (1996) offer a functional explanation for the position and orientation of the orbits.

What did *Myotragus balearicus* eat? – probably not typical caprine fare. The peculiar ever-growing rodent like incisors indicates much wear on these teeth. Their molars are very high crowned and in some mature to old aged individuals show bizarre wear patterns, and these features are associated with very large temporal fossae for large temporal muscles. Their diet must have been very tough and abrasive. Only South American vicunas have ever-growing central incisors among living Artiodactyla (MILLER 1924), but these occur together with a full complement of other incisors and canines. Vicunas are seen to nip off the grass close to the ground in contrast to relatives, who tend to pull out clumps of grass. *Maremmia haupti*, a Neogene fossil non-caprine bovid, may have had 3 ever-growing lower incisors, but they were very different in shape, and possibly represent a partially convergent ever-growing condition in a different subfamily (HÜRZELER 1983).

It is important to date the caves and levels within them as their faunas are studied, because this study shows that stratigraphic level even within one small

cave locality can be very important. This study has demonstrated changes in *Myotragus balearicus* through a relatively short time period. The change in centroid size of the metacarpal from a lower to an upper level of Son Muleta is about 1.3 standard deviations in about 10000–12000 or possibly fewer years. This is rapid evolution, but not as rapid as recorded in other well documented cases of island evolution (eg. LISTER 1989).

* * *

Acknowledgements – I am especially indebted to the WALDREN family who made me feel at home in Deià. WILLIAM WALDREN first invited me to view the collections and begin my analysis. I have been a guest at the Deià Archeological Institute during several visits, and especially enjoyed my associations with the Earth Watch projects there. WILLIAM WALDREN made the collections from Son Muleta, has preserved and curated them and has made them available for study by many scholars. ANTONI ALCOVER, of the CSIC, has allowed me to use extensive additional collections other than those from Deià, and expand the significance of this study. He has been encouraging and supportive through all of our contacts; and more than anyone else served as a useful critic on an earlier version of this paper – helping me to clarify many points, correct many errors, and has supplied many important additional references. PAUL SONDAAR spent considerable time looking at the materials with me and helping me to focus on the detailed metacarpal study. SANTIAGO REIG has visited Mallorca with me twice, and assisted in designing my measurement protocols, checking repeatability, and has been a constant source of ideas and feed back for this study. Many other colleagues in Spain have helped me with literature, access to specimens and feedback on the project. I am indebted to all of them. ROSS MACPHEE of the American Museum of Natural History has made important suggestions about *Myotragus balearicus* features, and arranged for American Museum support for one trip to Mallorca. He has shown considerable interest in *Myotragus* and the Balearics. The Polhemus 3D digitizer was purchased through a grant from PSC BHE of the City University of New York. TERRY WOJTOWICZ, GINA GOULD and ESTEBAN SARMIENTO all read early drafts and provided useful comments. FRED BOOKSTEIN suggested an approach that led to a test for the uniform component of variability.

REFERENCES

ALCOVER, J. A., MOYA OLA, S. & PONS, J. M. (1981) *Les Quimeres del Passat.* Edit. Moll, Ciutat de Mallorca. 260 pp.

ANDREWS, C. W. (1915) A description of the skull and skeleton of a peculiarly modified rupicaprine antelope (Myotragus balearicus, Bate), with a notice of a new variety M. balearicus var. major. *Phil. Trans. Royal Soc. London, Series B* **206:** 281–305.

ANGEL, B. (1966) El *Myotragus balearicus* Bate considerado como vertebrado mamifero troglobio. *Bol. Soc. Hist. Nat. Baleares* **7:** 89–94 (ALCOVER pers. comm.).

BOOKSTEIN, F. J. (1990) Introduction to methods for landmark data. Pp. 215–225. *In* ROHLF, F. J. *et al.* (eds): *Proc. Michigan Morphometrics Workshop.* Special Pub. 2, The Univ. Michigan Museum of Zoology, Ann Arbor.

BOOKSTEIN, F. J. (1996) Combining the tools of geometric morphometrics. Pp. 131–151. *In* MARCUS, L. F. *et al.* (eds): *Advances in Morphometrics.* Plenum Press, New York.

BOSOLD, P. VON KLAUS (1968) Geschlechts- und Gattungsunterschiede an Metapodien und Phalangien mitteleuropäischer Wildwiederkäuer. *Säugetierkundliche Mitteilungen* **16**(2): 93–153.

BURLEIGH, R. & CLUTTON-BROCK, J. (1980) The survival of Myotragus balearicus Bate, 1909, into the Neolithic on Mallorca. *J. Archeol. Science* **7:** 385–388.

CORNER, B. D., LELE, S. & RICHTSMEIER, J. T. (1992) Measuring precision of three-dimensional landmark data. *J. Quantitative Anthropol.* **3:** 347–359.

DEAN, D. (1996) Three-dimensional data capture and visualization. Pp. 53–69. *In* MARCUS, L. F. *et al.* (eds): *Advances in Morphometrics.* Plenum Press, New York.

ENCINAS, J. A. (1997) Inventari espeleològic de les Balears – ang 1997. *Endins* **21.**

ENCINAS, J. A. & ALCOVER, J. A. (1997) El jaciment fossilífer de La Cova Estreta (Pollença). *Endins* **21:** 83–92.

GENTRY, A. W. (1992) The subfamilies and tribes of the family Bovidae. *Mammal Review* **22**(1): 1–32.

GLIOZZI, E. & MALATESTA, A. (1980) The Quaternary goat of Capo Figari (Northeastern Sardinia). *Geoligica Roma* **19:** 295–347.

GREGORY, W. K. (1951) *Evolution Emerging. Vol. I.* MacMillan & Company, New York.

GUERIN, C. (1965) Gallogoral (nov. gen.) (Rutimeyer, 1878). Un Rupricaprine du Villafranchien d'Europe occidentale. *Documents des Laboratoires de Geologie de la Facultie des Sciences de Lyon* **11:** 1-353.

HAMILTON, J. (1984) The population structure of Myotragus balearicus from the Cave of Muleta, Mallorca. Pp. 71–97. *In* WALDREN, W. H. *et al.*: *The Deya Conference of Prehistory: Early Settlement in the Western Mediterranean Islands.* Part I. BAR International Series **229**(I): 71–88.

HÜRZELER, J. (1983) Un alcélaphiné aberrant (Bovidé, Mammalia) des «lignites de Grosseto» en Toscane. *C. R. Acad. Sc. Paris, Série II* **296:** 497–503.

KÖHLER, M. (1993) Skeleton and habitat of recent and fossil ruminants. *Münchner Geowissenschaftliche Abhandlungen. Reihe 1. Geologie und Pälaontologie* **25:** 1–88.

KURTÉN, B. (1968) *Pleistocene Mammals of Europe.* Aldine Publishing Company, New York.

LEINDERS, J. J. M. (1979) On the osteology and function of the digits of some ruminants and their bearing on taxonomy. *Z. Säugetierk.* **44:** 305–319.

LITTLE, R. J. A. & RUBIN, D. B. (1987) *Statistical Analysis with Missing Data.* John Wiley and Sons, New York, 278 pp.

LISTER, A. M. (1989) Rapid dwarfing of red deer on Jersey in the last interglacial. *Nature* **342:** 539–542.

MARCUS, L. F. (1995) Polhemus protocol. *In* Polhemus, Support Routines, Software [http://life.bio.sunysb.edu/morpho/]

MARCUS, L. F. & SARMIENTO, E. (1996) Variation in Myotragus balearicus and functional morphology of the skull and jaws compared to other ruminants. *J. Vertebrate Paleontology* **16**(3): 50a.

MCKENNA, M. C. & BELL, S. (1997) *Classification of the Mammals.* Columbia University Press, New York, 631 pp.

MILLER, G. S., JR. (1924) A second instance of the development of rodent-like incisors in an artiodactyl. *Proc. U. S. Nat. Museum* **65**(8): 1–4.

MOELLER, VON H. (1973) Nagezähne bei Eutheria and Metatheria. Ein Beitrag zur Kenntnis von konvergenzerscheinungen bei Säugern. *Säugetierkundliche Mittelungen* **74:** 112–121.

MOYA-SOLA, S. & PONS, J. M. (1981) Myotragus kopperi une nouvelle espece de Myotragus Bate 1909 (Mammalia, Artiodactyla, Rupicaprini). *Proc. Koninklijke Nederlandse Akademie van Wetenschappen. Series B* **84:** 57–69.

MOYA-SOLA, S. & PONS, J. M. (1982) Myotragus pepgonellae nov. sp., un primitivo representate del género Myotragus Bate, 1909 (Bovidae, Mammalia) en la isla de Mallórca (Baleares). *Acta Geol. Hispanica* **17**(1–2): 77–87.

NOWAK, R. W. (1991) *Walker's Mammals of the World.* 5th ed. The John Hopkins University Press, Baltimore.

PONS, J. M. (1990) Estratigrafia y fauna del yacimiento karstico de Cala Morlanda (Manacor, Mallorca). *Endins* **16:** 59–62.

ROHLF, F. J. (1996) Thin Plate Spline Relative Warp program for Windows. *In* Thin Plate Splines, Software [http:/life.bio.sunysb.edu/morph/]

SLICE, D. E. (1996) Three-dimensional generalized resistant fitting and the comparison of least squares and resistant fit residuals. Pp. 179–199. *In* MARCUS *et al.* (eds): *Advances in Morphometrics.* Plenum Press, New York.

SLICE, D. E., BOOKSTEIN, F. L., MARCUS, L. F. & ROHLF, F. J. (1996) Glossary for Geometric Methods. Appendix I. Pp. 531–551. *In* MARCUS *et al.* (eds): *Advances in Morphometrics.* Plenum Press, New York.

SNEDECOR, G. W. & COCHRAN, W. G. (1967) *Statistical Methods.* 6th ed. The Iowa State Univ. Press, Ames, Iowa, 593 pp.

SOKAL, R. R. & ROHLF, F. J. (1969) *Biometry.* W. H. Freeman, San Francisco, 776 pp.

SONDAAR, P. Y., MCMINN, M., SEGUI & ALCOVER, J. A. (1995) Paleontological interest of karstic deposits from the Gymnesic and Pityusic Islands. *Endins (Mon. Soc. Hist. Nat. Balears, 3* **20:** 155–170. [in Catalan and English]

SPOOR, C. F. (1988*a*) The body proportions in Myotragus balearicus Bate, 1909. *Proc. Koninklijke Nederlandse Akademie van Wetenschappen. Series B* **91:** 285–293.

SPOOR, C. F. (1988*b*) The limb bones of Myotragus balearicus Bate, 1909. *Proc. Koninklijke Nederlandse Akademie van Wetenschappen. Series B* **91:** 295–309.

STUCKENRATH, R. & MIELKE, J. E. (1972) Smithsonian Institution Radiocarbon Measurements VII. *Radiocarbon* **14**(2): 401–412.

TRIAS, M., PAVERAS, C. & GINES, J. (1979) Inventari espeleologic de les Balears. *Endins* **6:** 89–108.

WALDREN, W. H. (1982) Balearic prehistoric ecology and culture. The excavation and study of certain caves, rock shelters and settlements. *BAR International Series, Oxford* **149**(I): 1–401.

The oribatid species described by Berlese (Acari)

MAHUNKA, S. and L. MAHUNKA-PAPP

The authors had the opportunity for years to study the Oribatid species described by Berlese currently deposited in the Istituto Sperimentale per la Zoologia Agraria at Florence. The results of this series of studies are summarized in this volume.

The volume begins with an essay-like Introduction heavily relying on subjective opinions discussing the general questions of Oribatology. The following section lists Berlese's species placed in the modern system helping the specialists with morphological notes and many drawings; here also the condition of the specimens is discussed and lectotypes are designated.

The third, large section is the catalogue proper, wherein all the species are listed in the systematic order together with their combination and synonymic names. Here one may find all the literature data, usually missing from ordinary works, with reference to Description and Taxonomy, Distribution, with special emphasis on Catalogues whose references are partly unreliable. Where it was deemed necessary further information are added under the heading of Remarks. The volume closes with a very detailed list of literature.

ISBN 963 7093 27 3
325 pages with several figures. Soft bound.

Price: 40 US dollars excl. p. & p.

Order should be sent
to the Hungarian Natural History Museum, Library
Baross u. 13., Budapest, H–1088 Hungary
Fax: (36–1) 3171669

Acta Zoologica Academiae Scientiarum Hungaricae 44 (1–2), pp. 139–150, 1998

PHYLOGENY AND SIZE AND SHAPE CHANGES IN THE SKULL OF THE SOUTH AMERICAN RODENT PROECHIMYS*

CORTI, M., M. AGUILERA[+] and E. CAPANNA

Dipartimento di Biologia Animale e dell'Uomo, Universitá di Roma 'La Sapienza', via Borelli 50, I-00161, Roma, Italia
E-mail: corti@axrma.uniroma1.it
[+]Departamento Estudios Ambientales, Universidad Simón Bolívar Apartado 89000, Caracas, 1080–A, Venezuela

The rodent genus *Proechimys* has undergone rapid chromosomal speciation during late Pleistocene, resulting in several species and subspecies occurring in Venezuela. Here we present hypotheses for patterns of morphometric change in the skull based upon genetic relationships between two species of the "*guairae*" complex (*P. guairae* and *Proechimys* sp.) and *P. trinitatis*. Morphometrics of these species was studied using a geometric approach, and shape changes were visualised with respect to the branching in the allozymes tree. There is a consistency between morphometric change in the dorsal side of the skull and genetic variation, suggesting a phylogenetic explanation; however, there is incongruency between genetics and morphometrics of the ventral side of the skull. Incongruity may result from mutation rates which vary for both allozymes and morphometry and from the evolutionary forces which may act differently on the functional units (auditory, feeding, respiratory, olfactory) of the ventral side of the skull.

Key words: phylogeny, geometric morphometrics, rodents, *Proechimys*

INTRODUCTION

Speciation in rodents is common, fast, and often associated with transformations of the karyotype (CAPANNA & CORTI 1992, KING 1993). Phylogeny can therefore be reconstructed through chromosomal rearrangements and any other genetic or molecular data documenting speciation, provided that variation over short-term processes is mainly dependent on drift.

The genus *Proechimys* constitutes one of the best known cases of fast chromosomal speciation, which occurred during the Late Pleistocene in Venezuela with new species being characterised by increased diploid numbers, from 2n=42 to 2n=62 (AGUILERA *et al.* 1995, REIG *et al.* 1980). Genetic variation has been documented for this species complex (BENADO *et al.* 1979, PÉREZ-ZAPATA *et al.* 1992), as well as repetitive DNA and genome composition (GARAGNA *et al.* 1977). Moreover, traditional morphometrics (AGUILERA & CORTI 1994, CORTI

* Symposium presentation, 5th International Congress of Systematic and Evolutionary Biology, 1996, Budapest

& AGUILERA 1995) has suggested that size and shape changes in these species are consistent with the presumed phylogeny.

In this study we present a hypothesis for patterns of morphometric change in the skull that have characterised the evolution of some of these species based upon their genetic relationships (BENADO *et al.* 1979). Here we test the congruence between genetic and morphometric character sets, and between the two components of the skull analysed, i.e. dorsal and ventral, in order to ascertain whether or not they underwent the same kind of change during species evolution. This may provide information on rates of morphological evolution in cases of recent and fast speciation.

MATERIAL AND METHODS

Animals studied represent two species of the "*guairae*" complex, i.e. *P. guairae* (three subspecies included) and the undescibed *Proechimys* sp., and *P. trinitatis* (Fig. 1, Table 1). Divergence between *P. trinitatis* and the *guairae* complex occurred approximately 200,000 years before present, while divergence between species of the *guairae* complex is more recent, i.e. 50,000 yrs bp (BENADO *et al.*, 1979).

The 94 adult individuals examined come from the following collections: Colección de Vertebrados Terrestres – Universidad Simón Bolívar; Colección de la Estación Biológica de Rancho Grande; and Colección de Vertebrados de la Universidad de los Andes. Adults only were used (see AGUILERA & CORTI 1994).

Populations used were the same as in BENADO *et al.* (1979), with the exception of the 2n=48 *P. g. guairae* which, in our sample, is from the locality El Limon, approximately 150 km from the locality (San Antonio) sampled for genetic analyses. It should be remarked that *P. urichi* in BENA-

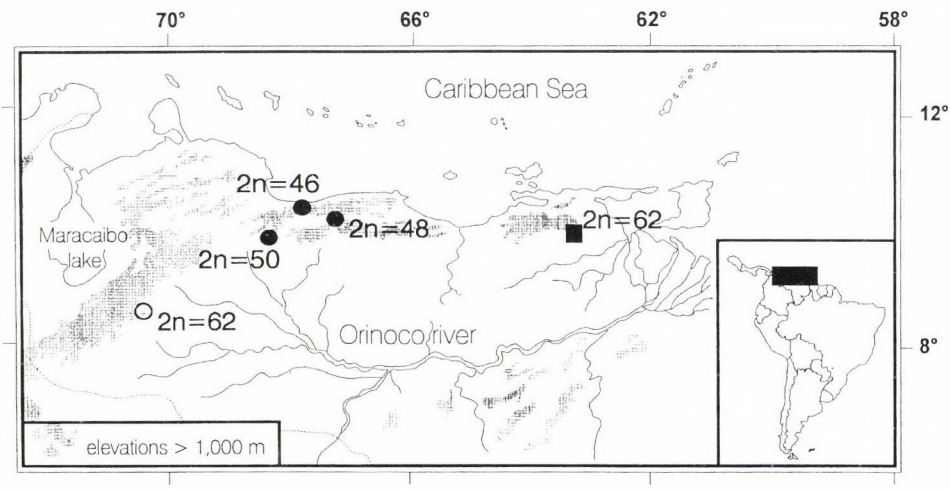

Fig. 1. Map of the northern part of South America with the locations of the species studied, with their diploid numbers. Filled circle = *P. guairae*; open circle = *Proechimys* sp.; filled square = *P. trinitatis*.

DO *et al.* (1979) is a junior synonym of *P. trinitatis* (AGUILERA *et al.* 1995), and that *Proechimys* sp. corresponds to the population of Barinitas in BENADO *et al.* (1979).

Images of the dorsal and ventral sides of the skulls were digitised with aid of a TV camera, and thirteen landmarks were collected for the dorsal and twenty two for the ventral side (Fig. 2, Table 2).

Table 1. Species, population, diploid number, geographic location and number of individuals used. The number of individuals for which sex is unknown is indicated into brackets

Species	2n	Population	Geographic location (latitude and longitude)	Males	Females	Total
P. guairae "Falcon"	46	La Trilla	10°24'N 67°45'W	9	8	17
P. g. guairae	48	El Limon	10°19'N 67°38'W	20	4	24
P. guairae "Llanos"	50	Palmero	9°44'N 68°34'W	5	7	12
Proechimys sp.	62	Barinitas	8°46'N 70°26'W	5	7	19 (7)
P. trinitatis	62	Cueva del Guacharo	10°10'N 63°33'W	10	12	22

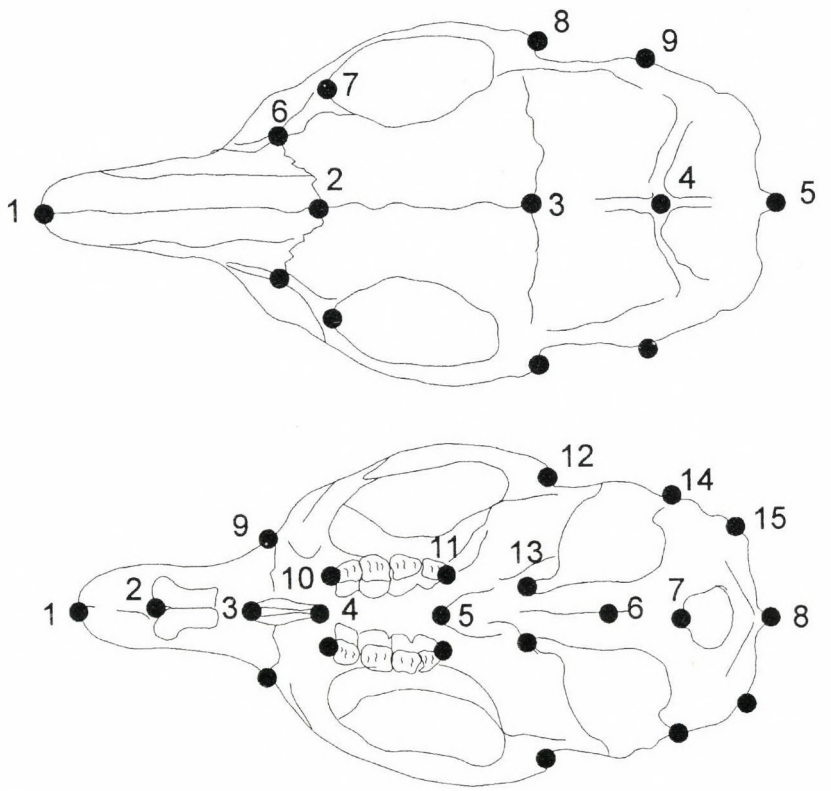

Fig. 2. Schematic drawing of the dorsal and ventral sides of the skull of *Proechimys* with the location of the landmarks collected. For landmarks description see Table 2

Table 2. Description of the landmarks collected on the dorsal and ventral sides of the skull. Numbers are as in Fig. 2.

Landmark	
DORSAL SIDE	
1	Prostion
2	Nasion
3	Bregma
4	Lambda
5	Opisthion
6	Foramen lacrimale
7	Inner anterior margin of the zygomatic arch
8	Posterior tip of the zygomatic arch
9	Posterior margin of the external acoustic opening
VENTRAL SIDE	
1	Prostion
2	Anterior margin of the incisive
3	Anterior margin of the palatine foramen
4	Posterior margin of the palatine foramen
5	Posterior edge of the palatine
6	Spheno-occipital synchondrosis
7	Basion
8	Opisthion
9	Infraorbital foramen
10	Anterior margin of M^1
11	Posterior margin of M^3
12	Posterior tip of the zygomatic arch
13	Muscular process
14	Posterior margin of the external acoustic opening
15	Paracondilar process

As the skull is a symmetrical structure, the left and right sides were averaged to avoid effects of lateral asymmetry. The new configurations were then reflected to obtain a complete representation of the skull for the visualisation of shape differences, with statistics performed on the averaged half configurations only.

Size is represented by the centroid size (the square root of the sum of the square of the distances between each landmark and the centroid, BOOKSTEIN 1991), and used to test for effects of sexual size dimorphism and to estimate size differences between populations and species.

Shape was represented by the Weight matrix of the Partial Warp Scores (ROHLF 1993*a*) to which the uniform component (BOOKSTEIN 1996) was appended. The consensus of each population was used to explore the overall diversity of shape in relation to the hierarchical arrangement of

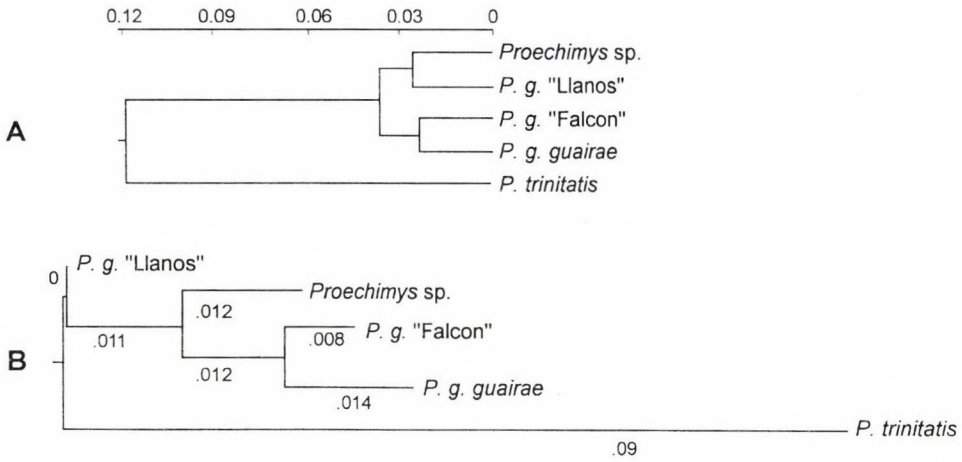

Fig. 3. Part A: UPGMA phenogram from NEI's genetic distances. Part B: Tree obtained using the Fitch-Margoliash Least Squares method; the tree has been outgroup rooted on *P. trinitatis*

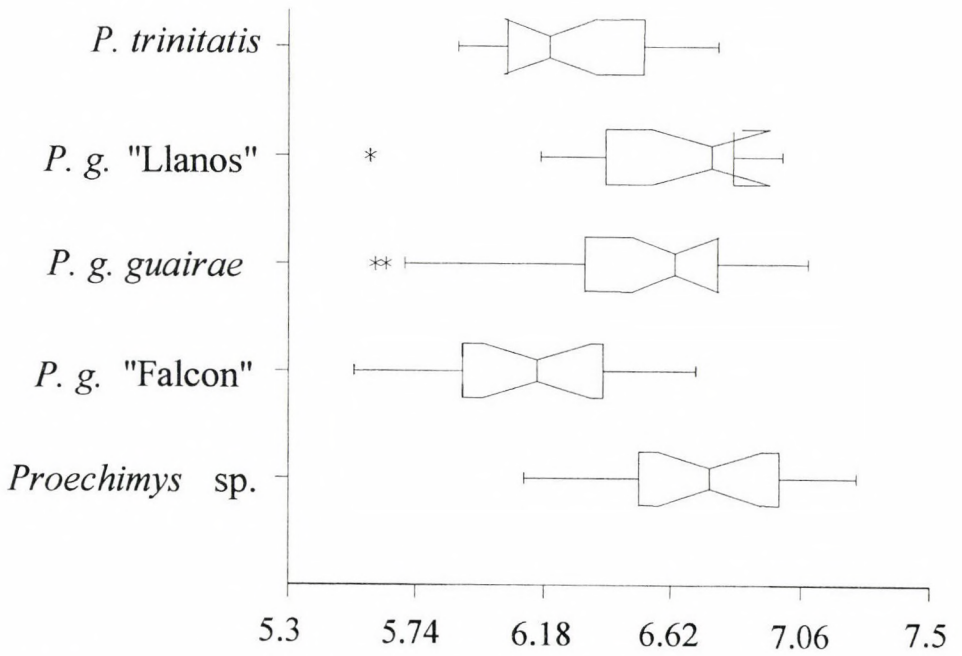

Fig. 4. Notched box plot of centroid size for the populations analysed. Medians are significantly different ($p < .05$) when the notches of the boxes do not overlap. Asterisks denote outliers. Note that *P. trinitatis* and *P. guairae* "Falcon" are significantly smaller than the other populations

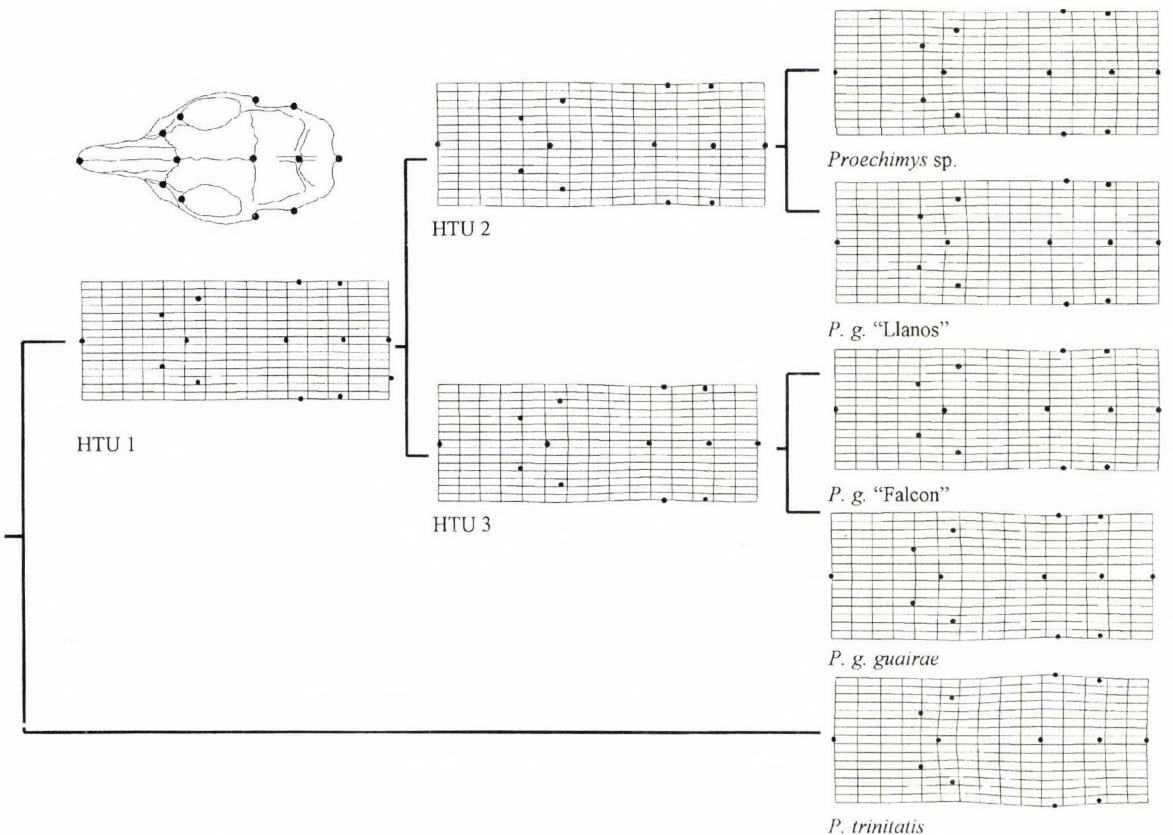

Fig. 5. Shape changes in the dorsal side of the skull (at the bottom left corner) shown as grid deformations from a thin-plate spline for all populations in the NEI's genetic distances UPGMA. Splines are ordered following the hierarchical arrangement of UPGMA phenogram in Fig. 3A. Thin-plate spline transformations are from the reference into those of each specimens. Splines of the internodes (HTUs 1, 2, 3) are computed by averaging the corresponding members of the cluster

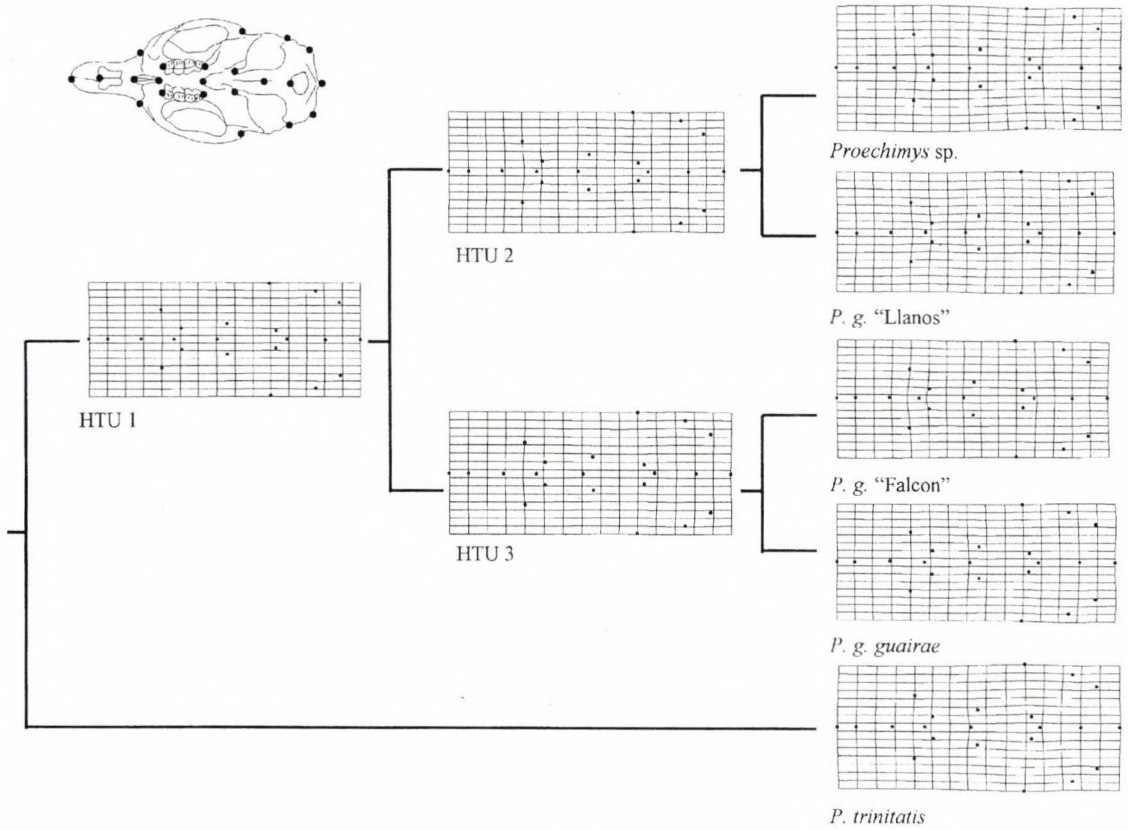

Fig. 6. Shape changes in the ventral side of the skull (at the bottom left corner) shown as grid deformations from a thin-plate spline for all populations in the NEI's genetic distances UPGMA. Splines are ordered following the hierarchical arrangement of UPGMA phenogram in Fig. 3A. Thin-plate spline transformations are from the reference into those of each specimen. Splines of the internodes (HTUs 1, 2, 3) are computed by averaging the corresponding members of the cluster

UPGMA based upon NEI's genetic distances (BENADO *et al.* 1979). Shape changes of taxa were shown as grid deformations from a thin-plate spline. Splines of the internal nodes were computed simply by averaging the corresponding members of the cluster.

The software MTV (UPTEGRAFF 1990–1993) was used for landmarks collection. The program GRF-ND (ver. 11–01–94, SLICE 1993) was used for the GLS procedure and to estimate centroid size, and the program TPSRW (ver. 10–2–93, ROHLF 1993*b*) to compute the weight matrix (ROHLF 1993*b*) and the uniform components (BOOKSTEIN 1996). The programs TpsTree (ver. 1.02, ROHLF 1996) was used to generate the UPGMA phenogram from NEI's genetic distances and to compute the thin-plate spline transformations from the reference into those of each taxon, including HTUs.

Programs GRF-ND, TPSRW and TpsTree are also available from the WWW server at http://Life.bio.SUNYSB.edu/morph/morph.html. All statistics were performed using the package SAS (ver. 6.11; SAS Institute Inc., 1996).

RESULTS

The UPGMA dendrogram derived from the NEI's genetic distances shows that *P. trinitatis* is the most differentiated (Fig. 3A). It has the highest genetic distances ($\overline{D} = 0.117$), while distances among populations of the *guairae* complex are lower (*D* value between 0.046 and 0.023). These latter form two clusters, one with the undescribed species *Proechimys* sp. and *P. guairae* "Llanos", the other with *P. g. guairae* and *P. guairae* "Falcon".

UPGMA clustering is in agreement with a chromosomal speciation hypothesis by increasing diploid number through centric fissions (REIG, 1980). Note that the hypothesis is relative to the *guairae* complex only, while the 2n=62 karyotype of *P. trinitatis* shows different and independent rearrangements (AGUILERA *et al.* 1995).

Since the correlation between centroid sizes of the two sides of the skull is very near to 1, the centroid size from the dorsal side was used for all statistical estimates.

There is no effect of sexual dimorphism in size as tested by two-way ANOVA (unbalanced design). However, populations display significant differences in size ($P < .001$), as also shown by the notched box plot (Fig. 4). *P. g.* "Falcon" and *P. trinitatis* are the smallest, with significant differences with the other populations, and *Proechimys* sp. is the biggest.

A multiple regression of the Weight matrix and the uniform component against centroid size did not show any significant pattern in both sides of the skull. Variation in size plays therefore no role in shape variation within the adult classes.

The Hotelling's T^2 test revealed that populations are all significantly different (at the .05 level) for both sides of the skull.

Major shape changes in the dorsal side between *P. trinitatis* and the *guairae* complex concern skull width at the insertion of the zygomatic arch, which is nar-

row at the rostral and larger at the squamosus part of the former (Fig. 5). The opposite tendency, i.e. a progressive enlargement at the base of the rostrum and a narrowing at the squamosus part, characterises the *guairae* complex line, starting from the internal node HTU 1 (Fig. 5). Further morphometric differentiation within the *guairae* complex concern the suture between frontal and nasal bones, with a shift backward occurring in *P. guairae* "Llanos" and *P. g. guairae*, therefore representing a parallelism.

Shape changes in the ventral side of the skull (Fig. 6) show patterns that are similar to the dorsal side. There is a process of lateral expansion at the base of the braincase, i.e. basisphenoid, pterygoids and palatines, occurring in *P. trinitatis*. The two lineages of the guairae complex (from HTUs 2 and 3) are characterised, respectively, by an incisive foramen shifted backwards and a fossa mesopterygoidea shifted forward. Further shape changes occurring in each species of the complex show some sort of parallelism as for the dorsal side, i.e. there is a lateral expansion of the rostral region in *Proechimys* sp. and *P. guairae* "Falcon", and a lateral expansion of the braincase in *P. guairae* "Llanos" and *P. g. guairae* (Figs 5 and 6).

Mantel comparisons between NEI's genetic distances and the dorsal and ventral Procrustes distances show that genetics is congruent with the dorsal shape variation ($r = .69$, $p = .015$) and not with the ventral one ($r = .07$, n.s.), although there is correspondence in shape change between the dorsal and ventral parts of the skull (matrix correlation between Procrustes distances is .51, $p = .05$). Procrustes distances of the ventral side of the skull increase rapidly in populations characterised by low genetic distances, and then even diminish as genetic distances increase (Fig. 7). On the contrary, the relations between genetic and dorsal Procrustes distances tend to be much more linear (Fig. 7).

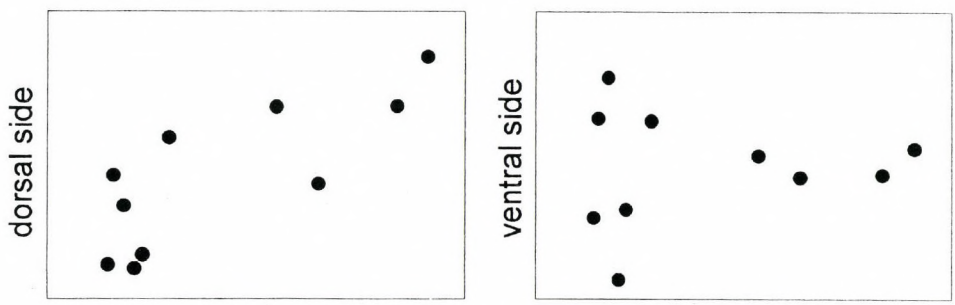

Fig. 7. Matrix plots between NEI's genetic distances (on the abscissa) and Procrustes distances for the dorsal (left) and ventral (right) sides of the skull

DISCUSSION

All these taxa occur in the same pedemontane habitat characterising the gallery forest below 1,000 m a.s.l., so that it is not possible to relate size and shape changes to adaptation for different environments. Previous studies (AGUILERA & CORTI 1994, AGUILERA 1995) invoked history (drift) as the main responsible for changes in morphometry, with possible additional effects from micro-niche shifts. Changes in morphology were therefore associated directly to the cladogenetic events of chromosomal speciation.

However, size variation across species is not consistent with the presumed phylogeny, although taxa show remarkable differences in size (Fig. 4). The taxa of the *guairae* complex are bigger with the exception of *P. guairae* "Falcon", which is even smaller than *P. trinitatis*. CORTI *et al.* (1998) have shown that all taxa of the *guairae* complex (not represented in this study) are bigger with few exceptions, so that the small size of *P. guairae* "Falcon" represents a parallelism with *P. trinitatis*.

Shape changes of the dorsal side of the skull are in agreement with the genetically based phylogeny but not those in the ventral side, as shown by the comparisons between distance matrices.

There are two main possible explanations on this concern: the mutation rate may be different in structural genes and morphology, and within each character system (e.g. the evolutionary forces acting on the structural subunits of the skull may differ in relation to their role in auditory, feeding, respiratory and olfactory functions).

The UPGMA clustering model adopted assumed that allozymes evolve at the same constant rate after speciation and that this kind of evolutionary clock occurs also in morphometric characters. Current assumptions consider that changes in morphology do not necessarily match those in allozymes (see for example AVISE 1994, WILSON *et al.* 1974), although, more recently, comparisons have shown that rates of molecular evolution are frequently correlated with rates of morphological evolution (OMLAND 1997). However, most of comparative studies did not focus on rates of morphological and genetic evolution in species complex where speciation, e.g. chromosomal, has been recent and rapid with little or none niche shift.

In *Proechimys*, fluctuating pressures of natural selection over morphology may have been unpredictable, with differential effects over the dorsal and ventral sides of the skull. Moreover, mutation rates in gene frequencies may have been different due to drift. A phylogenetic hypothesis with different adjusted branch lengths in the tree would be therefore more appropriate for comparison with morphological evolution.

As an example, we computed a tree using the Fitch-Margoliash least-squares approach (program Fitch of the PHYLIP package; FELSENSTEIN 1995), where pure drift without mutation was assumed to be responsible of change and the branch lengths are unconstrained (Fig. 3B). Except for *P. trinitatis*, the tree topology and the branch lengths are different from the UPGMA in Fig. 3A. However, the use of TpsTree program is limited to the 'evolutionary clock' hypothesis, so that the amount of morphological evolution represented in each branch length of the tree in Fig. 3B cannot be represented.

Finally, the different relationships between Procrustes distances from both sides of the skull and genetic distances shows how separate analyses of these two components of the skull can provide different information on species evolution. This would have been lost in a complete three-dimensional analysis of the entire skull, where it would have been difficult to locate the different contribution in terms of variation of the various subunits (see, as an example, FADDA & CORTI 1998), suggesting the need for new inquires into rates of morphological shape change during speciation.

REFERENCES

AGUILERA, M. & CORTI, M. (1994) Craniometric differentiation and chromosomal speciation of the genus Proechimys (Rodentia: Echimyidae). *Z. Säugetierkunde* **59**: 366–377.

AGUILERA, M., REIG, O. A. & PÉREZ-ZAPATA, A. (1995) G- and C-banding karyotypes of spiny-rats (Proechimys) of Venezuela. *Rev. Chil. Hist. Nat.* **68**: 185–190.

AVISE, J. C. (1994) *Molecular markers, natural history and evolution*. Chapman and Hall, New York, 520 pp.

BENADO, M., AGUILERA, M., REIG, O. A. & AYALA, F. J. (1979) Biochemical genetics of chromosome forms of Venezuelan spiny rats of the Proechimys guairae and Proechimys trinitatis superspecies. *Genetica* **50**: 89–97.

BOOKSTEIN, F. L. (1991) *Morphometric tools for landmark data*. Cambridge Univ. Press, Cambridge, 435 pp.

BOOKSTEIN, F. L. (1996) Standard formula for the uniform shape component in landmark data. Pp. 153–168. *In* MARCUS, L. F. *et al.* (eds): *Advances in Morphometrics*. NATO ASI Series A: Life Sciences, Vol. 284. Plenum Press, New York.

CAPANNA, E. & CORTI, M. (1991) Chromosomes, speciation and phylogeny in mammals. Pp. 355–370. *In* GHIARA, G. (ed.): *Symposium on the Evolution of Terrestrial Vertebrates. Selected Symposia and Monographs*. Mucchi, Modena.

CORTI, M. & AGUILERA, M. (1995) Allometry and chromosomal speciation of the casiraguas Proechimys (Mammalia, Rodentia). *J. Zool. Syst. Evol. Res.* **33**: 109–115.

CORTI, M., AGUILERA, M. & CAPANNA, E. (1998) Size and shape evolution in the skull of Proechimys (Rodentia). [submitted]

CORTI, M. & FADDA, C. (1996) Systematics of Arvicanthis (Rodentia, Muridae) from the Horn of Africa: A geometric morphometrics evaluation. *Ital. J. Zool.* **63**: 185–192.

FADDA, C. & CORTI, M. (1998) Geographic variation in Arvicanthis (Rodentia, Muridae) in the Nile Valley: a three dimensional geometric morphometrics evaluation. *Zeit. Säugetierkunde* **63**: 104–113.

FELSENSTEIN, J. (1995) PHYLIP. Phylogeny Inference Package, ver. 3.57c, University of Washington, Seattle.

GARAGNA, S., PÉREZ-ZAPATA, A., ZUCCOTTI, M., MASCHERETTI, S., MARZILIANO, N., REDI, C. A., AGUILERA, M. & CAPANNA, E. (1977) Genome composition in Venezuelan spiny-rats of the genus Proechimys (Rodentia, Echimyidae). I. Genome size, C-heterochromatin and repetitive DNAs in situ hybridization patterns. *Cytogenet. Cell Genet.* **78**: 36–43.

KING, M. (1993) *Species evolution. The role of chromosomal change.* Cambridge Univ. Press, Cambridge, 336 pp.

OMLAND, K. E. (1997) Correlated rates of molecular and morphological evolution. *Evolution* **51**: 1381–1393.

PÉREZ-ZAPATA, A., AGUILERA, M., & REIG, O. A. (1992) An allopatric karyomorph of the Proechimys guairae complex (Rodentia: Echimyidae) in Eastern Venezuela. *Interciencia* **17**: 235–240.

REIG, O. A. (1980) Modelos de especiacion cromosomica en las casiraguas (género Proechimys) de Venezuel. Pp. 149–190. *In* REIG, O. A. (ed.): *Ecologia y genética de la especiacion animal.* Equinoccio, Univ. S. Bolivar, Caracas, 295 pp.

ROHLF, F. J. (1993*a*) TPSRW. Thin Plate Spline Relative Warp. Software distributed at NATO A.S.I. 'Advances in morphometrics', July 1993, Italy.

ROHLF, F. J. (1993*b*) Relative warp analysis and an example of its application to mosquito wings. Pp. 131–190. *In* MARCUS, L. F. *et al.* (eds): *Geometrical Morphometrics.* Monografias Museo Nacional de Ciencias Naturales, Madrid, 264 pp.

ROHLF, F. J. (1996) TpsTree. Ecology and Evolution, Suny at Stony Brook, New York.

SAS Institute Inc. (1996) SAS/STAT Software: Changes and Enhancements through Release 6.11. Cary, NC.

SLICE, D. (1993) GRF-ND. Generalized rotational fitting of n-dimensional landmark data. Software distributed at NATO A.S.I. 'Advances in morphometrics', July 1993, Italy.

UPTEGRAFF, G. (1990–1993) MTV, *Measurement TV*, ver. 1.81, San Clemente, CA 92672.

WILSON, A. C., SARICH, V. M. & MAXSON, L. R. (1974) The importance of gene rearrangement in evolution: evidence from studies on rate of chromosomal, protein and anatomical evolution. *Proc. Natn. Acad. Sci. USA* **71**: 3028–3030.

Acta Zoologica Academiae Scientiarum Hungaricae 44 (1–2), pp. 151–164, 1998

A PARAPATRIC CONTACT AREA BETWEEN TWO SPECIES OF MOLES: CHARACTER DISPLACEMENT INVESTIGATED THROUGH THE GEOMETRIC MORPHOMETRICS OF SKULL*

LOY, A. and E. CAPANNA

Dipartimento di Biologia Animale e dell'Uomo
Università di Roma 'La Sapienza', 50 Via Borelli, 00161 Rome, Italy
E-mail: annaloy@caspur.it

Character displacement is investigated in sympatric populations of two related species of European moles, *Talpa europaea* and *T. romana*, along the zone of parapatric contact in Central Italy. Morphological variation of the two species is analysed through the geometric morphometrics of skulls by comparing sympatric to allopatric populations. The morphometric approach enabled us to consider separately the effect of size and shape on character displacement, while the analysis of relative warps allowed us to recognise and visualise specific regions of the skull involved in the phenomenon. Results suggest that size and shape can play a role in the local differentiation of the two species. Differences in size are sharper in the sympatric populations, while shape differences possibly related to character displacement are expressed by few relative warps in both the dorsal and the ventral view of the skull. Morphological features involved are concentrated in the zygomatic region, thus suggesting that character displacement is mainly related to the efficiency of food assumption and processing.

Key words: character displacement, geometric morphometrics, *Talpa*, Italy

INTRODUCTION

Moles are strictly fossorial insectivores widespread throughout the Holartic. Phylogenetic relationships among the European species belonging to the genus *Talpa* have been recently investigated with genetic, cytogenetic and morphometric analyses (KRATOCHVIL & KRAL 1972, CAPANNA 1981, FILIPPUCCI *et al.* 1987, RAMALHINO 1985, CORTI & LOY 1987, LOY *et al.* 1994). These studies definitely ascertained the occurrence of five distinct species: the widespread common mole (*Talpa europaea* L.), whose range extends to Europe and Asia; the blind mole *Talpa caeca*, confined to southern Europe, and three species occurring in peripheral regions of the genus range, i.e. *T. occidentalis* in Spain and Portugal, *T. romana* in Italy, and *T. stankovici* in the Balkans. This peculiar dis-

* Symposium presentation, 5th International Congress of Systematic and Evolutionary Biology, 1996, Budapest

tribution, coupled with the high genetic distances found between *T. europaea* and the last three taxa (FILIPPUCCI *et al.* 1987) suggests that *T. occidentalis*, *T. romana* and *T. stankovici* originated during the earlier Pleistocene glaciation, as the results of diversification in isolated southern European refuges (LOY 1992). Three of the European species occur in Italy: *T. caeca*, limited to the mountain areas; *T. europaea* occurring in north-central Italy, with a parapatric distribution with respect to *T. romana*, whose range is restricted to south-central Italy (Fig. 1). These last two species are morphologically very similar, and the only diagnostic character is represented by the shape of the upper molars, whose mesostyle is always bifid in *Talpa romana*, and only sometimes in *Talpa europaea* (CAPANNA 1981). Moreover, *T. romana* is usually bigger, but variation in size occurs throughout the range of the species (LOY *et al.* 1996). Following the discovery of sympatric populations of *Talpa europaea* and *Talpa romana* along their parapatric contact zone in Central Italy (FILIPPUCCI *et al.* 1987) we started extensive work in the area to clarify ecological and systematic relationships between the two species. In this paper we report first results of morphometric analyses carried out on the two sympatric populations and on three allopatric samples. Analyses were specifically directed to detect any evidence of character displacement that could be interpreted as an indication of competitive interactions between the two species. Geometric morphometrics of the skull (BOOKSTEIN 1991, 1996*a*) was used to explore shape and size differences among and within sympatric populations, following the high efficiency revealed by this approach in the description of intra- and inter-specific relationships among Talpidae (LOY *et al.* 1993, 1996, ROHLF *et al.* 1996).

MATERIAL AND METHODS

We analysed 102 adult moles belonging to five samples from Central Italy (three populations of *T. romana* and two of *Talpa europaea*, Fig. 1 and Table 1). Sixty-three moles were ex-

Table 1. List of *Talpa* material examined (102 specimens in total, 58 males and 44 females). For moles not captured in the field, the numbers superscript indicate the provenience of material (1 – Museo di Anatomia Comparata, University of Rome 'La Sapienza'; 2 – Museo La Specola, Firenze)

Species	Locality	Sample size
T. romana	Assisi	27 (10 males, 17 females)
T. romana	Roma[1]	15 (10 males, 5 females)
T. romana	Paliano[1]	5 (1 male, 4 females)
T. europaea	Assisi	33 (16 males, 17 females)
T. europaea	Barbano[2]	22 (21 males, 1 female)

pressly captured in the sympatric area, located in a hilly area near Assisi (Perugia), along the parapatric contact boundary of the two species. Moles were captured following a north to south transect intersecting the syntopic site reported by FILIPPUCCI *et al.* (1987), and crossing a variety of habitats, including open fields, cultivation, olive groves, and pastures. Skulls were prepared by papain digestion, while stomachs were preserved in formalin for bromathological analyses, and the carcasses frozen at -21°C for further genetic analyses (still in progress), which also allowed the correct classification of specimens. The remaining 42 skulls belong to three allopatric populations from Central Italy, one of *Talpa europaea* and two of *Talpa romana*, and were obtained from various museum collections (see Table 1 for details).

Morphometric analyses were run by recording 21 and 27 landmarks on the dorsal and the ventral view of the skull, respectively (Fig. 2, Table 2). Cartesian *x* and *y* co-ordinates of each landmark were collected by placing the skull under a video-camera connected to a monitor and a computer, using the program MTV (UPTERGRAFF 1990–1993). To rapidly detect recording errors, landmark configurations were first superimposed and visualised through GRF-ND software (SLICE 1993). To avoid the effect of lateral asymmetry, fixed original ASCII coordinate files were rotated by using a SAS (1985) procedure written by CARLO FADDA at the University of Rome, and the left and the right side of each skull were averaged. Centroid sizes and the U1 and U2 uniform components of shape (BOOKSTEIN 1996*b*) were extracted from the whole configurations through the TPSRELW program (ROHLF 1993). In contrast, only half configurations were used for subsequent statistical estimates, and resulting deformation grids were graphically reflected through Harvard Graphics (1991–1993) to obtain a complete representation of the skull for the visualisations of shape differences in the multivariate space. Half configurations were superimposed by using the General Least Square Procustes procedure (ROHLF & SLICE 1990) in the TPSRELW program

Fig. 1. Sample localities and distribution range of *Talpa europaea* and *Talpa romana* in Italy

Fig. 2. Landmarks recorded on the dorsal (above) and the ventral (below) projections of the skull. See Table 2 for detailed description of each landmark

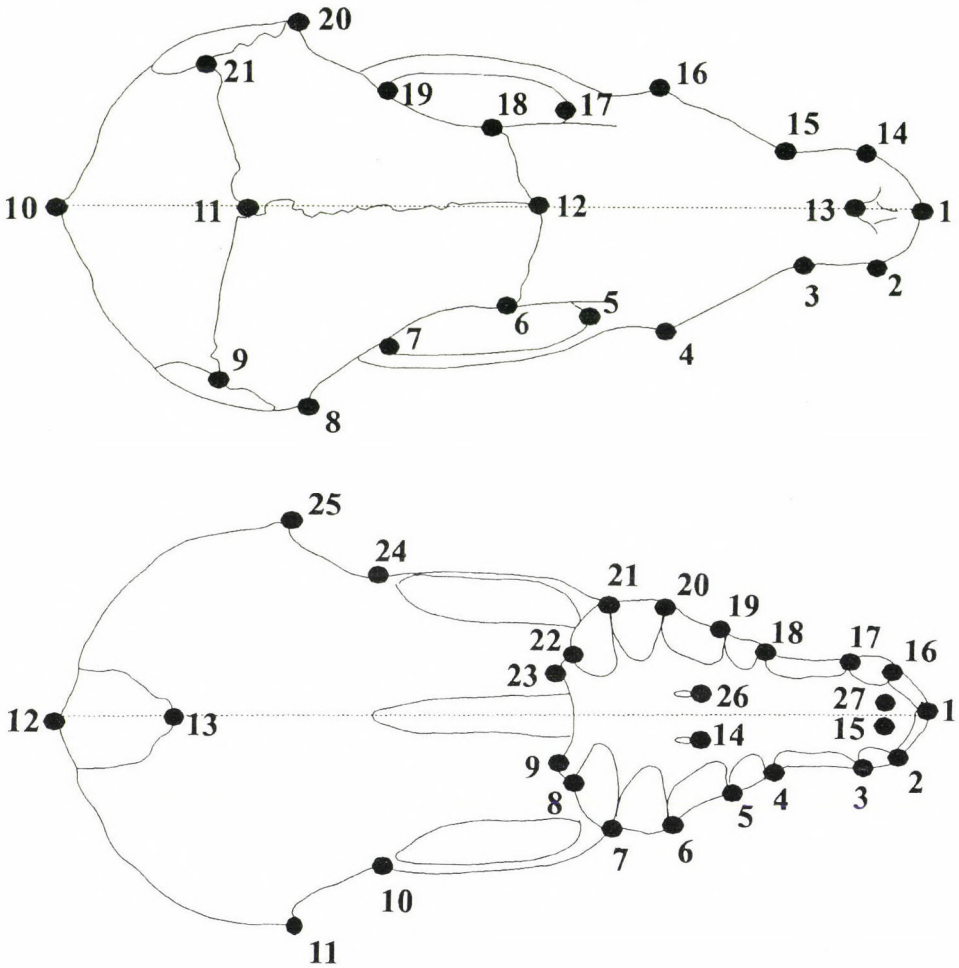

(ROHLF 1996*a*). In both cases the alpha value was set to 0, as recommended for exploratory analyses (ROHLF 1996*b*). Since sexual dimorphism did not show any effect on shape variation, as already assessed in other studies (LOY *et al.* 1993, 1996), sexes were considered separately only in the analysis of size variation. Ordination of specimens was obtained through the relative warp analysis of the residuals from superimposition (partial warp scores), through the TPSRELW programs. Relative warp scores, centroid sizes and uniform factors were then imported into the program STATISTICA (1993) to produce graphic plots and to run additional statistics. Relative warp scores and related grids were first plotted to elucidate shape differences among species. Population means of each relative warp were then examined in order to find out any pattern related to character displacement. Shape relationships between populations along the selected relative warp axes were visualised through the deformation grids extracted by pointing at the mean of each population in the relative warp space defined by the whole sample through the TPSRELW program.

Table 2. Description of the landmarks recorded on the dorsal and the ventral projections of the skull. Numbers are those reported in Fig. 2.

DORSAL	
1	Prosthion
2–14	Points of maximum curvature of the rostrum
3–15	Points of minimum breadth of rostrum
4–16	Points of maximum breadth of maxillar bone
5–17	Inner anterior point of curvature of the zygomatic arch
6–18	Intersection of coronal suture with the outline
7–19	Inner posterior point of curvature of the zygomatic arch
8–20	Points of maximum breadth of the braincase
9–21	Asterion
10	Opisthocranium
11	Lambda
12	Bregma
13	Nasion
VENTRAL	
1	Prosthion
2–16	Anterior margin of canine
3–17	Posterior margin of canine
4–18	Anterior margin of premolar row PM^{1-3}
5–19	Posterior margin of PM^4
6–20	Posterior margin of M^1
7–21	Posterior margin of M^2
8–22	Posterior margin of M^3
9–23	Posterior tips of pterigoids
10–24	Anterior margin of acoustic phoramen
11–25	Points of maximum breadth of the braincase
12	Opisthion
13	Basion
14–26	Maxillar foramina
15–27	Incisive foramina

RESULTS

Size variation. Centroid size variation of populations reveals that size represents a clear distinctive traits for the two species (Fig. 3), *T. romana* being signi-

Fig. 3. Box plots of centroid size for the five populations analysed (adult males only, from data on the ventral projection). Assisi is the sympatric locality. Upper and lower bars represents the mean plus and minus standard deviation respectively

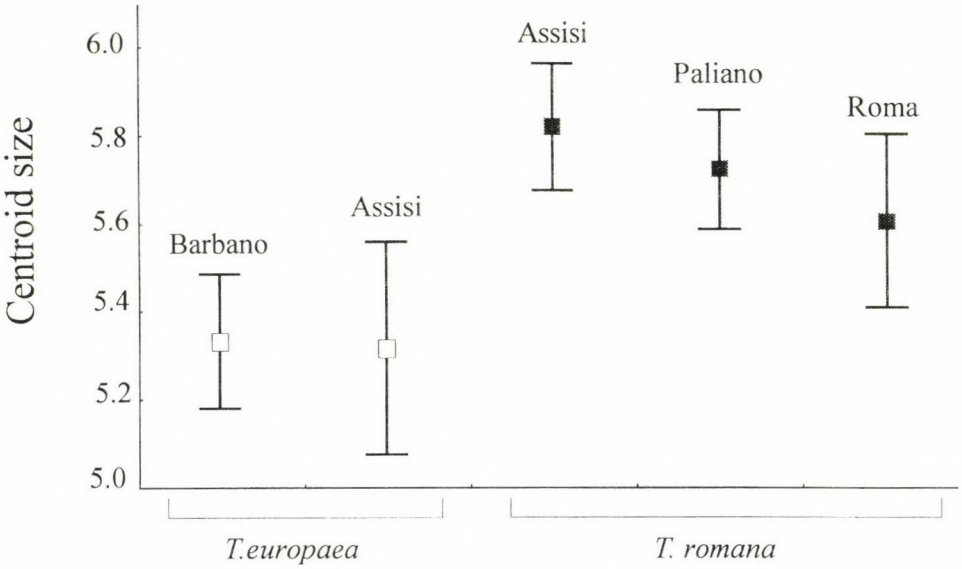

ficantly bigger than *T. europaea* (mean CS = 5.71 for *T. romana*; mean CS = 5.33 for *T. europaea*; *t*-test = – 10.957, $p < 0.0001$). The ratio of mean centroid size between the two species is 1.07; this value increases to 1.09 when considering only the two sympatric populations. Also, an opposite trend can be observed for the two species, with major size differences found between the two sympatric populations. This trend is only in part confirmed by the statistical inference, since only the mean centroid sizes of the three populations of *T. romana* differ significantly ($F^{CS} = 9.42$, $p < 0.0016$), while the two populations of *T. europaea* do not show any significant difference ($F^{CS} = 0.77$, $p < 0.38$).

Shape variation. The uniform components U1 and U2 do not contribute to species discrimination (Wilk's lambda = 0.968, $p = 0.515$), while the first relative warp computed on the residuals clearly differentiate *T. romana* and *T. europaea* in both the ventral (13.9% of total variation, including the uniform part) and the dorsal (41.09% of total variation) projection of the skull (Fig. 4). For the dorsal projections also the second relative warp (22.9% of total variation) also contributes to species discrimination. Deformation grids associated with the mean of each species along these axes reveal that shape differences are mostly related to the relative extension of the braincase, the zygomatic region, and the palatal bones, and within the latter, to the relative extension and width of the rostrum. As it is particularly evident from the dorsal view of the skull, the braincase in *T. eu-*

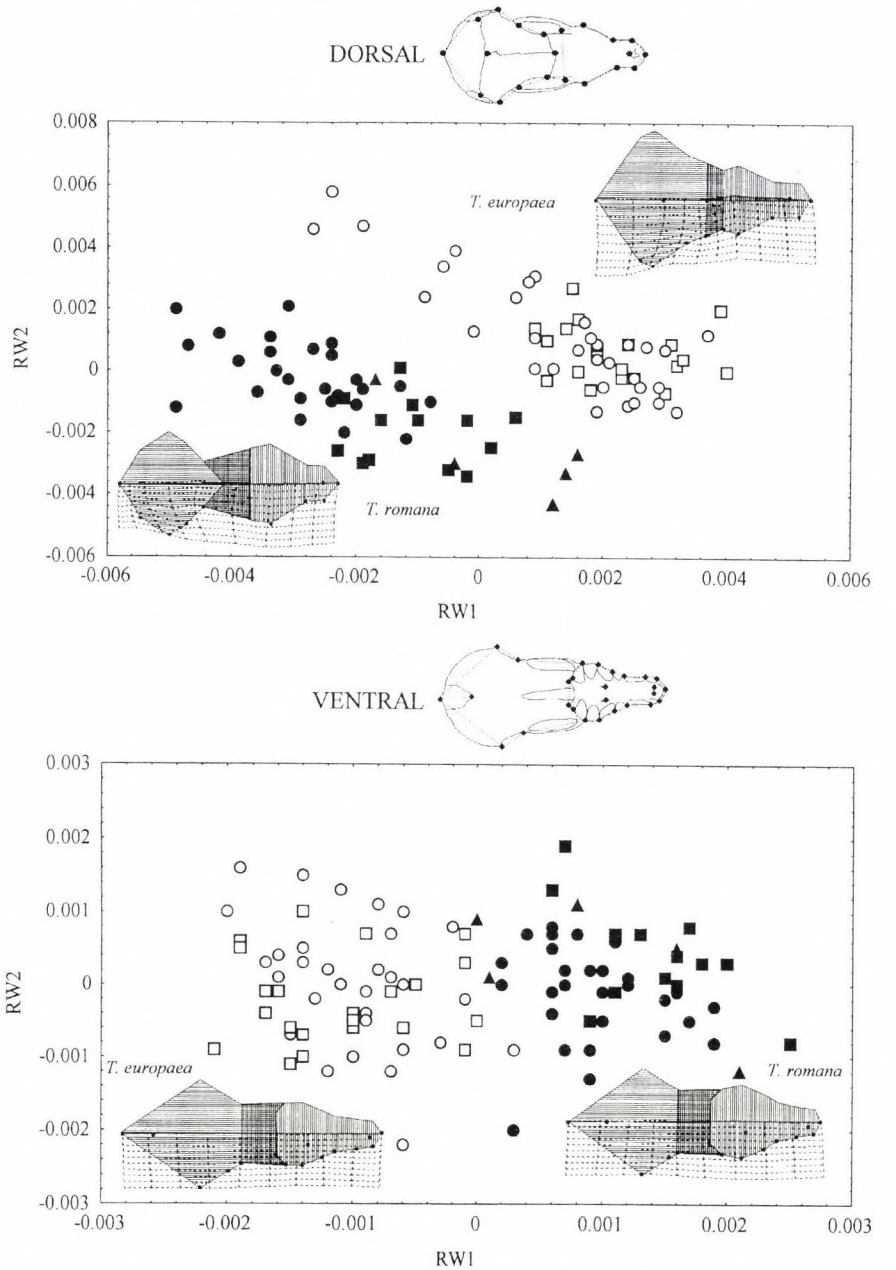

Fig. 4. Ordination of specimens along the first two relative warps, for the dorsal (top) and the ventral (bottom) projections of the skull. Deformation grids were derived by pointing at the mean values on RW1 and RW2 for each species in the TPSRELW program (ROHLF 1996*a*). Half configurations were then reflected through the graphic software Harvard Graphics. Empty circles = *T. europaea* from Assisi; filled circles = *T. romana* from Assisi; empty squares = *T. europaea* from Barbano; filled squares = *T. romana* from Roma; filled triangles = *T. romana* from Paliano

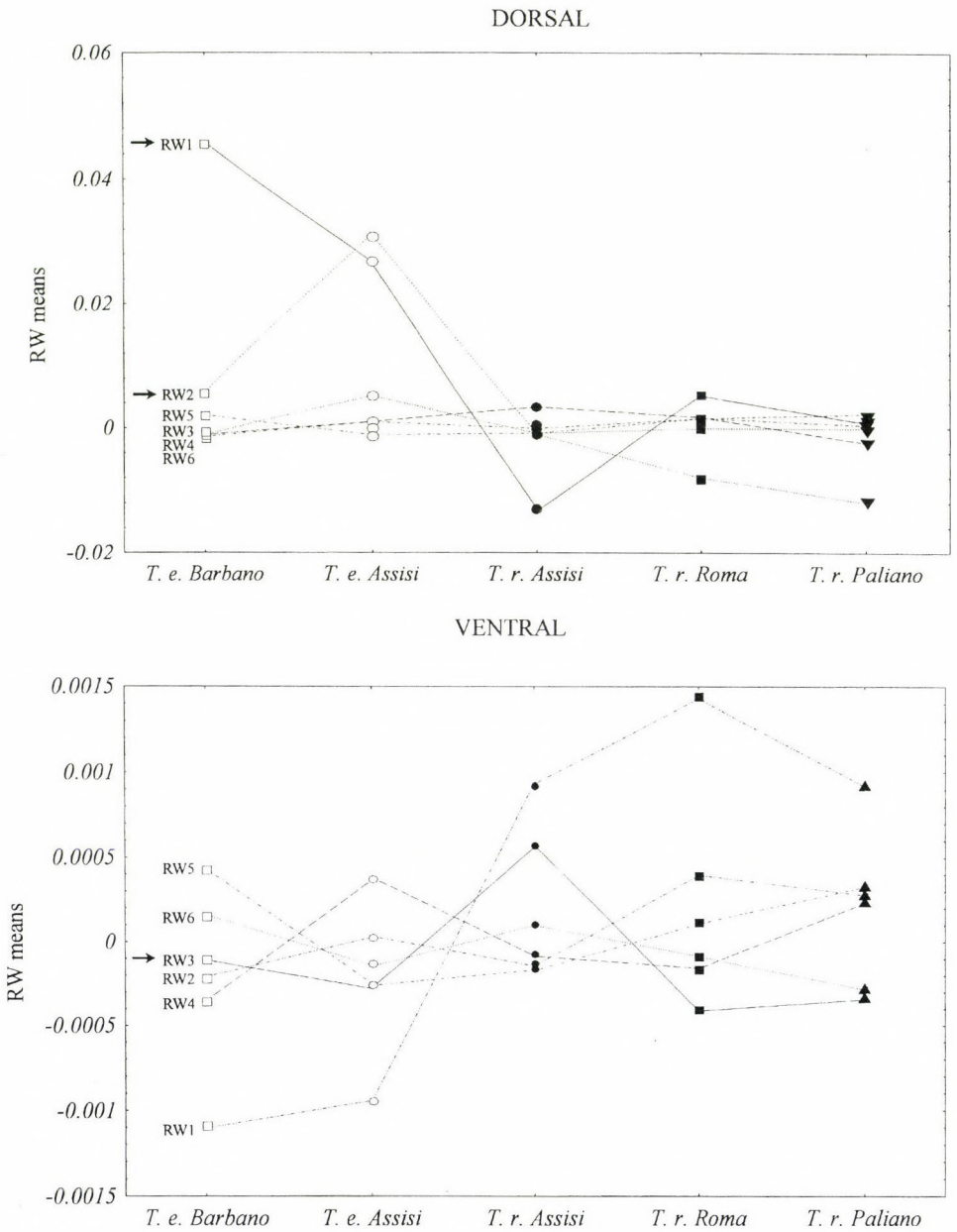

Fig. 5. Population means for the first six relative warps for the dorsal (top) and the ventral (bottom) projections. Means are plotted following a geographic cline from north to south. Arrows indicate relative warps which show a characteristic pattern of character displacement relatively to the sympatric populations (Assisi). The remaining relative warps are not shown, since they did not exhibited any specific pattern, and their addition would have caused confusion in the plot. *T. e.* = *T. europaea*; *T. r.* = *T. romana*

Table 3. Mahalanobis squared distances derived from canonical variate analysis on the first six relative warp scores (84.14% of total variation) for the dorsal projection of the skull. T. e. = *T. europaea*; T. r. = *T. romana*

	T. e. – Assisi	T. e. – Barbano	T. r. – Assisi	T. r. – Paliano	T. r. – Roma
T. e. – Assisi	–				
T. e. – Barbano	3.28	–			
T. r. – Assisi	19.22	15.39	–		
T. r. – Paliano	2.84	1.84	13.0	–	
T. r. – Roma	5.0	2.9	10.9	1.42	–

ropaea is much wider with respect to the palatal area, while in *T. romana* the two regions are mostly equivalent (Fig. 4, top). Moreover, *T. europaea* is characterised by a longer rostrum with respect to *T. romana*, while the latter has a more elongated zygomatic region.

In order to find out any shape displacement related to sympatric conditions, all relative warps were examined by plotting the population means of each relative warp according to their geographic location. Only few relative warps for each projection show a characteristic pattern (Fig. 5), with one or both sympatric populations highly different from the allopatric ones: the dorsal RW1 and RW2 (accounting for 41.09 % and 22.90 of total variance respectively), and the ventral RW3 (8.47% of total variation). F tests among populations are significant for all factors, with a highest value for the ventral RW3 (dorsal $F^{RW1} = 64.965$, $p < 0.001$; ventral $F^{RW3} = 9.25$, $p < 0.001$). Canonical variate analysis run on the first six relative warp scores for the dorsal view confirms the separation of populations, as shown in Table 3. The results of Tukey HSD tests for unequal sample sizes run on all pair of population comparisons for the dorsal RW1 and the ventral RW3 means are presented in Table 4. Highest differences are found between the two sympatric populations, with values always significant at $p < 0.0001$. Shape changes related to variation along the dorsal RW1 and RW2 and the ven-

Table 4. Probability levels from the Tukey HSD test for unequal sample sizes from post hoc comparisons between the ventral RW3 (below the diagonal) and the dorsal RW1 (above the diagonal) populations means. Differences significant at $p < 0.05$ are marked with an asterisk. T. e. = *T. europaea*; T. r. = *T. romana*

	T. e. – Assisi	T. e. – Barbano	T. r. – Assisi	T. r. – Paliano	T. r. – Roma
T. e. – Assisi	–	0.074	0.00011*	0.792	0.00016*
T. e. – Barbano	0.9245	–	0.00011*	0.130	0.00011*
T. r. – Assisi	0.0001*	0.0061*	–	0.00081*	0.0013*
T. r. – Paliano	0.9997	0.9772	0.1685	–	0.406
T. r. – Roma	0.9660	0.6753	0.0006*		–

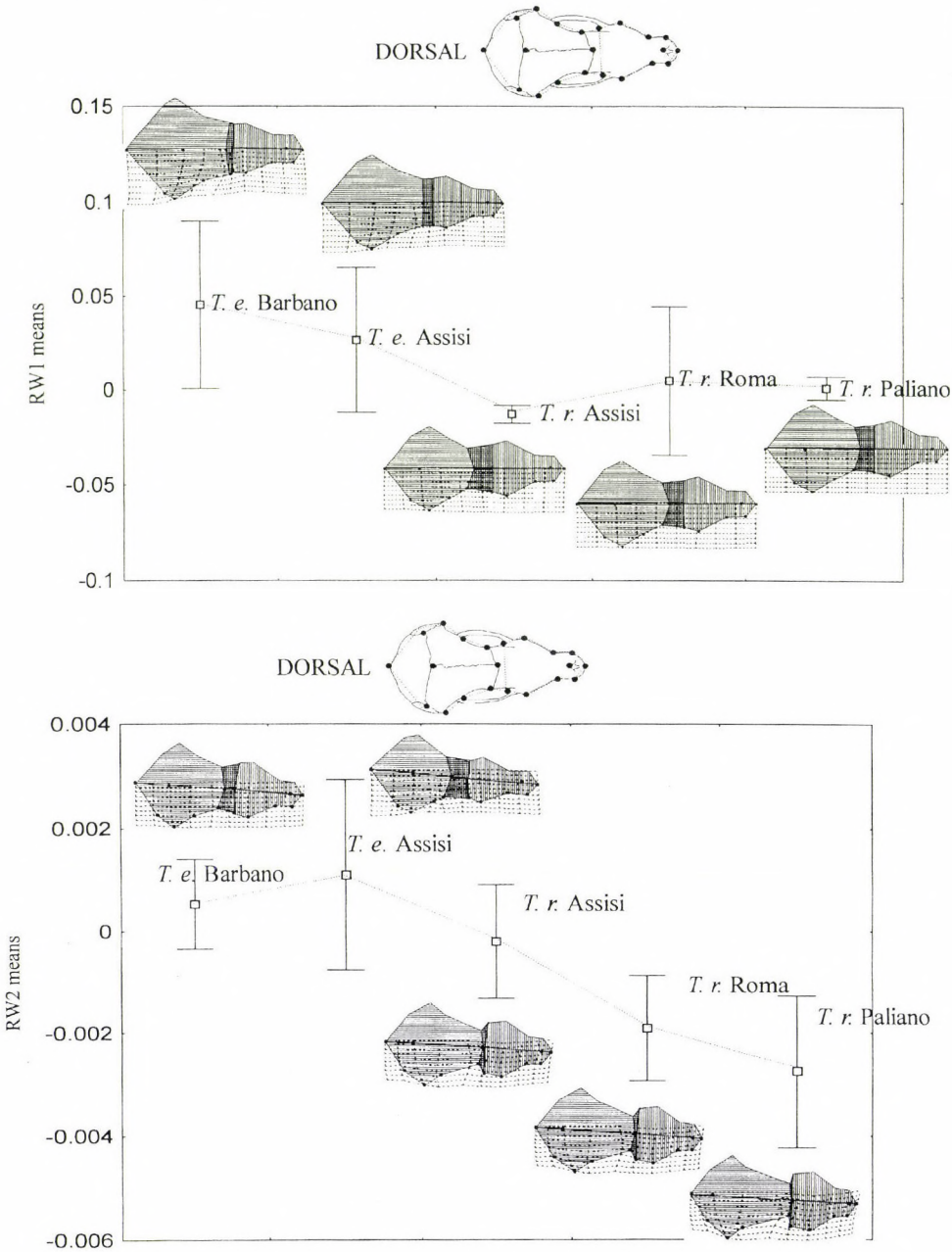

Fig. 6. Deformation grids related to variation along the dorsal RW1 (top), RW2 (bottom) and the ventral RW3 (facing page) population means, which show shape changes related to character displacement. Deformation grids for each population were produced through the TPSRELW program (ROHLF 1996*a*), by pointing at the population means for the corresponding relative warp scores. Half configuration were graphically reflected through Harvard Graphics. *T. e.* = *T. europaea*, *T. r.* = *T. romana*

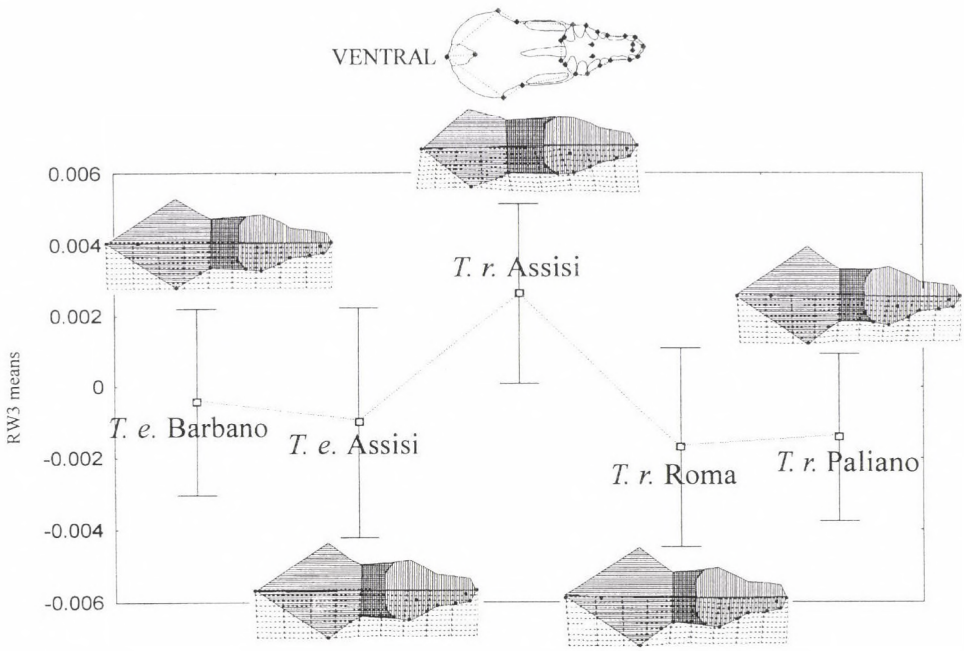

tral RW3 were then produced by visualising the deformation grids associated to the mean relative warp values for each population in the program TPSRELW (Fig. 6). The two species appear to respond differentially to sympatric conditions. Specifically the shape of the skull of *Talpa romana* tends to stress the typical *romana* shape: the braincase appears much narrower and the zygomatic arch more extended compared to the allopatric populations, both in the dorsal and in the ventral projections. Against our expectations, the shape changes along the dorsal RW2 reveals that the sympatric population of *T. europaea* shows the same tendency to the elongation of the zygomatic arch with respect to the allopatric one, as it is shown in *T. romana*.

DISCUSSION

The analysis of sympatric populations of *T. romana* and *T. europaea* revealed a different role played by the three components of variation (size, uniform and non-uniform) in the differentiation of sympatric populations. Size shows a clear evidence of character displacement, with major differences found between sympatric populations with respect to the allopatric ones. But the size ratio between the two sympatric populations is 1.09, which is less than the standard value

of 1.3 considered as the minimum degree of morphological divergence necessary to permit species coexistence under most conditions (HUTCHINSON 1959, PIANKA 1976, MAIORANA 1978), although the 1.3 rule has been contested by various authors (see for example SIMBERLOFF & BOECKLEN 1981, DAYAN *et al.* 1989). Since LOY *et al.* (1996) showed that size variation of *Talpa romana* follows a typical geographic cline, the phenomenon observed could be the result of different processes. It can be explained either as the result of competitive interactions, i. e. size shifting occurred through coevolution among competitors as a typical character displacement phenomenon (WAKE 1992), or it merely represents the extreme of a cline assessed independently, as the result of historical or ecological factors other than competition with *T. europaea*.

Although a few relative warps show greater differences between species for their sympatric populations than for their allopatric ones, they do suggest that competition plays a role in the local differentiation of the two species. Since the subterranean environment is mostly constant and characterised by few parameters that could affect interspecific competition (NEVO 1987), food may in fact represent the most limiting factor affecting the spatial distribution and abundance of moles (STONE 1990, BEOLCHINI *et al.* 1996). Characters involved in the local differentiation of the two species appear in fact to be strictly related to feeding activities. Character shifting is particularly evident in *Talpa romana*, in which the traits typically involved in the distinction from *Talpa europaea* (see Fig. 4) show the greatest emphasis in the sympatric population. These traits include the extreme elongation of the zygomatic bar, obtained through the dorsal shortening of the braincase, as the bregma and the lambda move posteriorly. This shortening is the result of the reduction of the parietals and the occipitals and of the extension of the frontal bones. The elongation of the zygomatic bar is also accompanied by the narrowing of the sphenoidal region, thus enlarging the opening of the temporal fenestra. The zygomatic bar represents the area of insertion of the muscular band of the deep masseter, while the temporal fenestra delimits the area containing the mass of the temporal muscle. Since both muscles take part in the complex movements of the mandible during chewing, an extension and enlargement of the zygomatic area leads to the expansion of the area on insertion of both muscles, thus increasing the efficiency of biting, grinding and chewing. The same tendency toward the elongation of the zygomatic region is also evident in the sympatric population of *Talpa europaea* with respect to the allopatric one, but in this case the sympatric population shows an opposite trend with respect to characteristic traits of the species (see Fig. 4).

These arguments suggest that in both species character shifting of the sympatric populations tends toward an increasing efficiency of food acquisition and processing. Whether this increased efficiency implies an extension of the spectrum of preys, i. e. an extension of the trophic niche of the species, or whether it

is directed toward a more effective exploitation of the same trophic niche, it can not be stated at present, due to the lack of information on the trophic niche of the two species in Italy. In fact much of the information available on the diet and food preference in the moles refer to *T. europaea* (SKOCZEN 1966, OPPERMANN 1968, FUNMILAYO 1977, STONE 1992), while very little is known on the diet of *T. romana*, the only available data being those collected by one of the authors in some localities of the species range (LOY 1992). These first data suggest that *T. romana* is a more opportunistic feeder with respect to *T. europaea*, that does not necessarily depend upon the availability of earthworms, and whose diet includes a wider prey spectrum with respect to that of *T. europaea*. Future analyses of the stomach contents of the sympatric specimens and of their habitat preference, which are still in progress, will likely help in the validation of alternative hypotheses and in the further clarification of ecological interactions between the two species.

* * *

Acknowledgements – Our gratitude goes to FRED BOOKSTEIN and CHRISTIAN PETER KLINGENBERG for their helpful comments and suggestions that contributed to improve the manuscript and to accomplish the objectives of this study. LESLIE F. MARCUS friendly encouraged the prosecution of the work, while FRANCESCA BEOLCHINI, SIMONA MARTULLO and ANTONELLA PALOMBI provided most of the sympatric specimens. The work was supported by the Ministero della Ricerca Scientifica and by the Consiglio Nazionale delle Ricerche, project N. 95.02178.CT04.

REFERENCES

BEOLCHINI F., DUPRE, E. & LOY, A. (1996) Territorial behaviour of Talpa romana in two different habitats: food resources and reproductive needs as potential causes of variation. *Z. Säugetierkunde* **61:** 193–201.

BOOKSTEIN, F. L. (1991) *Morphometric tools for landmark data.* Cambridge University Press, New York, 435 pp.

BOOKSTEIN F. L. (1996*a*) Biometrics, biomathematics and the morphometric synthesis. *Bull. Math. Biology* **58**(2): 313–365.

BOOKSTEIN F. L. (1996*b*) A standard formula for the uniform shape component in landmark data. Pp. 153–168. *In* MARCUS, L. F. *et al.* (eds): *Advances in Morphometrics.* NATO ASI Series, Vol. 284. Plenum Press, New York.

CAPANNA E. (1981) Cariotype et morphologie cranienne de Talpa romana de terra typica. *Mammalia* **45:** 71–82.

CORTI M., LOY, A., AZZAROLI M. L. & CAPANNA, E. (1987) Multivariate analysis of osteometric traits of Southern European moles (Insectivora, Talpidae). *Boll. Zool.* **54:** 187–191.

DAYAN, T., SIMBERLOFF D., TCHERNOV, E. & YOM-TOV Y. (1989) Inter- and intraspecific character displacement in mustelids. *Ecology* **70**(5): 1526–1539.

FILIPPUCCI M. G., NASCETTI, G., CAPANNA, E. & BULLINI, L. (1987) Allozyme variation and systematics of European moles of the genus Talpa (Mammalia, Insectivora). *J. Mammalogy* **68**(3): 487–499.

HARVARD GRAPHICS (1991–1993) Version 2.0. Software Publishing Corporation.

HUTCHINSON G. E. (1959) Homage to Santa Rosalia, or why there are so many kinds of animals? *Am. Nat.* **93:** 145–159.

LOY, A. (1992) Biologia evolutiva delle talpe europee (genus Talpa, Mammalia, Insectivora, Talpidae). Ph. D. Dissertation. University of Rome 'La Sapienza', 148 pp.

LOY, A., CORTI M. & MARCUS, L. F. (1993) Landmark data: size and shape analysis in systematics. A case study on Old World Talpidae (Mammalia, Insectivora). Pp 215–240. *In* MARCUS L. F. *et al.* (eds): *Contribution to Morphometrics.* Monographias 8, Museo Nacional de Ciencias Naturales, 264 pp.

LOY, A., CAPOLONGO, D. & DI MARTINO, S. (1996) Patterns of geographic variation of Talpa romana Thomas (Insectivora, Talpidae). Preliminary results derived from a geometric morphometric approach. *Mammalia* **60:** 77–89.

MAIORANA, V. C. (1978) An explanation of ecological and developmental constants. *Nature* **273:** 375–377.

OPPERMANN J. (1968) Die nahrung des Maulwurfs (Talpa europaea L., 1758) in Unterschiedlichen Lebensraumen. *Pedobiologia* **8:** 59–74.

PIANKA, E. R. (1976) Competition and niche theory. Pp. 114–141. *In* MAY, R. M. (ed): *Theoretical ecology.* Saunders, Philadelphia.

ROHLF, F. J. (1996*a*) TPSRELW – Thin plate spline relative warp. Version 1.0, Stony Brook, New York.

ROHLF F. J. (1996*b*) Morphometric spaces, shape components and the effects of linear transformations. Pp. 117–129. *In* MARCUS, L. F. *et al.* (eds): *Advances in Morphometrics.* NATO ASI Series, vol. 284, Plenum Press, New York.

ROHLF, F. J. & SLICE, D. (1990) Extensions of the Procustes method for the optimal superimposition of landmarks. *Syst. Zool.* **39:** 40–59.

ROHLF, F. J., LOY, A. & CORTI, M. (1996) Morphometric analysis of Old World Talpidae (Mammalia, Insectivora) using partial warp scores. *Syst. Biol.* **45**(3): 344–362.

SAS (1985) SAS Statistical program package. SAS Institute, Version 6.0 Cary, USA

SIMBERLOFF, D. & BOECKLEN, W. (1981) Santa Rosalia reconsidered: size ratio and competition. *Evolution* **35**(6): 1206–1228.

SKOCZEN, S. (1966) Stomach contents of the mole, Talpa europaea Linnaeus, 1758, from southern Poland. *Acta Theriol.* **11**(28): 551–575.

SLICE, D. (1993) GRF-ND. Generalized rotational fitting of N-dimensional data. Department of Ecology and Evolution, State University of New York, Stony Brook.

STATISTICA for Windows (1993) Version 4.3B StatSoft Inc.

STONE, R. D. (1992) *The mole.* Shire Natural History Series 61. Christopher Helm, London, 138 pp.

TAPER, M. L. & CASE, T. J. (1992) Coevolution among competitors. Pp. 289–346. *In* FUTUYMA, D. & ANTONOVICS, J. (eds): *Oxford Surveys in Evolutionary Biology, 9.*

UPTERGRAFF, G. (1990) MTV, Measurement TV, version 1.81, San Clemente, CA.

WAKE, M. H. (1992) Morphology, the study of form and function. Pp. 289–346. *In* FUTUYMA, D. & ANTONOVICS, J. (eds): *Oxford Surveys in Evolutionary Biology* 9.

Acta Zoologica Academiae Scientiarum Hungaricae 44 (1–2), pp. 165–175, 1998

CHARACTER DISPLACEMENT IN MANDIBLE SHAPE AND SIZE IN TWO SPECIES OF WATER SHREWS (NEOMYS, MAMMALIA: INSECTIVORA)*

RÁCZ, G.** and A. DEMETER***

Department of Zoology, Hungarian Natural History Museum
Budapest, Baross u. 13, H–1088 Hungary

Landmark coordinates were digitized from images of mandibles of trapped specimens of two species of water shrews (*Neomys fodiens* and *Neomys anomalus*, Mammalia: Insectivora), and unidentified mandibles from owl pellets collected in Hungary. Discriminant analyses based on variables describing size, affine and nonaffine shape changes were carried out using positively identified specimens as training sets. The results indicate that the two species can be separated using both size and shape variables, but the best discrimination can be achieved by using both set of variables.

The two species were found to be more different at localities where they occur sympatrically. The more abundant *Neomys anomalus* is more stable in its characters, while the less abundant species, *Neomys fodiens*, appears to lessen competition by shifting its characters at localities where both species co–occur.

Key words: *Neomys*, water shrews, geometric morphometrics, landmarks, character displacement

INTRODUCTION

Two species of water shrews, *Neomys* (Mammalia: Insectivora) can be found in most part of Europe, occurring sympatrically throughout most of their ranges (SPITZENBERGER 1990). Despite clear anatomical differences in the glans penis and the os coxae (PUCEK 1964, RICHTER 1965), in some cases it is not easy to distinguish between the two species using external characters such the number and distribution of digital pads, or the presence or absence and development of a fringe of long hairs on the underside of the tail (keel).

There is a general consensus among European mammalogists that there are two separate species that can be distinguished primarily by the height of the coronoid process (BUHALCZYK *et al.* 1961). This line of study was followed up by

* Symposium presentation, 5th International Congress of Systematic and Evolutionary Biology, 1996, Budapest

** Present address: Department of Biology, Castetter Hall, University of New Mexico, Albuquerque, NM 87131, U.S.A.

*** Present address: Department of Nature Conservation, Authority for Nature Conservation, Ministry of the Environment, Budapest, Költő u. 21, H-1121 Hungary

BÜHLER (1964) using a kind of discriminant analysis of six linear measurements. He found three measurements to be discriminating for the two species. This finding provoked a fierce debate. PIEPER (1966) examined specimens from owl pellets from different localities in Europe, and concluded that BÜHLER's discriminant function varied among different locations, and for this reason, could not work well in every case. Replying to this, REMPE and BÜHLER (1969), using mandibles from owl pellets, found that the discriminant function worked well in 99% of the cases. They also mentioned that using additional measurements could result in better separation of the two species. Later, PIEPER and REICHSTEIN (1980) found the discriminant function to fail in 23% of the cases. This was supported by REMPE (1982) who suggested some modification to the discriminant functions, thereby converting the constant in BÜHLER's equation to a variable in itself.

Other studies disregarded the continuing debate, and used BÜHLER's results in discriminating the two species. It is notable that HAMAR *et al.* (1964) found differences between the two species in a sample of shrews from Romania using all five measurements suggested by BÜHLER. Unfortunately, their sample sizes were very small. SCHMIDT (1969) found that distinguishing the two species could be unequivocal in the Carpathian Basin. They separate well in Hungary but there is some overlap between them in Slovakia.

At present it is obvious that we are dealing with two clearly separate species. The genetic distance between the two species using protein electrophoretic data is high enough to distinguish them at the specific level (CATZEFLIS 1984). Part of the problem is due to the fact that the two species occur not only sympatrically, but also syntopically (NIETHAMMER 1977). It is still poorly known how the two species share resources. Several authors describe differences in the microhabitat preference of the two species (see SPITZENBERGER, 1990): these reports are based on local observations and therefore may be very variable. It is said that *N. fodiens* is more aquatic and that there are differences between the two species in preferred water quality. The two species also partition habitats in mountains; *N. fodiens* is usually found at higher elevations. It also appears that there are trophic differences (summarized in SPITZENBERGER 1990), with *N. fodiens* being a more opportunistic feeder (CHURCHFIELD 1994). In general, it can be stated that *N. fodiens* is larger and that there are behavioural mechanisms which help the two species in intraspecific individual recognition (KRUSHINSKA & PUCEK 1989).

The original purpose of this study was to elucidate the distribution of the two water shrew species in Hungary, and to describe their morphometric variation in terms of their ecology, using a battery of modern landmark-based methods (BOOKSTEIN 1991, MARCUS *et al.* 1996). Although there is nothing *a priori* wrong with traditional morphometric methods that use distances between land-

marks (CORTI 1996), which can yield similar separation of the groups as the newer methods, geometric morphometrics have the advantage that they partition changes in size and shape, and can distinguish between affine and nonaffine shape changes.

We have set about the above-mentioned objective by teasing apart the size and shape variation in order to see whether character displacement (BROWN & WILSON 1956) might be the underlying cause of the uncertainty in morphometric description of the water shrews. This is also an excellent opportunity to interprete morphology in light of ecology through behaviour, under the ecomorphological rubric advocated by RICKLEFS and MILES (1994).

MATERIALS AND METHODS

All studied specimens are from the Mammal Collection of the Department of Zoology of the Hungarian Natural History Museum, Budapest. Two sets of samples were used: specimens collected by trapping, and to increase sample sizes, specimens from owl pellets. Most of the trapped specimens have been collected in the Carpathian Basin, but newer acquisitions are exclusively from Hungary. The same is true for the owl-pellet material. If available, the skin of the trapped specimen was also examined besides its skull in order to arrive at an *a priori* taxonomic identification. The length of the keel of bristles on the tail, the thickness of the brush of fringing hair on the hind foot, and size and coloration of the animals were used as key characters. This training set consisted of 178 positively identified specimens, 41 specimens were questionably allocated.

Images of 256 left mandibles of trapped specimens and 444 mandibles from owl pellets were digitized viewed from the lingual side. The images taken by a high resolution camera connected to a computer were recorded using IMAGOES, a software for morphometric image and data collection (DEMETER *et al.* 1996). Two-dimensional coordinates of 17 landmarks on the images of the mandibles have been digitized (Fig. 1). The coordinates of landmark number 12 were fixed as the origin of the coordinate system and landmark number 2 determined the direction of the X axis. This way the landmark coordinates of every mandible were translated to the same axis and rotated to the same direction.

Missing coordinate values in damaged specimens (especially among mandibles from owl pellets) were replaced by mean values. Size and shape variables were computed using the pro-

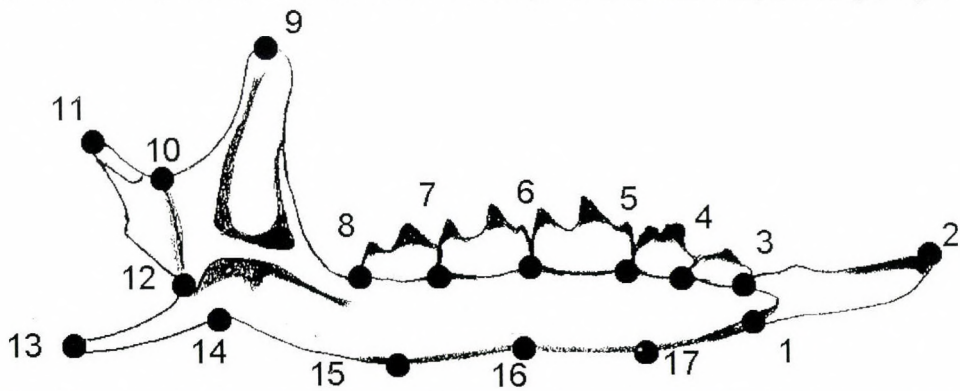

Fig. 1. Schematic drawing of the left mandible of the water shrew from lingual view, showing the landmark positions

gramme UNIGRAPH written by LESLIE F. MARCUS. Centroid size and uniform components for affine shape changes in the direction of axis X and Y were stored and the original coordinates were transformed to size-independent shape coordinates (BOOKSTEIN 1991). Nonaffine shape changes in each landmark were calculated by the TPSRW computer programme written by F. JAMES ROHLF and the partial warp scores were used as input for further analyses.

Specimens positively identified from their skins were used as training sets for calculating discriminant coefficients; unknown mandibles from owl pellets were allocated by calculating the discrimant scores. Variables describing size, affine and nonaffine shape changes were used together for discrimination. Outputs from discriminant analyses were also employed to determine the importance of variables for overall separation between the two species. Shape differences between the two species were visualized by the TPSREGR computer programme (written by F. JAMES ROHLF), using the canonical scores from the discriminant analysis as independent variable and affine and nonaffine shape components as dependent variables.

For analyzing differences between the two species at different localities, the whole sample was grouped by locality and species. A bivariate plot of centroid size and Procrustes distance was used to compare the groups. These two variables that describe size and shape differences were used in HOTELLING's T^2 test to detect significant differences between the two species, and among allopatric and sympatric populations of the same species.

RESULTS

There exist clear differences in size and shape between the two species. The discriminant analysis in which the size and shape variables were pooled performed well (Wilk's lambda = 0.19924) and the discriminant scores separate the two species completely (Fig. 2). The results of the discriminant analyses indicate that the size variable plays a substantial role in discrimination of the two species, because the analysis performed poorer when centroid size was excluded from the variables. *N. fodiens* specimens are larger as regards centroid size (Fig. 3), but the size ratio depends on whether they were collected in sympatry or allopatry with *N. anomalus*. Comparing character displacement graphically (Fig. 3), the two species may be separated well using centroid size, but the differences between the two species are greater in localities of sympatry. HOTELLING's T^2 test corroborates the notion that different populations of *N. anomalus* do not, while those of *N. fodiens* do show diverged morphological characters in respect of centroid size and Procrustes distance when occurring in sympatry (Table 1). The difference in Procrustes distance of sympatric and allopatric populations of *N. fodiens* is hardly noticeable in the bivariate plot, but running a *t*-test on this variable indicated significant although moderate differences ($t = 2.2559$, $p = 0.026$).

Pure shape differences are hardly noticeable, but they do exist (Fig. 2). Although splines on both side of the graph represent extreme shape variants within each species, the deformation grids show well the major differences in shape between the two species. The splines show that *N. fodiens* has a much more robust ramus of the mandible and we can also detect slight shape differences in the re-

Table 1. The result of pairwise Hotelling's T^2–tests (p-values in parentheses) to compare size and shape variables of syntopic and allopatric populations of the two water-shrew species

	N. anomalus sympatry	*N. anomalus* allopatry	*N. fodiens* sympatry	*N. fodiens* allopatry
N. anomalus sympatry	–	1.47 (0.4787)	547.45 (<0.0001)	238.57 (<0.0001)
N. anomalus allopatry	–	–	740.75 (<0.0001)	302.1 (<0.0001)
N. fodiens sympatry	–	–	–	33.99 (<0.0001)
N. fodiens allopatry	–	–	–	–

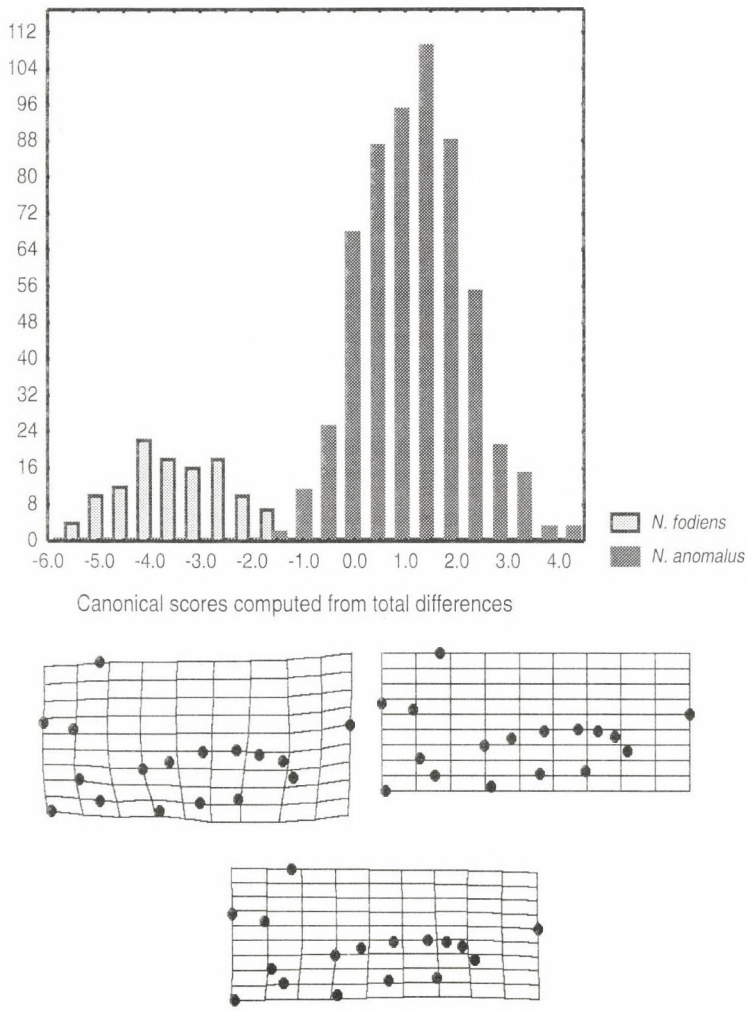

Fig. 2. Histogram of discriminant scores computed from size and shape variables (weight matrix) for the two species of water shrews. Splines on both sides illustrate extreme variation in shape, while the one in the middle shows the calculated consensus configuration

gion of the coronoid process of the mandible. The mandible of *N. fodiens* also looks more upward-curved because the tip of the incisor is relatively higher.

DISCUSSION

The term character displacement was originally coined by BROWN and WILSON (1956). Although they and others have published several examples, the validity of these was later questioned by GRANT (1972). It has been suggested that character displacement is rare in nature (MACARTHUR & LEVINS 1967, MACARTHUR 1972). These works elicited more research in this direction and since then a number of publications have reported the phenomenon in a wide range of species. For instance, OTTE (1989) considered it to be very common in Hawaian crickets. PIMM (1991) provided a compelling example of community-wide character displacement in mustelids and felids.

This report gives another example of character displacement. Many analyses of character displacement have been carried out by pooling samples over a huge geographic area. Most of these cases can be disputed on the basis that environmental factors, for example latitudinal gradients, can be responsible for the

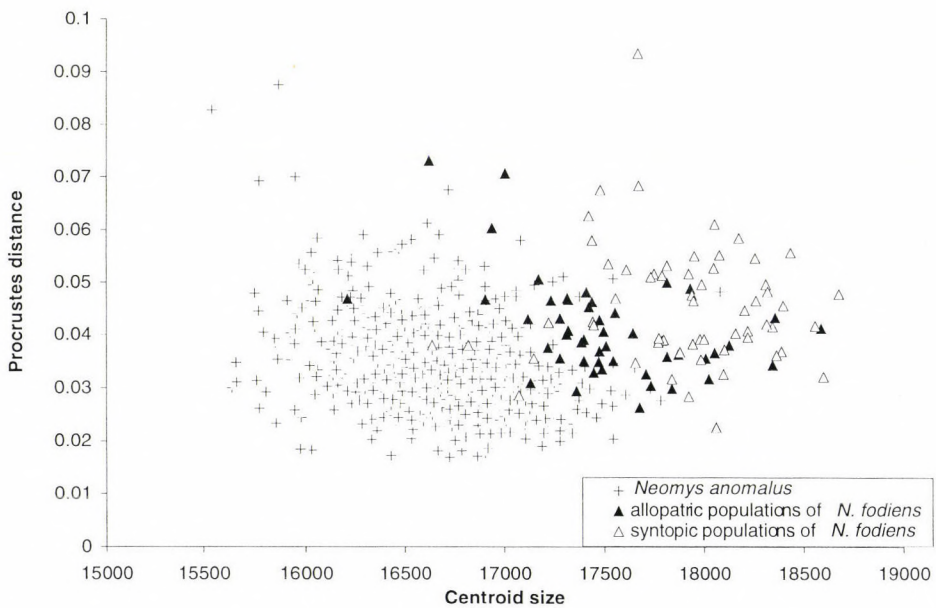

Fig. 3. Bivariate plot of centroid size and Procrustes distance showing variation in size and shape. Individuals were grouped by species and whether found in sympatry or allopatry with the other species

observed pattern (GRANT 1972). In the present survey, this kind of error is greatly reduced. Even more, we can say that not only sympatric species, but also syntopic populations were examined. The area of the survey covers the Carpathian Basin which, although very diverse in habitats, can still be regarded as a relatively small area on a geographic scale. Because most of the survey was based on owl pellets, we cannot completely exclude the error term, given that samples were pooled from different habitats within a home range of an owl. Trapping data in Hungary provide evidence for syntopic occurrence of the two species, so it can be said that in localities where both species were found, the two species are in such close contact that competition may be in operation. This way the present example can be viewed in the framework of Grant's more stringent determination of character displacement.

There are several genetic models for character displacement (see TAPER & CASE 1992), but there is not one which is generally accepted. A simple and possible explanation may be that there is selective retention of invading species (TAPER & CASE 1985). In this model, one of the species remains unchanged, while the other one shifts its character or suite of characters. This model would explain why in this case *N. anomalus* remains the same, while the other, less abundant species, *N. fodiens*, shows diverged characters in syntopy. A similar cases was observed in two sympatric species of shrews (*Sorex*) in Europe (MALMQUIST 1985). Theoretically, character displacement alone cannot explain differences between sympatric species. Another plausible explanation for the phenomenon is that in this way sympatric species can strengthen mate recognition systems and avoid interbreeding. In this example, this possibility cannot be completely excluded, but it has been shown in several studies that prey size is highly correlated with the predator's jaw size. Beside differences in the glans penis (PUCEK 1964), there must be other factors that can help interspecific recognition. This can be concluded from the high level of aggressiveness between members of the opposite species of water shrews (KRUSHINSKA 1994). For this reason, it is more probable that differences in mandible size and shape can be explained by differences in foraging strategies, an assumption supported by food analyses of the two species (SPITZENBERGER 1990). Other studies suggests that niche overlap calculated from food resources can decrease as more and more competing species are present in the community (CHURCHFIELD 1991). The decreased niche breadth was explained by the fact that this way the otherwise opportunistic and generalist feeder shrew species can ease competition with each other by specializing on certain food types. RYCHLIK and PUCEK (1996) found that in a lowland forest *N. fodiens* preferred microhabitats with direct access to open and deep water, whereas *N. anomalus* was found more often in wet flooded microhabitats with shallow water.

In our study, character displacement between different population of *N. fodiens* is caused by differences both in size and shape. Sympatric populations of *N. fodiens* tend to be more different from *N. anomalus* with respect to size and shape then allopatric populations of the two species. The importance of size in discriminating the two species is underlined by the fact that size is described by a single variable, while shape changes are described by multiple variables. The exclusion of one variable like size has a similar effect on discrimination than the exclusion of multiple variables describing shape, such as the weight matrix. However, we have to remember that size and shape variables are incommensurable (BOOKSTEIN 1990). In our study, we have to keep in mind that discrimination is based on both size and shape.

Another implication of this study is that it is possible to understand why BÜHLER's discriminant function did not perform equally well in different samples. When comparing the two species, one has to consider not only environmental differences but also whether they are sympatric or not. Using total variation in mandible size and shape the two species are clearly separated. This supports the assumption that the morphological differences between the two species are sufficient to separate them completely. It must be mentioned that taxonomic decision was made counter to those of the analysis when using skins for determining species. This can originate from the problem that the external features are very variable and our notion about typical external characters is not yet exact.

The geometric morphometric methods employed in this study were found to posses a high degree of sensitivity. Similarly, LOY *et al.* (1996) found landmark-based morphometrics to be very useful in elucidating ecogeographic variation in cranial characters of Italian moles. As for shrews, SARÁ (1996) also provides another example when geometric morphometrics is more powerful than traditional distance-based analysis. In a preliminary analysis not detailed here, distances between landmarks lacked the level of resolution demonstrated here for landmark data, despite the fact that the starting variable set contained the same 17 landmarks. The benefit of better separation can falsify the use of a more complicated method. However, researchers do not have to discard calipers and traditional methods. Using distance data has the advantage of simplicity as well as the fact that distance data may incorporate the most relevant changes into few variables. For example, BÜHLER (1964) suggested three measurements for discrimination (inter–landmark distances 1–11, 9–14 and 6–16, *cf.* Fig. 1). A different kind of shape change may be reflected in these three variables. Distance 1–11 is the total length of the mandible and may be a good measure of overall size. On the other hand, the other two distances can incorporate the uniform and nonuniform shape changes that are more pronounced in the same direction in which those measurements were taken.

The results of the foregoing morphometric analyses of the two species of water shrews conclusively demonstrate that there exists at least one mechanism to reduce interspecific competition when the two species occur sympatrically. This mechanism is traditionally known as character displacement. In the classic studies of the phenomenon, character displacement was displayed equally by the sympatrically (or parapatrically) occurring species being studied. However, in the case of the two congeneric shrew species studied herein, only one of the two species displays displacement in morphometric variables when occurring in sympatry. This may represent a novel phenomenon within the framework of character displacement, and will bear further study in shrews and other organisms.

* * *

Acknowledgement – Funds for this project were provided in part by OTKA grant number 3177/91 to A. DEMETER. We are grateful to CHRIS KLINGENBERG and FRED BOOKSTEIN for their valuable comments on the manuscript.

REFERENCES

BROWN, J. & WILSON, E. O. (1956) Character displacement. *Syst. Zool.* **5:** 49–64.

BOOKSTEIN, F. L. (1990) Introduction and overview: geometry and biology. Pp. 61–74. *In* ROHLF, F. J. & F. L. BOOKSTEIN (eds): Proc. Michigan Morphometrics Workshop, Spec. Publ. No. 2. Univ. Michigan Museum of Zoology, Ann Arbor.

BOOKSTEIN, F. L. (1991) *Morphometric tools for landmark data. Geometry and biology.* Cambridge University Press, New York, 435 pp.

BOOKSTEIN, F. L. (1996) Combining the tools of geometric morphometrics. Pp. 131–151. *In* MARCUS, L. F., M. CORTI, A. LOY, G. J. P. NAYLOR & D. E. SLICE (eds): Advances in Morphometrics. Plenum Press, New York.

BUCHALCZYK, T. & RACZYNSKY, J. (1961) Taxonomischer Wert einiger Schädelmessungen inländischer Vertreter der Gattung Sorex Linnaeus, 1758 und Neomys Kaup, 1829. *Acta theriol.* **5**: 115–124.

BÜHLER, P. (1964) Zur Gattungs- und Artbestimmung von Neomys-Schädeln – Gleichzeitig eine Einführung in die Methodik der optimalen Trennung zweier systematischer Einheiten mit Hilfe mehrerer Merkmale. *Z. Säugetierk.* **29**: 65–93.

CATZEFLIS, F. (1984) Différenciation génétique entre populations des espèces Neomys fodiens et N. anomalus par électrophorse des protéines (Mammalia, Soricidae). *Rev. suisse Zool.* **91**: 835–850.

CHURCHFIELD, S. (1991) Niche dynamics, food resources, and feeding strategies in multispecies communities of shrews. Pp. 23–34. *In* FINLEY, J. S. & T. L. YATES (eds): *The biology of Soricidae.* Spec. Publ. Museum of Southwestern Biology 1.

CHURCHFIELD, S. (1994) Foraging strategies of shrews, and the evidence from field studies. *Carnegie Museum of Natural History Spec. Publ.* **18**: 77–87.

CORTI, M. (1996) Introduction to comparison of similar objects whose group identity is known. Pp. 355–357. *In* MARCUS, L. F., M. CORTI, A. LOY, G. J. P. NAYLOR & D. E. SLICE (eds): *Advances in Morphometrics.* Plenum Press, New York.

DEMETER, A., VÁMOSI, J., PEREGOVITS, L. & TOPÁL, GY. (1996) An image-capture and data-collection system for morphometric studies. Pp. 91–101. *In* MARCUS, L. F., M. CORTI, A. LOY, G. J. P. NAYLOR & D. E. SLICE (eds): *Advances in Morphometrics.* Plenum Press, New York.

GRANT, P. R. (1972) Convergent and divergent character displacement. *Biol. J. Linnean Soc.* **4**: 39–68.

HAMAR, M. & KOVACS, A. (1964) Neue Daten über die Gattung Neomys Kaup (1829) in der Rumänischen Volksrepublik. *Acta theriol.* **9**: 377–380.

KRUSHINSKA, N. L. & PUCEK, Z. (1989) Ethological study of sympatric species of European water shrews. *Acta theriol.* **34**: 12–28.

LOY, A., MARTINO, S. DI & CAPOLONGO, D. (1996) Patterns of geographic variation of Talpa romana Thomas (Insectivora, Talpidae). Preliminary results derived from a geometric morphometric approach. *Mammalia* **60**: 77–89.

MACARTHUR, R. H. (1972) *Geographical ecology.* Harper and Row, New York, 269 pp.

MACARTHUR, R. H. & LEVINS, R. (1967) The limiting similarity, convergence and divergence of coexisting species. *Amer. Natur.* **101**: 377–385.

MALMQUIST, M. G. (1985) Character displacement and biogeography of the pygmy shrew in Northern Europe. *Ecology* **66**: 372–377.

MARCUS, L. F., CORTI, M., LOY, A., NAYLOR, G. J. P. & SLICE, D. E. (eds) (1996) *Advances in Morphometrics.* Plenum Press, New York, 587 pp.

NIETHAMMER, J. (1977) Ein syntopes der Wasserspitzmäuse Neomys fodiens und N. anomalus. *Z. Säugetierk.* **42**: 1–6.

OTTE, D. (1989) Speciation in Hawaian crickets. Pp. 482–526. *In* OTTE, D. & ENDLER, J. A. (eds): *Speciation and its Consequences.* Sinauer Associates, Inc., Sunderland.

PIEPER, H. (1966) Über die Artbestimmung von Neomys-Mandibeln mit Hilfe der Fischerschen Diskriminanz-Analyse. *Z. Säugetierk.* **31**: 402–403.

PIEPER, H. & REICHSTEIN, H. (1980) Zum frühgeschichtlichen Vorkommen der Sumpfspitzmaus (Neomys anomalus Cabrera, 1907) in Schleswig-Holstein. *Z. Säugetierk.* **45**: 65–73.

PIMM, S. L. (1991) *The Balance of Nature? Ecological Issues in the Conservation of Species and Communities.* The University of Chicago Press, Chicago, 434 pp.

PUCEK, Z. (1964) The structure of the glans penis in Neomys Kaup, 1929 as a taxonomic character. *Acta theriol.* **9**: 374–377.

REMPE, U. (1982) Die Trennung von Neomys-Mandibeln aus verschiedenen Teilen Mitteleuropas. *Säugetierk. Mitt.* **30**: 118–126.

REMPE, U. & BÜHLER, P. (1969) Zum Einfluß der geographischen und altersbedingten Variabilität bei der Bestimmung von Neomys-Mandibeln mit Hilfe der Diskriminanzanalyse. *Z. Säugetierk.* **34**: 148–164.

RICHTER, H. (1965) Die Unterscheidung von Neomys anomalus milleri Mottaz, 1907, und Neomys fodiens fodiens (Schreber, 1777) nach dem Hüftbein (Os coxae) nebst einer Mitteilung über neue Funde erstgenannter Unterart aus dem Erzgebirge und dem Vogtland und Ostthüringen. *Säugetierk. Mitt.* **13**: 1–4.

RICKLEFS, R. E. & MILES, D. B. (1994) Ecological and evolutionary inference from morphology: an ecological perspective. Pp. 13–41. *In* WAINWRIGHT, P. C. & REILLEY, S. M. (eds): *Ecological Morphology. Integrative Organismal Biology.* The University of Chicago Press, Chicago.

RYCHLIK, L. & PUCEK, Z. (1996) Biotope requirements of Neomys fodiens and Neomys anomalus lowland zone of their sympatric occurrence. Pp. 95-96 *In* Seminar on the biology and conservation of European desmans and water shrews (Galemys pyrenaicus, Desmana moschata, Neomys spp.). Ordesa, Spain, 7-11 June, 1995. Environmental Encounters No. 25. Council of Europe Publishing.

SARÁ, M. (1996) A landmark-based morphometrics approach to the systematics of Crocidurinae. Pp. 335–344. *In* MARCUS, L. F., M. CORTI, A. LOY, G. J. P. NAYLOR & D. E. SLICE (eds): *Advances in Morphometrics.* Plenum Press, New York.

SCHMIDT, E. (1969) Über die Koronoidhöhe als Trennungsmerkmal bei den Neomys-Arten in Mitteleuropa sowie über neue Neomys-Fundorte in Ungarn. *Säugetierk. Mitt.* **17**: 132–136.

SPITZENBERGER, F. (1990) Gattung Neomys. Pp 313–374. *In:* NIETHAMMER, J. N. & F. KRAPP (eds): *Handbuch der Säugetiere Europas. Insektenfresser, Primates 3/I.* AULA-Verlag GmbH, Wiesbaden

TAPER, M. L. & CASE, T. J. (1985) Quantitative genetic models for the coevolution of character displacement. *Ecology* **66**: 355–371.

TAPER, M. L. & CASE, T. J. (1992) Models of character displacement and theoretical robustness of taxon cycles. *Evolution* **46**: 317–333.

APPENDIX

List of localities (all from Hungary if otherwise not stated*) with sample sizes (number of *N. anomalus*/*N. fodiens*)

Agárd: 6/0; Alsónyék: 1/0; Aranyosgadány: 1/0; Bácsborsod: 3/0; Banská Bystrica (Besztercebánya) (SLO): 4/6; Bódvaszilas: 4/5; Bóly: 2/0; Baisoara (Járabánya) (ROM): 0/31; Baja: 9/0; Bakonygyirót: 1/0; Balassagyarmat: 1/0; Balatonlelle-felső: 3/0; Balatonszéplak: 4/0; Baranyaszentgyörgy: 1/0; Bikács: 3/0; Bodorfa: 6/0; Brennbergbánya: 1/1; Budajenő: 5/0; Budakalász: 1/0; Csákvár: 10/0; Csala: 1/0; Csíkoséger: 5/0; Csokonavisonta: 2/0; Dabas: 1/0; Dunakeszi: 23/0; Esztergom: 2/0; Felsődobsza: 12/0; Gemenelc (ROM): 1/1; Gönc: 3/0; Gura Zlata (ROM): 0/8; Gyula: 1/0; Hédervár: 0/1; Hejce: 1/0; Hernádszentandrás: 11/0; Izsákfa: 1/0; Kács: 2/0; Kéthely: 11/4; Körmend: 1/0; Kamond: 1/1; Kis-Balaton: 44/18; Kiskorpád: 4/0; Lillafüred: 5/1; Lippó: 10/0; Liptovská Teplicka (Teplicska) (SLO): 0/2; Mátraalmás: 2/0; Méra: 2/0; Makkoshotyka: 3/0; Malnas (Málnás) (ROM): 0/1; Martonvásár: 2/0; Miske: 1/0; Németbánya: 9/0; Nagydorog: 1/0; Nagyiván: 1/0; Nagyvenyim: 1/0; Novajidrány: 1/0; Nyírbátor: 0/1; Okula (UKR): 1/0; Oravita (Oravicabánya) (ROM): 1/0; Ócsa: 20/1; Ómassa: 30/0; Pavcina Lehota (Paucsinalehota) (SLO): 1/1; Pákozd: 61/2; Pánd: 17/0; Pécs: 7/0; Pécska: 1/0; Pacsa: 11/14; Pilisborosjenő: 25/0; Piliscsév: 2/0; Pilisszántó: 3/0; Pilisszentiván: 5/0; Pilisvörösvár: 26/1; Pomáz: 3/0; Råstolita (Ratosnya) (ROM): 0/1; Rudolf-tanya: 2/0; Sály: 2/0; Sajószöged: 1/0; Sajóvelezd: 10/0; Solymár: 2/0; Somogyfajsz: 2/0; Sopron: 2/0; Stary Smokovec (Ótátrafüred) (SLO): 0/2; Stinceni (Gödemesterháza) (ROM): 0/1; Stirovaca (CRO): 1/0; Szögliget: 13/0; Szederkény: 1/0; Szentendre: 9/0; Szentmártonkáta: 2/0; Szin: 2/0; Šamorín (Somorja) (SLO): 0/1; Tápiószág: 2/0; Töttös: 4/0; Tatabánya: 6/0; Telki: 11/0; Tihany: 2/0; Tihucza: 1/0; Tornyosnémeti: 6/0; Vác: 3/0; Velence: 8/0; Zamárdi-felső: 1/0; Zuberec (SLO): 3/3.

* CRO – Croatia, ROM – Romania, SLO – Slovakia, UKR – Ukraine.

Acta Zoologica Academiae Scientiarum Hungaricae 44 (1–2), pp. 177–194, 1998

THE IDENTIFICATION OF AFRICANIZED HONEY BEES: AN ASSESSMENT OF MORPHOMETRIC, BIOCHEMICAL, AND MOLECULAR APPROACHES

T. E. RINDERER

USDA-ARS Honey-Bee Breeding, Genetics & Physiology Laboratory
1157 Ben Hur Road, Baton Rouge, Louisiana 70820, U.S.A.
E-mail: trindere@asrr.arsusda.gov

African honey bees (*Apis mellifera scutellata*) were introduced into Brazil in 1955 with the intention of providing improved honey bee breeding stock for Brazilian apiculture. The spread of the descendants of the introduced African bees, known as Africanized bees, was a matter for scientific study and regulatory concern. This attention produced the need for an identification tool that could be employed in research, survey, and detection and regulation. In part due to a long history of study and in part due to its intrinsic value, the discriminant analysis of morphometric data has become the tool of choice for identifying Africanized honey bees. Cost of analysis led to the development of simple methods to screen large numbers of samples without sacrificing the overall quality of identifications. With these screening procedures, all colonies that are determined to be European at a $P \geq 0.99$ are considered European. All colonies that are not determined to be European are considered unidentified. Samples which remain unidentified after the initial screening are identified by a more complex morphometric procedure called USDA-ID. USDA-ID was developed primarily to provide several laboratories that were established to morphologically identify honey bees for regulatory purposes more accurate identification tools based on new discriminant analysis procedures. The characteristics of these procedures are discussed and their weaknesses and strengths are compared to those of several other identification tools.

Key words: *Apis mellifera scutellata*, Africanized bees, morphometrics, biochemical identification, molecular identification

INTRODUCTION

African honey bees (*Apis mellifera scutellata*) were introduced in 1955 with the intention of providing improved honey bee breeding stock for Brazilian apiculture (KERR 1957). In 1956, some of this stock was released. The released stock interbred with previously imported honey bee stocks from Europe, producing hybrid progeny known as Africanized honey bees. The success of Africanized honey bees in the New World was tremendous. The rapid and widespread colonization by Africanized bees of much of South America, all of Central America, and finally the southern portions of North America, including all of Mexico and portions of the southern United States, is one of the most remarkable ecological events of this century. Within three decades a small experimental im-

portation of honey bees became a population of many millions of colonies which now occupy about 25 million square kilometers.

Africanized honey bees are noted for several other traits beyond their remarkable potential for reproduction and range extension in the New World. Foremost among these traits is their intense level of stinging in defense of their nests (COLLINS & RINDERER 1991). Stinging, along with poor honey production (RINDERER *et al.* 1984) and generally poor apicultural value (DANKA *et al.* 1987) have generated scientific, regulatory and apicultural concerns about Africanized honey bees (RINDERER *et al.* 1993*b*). Proper study and regulation (survey, detection and control) efforts concerning Africanized honey bees require the ability to quickly and accurately identify Africanized honey bees. Scientific needs of identification will vary according to the specific study. For example, population genetic studies of the Africanization process benefit from having data from several measurement systems. However, for regulatory purposes, a useful method for identifying Africanized honey bees should depend upon one technique that can be applied uniformly by personnel from several laboratories having only brief training and limited equipment. Many countries and their states, provinces and even local jurisdictions have an interest in identifying Africanized honey bees. Ideally, all of them would use the same procedures and be able to reach quite similar identification conclusions. Many of these identification services would necessarily need to use relatively unskilled labor and could not afford elaborate or expensive equipment. At the same time, the technique should access a reasonably large portion of the genome in order to provide a clear identification of a variety of intermediate types arising from hybridization.

These identification needs arose in the context of a long tradition of honey bee taxonomy. The genus *Apis* is comprised of nine species which are easily distinguished by morphology and life history details. However, one species, *Apis mellifera*, has been the subject of intense taxonomic study. This study is motivated by *A. mellifera*'s economic value as a hive bee in combination with its wide range of subspecies diversity. The home range of *A. mellifera* includes all of Africa, most of Europe and most of the Arabian peninsula. The wide range of locally adapted ecotypes in this species has a correspondingly wide range of desirability for various economical characteristics. This variance in economic value has led to a long history of research efforts concerning the subspecific taxonomy of *A. mellifera*.

HISTORICAL ORIGINS

Research concerning the identification of Africanized honey bees was founded on the products of prior subspecific honey bee taxonomy. In many re-

gards, efforts to identify Africanized honey bees extended that work, especially in regard to choices and uses of statistical methods. However, the procedures developed to identify Africanized honey bees were produced in response to a practical need to have a fast, inexpensive and easily transferable identification technology.

Early interest in subspecific variation in *A. mellifera* led to the introduction of a tri-nomial classification system (VON BUTTEL-REPEN 1906). In the next half century, the application of this system in addition to other taxonomic work resulted in 600 different names in the literature by 1953 for honey bees. In a revision of the genus, MAA (1953) retained 146 names from his compilation of 600. RUTTNER (1987) extended this move toward recognizing fewer species and subspecies and in his revision used 37 names for the genus, with 24 of them used for subspecies of *A. mellifera*.

RUTTNER's 1987 work culminated efforts by himself and others to base a taxonomy of honey bees on morphometric data. The application of morphometric data to honey bee questions arose in Russia with the work of COCHLOV (1916), who compared groups using univariate measurements. Quite quickly, this work was extended to include multivariate measurements and studies of ecological correlates to geographical trends in morphology (ALPATOV 1929). GOETZE (1930) contributed to the development of honey bee morphometrics by studying ratios of lengths of wing veins as a way to include the geometry of wing venation and by suggesting that morphometric values could be used as breeding values indicating the presence of economically desirable characters which were correlated to morphometric characters. DUPRAW (1964), in an attempt to develop a numerically based non-Linnean taxonomy, overcame certain mathematical difficulties in using ratios of lengths of wing veins by using measurements of the angles formed by vein intersects and introducing more advanced forms of multivariate statistics. Hence, when African honey bees were released in Brazil in 1956-57, the morphometric study of subspecies variation in honey bees was already advanced and able to serve as a foundation for the development of identification procedures based on morphological evaluation.

MORPHOMETRIC APPROACHES TO IDENTIFYING AFRICANIZED HONEY BEES

Early Procedures

The release of African honey bees resulted in a population of honey bees in the Americas called Africanized honey bees which to some degree were the products of hybridization between African honey bees and various European subspecies of honey bees. Thus, the problem of identifying them included two as-

pects new to the morphometric study of subspecies variation. First, the group requiring identification was not a subspecies. Second, the group requiring identification had some parentage from the contrasting group, a collection of European subspecies. Hence, the problem of identifying Africanized bees could not rely on previously established descriptions for subspecies.

Early attempts to find a univariate character which provided certain identification of Africanized honey bees were not successful (DALY 1991). This result led DALY and BALLING (1978) to develop a multivariate morphometric procedure to distinguish between the Africanized honey bees of South America and the European honey bees of North America. To do so, they built discriminant functions from base-line data derived from 101 colonies of Africanized honey bees from South America and 297 colonies of European honey bees from North America. Ten worker bees from each colony were dissected and 25 morphometric characters were measured for each bee. The measurements were made for forewing, hindwing, hindleg, and sternite characteristics which were mainly either linear measurements or angular measurements (Fig. 1), although the number of wing hooks was also included. Using classification at the highest group probability, the expected misclassification rate was 0.5%.

DALY *et al.* (1982) provided an innovative development to morphological studies generally by adapting computers to assist in the measurement and analysis of data. A projecting microscope projects an image of dissected body parts onto the surface of a digitizing pad. Points are digitized and linear or angular data are interpreted by a program designed to receive data input. The data can then be submitted to analysis programs structured for specific purposes.

Current procedures

Screening with Simple Techniques. Currently used morphometric systems are both simplifications and developments of the foundations supplied by DALY and BALLING (1978) and DALY *et al.* (1982). It is costly to provide a full morphometric analysis of every sample from survey and detection programs or other programs that produce a large number of samples. This cost led to the development of simple methods to screen large numbers of samples without sacrificing the overall quality of identifications. RINDERER *et al.* (1986*a*) developed two simplified techniques appropriate for field or laboratory use. The simplest approach used a single character (forewing length) and correctly identified 86% of 136 colony samples at $P > 0.90$. The second approach used four morphometric measurements (forewing length, partial hindwing length, femur length and "clean" weight) and correctly identified 91% of colony samples at $P > 0.90$.

The procedures of RINDERER *et al.* (1986*a*) were used in the regulatory quarantine when Africanized honey bees were found in California, USA (GARY *et al.* 1985). Approximately 25,000 colonies were identified before the quaran-

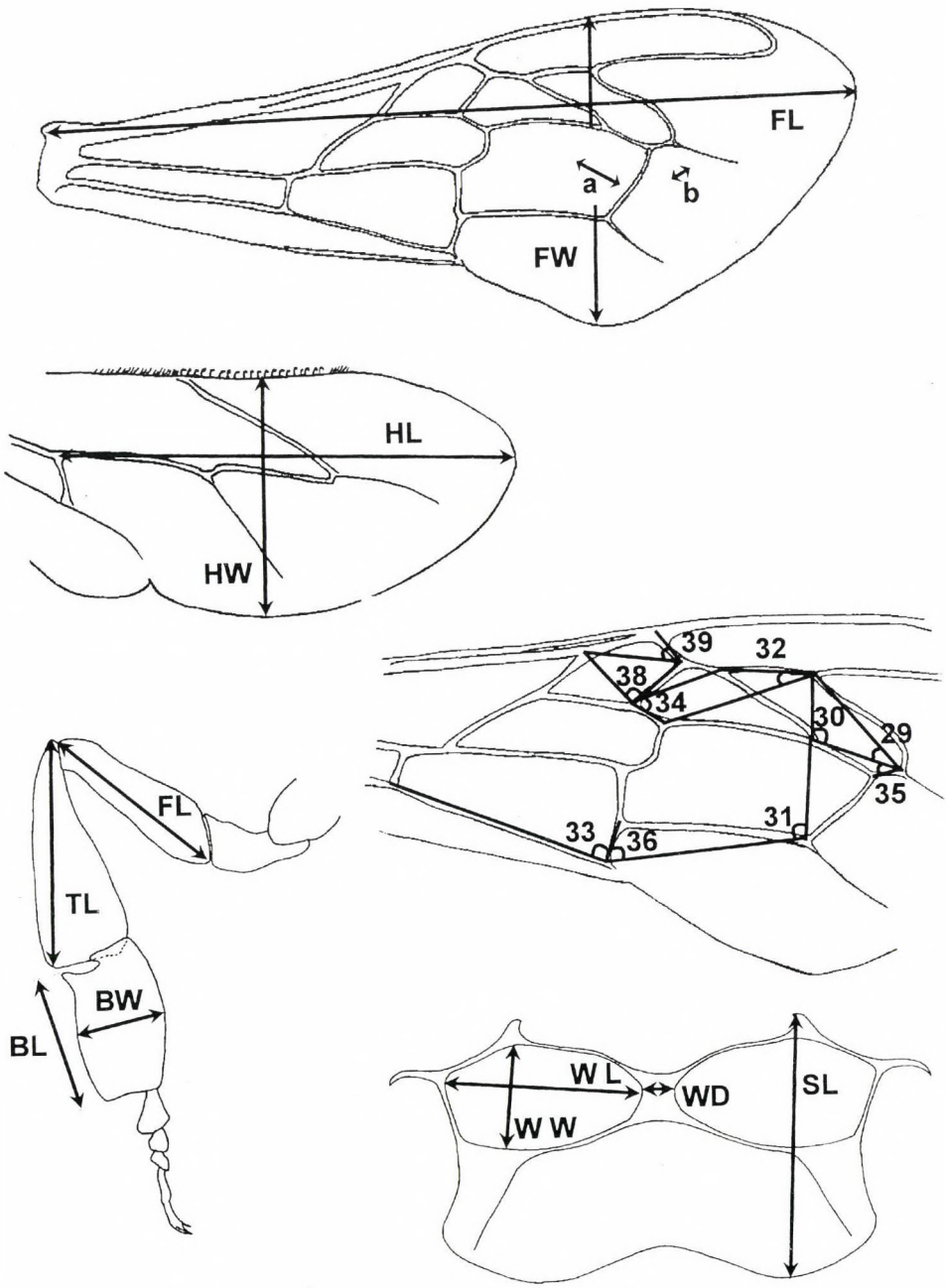

Fig. 1. Ten worker bees from each colony were dissected and 25 morphometric characters were measured for each bee. The measurements were made of forewing, hindwing, hindleg, and sternite characteristics which were mainly either linear measurements or angle measurements as illustrated, although the number of wing hooks was also included

tine was ended. These identifications were made during a 12-week period in a temporary laboratory using, for the most part, unskilled help. All colonies that were determined to be European at a $P \geq 0.99$ were considered European. All colonies that were not determined to be European were considered unidentified and were then identified using the procedures of (DALY *et al.* 1982). Periodically, (two to four a day) quality-control samples of Africanized honey bees were placed as "blind" samples among the unknown samples being processed. Every quality control sample was identified as Africanized.

Although the procedures of RINDERER *et al.* (1986*a*) were successful in the California regulatory action, possible ways to improve the procedures became apparent. In response to this need, RINDERER *et al.* (1987) provided eight simple identification techniques to identify Africanized and European honey bees. These techniques are based on measurements of dry weights, wet weights, forewing lengths, femur lengths and various groups of two or three of these characters (Fig. 2). Two of these techniques have seen regulatory and research use. Forewing length is a convenient measure which can be made on most samples of honey bees regardless of the way in which they have been collected or preserved. Hence, most programs interested in identifying Africanized honey bees have relied on forewing length as their first identification screen. Some regulatory and research programs having access to fresh samples and skilled technicians to identify the samples have used measurements of wet weight for this purpose.

Full morphometric procedures. In the last few years, spreading populations of Africanized honey bees have entered the states of Texas, New Mexico, Arizona, and California in the United States. As Africanized honey bees spread further into the United States, several laboratories were established to morphologically identify honey bees for regulatory purposes. To provide these laboratories with more accurate identification tools, new discriminant analysis procedures were developed to identify Africanized and European honey bees (RINDERER *et al.* 1991*a*, 1993*a*). These procedures are improved over those of DALY and BALLING (1978) in several respects. First, sample sizes of both Africanized and European bees are much larger than those previously used and hence can be expected to include more of the variation of both groups. Second, feral European honey bees and commercially kept European honey bees are well represented, reducing the chance of misclassifying feral European honey bees as Africanized. Third, Africanized honey bees reared in hives having European comb foundation and feral Africanized honey bees are well represented, reducing the chance of Africanized honey bees being misclassified as European. Fourth, the classification of base-line colonies as Africanized or European is determined by whether or not the general population was considered to be Africanized at the time of collection and the specific history of the queen that produced the colony. This eliminates the bias inherent in making decisions based on field behavior which likely led to

only the most clearly Africanized members of the sampled populations being collected as base-line material. Fifth, the measurement of two wing angles used by DALY and BALLING (1978) which have been difficult to standardize between laboratories has been eliminated.

The data from 2,500 colony samples of honey bees collected from colonies from several locations in the Western Hemisphere and Kangaroo Island, Australia, were reviewed to assign them as feral colonies, rustic colonies (hived without comb foundation or requeening) or commercial (hived with comb foundation or requeening) and to assure that they could be considered random samples of clearly Africanized or European populations based on their date of collection and other information. Additional samples from colonies were collected from several locations, including northern Mexico and several southwestern states in the U.S. in order to increase the geographical and biological variability of the samples. Overall, data from 2,103 colonies were used in the final analysis. This total includes 177 hived Africanized colonies which, with only occasional exception, had bees reared on European comb foundation, 414 feral and rustic (hived without comb foundation or requeening) Africanized colonies, 331 commercial European colonies, 1,111 feral and rustic European colonies, and 70 European colonies from unknown hives (swarms and other unknowns).

A sub-set of 87 Africanized and 48 European colonies was used to evaluate the potential of 40 morphological measurements to contribute to the identification of Africanized and European honey bees. Morphological measurements of 40 characteristics were taken from the dissected body parts of ten worker bees from each colony in the subset according to the guidelines of RUTTNER (1987). These data were analyzed using a step-wise discriminant analysis which permitted the average squared canonical correlation to be used to estimate the additional variance contribution of the characters not used by DALY and BALLING (1978). According to the analysis, the 25 characteristics selected by DALY and BALLING (1978) provided an analysis that was based on 93.6% of the total variance. The addition of the other 15 characters increased the total variance assessed by the analysis to 95.9%, indicating that generally these characters collectively added 2.3% to the variance accessed by the analysis. The range of additional proportions of the total variance added to the analysis by each of the 15 characters was from 1.0% to 0.000001%. The strongest characters of this group were angle L13 (RUTTNER 1987) and the length of the right distal segment of the proboscis. These characters were judged either to be difficult to obtain from field samples collected by different persons using different methods or difficult to standardize among laboratories. Of the 25 characters chosen by DALY and BALLING (1978) as the most valuable contributors to the multivariate analysis, two measurements, Angles 38 and 39, contributed little to the power of the discriminant analysis. When their contribution to the analysis was evaluated with a step-wise discrimi-

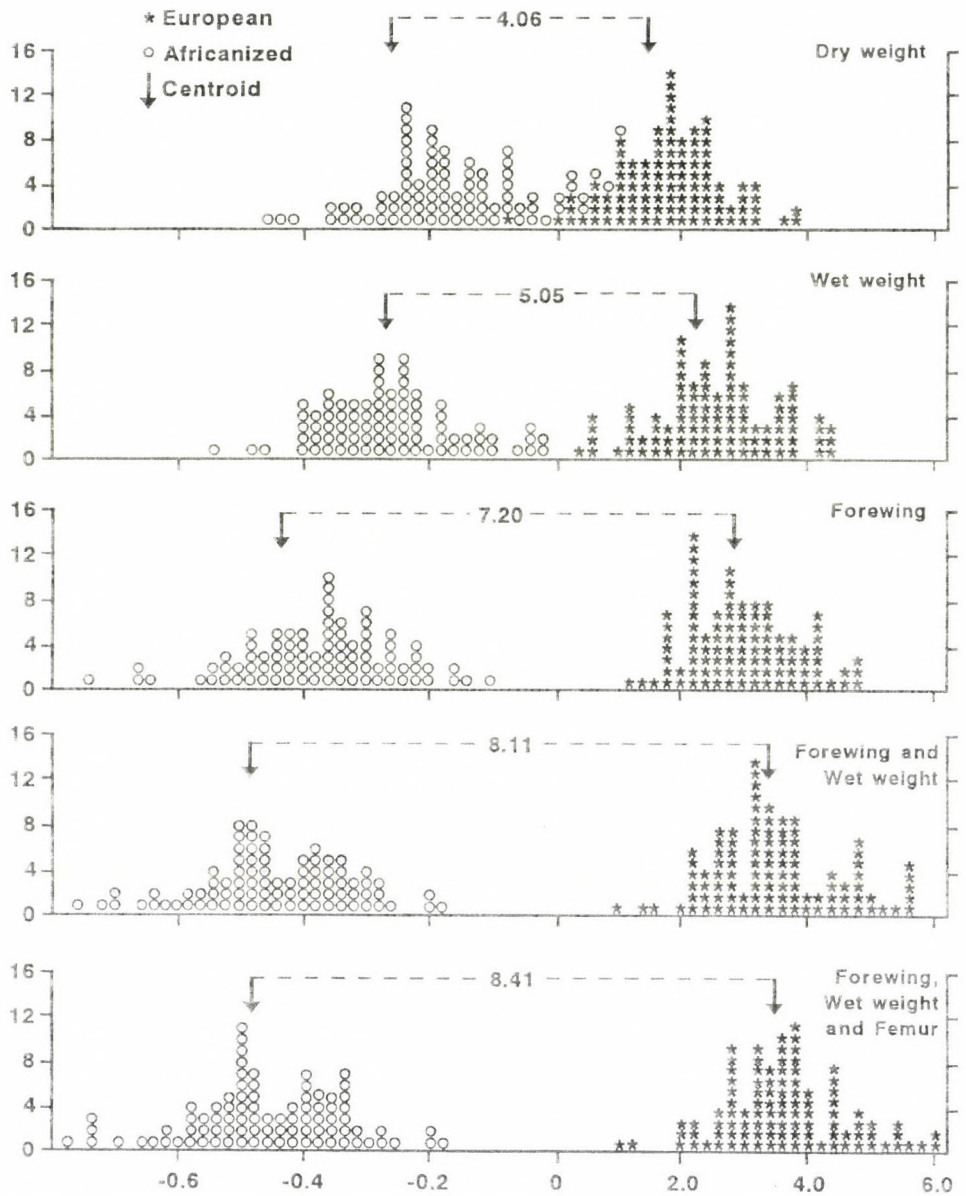

Fig. 2. Histograms of the placement of individual observations on a common discriminant axis for dry weights, wet weights, forewing lengths, the combination of forewing lengths and wet weights and the combination of forewing lengths, wet weights, and femur lengths. Numbers between arrows indicate Mahalanobis distances between group centroids

nate analysis that used an early subset of 1,637 colonies, the proportion of the variance that these two characters added to the overall analysis was only 0.22%. A cross validation analysis in which each of the 1,637 colonies was individually held from the data set and analyzed according to the measurements made on the other colonies produced the same results whether or not these two angles were included. These angles are formed from the intersections of thick veins and their measurement requires judging the geometric center of the intersection. This skill is difficult to teach and different persons will make the measurement in consistently different ways. For these reasons, these two wing venation angles were eliminated as components of the final procedure.

The importance of the groups of measurements made on various body parts to the accuracy of identification was also evaluated using an early subset of 1,926 colonies. All body parts included in the final set contributed reductions in the rate of misclassifications and were considered important to include in the final procedure.

Colony samples provided twenty-three measurements from each of ten worker bees. Sample means were calculated for each measurement and were used to estimate population means and variances. Measurements of commercial and feral Africanized honey bees, commercial, feral, and rustic European honey bees are different for some univariate measurements within major groups. However, these differences are minor when compared to the differences between the major groups of Africanized and European honey bees.

Multivariate discriminant analyses with more than three groups showed considerable overlap of the different Africanized and the different European groups. Based on the results of these preliminary multivariate discriminant analyses and the univariate analyses, three groups were chosen to be represented in the final multivariate discriminant analysis: 591 colonies of Africanized honey bees (combining feral, rustic, and managed colonies), 401 colonies of European bees (combining managed colonies and colonies of unknown origin), and 1,111 colonies of feral European bees (combining rustic and feral honey bees). Multivariate analyses of the colonies in these groups produced discriminant functions and coefficients that can be used to identify Africanized honey bees and commercial and feral European honey bees.

A multivariate analysis of variance (MANOVA) of the 23 characteristics showed that significant differences existed among the three groups (Wilks' Lambda = 0.1295, $p = 0.0001$). A post-MANOVA analysis of the Mahalanobis distances among the centroids of the groups revealed that each group was significantly different from the other two groups (Fig. 3).

The multivariate discriminant analysis correctly identified 565 (95.60%) of the 591 Africanized colonies and correctly identified all of the 1,512 European colonies (Table 1) according to our recommended regulatory standards (Table 2;

Fig. 3). In 19 (3.21%) cases, Africanized colonies were declared to be European with evidence of the introgression of Africanized genes and in 7 (1.19%) cases were declared to be European. Perhaps they were, since the sole criterion for inclusion in the Africanized group was to be found in an area considered to be generally Africanized. If an imported European colony somehow was involved in the sample's parentage it would nonetheless have been considered to be Africanized. This rate of misclassification is low and not likely to trouble commercial beekeeping, since in sensitive situations such as breeding programs, those colonies that are declared to be European with evidence of the introgression of Africanized genes would be culled from use. Three (0.14%) European colonies were

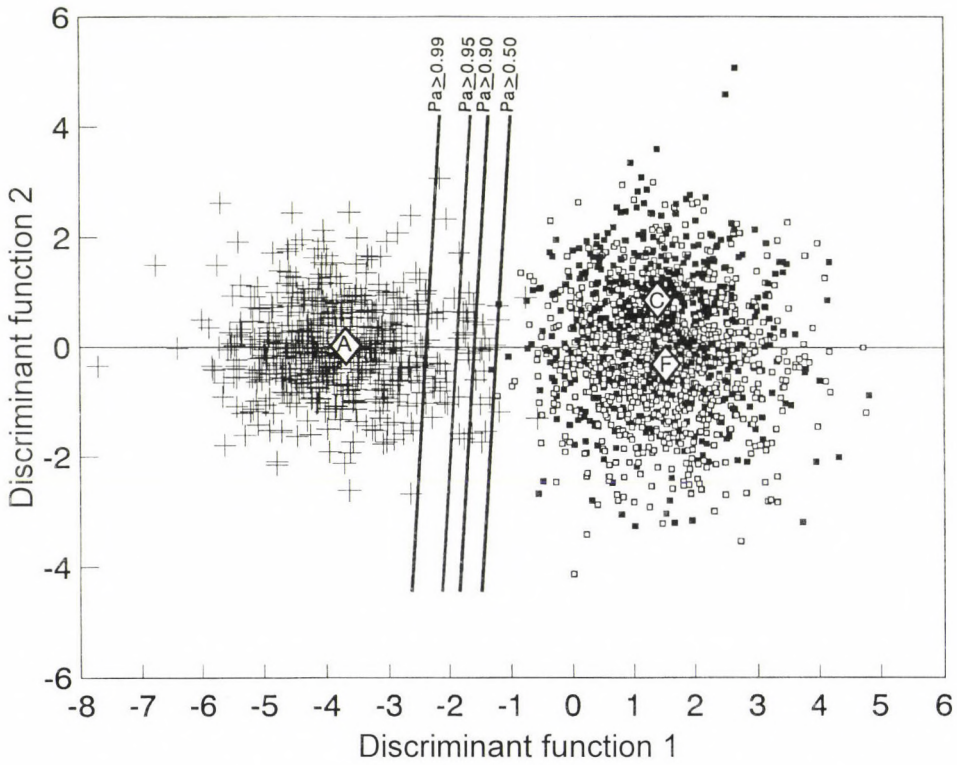

Fig. 3. Scatterplot of the results of the multivariate discriminant function analyses of Africanized and European honey bees: each + represents an Africanized colony, each ❒ represents a feral European colony and each ■ represents a commercial European colony. Some colony indicators are not visible due to the large number of colonies represented in the figure. The centroid for each group is marked by a ◊ : A = Africanized; F = feral European; C = commercial European. Using a pooled covariance matrix, the Mahalanobis distances between centroids are: Africianized to commercial European = 27.075; Africanized to feral European = 27.525; and commercial European to feral European = 1.356. Solid lines indicate a domaine to the left of the line which includes colonies with a probability of being Africanized of ≥ 0.99, ≥ 0.95, ≥ 0.90, and ≥ 0.50.

Table 1. Classification results (numbers and (percentages)) of the multivariate discriminate analysis

From the known group	To the classified group			
	Africanized	Africanized with evidence of the introgression of European genes	European with evidence of the introgression of African genes	European
Africanized	545 (92.22)	20 (3.38)	19 (3.21)	7 (1.19)
European (Commercial)	0	0	0	401 (100.00)
European (Feral)	0	0	3 (0.2)	1,108 (99.73)

The accuracy of the multivariate discriminate analysis was determined by withholding and classifying 250 randomly selected colonies at a time as independent samples. Classification is based on probabilities of group membership as shown in Table 2.

sufficiently Africanized-like to be suspected of having some Africanized genes. They may have as a consequence of early and undetected intrusion of Africanized bees into some of the collection sites (GARY *et al.* 1985). Alternately, they may be extreme samples from the European population. When the colonies were classified based strictly on their greatest probability of group membership, three colonies from the Africanized group were declared European with probabilities of being Africanized (pA) of 0.00004, 0.036, and 0.066 for colonies from the llanos of Venezuela, the Andes mountains of Venezuela, and the suburbs of Rio de Janeiro, Brazil. Two colonies from the European group were declared Africanized with pA of 0.544 and 0.668 for a colony from Mexico and for a feral colony from the desert of California. Additionally, the analysis was able to differentiate between commercial European and feral European colonies about 71% of the time.

Unstandardized function coefficients and constants are necessary to apply the discriminant analysis results to the identification of unknown samples. Mean body part measurements from an unknown sample of ten worker bees are multi-

Table 2. Guidelines for evaluating posterior probabilities of group membership in the identification of unknown samples

Probabilities	Determination
$0.990 \leq p\text{A} \leq 1.00$	Africanized
$0.900 \leq p\text{A} \leq 0.990$	Africanized with evidence of the introgression of European genes
$0.500 \leq p\text{A} \leq 0.900$	European with evidence of the introgression of African genes
$0.000 \leq p\text{A} \leq 0.500$	European

pA: probability of belonging to the Africanized group.

plied by the corresponding coefficients for each of the two functions. The two sums of these products are added to the appropriate constants to calculate the two function values required to determine the probability of group membership (RINDERER *et al.* 1993*a*).

With *a* as Africanized, *e* as commercial European and *f* as feral European, a first step in calculating exact probabilities of group membership (SAS Institute, 1982) is to determine three generalized square distances according to the general formula (in matrix notation),

$$D_i^2 = (X - \bar{X}_i) (\sum^{-1})^{1/2} (X - \bar{X}_i)' ,$$

where i is a, e, f.

Individual generalized square distances for unknown samples are based on derived functions. Character set measurements are multiplied by coefficients produced by the analysis of the baseline population data and the sums of these products are added to a function constant. Two derived functions are used to calculate exact probabilities of group membership:

$$D_i^2 = (\text{Function 1} + \text{Constant}_{i1})^2 / \text{Constant}_{i2} + (\text{Function 2} - \text{Constant}_{i3})^2 / \text{Constant}_{i4}$$

Each of the three posterior probabilities of group membership of a sample is then given by:

$$P_i = \frac{\exp(-0.5\, D_i^2)}{\sum_{t=a,e,f} \exp(-0.5 D_i^2)}$$

The determination of group membership for unknown samples is based on an interpretation of posterior probabilities of group membership. As hybridization of Africanized and European honey bees continues (BUCO *et al.* 1987, DEL LAMA *et al.* 1990, LOBO *et al.* 1989, HALL 1990, RINDERER *et al.* 1991*b*, 1992, SHEPPARD *et al.* 1991*a, b*, MORITZ & MEUSEL 1992, MCMICHAEL 1994), especially as Africanized bees continue their range expansion into areas having more temperate climates (SHEPPARD *et al.* 1991*a*), some samples will have probabilities of group membership which are intermediate between classification as clearly Africanized or clearly European. Intermediate probabilities are an indication of a colony possibly resulting from extensive hybridization. Intermediate scores may arise for individual colonies as the result of hybridization or simply because the colonies are rare cases sampled from the extremes of variation of one or another group. We evaluated 192 experimentally produced F_1 colonies. These colonies were generally intermediate between Africanized and European colonies (Fig. 4).

These morphometric procedures are used by the national governments of the United States, Mexico, Canada, Australia, New Zealand, and the United Kingdom as well as regional governments within these countries as the "offi-

cially recognized" means to identify Africanized honey bees. Scientists and regulators in other countries also rely on the procedures without them being designated as "officially recognized". The Agricultural Research Service of the United States Department of Agriculture has made the procedures accessible by providing training, a detailed manual for dissections, sample preparation, data entry and analysis (RINDERER *et al.* 1991*a*) and software programs (called USDA-ID) which guide data entry and provide analysis and identification.

The weaknesses and strengths of morphometric identification are often one and the same attribute. Since morphology is an old pursuit, it is sometimes considered outdated, but its long tradition makes it well established. It has a less perfect link to genes than DNA-based analyses but most of the characteristics have high heritabilities (OLDROYD & RINDERER 1991) and collectively the characteristics measured represent a far wider array of genes than could be reasonably ac-

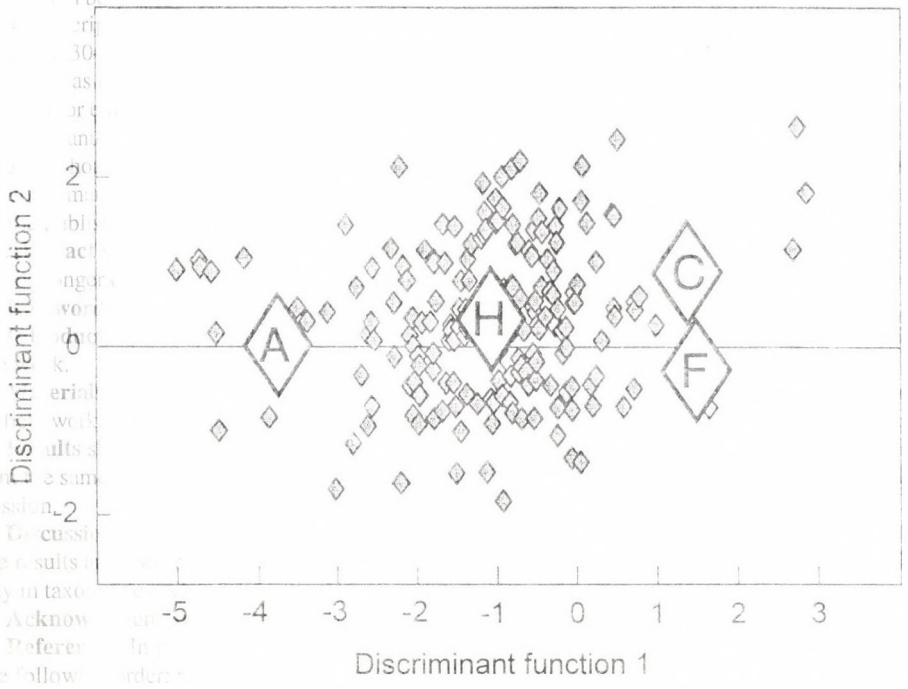

Fig. 4. Scatterplot of the results of classifying 192 experimentally produced F_1 colonies. These colonies were generally intermediate between Africanized and European colonies. Each ♦ represents one of these colonies. The centroid for the group is marked by a ◊ containing an H. The centroids of the groups used to derive the discriminant functions are each marked by a ◊ : A = Africanized, F = feral European, C = commercial European. The Mahalanobis distances between centroides are: hybrid to Africanized = 8.070; hybrid to feral European = 8.143; and hybrid to commercial European = 7.423.

cessed through DNA-based analyses. It is not suited to detect minor gene flow and hence not a fine-grained tool to study population genetics. However, because of this characteristic, it will only declare a sample to be Africanized or European with evidence of Africanized gene intrusion on very strong evidence. In the same regard, USDA-ID is structured to provide clear Africanized or European identifications. This is necessary for regulators to have unambiguous identifications. However, it also fosters a misinterpretation that samples with intermediate morphology are not found. Because of the clear identification produced by the program, it is not transparently easy to understand that samples that have intermediate morphology are interpreted by the software and assigned to either the Africanized or the European classifications.

OTHER TECHNOLOGIES

Many other approaches to identifying Africanized honey bees have been explored. For varied reasons they have proved less desirable than morphology, although several of them have value for scientific studies of various types.

Isozymes. Honey bees have far less isozyme variation than most organisms (SYLVESTER 1982). Only two enzymes, malate dehydrogenase (SYLVESTER 1982) and hexokinase (SPIVAK *et al.* 1988) show variation between Africanized and European honey bees. Using a known group of 12 Africanized and 19 European colonies, SPIVAK *et al.* (1988) used variation in these two enzymes to classify colonies. Thirteen percent of the Africanized group were misclassified as were 16% of the European colonies. Thus, the technique has little use for identification. It does have some application for detecting changes through time in population genetic studies.

DNA analyses. A variety of techniques fall within the general category of DNA analysis. The banding patterns produced by electrophoretically separating fragments of mitochondrial DNA produced by restriction enzymes (differential restriction fragment length patterns (mt-RFLP)) have been used in a variety of studies (ARIASD *et al.* 1990, HALL 1990, HALL & MURALIDHARAN 1989, RINDERER *et al.* 1991*b*, 1992, SHEPPARD *et al.* 1991*a*, SMITH *et al.* 1989, MCMICHAEL 1994, MORITZ & MEUSEL 1992). A serious weakness to using mt-RFLPs (or other ways of analyzing mt-DNA) as an identification tool is that mitochondria are only inherited from the maternal parent. Hence, backcrossing of an F_1 queen to the paternal parental type may produce colonies of honey bees that have a nuclear DNA subspecies constitution that differs substantially from that of the mt- DNA. Hence, in a recent survey, 17% of the Africanized honey bees of south Texas had European mitochondria (W. S. SHEPPARD, pers. comm.).

As with mt-DNA RFLP analysis, nuclear DNA RFLP analysis has been used to study the process of Africanization. One study (MCMICHAEL 1994) showed that as many as 50% of the alleles at certain loci in Africanized populations came from European parentage, indicating extensive hybridization in many Africanized populations. Thus, hybridization events negate the value of a limited number of loci as identification tools. In theory, direct examination of nuclear DNA using RFLP or other techniques will produce quality identifications. However, such analyses must be based on several loci.

The same conditions seem to hold when honey bee nuclear DNA is analyzed as variation in randomly amplified DNA segments (RAPD) (R. Page, pers. comm.). A large number of RAPD markers may produce information useful for identifications. However, the ability to identify unknowns is about the same as that of morphometric analysis and the costs of doing so are much higher. No identification procedures based on RAPD analysis of DNA have been published.

Much the same can be said of the analysis of the size variation of tandem repeat hypervariable microsatellite and minisatellite DNA regions. Although variation exists between parental populations, Africanized honey bees themselves do not have diagnostic nuclear DNA characteristics yet found which are qualitatively different (ESTOUP 1995). Frequency differences which are usually minor are common, and many of them could be combined to produce good identification systems. However, the costs, compared to the costs of morphometric analysis, are prohibitive.

Other Techniques. Behavioral characteristics such as flight behavior and stinging behavior, cuticular hydrocarbon components, the spectral analysis of pyrolysis products, etc., have all been evaluated as identification tools. All of them have proved unsuccessful because of cost efficiency, identification ability, or the lack of potential for many laboratories to conduct the techniques required for identification.

CONCLUSION

The pioneers of honey bee taxonomy who chose the study of numerical morphology as the way to describe subspecies chose well. Studies related to identifying Africanized honey bees have shown that numerical morphological characteristics are ideal in several ways. First, environmental circumstances, even extreme ones, have minimal effects on morphological characteristics of honey bees (DALY *et al.* 1995, OLDROYD & RINDERER 1991, RINDERER *et al.* 1986*b*). The effects of environment on morphology may be buffered since adults must care for honey bee brood. Second, the linkage between morphology and the honey bee genome is evidently close and broadly based. Most of the measured

characteristics have a very high heritability (OLDROYD & RINDERER 1991). Third, known genetically intermediate colonies overall have intermediate morphology with specific morphological characteristics having inheritance patterns that are often independent and indicative of polygenic origins. Hence, the entire pattern of morphology studied is regulated by a wide array of genes which mostly have additive rather than non-additive genetic effects (ROBERTS 1961, OLDROYD & MORAN 1987, RINDERER *et al.* 1990).

Morphological characters are therefore very suitable and currently superior to many other methods for distinguishing Africanized and European honey bees. The rapidity with which such determinations may be made (RINDERER *et al.* 1987) and the fact that morphology reflects many interacting aspects of the genome suggest that morphology may remain the method of choice for identifying honey bees subspecies and for studying dynamic genetic changes within and among populations of honey bees.

* * *

Acknowledgements – In cooperation with the Louisiana Agricultural Experiment Station.

REFERENCES

ALPATOV, W. W. (1929) Biometrical studies on variation and races of the honey bee Apis mellifera L. *Rev. Biol.* **4:** 1–57.

ARIASD, M. C., SOARES, A. E. E. & NOBREGA, F. G. (1990) Improvements to the mitochondrial restriction maps for Italian and Africanized honey bees. *Brazilian Journal of Genetics* **13:** 501–507.

BUCO, S. M., RINDERER, T. E., SYLVESTER, H. A., COLLINS, A. M., LANCASTER, V. A. & CREWE, R. (1987) Morphometric differences between South American Africanized and South African (Apis mellifera scutellata L.) honey bees. *Apidologie* **18(3):** 217–222.

BUTTEL-REEPEN, H. VON (1906) Apiacta. *Mitt. Zool. Mus. Berlin* **3:** 117–201.

COCHLOV, B. P. (1916) Investigations on the length of the bee tongue. *Min. Agric. Petrograd,* pp. 17–41. [in Russian]

COLLINS, A. M. & RINDERER, T. E. (1991) Genetics of defensive behavior I. Pp. 309–328. *In* SPIVAK *et al.* (eds): The "African" honey bee. Westview Press, Boulder, Colorado, U.S.A.

DALY, H. V. (1991) Systematics and identification of Africanized honey bees. Pp. 13–44. *In* SPIVAK *et al.* (eds): The "African" Honey Bee. Westview Press, Boulder, Colorado, U.S.A.

DALY, H. V. & BALLING, S. S. (1978) Identification of Africanized honey bees in the Western Hemisphere by discriminant analysis. *J. Kansas Entomol. Soc.* **51:** 857–869.

DALY, H. V., HOELMER, K., NORMAN, P. & ALLEN, T. (1982) Computer-assisted measurement and identification of honey bees (Hymenoptera: Apidae). *Ann. Entomol. Soc. Am.* **75:** 591–594.

DALY, H. V., DANKA, R. G., HOELMER, K., RINDERER, T. E. & BUCO, S. M. (1995) Honey bee morphometrics: Isometry and classification tested with European worker bees reared by varying ratios of nurse bees. *J. Apic. Res.* **34:** 129–145.

DANKA, R. G., RINDERER, T. E., COLLINS, A. M. & HELLMICH, R. L. (1987) Responses of Africanized honey bees (Hymenoptera: Apidae) to pollination management stress. *J. Econ. Entomol.* **80**(3): 621–624.

DEL LAMA, M. A., LOBO, J. A., SOARES, A. E. E. & DEL LAMA, S. N. (1990) Genetic differentiation estimated by isozymic analysis of Africanized honeybee populations from Brazil and from Central America. *Apidologie* **21:** 271–280

DUPRAW, E. (1964) Non-Linnean taxonomy. *Nature* **202:** 849–852.

ESTOUP, A., GARNERY, I., SOLIGNAC, M. & CORNUET, J-M. (1995) Microsatellite variation in honey bee (Apis mellifera L.) populations: Hierarchical genetic structure and test of the infinite allele and stepwise mutation models. *Genetics* **140:** 679–695.

GARY, N. E., DALY, H. V., LOCHE, S. & RACE M. (1985) The Africanized honey bee: Ahead of schedule. *California Agric.* **39:** 4–7.

GOETZE, G. (1930) Variabilitäts- und Züchtungsstudien an der Honigbiene mit besonderer Berücksichtigung der Langrüssligkeit. *Arch. Bienenkund* **11:** 135–274.

HALL, H. G. (1990) Parental analysis of introgressive hybridization between African and European honeybees using nuclear DNA RFLPs. *Genetics* **125:** 611–621.

HALL, H. G. & MURALIDHARAN, K. (1989) Evidence from mitochondrial DNA that African honey bees spread as continuous maternal lineages. *Nature* **339:** 211–213.

KERR, W. E. (1957) Introdução de abelhas africanas no Brasil. *Brasil Apicola* **3:** 211–213.

LOBO, J. A., DEL LAMA, M. A. & MESTRINER, M. A. (1989) Population differentiation and racial admixture in the Africanized honeybee (Apis mellifera L.). *Evolution* **43:** 794–804.

MAA, T. (1953) An inquiry into the systematics of the tribus Apidini or honey bees (Hym.). *Treubia* **21:** 525–640.

MCMICHAEL, M. A. (1994) *Genomic DNA restriction fragment length polymorphisms at a highly polymorphic locus distinguish Old and New World subspecies of the honey bee.* PhD Dissertation. Univ. Florida, Gainesville, Florida, U.S.A.

MORITZ, R. F. A. & MEUSEL, M. S. (1992) Mitochondrial gene frequencies in Africanized honeybees (Apis mellifera L.): Theoretical model and empirical evidence. *J. Evol. Biol.* **5:** 72–81.

OLDROYD, B. P. & MORAN, C. (1983) Additive and heterotic genetic effects in the haplo-diploid honey bee, Apis mellifera. *Aust. J. Biol. Sci.* **36:** 323-332.

OLDROYD, B. P. & RINDERER, T. E. (1991) Heritability of morphological characters used to distinguish European and Africanized honey bees. *Theor. & Appl. Genetics* **82:** 499–504.

RINDERER, T. E., BOLTEN, A. B., COLLINS, A. M. & HARBO, J. R. (1984) Nectar–foraging characteristics of Africanized and European honeybees in the neotropics. *J. Apic. Res.* **23**(2): 70–79.

RINDERER, T. E., SYLVESTER, H. A., BROWN, M. A., VILLA, J. D., PESANTE, D. & COLLINS, A. M. (1986*a*) Field and simplified techniques for identifying Africanized and European honey bees. *Apidologie* **17:** 33–48.

RINDERER, T. E., SYLVESTER, H. A., COLLINS, A. M. & PESANTE, D. G. (1986*b*) Identification of Africanized and European honey–bees: Effects of nurse–bee genotype and comb size. *Bull. Entomol. Soc. Am.* **32:** 150–152.

RINDERER, T. E., SYLVESTER, H. A., BUCO, S. M., LANCASTER, V. A., HERBERT, E. W., COLLINS, A. M. & HELLMICH, R. L. (1987) Improved simple techniques for identifying Africanized and European honey bees. *Apidologie* **18:** 179–197.

RINDERER, T. E., DALY, H. V., SYLVESTER, H. A., COLLINS, A. M., BUCO, S., HELLMICH, R. L. & DANKA, R. G. (1990) Morphometric differences among Africanized and European honey bees and their F1 hybrids (Hymenoptera: Apidae). *Ann. Entomol. Soc. Am.* **83:** 346–351.

RINDERER, T. E., BUCO, S. M., SYLVESTER, H. A. & STELZER, J. A. (1991*a*) *Manual for the laboratory preparation of honey bee samples and their analysis with the Universal System for the Detection of Africanized Bees.* USDA-ARS, Baton Rouge, Louisiana, U.S.A.

RINDERER, T. E., STELZER, J. A., OLDROYD, B. P., BUCO, S. M. & RUBINK, W. L. (1991*b*) Hybridization between European and Africanized honey bees in the neotropical Yucatan Peninsula. *Science* **253:** 309–311.

RINDERER, T. E., STELZER, J. A, OLDROYD, B. P., BUCO, S. M. & RUBINK W. L. (1992) Out of Africa: Hybrid bees. *Science* **256:** 720–721.

RINDERER, T. E., BUCO, S. M., RUBINK, W. L., DALY, H. V., STELZER, J. A., RIGGIO, R. M. & BAPTISTA, F. C. (1993*a*) Morphometric identification of Africanized and European honey bees using large reference populations. *Apidologie* **24:** 569–585.

RINDERER, T. E., OLDROYD, B. P. & SHEPPARD, W. S. (1993*b*) Africanized honey bees in the Americas. *Scientific American* **269:** 84–90.

ROBERTS, W. G. (1961) Heterosis in the honey bee as shown by morphological characters of inbred and hybrid bees. *Ann. Entomol. Soc. Amer.* **59:** 878–882.

RUTTNER, F. (1987) *Biogeography and taxonomy of honey bees.* Springer-Verlag, Berlin, 284 pp.

SAS Institute (1982) *SAS User's Guide: Statistics.* SAS Institute, Cary, N. C., U.S.A.

SHEPPARD, W. S., RINDERER, T. E., MAZZOLI, J. A., STELZER, J. A. & SHIMANUKI, H. (1991*a*) Gene flow occurs between Africanized and European–derived honey bee populations in Argentina. *Nature* **349:** 782–784.

SHEPPARD, W. S., SOARES, A. E. E., DEJONG, D. & SHIMANUKI, H. (1991*b*) Hybrid status of honey bee populations near the historic origin of Africanization in Brazil. *Apidologie* **22:** 643–652.

SMITH, D. R., TAYLOR, O. R. & BROWN, W. M. (1989) Neotropical Africanized honey bees have African mitochondrial DNA. *Nature* **339:** 213–215.

SPIVAK, M., RANKER, T., TAYLOR, O. Jr., TAYLOR, W. & DAVIS, L. (1988) Discrimination of Africanized honey bees using behavior, cell size, morphometrics, and a newly discovered isozyme polymorphism. Pp. 311–324. *In* NEEDHAM *et al.* (eds): *Africanized Honey Bees and Bee Mites.* Ellis Horwood, Chichester, United Kingdom.

SYLVESTER, H. A. (1982) Electrophoretic identification of Africanized honey bees. *J. Apic. Res.* **21:** 93–97.

ACTA ZOOLOGICA
ACADEMIAE SCIENTIARUM HUNGARICAE

An international journal of animal taxonomy and ecology

Instruction to authors

Submission of a paper implies that it has not been published previously, that is not under consideration for publication elsewhere, and that if accepted for the Acta Zoologica Hungarica, the authors will transfer copyright to the Hungarian Academy of Sciences/the Hungarian Natural History Museum as is customary. Articles and illustrations become the property of the HAS/HNHM.

Papers must be in English with British spelling, and be original contributions in the field of animal taxonomy, systematics, zoogeography and ecology. All manuscripts must be submitted to one of the editors (editor, assistant editor).

Entire manuscripts must be submitted on IBM compatible floppy disk and in duplicate printed copies and the author should retain a copy. In the case of multiple authors, the corresponding author should be indicated. Series of numbered papers will not be considered.

Manuscripts must be printed with double spacing (including the reference list), and with wide margins (30–35 mm) on the left side of the paper only. Authors are requested to keep their communications as concise as possible. Footnotes should be avoided or minimized, and italics should not be used for emphasis. A running head of not more than 30 letters should be supplied.

The manuscript should contain the following information:

Title should be followed by the name and full address of the author(s). Where possible, the fax and/or e-mail number of the corresponding author should be supplied with the manuscript, for use by the publisher.

Abstract should be a brief summary of the contents and conclusions of the paper, and should not be longer than 200 words and should not contain references.

Key words should not be more than five (exceptionally 6) key word entries.

Introduction should contain a brief survey of the relevant literature and the reasons for doing the work.

Materials and Methods supply sufficient information to permit repetition of the experimental or field work. The technical description of methods should be given only when such methods are new.

Results should be presented concisely. Only in exceptional cases will it be permissible to present the same set of results in both table and a figure. The results section should not be used for discussion.

Discussion should be separate from the results section and should deal with the significance of the results and their relationship to the object of the work (and, this is the place of the identification key in taxonomic revisions).

Acknowledgements (at most in 10 lines).

References. In principle the Harvard system is to be followed. References should be detailed in the following order: authors' names and initials, date of publication (in parentheses), the title of the article, the name of the journal as abbreviated in the World List of Scientific Periodicals (4th edn 1963), the volume, and the first and last pages of the article, e.g.

NORRBOM, A. L. and KIM, K. C. (1985) Taxonomy and phylogenetic relationships of Copromyza Fallén (s.s.) (Diptera: Sphaeroceridae). *Ann. Entomol. Soc. Am.* **78**: 331–347.

For books the author's names, date of publication, title, edition, page reference, publisher's name and the place of publication should be given, e.g.

HINTON, H. E. (1981) *Biology of insect eggs*, vol. 2. Pergamon Press, New York.

or

MCALPINE, J. F. (1981) Morphology and terminology, adults, pp. 9–63. *In* MCALPINE *et al.* (eds) *Manual of Nearctic Diptera*, vol. 1. Agriculture Canada, Ottawa.

In the text references should be given as MARSHALL (1992) or (MARSHALL 1992). When a citation includes more than two authors, e.g. GREY, BLACK and WHITE, the paper should be referred to in the text as GREY *et al.*, provided that this not ambiguous. If papers by the same author(s) in the same year are cited, they should be distinguished by the letters, *a, b, c,* etc., e.g. MARSHALL (1992*a*).

References to papers "in press" must mean that the article has been accepted for publication. References to "personal communications" and unpublished work are permitted in the text only: references to papers in preparation or submitted are not permissible.

All necessary **illustrations** should accompany the manuscript, but should not be inserted in the text. All photographs, graphs and diagrams should be numbered consecutively in Arabic numerals in the order in which they are referred to in the text. Glossy photographs or positive prints should be sent unmounted wherever possible and should be kept to a minimum. Figures should be of good quality. Explanation of lettering and symbols should be given in the figure caption and only exceptionally in the figures. Lettering and symbols to appear on the illustration should be of sufficient size to allow for considerable reduction where necessary (usually proper for a 50% reduction in size). Scales must be indicated on micrographs, not by magnifications in the legends. Figure size must not exceed 24×30 cm. On the back of each illustration should be indicated the author's name, the figure number (in Arabic numerals), and the top of the illustration, where this is not clear. Half-tones should be included only when they are essential. Details and quotation of publication of colour plates should be made to the editors. The following symbols should be used on line drawing: ● ■ ○ ❑ ▲ ◆ ♦ etc.

Legends to figures should be typed on a separate sheet. They should give sufficient data to make the illustration comprehensible without reference to the text.

Tables and appendices should be constructed so as to be intelligible without reference to the text, numbered in Arabic numerals and typed on separate sheets. Every table should be provided with an explanatory caption and each column should carry an appropriate heading. Units of measure should always be indicated clearly (metric units are preferred). All tables and figures must be referred to in the text.

Only standard **abbreviations** should be used. Arbitrary abbreviations and jargon will not be accepted.

The Latin names should be given for all species used in the investigation, although taxonomic affiliation and authority need not be provided in the title.

Page proofs will be sent to the author (or the first-mentioned author in a paper of multiple authorship) for checking. Corrections to the proofs must be restricted to printers' errors. Any substantial alterations other than these may be charged to the author. Authors are particularly requested to return their corrected proofs as quickly as possible in order to facilitate rapid publication. Please note that authors are urged to check their proofs carefully before return, since late corrections cannot be guaranteed for inclusion in the printed journal.

Fifty reprints free of charge will be sent to the first author; extra copies of the issue (at a specially reduced rate) can be ordered on the form which will accompany the proofs. These should be returned to: The Editorial Office of the Acta Zoologica, Hungarian Natural History Museum, Budapest, Baross u. 13, H–1088, Hungary

The **page charge** required from authors outside Hungary is USD 15 per printed page. In exceptional cases, the page charge may be waived. Please contact the editor in before submitting a paper if you ask for a waiver. Authors of papers exceeding 16 printed pages are asked to pay USD 40 (or HUF equivalent) for each such page, i.e. all costs of publication (irrespective of their nationality).

FOR FURTHER INFORMATION PLEASE CONTACT US
The Editorial Office of the Acta Zoologica
H–1088 Budapest, Baross u. 13, Hungary
Fax: (36–1) 3171669
http:/actazool.nhmus.hu/
E-mail: perego@zoo.zoo.nhmus.hu

SUBSCRIPTION INFORMATION

Orders should be addressed to

Editorial Office of the Acta Zoologica
Hungarian Natural History Museum
H–1088 Budapest, Baross u. 13, Hungary
Fax: (36–1) 3171669
E-mail: perego@zoo.zoo.nhmus.hu

Typeset: Pars Ltd., Budapest.
Printed by mondAt Ltd., Hungary

CONTENTS

HU ISSN 1217–8837

Acta Zoologica

Academiae Scientiarum Hungaricae

VOLUME 44 - NUMBER 3 - 1998

HUNGARIAN NATURAL HISTORY MUSEUM, BUDAPEST

ACTA ZOOLOGICA
ACADEMIAE SCIENTIARUM HUNGARICAE

AN INTERNATIONAL JOURNAL OF
ANIMAL TAXONOMY AND ECOLOGY

Acta Zoologica Academiae Scientiarum Hungaricae is published quarterly from February 1994 (other issues in May, August and November) by the Hungarian Natural History Museum and the Biological Section of the Hungarian Academy of Sciences with the financial support of the Hungarian Academy of Sciences.

For detailed information (contents, journal status, instructions for authors, subscription, and from Volume 40 onward title, author, authors' addresses, abstract, keywords and a searchable taxon index) please visit our website at

http://actazool.nhmus.hu/

Acta Zoologica Academiae Scientiarum Hungaricae 44 (3), pp. 195–203, 1998

ON THE INTERPRETATION OF PLEXUS DIAGRAMS: AN EXAMPLE OF CANADIAN MICROCRUSTACEAN COMMUNITIES

MOSKÁT, C.[1] and L. FORRÓ[2]

[1]*Animal Ecology Research Group, Hungarian Academy of Sciences*
c/o Hungarian Natural History Museum, H-1088 Budapest, Baross u. 13, Hungary
E-mail: moskat@zoo.zoo.nhmus.hu
[2]*Department of Zoology, Hungarian Natural History Museum*
H-1088 Budapest, Baross u. 13, Hungary
E-mail: forro@zoo.zoo.nhmus.hu

Microcrustacean communities and chemical variables measured in Canadian saline lakes were analyzed to demonstrate the usefulness of plexus diagrams with the aim to elucidate structure in species-environmental complexes. Some of the alternative multivariate techniques to calculate and draw plexus diagrams were also examined. It was shown that, depending on the type of transformation of the rank correlation matrix, both the highly negative and the highly positive values can have the same effect, a tendency for points to get closer on the diagram. This type of plexus diagrams emphasises the high associations including negative relationships, like the avoidance of a habitat component. It is also shown that plexus diagrams are suitable to display community structure hierarchically by the strength of associations at different significance levels. The plexus diagram helped identify species preferring saline lakes, generalists, and species avoiding saline waters.

Key words: multivariate analysis, plexus diagram, ordination, community structure, Branchiopoda, Copepoda, saline waters, British Columbia

INTRODUCTION

It can be seen from past uses (WHITTAKER 1967, MCINTOSH 1978, MATUS & TÓTHMÉRÉSZ 1990) that plexus diagrams are useful tools to elucidate the structure of complex data-sets. The plexus technique is particularly suited to examination of species-habitat associations when two or more subsets of data can be separated on a logical basis, such as abundance data of a bird community, vegetation physiognomical data, vegetation floristical data. The multivariate plexus concept (MOSKÁT 1991) offers a flexible framework to analyze and display wildlife-habitat relationships. As there are many techniques for plexus analysis, the plexus diagram can be drawn in several ways. Our aim in this paper is to review techniques, and to examine what type of information can be gained when they are applied in community-environment analysis. A data set from saline lakes in British Columbia, including species of Branchiopoda, and Copepoda, and chemical parameter data, serves as an illustration of the method.

MATERIAL AND METHODS

Study area

The microcrustacean fauna of saline lakes on the southern Interior Plateau in British Columbia was investigated. The climate of this region is semi-arid to subhumid, annual precipitation is 300–400 mm, with cold winters and warm summers. Vegetation varies with elevation and latitude from dry bunch grass and sagebrush communities to mountain closed forest. The geology is highly variable and consequently the chemical properties of the saline waters are very diverse (HAMMER 1986). RENAUT (1990) established two main groups: alkaline waters with Na^{+}-CO_3^{--}, and more neutral ones with Mg^{++}-Na^{+}-SO_4^{--} dominance. All lakes studied are relatively small and shallow. Further information on the chemistry and biology of these waters can be found in TOPPING & SCUDDER (1977), HAMMER & FORRÓ (1992) and BOS *et al.* (1996).

Sampling

Zooplankton populations from 17 lakes were sampled in August 1990 by wading into the water from the shore. Qualitative samples were taken by using a plankton net of 100 μm mesh size. Samples were fixed with formol immediately after collecting. Five abundance categories were established for the species.

Preparing the plexus diagram

As originally suggested by MATTHEWS (1978), a plexus diagram is the graphical representation of multidimensional inter-species similarities in a two-dimensional network often relying on sorting of similarity coefficients by eye. A plexus diagram is composed of subgraphs in which connection between a pair of elements is established if they are significantly associated. WHITTAKER (1967) found a variety of similarity coefficients to be useful in ecology. In multivariate plexus analysis (MPA) coordinates of elements are calculated, using metric or non-metric multidimensional scaling (MATTHEWS 1978, WHITTAKER 1987, MOSKÁT 1991).

The evolution of the multivariate plexus analysis

Multivariate plexus analysis is a multistep procedure developed for the analysis of comp[redacted] structures, especially species-environment relationships. A brief account of MPA and its uses is a[redacted] propriate:

(1) WHITTAKER (1967) considered the species-plexus idea useful for a graphical represent[redacted] tion of plant species associations according to ecological similarities.

(2) MCINTOSH (1978) considered the conjunction of the plexus technique with multivariate ordination, and recommended it particularly for the analysis of highly heterogeneous data sets.

(3) MATTHEWS (1978) combined the plexus technique with non-metric multidimensional scaling, by constructing an objective species plexus based on species correlations using the PEARSON's correlation coefficient.

(4) WHITTAKER (1987) developed a four-stage computational procedure for analyzing vegetation-environment relationships. He used detrended correspondence analysis scores of vegetation with environmental variables, and replaced the correlation coefficient by the more robust Kendall rank correlation.

(5) The multivariate plexus concept (MPC), a general framework for multivariate plexus analysis (MPA) developed by MOSKÁT (1991), consists of the following steps:

(i) An eigenordination (principal components analysis, correspondence analysis, principal coordinates analysis, etc.) is performed to simplify the data structure of any submatrix of data. MPC makes it possible to choose the type of analysis most appropriate to the characteristics of the data and to the problem.

(ii) Kendall rank correlations are computed between the components derived by eigenvector ordinations or between the components and the original variables.

(iii) Rank correlations are transformed prior to further analysis (e.g. $\tau'=1-abs(\tau)$).

(iv) Non-metric multidimensional scaling (NMDS) is used to analyze the transformed rank correlation matrix. Coordinates from NMDS are used for drawing the positions of the components or the components and the original variables in the ordination space.

(v) Between the components or the original variables, where rank correlations showed significant values, connections are drawn by lines of different type indicating the level of significance.

(vi) Negative and positive relationships are shown by '-' or '+' signs over the lines.

Steps (iv)-(vi) lead to the plexus diagram. WHITTAKER (1987) used predefined categories of the values of rank correlations to make connections between associated elements, but MOSKÁT (1991) suggested use of the significance levels of the Kendall rank correlations, because with the latter one can test associations under specific conditions (SOKAL & ROHLF 1981). In the case of plexus diagrams the independence criterion is not supported, and the test is applied for the sake of illustration only.

Resolution levels on the plexus diagram

Connections between elements on the plexus diagrams are drawn according to the significance levels of the associations. Only in this sense can we speak about resolution levels of the association structure. When the association is highly significant (e.g. $p<0.0001$, or $p<0.001$) it suggests a strong relationship, but at weaker levels (e.g. $p<0.05$) the effect of pure chance is larger. Practically, researchers have to take into consideration if weaker relationships are useful in interpreting community structure, or whether to omit them from the diagram, especially when the number of cases is low. Sometimes there are too many relationships depicted in the diagram, and omission of the weakest ones makes the picture more interpretable.

Multivariate plexus analysis of microcrustacean communities

The multivariate plexus analysis was carried out as follows. The data matrix of the abundances of Branchiopoda and Copepoda was joined with the matrix of chemical parameters. Kendall rank correlation (τ) for species and chemical components obtained by PCA was computed based on the joined data matrix. Rank correlations were transformed in five different ways:

(1) $\tau'=1-abs(\tau)$,

(2) $\tau'=1-\tau$,

(3) $\tau'=sqrt(1-\tau)$,

(4) $\tau'=sqrt(1-\tau^2)$,

(5) $\tau'=1-(\tau+1)/2$.

Non-metric multidimensional scaling analyses were carried out using the matrices of transformed rank correlations to obtain ordinations of the species-environmental plexus.

Computations were performed by the PLEXUS computer program package (MOSKÁT *et al.* in prep.).

RESULTS AND INTERPRETATION

The structure of the Branchiopoda and Copepoda communities in relation to chemical parameters of saline lakes in British Columbia

Sixteen species were found in the samples, including 2 Anostraca, 8 Cladocera and 6 Copepoda. The number of species per sampling unit varied between 1 to 6. The most common species was *Diaptomus sicilis*, found in 13 samples.

Two cladocerans, *Daphnia similis* and *Ceriodaphnia quadrangula* were encountered in 6 localities, the remaining species were restricted to only few water bodies. Rare species, occurring in only one sample were omitted from the data set, so twelve species were used for subsequent analyses.

Salinity of the waters from where samples were taken covered a wide range (conductivity varied from 1.5 to 64 mS), however, in 11 waters the conductivity was below 10 mS. In only three samples was conductivity above 50 mS.

Before the plexus analysis a principal components analysis (PCA) was carried out on the original chemical data, in order to reduce the number of environmental components, and to reveal their interrelationships. For plexus analysis only the first two components were used. The corresponding two eigenvalues represented about 47% and 29% of the total variance, respectively. Component 1 ("C1") was interpreted as the salinity component, combining the original variables with high positive loadings: conductivity, Na^+, K^+, HCO_3^-, CO_3^{--}, and Cl^- (Table 1). Component 2 ("C2") represents a combination of the bivalent cations: pH (+), Ca^{++} content (-), Mg^{++} content (-), and the $(Na^+ + K^+)/(Mg^{++} + Ca^{++})$ ratio (+).

The plexus diagram (Fig. 1*a*) revealed the between-element relationships on three hierarchical levels: weak relationships ($p<0.1$), intermediate relationships ($p<0.01$), and strong relationships ($p<0.001$). Generally, these levels of significance can be chosen flexibly, adjusted to the properties of the given data set. The diagrams show only the relationships between chemical components and species.

Our data set included samples taken along a salinity gradient. We expect that microcrustacean species preferring saline waters would show relationships

Table 1. Component correlations of 11 chemical variables with the first two components (PC I and PC II), obtained by principal components analysis (PC I and II explain 76% of the total variance.)

Chemical variables	PC I	PC II
pH	0.192	0.677
conductivity	0.799	-0.518
Na^+	0.923	-0.261
K^+	0.862	-0.182
Ca^{++}	0.012	-0.955
Mg^{++}	0.035	-0.887
HCO_3^-	0.909	0.203
CO_3^{--}	0.813	0.370
Cl^-	0.871	0.023
$Na^+ + K^+/Mg^{++} + Ca^{++}$	0.655	0.616
HCO_3^-/Cl^-	-0.484	0.381

with the salinity component ("C1"). In fact we found that the two species belonging to this category, namely *Artemia franciscana* and *Moina hutchinsoni* showed strong positive relationships with C1, while some other species, including generalists and species avoiding saline waters such as *Daphnia schoedleri* and *Ceriodaphnia quadrangula*, showed negative associations with the salinity component. Chemical component 2 ("C2"), which was interpreted as a gradient of bivalent cations, shows only weak relationships with microcrustaceans. The picture became quite clear when we presented interspecies relationships in a plexus diagram (Fig. 1*b*). For example the species *Diaptomus connexus* is known to prefer saline waters, it has no direct relationships with C1, the salinity component, but it has a positive connection to the species *Artemia franciscana*, a species directly connected to C1. We think that white noise in sampling marked the relationship, but indirectly it surfaces in the relationship with *Artemia*.

The plexus diagram is hierarchical as regards levels of resolution (e.g. $p<0.1$, $p<0.01$, $p<0.001$ in our example). It is possible to choose a higher level of the minimum significance to show only the stronger relationships (Fig. 1.c).

The effect of transformation of rank correlations on the plexus diagram

For non-metric multidimensional scaling the values of Pearson correlation coefficient or Kendall rank correlation coefficient need to be transformed, because both coefficients have values in the range [-1, 1], but the input values in NMDS must be non-negative. MATTHEWS (1978) applied the y=1–x transformation, and one of us (MOSKÁT 1991) used y=1–abs(x). When this transformation is applied, both the highly negative and highly positive values have the same effect on the diagram. The signs in the graphs (Figs 1*a, d*) indicate the signs of the relationship whether positive or negative. Figures 1*a, d* show the effect of transformations (1) and (5) on the plexus diagram. Although five transformations were applied, and each of them yielded different values of the resemblance function, only two different diagrams were produced. For this reason only these two different result were displayed on the diagram (Figs 1*a, d*). As the NMDS is based on the rank order of the values, not on the exact values, transformations $\tau'=1-\text{abs}(\tau)$ and $\tau'=\text{sqrt}(1-\tau^2)$ gave the same results. On the other hand transformations $\tau'=1-(\tau+1)/2$, $\tau'=1-\tau$ and $\tau'=\text{sqrt}(1-\tau)$ produced the same diagram. We note that notwithstanding the present example, sometimes the transformations may lead to slightly different results. The reason is the stress function, an indicator of goodness of the solution for rearrangements of points, uses not only the rank order of the elements. While transformations $\tau'=1-\text{abs}(\tau)$ and $\tau'=\text{sqrt}(1-\tau^2)$ emphasize the strong associations, regardless whether positive or negative, transformations $\tau'=1-(\tau+1)/2$, $\tau'=1-\tau$ and $\tau'=\text{sqrt}(1-\tau)$ follow the idea of the traditional ordination diagrams, that is more different objects are placed far apart in the NMDS ordination space.

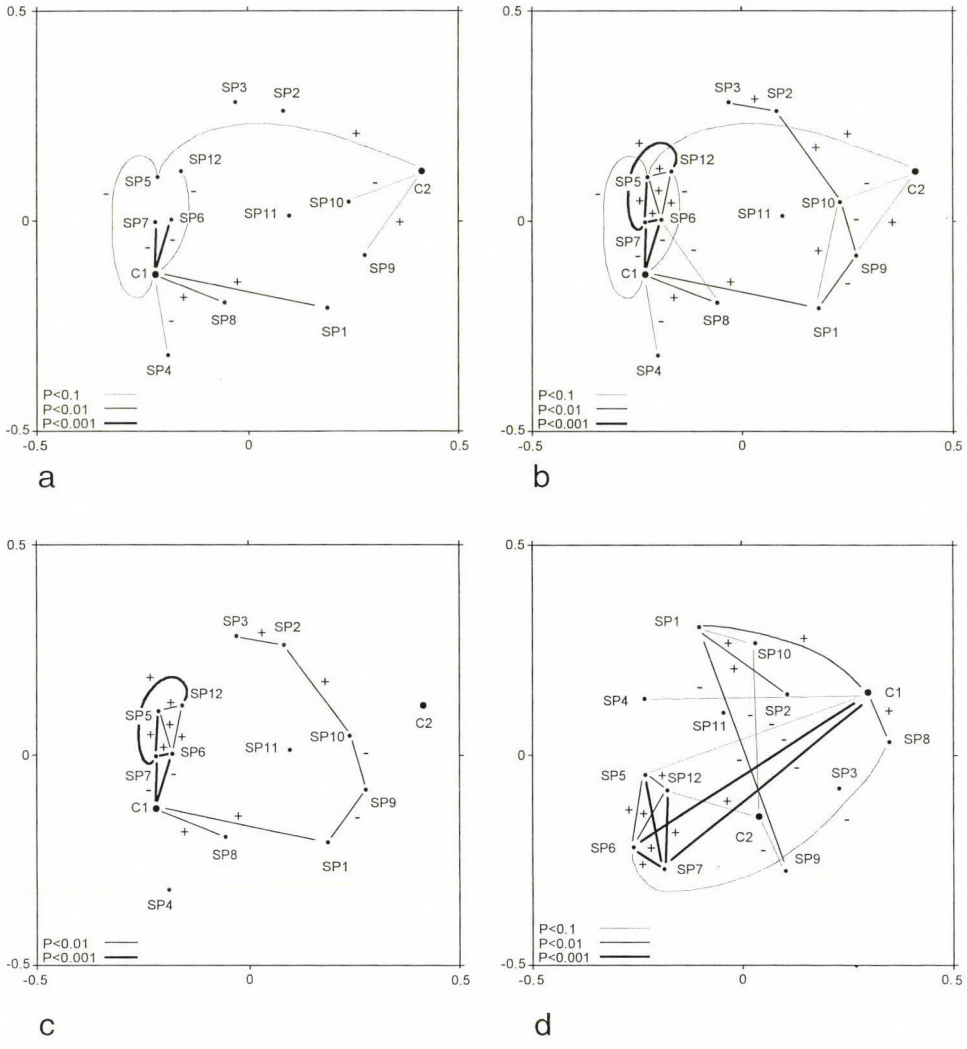

Fig. 1.(a-d) Plexus diagram produced by multivariate plexus analysis on 12 microcrustacean species and 2 environmental components. Multivariate plexus analysis was carried out by non-metric multidimensional scaling on the pooled Kendall rank correlation matrix. Environmental components were derived by principal components analysis of 11 chemical variables. Large dots represent environmental components (C1 salinity component, C2 bivalent cations). Small dots indicate microcrustacean species (SP1=*Artemia franciscana*, SP2=*Branchinecta mackini*, SP3=*Daphnia similis*, SP4=*Daphnia pulex*, SP5=*Daphnia schoedleri*, SP6=*Ceriodaphnia quadrangula*, SP7=*Scapholeberis rammneri*, SP8=*Moina hutchinsoni*, SP9=*Diaptomus sicilis*, SP10=*Diaptomus connexus*, SP11=*Diaptomus nevadensis*, SP12=*Acanthocyclops robustus*). Figs (a)-(d) differ in (i) the type of transformation of the pooled rank correlation matrix before non-metric multidimensional scaling (Figs (a)-(c): $\tau'=1-\text{abs}(\tau)$, (d): $\tau'=1-\tau$); (ii) threshold levels of associations presented on the diagram (Figs (a), (b), and (d): $p<0.1$, $p<0.01$, and $p<0.001$, and (c): $p<0.01$, $p<0.001$); (iii) restrictions on displaying relationships (Figs (b)-(d): all, (a): only between environmental components and species).

DISCUSSION

It is necessary to distinguish between plexus diagrams created in the classical way, where the positions of the elements are arbitrary, and those in which positions of the points are coordinates derived from non-metric multidimensional scaling or other ordination. In vegetation ecology plexus techniques were very popular. The connections in the plexus diagram display the strength of similarity between the objects or characters. This was typically so in the case of MCINTOSH (1978). Plexus diagrams were most commonly applied to represent a pattern of species as points linked by positive similarity coefficients (WELCH 1960, AGNEW 1961, JUHÁSZ-NAGY 1963). Occasionally negative and positive interrelationships were also recognized (MCINTOSH 1957). In these plexus graphs, the distance between elements was approximately proportional to the magnitude of association. Connecting lines were drawn when the level of association reached a predefined value. In an early variant of the multivariate plexus analysis MATTHEWS (1978) used a plexus diagram to express the correlation structure in a sample of plant species. This plexus diagram, similar to the early constructions, represented the correlations according to value categories ($r>0.50$, $r>0.40$, $r>0.30$, $r>0.25$). WHITTAKER's plexus diagram (WHITTAKER 1987), changed this in that it displayed relationships between elements of the two sets of the observational data, plant species and environmental variables, where the value of the rank correlation has reached significance at $p>0.001$ for τ in three categories ($\tau>0.5$, $\tau>0.4$, $\tau>0.3$). WHITTAKER used the Kendall rank correlation instead of the Pearson product-moment correlation coefficient. This type of plexus diagram showed well-structured relationships, where environmental variables were clustered around detrended correspondence analysis (DCA) axes of the plant species data. As plant species were not represented, only the DCA axis, this diagram revealed little about correlations among species, but still gave valuable information on the effects of the environmental variables on the species as a group. MOSKÁT (1991) and MOSKÁT & FUISZ (1995) also applied Kendall rank correlation coefficient, but connected the elements of the graph according to significance levels ($p<0.5$, $p<0.01$, $p<0.001$). This type of plexus diagram emphasized both the strong negative and positive relationships. We mention that MOSKÁT's multivariate plexus analysis applied the $\tau'=1-\text{abs}(\tau)$ transformation for the rank correlations prior to non-metric multidimensional scaling. The present paper examined the effect of this type of transformation with respect to the traditional ones. Altogether five transformations were applied, including the $r'=1-r_{ij}$ type, which was used by MATTHEWS (1978) for the transformation of the PEARSON product-moment correlation coefficient. Based on the results, we recommend the application of transformations $\tau'=1-\text{abs}(\tau)$ which yields a plexus diagram emphasizing strong associations by close positions, and weak relationships by greater distance.

Generally, the plexus diagram becomes less clear when the transformation $\tau'=1-\tau$ or its relatives are applied.

Plexus diagrams display significant relationships between elements. If the number of significant relationships is high, the diagram can be overwhelmed by lines. In this case only the highly significant relationships should be drawn. This "weeding out" of elements may be necessary also when white noise is extensive due to sampling effects, low sample size, rare species etc. Although multivariate plexus analysis could be done on a simple rank correlation matrix, similar to classical plexus analysis (e.g. WHITTAKER 1967), and its result plotted as a plexus diagram, the main advantage of the multivariate plexus analysis can be understood when the analysis is carried out on complex data structures. In this case two or more different, logically separate subsets of data are used, such as vegetation and environmental. In this case the relationships between the pairs of elements belonging to two different subsets are of main interest to be displayed. Taking into consideration that all relationships are responsible for the position of the variables on the diagram, the plot is natural. In this case preliminary ordination analysis may be desired on one or more subsets of data. Principal components analysis for vegetation physiognomical data, and correspondence analysis for vegetation floristical data have been used in the analysis of bird-habitat relationships (MOSKÁT 1991). In this case the components are uncorrelated, at least linearly, thus expressing the relationships between environmental components seems to be superfluous. The only exception is when strong non-linear association has been detected. In contrast, the present study showed that displaying the between-species associations can be important in understanding the structural relationships. Connecting elements may reflect the relationships between elements, which are not connected directly to each other. We think that albeit a plexus diagram appears to be a static demonstration of the species-environmental complex, plexus diagrams in fact are rather dynamic, since the resolution levels displayed on the diagram can be chosen to reveal different aspects of relationships. Generally, some of the important structural relationships cannot be realized directly because of several methodological problems, but varying threshold levels and connecting elements between two distinct elements may reflect these. We think that plexus diagrams should be used widely when the objective is to reveal the structure of species-environmental interrelationships.

* * *

Acknowledgements – The authors are indebted to J. PODANI, L. ORLÓCI and B. TÓTHMÉRÉSZ for their comments on the manuscript. The study was supported by the Hungarian Scientific Research Fund (OTKA) Nos T12832 and T16510 to C. M. One of us (L. F.) would like to thank Professor U. T. HAMMER for his invitation and financial support which made the study of the microcrustacean fauna possible.

REFERENCES

AGNEW, A. D. Q. (1961) The ecology of Juncus effusus L. in North Wales. *J. Ecol.* **49:** 83–102.

BOS, D. G., CUMMING, B. F., WATTERS, C. E. & SMOL, J. P. (1996) The relationship between zooplankton, conductivity and lake-water ionic composition in 111 lakes from the Interior Plateau of British Columbia, Canada. *Int. J. Salt Lake Res.* **5:** 1–15.

HAMMER, U. T. (1986) *Saline lake ecosystems of the world.* Dr. W. Junk Publishers, The Hague, 602 pp.

HAMMER, U. T. & FORRÓ, L. (1992) Zooplankton distribution and abundance in saline lakes of British Columbia, Canada. *Int. J. Salt Lake Res.* **1:** 65–80.

JUHÁSZ-NAGY, P. (1963) Investigations on the Bulgarian vegetation. Some hygrophilous plant communities. (I-III.) *Acta Biol. Debrecina (Acta Univ. Debrecen, Ser. 2)* **2:** 47–70.

MATTHEWS, J. A. (1978) An application of non-metric multidimensional scaling to the construction of an improved species plexus. *J. Ecol.* **66:** 157–173.

MATUS, G. & TÓTHMÉRÉSZ, B. (1990) The effect of grazing on the structure of a sandy grassland. Pp. 23–30. *In* KRAHULEC, F., AGNEW, A. D. Q., AGNEW, S. & WILLEMS, J. H. (eds): *Spatial processes in plant communities.* SPB Academic Publishing, The Hague.

MCINTOSH, R. P. (1957) The New York Woods, a case history of forest succession in southern Wisconsin. *Ecology* **38:** 29–37.

MCINTOSH, R. P. (1978) Matrix and plexus techniques. Pp. 151–184. *In* WHITTAKER, R. H. (ed.): *Ordination of plant communities.* Dr. W. Junk Publishers, The Hague.

MOSKÁT, C. (1991) Multivariate plexus concept in the study of complex ecological data: an application to the analysis of bird-habitat relationships. *Coenoses* **6:** 79–89.

MOSKÁT, C & FUISZ, T. (1995) Bird community and vegetation structure in Central-European deciduous forests: a multivariate study. Pp. 643–647. *In* BISSONETTE, J. A. & KRAUSMAN, P. R. (eds): *Integrating people and wildlife for a sustainable future.* Proc. First Intern. Wildlife Management Congr. The Wildlife Society, Bethesda, MD, USA.

RENAUT, R. W. (1990) Recent carbonate sedimentation and brine evolution in the saline lake basins of the Cariboo Plateau, British Columbia, Canada. *Hydrobiologia* **197**: 67–81.

TOPPING, M. S. &. SCUDDER, G. G. E. (1977) Some physical and chemical features of saline lakes in central British Columbia. *Syesis* **10:** 145–166.

WELCH, J. R. (1960) Observations on deciduous woodland in the eastern province of Tanganyika. *J. Ecol.* **48:** 557–573.

WHITTAKER, R. H. (1967) Gradient analysis of vegetation. *Biol. Rev.* **42:** 207–264.

WHITTAKER, R. J. (1987) An application of detrended correspondence analysis and non-metric multidimensional scaling to the identification and analysis of environmental factor complexes and vegetation structure. *J. Ecol.* **75:** 363–376.

Received 26th January, 1998, accepted 30th September, 1998, published 28th December, 1998

Acta Zoologica Academiae Scientiarum Hungaricae 44 (3), pp. 205–281, 1998

TWENTY TWO NEW SPECIES AND SIX NEW SUBSPECIES OF NOCTUIDAE FROM TURKMENISTAN AND ADJACENT REGIONS (LEPIDOPTERA)

RONKAY, L.[1], VARGA, Z.[2] and M. HREBLAY[3]

[1]*Department of Zoology, Hungarian Natural History Museum*
Baross u. 13, H–1088 Budapest, Hungary, E-mail: ronkay@zoo.zoo.nhmus.hu
[2]*Department of Zoology and Evolution, Kossuth Lajos University*
H–4010 Debrecen, Hungary, E-mail: zvarga@tigris.klte.hu
[3]*Somfa u. 15, H–2030 Érd, Hungary*

Descriptions of *Euxoa sayvana*, *Eicomorpha firyuza*, *Cucullia petrophila*, *C. xerophila*, *C. apo*, *Omphalophana turcomana*, *Allophyes sericina*, *Episema minutoides*, *Dasypolia nebulosa*, *D. ipaykala*, *Polymixis pericaspicus*, *P. schistochlora*, *P. fabiani*, *P. achrysa*, *P. csorbagabori*, *Agrochola turcomanica*, *Cryphia basivittata*, *C. duskeimima*, *Gortyna roseago*, *Chilodes repeteki*, *Haemerosia albicomma*, *H. ionochlora* spp. n. and *Periphanes delphinii tekke*, *Conisania vidua eupepla*, *Dasypolia templi dushaki*, *Bornolis crinomima diluta*, *Agrochola oropotamica archar* and *Autophila luxuriosa arnyekolta* sspp. n. are given. The taxonomic states of some species recently described from Turkmenistan are discussed, new synonymies, new status and combinations are established. With 175 figures.

Key words: new species and subspecies, Noctuidae, Turkmenistan

INTRODUCTION

During six expeditions made into Turkmenistan between the years 1990–1992, a surprisingly high number of new Noctuidae taxa were collected. Many of them have closely related vicariant taxa (species or subspecies) in the neighbouring territories, mostly in Transcaucasia and in the Elburz Mts. Therefore the Kopet-Dagh Mts fully satisfie the criterion of an "area of endemism" (sensu HAROLD & MOOR 1994).

The very high number of species, including numerous endemic ones, within a relatively restricted and not very high montaineous region can be explained by two major sources of high species-diversity.

The Kopet-Dagh Mts, together with the neighbouring mountains of Khorassan (NE Iran, see the map, Fig. 49) had been a large island or at least peninsula during the late Tertiary and Quaternary transgression phases of the Ponto-Caspian inland sea.

In addition, in the arboreal refuges of the gorge-like valleys of these mountains, which are well-known centres of genetic diversity of native flora and culti-

vated plants as well, many Tertiary relict species could survive the glacial phases and also the arid periods of post-glacial times.

Thus, within this area, there are favourable conditions both for relict-like survival of ancient taxa and for autochtonous speciation.

Abbreviations: Zoologisches Forschungsinstitut und Museum Alexander Koenig, Bonn; BIN – Biological Institute, Russian Academy of Sciences, Novosibirsk; HM – HREBLAY MÁRTON; HNHM – Hungarian Natural History Museum, Budapest; MNHU – Museum für Naturkunde, Humboldt-Universität, Berlin; NHM – Naturhistorisches Museum, Vienna; PL - JACQUES PLANTE; RL – RONKAY LÁSZLÓ; VZ – VARGA ZOLTÁN; ZIN – Zoological Institute, Russian Academy of Sciences, St. Petersburg; ZM – Zoological Museum, Copenhagen.

The holotypes, deposited in the private collections of GY. FÁBIÁN, M. HREBLAY and G. RONKAY, are available for studies through the Hungarian Natural History Museum, Budapest.

TAXONOMIC AND BIOGEOGRAPHIC COMMENTS ON SOME SPECIES AND GENERA OCCURRING IN TURKMENISTAN

During the treatment of a late autumn noctuid material, two new *Pseudopseustis* species *P. miatleuski* and *P. turcmana* were described from Turkmenistan by BERGMANN and THÖNY (1996). The specimens of the type series of these species, however, represent the two colour forms of *Pseudohadena (Jaxartia) elinguis* (PÜNGELER, 1914), a desert species rather widespread in the Kara-Kum and the Kizyl-Kum. The differences of the male genitalia mentioned in the diagnoses are small, matching well with the variation of *P. elinguis*; in addition the unusual configuration of the vesica of the holotype of *P. miatleuski* is a result of incomplete eversion. The taxonomic analysis of the genus *Pseudohadena* and its subgenera are given by RONKAY *et al.* (1995); the two taxa under discussion are here formally synonymized with *P. elinguis (P. miatleuski* and *P. turcmana*, syn. n.).

In 1998, a new *Polymixis* species, *P. remmi* was described by LUIG, MIATLEWSKI et SALDAITIS (1998) which is conspecific (and con-subspecific) with *Polymixis (Parabrachionycha) atossa limula* SUKHAREVA, 1978, described from the Kizyl-Kum area. The taxonomy of this widespread species, distributed from SE Turkey and N Iraq throughout the Middle Asian mountain systems and their foothills to the Pamir and the eastern Tien Shan massif, is rather difficult as the local populations are often conspicuously different. The genitalia of these "subspecies", however, are highly uniform, displaying no significant differences and the individual variation within the populations is rather large. *P. remmi* is here formally synonymized with *P. atossa* WILTSHIRE, 1941 (syn. n.).

DESCRIPTIONS OF NEW TAXA

Euxoa sayvana VARGA et RONKAY sp. n.
(Figs 3, 4, 50, 51, 89, 90)

Holotype: male, Turkmenistan, Kopet-Dagh Mts, 1300 m, Sayvan valley, cca 10 km N of Sayvan, 11.X.1991, No. L41, leg. A. PODLUSSÁNY, L. RONKAY & Z. VARGA (Coll. Z. VARGA, ZIUD).

Paratypes: Turkmenistan. 33 males, 19 females, from the following localities: Kopet-Dagh Mts, 1300 m, Sayvan valley, cca 10 km N of Sayvan, 11.X.1991, No. L41; 25 km E of Nochur, Karayalchi valley, 1600 m, 57°09'E, 38°21'N, 05.X.1991, No. L36; 20 km E of Nochur, Karayalchi valley, 800 m, 57°12'E, 38°23'N, 04.X.1991, No. L35; Kurkulab, 6 km W Germob, 1000 m, 03.X.1991, No. L34; Vanovskiy, 5 km NE Firyuza, 400 m, 58°06'E, 38°00'N, 27.09.1991, No. L29; Firyuza, 4–600 m, 58°05'E, 37°59'N, 28.09.1991, No. L30; Kopet-Dagh Mts., 700–800 m, 5 km S of Chuli, 58°01'E, 37°56'N, 30.09.1991, No. L32; Parkhay, 6 km NW of Kara-Kala, 400 m, 56°13'E, 38°22'N, 09.X.1991, No. L39, leg. A. PODLUSSÁNY, L. RONKAY & Z. VARGA (Coll. HNHM, GY. FÁBIÁN, P. GYULAI, B. HERCZIG, M. HREBLAY, G. RONKAY and Z. VARGA); 2 males, W Kopet-Dagh, Sunt-Khasardagh, southern foothills of Mt Sunt, 9.X.1996, leg. O. TARGONJA (Coll. Z. KLYUCHKO).

Slide Nos HACKER 10706, VZ6650, VZ6711 (males), RL5993, VZ6748 (females).

Diagnosis: A relatively large *Euxoa* species (wingspan 33–38 mm) with regular, contrasting markings and black and light grey-white general colouration. The male antenna, wing shape and wing pattern are generally reminiscent of *E. temera* (HÜBNER, [1808]), but *E. sayvana* is more contrasting in wing pattern and colouration. Its ground colour is lighter grey with a very delicate ochreous hue, the brownish colouration is practically reduced to the darker blackish-brown markings of the maculation and the transverse lines; the male antenna is slightly shorter pectinated than in *E. temera*. *E. sayvana* shows some external similarity also to three not very closely related *Euxoa* species. *E. adjemi* BRANDT, 1941 is externally quite similar, but is more long-winged, the ground colour is more brownish, and the pectination of the male antenna is much shorter. *E. dsheiron* BRANDT, 1938 has similarly bipectinated antenna, but the pectination is more equal on both sides of antenna, it is shorter-winged and has a typical yellowish/brownish coloration. *E. emolliens* WARREN, 1909 (= *E. amplexa* CORTI, 1931) is also shorter-winged, more ochreous-brownish in colouration and has shortly pectinated antennae. The latter species has two colour forms, as in most *Euxoa* species, while the rather large type series of *E. sayvana* is fairly homogeneous.

The male genitalia of *E. sayvana* are of the same basic type as those of *E. temera*, but the ventral processus of sacculus is stronger, longer, more curved, and the vesica is broader, more recurved. The female genitalia are also similar to those of *E. temera*, but the papillae anales are more conical, the apophyses are shorter, the ductus bursae is slighly curved, the appendix bursae is broader, triangular, and the corpus bursae is also broader. The genitalia of the externally simi-

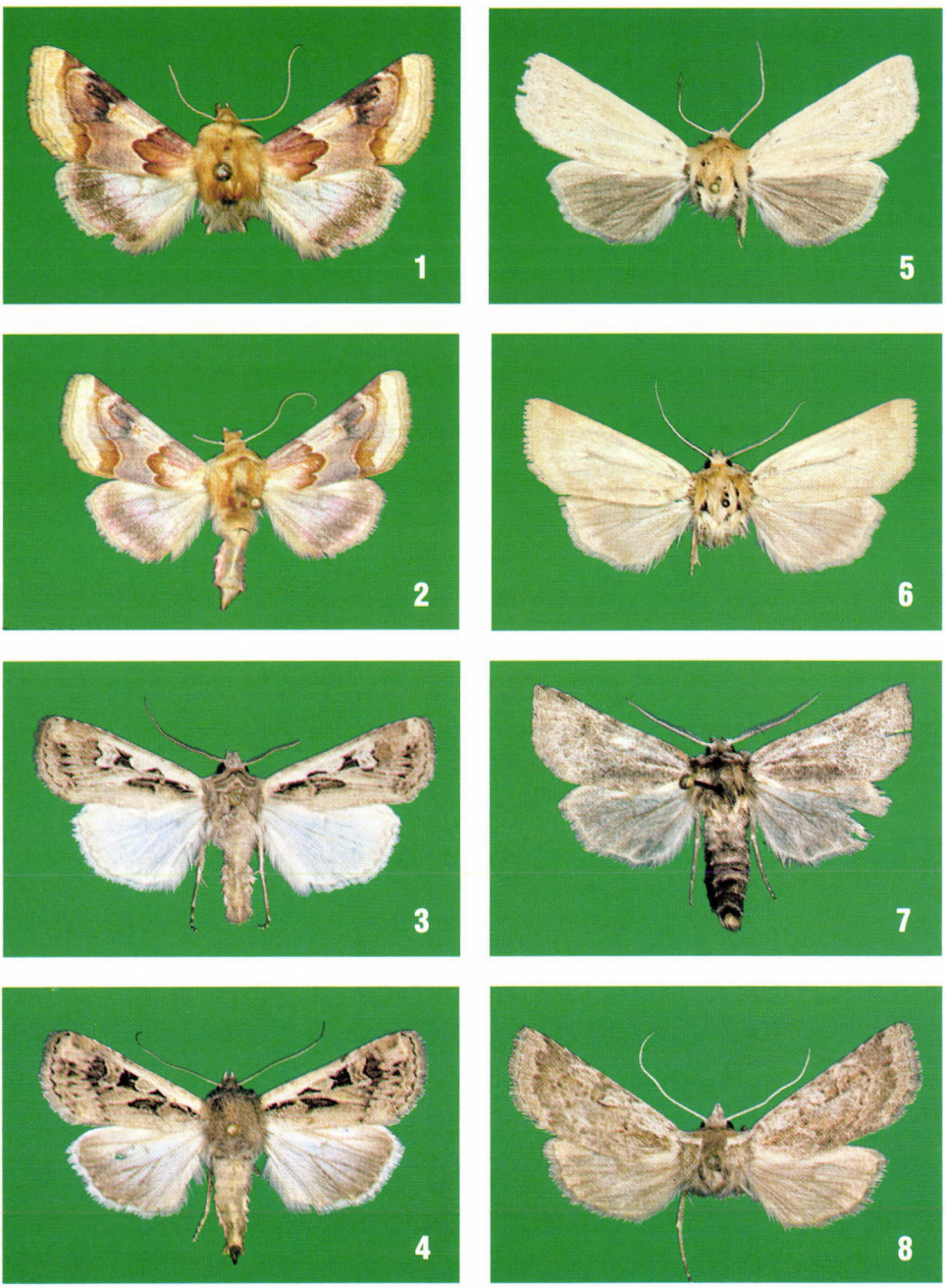

Figs 1–8. 1–2 = *Periphanes delphinii tekke* ssp. n.; 3–4 = *Euxoa sayvana* sp. n.; 5–7 = *Eicomorpha antiqua* STAUDINGER, 1888; 8 = *E. epipsilioides* BOURSIN, 1970

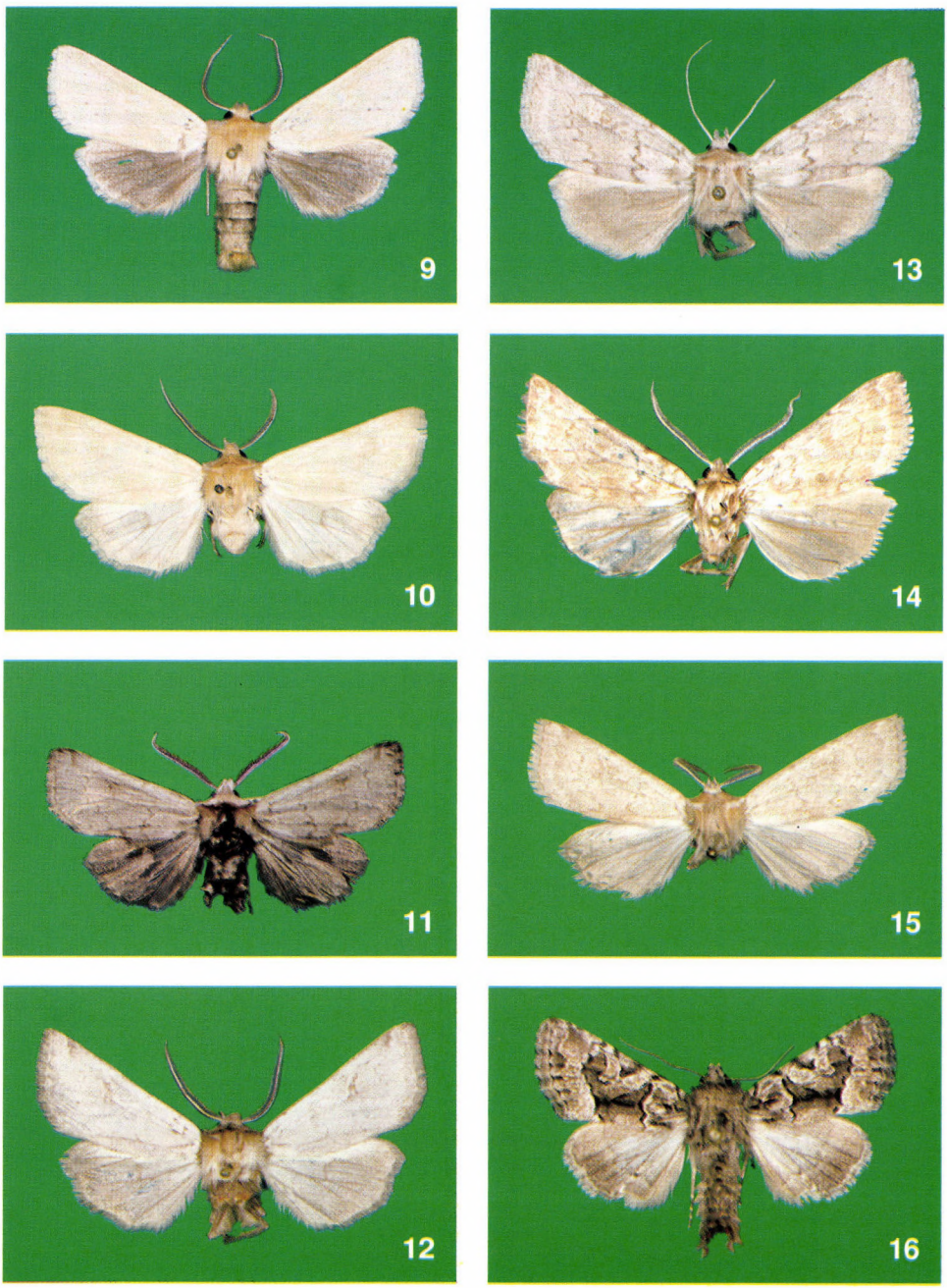

Figs 9–16. 9–10 = *Eicomorpha kurdestanica* DE FREINA et HACKER, 1985; 11–13 = *E. koeppeni* ALPHERAKY, 1894 (11 = lectotype); 14–15 = *Eicomorpha firyuza* sp. n. (14 = holotype); 16 = *Conisania vidua eupepla* ssp. n., holotype

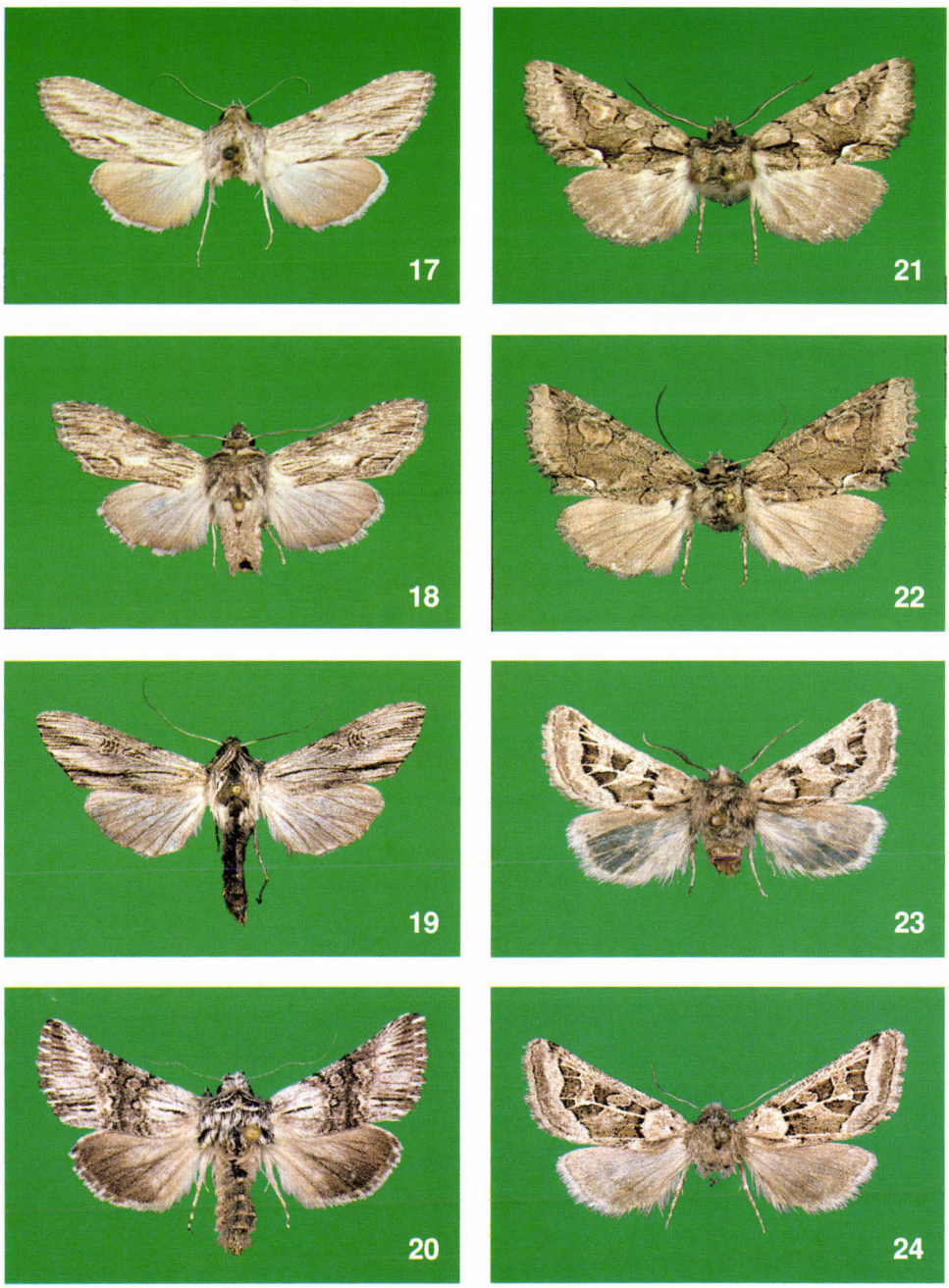

Figs 17–24. 17 = *Cucullia petrophila* sp. n., holotype; 18 = *C. xerophila* sp. n., holotype; 19 = *C. apo* sp. n., paratype; 20 = *Omphalophana turcomana* sp. n., holotype; 21–22 = *Allophyes sericina* sp. n., paratypes; 23–24 = *Episema minutoides* sp. n. (23 = holotype)

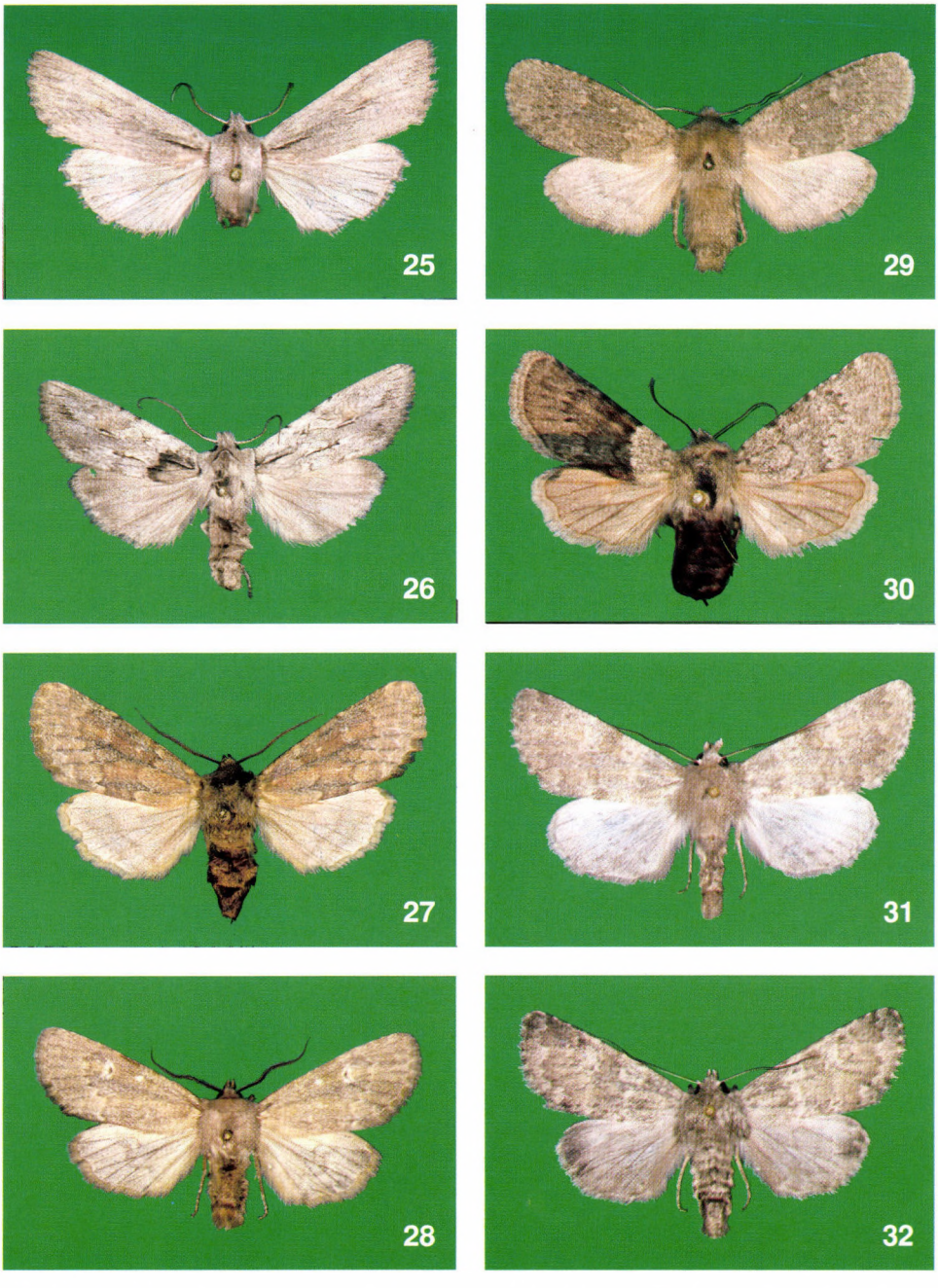

Figs 25–32. 25–26 = *Lithophane alaina* BOURSIN, 1957, Turkmenistan; 27 = *Dasypolia templi dushaki* ssp. n., holotype; 28–29 = *Dasypolia nebulosa* sp. n., (28 = holotype); 30 = *Dasypolia ipaykala* sp. n., holotype; 31–32 = *Polymixis schistochlora* sp. n. (31 = holotype)

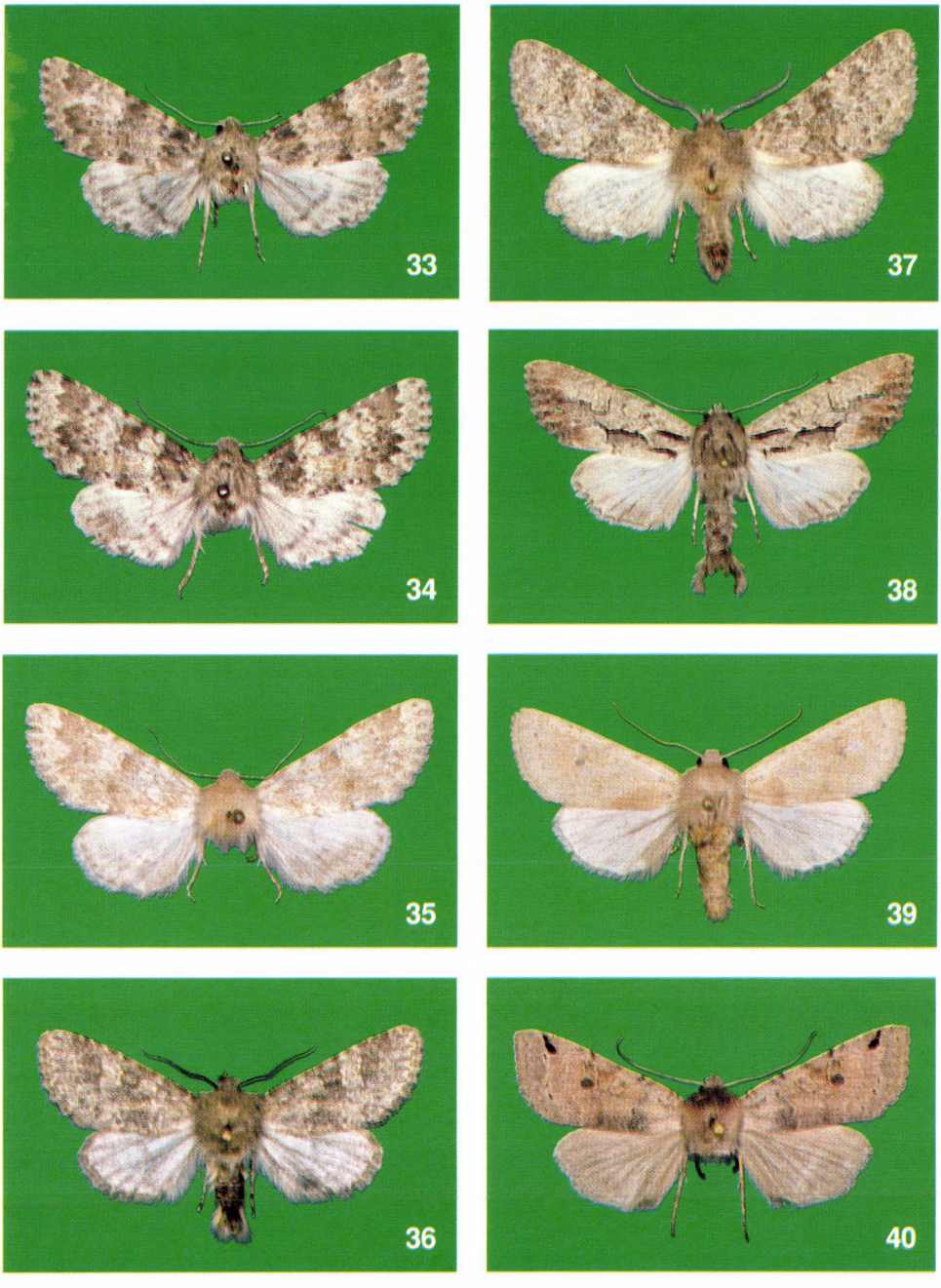

Figs 33–40. 33–34 = *Polymixis fabiani* sp. n., paratypes; 35 = *P. pericaspicus* sp. n., holotype; 36 = *P. achrysa* sp. n., holotype; 37 = *P. csorbagabori* sp. n., paratype; 38 = *Bornolis crinomima diluta* ssp. n., holotype; 39 = *Agrochola oropotamica archar* ssp. n., paratype; 40 = *A. turcomanica* sp. n., holotype

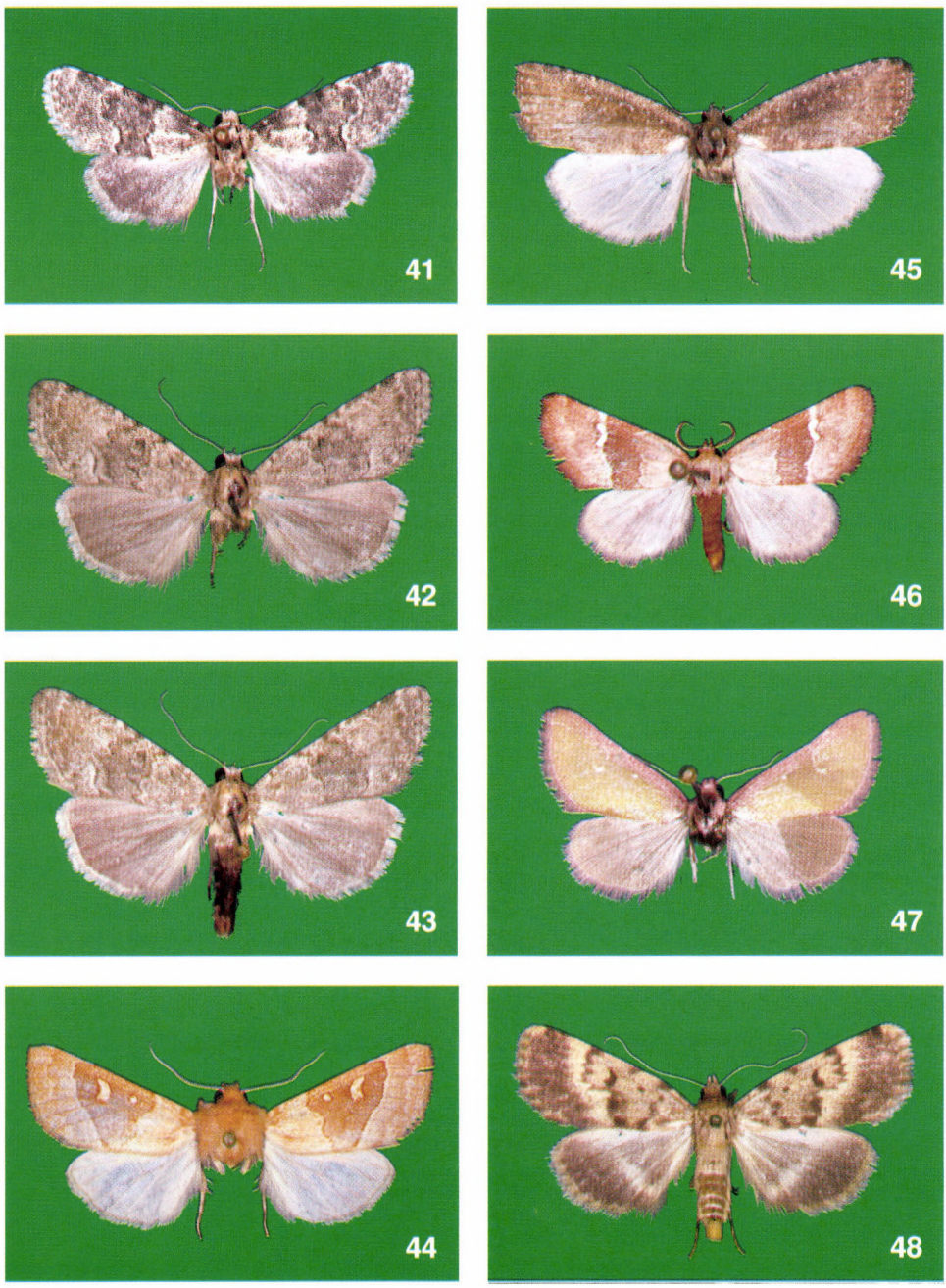

Figs 41–48. 41 = *Cryphia basivittata* sp. n., holotype; 42–43 = *C. duskeimima* sp. n., (42 = holotype); 44 = *Gortyna roseago* sp. n., holotype; 45 = *Chilodes repeteki* sp. n., holotype; 46 = *Haemerosia albicomma* sp. n., holotype; 47 = *H. ionochlora* sp. n., holotype; 48 = *Autophila luxuriosa arnyekolta* ssp. n., holotype

lar species indicate that they belong to different species groups: *E. dsheiron* is related to *E. distinguenda* LEDERER, 1857 while *E. adjemi* and *E. emolliens* are related to *E. aquilina* ([DENIS et SCHIFFERMÜLLER], 1775).

Description: Wingspan 33–38 mm, length of forewing 16–18 mm. Male. Head and base of collar ochreous grey, palpi laterally darker brownish grey. Antenna rather shortly, asymmetrically bipectinate, branches about twice as long on upper (fore) side. Upper half of collar dark greyish brown with fine black medial line, tegulae large, dark grey-brown mixed with a few ochreous grey and blackish scales, prothoracic tuft ochreous, metathorax somewhat paler than tegulae. Abdomen ochreous whitish, dorsal crest weak, consisting of small, pale ochreous-brownish tufts. Forewing elongated, narrow, with apex finely pointed, ground colour pale greyish brown with intense ochreous shine and scarce dark brown irroration. Costal area widely suffused with pale ochreous grey or whitish grey from base to postmedial line, streak of submedian fold short, blackish, defined with some ochreous; veins finely covered with darker brownish. Ante- and postmedial lines usually diffuse, often obsolescent, double, dark brown or blackish, filled with ground colour; antemedial oblique, waved, postmedial sinuous, represented by dark inner line and row of darker spots on veins; medial line regularly absent. Stigmata sharply defined, orbicular and reniform large, rounded, more or less completely encircled with blackish and ochreous-whitish outlines, filled with pale ochreous grey, claviform long, wedge-shaped, blackish with paler brown filling. Subterminal sinuous, more or less continuous, whitish, defined by small, triangular blackish brown arrowheads. Terminal line blackish brown, cilia as ground colour, chequered by ochreous whitish. Hindwing shiny silky white, veins pale brownish, marginal area with a few brownish scales, mostly at apical part. Underside of wings shiny whitish, forewing with stronger grey-brownish suffusion, discal spots often present but pale, diffuse. Female. As male, antenna filiform, ovipositor long, protruding; forewing narrower, wing pattern regularly more sharply defined, hindwing greyish white with diffuse but wide brownish marginal suffusion and well discernible discal spot, underside of both wings somewhat darker, discal spots and traces of transverse lines stronger, darker.

Male genitalia (Figs 50, 51): uncus long, slender, apex finely pointed, tegumen rather low, penicular lobes small, densely hairy. Fultura inferior high, subdeltoidal with weakly incised apical part, vinculum short, strong, V-shaped. Valvae almost symmetrical, narrow, curved at middle, costa with rounded lobe at this curve. Cucullus short, slightly dilated, foot-shaped, with apex pointed, corona long. Sacculus long, clavus reduced, tubercle-like, saccular extensions very long, extending over ventral angles of valvae; dorsal saccular processus small, rounded triangular, sclerotized lobe, harpe long, slender, finely arcuate. Aedeagus short, cylindrical, carina with two long, sclerotized lateral bars. Vesica broadly tubular, everted forward, recurved dorsally; basal part with two small, semiglobular diverticula, ventral one armed with minute spinule at its base. Distal, recurved part inflated, finely scobinate, having large, curved diverticulum at inner arch of main tube.

Female genitalia (Figs 89, 90): ovipositor medium-long, strong, conical, papillae anales covered with short setae; gonapophyses medium-long, strong. Ostium bursae calyculate, ductus bursae narrow, tubular, flattened, both surfaces with continuous, smooth sclerotized plates running from posterior end of ostium to proximal part of ductus bursae. Appendix bursae large, conical, pointed, projected laterally, corpus bursae elliptical-sacculiform, finely scobinate.

Bionomics and distribution: At the end of summer and early autumn, *E. sayvana* seems to be widely distributed and frequent species in the moderate altitudes of the whole Kopet-Dagh Mts. Its habitats are scrub-forest and grassland mosaic-complexes with rich vegetation and also with other endemic species of Noctuidae.

Etymology: a large part of the new species was collected in the Sayvan valley, Kopet-Dagh Mts.

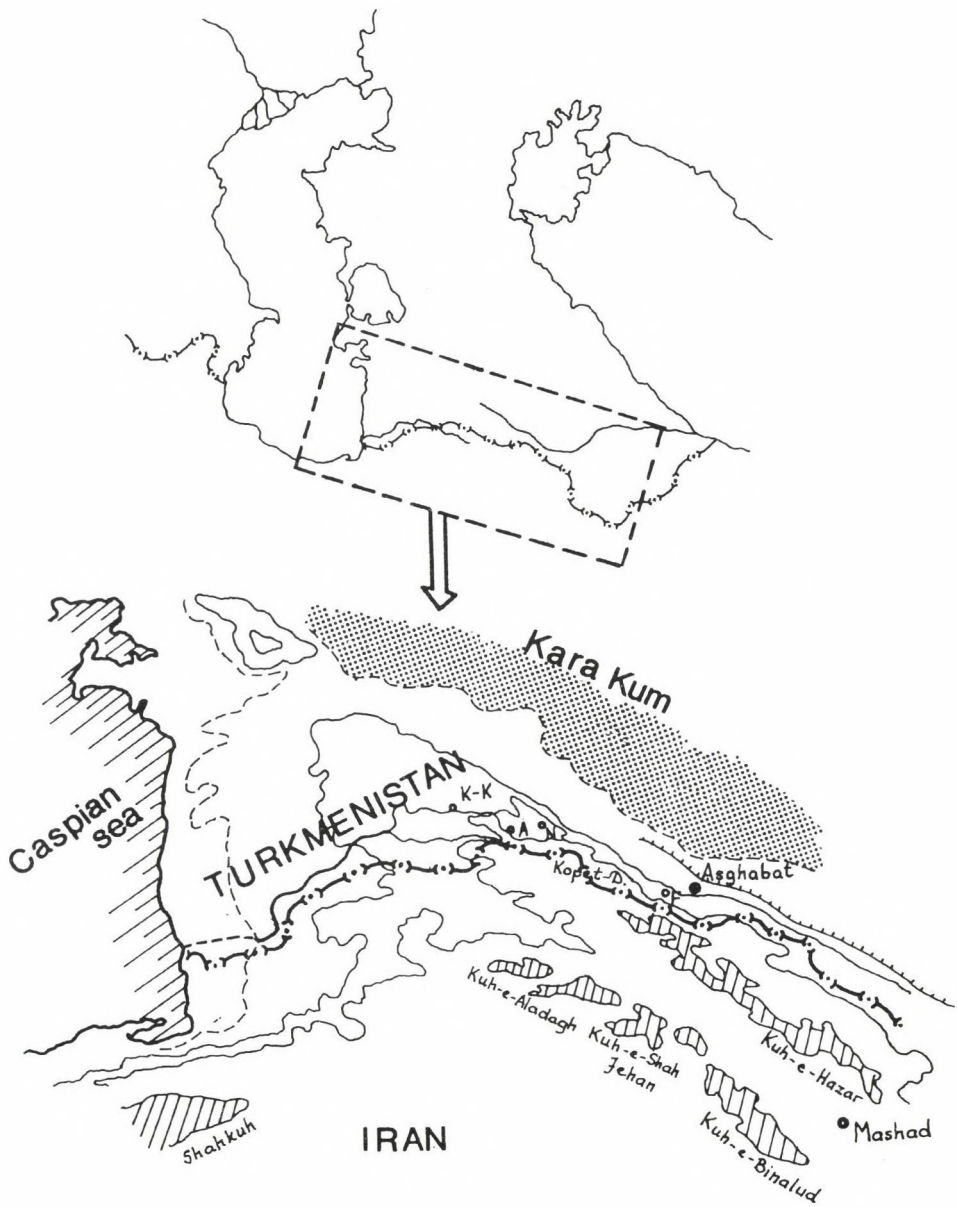

Fig. 49. Map of the Kopet-Dagh region

Eicomorpha STAUDINGER, 1888

Type species: *Eicomorpha antiqua* STAUDINGER, 1888

List of species
– *antiqua* STAUDINGER, 1888
– *kurdestanica* DE FREINA et HACKER, 1985
– *koeppeni* ALPHERAKY, 1894
– *epipsilioides* BOURSIN, 1970
– *firyuza* sp. n.

The identification of the *Eicomorpha* STAUDINGER, 1888 species and the distinction of the specimens by their external characters is often difficult, because of the wide range of variation of the colouration and wing pattern. In addition, the male genitalia are rather simple and also variable in the shape of the bifurcate uncus, the fultura inferior and the valva. Some parts of the valva are reduced: the sacculus is simple, the cucullus is usually wedge-shaped, lacking the corona, the harpe is represented by its basal plate and the ampulla is absent. The configuration of the aedeagus and the vesica is highly uniform within the genus, displaying no specific features. The aedeagus is cylindrical, straight, the carina is strongly sclerotized bearing a well-developed spine, the vesica is simple, short, tubular, membranous, recurved near to its base. In females, the ovipositor is large, strongly sclerotized, the ostium and ductus bursae are short, also strongly sclerotized, the corpus and appendix bursae are simple, small, membranous. These parts of the female genitalia show a considerable variation, and no key features were found in them.

Eicomorpha antiqua STAUDINGER, 1888
(Figs 5–7, 92–94)

Type material examined: syntypes from Samarkand and Namangan (Coll. MNHU Berlin, Coll. STAUDINGER and PÜNGELER)

Additional material examined. Uzbekistan: 1 male, 1 female, Kuramin Mts, Kamchik Pass, 2300 m, 8.VII.1991, leg. DANILEVSKY; 1 male, Tien Shan, Chimgan, 7–10.VI.1990, leg. V. KFENEK; 1 male, Tien Shan Mts, Mt. Chimgan, 1600 m, 26.VI.1981; 6 males, 11 females, W Tien Shan, 1200 m, Tschatkal Reserve, Bash-Kizil-say, 27.V.-3.VI.1982, leg. PEREGOVITS and 30.V.-4.VI.1983, leg. P. FEHÉR and F. HORVÁTH; 1 male, Fergana, 10.VII.1985. Kazakhstan: 2 males, Alma-Ata, Medeo, 4–8.VII.1987, 1700 m, leg. L. HLAVACKAVA; 1 male, Zailiski Alatau, Kaskaler Schlucht, 2400–2800 m, 29.VII.1995; 1 male, Mt. Tien Shan, Transiliskij Ala-tau, Tschimbulak, 2500–2700 m, 5–8.VII.1980; 1 male, Bakanas, 3–5.V.1995, leg. TOROPOV. Kirghisia: 1 male, Chatkal Mts, 1600 m, Sumsar, 16.VI.1993, leg. DANILEVSKY. Tadjikistan: 1 male, Pamir, Chorog, leg. KRUSEK; 2 m, Pamir Mts, Mt. Pervopetrovo, Ganishou, 2200 m, 12–20.VI.1990, leg. K. GASKÓ; 1 female, Hissar Mts, Romit, 27.V.1978, leg. DANILEVSKY. Afghanistan: 2 males, 1 female, Nord Salang, ca. 2800 m, 5–8. VII. 1976, leg. RESHÖFT. China: 1 male, Korla.

The material examined is preserved in the collections of the HNHM, M. HREBLAY and G. RONKAY.

Slide Nos HM2711, HM2712, HM2713, HM2718, HM3498, HM3509, HM3514, HM3515, HM3526, HM10469, HM10470, HM10476 (males), HM3510, HM3512, HM3517 (females).

Diagnosis: The largest species of the genus, especially some females have large wingspan. The forewing colouration is highly variable, pale ochreous, rufous or greyish or darker reddish-brown to brown. The intensity of pattern is also variable, sometimes fully reduced, in other cases the darker submarginal area and the darker reniform are well discernible. In the male genitalia (Figs 92, 93) this species has the most elongated cucullus within the genus, its major part curved laterally; the incision of the bifurcate cucullus is weaker than in the other species.

Eicomorpha kurdestanica DE FREINA & HACKER, 1985
(Figs 9, 10, 95–97)

Material examined. Turkey: a large series, Prov. Agri, 5 km E of Sarican, 1800 m, 12–15.VI.1991, 42°39'E, 39°49'N, leg. M. HREBLAY; Prov. Agri, Tahir Gecidi, Toytaci, 2780 m, 7–8. VII.1986, leg. W. PAVLAS; 5 males, Prov. Bingöl, Buglan-Pass, 1600 m, 9.VI.1985, leg. THÖNY; (Coll. HREBLAY and HNHM); 1 male, from the same locality, 6.VI.1985, leg. K. HUBER; a series of males, Prov. Agri, 15 km E of Horasan, Hayrangöl Köyü, 1500 m, 42°18'E, 40°05'N, 12–15.VI.1991, leg. CS. SZABÓKY (HNHM, G. RONKAY).

Slide Nos HM2710, HM2714, HM2715, HM3513 (males), HM3511, HM3520, HM3522 (females).

Diagnosis: Externally close to *E. antiqua* but somewhat smaller in size, the wing pattern reduced, sometimes the postmedial line presented as a row of spots on the veins. The hindwing is regularly darker than the forewing, in spite of the other taxa of the genus. The valva of the male genitalia (Figs 95, 96) is relatively short, the broadest within the genus.

Eicomorpha koeppeni ALPHERAKY, 1894
(Figs 11–13, 98–100)

Type material examined. Lectotype: male, Samarkand, HERZ, Slide No. 8277 RYABOV (Coll. ZIN, St. Petersburg), here designated. Paralectotypes: 1 male, 1 female, with the same data as the lectotype (Coll. ZIN St. Petersburg).

Additional material examined. Turkmenistan: 20 males, Kugitang-Tau Mts, 4 km SW of Airi-Baba peak, 2000 m, 22.V.1991, 66°34'E, 37°50'N, No L24; 9 males, 1 km SW of Airi-Baba Peak, 2500 m, 66°34'E, 37°52'N, 20–21.V.1991, No. L23, leg. M. HREBLAY & G. RONKAY; 2 males, Kopet-Dagh Mts, 400–600 m, Firyuza, 58°05'E, 37°54'N, 30.IV.-5.V.1991, leg. G. CSORBA, GY. FÁBIÁN, B. HERCZIG, M. HREBLAY & G. RONKAY. Uzbekistan: 1 male, Kuramin Mts, Kamchik Pass, 2300 m, 8.VII.1991, leg. DANILEVSKY. Kirghisia: 3 males, Chatkal Mts, 1600 m, Sumsar, 16.VI.1993, leg. DANILEVSKY (Coll. HREBLAY).

Slide Nos HM2708, HM2709, HM2717, HM3524, HM3525, HM10466, HM10468, HM10471 (males), HM10472, HM10473 (females).

Diagnosis: This species is somewhat smaller than *E. antiqua*, and has the broadest forewing within the genus. The ground colour of the forewing is most often pale ashy greyish, and the ante- and postmedial lines are fine, dark, sinuous. In the male genitalia (Figs 98, 99) the valva is as large as that of *E. antiqua*, but the cucullus is less elongated and less curved laterally; the uncus is with deeper medial incision.

Eicomorpha epipsilioides BOURSIN, 1970
(Figs 8, 101, 102)

Material examined. Afghanistan: 1 male, Kotal-e-Salang, 2700 m, 19.VI.1974, leg. Dr. RESHÖFT; 1 female, Tang-i-Gharu, 1700 m, 19.V.1975, leg. Dr. RESHÖFT.

Pakistan: 1 male, Hindukush Mts, Shandur Pass, 36°05'N, 72°32'E, 3600 m, 21.VI.1992, leg. M. HREBLAY & G. CSORBA, (Coll. M. HREBLAY).

Slide Nos HM3452, HM10462, (males), HM10463 (female).

Diagnosis: The smallest *Eicomorpha* species which has the strongest forewing pattern and the smallest male and female genitalia (Figs 101, 102). The medial incision of the uncus is the deepest within the genus.

Eicomorpha firyuza sp. n.
(Figs 14, 15, 103–105)

Holotype: male, "USSR, Turkmenistan, Kopet-Dagh Mts. 400–600 m, Firyuza, 58°05'E, 37°54'N, 30.IV.-5.V.1991, No. L13, leg. G. Csorba, Gy. Fábián, B. Herczig, M. Hreblay & G. Ronkay", Slide No. HM10467 (Coll. M. HREBLAY).

Paratypes. Turkmenistan: 4 males, 4 females, same data as the holotype, 3 males, 10 females, Kopet-Dagh Mts, 400–600 m, Firyuza, 58°05'E, 37°54'N, 12–16.V.1991, No. L19; 1 female, Kopet-Dagh Mts, 5km S of Chuli, 14.V.1991, 700–800 m, 58°01'E, 37°56'N, No. L21, leg. G. CSORBA, GY. FÁBIÁN, B. HERCZIG, M. HREBLAY & G. RONKAY (Coll. HNHM, GY. FÁBIÁN, P. GYULAI, B. HERCZIG, M. HREBLAY, G. RONKAY), 1 male, 1 female, 4 km NW Germob, 1000 m, 20.IV.1993, 57°48'E, 38°01'N, No. L90, leg. M. HREBLAY, GY. M. LÁSZLÓ and A. PODLUSSÁNY (G. RONKAY); 2 males, 1 female, Dushak Mt., 1800 m, 23.VI.1992, leg. M. DANILEVSKY (P. GYULAI). Kirghisia: 1 male, Frunze region, Tien Shan, Alaarcha river, 1800–2300 m, 24–28.V.1980 (Coll. BEHOUNEK). Uzbekistan: 1 male, Mt. Alai, 3600–4000 m, Pik Spartakiada, 15.VII.1979, leg. KRUSEK (Coll. BEHOUNEK).

Slide Nos BEHOUNEK 424; HM2716, HM3523, HM10465, HM10697 (males), HM3516, HM3521 (females).

Diagnosis: *Eicomorpha firyuza* sp. n. is closely related to *E. koeppeni*, but somewhat smaller in size, the forewing ground colour is more brownish grey, and the crosslines and the stigmata are more sharply defined. The male genitalia of

the new species are generally smaller than those of *E. antiqua* and *E. koeppeni*, the cucullus is less elongated, more or less straight, and the ventral margin of the sacculus is also more rounded.

Description: Wingspan: 40–43 mm, length of forewing 19–20 mm. Male. Pubescence of head and thorax pale brownish grey mixed with whitish and greyish beige hairs, abdomen whitish grey. Antenna bipectinated, branches rather long. Forewing broad, triangular with apex acute, ground colour pale grey with strong brownish-beige shade, medial and marginal areas irrorated with a few darker brownish scales. Ante and postmedian lines darker grey-brown, sinuous, followed by weak paler zones on both sides; median line missing or diffuse, darker brownish shadow. Orbicular and reniform stigmata present, although often diffuse, relatively small, narrow, encircled by pale whitish-grey scales, filled with ground colour, former elongated, latter elliptical. Subterminal line diffuse, sinuous, pale whitish grey stripe, defined by darker greyish inner zone. Terminal line fine, more or less interrupted, dark grey-brown, cilia slightly paler than marginal field. Hindwing greyish brown, veins darker, discal spot and transverse line usually indistinct, marginal suffusion narrow, inner half of it somewhat darker, darkest part of wing. Undersides of wings greyish, veins somewhat darker, marginal area paler, transverse lines and discal spots present but diffuse on both wings.

Female. As male, but forewing more elongated and acute, wing pattern usually somewhat stronger. Antenna filiform (but with bald eye appearing as finely serrate, due to its coverage of pale greyish scales arranged into smaller groups).

Male genitalia (Figs 103, 104): Genital capsula strongly sclerotized, uncus bifurcate with deep medial incision, tegumen low, vinculum strong, rather short, U-shaped. Fultura inferior drop-shaped, dorsal part with stronger sclerotization. Valva elongated, distally tapering, cucullus streched with finely rounded apex. Sacculus short, saccular plate present, harpe and ampulla absent. Aedeagus cylindrical, straight, carina strongly sclerotized, bearing well-developed spine. Vesica simple, short, tubular, membranous, recurved near base.

Female genitalia (Fig. 105): Ovipositor large, strongly sclerotized, more or less conical, posterior apophyses long, slender, anterior ones rather short, stick-like. Ostium bursae short, broad, ductus bursae rather short, flattened, partly folded, heavily sclerotized. Appendix bursae small, semiglobular, corpus bursae elliptical, small, membranous.

Bionomics and distribution. The new species is characteristic for the medium high, xerothermic slopes of the Kopet-Dagh Mts, covered with rather open rocky grasslands. The imagines are on wing in the mid-spring, from the second part of April to the middle of May and are strongly attracted by the artificial light.

Remarks. The only specimen known from Kirghisia shows some differences in the colouration, the forewing is more rufous but the male genitalia are typical of the new species. A more detailed taxonomic analysis requires further material.

Periphanes delphinii tekke ssp. n.
(Figs 1, 2, 106–108)

Holotype: male, "TURKMENISTAN, 50 km N of Ashkhabad, 100 m, 17.IV.1993, No L88, 58°33'E, 38°22'N, leg. M. Hreblay, Gy. László & A. Podlussány", slide No. HM10453 (Coll. M. HREBLAY).

Paratypes. Turkmenistan: a large series of both sexes from the following localities: Kopet-Dagh Mts, 3 km N of Kara-Kala, 500 m, 20.IV.1991, 56°17'E, 38°25'N, No. L5; Kopet-Dagh Mts, 5 km NW of Tutlikala, 800–900 m, 22.IV.1991, 56°44'N, 38°26'N, No. L7; 50 km N of Ashkhabad, 29.IV.1991, 100 m, 58°33'E, 38°21'N, No. L12; 50 km SE of Tedjen, 7.V.1991, 200–300 m, 60°53'E, 36°56'N, No. L15; Kopet-Dagh Mts, 5 km S of Chuli, 14.V.1991, 700–800 m, 58°01'E, 37°56'N, No. L21, leg. G. CSORBA, GY. FÁBIÁN, B. HERCZIG, M. HREBLAY, G. RONKAY; 50 km N of Ashkhabad, 100 m, 17.IV.1993, No. L88, 58°33'E, 38°22'N, leg. M. HREBLAY, GY. M. LÁSZLÓ & A. PODLUSSÁNY; Kugitang-Tau Mts, 7 km SW of Airi-Baba Peak, Kara-Bilent, 11–15.V.1991, 1500 m, 66°32'E, 37°50'N, No. L26, leg. M. HREBLAY and G. RONKAY; 1 female, Mari, 12–15.IV.1993, leg. KLIMENKO (Coll. the collectors, HNHM Budapest, P. FASTRÉ, P. GYULAI and Z. VARGA). Uzbekistan: 2 females, Nuratau, Nuratau Nature Conservation Area, 900 m, 3-15.V.1995, leg Z. KLYUCHKO (Coll. Z. KLYUCHKO).

Slide Nos HM4421 (male), HM10454 (female).

Diagnosis: The new subspecies differs from the nominate subspecies by its conspicuously paler forewing colouration, externally resembling the NW African (Morocco, Tunesia, Algeria) *P. d. darollesi* (OBERTHÜR, 1876). The colouration of the populations occurring in Turkmenistan is ochreous-pinkish, the paler areas are yellowish-ochreous on both wings. The forewing ground colour of the typical populations of *P. delphinii delphinii* (LINNAEUS, 1758) is crimson-violet and the paler areas are usually clear white; the forewing pattern of *P. d. tekke* ssp. n. is more indistinct than in *P. delphinii delphinii*. The genitalia of both sexes show no remarkable differences in the three subspecies of *P. delphinii*.

Description: Wingspan 28–32 mm, length of forewing 13–16 mm. Head, collar, tegulae and thorax pale ochreous, irrorated with some rufous. Abdomen whitish-ochreous mixed with pinkish on ventral side. Antenna of male ciliate, that of female filiform. Forewing triangular, rather broad, with apex acute, outer margin slightly concave below apex. Ground colour pale ochreous pink, subbasal area pale, basal area somewhat darker pinkish, antemedial line even darker, sinuous. Medial line absent or obsolete, postmedial line more or less S-shaped, double with diffuse inner line, filled with pale ochreous. Medial area indistinct, pinkish grey, costa irrorated with whitish-ochreous. Orbicular most often reduced, sometimes represented by a few darker scales, reniform large, connected with costa, dark greyish pink. Inner part of marginal area pinkish-ochreous, generally darker than pale ochreous-pinkish outer half; cilia ochreous-pinkish. Hindwing ochreous with pinkish sheen, veins darker, marginal suffusion broad, dark brown defined with pale pinkish at both sides; cilia whitish. Underside of both wings light whitish-ochreous, with indistinct, pale pinkish pattern.

Male genitalia (Figs 106, 107): Uncus long, slender, tegumen high with setose penicular lobes. Fultura inferior simple, subdeltoidal, vinculum V-shaped. Valva elongated, distally somewhat broadened, cucullus rounded, finely setose; corona present. Sacculus short, simple, ampulla and harpe reduced. Aedeagus short, cylindrical, slightly curved, carina weakly sclerotized. Vesica tubular, recurved near its basis, bearing bifurcate diverticulum; shorter arm of this diverticulum turned back to aedeagus, longer arm sometimes also bifurcate, these diverticula armed with small stick-like cornuti; main tube of vesica distally broader, having two small diverticula, proximal one with minute cornutus.

Female genitalia (Fig. 108): Ovipositor short, conical, gonapophyses slender. Ostium bursae short, calyculate, ductus bursae narrow, proximally heavily ribbed. Appendix bursae broad, rounded, corpus bursae large, elongate, simple sac, without signa.

Bionomics and distribution. The eastern subspecies of the species is distributed in the Kara-Kum desert and the bordering mountain chains up to 600–

800 m altitudes. The imagines are on wing from middle April (in the deserts) to the end of May (in the mountains).

Conisania vidua eupepla ssp. n.
(Figs 16, 109–111)

Holotype: male, "Turkmenistan, Kopet-Dagh Mts, 6 km S of Ipay-Kala, 1600 m, 57°07'E, 38°17'N, 16–23.VIII.1992, No. L74, leg. M. Hreblay, Gy. László and G. Ronkay" (Coll. HNHM).

Paratypes: Turkmenistan, a large series of both sexes (more than 300 specimens) with the following data: Kopet-Dagh, Dushak, 3–13.VII.1990, leg. DUBATOLOV & DUBATOLOVA; Kopet-Dagh, Dushak, 9.V.1987, leg. DUBATOLOV; Kopet-Dagh Mts, 800–1500 m, Ipay-Kala, 57°07'E, 38°17'N, 30.VI – 4.VII.1992, No. L63; Kopet-Dagh Mts, 2300 m, Dushak, 57°54'E, 37°57'N, 6–8.VII.1993, No. L64, leg. GY. FÁBIÁN, B. HERCZIG, A. PODLUSSÁNY and Z. VARGA; Dushak Mt., 1500 m, 57°56'E, 37°54'N, 1500 m, 7–8.VIII.1992, No. L69; Dushak Mt., 57°54'E, 37°57'N, 2400 m, 9–10.VIII.1992, No. L70, Dushak Mt., 2300 m, 11–12.VIII.1992, No. L71; Kopet-Dagh Mts, 6 km S of Ipay-Kala, 1600 m, 57°07'E, 38°17'N, 16–23.VIII.1992, No. L74, leg. M. HREBLAY, GY. M. LÁSZLÓ and G. RONKAY (Coll. HNHM, GY. FÁBIÁN, P. GYULAI, B. HERCZIG, M. HREBLAY, G. RONKAY, Z. VARGA).

Slide Nos RL3686, RL6006 (males), RL6007 (female).

Diagnosis: The westernmost populations of *Conisania vidua* occurring in the higher parts of the Kopet-Dagh Mts represent a distinct geographic subspecies. It differs from the nominotypical *C. vidua* (STAUDINGER, 1888) by its smaller size, shorter forewing, light tobacco-brown ground colour with fine ochreous shine, finer, more sharply defined crosslines and stigmata, with stronger whitish definition. The genitalia of both sexes show no conspicuous differences compared with the other more easterly populations occurring from the Tien Shan massif to the western Himalayas. The male genitalia of the species are illustrated by HACKER *et al.* (1996: 406, Fig. 14; India, Himachal Pradesh).

Description: Wingspan 23–26 mm, length of forewing 10–12 mm. Head and thorax tobacco-brown mixed with whitish grey hairs, collar and tegulae marked with fine blackish lines. Antenna filiform in both sexes. Abdomen somewhat paler, more ochreous-greyish, dorsal crest consisting of tiny dark tufts. Forewing short, rather broad with apex pointed, ground colour shiny tobacco-brown with ochreous shade, basal and marginal areas strongly, medial field usually weakly irrorated with pale ochreous grey. Wing pattern sharply defined, ante- and postmedial crosslines sinuous, blackish, former defined with ochreous grey, latter with whitish; medial line diffuse, blackish brown shadow. Stigmata present, orbicular and reniform encircled with blackish and whitish outlines, filled with ochreous grey and a few brownish, former surrounded by broader ochreous grey patch extending widely below cell. Claviform medium-long, blackish brown arrowhead, filled with ground colour. Subterminal sinuous, whitish forming a rather indistinct W-mark at lower edge of cell, defined by a few short dark streaks, inner half of marginal area often irrorated with whitish grey. Terminal line fine, blackish, marked with minute black dots between veins, cilia as ground colour, with fine, pale ochreous lines. Hindwing whitish-ochreous, veins, costal and marginal areas covered with brown, discal spot and transverse line variably strong, usually pale but well visible. terminal line fine, dark brown, cilia white with brown inner line. Underside of wings whitish grey, forewing and costal area of hindwing irrorated with brown, discal spots and transverse lines present on both wings.

Male genitalia (Figs 109, 110): Uncus short, slender, flattened, with apex finely rounded, tegumen low, broad, penicular lobes narrow, densely hairy. Fultura inferior divided into two parts, upper part considerably larger, rather weak, drumstick-like, lower part smaller, strongly sclerotized, Y-shaped; vinculum strong, V-shaped. Valvae symmetrical, sclerotized, saccular part broad, medial part tapering to neck of cucullus. Cucullus small, elliptical, densely setose. Sacculus strong, broad, without well-developed saccular extension. Clavus large, lobate, dorsal surface covered with minute setae. Basal plate of harpe large, triangular, distal part long, sclerotized crest fused with costal plate, subapical costal process small, pointed. Aedeagus rather short, cylindrical, carina with two dorso-lateral, acute sclerotized plates, one of them armed with strong spine. Vesica tubular, curved ventrally, membranous with fine scobination, basal third with a strong, relatively short wide-based thorn, medial third with small, semiglobular diverticulum.

Female genitalia (Fig. 110): Ovipositor strong, conical, posterior papillae small, acute, gonapophyses strong. Ostium bursae broad, calyculate, strongly sclerotized, fused with large, flattened, medially dilated, strongly, granulosely sclerotized ductus bursae. Appendix bursae small, elongate, apically rounded, membranous with fine wrinkles, corpus bursae sacculiform, hyaline, without signa.

Bionomics and distribution. The new subspecies represents the westernmost populations of the widespread species, distributed in the large mountain systems of Central Asia from the Kopet-Dagh throughout the whole area of the Tien Shan massif, the Hissar Mts, the Pamir region, the eastern parts of the Hindukush to the Karakoram and the north-western Himalayas. The new subspecies is rather frequent in the medium high and higher elevations of the Kopet-Dagh, inhabiting xerothermic rocky grasslands and scrubby steppes.

Cucullia petrophila RONKAY et RONKAY sp. n.
(Figs 17, 112–114)

Holotype: female, "Tian-Shan oc., ms. Bolshoj Tshimgan (prope Tshimgan), 2500 m. alt., lumine, 1.VIII.1934, L. Sheljuzhko leg.", slide No. RL2907 (Coll. HNHM, Budapest).

Paratypes: Uzbekistan. 17 males, 12 females, W Tien Shan, Mt. Chimgan, 800–2000 m, 68°58'E, 41°32'N, 15–25.VII.1990, leg. P. GYULAI and M. HREBLAY (P. GYULAI, H. HACKER and M. HREBLAY); 1 male, from the same locality, 28.VI.–10.VII.1993, leg. VODYANOV (P. GYULAI); 2 females, Tshatkal Mts, Terek-Sal, 1300–1700 m, 71°18'E, 41°25'N, 22–23.VII.1993, leg. LUKHTANOV (P. GYULAI); 2 males, Tshatkal Mts, 2200 m, Besh-Aral, 71°27'E, 42°00'N, 27.VII.1993, leg. LUKHTANOV (P. GYULAI); 1 male, 3 females, Kuramin Mts, Kamchik Pass, 150 km SE Tashkent, 7.VII.1991, leg. GASKÓ (P. GYULAI); 4 males, 1 female, from the same locality, 2300 m, 8.VII.1991, leg. DANILEVSKY (Coll. THÖNY, HNHM and M. HREBLAY); 1 female, Nuratau Mts, Sarmitau, 40 km W Farish, 1300 m, 11–13.VI.1994, leg. LUKHTANOV (P. GYULAI); 17 specimens, Nuratau, Nuratau Nature Conservation Area, 900 m, 3-15.V.1995, leg Z. KLYUCHKO (H. HACKER and Z. KLYUCHKO). Tadjikistan: 3 males, 2 females, Hissar Mts, 25 km S Pedzhikent, 1800 m, 10.VII.1994, leg. LUKHTANOV (P. GYULAI). Afghanistan. 4 males, 5 females, Paghman, 30 km NW Kabul, 2200 m, 3.VIII.1963, leg. KASY & VARTIAN (Coll. E. VARTIAN, NHMV; HNHM); 2 males, 2 females, Band-e-Amir, 2800 m, 9–12.VII.1975, leg. W. THOMAS (H. HACKER and J. PLANTE).

Slide Nos HACKER 8609, PL436, RL2698, RL6016 (males), HACKER 8616, RL2474, RL2816 (females).

Diagnosis: The new species, together with *C. xerophila* sp. n., described below, belongs to the *C. boryphora* species-group, forming an allopatric species-pair. *C. petrophila* differs externally from *C. xerophila* by its somewhat larger size, more elongate forewing with much paler, regularly whitish slate-grey or ash-grey ground colour, less distinct crosslines, less conspicuous whitish patch at place of claviform and paler hindwing. The genitalia of the two species are very close, but *C. petrophila* has a shorter, less curved uncus, a longer, apically more tapering valva with more acute cucullus, significantly longer harpe and the bigger cornutus of the vesica is also longer. In the females the ostium bursae of *C. petrophila* is narrower but with broader V-shaped ostial ligula, the ductus bursae is narrower, more tubular, the gelatinous appendage of cervix (= appendix) bursae is smaller, more conical, the cervix-like lobe is larger, broader.

C. petrophila is rather similar to two other Asian species of the group, *C. improba* CHRISTOPH, 1885 and *C. boryphora* FISCHER VON WALDHEIM, 1840, but the forewing of the new species is shorter, somewhat broader with the apex less acute, the ground colour is paler, more greyish without the bluish shade, being characteristic to the other two species, the crosslines are significantly paler, more indistinct, the dark covering of the veins are also less expressed, not blackish but paler brown-grey. The male genitalia of *C. petrophila* (and of *C. xerophila*) differ from those of *C. improba* by their much narrower valva with evenly tapering distal end, narrow cucullus with short, weak corona, almost symmetrical, slightly S-shaped harpes and the configuration of the vesica, having two large, inequal cornuti (*C. improba* has only one, which is the largest in the species group). The female genitalia of the two species are easily distinguishable, the ostial ligula and the ductus bursae are much narrower in *C. petrophila*, the appendix bursae is without gelatinous appendage but with considerably longer, rugulose, rounded cervix-like lobe.

The differences in the male genitalia of *C. petrophila* and C. *boryphora* are almost the same as mentioned in the comparison of *C. petrophila* and *C. improba*, only that *C. boryphora* also has two, but more inequal cornuti in the vesica. In the female genitalia *C. boryphora* has much broader ostial ligula, a longer, broader ductus bursae and a narrower, higher, conical cervix-like lobe.

Description: Wingspan 30–36 mm, length of forewing 14–16 mm. Head and thorax pale ash-grey or slate-grey, mixed with some darker grey and brownish, collar striolate with blackish, tegulae marked with darker grey-brown. Abdomen more greyish, dorsal crest consisting of small, blackish-brown tufts. Forewing rather short, broadly triangular with apex acute, ground colour pale, ash-grey or slate-grey with fine ochreous shiny, irrorated sparsely with darker grey-brown. Streak of submedian fold fine, long, rather pale, veins and inner margin covered finely with blackish grey. Ante- and postmedial lines rather indistinct, strongly sinuous, double, postmedial represented by an oblique blackish brown stripe near tornal streak, defined by whitish line at outer side. Orbicular and reniform stigmata obsolete or fully reduced, reniform often marked by fine blackish arch below cell. Medial area narrow, often irrorated with whitish below cell, claviform represented by stronger whitish patch. Subterminal diffuse, whitish, more or less shadow-like, defined by indistinct tobac-

co-brown spots and two rather sharply defined, blackish streaks, weaker, shorter line at lower extremity of cell and much stronger tornal stripe. Terminal line a row of blackish dots, cilia whitish grey, spotted with dark brown. Hindwing shiny, slightly transparent ochreous white, veins and marginal suffusion pale fuscous, much stronger in females; discal spot and transverse line absent, cilia white with pale brown inner line. Underside of wings patternless silky white, forewing intensely, hindwing weakly suffused with pale greyish.

Male genitalia (Figs 112, 113): Uncus relatively long, strong, curved at basal third, medial part almost straight, apex finely hooked. Tegumen high, narrow, penicular lobes elongate, covered with long setae. Fultura inferior subdeltoidal, large, high, vinculum short, rather strong, more or less U-shaped. Valva narrow, long, strongly tapering to apex, cucullus narrow triangular with apex finely acute, corona short, weak. Sacculus long, narrow, clavus medium-long, digitiform, harpe very long, slender, slightly S-shaped with finely hooked, sclerotized tip. Aedeagus cylindrical, rather thick and short, carina with two narrow, lateral sclerotized bars. Vesica broadly tubular, everted forward, recurved dorso-laterally, basal part with two medium-long, more or less tubular diverticula and long, sclerotized, serrate half-ring between them; both diverticula armed with long, sclerotized, nail-shaped cornutus, that of ventro-lateral diverticulum considerably shorter. Distal, recurved part of vesica membranous, terminal part scobinate, medial part with small, subconical diverticulum near ductus ejaculatorius.

Female genitalia (Fig. 114): Ovipositor short, weak, conical, apophyses posteriores short, fine. Ostium bursae membranous, narrow, cup-shaped, posterior half finely scobinate, ostial ligula rather big, V-shaped. Ductus bursae medium-long, tubular, flattened, both surfaces finely cristate. Appendix bursae large, elliptical-sacculiform, with a cervix-like, flattened-conical, membranous lobe and small, rounded-triangular, gelatinous plate at junction of ductus bursae.

Bionomics and distribution. The new species is known from the westernmost parts of the Tien Shan massif, the Hissar Mts and the western and central parts of the Hindukush (Band-i-Amir, Paghman) in Afghanistan. It occurs in rather low and medium high ranges of the mountain systems, inhabiting hot, dry rocky grasslands. The adults are on wing in the midsummer period, and are easily attracted to artificial light.

Cucullia xerophila RONKAY et RONKAY sp. n.
(Figs 18, 115–117)

Holotype: male, "Turkmenistan, Kopet-Dagh Mts, Dushak Mt. 57°56'E, 37°54'N, 1500 m, 7–8.VIII.1992, No. L69, leg. M. Hreblay, Gy. László and G. Ronkay", slide No. RL4311 (Coll. G. RONKAY).

Paratypes: Turkmenistan. 1 male, with the same data as the holotype (Coll. M. HREBLAY); 1 female, Turkmenia, Kopet-Dagh Mts, 700–800 m, 5 km S of Chuli, 58°01'E, 37°56'N, 10.07.1992, No. L65, leg. GY. FÁBIÁN, B. HERCZIG, A. PODLUSSÁNY and Z. VARGA (HNHM).

Slide No. RL5401(female)

Diagnosis: *C. xerophila* is the sister species of *C. petrophila*, the detailed comparison is given under the latter species. It is also similar to the other members of the *C. boryphora* species group, easily distinguishable from *C. improba* and *C. boryphora* by its significantly darker, more brownish, not pale (bluish-)-

grey forewing ground colour, shorter, less elongate forewing shape and a series of differences in the genitalia of both sexes.

Description: Wingspan 31–32 mm, length of forewing 13–14 mm. Male. Head and thorax dark grey mixed with some brownish, whitish grey and black hairs, collar ochreous-whitish, striolate with blackish, tegulae indistinctly marked with dark grey-brown. Abdomen more greyish, dorsal crest consisting of small, blackish-brown tufts. Forewing rather short, broad triangular, with apex acute, ground colour dark, less shiny grey, irrorated with brownish and greyish white. Streak of submedian fold fine, long, rather pale, veins and inner margin with weak blackish shade. Ante- and postmedial lines diffuse, strongly sinuous, double, dark grey-brown, marked with whitish-grey, tornal part of postmedial strong, oblique blackish stripe defined by white. Medial area narrow, often irrorated with whitish below cell, orbicular and reniform stigmata obsolete, claviform represented by conspicuous whitish patch. Subterminal obsolescent, marginal area variegated with short whitish streaks between veins and two blackish streaks, weaker, shorter line and much stronger stripe, former at cell, latter at tornus. Terminal line a row of blackish dots with white line outside, cilia dark brownish grey, chequered with whitish. Hindwing greyish white, veins and marginal suffusion fuscous, discal spot and transverse line absent, cilia white with pale brown inner line. Underside of wings whitish, forewing and marginal area of hindwing intensely suffused, other parts of hindwing sparsely irrorated with dark greyish brown. Female. As male but generally darker in colouration, forewing suffused with dark brownish, crosslines somewhat sharper, white patch at place of claviform more conspicuous, dark suffusion of hindwing stronger, underside of both wings suffused with dark greyish brown.

Male genitalia (Figs 115, 116): Uncus long, strong, curved at basal third, apex finely hooked. Tegumen high, narrow, penicular lobes elongate, covered with long setae. Fultura inferior subdeltoidal, large, high, vinculum short, rather strong, more or less U-shaped. Valva narrow, long, evenly tapering towards apex, cucullus small, with apex finely rounded, corona short, weak. Sacculus long, narrow, clavus medium-long, digitiform, apically slightly dilated, covered with short setae. Harpe long, slender, slightly S-shaped, apex with short, acute, sclerotized tip. Aedeagus cylindrical, rather thick and short, carina with two narrow, lateral sclerotized bars. Vesica broadly tubular, recurved dorso-laterally, basal part with two medium-long, tubular diverticula and long, sclerotized, serrate medial half-ring; both diverticula bear long, sclerotized, nail-shaped cornuti, that of dorso-lateral diverticulum considerably longer. Distal, recurved part of vesica membranous, with small, subconical diverticulum near ductus ejaculatorius.

Female genitalia (Fig. 117): Ovipositor short, weak, conical, apophyses short, fine. Ostium bursae membranous, more or less lyriform, posterior half finely scobinate, ostial ligula rather large, narrow V-shaped. Ductus bursae medium-long, tubular, flattened, both surfaces finely cristate, crests of dorsal surface stronger, longer. Appendix bursae large, elliptical-sacculiform, with rounded conical cervix-like lobe, gelatinous plate at junction of ductus bursae small, flattened, rounded-elliptical.

Bionomics and distribution. The new species is the allopatric, western sibling taxon of *C. petrophila*, occurring in the very dry, sparsely vegetated rocky slopes at the medium high altitudes of the Central Kopet-Dagh.

Cucullia apo RONKAY et RONKAY sp. n.
(Figs 19, 118–122)

Holotype: male, "Turkmenistan, Kopet-Dagh Mts, 2300 m, Dushak Mt., 57°54'E, 37°57'N, 06–08.07.1992, No. L64, leg. Gy. Fábián, B. Herczig, A. Podlussány and Z. Varga" (Coll. G. RONKAY).

Paratypes. Turkmenistan: 4 males, 3 females, Kopet-Dagh Mts, 2300 m, Dushak, 57°54'E, 37°57'N, 6–8.VII.1992, No. L64; 1 male, Kopet-Dagh Mts, 800 m, Ipay-Kala, 57°07'E, 38°20'N, 26.06.1992, No. L58, leg. GY. FÁBIÁN, B. HERCZIG, A. PODLUSSÁNY and Z. VARGA (Coll. HNHM, B. HERCZIG and G. RONKAY), 1 female, Kopet-Dagh Mts, Dushak Mt., 1800 m, 30.VI.1990, leg. DANILEVSKY (Coll. THÖNY, HNHM).

Slide Nos RL4400, RL5375 (males), RL4765 (female).

Diagnosis: *C. apo* sp. n. is the sister species of *C. heinickei* BOURSIN, 1968. The two species are relatively easily distinguishable as *C. apo* has longer, narrower forewing with darker, more unicolorous bluish grey ground colour and longer, more or less continuous blackish line running from the base of wing to the tornal angle (like in *C. santonici* (HÜBNER, [1813]) and *C. aksuana* DRAUDT, 1935), the dark brownish suffusion of the hindwings is also stronger in both sexes. The male genitalia of the new species are very similar to those of *C. heinickei*, but the uncus is somewhat longer, more curved, the cucullus is more rounded ventrally, both harpes are longer, their apical parts more curved and dilated, the bigger cornutus of the vesica longer, finer, more curved. The female genitalia of *C. apo* has stronger ostial ligula, distally narrower, proximally broader ductus bursae without stronger ventro-lateral projection of ventral plate, which is well expressed in *C. heinickei*, the cervix-like lobe and the cervix (= appendix) bursae itself are considerably larger.

Description: Wingspan 38–39 mm, length of forewing 18–19 mm. Head and thorax bluish ash-grey, mixed with dark grey, brown and whitish, collar paler, striolate with blackish, tegulae and metathorax indistinctly marked with dark hair-scales; abdomen darker, more brownish, dorsal crest strong, blackish. Forewing elongate, narrow with apex acute, ground colour variably bluish ash-grey, irrorated with some whitish, brown and violaceous-grey. Wing pattern variably strong, cross-lines regularly diffuse or obsolescent, strongly sinuous, double, antemedial line stronger, blackish grey, medial fascia and postmedial line most often reduced or shadow-like. Subterminal indistinct, marked with blackish and whitish streaks, and patches. Streak of submedian fold very long, fine, black, continued as thicker black stripe at place of claviform, fused with tornal streak, forming continuous black stripe from base of wing to outer angle. Orbicular and reniform stigmata relatively small, rather sharply defined, encircled with blackish, filled with whitish and brown, former oblique, flattened, latter more or less lunulate. Terminal line black, cilia whitish, spotted with dark grey-brown. Hindwing pale greyish, suffused with darker brown, veins and marginal area darker, discal spot pale, diffuse. Underside of wings whitish grey, forewing and marginal area of hindwing suffused strongly with dark grey-brown, discal spot diffuse but well discernible.

Male genitalia (Figs 118–121): Uncus long, rather slender but strong, curved, apex finely hooked. Tegumen high, narrow, penicular lobes elongate, covered with long setae. Fultura inferior pentagonal, relatively weak, vinculum short, V-shaped. Valva long, narrow with almost parallel margins, cucullus small, only slightly dilated, with apex finely pointed, corona long. Sacculus medium-long, narrow, clavus long, finger-like, apically slightly dilated, setose. Harpes narrow, digitiform, asymmetric, right harpe about twice as long as left harpe, both finely arcuate, their tips rounded. Aedeagus cylindrical, rather thick, short, carina with two narrow, lateral sclerotized bars. Vesica everted forward, recurved dorso-laterally; proximal part finely scobinate, with spacious, subsphaerical basal and short, tubular submedial diverticulum, with long, sclerotized, serrate half-ring between them. Basal diverticulum armed with short, thorn-like spine (reduced in one of the specimens), submedial one with long, strongly curved cornutus, both cornuti having wide basal plate. Distal part upturned dorsally, membranous, terminal part scobinate.

Female genitalia (Fig. 122): Ovipositor short, weak, conical, apophyses short, fine. Ostium bursae membranous, infundibuliform, constricted proximally, posterior half finely scobinate, ostial ligula weakly sclerotized, finely prominent V-shaped bar. Ductus bursae tubular, flattened, proximally dilated, inequally sclerotized, ventral plate larger, finely cristate, dorsal plate smaller but stronger, proximally tapering. Appendix bursae large, elliptical-sacculiform, with subconical cervix-like appendage at junction of ductus bursae and gelatinous plate at opposite side.

Bionomics and distribution. *C. apo* is the western vicariant of *C. heinickei*, which is known from the Pamir region. *C. apo* was found in the medium high and high regions of the Central Kopet-Dagh, its habitats are xerophilous rocky steppes.

Etymology. The new species is dedicated to Dr. B. HERCZIG ("Apo"), one of the collectors of it.

Omphalophana turcomana sp. n.
(Figs 20, 126–128)

Holotype: male, "USSR, Turkmenia, Kopet-Dagh Mts., 800–900 m, 5 km NW of Tutlikala, 56°44'E, 38°26'N, 22.IV.1991, No. L7, leg. G. Csorba, Gy. Fábián, B. Herczig, M. Hreblay & G. Ronkay" (Coll. HNHM).

Paratypes: Turkmenistan. A large series of both sexes from the following localities: Kopet-Dagh Mts, Firyuza, 30.IV.- 5.V., 15–19.IV.1991, 400–600m, 58°05'E, 37°59'N, Nos L1, L13; Kopet-Dagh Mts, 5 km NW of Tutlikala, 800–900 m, 22.IV.1991, 56°44'N, 38°26'N, No. L7; Kopet-Dagh Mts, 12 km W of Kara-Kala, 24–25.IV.1991, 300 m, 56°08'E, 38°19'N, No. L8; Kopet-Dagh Mts, 3 km N of Kara-Kala, 500 m, 20.IV.1991, 56°17'E, 38°25'N, No. L9; Kopet-Dagh Mts., 5km S of Chuli, 18.IV., 14.V.1991, 700–800m, 58°01'E, 37°56'N, No. L21; Kopet-Dagh Mts, Aidere, 21–23.IV.1991, 600–1000 m, 56°46'E, 38°19'N, No. L6; 50 km N of Ashkhabad, 29.IV.1991, 100 m, 58°33'E, 38°21'N, No. L12, leg. G. CSORBA, GY. FÁBIÁN, B. HERCZIG, M. HREBLAY, G. RONKAY; Parkhay, 6 km NW of Kara-Kala, 400 m, 56°13'E, 38°22'N, 09.X.1991, No. L39, leg. A. PODLUSSÁNY, L. RONKAY & Z. VARGA; 4 km NW Germob, 1000 m, 20.IV.1993, 57°48'E, 38°01'N, leg. M. HREBLAY, GY. M. LÁSZLÓ and A. PODLUSSÁNY (Coll. HNHM, the collectors and P. GYULAI); 2 males, Ai-Dere, 29.V.1952, leg. KUZNETSOV (HNHM); 3 specimens, Ai-Dere, 25-26.IV.1997, leg. Z. KLYUCHKO and O. TARGONJA (Coll. BISCHOF); 3 males, Kopet-Dagh, Annau, 12, 17.V.1987, leg. DUBATOLOV (HNHM); Mari, 12–15.IV.1993, leg. KLIMENKO; Kara-Kala, V.1993, leg. MAGUS (Coll. P. GYULAI); 12 specimens, W Kopet-Dagh, Sunt-Khasardagh, southern foothills of Mt Sunt, 9.X.1996, leg. O. TARGONJA (Coll. BISCHOF and KLYUCHKO). Tadjikistan: 5 males, 1 female, Babatag Mts, 1200 m, 50 km W Kurgan Tyube, 5.V.1994, leg. LUKHTANOV (Coll. P. GYULAI and G. RONKAY); Kopet-Dagh, Kara-Kala, IV-V.199; Kopet-Dagh, Chuli, IV.1995 (Coll. P. FASTRÉ and A. LEGRAIN). Uzbekistan: 1 female, Bukhara, vic. Katan, V.1994, leg. ROMANOV; 2 females, Bukhara region, Kagan, 22.IV-5.V., 5–11.V.1994, leg. KLIMENKO (Coll. P. GYULAI).

Slide Nos HACKER 10718, HM4434, RL4347, RL4388, RL4389 (males), RL6004 (female).

Diagnosis: The new species is an allopatric, eastern sibling taxon of *O. anatolica* (LEDERER, 1857), which is distributed in the eastern part of the Mediterranean eastwards to Eastern Turkey and Armenia, while *O. turcomana* is known from Turkmenistan, Uzbekistan and Tadjikistan. *O. turcomana* differs ex-

ternally from its sister species by its broader, more pointed forewing, less darkened medial area with paler crosslines but with more sharply defined stigmata, less conspicuous blackish streaks in marginal area and darker hindwing with broader marginal suffusion.

The male genitalia of *O. turcomana* has, as compared with *O. anatolica*, narrower distal part of valva with shorter, more straight apical extension, shorter clavus, finer, more straight harpe, more globular dorsal plate of carina, larger amount of spiniform cornuti and weaker, smaller terminal cornutus in the vesica. The female genitalia of the new species differ from those of *O. anatolica* by its shorter but broader, caudally more dilated ostium bursae, bigger, more rounded appendix bursae and shorter signa of corpus bursae.

Description: Wingspan 22–29 mm, length of forewing 12–14 mm. Male. Head and thorax pale bluish grey mixed with whitish and blackish hairs, frons, collar and tegulae marked with black

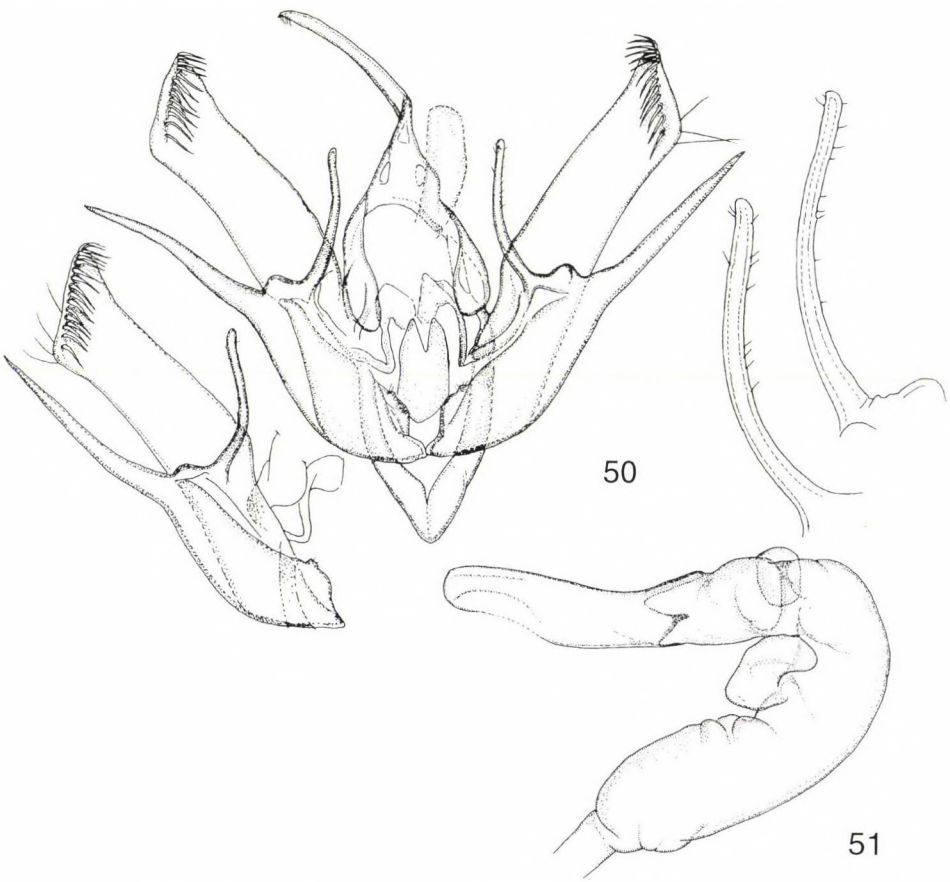

Figs 50–51. Male genitalia of *Euxoa sayvana* sp. n., paratypes

and whitish lines, tip of collar producing short, pointed hood; antenna shortly ciliate. Abdomen grey mixed with brown and whitish, dorsal crest consisting of one large and a few (1–2) small blackish tufts. Forewing rather short, acute triangular, outer margin evenly arcute. Ground colour pale bluish grey irrorated with a few blackish scales, veins often darker, especially in marginal area. Basal area wide, clear, streak of submedian fold short, fine, black. Ante- and postmedial lines more or less straight, slightly sinuous, double, blackish filled with ochreous. Medial area very narrow, suffused with dark grey-brown, darkest part of wing, medial fascia diffuse, rather wide, dark brown. Orbicular and reniform stigmata small, former sharply defined, rounded, encircled with blackish, outline of reniform incomplete, blackish, defined with pale grey; claviform tiny blackish circle. Subterminal obsolescent, upper part usually visible as arcuate, dark grey shadow, lower half regularly missing. Marginal area wide, apical and tornal parts with fine blackish streaks between veins. Terminal line diffuse, greyish, cilia dark grey-brownish, chequered with white. Hindwing pale ochreous, irrorated with brownish, veins and wide marginal area dark brown. Terminal line dark brown, cilia whitish with interrupted brown medial line. Underside of forewing unicolorous, dark greyish brown, upper part of transverse line variably strong, blackish stripe, defined with a few whitish grey, cilia, as on upper side, hindwing whitish, costal area irrorated, veins and marginal area covered with brown, discal spot small dot, transverse line usually present, diffuse.

Male genitalia (Figs 126, 127): Uncus short, strong, with small medial hump dorsally, tegumen high, narrow, penicular lobes elongate, setose. Fultura inferior shield-like, sometimes folded medially; vinculum strong, V-shaped. Valva elongate, narrow, costal margin arcuate distally, cucullus sclerotized, terminated in acute, beak-shaped extension; corona absent. Sacculus strong, large, distally tapering, clavus long, digitiform. Harpe wide-based, slender, cuneiform with strong, short apical thorn. Aedeagus short, thick, carina with rounded, flattened, serrate dorsal plate. Vesica membranous, broadly tubular, recurved ventrally, basal two-third inflated, covered with numerous spiniform cornuti arranged into long cornuti fields. Distal part slightly tapering, with two short diverticula armed with spiniform cornuti, terminal part finely scobinate, with big, flattened, lanceolate cornutus.

Female genitalia (Fig. 128): Ovipositor strong, short, conical, apophyses slender, rather long. Ostium bursae sclerotized, flattened, trapezoidal with widened caudal end and stronger, folded lateral margins. Ductus bursae inflated, membranous with fine scobination and stronger wrinkles. Appendix bursae semiglobular, slightly scobinate, corpus bursae elliptical, membranous, with two broad, ribbon-like, inequal signa.

Bionomics and distribution. The new species occurs in the foothills and the medium high zones of the Kopet-Dagh, the western Pamir and the Saravshan chains, appearing as relatively frequent in dry, very hot scrubby grasslands and steppes. Most specimens were collected at the early and mid-spring, a single datum is known from the beginning of October which may refer to its partial second generation.

Etymology: The specific name refers to the distribution of the species.

Allophyes sericina sp. n.
(Figs 21, 22, 52, 53, 129)

Holotype: male, "USSR, Turkmenia, Kopet-Dagh Mts., 5 km S of Chuli, 700–800 m, 58°01'E, 37°56'N, 11.XI.1991, No. L47. leg. M. Hreblay & G. Ronkay" (Coll. HNHM, donated by G. RONKAY).

Paratypes. Turkmenistan: 7 males, 2 females, with the same data as the holotype; 1 male, Kopet-Dagh Mts, 400–600 m, Firyuza, 58°05'E, 37°59'N, 8–13.XI.1991, No. L46; 1 male, Kopet-Dagh Mts, 15 km SE of Nochur, 1300–1400 m, 57°09'E, 38°21'N, 13–14.XI.1991, No. L49, leg. M. HREBLAY & G. RONKAY (Coll. HNHM, P. GYULAI, M. HREBLAY and G. RONKAY); 13 specimens, Kopet-Dagh, Kara-Kala, 20.X.-10.XI.1994, leg. MIATLEUSKI (Coll. FASTRÉ); 1 male, Kopet-Dagh, Firyuza, 29.X.1990, leg. DUBATOLOV; 1 female, Kopet-Dagh, Dushak, 27.IX.1988, leg. DUBATOLOV.

Slide Nos RL4119, RL4120, RL5985 (males), RL5999 (female).

Diagnosis: The new species has an intermediate position between the *A. asiatica* STAUDINGER, 1891 – *A. metaxys* BOURSIN, 1953 and the *A. heliocausta* BOURSIN, 1957 species groups, its closest relative is *A. heliocausta*. The new species differs externally from *A. heliocausta* by its more unicolorous greyish brown ground colour with less contrasting forewing pattern. The blackish patches of the submedian area, being typical of *A. heliocausta* are missing in *A. sericina*. The members of the *A. asiatica-metaxys* group have characteristically paler, whitish or pale greyish hindwing in both sexes while that of *A. sericina* is uniformly dark brown.

The male genitalia of *A. sericina* differ from those of *A. heliocausta* by the absence of the strong ampullar process on the right valva (the most typical feature of *A. heliocausta*), the longer ventral costal extension on the right valva and the broader distal plate of the left valva having shorter ventral extension, the somewhat longer uncus with narrower, apically not dilated arms and the smaller, thicker cornuti of the proximal part of the vesica. The members of the *A. asiatica* species group have broader but shorter uncus with apically dilated arms and the valval shape, the length of the costal and saccular extensions and the cornuti of the proximal part of the vesica are also clearly different. *A. asiatica* has shorter, lobate ventral extension on left valva while the saccular extension is fully reduced on right valva; *A. benedictina* has significantly narrower valvae with long, slender saccular processus but reduced costal extension on right valva and the ventral extension of the right valva is reduced; *A metaxys* has significantly longer, stronger saccular process but shorter and weaker costal extension on the right valva, and the cornuti of the proximal part of the vesica are considerably larger. The male genitalia of the species discussed above are illustrated by BOURSIN (1953, 1957).

Description: Wingspan 38–40 mm, length of forewing 19–20 mm. Male. Head and thorax grey-brown, mixed with whitish grey and some greenish; pubescence consisting of rather large, hair-like scales. Collar with blackish line and pale grey tip, tegulae with weak darker margins. Antenna of male shortly, symmetrically bipectinate with rather thick branches, Abdomen paler grey-brown, with some dark grey hairs, dorsal crest strong. Forewing relatively long, broad, with apex pointed, outer margin crenulate, tornal angle almost rectangular. Ground colour dark greyish brown with fine red-brownish shade and variably strong ochreous-brownish and metallic green irroration. Wing pattern sharply defined, ante-and postmedial lines black(ish), sinuous, simple, defined partly with whitish grey, latter with conspicuous white patch above inner margin; streak of submedian fold strong, fine, black. Stigmata present, large, encircled with fine black lines, their filling slightly

paler than ground colour. Subterminal line diffuse, interrupted, whitish-ochreous, marked with one or two black streaks at costa and a few darker brown patches at lower half. Terminal line row of fine blackish arches, defined by a few fine blackish streaks at tornus, cilia as ground colour, spotted with ochreous. Hindwing almost unicolorous, dark grey-brown with greasy shine, basal bart slightly paler, more ochreous grey, traces of transverse line and light spot at outer angle usually visible. Terminal line fine, dark, cilia ochreous with wide, dark grey-brown outer stripe. Underside of wings more or less unicolorously brownish grey, hindwing somewhat paler, wing pattern reduced to a whitish lunule at place of reniform and obsolescent, wide brownish stripe on hindwing. Female. As male, antenna very shortly serrate, forewing broader, darker, more unicolorous, dark pattern less conspicuous.

Male genitalia (Figs 52, 53): Uncus bifurcate with slender, apically rounded, hairy distal arms, tegumen low, penicular lobes narrow, less hairy. Fultura inferior broad, sclerotized, shield-like, vinculum long, strong, more or less V-shaped. Valvae elongate, constricted above sacculus, strongly asymmetrical; right valva with long, cuneate cucullus and long, strong, curved ampullar process; left valva with shorter cucullus, broader, more trapezoidal distal lamina with ampullar process reduced to small, pointed, triangular extension. Right harpe long, hooked, its base with medium long, slender extension fused with ventral margin, left harpe longer, finer, its base without extension. Sacculi symmetric with lobate, setose clavus, small, erected, triangular processus below clavus and short, small extension at ventral extremity. Aedeagus cylindrical, arcuate, carina with sclerotized, smooth dorsal plate having serrate margin. Vesica broadly tubular, recurved ventrally,

Figs 52–53. Male genitalia of *Allophyes sericina* sp. n., paratypes

its walls hyaline. Basal half with numerous (45–55) small and very small, pointed, usually wide-based cornuti, medial third with one or two huge, cristate or acute cornuti with large, granulosely sclerotized basal plates, terminal part with big, semiglobular diverticulum covered with fine spiculi and partly sclerotized, apically rounded, flattened terminal lobe.

Female genitalia (Fig. 129): Ovipositor rather short but strong, conical, papillae anales pointed, covered with long setae; apophyses slender, long. Lamella antevaginalis sclerotized, with rounded triangular ventro-lateral appendages. Ostium bursae broad, low, cup-shaped, ductus bursae granulosely sclerotized, very strongly folded, constricted at posterior third, dilated anteriorly. Appendix bursae flattened, heavily sclerotized, more or less discoidal with pointed tip. Corpus bursae spacious, elliptical-ovoid, its walls membranous with fine scobination and variably strong wrinkles.

Bionomics and distribution. The species appears as endemic to the central parts of the nothern chain of the Kopet-Dagh, occurring in shrubby steppes and open *Acer turcomanica* forest patches in medium high and higher elevations. The imagines are on wing in the very late autumn and are attracted better to sugar baits, less to artificial light.

Etymology. The specific name refers to the silky shine of the forewings.

Lithophane alaina BOURSIN, 1957
(Figs 130–132)

Type material examined: holotype female, Alai Mts (Coll. PÜNGELER, MNHU).

Additional material examined: Uzbekistan: 1 female, W Tien Shan, 1200 m, Tshatkal Reserve, Bash-Kizil-Say, 27.V.- 3.VI.1982, leg. PEREGOVITS (HNHM). Kazakhstan: 8 specimens, Aksu-Dzhabagli (ZIN). Turkmenistan: 3 males, 1 females, Kugitang-Tau Mts, 1 km SW of Airi-Baba peak, 2500 m, 20–21.V.1991, 66°37'E, 37°52'N, No. L23, leg. M. HREBLAY & G. RONKAY; 3 males, 1 female, Kopet-Dagh Mts, 15 km SE of Nochur, 1300–1400 m, 13–14.XI.1991, 58°01'E, 37°56'N, No. L49, leg. M. HREBLAY & G. RONKAY; a long series, Kopet-Dagh Mts, 6 km S of Ipay-Kala, 1600 m, 8–12.IV.1993, No. L86, 57°07'E, 37°17'N, leg. M. HREBLAY, GY. M. LÁSZLÓ & A. PODLUSSÁNY (Coll. HNHM, GY. FÁBIÁN, M. HREBLAY, G. RONKAY).

Slide Nos HM2736, HM2753, HM2775, HM2745, HM2747, HM2748, HM2749 (males), HM2747, HM2776, HM4246, HM4250, HM4251 (females).

Description: Male genitalia (Figs 130, 131): Uncus slender, with fine apical hook, tegumen high, vinculum U-shaped. Fultura inferior subdeltoidal with long dorsal arm. Valva elongate, distally tapering, cucullus bifurcate with apex acute; corona absent. Sacculus short, clavus simple, flat, rounded. Harpe very long, slender, distal part recurved to costal margin; ampulla absent. Aedeagus curved ventrally in right angle at its distal fourth, carina strongly slerotized, rounded. Vesica tubular, about twice as broad as the tube of aedeagus, terminal part with two small fields of fasciculate cornuti.

Female genitalia (Fig. 132): Ovipositor short, conical, ostium bursae broad, trapezoidal-calyculate, caudal edge deeply arcuate. Ductus bursae flattened, distally tapering both surfaces with sclerotized plates, ventral plate considerably larger, extending into corpus bursae. Appendix bursae very small, wrinkled, corpus bursae globular-discoidal, membranous with fine wrinkles and with four weak but long signum-stripes.

Remarks. The specimens found in Turkmenistan shows some differences in the ground colour and the intensity of the wing pattern as compared with the few

known specimens from the western Tien Shan area, but the genitalia of both sexes are almost identical.

Dasypolia templi dushaki ssp. n.
(Fig. 27)

Holotype: male, "USSR, Turkmenia, Kopet-Dagh Mts., 15 km SE of Nochur, 1300–1400 m, 57°09'E, 38°21'N, 13–14.XI.1991, No. L49, leg. M. Hreblay & G. Ronkay", slide No. HM2909 (Coll. M. HREBLAY).

Paratypes: Turkmenistan: 6 males, Turkmenia, Kopet-Dagh Mts, 15 km SE of Nochur, 1300–1400 m, 57°09'E, 38°21'N, 13–14.XI.1991, No. L49, leg. M. HREBLAY & G. RONKAY (Coll. HNHM, M. HREBLAY and G. RONKAY).

Slide Nos HM2902, RL6091 (males).

Diagnosis: The population occurring in the central part of the Kopet-Dagh Mts differs from the geographically closest known races, *D. templi armeniaca* RONKAY et VARGA, 1985 (eastern Caucasus, eastern Turkey), *D. templi anatolica* HACKER, 1990 (central Turkey) and *D. templi hortensis* RONKAY et VARGA, 1990 (Pamir Mts). The males of *D. templi dushaki* have broad, olive-brownish

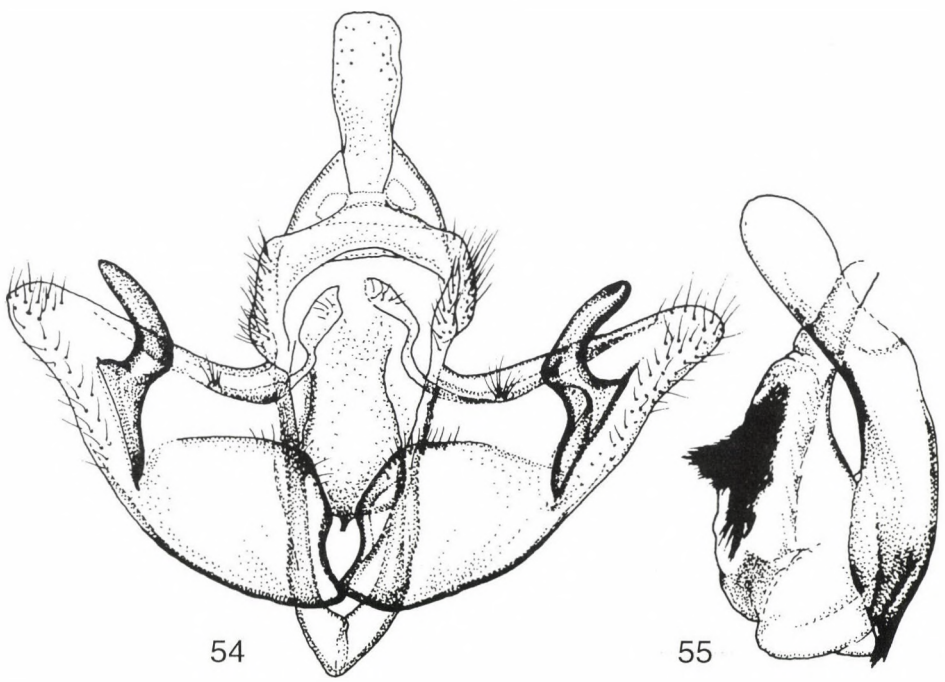

Figs 54–55. Male genitalia of *Episema minutoides* sp. n., holotype

forewing with fine reddish and dark olive-grey irroration, the forewing pattern is relatively strong, the crosslines are diffuse but well visible, strongly sinuous, and the stigmata clearly visible. The males of *D. templi anatolica* are similarly large in size, but much paler, ochreous without darker brownish irroration and the wing pattern is more diffuse, more indistinct. *D. templi armeniaca* is smaller in size (wingspan 39–50 mm), the forewings narrower, and the colouration variable from ochreous-brown to dark olive-brown or olive-greyish, the crosslines are regularly more diffuse, less sinuous. The males of *D. templi hortensis* are also smaller, the forewing is characteristically pale ochreous-reddish brown with obsolescent forewing pattern. The male genitalia show no significant differences compared with the other Asian races of the species.

Description: Wingspan 53–55 mm, length of forewing 25–26 mm. Male. Pubescence of head and thorax dark olive-brownish mixed with reddish and dark grey hairs, antenna strongly bipectinate, with long, fasciculate cilia. Abdomen similarly olive-greyish, anal tuft slightly more ochreous. Forewing elongate, broad, with apex finely rounded, scaling long, dense, hair-like. Ground colour olive-brown, mixed with whitish grey and reddish brown, medial area with stronger dark irroration. Wing pattern relatively diffuse but well discernible, ante- and postmedial lines strongly sinuous, simple, dark brownish grey defined with a few whitish-greyish scales, medial line pale, shadow-like, subterminal line interrupted, diffuse, defined by some ochreous at outer side. Orbicular stigma pale ochreous, small, round(ed), reniform less distinct, ochreous-whitish without darker outline. Terminal line fine, dark grey-brown line, cilia as ground colour, variegated with pale ochreous. Hindwing shiny whitish-ochreous, suffused with with darker grey-brownish, veins regularly slightly darker, transverse line often present but diffuse; discal spot may also be present, small, shadow-like. Terminal line fine dark brown-grey, cilia orange-ochreous. Underside of wings shiny, pale ochreous grey, irrorated with brownish, transverse lines and discal spots diffuse, often present on both wings, stronger on hindwing. Female unknown.

Distribution. *D. templi dushaki* was found in a rather low site at the northern slope of the Dushak massif.

Dasypolia nebulosa sp. n.
(Figs 28, 29, 56, 57, 134, 135)

Holotype: male, "USSR, Turkmenia, Kopet-Dagh Mts., 400–600 m, Firyuza, 58°05'E, 37°59'N, 8–13.XI.1991, L46. leg. M. Hreblay & G. Ronkay", deposited in Coll. HNHM, donated by G. RONKAY.

Paratypes. Turkmenistan: 15 males, 1 female, with the same data as holotype; 9 males, Kopet-Dagh Mts, 15 km SE of Nochur, 1300–1400 m, 57°09'E, 38°21'N, 13–14.XI.1991, No. L49, leg. M. HREBLAY & G. RONKAY; 23 males, 1 female, Kopet-Dagh Mts, Firyuza, 400–600 m, 58°05'E, 37°59'N, 22–26.XI.1991, No. L55, leg. M. HREBLAY & G. RONKAY; 16 females, Kopet-Dagh Mts, Dushak Mt., 1800 m, 57°56'E, 37°54'N, 2–3.IV.1993, No. L82, leg. M. HREBLAY, GY. M. LÁSZLÓ and A. PODLUSSÁNY (Coll. HNHM, GY. FÁBIÁN, P. GYULAI, B. HERCZIG, M. HREBLAY and G. RONKAY).

Slide Nos HM2901, HM2908, RL5975 (males), HM10474, RL5976 (females).

Diagnosis: The taxonomy of the D. *ferdinandi* RÜHL, 1892 species-group (s. l.) is rather difficult, as the externally often conspicuously different popula-

tions display only slight differences in the genitalia, the individual variation within the populations is often rather large, the variations of the distinct, presumably isolated populations are partly overlapping even in the features considered as taxonomically important within the whole genus. The taxa of the species group are easily separable for two major groups, the western Palaearctic and the Central Asian species are clearly distinguishable by their external and genital features (the only member of the *D. afghana* BOURSIN, 1967 line which occurs in eastern Turkey, *D. altissima* HACKER et MOBERG, 1988 shows good specific features in the male genitalia, too). The western Palaearctic species (the *D. ferdinandi*-group s. str.) belong to two parallel lineages, occurring often sympatrically and syntopically in Anatolia, E Turkey, Transcaucasia and the Kopet-Dagh Mts (and probably also in the Atlas Range), while only *D. ferdinandi* is known from the Alps and the other high mountains of Europe. It is rather subjective to estimate the taxonomic rank of the taxa distributed outside Europe, but it is easy to conclude that they cannot represent different subspecies of the same species, *D. ferdinandi*. It seems most probable that *D. ferdinandi*, *D. dichroa* RONKAY et VARGA, 1985, *D. nebulosa* sp. n. and an undescribed population occurring in the High Atlas form one of the main lineages while *D. haroldi* RUNGS, 1950, *D. transcaucasica* RONKAY et VARGA, 1985 and *D. ipaykala* sp. n. (described below) represent the parallel species complex. These taxa are considered here – tentatively – as distinct species and not subspecies of two rather widespread twin species.

D. nebulosa differs conspicuously from the related taxa distributed in the adjacent mountain systems (*D. dichroa* RONKAY et VARGA, 1985, central and eastern Turkey, *D. transcaucasica* RONKAY et VARGA, 1985, eastern Turkey, Armenia, *D. altissima* HACKER et MOBERG, 1988, eastern Turkey, and from the other members of the *D. afghana* BOURSIN, 1967 species-complex, widespread in Central Asia) by its larger size, pale ochreous-olive forewing ground colour with obsolescent, diffuse crosslines. *D. nebulosa* mostly resembles the typical populations of *D. ferdinandi* occurring in the Alps by its pale forewing but the antemedial crossline is more oblique and sinuous, the dark centre of the reniform is regularly more sharply defined and the hindwing has a stronger greyish suffusion.

The male genitalia show no conspicuous differences compared with *D. dichroa* and *D. ferdinandi*, although on average the cucullus seems more elongate, and the costal extension longer, more acute in average in the new species than in the other related taxa, and in the females the ductus bursae of *D. nebulosa* is somewhat broader, stronger, and more straight.

Description: Wingspan 40–48 mm, length of forewing 18–23 mm. Male. Pubescence of head and thorax rather homogeneous, pale olive-brown mixed with ochreous and darker grey hairs, antenna bipectinate with relatively short branches having long, fasciculate cilia. Abdomen more ochreous-grey, covered with long hairs, dorsal crest rather indistinct. Forewing elongate, narrow,

with apex finely rounded, scaling long, dense, hair-like. Ground colour pale olive-grey with ochreous sheen, mixed with ochreous and whitish grey. Wing pattern obsolescent, ante- and postmedial lines sinuous, simple, darker brownish grey defined with few whitish-greyish scales, medial fascia and subterminal line missing. Orbicular stigma absent or tiny ochreous dot, reniform also indistinct, ochreous, without darker outline, sometimes with darker medial spot. Terminal line interrupted, grey-brown, cilia as ground colour, variegated with pale ochreous. Hindwing shiny ochreous grey, suffused with darker brownish, veins regularly slightly darker, transverse line often present but diffuse, shadow-like; a small, diffuse discal spot may also present. Terminal line dark brown-grey, cilia ochreous grey. Underside of wings shiny, pale ochreous grey, irrorated with brownish, transverse lines and discal spots diffuse, often present on both wings, stronger on hindwing. Female. As male, but forewing shorter, somewhat broader with more rounded apex, antenna filiform.

Male genitalia (Figs 56, 57): Uncus short, rather strong, apically finely hooked, tegumen broad, low, penicular lobes small, rounded, densely hairy. Fultura inferior more or less cordiform, apical incision deep, with long, strongly sclerotized marginal bars and medium-long, finely pointed medial process; vinculum long, strong, V-shaped. Valva elongate, apically tapering, cucullus medium-long, with apex pointed, corona reduced. Sacculus short, triangular, clavus relatively strong, digitiform, setose, harpe long, slender, S-shaped, basal bar long, strong, costal extension well-developed, cuneate. Aedeagus long, tubular, finely curved at middle, carina with a small, strong, dentated dorsal plate. Vesica membranous, tubular, everted forward, recurved at middle, basal part slightly dilated at base, evenly tapering distally. Medial area finely scobinate, bearing two rather long, narrowly tubular, pointed diverticula.

Female genitalia (Figs 134, 135): Ovipositor short, conical, rather strong, posterior gonapophyses long, slender, anterior ones very short, weak. Ostium bursae relatively broad, quadrangular with two sclerotized, triangular ventro-lateral plates. Ductus bursae long, tubular, flattened, dorsal and ventral surfaces more or less equally, granulosely sclerotized, gelatinous dorsal pocket oblique, narrow, only slightly projected over lateral margin. Appendix bursae short, conical, finely wrinkled, corpus bursae spacious, ovoid, weakly membranous.

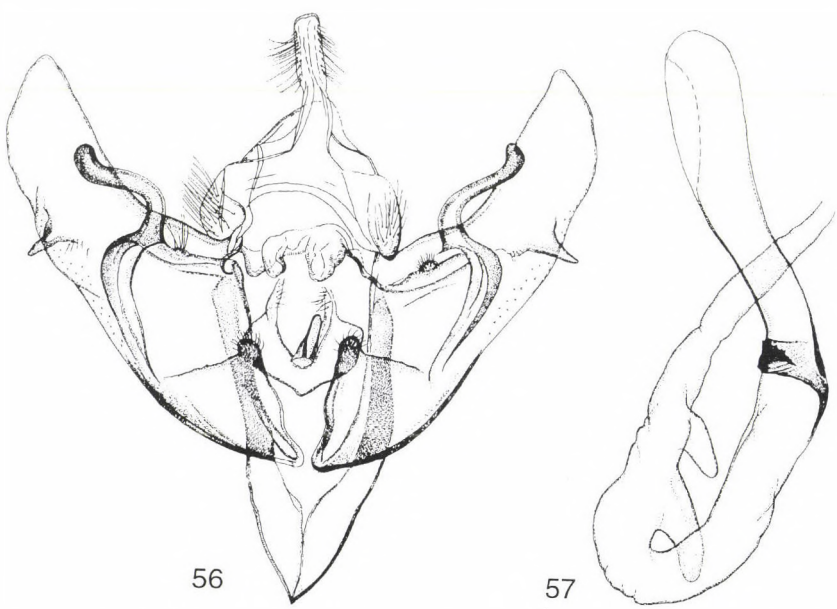

Figs 56–57. Male genitalia of *Dasypolia nebulosa* sp. n., paratype

Bionomics and distribution. The new species was found in the lower and medium high zones of the northern main chain of the Kopet-Dagh Mts. The localities are dry, rocky slopes with scarce herbaceous vegetation. The freshly emerged moths appear very late in the year, usually in the second part of November, the overwintered females were collected in the mid-spring; the moths are attracted strongly to artificial light.

Etymology. The specific name refers to the obsolescent forewing markings.

Dasypolia ipaykala sp. n.
(Figs 30, 136, 137)

Holotype: female, "Turkmenistan, Kopeth-Dagh Mts, 6 km S of Ipaj-Kala, 1600 m, 8–12. IV. 1993, No L86, 57°07'E, 37°17'N, leg. M. Hreblay, Gy. László & A. Podlussány", slide No. HM4260 (Coll. M. HREBLAY).

Diagnosis: *Dasypolia ipaykala* sp. n. belongs to the *D. ferdinandi* species-group, its closest relatives are *D. dichroa* RONKAY et VARGA, 1985 and *D. transcaucasica* RONKAY et VARGA, 1985. *D. ipaykala* sp. n. is smaller in size than *D. dichroa*, having much darker colouration of both wings. Compared with *D. transcaucasica*, the new species has broader forewing and darker hindwing. In addition, *D. ipaykala* sp. n. differs from the other species of this species group by the absence of the orbicular and reniform stigmata. In the female genitalia the ductus bursae of the new species is shorter than those of the related species.

Description: Wingspan 34 mm, length of forewing 15 mm. Female. Head and thorax densely covered with long olive-greyish and brown hairs, eye-lashes long, blackish. Antenna filiform with scarce cilia. Forewing rather short, broadly triangular with apex rounded, outer margin evenly arcuate. Ground colour dark brownish-grey with olive-green shade, mixed with darker brown and ochreous scales. Wing pattern rather diffuse, crosslines present, sinuous, costal spots rather strong, postmedial line more or less S-shaped, subterminal line a diffuse shadow. Median area darker than other parts of wing, stigmata deleted. Terminal line fine, dark, cilia long, paler than ground colour. Hindwing brownish grey, veins somewhat darker, discal spot visible as weak line; terminal line darker brown, cilia ochreous. Underside of wings greyish, forewing suffused with grey-brown, transverse lines diffuse, discal spot of hindwing present, tiny. Male unknown.

Female genitalia (Figs 136, 137): Ovipositor short, conical, rather weak, posterior papillae finely setose, gonapophyses slender, weak. Ostium bursae low but rather broad, more or less cordiform, caudal edges angular. Ductus bursae narrow, flattened, long, dorsal and ventral surfaces with inequal, granulose sclerotization; dorsal pocket reduced. Appendix bursae minute, corpus bursae long, weakly membranous.

Bionomics and distribution. The unique known specimen is an overwintered female, found in the first part of April, at higher elevations of the central Kopet-Dagh Mts.

Episema minutoides sp. n.
(Figs 23, 24, 54–55, 133)

Holotype: male, "USSR, Turkmenia, Kopet-Dagh Mts., 1000 m, Kurkulab, 6 km W Germob, 57°50'E, 38°04'N, 03.X.1991, No. L34, leg.: A. Podlussány, L. Ronkay & Z. Varga". Slide No. RL5958 (Coll. HNHM).

Paratype: 1 female, with the same data as the holotype (Coll. G. RONKAY).
Slide No. RL6002 (female).

Diagnosis: The new species is closely related to *Episema minuta* EBERT, 1971, described from Afghanistan, based on the unique male holotype. *E. minutoides* differs externally from this specimen of *E. minuta* by its dark fumous grey ground colour (probably variable in both species!), stronger, blackish ante- and postmedial crosslines, sharper whitish covering of veins, smaller, darkened reniform stigma and the generally darker hindwing, intensely suffused by grey-brown. The male genitalia of the new species are very similar to those of *E. minuta* but the distal half of the uncus is broader with more parallel lateral margins, the fultura inferior is larger, wider, more quadrangular, the carina penis is much broader distally, and the dorso-lateral plates are armed with different spines and teeth.

The new species externally also resembles *E. lederi* CHRISTOPH, 1885, but is smaller in size, the pectination of the male antenna is about half of that in *E. lederi*, and the corneous frontal plate is stronger, more expressed, having a central process. The genitalia differ from those of *E. lederi* by their broader, shorter, apically more tapering valvae with shorter, broader triangular cucullus, larger, more quadratic fultura inferior, and the more slender, apically less rounded harpe. The configuration of the carina is strongly dissimilar in the two species, both plates are projected dorso-laterally and fused with the main wall of carina in *E. minutoides*, while one of them is a separate spine in *E. lederi* and the second is projected ventrally, armed with a pointed tooth. The female genitalia of *E. minutoides* differ from those of *E. lederi* by their narrower ostium bursae, the smaller, proximally slightly dilated, more quadratic ductus bursae, the more rounded, anteriorly more constricted appendix bursae and the smaller, elliptical corpus bursae.

Description: Wingspan 24–27 mm, length of forewing 11–13 mm. Male. Head small, frons covered with whitish hairs, frontal corneous plate rounded, strong, with short central prominence. Antenna rather shortly bipectinated, pubescence of thorax less distinct, dark grey mixed with whitish and dark brown, collar with darker apical third; metathoracic tuft large, dark grey. Abdomen paler greyish, anal tuft paler, dorsal crest absent. Forewing short, broadly triangular, apically pointed, ground colour dark fumous grey, irrorated with brown, whitish-grey and black; veins whitish. Basal area narrow, suffused with whitish grey, costal area chequered with whitish between crosslines. Ante and postmedial lines interrupted, simple, black, former arcuate, latter slightly sinuous. Orbicular and reniform stigmata rather sharply defined, incompletely encircled with blackish, filled with whitish and with ground colour. Suborbicular patch larger, rather diffuse, reniform elliptical, without extension at lower extremity; claviform missing. Subterminal indistinct, slightly sinu-

ous, defined by dark grey costal spot and wide, pale grey zone between postmedial and subterminal lines, outer part of marginal area darker grey. Terminal line fine, continuous, blackish brown, cilia pale grey, spotted with brownish grey. Hindwing greyish white, basal area irrorated, wide marginal area suffused with brownish grey, transverse line diffuse, darker brownish. Terminal line brown, cilia whitish, spotted with pale brownish. Underside of wings whitish grey, forewing and marginal area of hindwing suffused with greyish brown, traces of stigmata and crosslines well visible. Female. As male, forewing longer, more acute, colouration less contrasting, whitish grey irroration weaker, outlines of stigmata sharper, hindwing much darker, more or less concolorous with diffuse transverse line.

Male genitalia (Figs 54–55): Uncus short, flattened, distal half slightly dilated, quadrangular-spatulate with almost parallel margins, apex finely rounded. Tegumen narrow, low, penicular lobes elongate, densely setose. Fultura inferior sclerotized, quadrangular, high, vinculum short, thick, V-shaped. Valva rather short, triangular, apically strongly tapering, cucullus short, triangular with apex rounded, setose, corona absent. Sacculus more or less triangular, big, clavus rounded, setose lobe, harpe strong, flattened, evenly curved, with apex rounded, basal bar heavily sclerotized; pulvillus minute, rounded densely setose prominence. Aedeagus short, cylindrical, arcuate, carina with two dorso-lateral, sclerotized plates, one of them covered with acute teeth, second one armed with flattened, spiniform tooth. Vesica rather short, membranous, everted ventrally, recurved to coecum penis. Basal part broad, distal half strongly tapering, ventral surface bearing two long, narrow bundles of rather short, acute spinules.

Female genitalia (Fig. 133): Ovipositor medium-long, rather weak, papillae anales broad, densely setose, apophyses fine, slender. Ostium bursae wide, very short, forming a sclerotized ring; ductus bursae sclerotized, short, almost quadrate, proximally slightly dilated. Appendix bursae ovoid-elliptical, flattened, partly gelatinous and scobinate, constricted above corpus bursae. Corpus bursae weakly membranous, elliptical-ovoid, without signum.

Bionomics and distribution. The two sister species, *E. minuta* and *E. minutoides* are known from a total of three specimens only, the holotype of *E. minuta* was discovered in the vicinity of Herat, NE Afghanistan, the pair of *E. minutoides* was collected in a deep rocky gorge west from the Germob Basin, situated between the two northern chains of the Turkmenian Kopet-Dagh. It is hard to estimate their ranges but they seem to represent an allopatric species pair. The exact locality of *E. minutoides* is the opening of the long, narrow, deep gorge surrounded by small hills, a very hot and dry grassland with sparse rocky vegetation.

Etymology. The specific name refers to the high similarity of the new species with its closest relative, *E. minuta*.

Polymixis pericaspicus sp. n.
(Figs 35, 58, 59, 138)

Holotype: male, "USSR, Turkmenia, Kopet-Dagh Mts., 1000 m, Kurkulab, 6 km W Germob, 57°50'E, 38°04'N, 03.X.1991, No. L34, leg.: A. Podlussány, L. Ronkay & Z. Varga". Slide No. RL4253 (Coll. HNHM).

Paratypes. Turkmenistan: 1 male, with the same data as the holotype (Coll. Z. VARGA), 1 female, Kopet-Dagh Mts, 800 m, 20 km E of Nochur, Karayalchi valley, 57°12'E, 38°23'N, 04.10.1991, No. L35, leg. A. PODLUSSÁNY, L. RONKAY & Z. VARGA (Coll. P. GYULAI). Iran: 1 female, Derbend, 25 km NW Teheran, 2000 m, 5–17.10.1963, leg. VARTIAN (Coll. G. RONKAY).

Slide No. RL5974 (female).

Diagnosis: The new species is an allopatric sibling taxon of *P. zagrobia* (WILTSHIRE, 1941), which is described from SW Iran. *P. pericaspicus* differs from the darker olive-brownish *P. zagrobia* by its much paler ochreous-brownish or buff forewing ground colour with fine pinkish shade and intense ochreous shine and the clearer, paler ochreous reniform and orbicular stigmata. The male genitalia of the two species are rather similar but *P. pericaspicus* has larger and broader uncus, longer, more acute costal triangles, finer, shorter, symmetrical harpes, and longer, more asymmetrical, acute costal extensions, and the tooth on the ventro-lateral bar of the carina is stronger, narrower, more thorn-like. The male genitalia of the holotype of *P. zagrobia* are illustrated by WILTSHIRE (1993: Fig. 8).

The species also resembles *P. (Brandticola) dubiosa roseotincta* (BRANDT, 1941) by its pinkish shade of the forewings but the wing is more elongate, the wing pattern is more diffuse, less mosaic-like, the stigmata are paler, etc. and the genitalia of both sexes show good distinguishing characters (see HACKER & RONKAY 1992).

Description: Wingspan 34–39 mm, length of forewing 16–19 mm. Head and thorax pale ochreous mixed with some clay-brownish hairs, pubescence long, rather homogeneous, tegulae and metathoracic tuft less distinct. Palpi short, slightly upturned. Antenna of male shortly bipectinate with long, fasciculate cilia, that of female filiform. Abdomen similarly pale, dorsal crest present, consisting of tiny, dark brown tufts. Forewing relatively narrow, elongate with apex acute, outer margin evenly arcuate. Ground colour pale, shiny ochreous-brownish or buff, with fine pinkish

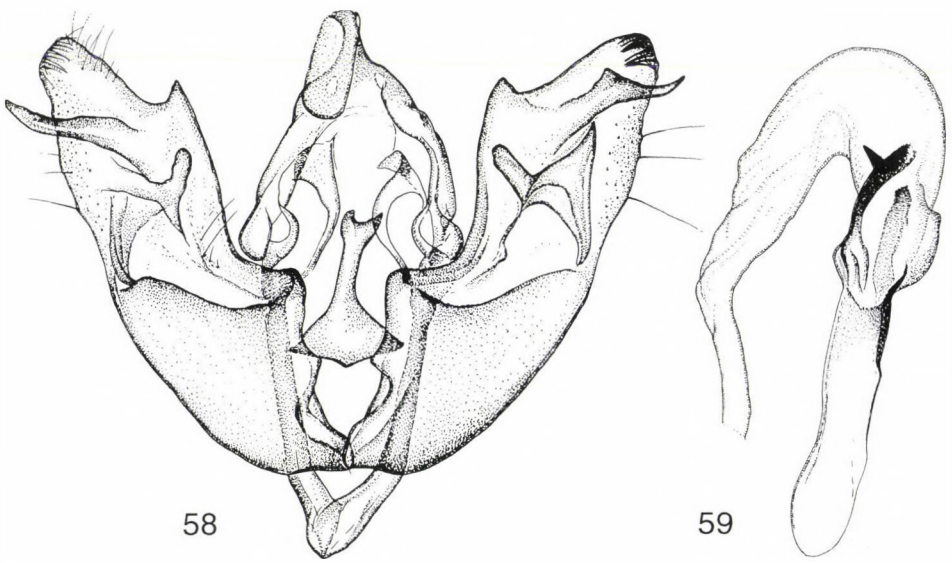

Figs 58–59. Male genitalia of *Polymixis pericaspicus* sp. n., holotype

hue, irrorated with pale ochreous, especially in outer half of marginal area. Antemedial crossline double, sinuous, brownish, filled with whitish ochreous, medial line diffuse, narrow brownish stripe, postmedial line represented by row of dark brownish spots on veins and their paler ochreous definition. Orbicular and reniform stigmata well visible but rather diffuse, paler than ground colour but without sharper outlines; claviform deleted. Orbicular small, round, ochreous with more or less conspicuous dark medial spot, reniform large, broadly quadrangular, both pale ochreous with a few scattered darker brownish scales. Subterminal line strongly sinuous, whitish-ochreous, dividing marginal area into dark inner and pale outer halves. Terminal line brownish, interrupted, cilia pale ochreous, spotted with ground colour. Hindwing shiny whitish-ochreous, veins brownish, marginal area with weak darker brown irroration forming two rather indistinct, parallel stripes. Terminal line brown, cilia whitish with a few darker scales. Underside of wings milky whitish with scarce brownish irroration, discal spots and transverse lines very pale or obsolete.

Male genitalia (Figs 58, 59): Uncus moderately long, distal two-thirds broad, flattened, with apex rounded, tegumen narrow, relatively high, penicular lobes small, rounded. Fultura inferior subdeltoidal, with narrow, high, terminally incised apical extension, vinculum short but strong, V-shaped. Valvae slightly asymmetrical, elongate, cuculli more or less triangular with rounded apices and short, weak corona, costal margin with rather long, acute subapical lobes. Sacculus strong, clavus broad, digitiform, relatively short, with apex rounded, harpe slender, pointed, finely setose, its base forming large, triangular, sclerotized plate. Costal extensions asymmetrical, left extension longer, more curved but with smaller dorsal crest. Aedeagus relatively short, tubular, carina with large, granulosely sclerotized, wrinkled, eversible laminae, ventro-lateral lamina with strong but rather short, thorn-like distal tooth. Vesica broadly tubular, everted forward, recurved laterally, constricted at curve. Basal third membranous, constricted part with finely sclerotized dorsal plate bearing stronger wrinkles, distal part finely scobinate, evenly tapering.

Female genitalia (Fig. 138): Ovipositor short, weak, gonapophyses short, fine. Ostium bursae broad but short, sclerotized, dorsal surface with two elliptical depressions having stronger margins. Ductus bursae elongate, flattened, distal end broader, proximally slightly tapering. Both surfaces strongly, granulosely sclerotized, margins even stronger, slightly folded, longer, stronger on left side. Appendix bursae small, shortly conical, finely wrinkled, corpus bursae ovoid, hyaline with very fine scobination and with four long, strong signum-stripes.

Bionomics and distribution. The new species is known only by a very few specimens collected in extremely dry, rocky grasslands. It seems as a rarity, single specimens were found in huge materials from these regions, e.g. in the whole Iranian material we had the opportunity to study, a sole female was present in the unset doublettes of *P. dubiosa* from the Elburs Mts of the VARTIAN collection.

Etymology. The specific name refers to the area of the species, occurring in the large mountains at the southern edge of the Caspian Sea.

Polymixis schistochlora sp. n.
(Figs 31, 32, 60, 61, 139)

Holotype: male, "USSR, Turkmenia, Kopet-Dagh Mts., 800 m, 20 km E of Nochur, Karayalchi valley, 57°12'E, 38°23'N, 04.X.1991, No. L35, leg.: A. Podlussány, L. Ronkay & Z. Varga" (Coll. HNHM).

Paratypes. Turkmenistan: 1 male, 8 females, with the same data as the holotype; 4 males, 2 females, Kopet-Dagh Mts, 1600 m, 25 km E of Nochur, Karayalchi valley, 57°09'E, 38°21'N, 05.X.1991, No. L36, leg. A. PODLUSSÁNY, L. RONKAY & Z. VARGA (Coll. HNHM, GY. FÁBIÁN, P.

GYULAI, M. HREBLAY, G. RONKAY and Z. VARGA); 1 male, 1 female, Kopet-Dagh Mts. Garrygala, 20.X.-10.XI.1994, leg. MIATLEUSKI (Coll. P. GYULAI).

Slide Nos RL4060, RL4063, RL4233 (males), RL5963 (female).

Diagnosis: The new species is the westernmost known member of the *P. polymorpha* BOURSIN, 1960 species complex, representing an allopatric sibling species of *P. zophodes* BOURSIN, 1960. The external appearance of *P. schistochlora* is very characteristic, the forewing being almost unicolorous, dark olive-greyish with diffuse or obsolescent paler crosslines and stigmata, while *P. zophodes* is ochreous-brownish or ochreous grey with much stronger forewing pattern. The male genitalia of the two species are very close, the most conspicuous difference between them being the projection of the right costal extension which is divergent from the ventral arch of the basal plate of the harpe in *P. schistochlora* while they are strictly parallel in *P. zophodes*. In addition, the valvae of the new species are broader with more acute cucullus, the subapical costal lobe is smaller and the left costal extension is more curved. In the female genitalia the ostium of *P. schistochlora* is somewhat narrower with stronger ostial extension on dorsal side, the ductus bursae is stronger with parallel margins, not caudally widening as in *P. zophodes*, and the appendix bursae is broader, more rounded apically.

Description: Wingspan 38–40 mm, length of forewing 17–18 mm. Pubescence of head and thorax rather homogeneous, long, olive-greyish mixed with a few ochreous-brownish hairs. Palpi short, upturned. Antenna of male ciliate with short fasciculate cilia, that of female filiform. Abdomen more ochreous, mixed with dark grey, dorsal crest reduced to weak ochreous-greyish tufts. Forewing elongate, rather high triangular with apex acute, outer margin evenly arcuate. Ground colour dark olive-greyish with fine bronze sheen and fine, weak whitish irroration, medial and submarginal areas suffused partly with brownish olive. Ante- and postmedial crosslines diffuse, double, often interrupted, filled with whitish grey or pale ochreous grey, postmedial marked by some dark spots on veins. Medial line diffuse, usually narrow brownish-olive shadow. Orbicular and reniform stigmata present but less distinct, without sharply defined outlines; claviform absent. Orbicular rounded, reniform large, more or less quadrangular, both filled with whitish-greyish, reniform with plumbeous grey scales at lower third. Subterminal strongly sinuous, ochreous-whitish, outer part of marginal area irrorated strongly with whitish grey. Terminal line row of dark spots, cilia whitish, spotted with grey-brown. Hindwing milky whitish, scarcely (males) or rather strongly (females) irrorated with dark greyish brown. Veins dark, transverse line and discal spot diffuse but usually visible. Terminal line brown, cilia white, spotted with brown. Underside of wings milky whitish, with variably strong greyish-brownish suffusion, regularly stronger, darker in females. Traces of transverse lines most often present on both wings, discal spot absent or only pale shadow on forewing.

Male genitalia (Figs 60, 61): Uncus short, slender, curved, with apex finely pointed, tegumen wide, relatively high, penicular lobes small, rounded. Fultura inferior subdeltoidal, with narrow, high, terminally incised apical extension, vinculum short but strong, V-shaped. Valvae asymmetrical, elongate, cucullus more or less triangular with pointed apex, corona short, weak; costal margin with wide, triangular subapical lobe. Sacculus long, strong, clavus sclerotized, triangular lobe. Harpe reduced to flattened, arcuate, sclerotized basal plate. Costal extensions asymmetrical, left extension strong, acute, curved at middle, directed apically, right extension longer, more slender, projected ventrally, its distal part diverging from ventral arch of harpe. Aedeagus cylindrical, finely arcuate, carina with narrow, serrate ventro-lateral bar and much longer, ventrally serrate

lamina curved into dorso-lateral side of carina, dorsal part finely dentate, terminated in small, subconical extension. Vesica membranous, main part inflated, more or less globular, distal part finely scobinate, evenly tapering into ductus ejaculatorius.

Female genitalia (Fig. 139): Ovipositor medium-long, weak, papillae anales densely hairy; apophyses short, fine. Ostium bursae lyriform, with wide, short ostial extension, lamella antevaginalis strong, laterally rounded. Ductus bursae flattened, posterior part quadrangular, granulosely sclerotized, proximal part membranous with strong scobination and wrinkles, and cristate lamina at anterior edge. Appendix bursae subconical with rounded apical part, covered with finely sclerotized wrinkles, corpus bursae ovoid, hyaline with four long, narrow signum-stripes.

Bionomics and distribution. The new species inhabits semi-desert like open rocky grasslands in medium high and higher altitudes of the Karayalchi valley; all known specimens were collected at light.

Etymology. The specific name refers to the greenish-greyish forewing ground colour of the species.

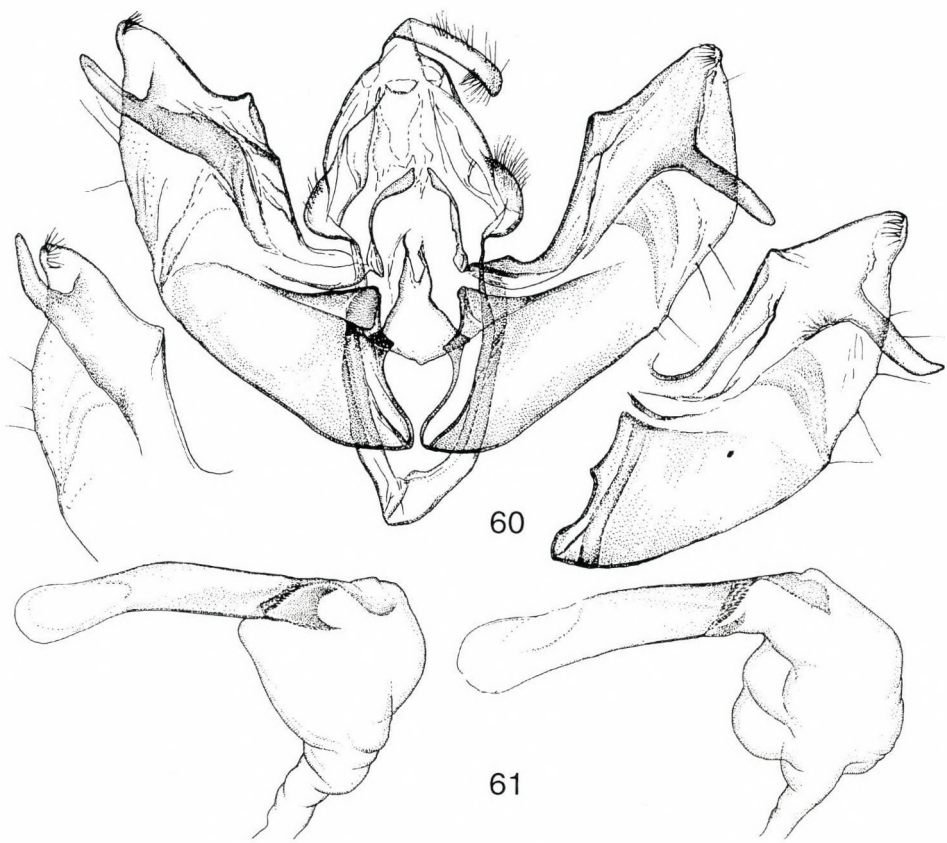

Figs 60–61. Male genitalia of *Polymixis schistochlora* sp. n., paratypes

Polymixis fabiani sp. n.
(Figs 33, 34, 64–66, 142)

Holotype: male, "Pakistan, Hindukush Mts, Shandur Pass, E slope, 3300 m, 72°38'E, 36°07'N, 29–31.VIII.1997, leg. Gy. Fábián & G. Ronkay" (Coll. GY. FÁBIÁN).

Paratypes. Pakistan: 7 males, 2 females, with the same data as the holotype; 2 males, 1 female, Karakoram Mts, Naltar valley, 2800 m, 74°12'E, 36°09,6'N, 11. and 18.X.1998, leg. GY. M. LÁSZLÓ and G. RONKAY (Coll. HNHM, GY. FÁBIÁN, P. GYULAI, G. RONKAY and Z. VARGA). Afghanistan: 1 male, Prov. Kunar, Nuristan, Lindai-Sin valley, vic. of Barg-e-Matal, 2200 m, 21.X.1970, leg. C. NAUMANN (Coll. NAUMANN, AKM Bonn).

Slide Nos RL5996, VZ4624 (males), RL6011 (female).

Diagnosis: The new species belongs to the *P. polymorpha* species-group, and is closely allied to *P. polymorpha*. *P. fabiani* is larger in size (wingspan of *P. fabiani* 40–45 mm, that of *P. polymorpha* 36–41 mm), the scaling is less reticulate, the wings are less glossy, the forewing pattern is more diffuse, the darker parts of wing, especially the basal area and the inner part of the marginal field are conspicuously darker, the crosslines are less distinct, and the subterminal is more sinuous with darker definition at inner side. The male genitalia of the two species

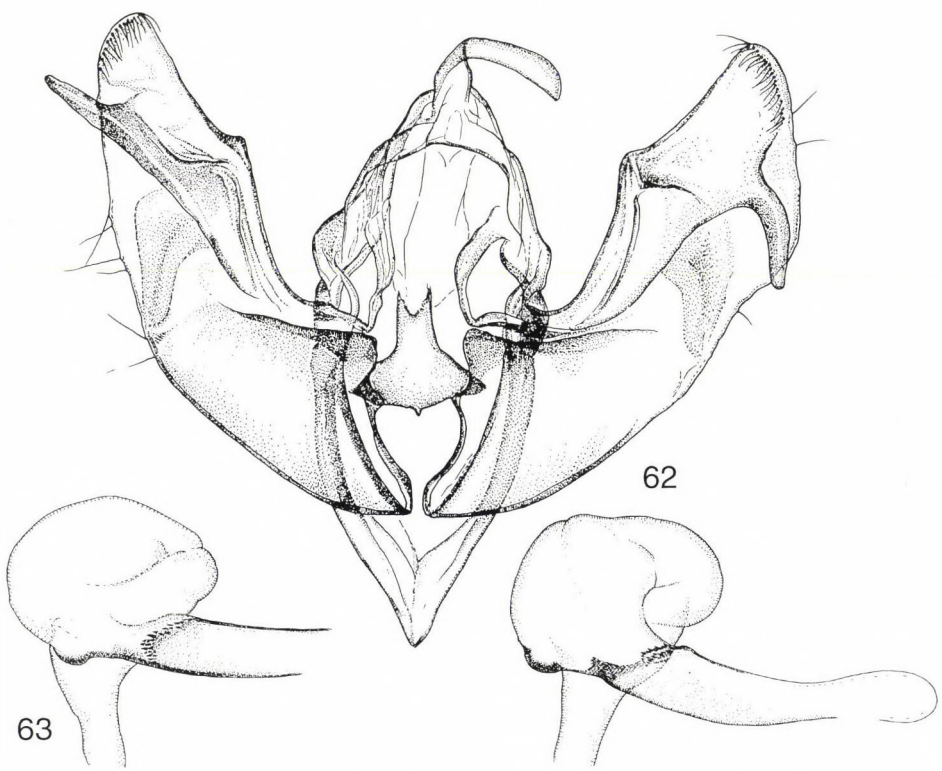

Figs 62–63. Male genitalia of *Polymixis zophodes* BOURSIN, holotype (clasping apparatus and left aedeagus) and paratype (right aedeagus)

are very similar, *P. fabiani* has a thicker uncus, larger costal lobes on both sides, broader basal plate of fultura inferior, longer right costal extension and stronger, more bifurcate dorso-lateral plate of the carina. The female genitalia of the two species differ in the shape of the ostium and the ductus bursae, the ostium is broader in *P. fabiani*, its ventral edge rounded triangular, without medial wave, the ductus bursae is somewhat longer, its sclerotization is stronger, and the right margin is folded, the distal end is conspicuously dilated at the right side forming a small postero-lateral lobe.

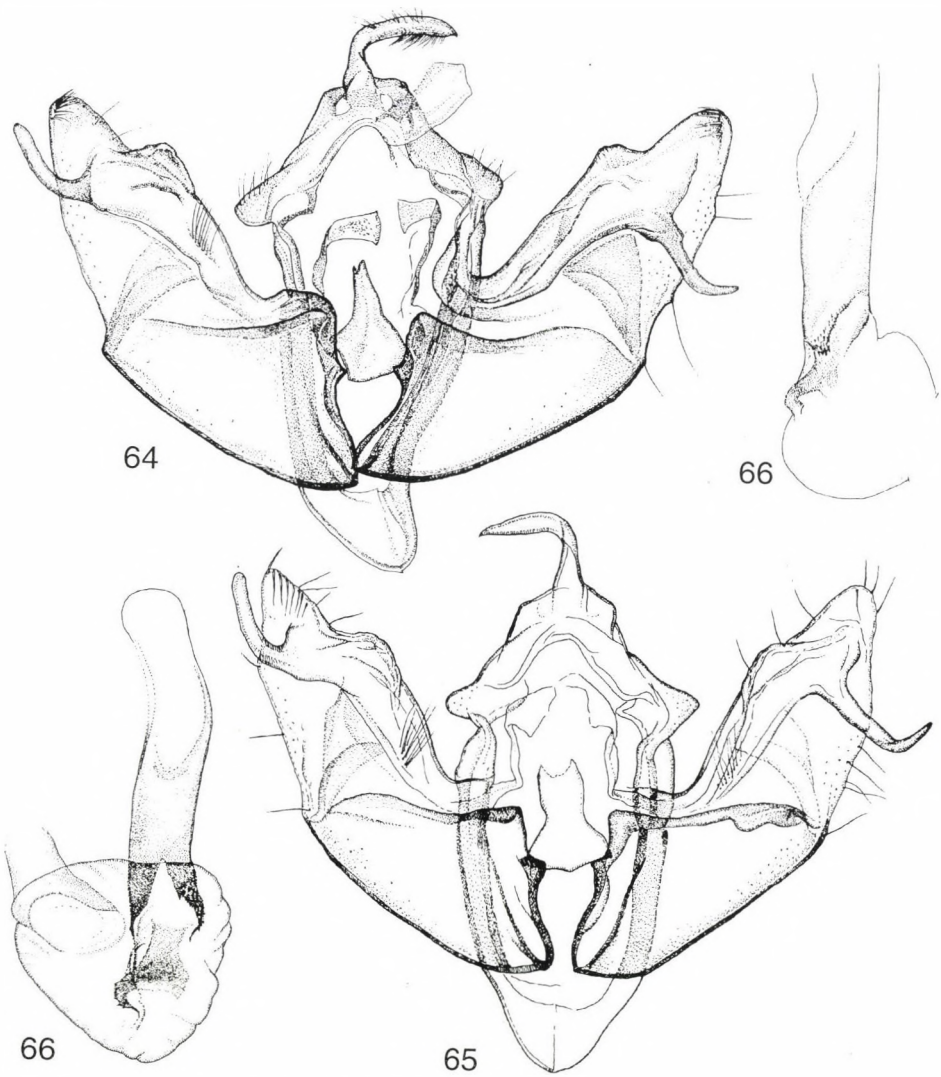

Figs 64–66. Male genitalia of *Polymixis fabiani* sp. n., paratypes

Description: Wingspan 40–45 mm, length of forewing 19–21 mm. Head and thorax ochreous grey mixed with dark olive-grey and yellowish, pubescence long, tegulae less distinct. Palpi short, porrect, covered laterally with dark brown hairs. Antenna of male ciliate with short fasciculate cilia, that of female filiform. Abdomen pale ochreous mixed with darker grey. Forewing elongate, narrow triangular with apex acute, ground colour shiny, dark olive-brown mixed with grey, variegated variably strongly with orange-ochreous and whitish. Wing pattern rather diffuse, ante- and postmedial crosslines double, often interrupted, dark brownish filled with ochreous, postmedial marked by some blackish spots on veins. Medial line shadow-like, strongest between orbicular and reniform stigmata. Orbicular and reniform stigmata large, orange-ochreous with a few olive-brownish spots, reniform often with narrow, lunulate, dark centre, outlines of both stigmata regularly missing; claviform absent. Subterminal strongly sinuous, ochreous-orange, inner half of marginal area dark olive-brownish, outer half irrorated strongly with ochreous and whitish scales. Terminal line fine, interrupted, dark grey, cilia orange-ochreous, spotted with grey-brown. Hindwing pale ochreous, marginal area scarcely (males) or rather strongly (females) irrorated with dark greyish brown. Veins dark, transverse line broad, diffuse, discal spot lunulate, pale but usually visible; cilia ochreous with fine, interrupted brownish inner line. Underside of wings milky ochreous with variably strong but usually weak greyish-brownish irroration. Traces of transverse lines most often present on both wings as blackish grey streaks on veins, discal spots small, diffuse.

Male genitalia (Figs 64–66): Uncus short, curved, distally slightly dilated with apex finely pointed, tegumen wide, low, penicular lobes elongate, apically rounded. Fultura inferior subdeltoidal, with terminally slightly incised apical extension, vinculum short but strong, V-shaped. Valvae asymmetrical, elongate, cucullus triangular with pointed apex, corona short, weak; subapical costal lobe wide, triangular, heavily sclerotized. Sacculus long, strong, clavus large, rounded triangular, partly folded lobe. Harpe reduced to flattened, arcuate, sclerotized basal plate. Costal extensions asymmetrical, left extension strong, curved at middle, distal part slender, with apex finely rounded; right extension as long as right harpe, basal and medial parts running parallel with harpe, terminal third curved upwards to apex. Aedeagus cylindrical, finely arcuate, carina with narrow, serrate ventro-lateral bar and significantly longer, larger, flattened, apically dilated dorsal plate having stronger apical hook. Vesica membranous, main part inflated, more or less globular, projected ventrally, distal part finely scobinate, recurved ventro-laterally, evenly tapering into ductus ejaculatorius.

Female genitalia (Fig. 142): Ovipositor medium-long, weak, papillae anales densely hairy; apophyses short, fine. Ostium bursae more or less triangular, broad with much narrower, lyriform dorsal plate having short V-shaped ostial extension, ventral plate heavily sclerotized, triangular, lamella antevaginalis laterally rounded. Ductus bursae flattened, posterior end strongly dilated, right margin folded, medial and distal parts strongly, granulosely sclerotized, proximal part membranous with strong scobination and wrinkles. Appendix bursae large, rounded, covered with finely sclerotized wrinkles, corpus bursae elliptical, membranous, with four long, narrow signum-stripes.

Bionomics and distribution. The new species occurs in the higher zones of the eastern Hindukush, known eastwards from the Paghman Mts where its area is partly overlapping that of its closest relative, *P. polymorpha*. The habitats are xerothermic, steep slopes vegetated with xerophilous *Juniperus* forests with diverse scrubs and grasslands.

Remarks. There are a few specimens from the central part of the Afghan Hindukush (Prov. Bamian: Band-e-Amir, Dasht-e-Nawar) with smaller size and much paler, shiny olive-ochreous forewings irrorated with darker olive-grey, the genitalia of which are closer to those of *P. fabiani* than to those of the typical populations of *P. polymorpha* (and its form *niviplaga* BOURSIN, 1960, syn. n.)

occurring in the eastern Hindukush (Paghman, Salang). The taxonomic interpretation of this (these) population requires further material.

Etymology. The new species is dedicated to Mr GY. FÁBIÁN, one of the discoverers of the new species.

Polymixis achrysa sp. n.
(Figs 36, 73, 77, 78, 146)

Holotype: male, "USSR, Turkmenia, Kopet-Dagh Mts., 400–600 m, Firyuza, 58°05'E, 37°59'N, 12.X.1991, No. L42, leg. A. Podlussány, L. Ronkay & Z. Varga" (Coll. HNHM).

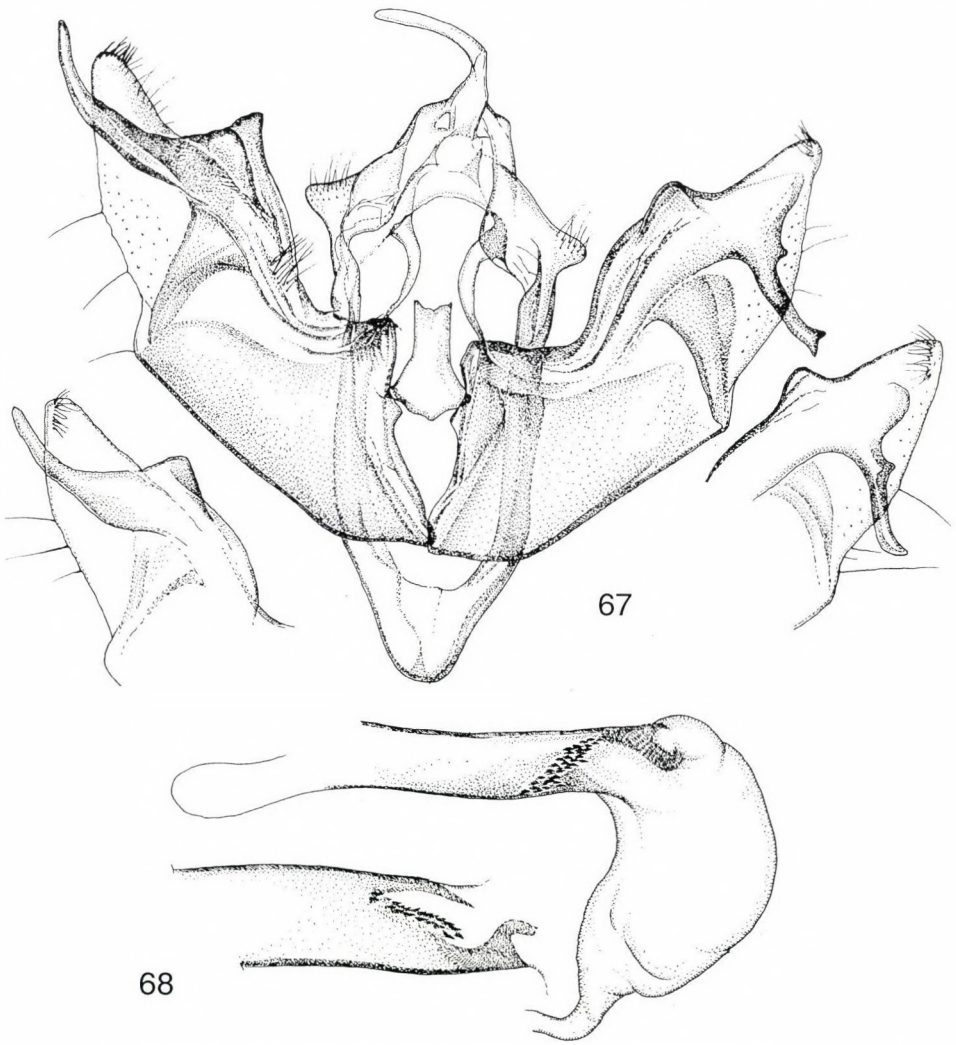

Figs 67–68. Male genitalia of *Polymixis polymorpha* BOURSIN

Paratypes. Turkmenistan: 4 males, Kopet-Dagh Mts, 1000 m, Kurkulab, 6 km W Germob, 03.X.1991, No. L34; 8 males, Kopet-Dagh Mts, 800 m, 20 km E of Nochur, Karayalchi valley, 57°12'E, 38°23'N, 04.X.1991, L35; 29 males, Kopet-Dagh Mts, 1600 m, 25 km E of Nochur, Karayalchi valley, 57°09'E, 38°21'N, 05.X.1991, L36; 12 males, 1 female, 400–600 m, Firyuza, 58°05'E, 37°59'N, 12–14.X.1991, L42, L. 44; 2 males, Kopet-Dagh Mts, 1300 m, Sayvan valley, cca 10 km N of Sayvan, 11.X.1991, No. L41; 1 male, Kopet-Dagh Mts, 700–800 m, 5 km S of Chuli, 58°01'E, 37°56'N, 30.09.1991, No. L32, leg. A. PODLUSSÁNY, L. RONKAY & Z. VARGA (Coll. HNHM, GY. FÁBIÁN, P. GYULAI, B. HERCZIG, M. HREBLAY, G. RONKAY and Z. VARGA).

Azerbaijan: 1 male, Nakhichevan, Dzhuga, Dzhulfa, Arax valley, 3.XI.1931, leg. RYABOV (Coll. NHM, Vienna).

Slide Nos: RL4205, RL4220 (males), RL4256 (female).

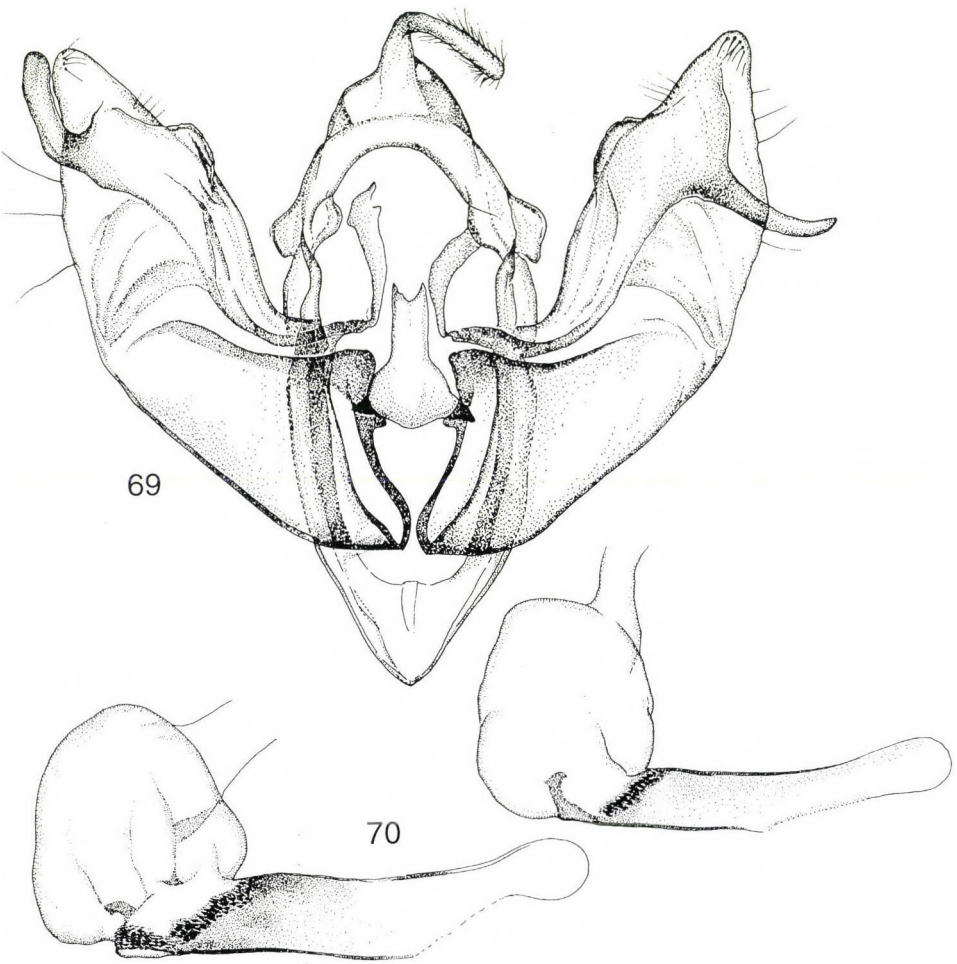

Figs 69–70. Male genitalia of *Polymixis pamiridia* BOURSIN.

Diagnosis: *P. achrysa* belongs to the *P. philippsi* (PÜNGELER, 1911) - *chrysographa* (WAGNER, 1931) species group, differing from the related taxa by a series of rather conspicuous external and some smaller but characteristic genital features: the forewing ground colour of the new species is darker, more unicolorous olive-grey without the ochreous-reddish irroration, which is typical of the other members of the group; the forewing pattern is more obsolescent, and the dark suffusion of the hindwing is stronger. The male genitalia of *P. achrysa* (Figs 73, 77–78) differ from those of *P. philippsi* (Figs 74, 79) by the more slender valva having almost parallel margins, stronger processi on outer margin of cucullus, broader clavus, stronger ampulla, significantly shorter eversible bar of carina armed with longer spines arranged into a more compact bundle, larger basal but smaller medial diverticula of vesica, terminal bundle of cornuti consisting of considerably shorter spinules. In the case of *P. perchrysa* HACKER et RONKAY, 1993 and *P. chrysographa* the valvae are narrower, apically more tapering, the cucullus is more elongate, less sclerotized with weaker or reduced medial process but with much stronger costal extension, the eversible bar of the carina is weak, bearing no spines, the tube of vesica is more simple with partly or fully reduced diverticula but much stronger terminal bundle of spinules, and has, in addition, one or two large, thorn-like cornuti. The female genitalia of the new species have broader, more sclerotized ostium bursae and posterior part of ductus bursae than those of *P. philippsi* where the ostium is longer, narrower, more calyculate, and the ventral plate has stronger scobination; the posterior part of ductus bursae is narrower with parallel margins in *P. philippsi*, broader, distally tapering in *P. achrysa*.

Description: Wingspan 34–36 mm, length of forewing 15–16 mm. Head and thorax dark olive-grey mixed with ochreous, pubescence long, more or less homogeneous. Palpi short, porrect, laterally darker grey, antenna of male shortly bipectinate, that of female filiform. Abdomen paler, ochreous grey, dorsal crest less conspicuous, consisting of small greyish tufts. Forewing rather short, broadly triangular with apex pointed, ground colour more or less concolorous dark olive-grey, basal and marginal areas with scarce whitish-greyish scales, ochreous irroration reduced or very weak. Wing pattern diffuse, ante- and postmedial crosslines shadow-like, dark greyish defined with a few whitish or ochreous scales. Medial and subterminal lines obsolete, latter usually marked by fine, interrupted whitish line and a few darker dots. Orbicular and reniform stigmata large, incompletely encircled by dark olive-grey, filled with pale olive-grey or whitish and ochreous; claviform absent. Terminal line fine, blackish grey, cilia ochreous, spotted with ground colour. Hindwing pale whitish grey, irrorated with dark greyish brown. Veins darker, transverse line and discal spot poorly visible or missing; cilia ochreous with grey-brownish stripe. Underside of wings greyish white with regular weak greyish-brownish irroration, traces of transverse lines and discal spots most often present on both wings.

Male genitalia (Figs 73, 77, 78): Uncus short, weak, finely hooked, tegumen broad, low, penicular lobes small, narrow, densely hairy. Fultura inferior big, shield-like with moderately wide apical incision, fultura superior with spiny lobes above it; vinculum short, more or less V-shaped with short apical spine. Valva elongate with almost parallel margins, costa heavily sclerotized; costal margin slightly curved and convex above ampulla, ventral margin finely arcuate. Cucullus well-developed, more or less triangular, sclerotized, densely setose; apex finely rounded, outer margin

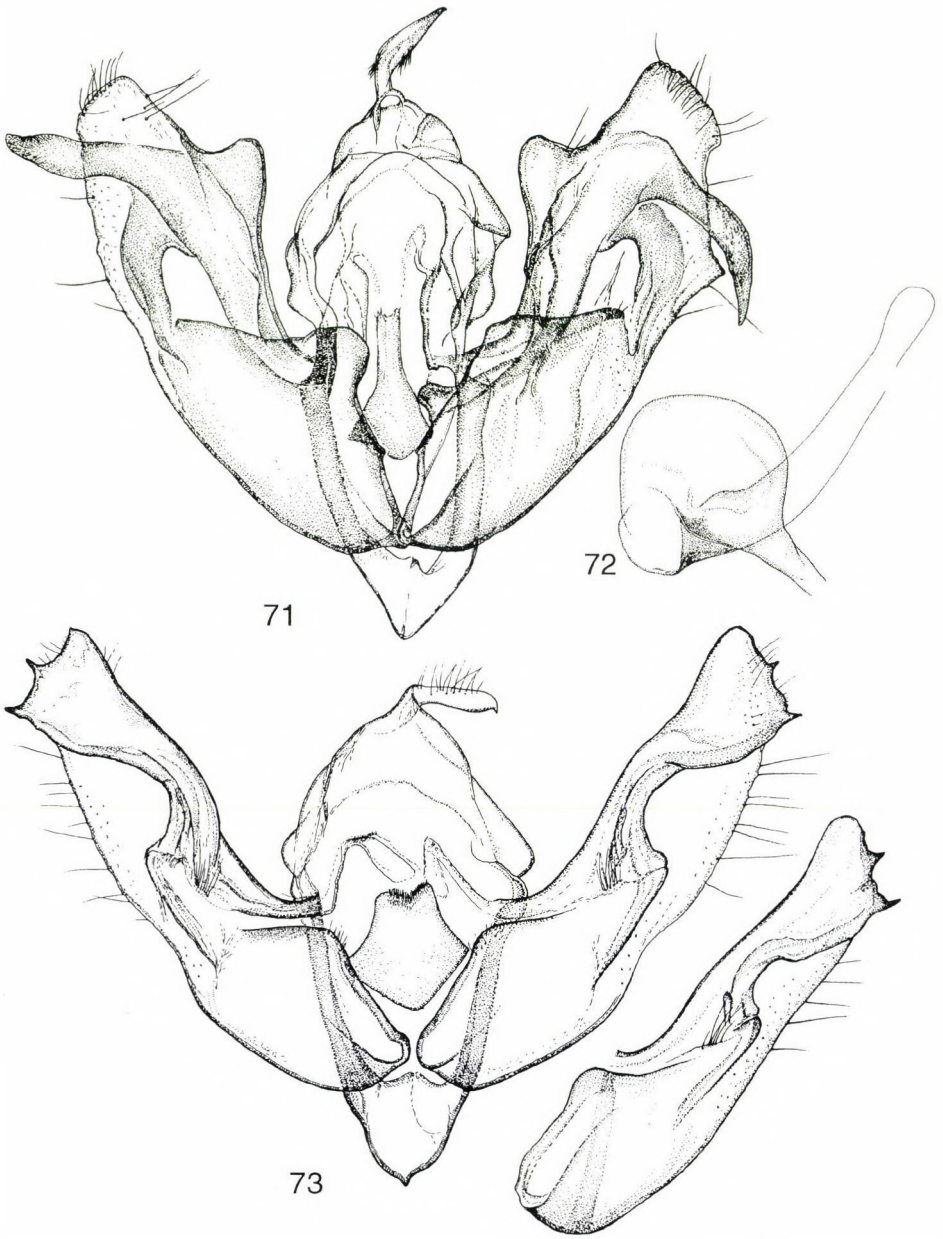

Figs 71–73. Male genitalia of *Polymixis* species. 71–72 = *P. stictineura* BOURSIN; 73 = *P. achrysa* sp. n., paratypes

with two short but strong, acute processi at middle and at ventral extremity. Sacculus short, rather weak, clavus rounded, finely setose. Harpe reduced to its narrow basal bar; ampulla slender, weak, digitiform, apically dilated, rounded. Costal extension heavily sclerotized, its ventral margin fused with cucullus. Aedeagus long, tubular, slightly curved at distal end. Carina with sclerotized ventral plate and long, eversible dorsal bar armed with bundle of long, strong, thorn-like spines. Vesica tubular, everted ventrally, basal third broader, armed with a few weak spiculi and an elongate distal diverticulum, medial third tubular, hyaline, distal third with relatively long, tubular terminal diverticulum and bundle of fine, long spinules at its base.

Female genitalia (Fig. 146): Ovipositor short, weak, papillae anales densely hairy; apophyses short. Ostium bursae short, relatively broadly trapezoidal, ventral plate shorter but broader, dorsal plate more elongate, narrower, both surfaces granulosely sclerotized. Ductus bursae rather long, posterior part narrow, flattened, sclerotized, its margins folded with stronger sclerotization. Medial part strongly dilated, discoidal, gelatinous-scobinated, with small, tubular diverticulum, anterior part narrow, tubular, membranous with fine wrinkles. Appendix bursae small, rounded conical, membranous, wrinkled, corpus bursae elongate-elliptical, weakly membranous, with short, narrow signum close to ductus bursae.

Bionomics and distribution. The typical populations of *P. achrysa* occur in the northernmost main chain of the Kopet-Dagh where the species may occur in high numbers; a few other specimens were found along the Arax valley, they have somewhat paler, more variegated forewing. The adults are on wing in the middle of the autumn.

Etymology. The specific name refers to the lack of the ochreous-reddish ("golden") irroration, present in the other taxa of the species-group.

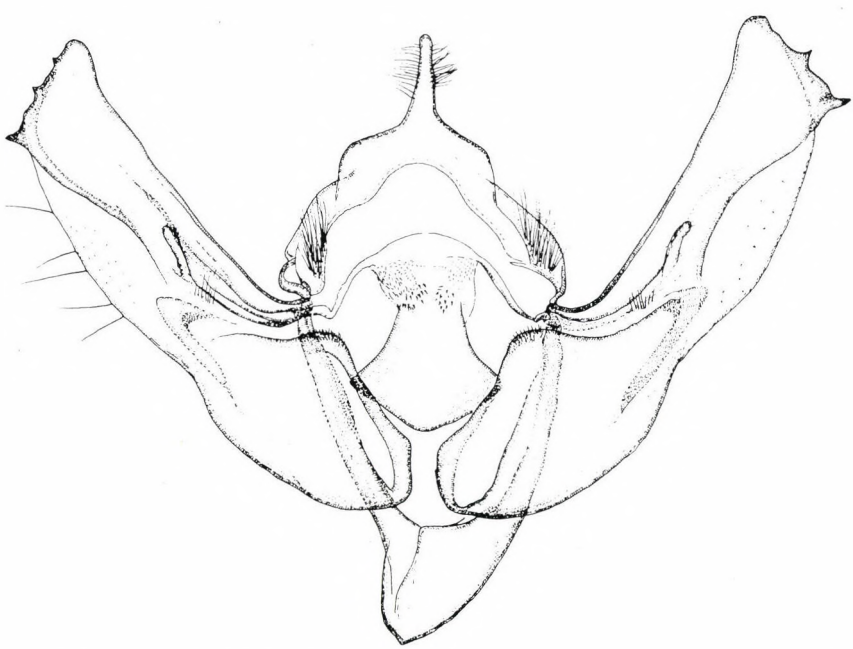

Fig. 74. Male genitalia of *P. philippsi* (PÜNGELER)

Polymixis csorbagabori sp. n.
(Figs 37, 75, 76, 148)

Holotype: male, "Turkey, Prov. Van, 2300 m, Kuzgunkiran Gecidi, 42°46'E, 38°17'N, 14.X.1989, leg. Ronkay and Csorba" (Coll. HNHM, donated by G. RONKAY).

Paratypes. Turkey: 1 female, with the same data as the holotype (HNHM); 5 males, from the same locality, 22.X.1992, leg. M. HREBLAY and G. RONKAY (Coll. M. HREBLAY and G. RONKAY). Armenia: 2 males, Garny, 1–9.X., 12–14.X.1992, leg. KAZARJAN (Coll. P. GYULAI).

Slide Nos: HM3701, RL6005, RL6097 (males), RL4254 (female).

Diagnosis: The SE Turkish and Armenian species, *P. csorbagabori* differs from the more unicolorous, greyish-olive southern Caspian – Transcaspian and Azeri *P. achrysa* populations by its more grey-brownish forewing ground colour and intense orange-yellowish irroration, especially along the crosslines and in the stigmata. The shape of the forewing is somewhat more elongate, higher with more acute apex and the pectination of the male antenna is also somewhat longer. In the male genitalia the valvae of *P. csorbagabori* are broader, more arcuate, and the cucullus has stronger triangular processi, resembling those of *P. philippsi*, the teeth of the carina and the diverticula of the vesica are larger. The configuration of the female genitalia is very similar, though the medial part of the ductus bursae is stronger, more sclerotized in *P. csorbagabori*.

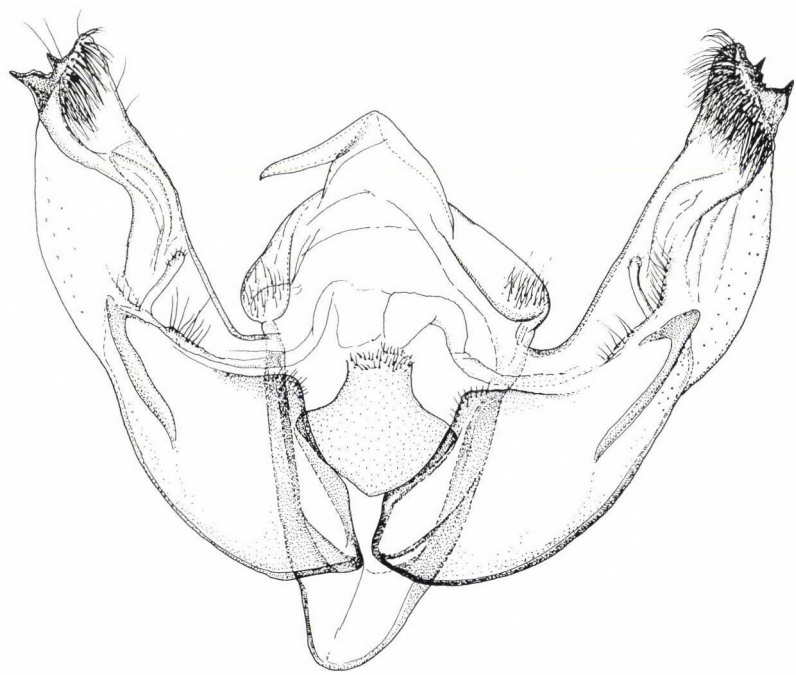

Fig. 75. Male genitalia of *P. csorbagabori* sp. n., paratype

Description: Wingspan 33–37 mm, length of forewing 15–17 mm. Head, thorax and forewing dark olive-grey mixed with orange-ochreous, abdomen whitish grey mixed with dark grey-brown. Antenna of male bipectinate with rather long branches, that of female filiform. Forewing elongate, broadly triangular with apex pointed, ground colour dark olive-brown, mixed with grey and ochreous-orange, especially in basal and marginal areas. Wing pattern diffuse, ante- and postmedial crosslines sinuous, dark grey-brown, defined with ochreous-orange, medial and subterminal lines poorly visible. Orbicular and reniform stigmata large, without sharper outlines, filled with greyish and orange-ochreous; claviform absent. Terminal line fine, brown-grey, cilia ochreous-orange, spotted with ground colour. Hindwing milky whitish, veins darker, marginal suffusion rather weak, dark greyish brown; transverse line and discal spot reduced, cilia orange with pale grey-brownish stripe. Underside of wings milky whitish, sparsely irrorated with darker greyish-brownish, traces of transverse lines and discal spots most often present as short streaks on veins.

Male genitalia (Figs 75, 76): Similar to those of *P. achrysa*. Fultura inferior sclerotized, shield-like with deep apical incision, spines of fultura superior rather strong. Valvae elongate with arcuate ventral margin, heavily sclerotized, almost straight costa and triangular, sclerotized cucullus with apex acute. Cucullus densely setose, outer margin with two relatively long, strong, acute processi at middle and at ventral extremity. Clavus narrower, more pointed, ampulla slightly stronger. Spines of carina longer, stronger, diverticula of vesica generally broader, larger, less tubular.

Female genitalia (Fig. 148): Similar to those of *P. achrysa*, ostium bursae somewhat longer, slightly more cup-shaped. Ductus bursae slightly more sclerotized, especially medial part, having stronger scobination and thicker, gelatinous-chitinous covering.

Bionomics and distribution. The three species of the *P. philippsi* group seemingly have an allopatric distribution, *P. philippsi* is known only from the vicinity of Sultanabad, *P. achrysa* occurs in the Kopet-Dagh and in the Arax valley while *P. csorbagabori* is found in the high mountains at the southern shore of the Lake Van and in a deep rocky gorge in Armenia, not far eastward from Yerevan.

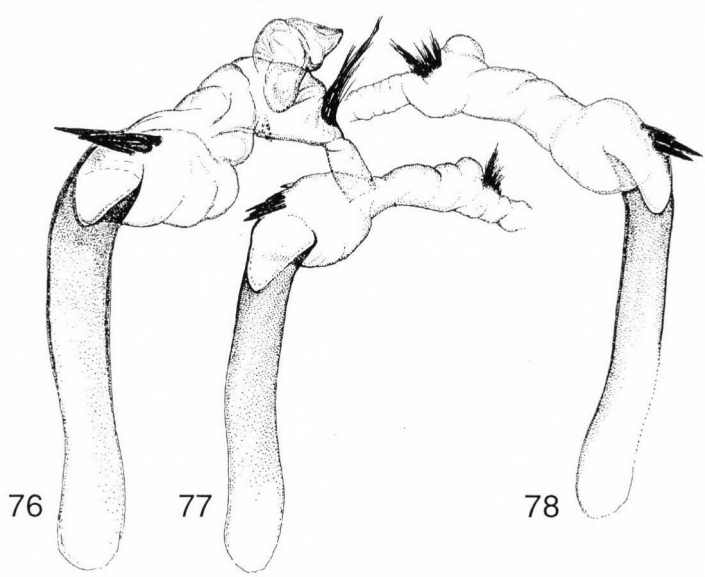

Figs 76–78. Male genitalia of *Polymixis* species. 76 = *P. csorbagabori* sp. n., paratype; 77–78 = *P. achrysa* sp. n., paratypes

Etymology. The new species is dedicated to Dr. GÁBOR CSORBA, a specialist of small mammals, a talented field worker, and discoverer of numerous new insect taxa.

Bornolis crinomima diluta ssp. n.
(Figs 38, 149–151)

Holotype: male, "USSR, Turkmenia, Kopet-Dagh Mts., 1600 m, 25 km E of Nochur, Karayalchi valley, 57°09'E, 38°21'N, 05.X.1991, No. L36, leg. A. Podlussány, L. Ronkay & Z. Varga" (Coll. HNHM).

Paratypes. Turkmenistan: a large series of both sexes from the following localities: Kopet-Dagh Mts, 1000 m, Kurkulab, 6 km W Germob, 03.X.1991, No. L34; Kopet-Dagh Mts, 800 m, 20 km E of Nochur, Karayalchi valley, 57°12'E, 38°23'N, 04.X.1991, No. L35; Kopet-Dagh Mts, 1600 m, 25 km E of Nochur, Karayalchi valley, 57°09'E, 38°21'N, 05.X.1991, No. L36; Kopet-Dagh Mts, 400–600 m, Firyuza, 58°05'E, 37°59'N, 12–14.X.1991, Nos L42, L43, L44; Kara-Kum desert, 100 m, 42 km N of Ashkhabad, 58°33'E, 38°21'N, 15.X.1991, No. L45, leg. A. PODLUSSÁNY, L. RONKAY & Z. VARGA; Kopet-Dagh Mts, 400–600 m, Firyuza, 58°05'E, 37°59'N, 8–13.XI.1991, No. L46; Kopet-Dagh Mts, 5 km S of Chuli, 700–800 m, 58°01'E, 37°56'N, 11.XI.1991, No. L47; 80 km SE of Tedjen, 200–300 m, 60°53'E, 36°56'N, 17.XI.1991, No. L50; 80 km SE of Serahs, 600 m, 61°28'E, 35°52'N, 19.XI.1991, No. L53, leg. M. HREBLAY & G. RONKAY; Kopet-Dagh, Kara-Kala, 20.X.-10.XI.1994, leg. MIATLEUSKI (Coll. HNHM, GY. FÁBIÁN, P. FASTRÉ, P. GYULAI, B. HERCZIG, J. PLANTE, G. RONKAY and Z. VARGA). Armenia: 1 male, Garny, 1–9–X.1992, leg. KAZARJAN (Coll. P. GYULAI). Turkey: 1 female, Prov. Van, Kuskunkiran, 22.X.1992, leg. M. HREBLAY and G. RONKAY (Coll. G. RONKAY).

Slide Nos RL5969, RL5971 (males), RL5970 (female).

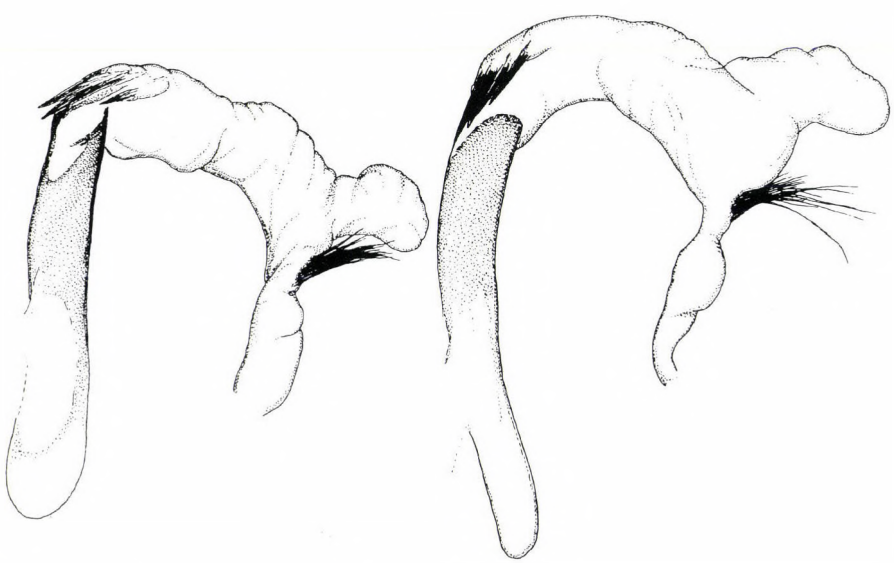

Fig. 79. Male genitalia of *Polymixis philippsi* (PÜNGELER)

Diagnosis: The populations inhabiting the Kopet-Dagh Mts and the southern coast of Lake Van have an intense pale ochreous-greyish suffusion in the costal and inner areas of the forewing which is darker, more unicolorous brownish in the typical *B. crinomima* (WILTSHIRE, 1946) population occurring in Farsistan. The genitalia show only slight differences in the shape and position of the subapical costal lobe and the asymmetrical costal extensions.

Description: Wingspan 45–47 mm, length of forewing 20–21 mm. Male. Head and thorax pale tobacco-brown mixed with whitish grey and blackish brown, frons somewhat paler ochreous, collar with sharp blackish line at middle; tegulae marked with dark grey-brown lines. Abdomen ochreous grey, dorsal crest well-developed, anal tuft ochreous. Forewing elongate, rather broadly triangular with apex acute, outer margin finely crenulate. Ground colour pale tobacco-brown, irrorated densely with ochreous-grey, especially in inner area and inner half of marginal field. Wing pattern sharply defined, blackish, ante- and postmedial crosslines simple, sinuous, defined with whitish, medial line diffuse, rather pale brown. Streak of submedian fold strong, long, black, basal area with an additional, shorter black line at inner margin. Orbicular and reniform stigmata sharply defined, blackish filled with ground colour and a little ochreous, claviform more or less rounded, fused partly with strong black stripe connecting antemedial and postmedial lines. Subterminal whitish-ochreous, strongly sinuous, less distinct, defined by blackish wedge-shaped marks and red-brownish patches often unified into long belt. Terminal line fine, blackish, with small dots between veins, cilia as ground colour, spotted with whitish. Hindwing shiny milky whitish, veins brownish,

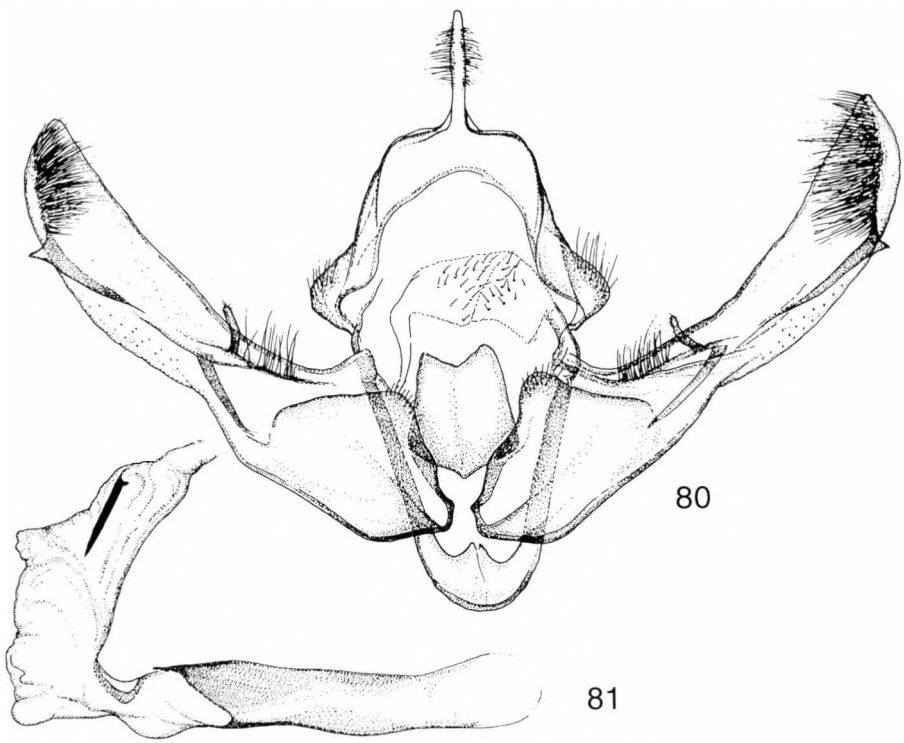

Figs 80–81. Male genitalia of *Polymixis chrysographa* (WAGNER)

marginal area diffuse, pale brownish, discal spot rather strong, small. Underside of wings ochreous-whitish with scarce brownish irroration, traces of transverse lines present, diffuse, discal spots strong, dark brown. Female. As male but smaller in size with forewing less elongate and acute, more unicolorous brownish with stronger red-brownish suffusion, hindwing essentially darker, fuscous, underside with stronger brown irroration.

Male genitalia (Figs 149, 150): Uncus medium-long, slender, curved at middle, apically slightly dilated. Tegumen high, rather narrow, penicular lobes large, more or less angular. Fultura inferior high, narrowly subdeltoidal with finely dilated apical end, vinculum strong but short, U-shaped. Valva large, more or less triangular, broad at base, apically strongly tapering, costa with large, pointed triangular subbasal lobe, cucullus triangular with apex acute, corona short, weak; sacculus very broad, sclerotized, clavi symmetrical, broadly digitiform, flattened processi projected medially; harpe reduced to its broad, flat, arcuate basal plate, costal extensions asymmetrical, smaller, more rounded on left valva, larger, ventral edge more elongate on right valva. Aedeagus long, tubular, arcuate, carina with two narrow, sclerotized dorso-lateral bars and large, triangular, curved ventral lamina terminated in small, triple-peaked tooth. Vesica tubular, everted forward, recurved ventrally, membranous with fine scobination, slightly dilated at main curve, tapering terminad.

Female genitalia (Fig. 151): Ovipositor rather long, conical, apophyses posteriores long, slender, anteriores short, fine. Ostium bursae broad, short, ventral lamina quadrangular, heavily sclerotized, dorsal lamina much narrower, weaker, with strong horizontal, dentate crest at middle. Ductus bursae long, flattened, heavily sclerotized, anterior end folded laterally, posterior end strongly dilated. Appendix bursae subconical, sclerotized, with strong, sclerotized wrinkles, corpus bursae rounded quadratic, membranous with four parallel signum stripes, one of them sinuous, separated into smaller patches.

Etymology. The subspecific name refers to the lighter forewing ground colour of the specimens.

Remarks. *Eremophysa jabaliya* WILTSHIRE, 1987 represents the southernmost subspecies of *B. crinomima*, differing from the other two races by its conspicuously darker wings. The genitalia of *jabaliya* display only small differences compared to those of *P. c. crinomima* and *P. c. diluta* [(*Bornolis crinomima jabaliya* (WILTSHIRE), 1987, stat. rev., comb. n.)].

Agrochola oropotamica archar ssp. n.
(Figs 39, 82, 83, 152)

Holotype: male, "USSR, Turkmenia, 80 km SE of Tedjen, 200–300 m, 60°53'E, 36°56'N, 17.XI.1991, No. L50, leg.: M. Hreblay & G. Ronkay" (Coll. G. RONKAY).

Paratypes. Turkmenistan: a series of about 250 specimens, with the same data as the holotype and from the following localities: Kopet-Dagh Mts, 400–600 m, Firyuza, 58°05'E, 37°59'N, 8–13.XI.1991, No. L46; Kopet-Dagh Mts, 5 km S of Chuli, 700–800 m, 58°01'E, 37°56'N, 11.XI.1991, No. L47; 20 km SE of Serahs, 400 m, 61°20'E, 36°22'N, 18.XI.1991, No. L52; 80 km SE of Serahs, 600 m, 61°28'E, 35°52'N, 19.XI.1991, No. L53, leg. M. HREBLAY & G. RONKAY (Coll. HNHM, GY. FÁBIÁN, P. GYULAI, B. HERCZIG, M. HREBLAY and G. RONKAY); 1 male, Firyuza, 27.X.1990, leg. DUBATOLOV (Coll. BIN); 2 specimens, Kopet-Dagh, Kara-Kala, Sumbar valley, 1.XI.1994, leg. MIATLEUSKI (Coll. P. FASTRÉ).

Slide Nos HM2915, HM2916, RL5977 (males), RL5978 (female).

Diagnosis: *A. oropotamica* (WILTSHIRE, 1941) is a species typical for the NW and SW Iranian mountainous regions, the subspecies *A. o. thermopotamica*

(WILTSHIRE, 1941) is known from Farsistan. The populations occurring in the Kopet-Dagh and in the southern lowlands of Turkmenistan descending to the Badhyz area differ from these subspecies by the generally lighter colouration with paler, less conspicuous forewing pattern. In the male genitalia, the harpe is larger, and the lateral projection is larger, more angulate than in the other subspecies (see BOURSIN 1956, Fig. 4).

Description: Wingspan 31–34 mm, length of forewing 14–16 mm. Male. Head and thorax pale orange-brown or ochreous brown mixed with pale greyish and dark brown, pubescence rather homogeneous; antenna shortly ciliate. Abdomen darker greyish, dorsal crest reduced. Forewing elongate, narrow, with apex pointed, ground colour pale ochreous-brown or orange-brown (sometimes pale greyish) with fine pinkish-orange shade and scarce brownish grey irroration. Wing pattern pale, rather indistinct, ante- and postmedial crosslines double, sinuous, marked with a few dark brown scales, filled with ochreous, medial line diffuse greyish stripe. Orbicular and reniform stigmata encircled with ochreous, former small, often flattened, latter narrow, high, slightly constricted at middle; both stigmata filled with greyish brown, that of reniform regularly much darker, darkest element of pattern. Subterminal interrupted, pale ochreous, defined by small, variably strong, dark grey or blackish dots. Terminal line ochreous, cilia as ground colour. Hindwing shiny whitish ochreous, veins darker, costal area weakly irrorated with brownish, marginal suffusion reduced to a few brownish scales. Discal spot and transverse line most often poorly visible. Terminal line diffuse, greyish, cilia ochreous. Underside shiny whitish or ochreous with weak brownish irroration, discal spots present on both wings, regularly much stronger on forewing, transverse line usually obsolete. Female. As male, antenna filiform, forewing shorter, abdomen darker brownish grey, and hindwing with somewhat stronger dark greyish irroration.

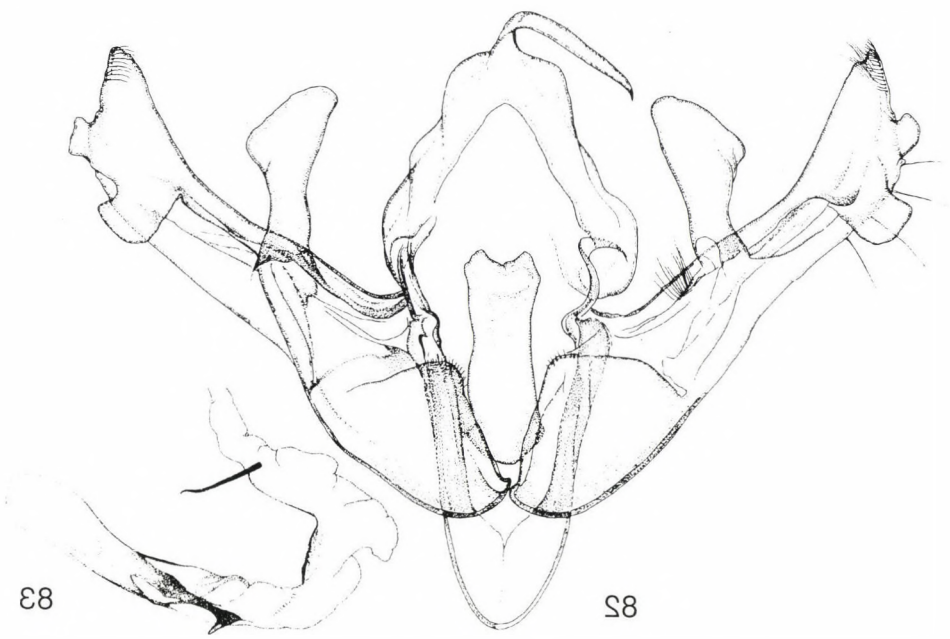

Figs 82–83. Male genitalia of *Agrochola oropotamica archar* ssp. n., paratype

Male genitalia (Figs 82, 83): Uncus short, slender, finely hooked, tegumen moderately high, penicular lobes relatively large, elliptical. Fultura inferior large, high and narrowly quadrangular, dorsal part with two low but strong pyramidoid extensions; vinculum short but strong, more or less V-shaped. Valva elongate, tapering, finely curved below apex, costa heavily sclerotized. Cucullus triangular with apex acute, corona short, weak. Sacculus short, strong, clavus less prominent, rounded, setose lobe. Basal bar of harpe short, strong, erected part very strong, flattened, distal part dilated, with triangular lateral lobe. Costal extension double-peaked, apical one much shorter, both extensions more or less quadratic. Aedeagus long, cylindrical, slightly arcuate, carina with stronger dorsal plate and heavily sclerotized, medially twisted, long ventral extension armed with two strong, cuneate thorns. Vesica rather complex, broadly tubular, membranous with variably strong scobination; proximal part narrow, curved ventro-laterally, having long, narrow field of numerous short spinules; distal part slightly dilated, with medial and two terminal, semiglobular diverticula, as well as long, stick-like, finely arcuate terminal cornutus and small spinulose field at base of terminal cornutus.

Female genitalia (Fig. 152): Ovipositor very long, acute, apophyses slender, very long. Ostium bursae broad but short, calyculate with heavily sclerotized, broad caudal ring. Ductus bursae long, flattened, caudally dilated, both surfaces with strong granulation arranged into two, partly folded ribbons, one of them extending into base of appendix bursae. Appendix bursae large, lateral, rounded, membranous with broad, medial sclerotized area. Corpus bursae rounded quadratic, membranous, with three small, weak signum-plates.

Agrochola turcomanica sp. n.
(Figs 40, 84, 85, 153)

Holotype: male, "USSR, Turkmenia, Kopet-Dagh Mts., 1300 m, Sayvan valley, cca 10 km N of Sayvan, 56°52'E, 38°25'N, 11.X.1991, No. L41, leg. A. Podlussány, L. Ronkay & Z. Varga", slide No. RL4065 (Coll. HNHM).

Paratypes. Turkmenistan: 1 male, with the same data as the holotype (HNHM); 1 female, Kopet-Dagh Mts, 400–600 m, Firyuza, 58°05'E, 37°59'N, 8–13.XI.1991, No. L46; 1 male, 1 female, Kopet-Dagh Mts, 15 km SE of Nochur, 1300–1400 m, 57°09'E, 38°21'N, 13–14.XI.1991, No. L49, leg. M. HREBLAY & G. RONKAY (Coll. M. HREBLAY and G. RONKAY); 1 male, Firyuza, 30.X.1990, leg. DUBATOLOV (HNHM); 21 specimens, Kopet-Dagh, Kara-Kala, Sumbar valley, 1.XI.1994, leg. MIATLEUSKI (Coll. P. FASTRÉ).

Slide Nos RL5980 (male), RL6001 (female).

Diagnosis: The new species represents the easternmost known member of the *A. litura* (LINNAEUS, 1761) species group, the closest relatives are *A. luteogrisea* WARREN, 1911 and *A. sairtana* DERRA, 1990, both occurring in Turkey. *A. turcomanica* differs from the related species by its more unicolorous brownish forewing ground colour, but otherwise the external appearance of the taxa of the group is very uniform with partly overlapping variation, and the study of the genitalia is necessary for the separation of the species. The male genitalia of the four species are very similar, *A. turcomanica* has almost straight valva with the apical third not at all or only very slightly arcuate, while those of *A. litura* and *A. luteogrisea* are clearly arcuate, and in the new species the dentition of the costal plate is the strongest, and the harpe is the longest. The shape of the fultura inferior is also different in these three species: *A. turcomanica* has the basal plate

transversally rather narrow with broader, terminally less dilated dorsal extension, since the basal plate is broader in *A. litura* and *A. luteogrisea*, and the apical extension is narrower. The terminal cornutus of the vesica is the longest, and the curved tubular diverticulum of the distal tube strongest in *A. turcomanica*. *A. sairtana* has the shortest terminal cornutus within the species group, the valva is broader and the harpe is thicker than those of the related taxa.

The female genitalia of the new species has the most deeply calyculate plate of ostium bursae and the strongest and highest sclerotized lateral pocket within the four species under discussion; the shape of the corpus bursae is characteristically quadratic.

Description: Wingspan 32–33 mm, length of forewing 15mm. Head and thorax dark ochreous brown mixed with paler grey and red-brown, frons and metathorax paler, more ochreous-greyish. Antenna filiform in both sexes. Abdomen slightly paler, more brownish, dorsal crest weak, consisting of small, darker brown tufts. Forewing narrow, elongate, apex pointed, outer margin evenly arcuate. Ground colour dark ochreous brown, irrorated with reddish brown, ochreous grey and some dark brown. Crosslines less distinct, ante- and postmedial lines sinuous, double, often interrupted, brown-grey filled with pale ochreous grey, defined with darker red-brown. Medial line diffuse, reddish brown shadow, forming larger, darker patch between orbicular and reniform stigmata. Orbicular oblique, slightly flattened, reniform elliptical, relatively narrow, both encircled

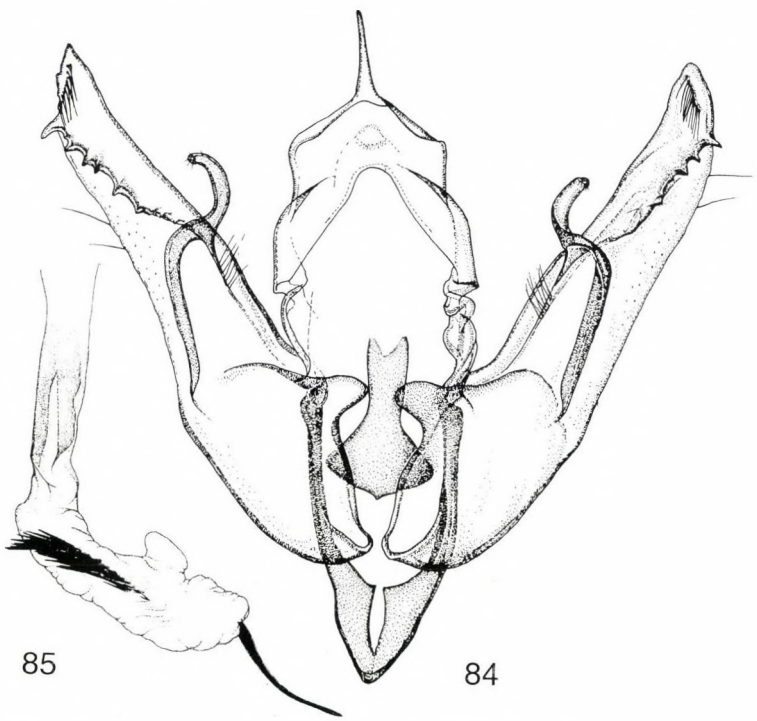

Figs 84–85. Male genitalia of *Agrochola turcomanica* sp. n., holotype

with fine ochreous and red-brownish rings, filled with ground colour and some darker grey-brown, lower half of reniform regularly plumbeous grey; claviform missing. Subterminal obsolescent, ochreous, slightly sinuous, defined by two sharp black costal spots and a few tiny blackish dots between veins. Terminal line fine, brown, cilia as ground colour, spotted with ochreous. Hindwing strongly suffused with dark brown, veins and marginal area somewhat darker, terminal line brown, cilia ochreous with brown medial line. Underside of wings pale ochreous-greyish, inner area of forewing strongly suffused, apical part of forewing and hindwing densely irrorated with dark greyish brown. Discal spots and traces of transverse lines present, rather diffuse.

Male genitalia (Figs 84, 85): Uncus very short, slender, finely hooked, tegumen small, quadrangular with small, narrow penicular lobes. Fultura inferior large, subdeltoidal with high dorsal process, incised weakly at apex; vinculum short but strong, V-shaped. Valva elongate, evenly tapering to apex, costa heavily sclerotized. Cucullus short, triangular, with acute apex, corona short, rather weak. Sacculus short, strong, clavus rather long, rounded triangular, densely setose, directed medially. Basal bar of harpe long, slender, erected part short, arcuate with finely setose tip. Costal extension heavily sclerotized, ventral margin serrate with four-five teeth, terminal one longer than others. Aedeagus long, cylindrical, slightly arcuate, carina with stronger ventral plate. Vesica broadly tubular, membranous with variably strong scobination; basal part narrow, with long, subconical, apically twisted diverticulum, distal two-third dilated, armed with long ventral field of cornuti consisting of strong spines, big, curved tubular-subconical diverticulum dorso-laterally and very long, sword-like, arcuate terminal cornutus.

Female genitalia (Fig. 153): Ovipositor very long, acute, apophyses slender, very long. Ostium bursae calyculate with heavily sclerotized, arcuate ventral plate. Ductus bursae rather short, broad, flattened, slightly tapering caudally, both surfaces partly sclerotized, junction to corpus bursae with stronger scobination. Appendix bursae large, situated laterally, heavily sclerotized, folded, apically rounded pocket, continued as long, broad zone with weaker sclerotization in corpus bursae, terminated as a rounded conical, heavily sclerotized lobe. Corpus bursae quadratic, membranous with fine scobination and with three small but strong signum-plates.

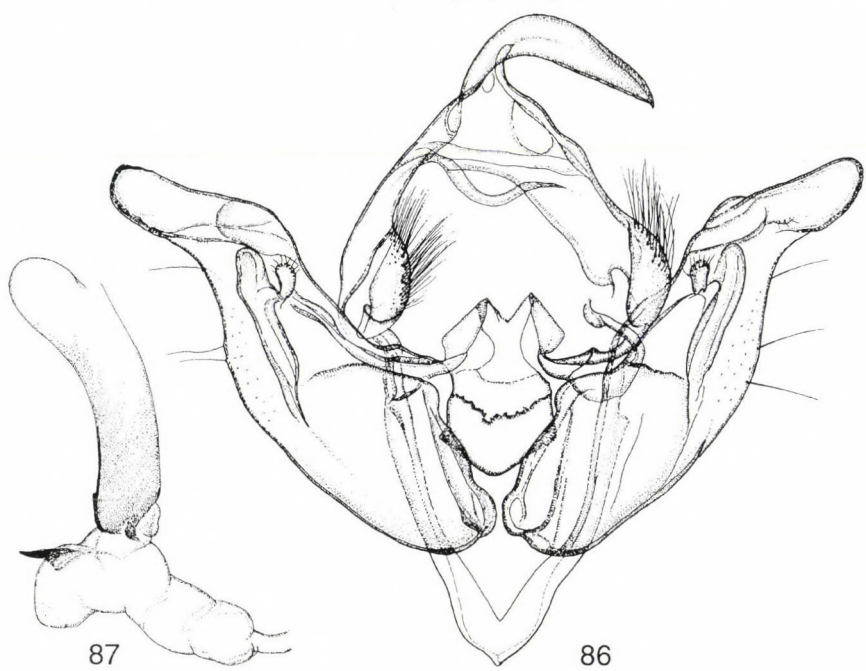

Figs 86–87. Male genitalia of *Gortyna roseago* sp. n., holotype

Bionomics and distribution. The new species occurs in the central part of the northern chain of the Kopet-Dagh Mts. Its habitats are open forest edges, xerothermic slopes with mosaics of scrubs and rocky grassland patches at medium high altitudes.

Etymology. The specific name refers to the homeland of the species.

Cryphia basivittata sp. n.
(Figs 41, 154, 155)

Holotype: male, "Turkmenistan, Kopet-Dagh Mts, Dushak Mt., 57°54'E, 37°57'N, 2400 m, 9–10.VIII.1992, No. L70, leg. M. Hreblay, Gy. László and G. Ronkay", slide No. RL4650 (Coll. HNHM, donated by G. RONKAY).

Paratypes: 2 males, with the same data as the holotype (Coll. M. HREBLAY and G. RONKAY).

Diagnosis: The new species belongs to the *C. plumbeola* (STAUDINGER, 1881) – *C. salomonis* BOURSIN, 1954 species group, representing an isolated taxon, being rather remote from all known relatives. It differs from the other species of the group by its characteristic, sharply defined (ochreous-)white basal streak, narrower, more acute forewing and darker greyish brown hindwing. The male genitalia differ from those of the related taxa (illustrated by BOURSIN 1954, Figs 6–13; HERCZIG *et al.* 1991 – *C. uzahovi* RONKAY et HERCZIG, 1991) by its rather short, broad valva with stronger, thicker harpe and the minute cornutus of the vesica.

Description: Wingspan 25 mm, length of forewing 11 mm. Head small, frons ochreous white, vertex, collar and thorax covered with whitish hair-scales, mixed with dark greenish grey, antenna finely ciliate. Forewing narrow, elongate with apex more or less acute, scaling rather granulose. Ground colour whitish ochreous, basal and marginal areas irrorated, median field suffused with dark bluish-greenish grey. Basal area wide, submedian fold with sharply defined ochreous-white streak, ante- and postmedial lines sinuous, dark grey, defined with whitish scaling, medial fascia obsolete. Orbicular and reniform stigmata indistinct, darker greyish patches with very pale, interrupted outlines. Marginal area rather concolorous, subterminal deleted, terminal line fine, dark brown, cilia whitish, chequered with brownish grey. Basal part of hindwing whitish, other parts strongly suffused with dark greyish brown, discal spot a slightly darker shadow, cilia ochreous white. Underside of wings shiny ochreous white, forewing and marginal area of hindwing intensely irrorated with grey-brown. Transverse lines obsolete, discal spots of both wings rather strong, rounded, dark brown. Female unknown.

Male genitalia (Figs 154–155): Uncus relatively short, flattened, with strong apical hook, tegumen moderately high, penicular lobes narrow, fultura inferior subdeltoidal with wide apical part and weak medial incision, fultura superior arcuate ribbon; vinculum short but strong, more or less V-shaped. Valva elongate, slightly constricted at middle, distal half dilated medially, then tapering apically. Cucullus short, with apex acute, corona reduced. Sacculus broad, rather short, harpe long, heavily sclerotized, arcuate with acute tip. Aedeagus short, cylindrical, carina with slightly stronger ventral plate. Vesica short, membranous, scobinate at base, medial part inflated, subsphaerical, with small diverticulum projected dorsally, bearing fine, small, acute spine, distal tube directed ventrally.


89

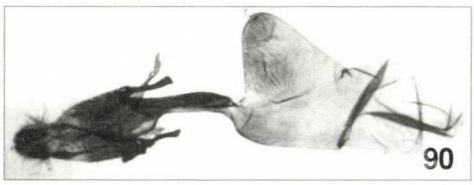
90

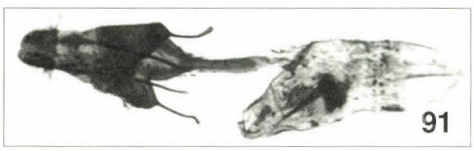
91

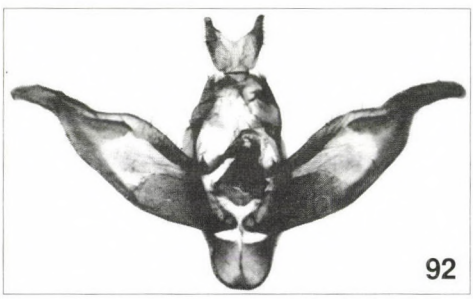
92

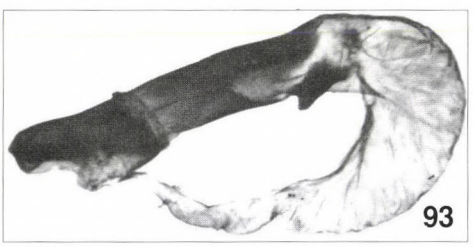
93

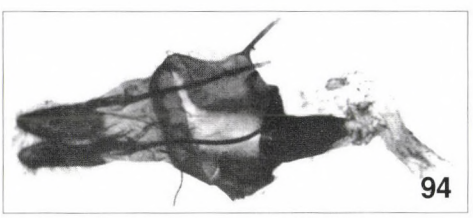
94

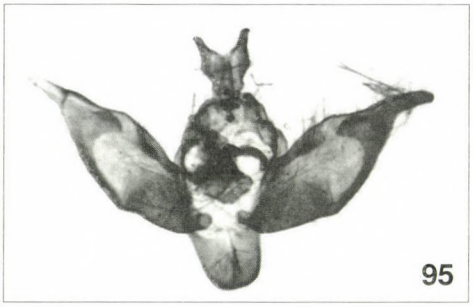
95

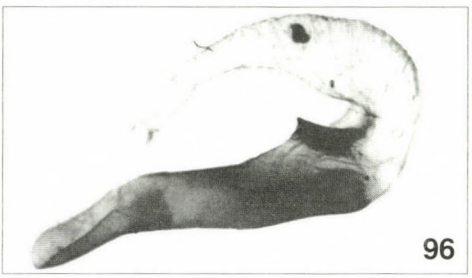
96

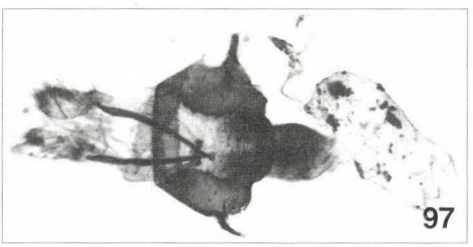
97

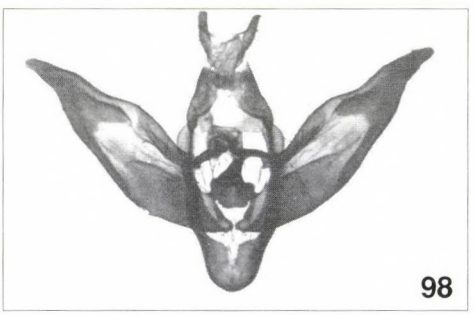
98

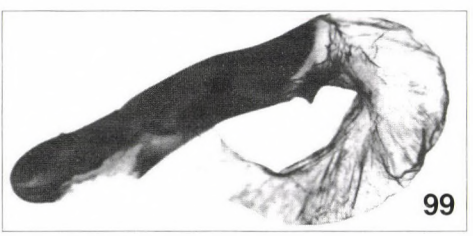
99

Bionomics and distribution. The species is known from the high limestone plateau of the Dushak Mts, with scarce *Juniperus* forest patches and calciphilous, xeric oreal plants (e.g. scrub polsters of *Acantholimon*, *Ephedra*, etc.).

Etymology. The specific name refers to the white subbasal streak of the forewing.

Cryphia duskeimima sp. n.
(Figs 42, 43, 156, 157)

Holotype: male, Turkmenistan, Kopet-Dagh Mts, 6 km S of Ipay-Kala, 1600 m, 57°07'E, 38°17'N, 16–23.VIII.1992, No. L74, leg. M. Hreblay, Gy. László and G. Ronkay", slide No. HM10458 (Coll. M. HREBLAY).

Paratypes. Turkmenistan: a large series of specimens with the same data as the holotype (HNHM, Coll. GY. FÁBIÁN, P. GYULAI, B. HERCZIG, M. HREBLAY and G. RONKAY); 1 male, Kopet-Dagh Mts, Dushak, 25.VIII.1988, leg. DUBATOLOV (BIN); 2 males, W Kopet-Dagh, Sunt-Khasardagh, southern foothills of Mt Sunt, 9.X.1996, leg. O. TARGONJA (Coll. H. HACKER and Z. KLYUCHKO); 2 males, from the same locality, 5-13.X.1996 (Coll. BISCHOF).

Slide Nos HACKER 10705, 10708, RL4122 (males).

Diagnosis: *C. duskeimima* is also a member of the *C. plumbeola* – *C. salomonis* species group. It differs from the related taxa by its narrower forewing with rather obsolescent pattern, and without stronger light markings. The most characteristic feature of the male genitalia is the strongly dentate, sclerotized collar-like basal plate of the vesica, in addition the valva is shorter, the distal part is narrower than those of the related taxa and the harpe is the strongest and longest within the species group.

Description: Wingspan 26–29 mm, length of forewing 14–15 mm. Head and thorax dark greenish grey mixed with whitish scales. Antenna of male finely ciliate, that of female filiform. Abdomen slender, long, paler brownish grey, dorsal crest represented by a few very small dark tufts. Forewing long, narrow, apex pointed, scaling finely reticulate. Ground colour dark metallic grey with fine bluish-greenish shine, strongly irrorated with whitish grey. Wing pattern rather diffuse, ante- and postmedial lines sinuous, whitish defined with fine dark grey lines, often with some blackish patches below cell, medial line obsolete or completely missing. Orbicular and reniform stigmata indistinct, former rather large, rounded, encircled with whitish, filled with darker greyish, reniform diffuse whitish grey patch with very pale, interrupted outline and relatively strong, fine, blackish grey inner line or lunule. Marginal area narrow, subterminal whitish grey, fine, sinuous, more or less interrupted. Terminal line row of fine blackish spots, cilia as ground colour, striolate with whitish at outer half. Hindwing suffused with dark greyish brown, veins even darker, discal spot often visible as diffuse, shadow-like dot, cilia pale greyish. Underside of wings whitish, forewing strongly suffused with brownish grey, marginal area of hindwing with darker brownish irroration. Transverse lines missing or very pale, discal spot of hindwing regularly present, rounded, that of forewing absent or poorly visible lunule.

Figs 89–99. Genitalia figures. 89–90 = *Euxoa sayvana* sp. n., paratypes; 91 = *E. temera* (HÜBNER); 92–94 = *Eicomorpha antiqua*; 95–97 = *E. kurdestanica*; 98–99 = *E. koeppeni*

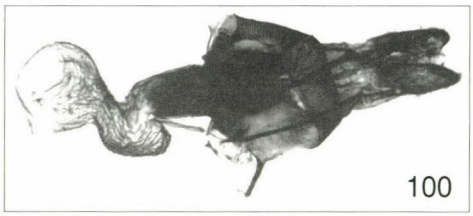

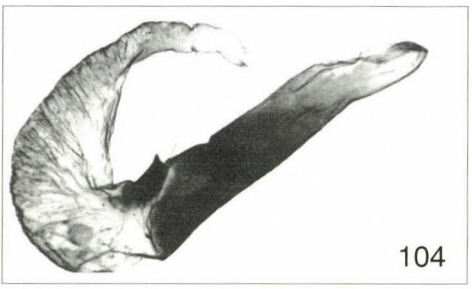

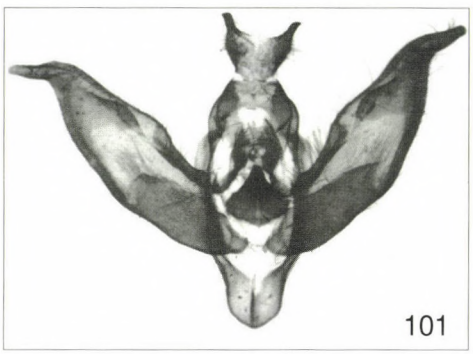

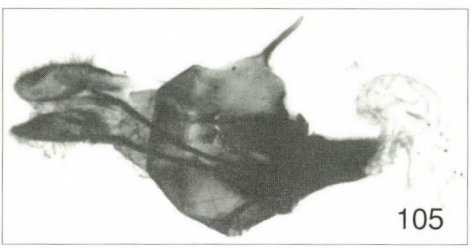

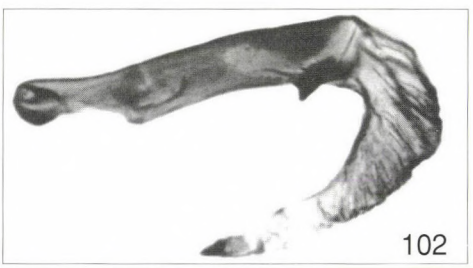

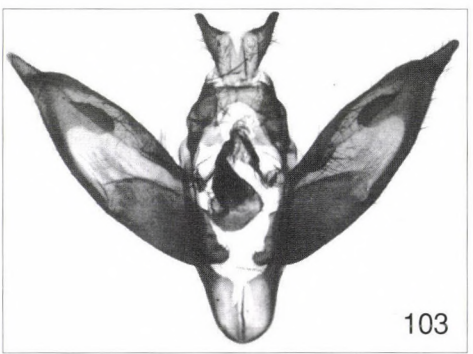

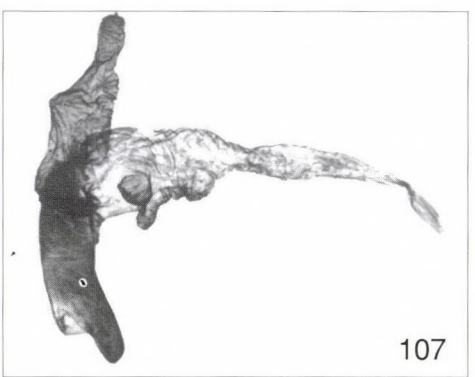

Figs 100–107. Genitalia figures. 101–102 = *E. epipsilioides*; 103–105 = *E. firyuza* sp. n., 103–104 = holotype, 105 = paratype; 106–107 = *Periphanes delphinii tekke* ssp. n., holotype

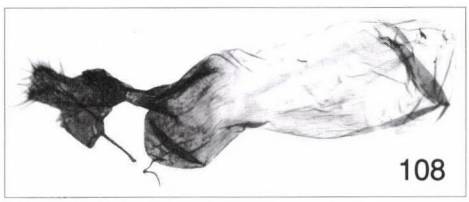

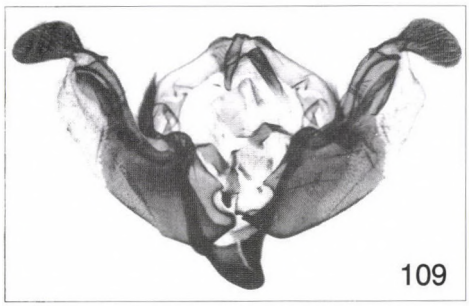

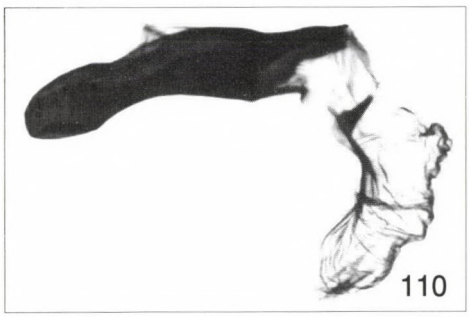

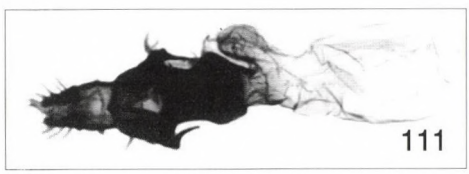

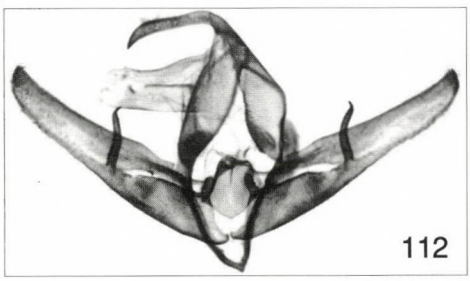

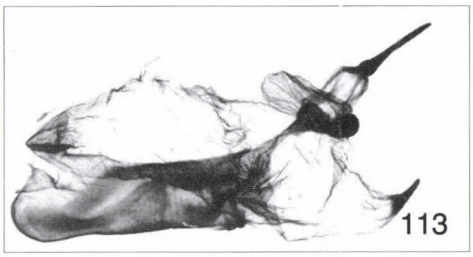

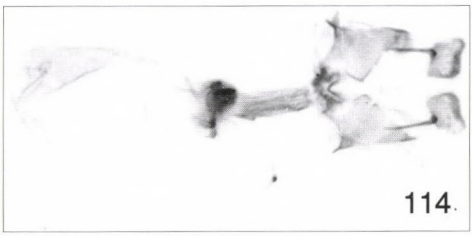

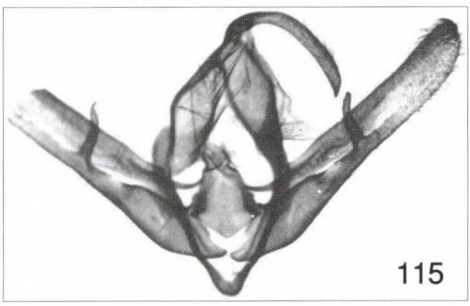

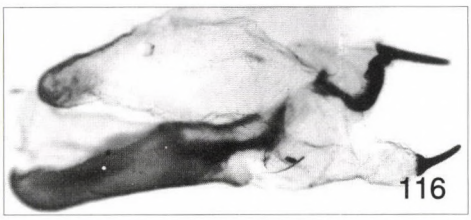

Figs 108–117. Genitalia figures. 108 = *Periphanes delphinii tekke* ssp. n., paratype; 109–111 = *Conisania vidua eupepla* ssp. n., paratypes; 112–114 = *Cucullia petrophila* sp. n., paratypes; 115–117 = *Cucullia xerophila* sp. n., 115–116 = holotype, 117 = paratype

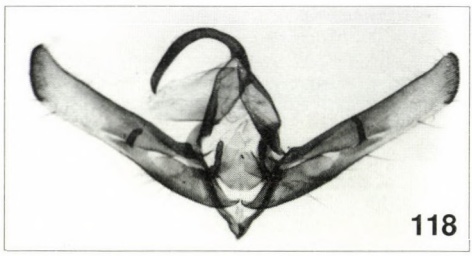

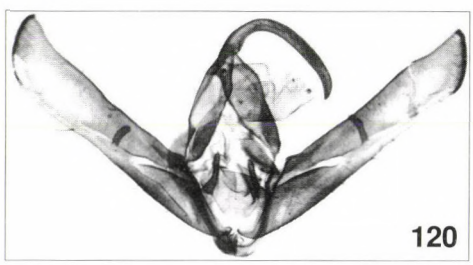

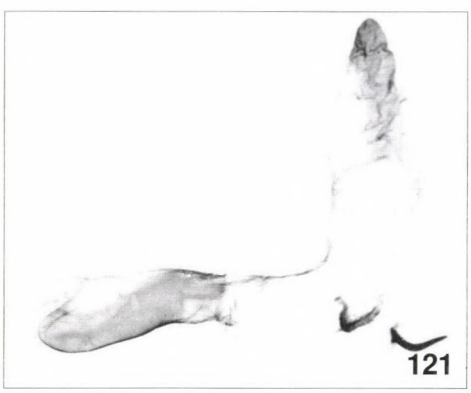

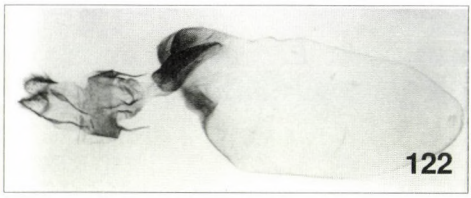

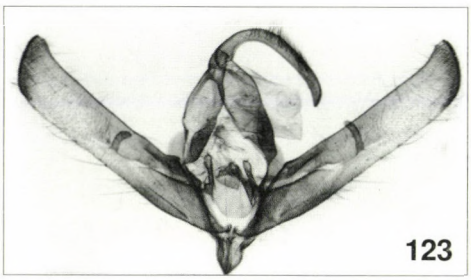

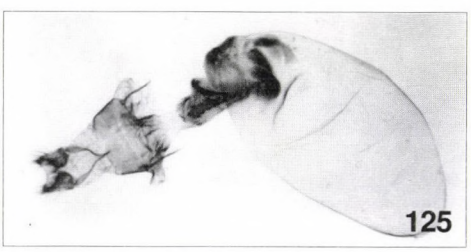

Figs 118–125. Genitalia figures. 118–122 = *Cucullia apo* sp. n., paratypes; 123–125 = *C. heinickei* BOURSIN

Male genitalia (Figs 156, 157): Uncus relatively long, curved at base, slightly concave at middle, apically finely hooked. Tegumen high, penicular lobes narrow, long, fultura inferior deltoidal, wide, rather low, sclerotized, fultura superior regular, fine, arcuate plate; vinculum short but strong, U-shaped. Valva medium-long, narrow, apically tapering, slightly constricted at base of harpe. Cucullus sclerotized, narrow, with apex acute, corona missing. Sacculus long, sclerotized, with small, setose depression at place of clavus. Harpe very long, falcate, broad, flattened at base; tip pointed. Aedeagus short, thick, carina with slightly stronger ventral plate. Vesica short, tubular, basal third with large, broad, sclerotized half-ring covered with strong spinules, medial third slightly dilated, with small, membranous diverticulum and short but thick spine with large, conical base, and distal third turned ventrally, membranous, finely scobinate.

Gortyna roseago sp. n.
(Figs 44, 86, 87)

Holotype: male, "Turkmenija, Kara-Kala, Ai-Dere, 1987. 10. 10, P. Ivinskis", slide No. RL4416 (ZM Copenhagen).

Paratypes. Turkmenistan: 1 male, with the same data as the holotype (Coll. J. NOWACKI, Poznan); 2 males, from the same locality, 14.X.1981, leg. V. V. DUBATOLOV (BIN, Novosibirsk); 1 male, Kopet-Dagh, 45 km E of Kara-Kala, 2-3.X.1996, leg. O. TARGONJA (Coll. Z. KLYUCHKO); 1 specimen, Kopet-Dagh, Kara-Kala, 20.X.-10.XI.1994, leg. MIATLEUSKI (Coll. P. FASTRÉ).

Slide Nos HACKER 10709, RL3440, RL3480 (males).

Diagnosis: *Gortyna roseago* is the sister species of *G. cervago* (EVERSMANN, 1844), and is known only from the south-western chains of the Kopet-Dagh Mts. The two species are often very similar externally, the three specimens of *G. roseago* are almost identical in colouration while *G. cervago* has a wide range of variation in colour and intensity of pattern. The colouration of the new species is less contrasting, more pastel-like, the crosslines are finer, the antemedial is more evenly sinuous, the stigmata are clearer, the hindwing is paler, without darker irroration, and the veins are also lighter. The male genitalia of the two sibling species are similar, although the new species has a more elongate, apically less curved valva with narrower, more elongate and apically pointed cucullus, and a somewhat broader, apically less incised fultura inferior; the aedeagus is slightly longer, and the basal part of cornutus is smaller, less conical.

Description: Wingspan 43–45 mm, length of forewing 20–21mm. Male. Head and thorax pale reddish brown mixed with ochreous, collar and tegulae less distinct. Antenna shortly bipectinate. Abdomen more ochreous, dorsal crest present, less conspicuous. Forewing relatively broadly triangular, with apex pointed, ground colour pale reddish brown with fine pinkish shade, basal third and marginal area strongly suffused, medial field sparsely irrorated with ochreous. Basal, ante- and postmedial crosslines sinuous, simple, red-brown defined with whitish, subterminal diffuse, waved ochreous line defined by darker red-brownish inner zone. Medial area more or less triangular, constricted below cell, darkest part of wing. Orbicular small, rounded, reniform narrow, lunulate, both stigmata encircled with red-brown, filled with whitish-ochreous. Terminal line fine, continuous, reddish brown, cilia as ground colour, spotted with ochreous. Hindwing shiny milky white, veins slightly darker, ochreous-brownish, cilia pure white. Underside of wings whitish-ochreous with

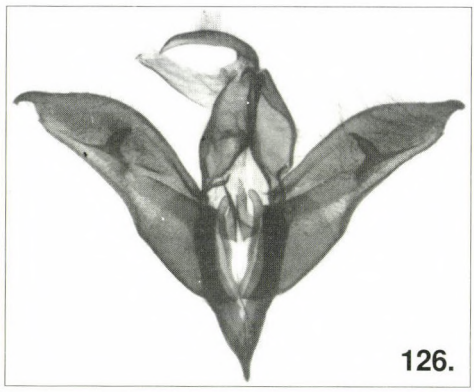

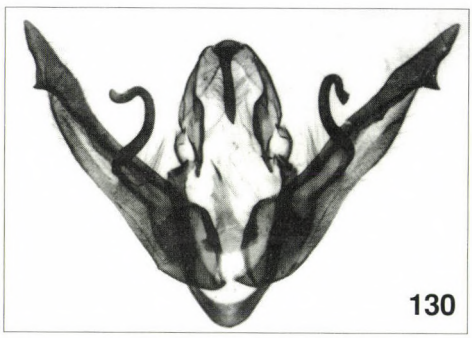

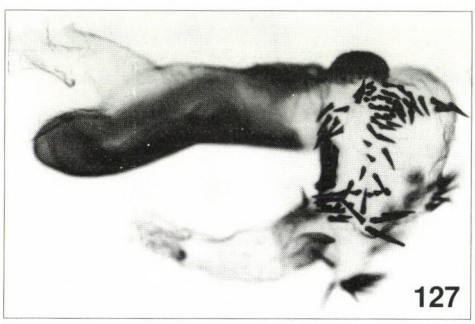

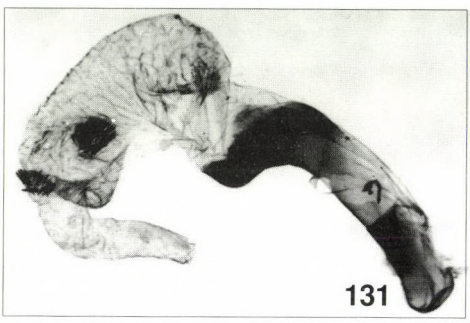

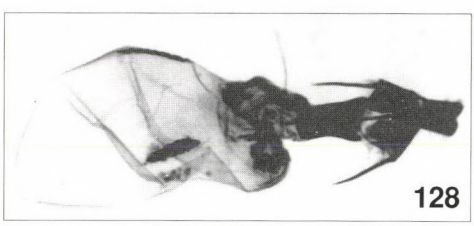

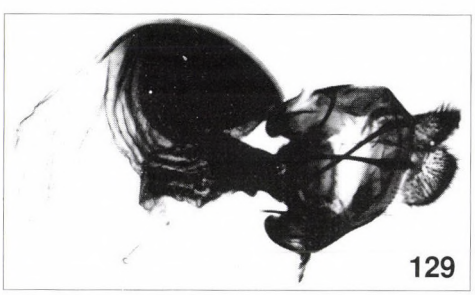

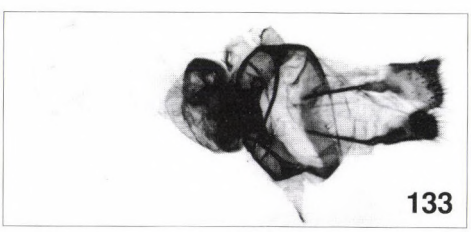

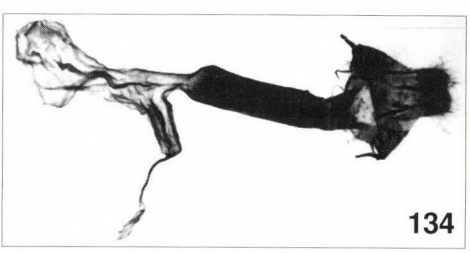

Figs 126–134. Genitalia figures. 126–128 = *Omphalophana turcomana* sp. n., paratypes; 129 = *Allophyes sericina* sp. n., paratype; 130–132 = *Lithophane alaina* BOURSIN; 133 = *Episema minutoides* sp. n., paratype; 134 = *Dasypolia nebulosa* sp. n., paratype

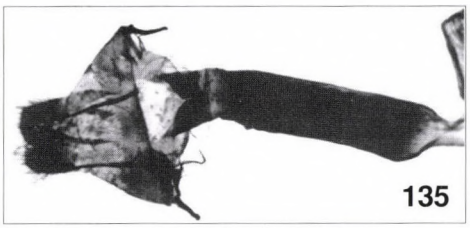

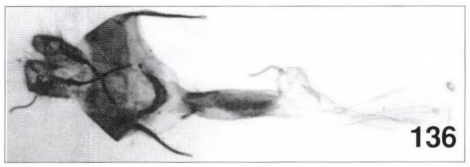

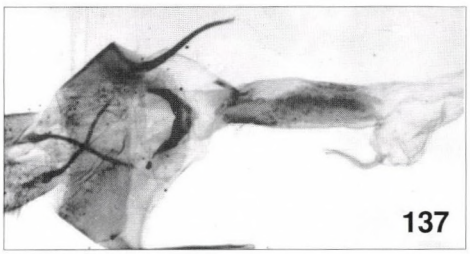

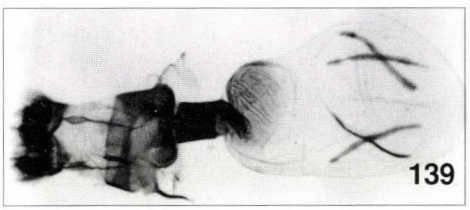

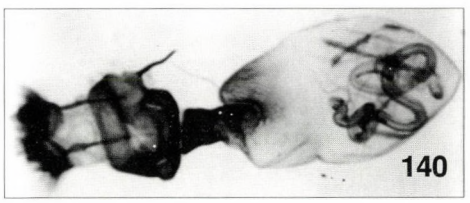

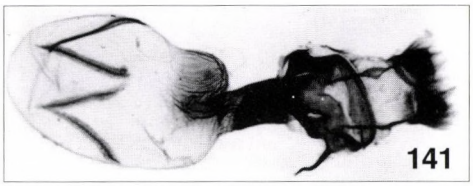

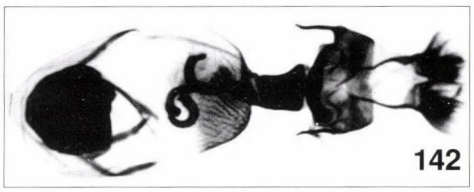

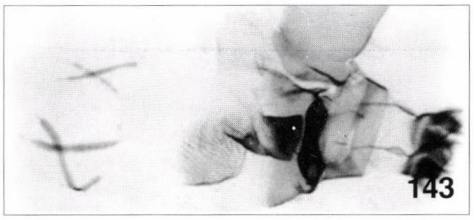

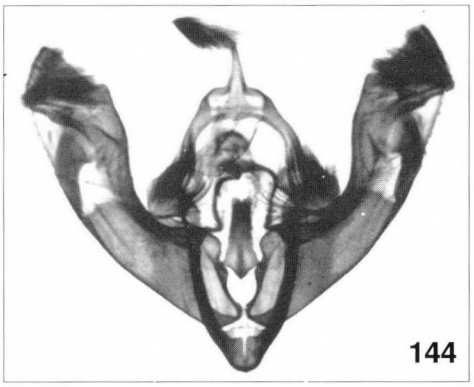

Figs 135–145. Genitalia figures. 135 = *Dasypolia nebulosa* sp. n., paratype; 136–137 = *D. ipaykala* sp. n., holotype; 138 = *Polymixis pericaspicus* sp. n., paratype; 139 = *P. schistochlora* sp. n., paratype; 140 = *P. zophodes* BOURSIN; 141= *P. pamiridia* BOURSIN; 142 = *P. fabiani* sp. n., paratype; 143 = *P. polymorpha* BOURSIN; 144–145 = *P. juditha* (STAUDINGER)

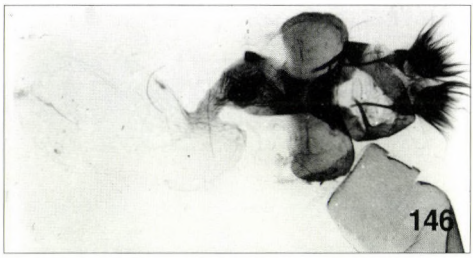

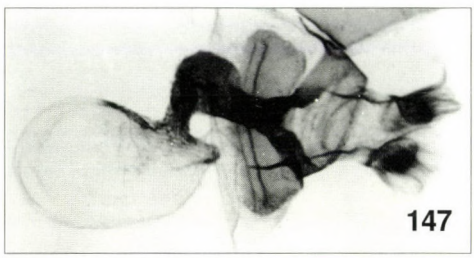

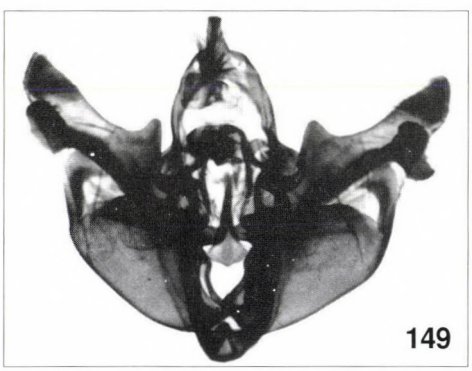

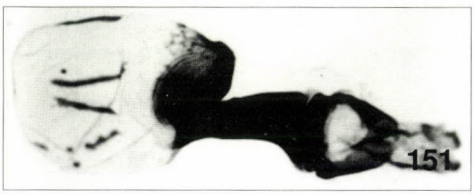

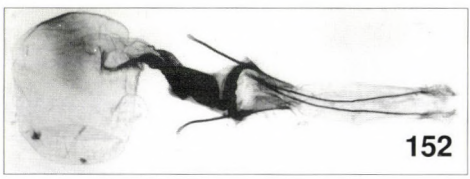

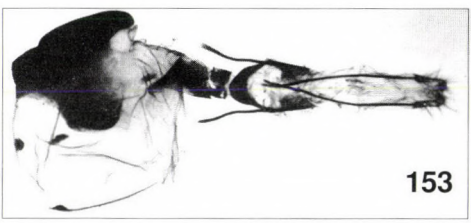

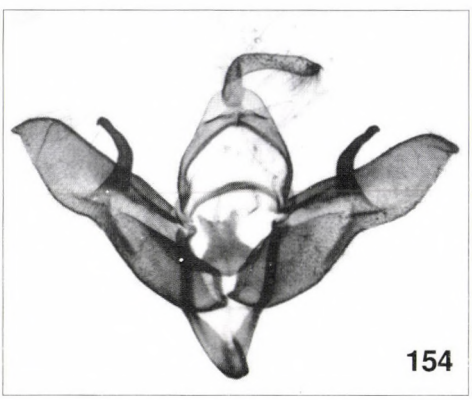

Figs 146–154. Genitalia figures. 146 = *Polymixis achrysa* sp. n., paratype; 147 = *P. philippsi* (PÜNGELER); 148 = *P. csorbagabori* sp. n., paratype; 149–151 = *Bornolis crinomima diluta* ssp. n., paratypes; 152 = *Agrochola oropotamica archar* ssp. n., paratype; 153 = *A. turcomanica* sp. n., paratype; 154 = *Cryphia basivittata* sp. n., holotype

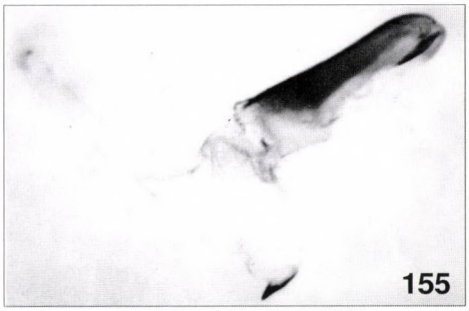

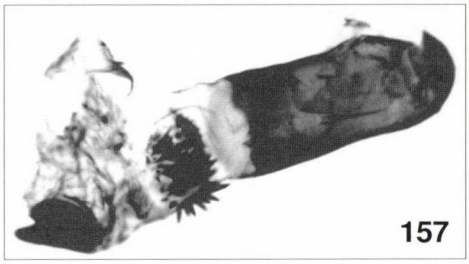

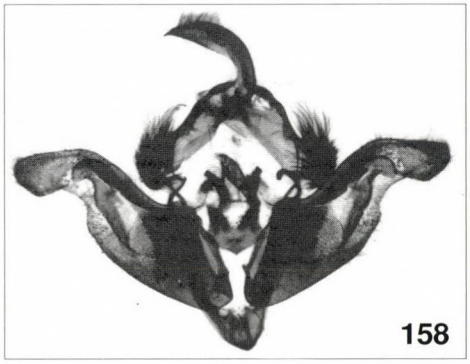

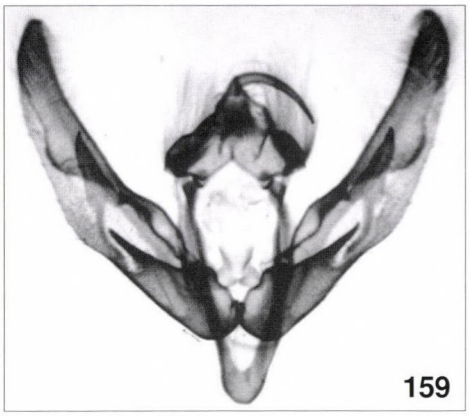

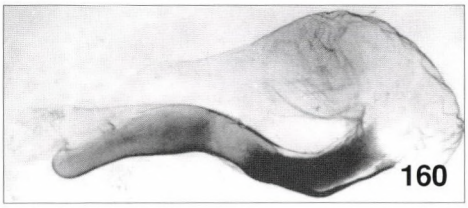

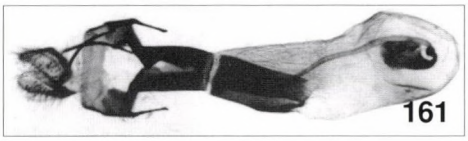

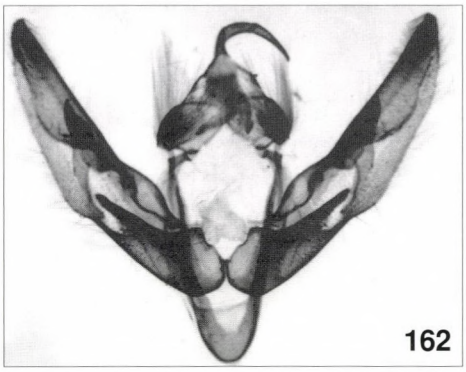

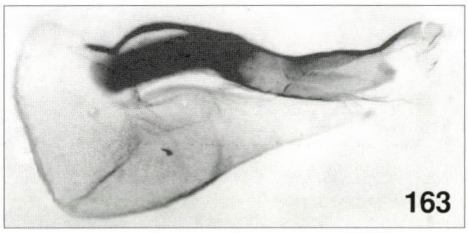

Figs 155–163. Genitalia figures. 155 = *Cryphia basivittata* sp. n., holotype; 156–157 = *Cryphia duskeimima* sp. n., holotype; 158 = *Gortyna cervago* (EVERSMANN); 159–161 = *Chilodes repeteki* sp. n., 159–160 = paratype, 161 = holotype; 162–163 = *C. distracta* (EVERSMANN)

weak red-brownish irroration, especially in medial and apical parts of forewing and costal area of hindwing, traces of orbicular and reniform stigmata well discernible. Female unknown.

Male genitalia (Figs 86, 87): Uncus medium-long, strong, curved, apical third slightly flattened, apex finely hooked. Tegumen broad, penicular lobes large, densely hairy. Fultura inferior sclerotized, relatively big, pentagonal with wide, rounded dorsal incision; vinculum short, strong, V-shaped. Valva elongate, distal part rather strongly tapering, curved before cucullus. Cucullus small, narrow triangular, setose, apex finely rounded. Sacculus big, rounded, clavus small, rounded, sparsely setose hump. Basal plate of harpe long, wide, flat, erected part small, mushroom-shaped, twisted at base, costal process ("ampulla") much larger, flattened, apically slightly dilated with apex rounded; pulvillus long, narrow, sclerotized, with long, fine setae. Aedeagus medium-long, cylindrical, arcuate, carina with small, serrate ventral and broader, less sclerotized, dentate plate. Vesica broadly tubular, everted forward, upturned dorsally. Basal part membranous, with rounded, weakly scobinate ventral diverticulum, bearing strong, wide-based, acute spine, upturned part narrower, apically tapering, medial third with strong scobination.

Distribution. The new species is known from the vicinity of Kara-Kala only.

Etymology. The specific name refers to the pinkish hue of the forewing.

Chilodes repeteki sp. n.
(Figs 45, 159–161)

Holotype: female, "USSR, Turkmenia, Kara-Kum desert, 200 m, 20 km SW of Repetek, 63°09'E, 38°25'N, 9.V.1991, No. L17, leg. G. Csorba, Gy. Fábián, B. Herczig, M. Hreblay & G. Ronkay", slide No. RL4570 (Coll. HNHM, donated by G. RONKAY).

Paratypes. Turkmenistan: 2 males, with the same data as the holotype (Coll. M. HREBLAY and G. RONKAY); 1 male, Seidi, 200 m, 18.VI.1992, leg. M. DANILEVSKY; 2 males, Mari, 12–15.IV.1993, leg. KLIMENKO (Coll. P. GYULAI). Kazakhstan: Bakanas, 12–13.V.1991 (Coll. P. GYULAI).

Slide No. RL4841 (male).

Diagnosis: The new species appears as an allopatric sibling taxon of *C. distracta* (EVERSMANN, 1848). The two species differ conspicuously in their external features, but the genitalia in both sexes are much closer, displaying small but characteristic differences. *C. repeteki* differs from *C. distracta* by its ochreous brown or sand-brown (not greyish!) forewing ground colour, obsolescent ante- and postmedial crosslines, smaller and less distinct orbicular and reniform stigmata. The best distinctive feature is the colouration of the hindwing, which is silky white in *C. repeteki*, without well-defined discal spot while the hindwing of *C. distracta* is greyish white, suffused with brownish grey, the marginal area being darker, and the discal spot rather strong. The third related species, *C. mollicella* (PÜNGELER, 1907), known from the Kuku-Noor region and from Mongolia, is smaller in size, the forewing pattern is more sharply defined, the whitish markings are stronger, and the hindwing is white with strong, dark discal spot. The male genitalia of *C. repeteki* differ from those of *C. distracta* by their longer

uncus, narrower, more cuneate harpe and somewhat broader, frontally less "humped" tube of vesica. The female genitalia of the two closely allied species differ in the shape, size and proportion of the ostium and the ductus bursae, both parts being longer and narrower and almost equally long in *C. repeteki*, while the ductus bursae is considerably longer than ostium bursae in *C. distracta*.

The fourth species of the genus, *C. maritima* (TAUSCHER, 1806) has the shape and proportion of the ostium and ductus bursae similar to those of *C. distracta*, but the ostium bursae is even shorter and slighly broader than in the latter species.

Description: Wingspan 29 mm, length of forewing 14 mm. Head and thorax ochreous brown, mixed with whitish and grey hair-scales, antenna of female filiform. Abdomen whitish grey with some darker hairs, dorsal crest absent. Forewing elongate, narrow, with apex pointed, outer margin arcuate. Ground colour shiny ochreous brown or sand-brown, costa irrorated with ashy grey, other parts of wing with whitish and darker brownish scales; veins partly covered with grey. Crosslines obsolete, represented by a few darker spots and their whitish definition. Orbicular and reniform stigmata present, small, more or less rounded, incompletely encircled by whitish, their filling greyish brown, darker than ground colour. Subterminal line indistinct, whitish-ochreous, slightly sinuous, terminal line row of tiny black dots in small whitish patches; cilia as ground colour, spotted with whitish. Hindwing pure white with intense silky shine, discal spot very pale shadow, terminal line whitish grey, cilia pure white. Underside of wings shiny white, forewing with stronger, costal area of hindwing with weaker brownish irroration, veins of forewing cell and discal spots of both wings darker grey-brown.

Male genitalia (Figs 159, 160): Uncus slender, weak, distally evenly tapering, with fine apical hook. Tegumen low, narrow, penicular lobes small, densely hairy. Fultura inferior small, relatively weak, X-shaped, vinculum long, strong. Valva long, slender, slightly dilated at medial third, cucullus elongate-triangular with apex pointed, corona rather long. Sacculus long, narrow, terminated in heavily sclerotized, narrow bar, clavus relatively large, rounded, densely setose lobe. Pulvillus small, setose tubercle, harpe long, flattened, cuneate, apically finely twisted, costal extension forming sclerotized, short, rounded lobe with fine wrinkles and crenulate margin. Aedeagus rather short, tubular, carina covered with minute denticles armed with three very long, eversible, granulosely sclerotized bars, two of them projected laterally, third situated ventrally. Vesica broadly tubular, membranous with fine scobination, everted forward, recurved dorsally; basal part with small ventral diverticulum, frontal and dorsal surfaces evenly arcuate, distal third strongly tapering.

Female genitalia (Fig. 161): Ovipositor short, weak, conical, papillae anales narrow, densely setose; apophyses slender, fine. Ostium bursae quadrangular, flattened, both surfaces posteriorly deeply incised, much deeper on dorsal plate. Ductus bursae similarly wide, flattened, granulosely sclerotized, only slightly longer than ostium bursae, lateral margin slightly folded at junction to appendix bursae. Appendix bursae long, conical, pointed, its walls membranous with fine wrinkles, corpus bursae elliptical-sacculifom, strongly scobinate.

Haemerosia albicomma sp. n.
(Figs 46, 166–168)

Holotype: male, "Turkmenistan, Kopet-Dagh Mts, 5 km S of Chuli, 700–800 m, 58°01'E, 37°56'N, 25.VIII.1992, No. L75, leg. M. Hreblay, Gy. M. László and G. Ronkay" (Coll. HNHM, donated by G. RONKAY).

Paratypes. Turkmenistan: 1 female, with the same data as the holotype; 4 males, 2 females, Kopet-Dagh Mts, 5 km S of Chuli, 700–800 m, 58°01'E, 37°56'N, 5.VIII.1992, No. L68; 2 males, Kopet-Dagh Mts, Ipay-Kala, 57°07'E, 38°20'N, 1100 m, 15.VIII.1992, No. L73; 1 male, 6 km S of Ipay-Kala, 1600 m, 57°07'E, 38°17'N, 16–23.VIII.1992, No. L74, leg. M. HREBLAY, GY. M. LÁSZLÓ and G. RONKAY (Coll. HNHM, GY. FÁBIÁN, B. HERCZIG, M. HREBLAY and G. RONKAY); 1 female, Kopet-Dagh, Germob, Kurkulab, 13–17.VII.1990, leg. DUBATOLOV & DUBATOLOVA (BIN); 1 male, Kopet-Dagh Mts, Garygala, 10.IX.1991, leg. MIATLEUSKI; 1 male, Kara-Kala, V.1993, leg. MAGUS (Coll. P. GYULAI).

Slide Nos RL5987 (male), RL4575 (female).

Diagnosis: The new species is the eastern twin species of *H. renalis* (HÜBNER, [1813]). It differs externally from its Holo-Mediterranean – Anatolian sister species by its narrower, apically more pointed forewing with essentially darker colouration, especially the narrower medial area is deep red-brownish, the crosslines are sharper, less sinuous, the reniform stigma is narrower, finer, and the hindwing is paler, more ochreous in both sexes. The male genitalia of *H. albicomma* and *H. renalis* are very similar but the valvae of the new species are distally broader, more rounded and the distal part of the aedeagus is broader, less curved subapically. The female genitalia of the two related taxa differ by the shape of the ostial appendage which is bigger, cordiform in *H. albicomma* but narrow, pendulous in *H. renalis*.

Description: Wingspan 21–22 mm, length of forewing 10 mm. Male. Head vivid red-brown, collar darker reddish, tegulae and metathorax more ochreous-pinkish. Antenna shortly bipectinate. Abdomen ochreous-reddish, covered with smooth scales, dorsal crest absent. Forewing short, broadly triangular with apex pointed, outer margin evenly arcuate. Ground colour pale, pinkish brown, basal field more ochreous, medial area strongly suffused with deep, pinkish red-brown. Basal area wide, ante- and postmedial crosslines simple, sinuous, white, defined by some brown, both marked with larger, ochreous-whitish patch at costa. Subterminal obsolescent, whitish-ochreous, slightly sinuous, defined by darker patch at costal margin and darker pinkish brown zone at inner side. Medial field narrow, contrastingly darkest part of wing, medial fascia often represented by slightly darker, diffuse brownish stripe. Orbicular stigma missing, reniform narrow, white lunule, often subdivided into more or less distinct spots. Terminal line fine, dark red-brown, cilia pinkish-reddish, outer half usually darker, more red-brownish. Hindwing shiny whitish-ochreous, medial and narrow marginal areas with scarce pale ochreous- or reddish brown hue, cilia whitish-ochreous. Underside of wings ochreous- or milky white, forewing with stronger, costal part of hindwing with usually weak red-brownish irroration, shadow of reniform and traces of transverse lines pale but visible. Female. As male, antenna ciliate, ground colour of forewing somewhat darker, more brownish, hindwing with stronger ochreous brown suffusion, underside of both wings with stronger brownish irroration.

Male genitalia (Figs 166, 167): Uncus medium-long, slender, curved, pointed, tegumen high, rather strong, with small, tubercular, densely setose subapical processi ("socii"), penicular lobes reduced. Fultura inferior broad, medium-high, quadrangular plate, vinculum short, strong, V-shaped. Valva short, broad, elliptical with rounded, finely setose apex, corona absent; costa with large,

Figs 164–173. Genitalia figures. 164 = *Chilodes distracta* (EVERSMANN); 165 = *C. maritima* (TAUSCHER); 166–168 = *Haemerosia albicomma* sp. n., paratypes; 169–171 = *H. renalis* (HÜBNER); 172 = *H. ionochlora* sp. n., holotype; 173 = *Autophila luxuriosa arnyekolta* ssp. n., paratype

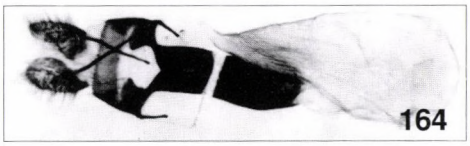
164

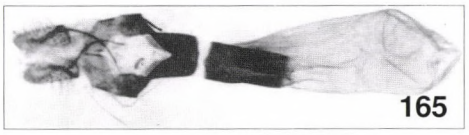
165

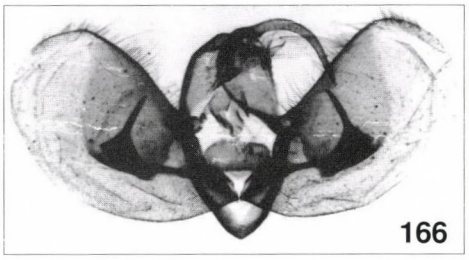
166

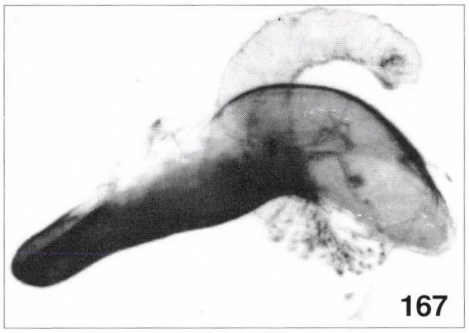
167

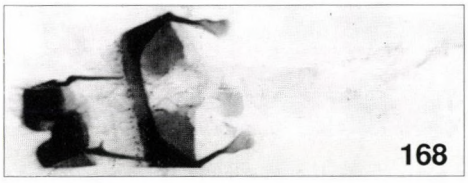
168

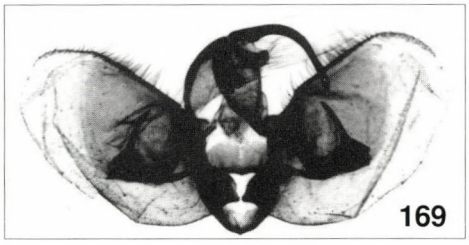
169


170

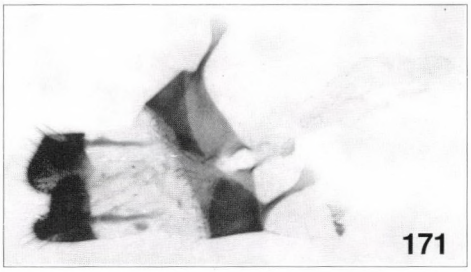
171

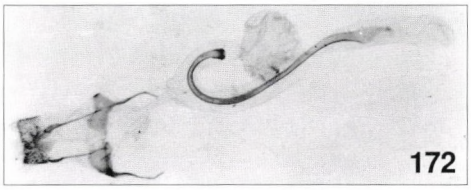
172

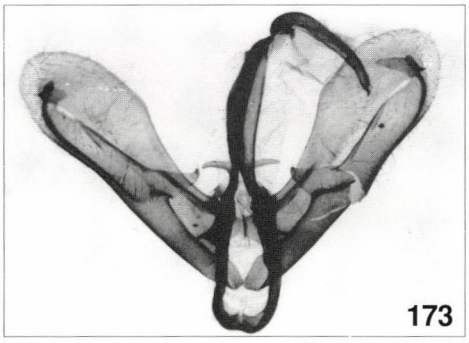
173

smoothly sclerotized plate at medial part. Sacculus very short, rounded, clavus setose, stronger plate. Harpe long, sclerotized, pin-like with large, conical base, basal bar long, narrow, sclerotized. Aedeagus short, distally thickened, curved ventrally, carina with sclerotized dorso-lateral plate. Vesica tubular, distally tapering, everted ventrally, recurved dorsally and directed forwards; basal third armed with numerous tiny, pointed spiculi, medial third with small, angular pocket, terminal part narrow tube.

Female genitalia (Fig. 168): Ovipositor short, rather broad, conical, papillae anales large, rounded triangular, covered densely with short setae; apophyses short but rather thick, terminally dilated. Ostium bursae membranous, fused with ductus bursae, with sacculiform dorsal appendage terminated in gelatinous, more or less pendulous-cordiform plate.

Etymology. The specific name refers to the fine white reniform stigma of the species.

Haemerosia ionochlora sp. n.
(Figs 47, 172)

Holotype: female, "USSR, Turkmenia, Kara-Kum desert, 100 m, 50 km N of Askhabad, 29. IV. 1991, 58°33'E, 38°21'N, 29.IV.1991, No. L12, leg. G. Csorba, Gy. Fábián, B. Herczig, M. Hreblay & G. Ronkay", slide No. RL4591 (Coll. G. RONKAY).

Diagnosis: The new species is rather remote from the other members of the genus, *H. renalis* (HÜBNER, [1813]), *H. albicomma* sp. n. and *H. vassilininei* BANG-HAAS, 1912, respectively. The other three species have the forewing ground colour and pattern similar while the forewing of *H. ionochlora* sp. n. is unicolorously mossy green with pinkish-crimson costal stripe and cilia, and with tiny whitish orbicular and reniform stigmata. The female genitalia of *H. ionochlora* differ from those of *H. renalis* and *H. albicomma* by its well-developed appendix bursae, longer corpus bursae and simple ductus bursae, without gelatinous plate which is present in the related species.

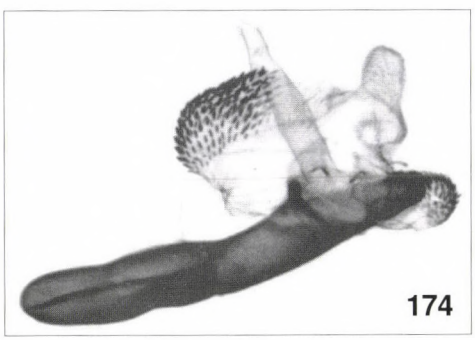

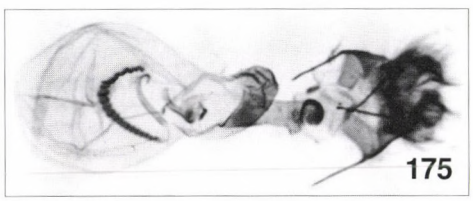

Figs 174–175. Aedeagus and female genitalia of *Autophila luxuriosa arnyekolta* ssp. n., paratypes

Description: Wingspan 20 mm, length of forewing 9 mm. Female. Head and thorax covered with flattened pinkish crimson hair-scales, frontal prominence long, cylindrical with crater-like tip, antenna filiform. Abdomen grey, dorsal crest reduced. Forewing short, broadly triangular with apex pointed, ground colour unicolorous, shiningly vivid mossy green, wide costal stripe and cilia pinkish crimson. Crosslines missing, orbicular tiny white dot, reniform small, narrow, consisting of three small white spots. Hindwing dark greyish brown, cilia dark pinkish. Underside of wings shiny, patternless, whitish ochreous with fine greenish shade, inner area of forewing irrorated with brownish grey scales.

Female genitalia (Fig. 172): Ovipositor rather short, weak, papillae anales quadratic, shortly setose, apophyses fine, slender. Ostium bursae membranous, infundibuliform, ductus bursae very short, narrowly tubular, weakly membranous. Appendix bursae complex, consisting of a narrow, arcuate, membranous basal tube and a broad, discoidal, wrinkled-gelatinous apical plate, terminated in ductus seminalis. Corpus bursae also weakly membranous, long, tubular, proximal end slightly dilated, finely wrinkled.

Bionomics and distribution. The unique female specimen was found in the southern edge of the Kara-Kum desert, overgrown by scattered *Haloxylon* trees and sparse grassy vegetation.

Etymology. The specific name refers to the green and pinkish colouration of the forewing.

Autophila luxuriosa arnyekolta ssp. n.
(Figs 48, 173–175)

Holotype: male, Turkmenistan, Kopet-Dagh Mts, 6 km S of Ipay-Kala, 1600 m, 8–12.IV.1993, 57°07'E, 38°17'N, 16–23.VIII.1992, No. L86, leg. M. Hreblay, Gy. László, A. Podlussány", (Coll. HNHM, donated by G. RONKAY).

Paratypes. Turkmenistan: 97 specimens, from the following localities: Kopet-Dagh Mts, 5 km NW of Tutlikala, 800–900 m, 22.IV.1991, 56°44'N, 38°26'N, No. L7; Kopet-Dagh Mts, 15 km SE of Nochur, 1300–1400 m, 28.IV.1991, 57°09'E, 38°21'N, No. L11, leg. G. CSORBA, GY. FÁBIÁN, B. HERCZIG, M. HREBLAY, G. RONKAY; Kopet-Dagh Mts, 800 m, Ipay-Kala, 57°07'E, 38°20'N,, 26.06., 30.06 – 04.07.1992, Nos L58, L63; Kopet-Dagh Mts, 1800 m, Sayvana valley, cca 8 km E of Sayvana, 29.06.1992, No. L61; Kopet-Dagh Mts, 1700 m, Sayvana valley, at the observatory, 29.06.1992, No. L62, leg. GY. FÁBIÁN, B. HERCZIG, A. PODLUSSÁNY and Z. VARGA; Kopet-Dagh Mts, Dushak Mt., 57°56'E, 37°54'N, 1500 m, 7–8.VIII.1992, No. L69; Kopet-Dagh Mts, 6 km S of Ipay-Kala, 1600 m, 57°07'E, 38°17'N, 16–23.VIII.1992, No. L74, leg. M. HREBLAY, GY. M. LÁSZLÓ and G. RONKAY; Kopet-Dagh Mts, Dushak Mt., 1800 m, 57°56'E, 37°54'N, 2–3.IV.1993, No. L82; Kopet-Dagh Mts, 6 km S of Ipay-Kala, 1600 m, 8–12.IV.1993, 57°07'E, 38°17'N, 16–23.VIII.1992, No. L86, leg. M. HREBLAY, GY. LÁSZLÓ, A. PODLUSSÁNY (HNHM, Coll. GY. FÁBIÁN, P. GYULAI, B. HERCZIG, M. HREBLAY and G. RONKAY).

Slide Nos RL5972 (male), RL5973 (female).

Diagnosis: *A. luxuriosa* ZERNY, 1931 is one of the polytypic *Autophila* species, represented by numerous geographic subspecies. The easternmost known populations of the species inhabiting the Kopet-Dagh Mts differ from *A. l. elbursica* BOURSIN, 1940, *A. l. taurica* BOURSIN, 1940, and *A. l. cyprogena* BOURSIN, 1940, by its more vivid ochreous-yellowish ground colour, more intensive darker pattern, especially the marginal suffusion is darker, stronger. *A.*

luxuriosa arnyekolta differs rather strongly from the SW Iranian (Farsistan) *A. l. clara* WILTSHIRE, 1952 by its darker ochreous-yellowish forewing ground colour and significantly stronger, more diffuse dark pattern, the hindwing is also darker. The other geographic subspecies of the species (*A. l. garmsira* WILTSHIRE, 1952 and *A. l. hormuza* WILTSHIRE, 1977) are generally paler with more diffuse pattern of both wings.

Description: Wingspan 35–37 mm, length of forewing 17–18 mm. Head and thorax ochreous-yellowish mixed with dark brown and greyish hair-scales, abdomen paler ochreous grey, anal tuft yellowish. Forewing rather short, broad with apex rounded, outer margin strongly convex, evenly arcuate. Ground colour bright ochreous-yellowish, basal and medial areas variably strongly irrorated with greyish brown scales, outer two-thirds of wide marginal area suffused with dark chocolate-brown. Wing pattern rather strong but diffuse, ante- and postmedial lines broad, strongly sinuous, simple, dark brown, latter strongly angled inwards below cell, medial fascia represented by stronger costal spot and brownish shadow below cell, fused partly with postmedial. Orbicular stigma tiny spot or missing, reniform stronger, more or less lunulate, claviform absent. Subterminal obsolete, usually represented by yellow apical spot and a few ochreous scales, defined mostly by darker brown shade of inner third of marginal suffusion. Cilia yellowish, chequered with dark brown. Hindwing shiny ochreous-yellowish, basal half strongly irrorated with brown scales, discal spot absent or slightly darker spot. Marginal suffusion broad, dark brown. Cilia as ground colour, spotted with brown. Underside of wings shiny ochreous-yellowish, marginal suffusion broad, strong, dark brown irrorated with yellowish scales, darker inner parts of both wings weakly visible. Discal spots absent or poorly visible, stronger on forewing; cilia as on upperside.

Male genitalia (Figs 173, 174): Uncus long, slender, curved at base, hooked apically. Tegumen high, very narrow, peniculi narrow, pointed, rather short. Fultura inferior broadly X-shaped, vinculum strong, medium-long, widely U-shaped. Valva elongate, distal half strongly dilated, with apex rounded, corona absent. Sacculus narrow, sclerotized, continued as long, flattened, sclerotized plate. Dorsal extension of sacculus flattened, acute triangular with setose apex, ventral extension terminated as double-peaked, medially folded lobe ("harpe"), these extensions being asymmetrical, left "harpe" considerably smaller, tips more rounded, right "harpe" larger, inner (dorsal) lobe elongate, acute triangular with pointed tip. Aedeagus tubular, rather short, slightly arcuate, carina with strong, bill-like ventral extension. Vesica everted dorsally, consisting of sphaerical basal part having two smaller, tubular subbasal diverticula and one much larger, semiglobular terminal diverticulum, all armed with numerous short spiculi, ductus ejaculatorius originating from between subbasal diverticula.

Female genitalia (Fig. 175): Ovipositor short, broad, subconical, papillae anales wide, densely hairy; apophyses fine, rather long. Ostium bursae membranous, more or less quadratic, with big, heavily sclerotized, subsphaerical appendage on dorsal surface. Ductus bursae relatively short, tubular, proximal half slightly dilated, with rather weak sclerotization on both surfaces. Appendix bursae big, membranous, elliptical, apical part with stronger wrinkles, corpus bursae spacious, ovoid, finely scobinate, signum well-developed, broad, slightly asymmetrical U-shaped.

* * *

Acknowledgements – The authors are indebted to G. CSORBA (Budapest), GY. FÁBIÁN (Budapest), P. GYULAI (Miskolc), B. HERCZIG (Baj), GY. M. LÁSZLÓ, A. PODLUSSÁNY and G. RONKAY (Budapest) and H. THÖNY (Poté, Brasil) for the opportunity to study their material, to V. M. KORSHUNOV (Ashkhabad) for the kind help and cooperation in the organization of the field expeditions to Turkmenistan. Our sincere thanks to V. V. DUBATOLOV (Novosibirsk), P. FASTRÉ (Marchin), H. HACKER (Staffelstein), M. R. HONEY (London), O. KARSHOLT (Copenhagen), I. YU. KOSTYUK (Kiev), V. I. KUZNETSOV (St. Petersburg), M. LÖDL (Vienna), A. LVOVSKY (St. Peters-

burg), W. MEY (Berlin), C. NAUMANN (Bonn), J. NOWACKI (Poznan), J. PLANTE (Martigny), W. SPEIDEL (Berlin), D. STÜNING (Bonn), I. L. SUKHAREVA (St. Petersburg), E. VARTIAN (Vienna) and E. P. WILTSHIRE (Cookham Rise) for the kind help loaning the necessary types and additional specimens for our investigations.

The research was supported by the Hungarian National Scientific Research Fund (OTKA), (No. 16465).

REFERENCES

BERGMANN, A. & THÖNY, H. (1996) Zwei neue Arten aus der Gattung Pseudopseustis Hampson, 1910, aus Turkmenien (Lepidoptera, Noctuidae, Amphipyrinae). *Facetta* **13(2)**: 11–15.

BOURSIN, CH. (1940) Beiträge zur Kenntnis der "Agrotidae-Trifinae", XXII. Neue palaearktische Arten und Formen mit besonderer Berüchsichtigung der Gattung Autophila Hb. *Mitt. münchn. ent. Ges.* **30**: 474–543

BOURSIN, CH. (1943) Contribution a l'etude de la Faune du Caucase et de l'Armenie. *Rev. fr. ent.* **10**: 75–84.

BOURSIN, CH. (1955) Description de nouvelles especes et formes du Bassin Mediterraneen (Lep., Phal.). *Bull. mens. Soc. linn. Lyon* **1955**: 252–255.

BOURSIN, CH. (1953) Über die Gattung "Allophyes" Tams nebst Bescreibung einer neuen Art aus Klein-Asien. Lep., Phalaenidae (Noctuidae) (Beiträge zur Kenntnis der "Agrotidae-Trifinae", LIX). *Mitt. münchn. ent. Ges.* **43**: 239–247.

BOURSIN, CH. (1954) Zwei neue Cryphia Hb. (Bryophila)-Arten aus dem vorderasiatisch-mediterranen Faunenkreis. *Z. wien. ent. Ges.* **39**: 85–89.

BOURSIN, CH. (1955) Eine neue Agrochola Hb. aus Algerien. *Z. wien. ent. Ges.* **40**: 246–248.

BOURSIN, CH. (1956) Eine neue südchinesische Agrochola Hb. (Orthosia auct.) aus Dr. H. Höne's China-Ausbeuten. *Z. wien. ent. Ges.* **41**: 35–37.

BOURSIN, CH. (1957) Eine neue Allophyes Tams aus Mittelchina. (Aus Dr. Höne's China-Ausbeuten) (Beiträge zur Kenntnis der "Agrotidae-Trifinae" XCIII). *Z. wien. ent. Ges.* **42**: 103–106.

BOURSIN, CH. (1960) Nouvelles "Trifinae" d'Afghanistan de l'expedition Klapperich (3me note). (Lep. Noctuidae)(Diagnoses preliminaires) (Contributions a l'etude des "Noctuidae-Trifinae" CIII). *Bull. mens. Soc. linn., Lyon* **29**: 136–152.

BOURSIN, CH. (1967) Description de 26 espéces nouvelles de Noctuidae Trifinae paléarctiques et d'un sous-genre nouveau des la sous-famille des Apatelinae. (Contributions a l'etude des Noctuidae-Trifinae, 160). *Entomops* **11**: 43–108.

BOURSIN, CH. (1969) Description de 40 espéces nouvelles de Noctuidae Trifinae paléarctiques et de deux genres nouveaux des sous-familles Noctuinae et Amphipyrinae I. *Entomops* **15**: 215–240.

BOURSIN, CH. (1970): Description de 40 espéces nouvelles de Noctuidae Trifinae paléarctiques et de deux genres nouveaux des sous-familles Noctuinae et Amphipyrinae II. *Entomops* **18**: 45–80.

BRANDT, W. (1938–1939) Beitrag zur Lepidopteren-Fauna von Iran. *Ent. Rundschau* **55**: 497–505, 517–523, 548–554, 558–569; **56**: 11–15, 23–24, 32–34, 59–61, 86–87, 109–111, 139–141.

BRANDT, W. (1941) Beitrag zur Lepidopteren-Fauna von Iran (3). Neue Agrotiden, nebst Faunenverzeichnissen. *Mitt. münchn ent. Ges.* **31**: 835–863.

CHRISTOPH, H. (1884): Lepidoptera aus dem Achal-Tekke Gebiete I. *In* ROMANOFF, N. M.: *Mém. Lép.* **1**: 93–138.

CHRISTOPH, H. (1887): Lepidoptera aus dem Achal-Tekke Gebiete III. *In* ROMANOFF, N. M.: *Mém. Lép.* **3**: 50–90.

CHRISTOPH, H. (1889): Lepidoptera aus dem Achal-Tekke Gebiete IV. *In* ROMANOFF, N. M.: *Mém. Lép.* **5**: 1–58.

DERRA, G. & SCHREIER, H.P. (1990) Beitrag zur Noctuidae-Fauna der Türkei (Lepidoptera). *Esperiana* **1**: 393–402.

DRAUDT, M. (1950) Beiträge zur Kenntnis der Agrotiden-Fauna Chinas. Aus den Ausbeuten Dr. H. Höne's (Beitrag zur Fauna Sinica). *Mitt. münchn. ent. Ges.* **40**: 1–174.

EBERT, G. (1971) Beiträge zur Kenntnis der Fauna Afghanistans (Noctuidae, Trifinae, Lep.). *Acta Mus. Moraviae* **61**: 175–189.

HACKER, H. (1990) Die Noctuidae Vorderasiens (Lepidoptera). *Neue ent. Nachr.* **27**: 1–707.

HACKER, H. (1990) Die Genera Cryphia HÜBNER, 1818 und Mniotype Franclemont, 1941 im himalayanischen Raum. *Esperiana* **1**: 359–375.

HACKER, H. & KUHNA, P. (1986): Drei neue Noctuidae-Arten aus der Türkei (Lepidoptera). *Nota lepid.* **9**: 179–190.

HACKER, H., KUHNA, P. & GROSS, F. J. (1986) 4. Beitrag zur Erfassung der Noctuidae der Türkei. Beschreibung neuer Taxa, Erkenntnisse zur Systematik der kleinasiatischen Arten und faunistisch bemerkenswerte Funde aus den Aufsammlungen von Gross und Kuhna aus den Jahren 1968–1984 (Lepidoptera: Noctuidae). *Mitt. münchn. ent. Ges.* **76**: 79–141.

HACKER, H. & MOBERG, A. (1988) Zwei neue Dasypolia Guenée, 1852 – Arten aus der östlichen Türkei (Lepidoptera, Noctuidae, Cuculliinae). *Mitt. münchn. ent. Ges.* **78**: 179–185.

HACKER, H. & WEIGERT, L.(1990) Übersicht über das Artenspektrum in Nordpakistan (Karakorum, Westhimalaya) im September und Oktober. *Esperiana* **1**: 237–275.

HACKER, H., KAUTT, P. & WEISZ, V. (1996) Noctuidae gesammelt von Kautt und Weisz im Sommer 1994 in Spiti Valley in Himachal Pradesh. *Esperiana* **4**: 395–417.

HACKER, H. & L. RONKAY (1992) Das Genus Polymixis HÜBNER [1820] mit Beschreibung einer neuen Art und Festlegung neuer Stati (Lepidoptera: Noctuidae). *Esperiana* **3**: 473–496.

HAROLD, A. S. & MOOR, R. D. 1994. Areas of endemism: Definition and recognition criteria. *Syst. Biol.* **43**: 261–266.

HERCZIG, B., L. RONKAY, A. M. BATHIEV, I. I. GIZATULIN, T. S. KOROLJ, T. Y. TOCHIEV & D. I. UZAHOV (1991) Contributions to the knowledge of the Noctuidae (Lepidoptera) fauna of the NE Caucasus II. *Annls hist.-nat. Mus. natn. hung.* **83**: 125–134.

HREBLAY, M. (1992) Neue Taxa und Synonyme der Gattung Conistra HÜBNER, [1821] (Lepidoptera: Noctuidae). *Esperiana* **3**: 531–544.

HREBLAY, M. (1993) Neue Taxa aus der Gattung Orthosia Ochsenheimer, 1816 (s.l.) II. (Lepidoptera, Noctuidae). *Acta zool. hung.* **39**(1–4): 71–90.

HREBLAY, M. (1996): Neue paläarktische Taxa aus der Gattung Perigrapha Lederer, 1857 (Lepidoptera, Noctuidae. *Esperiana* **4**: 65–94.

HREBLAY, M. & L. RONKAY (1995) New species of Dasypolia Guenée, 1852 (s. l.) from the Himalayan region (Lepidoptera, Noctuidae, Xylenini). *Acta zool. hung.* **41**(4): 349–378.

HREBLAY, M. & RONKAY, L. (1997) New Noctuidae (Lepidoptera) species from Taiwan and the adjacent areas (Lepidoptera). *Acta zool. hung.* **43**(1): 21–83.

KUZNETZOV, V. I. (1958) Neue und wenig bekannte Noctuiden-Arten (Lepidoptera, Noctuidae) aus westlichen Kopet-Dagh, Turkmenien. *Ent. Obozr.* **37**(1): 183–195.

KUZNETZOV, V. I. (1960) On the fauna and biology of Lepidoptera of of the western Kopet-Dagh. Fauna & ecology of Turkmenia. *Trudy zool. Inst. Akad. Nauk. SSSR, Moscow* **27**: 11–93.

LUIG, J., MIATLEWSKI & SALDAITIS, A. (1998) A new species of the genus Polymixis Hbner, [1820] from Western Turkmenistan (Lepidoptera, Noctuidae). *Atalanta* **28**: 153-156.

POLTAVSKY, A. N., NEKRASOV, A. V., PETCHEN, V. I. & HATCHIKOV, E. A. (1997) The Noctuidae fauna of Turkmenia (Lepidoptera). *Phegea* **25**(4): 173–183, **26**(1): 31–40.

POOLE, R. W. (1989): Noctuidae. *In Lepidopterorum Catalogus* (New Series, Fasc. 118). Brill, Leiden.

RONKAY, L. (1986) Taxonomic studies on the genus Autophila Hübner, 1823. I. *Acta zool. hung.* **32**(1–2): 141–159.

RONKAY, G. & RONKAY, L. (1988) Taxonomic studies on the Palaearctic Cuculliae (Lepidoptera, Noctuidae). Part IV. *Annls hist.-nat. Mus. natn. hung.* **80**: 91–103.

RONKAY, L. (1989) Taxonomic studies on the genus Autophila Hübner, 1823 (Lepidoptera, Noctuidae), II. *Acta zool. hung.* **35**(1–2): 111–141.

RONKAY, G. & RONKAY, L. (1994) *Cuculliinae I. Noctuidae Europaeae. Vol. 6.* Entomological Press, Sorø, 282 pp. + 10 colour plates.

RONKAY, G. & RONKAY, L. (1995) *Cuculliinae II. Noctuidae Europaeae. Vol. 7.* Entomological Press, Sorø, 224 pp. + 4 colour plates.

RONKAY, L. & VARGA, Z. (1985) Neue Noctuiden aus Armenien bzw. aus dem Kaukasus-Raum (Lepidoptera: Noctuidae). *Z. Arbgem. öst. Ent.* **36**: 86–94.

RONKAY, L. & VARGA, Z. (1990) Taxonomic and zoogeographical studies on the subfamily Cuculliinae (Lepidoptera, Noctuidae). Part II. *Esperiana* **1**: 471–497.

RONKAY, L. & VARGA, Z. (1993) Taxonomic studies of the genera Pseudohadena Alphéraky, 1889 and Auchmis Hübner, [1821] (Lepidoptera, Noctuidae), Part IV. *Acta zool. hung.* **39**(1–2): 211–252.

RONKAY, L. & VARGA, Z. (1994) On the taxonomy of the genus Ostheldera Nye, 1975 (Lepidoptera, Noctuidae, Cuculliinae). *Acta zool. hung.* **40**(2): 157–170.

RONKAY, L. & VARGA, Z. (1998) On the taxonomy of the genera Odontelia Hampson, 1905, and Thargelia Püngeler, 1900 (Noctuidae, Hadeninae). *Annls hist.-nat. Mus. natn. hung.* [in press]

RONKAY, L., VARGA, Z. & FÁBIÁN, GY. (1995) Taxonomic studies of the genus Pseudohadena Alpheraky, 1889. Part V. The revision of the genus Pseudohadena s. str. *Acta zool. hung.* **41**(3): 251–282.

VARGA, Z. (1996) New species and subspecies of Dichagyris, Chersotis and Rhyacia (Lepidoptera, Noctuidae) from Central Asia. *Acta zool. hung.* **42**(3): 195–230.

VARGA, Z. & RONKAY, L. (1991) Taxonomic studies of the Palaearctic Noctuidae (Lepidoptera) I. New taxa from Asia. *Acta zool. hung.* **37**(3–4): 263–312.

VARGA, Z. & RONKAY, L. (1994) Revision of the genus Eugnorisma Boursin, 1940, III. Additional notes with the description of a new species and redescription of two misidentified species (Lepidoptera, Noctuidae). *Acta zool. hung.* **40**(1): 87–97.

WILTSHIRE, E. P. (1946) Middle East Lepidoptera V. A new genus, a new species, and two new races from Iran, with taxonomic notes on other Persian Heterocera. *Proc. Royal ent. Soc., London,* **15**(9–10): 118–128.

WILTSHIRE, E. P. (1987) Middle East Lepidoptera 48: Eremophysa jabaliya sp. n., a further discovery from Northern Oman (Lepidoptera, Noctuidae). *Entomofauna* **8**: 441–446.

WILTSHIRE, E. P. (1993) Middle East Lepidoptera 50: Notes on some hitherto misunderstood forms near Polymixis bischoffi (Herrich-Schäffer, 1850) (Noctuidae). *Nota lepid.* **15**(3–4): 257–267.

Received 30th March, 1998, accepted 1st September, 1998, published 28th December, 1998

ACTA ZOOLOGICA
ACADEMIAE SCIENTIARUM HUNGARICAE

An international journal of animal taxonomy and ecology

Instruction to authors

Submission of a paper implies that it has not been published previously, that is not under consideration for publication elsewhere, and that if accepted for the Acta Zoologica Hungarica, the authors will transfer copyright to the Hungarian Academy of Sciences/the Hungarian Natural History Museum as is customary. Articles and illustrations become the property of the HAS/HNHM.

Papers must be in English with British spelling, and be original contributions in the field of animal taxonomy, systematics, zoogeography and ecology. All manuscripts must be submitted to one of the editors (editor, assistant editor).

Entire manuscripts must be submitted on IBM compatible floppy disk and in duplicate printed copies and the author should retain a copy. In the case of multiple authors, the corresponding author should be indicated. Series of numbered papers will not be considered.

Manuscripts must be printed with double spacing (including the reference list), and with wide margins (30–35 mm) on the left side of the paper only. Authors are requested to keep their communications as concise as possible. Footnotes should be avoided or minimized, and italics should not be used for emphasis. A running head of not more than 30 letters should be supplied.

The manuscript should contain the following information:

Title should be followed by the name and full address of the author(s). Where possible, the fax and/or e-mail number of the corresponding author should be supplied with the manuscript, for use by the publisher.

Abstract should be a brief summary of the contents and conclusions of the paper, and should not be longer than 200 words and should not contain references.

Key words should not be more than five (exceptionally 6) key word entries.

Introduction should contain a brief survey of the relevant literature and the reasons for doing the work.

Materials and Methods supply sufficient information to permit repetition of the experimental or field work. The technical description of methods should be given only when such methods are new.

Results should be presented concisely. Only in exceptional cases will it be permissible to present the same set of results in both table and a figure. The results section should not be used for discussion.

Discussion should be separate from the results section and should deal with the significance of the results and their relationship to the object of the work (and, this is the place of the identification key in taxonomic revisions).

Acknowledgements (at most in 10 lines).

References. In principle the Harvard system is to be followed. References should be detailed in the following order: authors' names and initials, date of publication (in parentheses), the title of the article, the name of the journal as abbreviated in the World List of Scientific Periodicals (4th edn 1963), the volume, and the first and last pages of the article, e.g.

NORRBOM, A. L. and KIM, K. C. (1985) Taxonomy and phylogenetic relationships of Copromyza Fallén (s.s.) (Diptera: Sphaeroceridae). *Ann. Entomol. Soc. Am.* **78**: 331–347.

For books the author's names, date of publication, title, edition, page reference, publisher's name and the place of publication should be given, e.g.

HINTON, H. E. (1981) *Biology of insect eggs*, vol. 2. Pergamon Press, New York.

or

MCALPINE, J. F. (1981) Morphology and terminology, adults, pp. 9–63. *In* MCALPINE *et al.* (eds) *Manual of Nearctic Diptera*, vol. 1. Agriculture Canada, Ottawa.

In the text references should be given as MARSHALL (1992) or (MARSHALL 1992). When a citation includes more than two authors, e.g. GREY, BLACK and WHITE, the paper should be referred to in the text as GREY *et al.*, provided that this not ambiguous. If papers by the same author(s) in the same year are cited, they should be distinguished by the letters, *a, b, c,* etc., e.g. MARSHALL (1992*a*).

References to papers "in press" must mean that the article has been accepted for publication. References to "personal communications" and unpublished work are permitted in the text only: references to papers in preparation or submitted are not permissible.

All necessary **illustrations** should accompany the manuscript, but should not be inserted in the text. All photographs, graphs and diagrams should be numbered consecutively in Arabic numerals in the order in which they are referred to in the text. Glossy photographs or positive prints should be sent unmounted wherever possible and should be kept to a minimum. Figures should be of good quality. Explanation of lettering and symbols should be given in the figure caption and only exceptionally in the figures. Lettering and symbols to appear on the illustration should be of sufficient size to allow for considerable reduction where necessary (usually proper for a 50% reduction in size). Scales must be indicated on micrographs, not by magnifications in the legends. Figure size must not exceed 24×30 cm. On the back of each illustration should be indicated the author's name, the figure number (in Arabic numerals), and the top of the illustration, where this is not clear. Halftones should be included only when they are essential. Details and quotation of publication of colour plates should be made to the editors. The following symbols should be used on line drawing: ● ■ ○ ❑ ▲ ◆ ♦ etc.

Legends to figures should be typed on a separate sheet. They should give sufficient data to make the illustration comprehensible without reference to the text.

Tables and appendices should be constructed so as to be intelligible without reference to the text, numbered in Arabic numerals and typed on separate sheets. Every table should be provided with an explanatory caption and each column should carry an appropriate heading. Units of measure should always be indicated clearly (metric units are preferred). All tables and figures must be referred to in the text.

Only standard **abbreviations** should be used. Arbitrary abbreviations and jargon will not be accepted.

The Latin names should be given for all species used in the investigation, although taxonomic affiliation and authority need not be provided in the title.

Page proofs will be sent to the author (or the first-mentioned author in a paper of multiple authorship) for checking. Corrections to the proofs must be restricted to printers' errors. Any substantial alterations other than these may be charged to the author. Authors are particularly requested to return their corrected proofs as quickly as possible in order to facilitate rapid publication. Please note that authors are urged to check their proofs carefully before return, since late corrections cannot be guaranteed for inclusion in the printed journal.

Fifty reprints free of charge will be sent to the first author; extra copies of the issue (at a specially reduced rate) can be ordered on the form which will accompany the proofs. These should be returned to: The Editorial Office of the Acta Zoologica, Hungarian Natural History Museum, Budapest, Baross u. 13, H–1088, Hungary

The **page charge** required from authors outside Hungary is USD 15 per printed page. In exceptional cases, the page charge may be waived. Please contact the editor in before submitting a paper if you ask for a waiver. Authors of papers exceeding 16 printed pages are asked to pay USD 40 (or HUF equivalent) for each such page, i.e. all costs of publication (irrespective of their nationality).

FOR FURTHER INFORMATION PLEASE CONTACT US
The Editorial Office of the Acta Zoologica
H–1088 Budapest, Baross u. 13, Hungary
Fax: (36–1) 3171669
http:/actazool.nhmus.hu/
E-mail: perego@zoo.zoo.nhmus.hu

SUBSCRIPTION INFORMATION

Orders should be addressed to

Editorial Office of the Acta Zoologica
Hungarian Natural History Museum
H–1088 Budapest, Baross u. 13, Hungary
Fax: (36–1) 3171669
E-mail: perego@zoo.zoo.nhmus.hu

Typeset: Pars Ltd., Budapest.
Printed by *mondAt Ltd.*, Hungary

CONTENTS

HU ISSN 1217–8837

Acta Zoologica

Academiae Scientiarum Hungaricae

VOLUME 44 - NUMBER 4 - 1998

HUNGARIAN NATURAL HISTORY MUSEUM, BUDAPEST

ACTA ZOOLOGICA
ACADEMIAE SCIENTIARUM HUNGARICAE

AN INTERNATIONAL JOURNAL OF
ANIMAL TAXONOMY AND ECOLOGY

Acta Zoologica Academiae Scientiarum Hungaricae is published quarterly from February 1994 (other issues in May, August and November) by the Hungarian Natural History Museum and the Biological Section of the Hungarian Academy of Sciences with the financial support of the Hungarian Academy of Sciences.

For detailed information (contents, journal status, instructions for authors, subscription, and from Volume 40 onward title, author, authors' addresses, abstract, keywords and a searchable taxon index) please visit our website at

http://actazool.nhmus.hu/

Acta Zoologica Academiae Scientiarum Hungaricae 44 (4), pp. 283–295, 1998

NEW OPPIID ORIBATID MITES FROM MEXICO (ACARI: ORIBATIDA), I.*

S. MAHUNKA and J. G. PALACIOS-VARGAS

Department of Zoology, Hungarian Natural History Museum
H-1088 Budapest, Baross u. 13, Hungary, E-mail: mahunka@zoo.zoo.nhmus.hu
Laboratorio de Ecología y Systemática de Microartropódos
Depto. Biología, Fac. Ciencias, UNAM. 04510 México, D. F., México
E-mail: jgpv@hp.fciencias.unam.mx

This study deals with oppiid mites from Mexico. Three new species are descibed, one of which represent a new genus (*Pararamusella* gen. n.), another two belong to new subgenera [*Arcoppia (Dysarcoppia)* subgen. n. and *Berniniella* (*Canaloppia*) subgen. n.]. Some notes are given regarding the systematics of this family.

Key words: Acari, Oribatida, Oppiidae, new taxa, Mexico

INTRODUCTION

In the framework of a project supported by the Hungarian Commission of Technical Development (OMFB) and the Mexican CONACyT we are studying the connection between the vegetation and the oribatid mite fauna of Mexico. During the sampling for this overall project, new species of oribatid mites are being encountered and are in need of description. In one such sample, collected in a cultivated area in Hidalgo State, the junior author and his co-workers have found an interesting fauna, that contains remarkably numerous species belonging to the superfamily Oppioidea.

Several species belonging to this superfamily have been described from Mexico, some by the senior author. Many of the records of Oppiidae from Mexico are represented simply at the family or genus level (see PALACIOS-VARGAS 1994).

In the following we list and describe some of the newly collected species. Even though we describe supraspecific taxa, the detailed elaboration of the systematics of the Oppioidea is prevented by space limitation. Nevertheless, it is necessary to give some comments in order to arrange the taxa correctly.

We believe that there is not enough information to create a phylogenetic system of the Oppioidea. Nevertheless, it is necessary to define precisely the relationships at a supraspecific level, regardless of the fact that the taxon later will

* Project: Biodiversity of Mexican mites (see BORHIDI *et al.* 1996). CONACyT, Mexico – OMFB, Hungary. This work was also sponsored by the Hungarian Research Fund (OTKA, grant no. 16729).

be given generic, subgeneric or subfamilial status. We regard as bad practice the continuous change of level and content of supraspecific taxa without synthesis. There is no point in unification or separation of taxa until a consensus is reached regarding the value of features separating them. Therefore we can not accept the opinion of FRANKLIN and WOAS (1992), who would argue to treat the *Arcoppia* species only as a subgenus of *Oppia*. The features separating the genera in our opinion would be given a lower evaluation this way. We can not agree with the practice by which the unification of species, subgenera or subfamilies (synonymisation) is not followed by exact diagnose, and the content of a new taxon is not given (see WOAS 1986: 215, or FRANKLIN & WOAS 1992: 11). Hereafter we follow the system of BALOGH (1983) and SUBIAS and BALOGH (1989).

When examining the following species a striking character, formerly known and used for the separation of genera (MAHUNKA 1996, 1997), was reexamined. This character is the distance separating acetabula III and IV. When large, it results in pronounced elongation of the discidium and a transformation of the whole epimeral region. This enlargement was recognised as an important character-trend by FRANKLIN and WOAS (1992: 14, 16), and it seems to reappear in several Oppiidae subfamilies (genera), indirectly proving their independence. We now find the less pronounced presence of this feature in the *Arcoppia* HAMMER, 1977 and *Ramusella* HAMMER, 1962 complex. We mainly separate taxa at generic or subgeneric level by this feature, with the evaluation of other characters.

In the descriptions we generally apply the terminology used in several publications by NORTON (*e. g.* 1982) and BEHAN-PELLETIER (*e. g.* 1984) based on GRANDJEAN's work, further elaborated and completed by the senior author (MAHUNKA 1996*b*).

LIST AND DESCRIPTIONS

Arcoppia (Dysarcoppia) subgen. n.

Diagnosis: Habitus, prodorsal structure and sculpture as in the genus *Arcoppia* HAMMER, 1977, rostrum tripartite. Notogaster with 10 pairs of setae. Position of the acetabula characteristic: acetabula IV far removed from acetabula III, discidium very long, without large, sharp distal apophysis. A longitudinal ridge runs along the discidial margin on the epimeral surface.

Type species: *Arcoppia (Dysarcoppia) mexicana* sp. n.

Remarks: The above mentioned combination of features was unknown in this genus.

Etymology: Named after the long distance between acetabula III and IV.

Arcoppia (Dysarcoppia) mexicana sp. n.
(Figs 1–8)

Measurements. – Length of body: 405–428 µm, width of body: 186–203 µm.

Prodorsum: Rostrum tripartite, rostral apex shorter than the lateral teeth (Fig. 2). Rostral incisions narrow, sometimes hardly discernible. Shape of costulae atypical, the basal (longitudinal) part of all three short or indistinct, consisting of small granules in front of bothridia. The unpaired median ones U-shaped, slightly concave or straight medially (Fig. 1). Bothridia relatively small, nearly quadrangular. Two pairs of sigillae present in the interbothridial region, some indistinct similar ones visible laterally. Behind the interbothridial sigillae and the bothridia an arched line is present, one pair of well sclerotised laths with a pair of porose areas (?) observable also in this region laterally. All four pairs of prodorsal setae strong but setiform, distinctly ciliate, setae *ex* shorter than the others, no essential difference exist among the latter, but lamellar and interlamellar setae equal in length, rostral ones slightly shorter. Sensillus long, without typical clavate head. Its branches (mostly 6) also conspicuously long (Fig. 4).

Notogaster: Well elongated. Median part of the dorsosejugal line thin, indistinct. Ten pairs of notogastral setae present, setae c_2 short, simple, all others long, some cilia well observable on them. Setae *la* arising clearly in front of *lm* (Fig. 1).

Lateral part of podosoma: Position of the acetabula of the legs are characteristic, acetabula IV located far posterior to acetabula III, distance of acetabula III and IV two and half times longer than the distance between acetabula I and II (Fig. 4). Exobothhridial region and field between acetabula II and III well granulated. Pedotecta I large, peddotecta II-III reduced, pedotecta IV very long, reaching acetabula IV.

Ventral parts of the body (Fig. 3): Epimeral borders and apodema partly weakly developed, *bo.* $_2$ short, with large sigillae laterally. Epimera III and IV very large, apodema IV arched and directed posteriorly to the acetabula IV. Epimera I and II well framed laterally by arched cuticular ridges, setae *1c* arising on them. Along pedotecta IV a straight longitudinal ridge present, directed toward acetabula IV (Fig. 5). Setae *4c* arise on pedotecta IV. Epimeral setae of normal size, setae *1c, 3c, 4b* and *4c* well ciliate, all others nearly smooth. Setae *3c, 4b* and *4c* longer and stronger than the others. Epimeral setal formula: 3 – 1 – 3 – 3.

Genital opening much smaller than anal one. Anogenital setal formula: 6 – 1 – 2 – 3. Position of the aggenital setae normal, but the posterior pair of adanal setae located far anteriorly and laterally, setae ad_1 in paraanal position, arising near posterior corner of anal opening. Adanal setae well ciliated.

Infracapitulum, chelicera and palps normal.

Legs: Tibia and tarsi of leg I and II moderately elongated, femora of these legs slightly incrassate. Tibia and tarsi of legs III and IV conspicuously long. All setae of femora I short, setae *d* well ciliate. Seta *l'* of genu IV much longer than the other setae, setae *v"* short and spiniform, seta *l'* much longer. Setae *v"* and *a"* plumose.

Legs setal formulae:

I: 1 – 5 – 2+1 – 4+2 – 20+2 – 1 (Figs 6–7).
IV: 1 – 2 – 2 – 3+1 – 10 – 1 (Fig. 8).

Material examined: Holotype: México: Hidalgo: near Pachuca. Cultivated field "La Estanzuela", 25.X.1997. leg. J. PALACIOS-VARGAS. 13 paratypes from the same sample. Holotype (1594–HO-98) and 7 paratypes (1594–PO-98) (with identification numbers of the specimens in the Collection of Arachnida) deposited in the Hungarian Natural History Museum, Budapest, 5 paratypes in the Laborátorio de Ecologia y Sistemática de Microartrópodos, Depto. Biologia, Fac. Ciencias, UNAM, México and 1 paratype in the Muséum d'Histoire naturelle, Geneve.

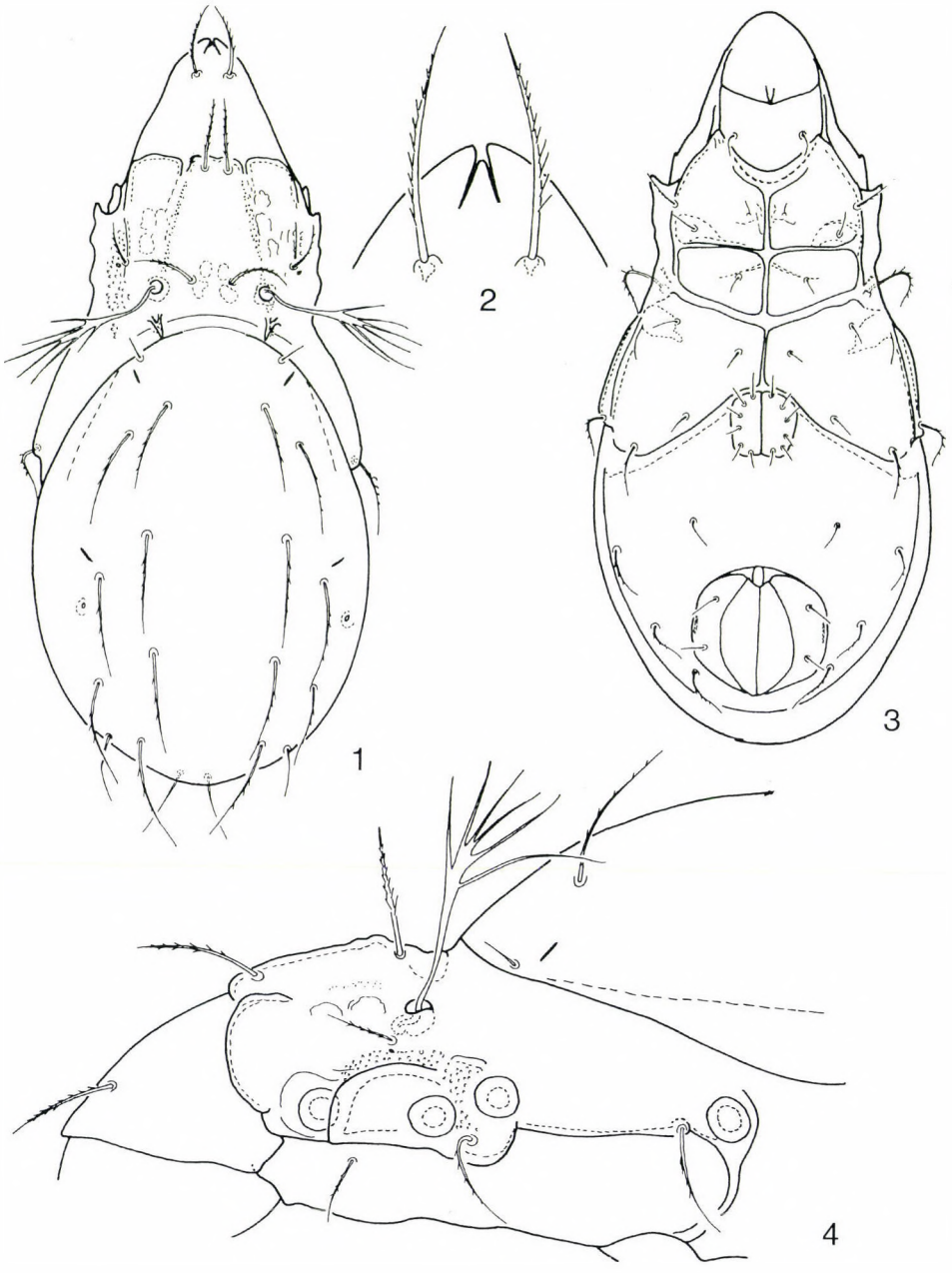

Figs 1–4. *Arcoppia (Dysarcoppia) mexicana* sp. n. 1 = body in dorsal view, 2 = rostrum, 3 = body in ventral view, 4 = lateral part of podosoma

Remarks: The new species is well characterised by the long distance between acetabula III-IV and by the longitudinal ridge along the discidium (see also below). The form of the basal part of

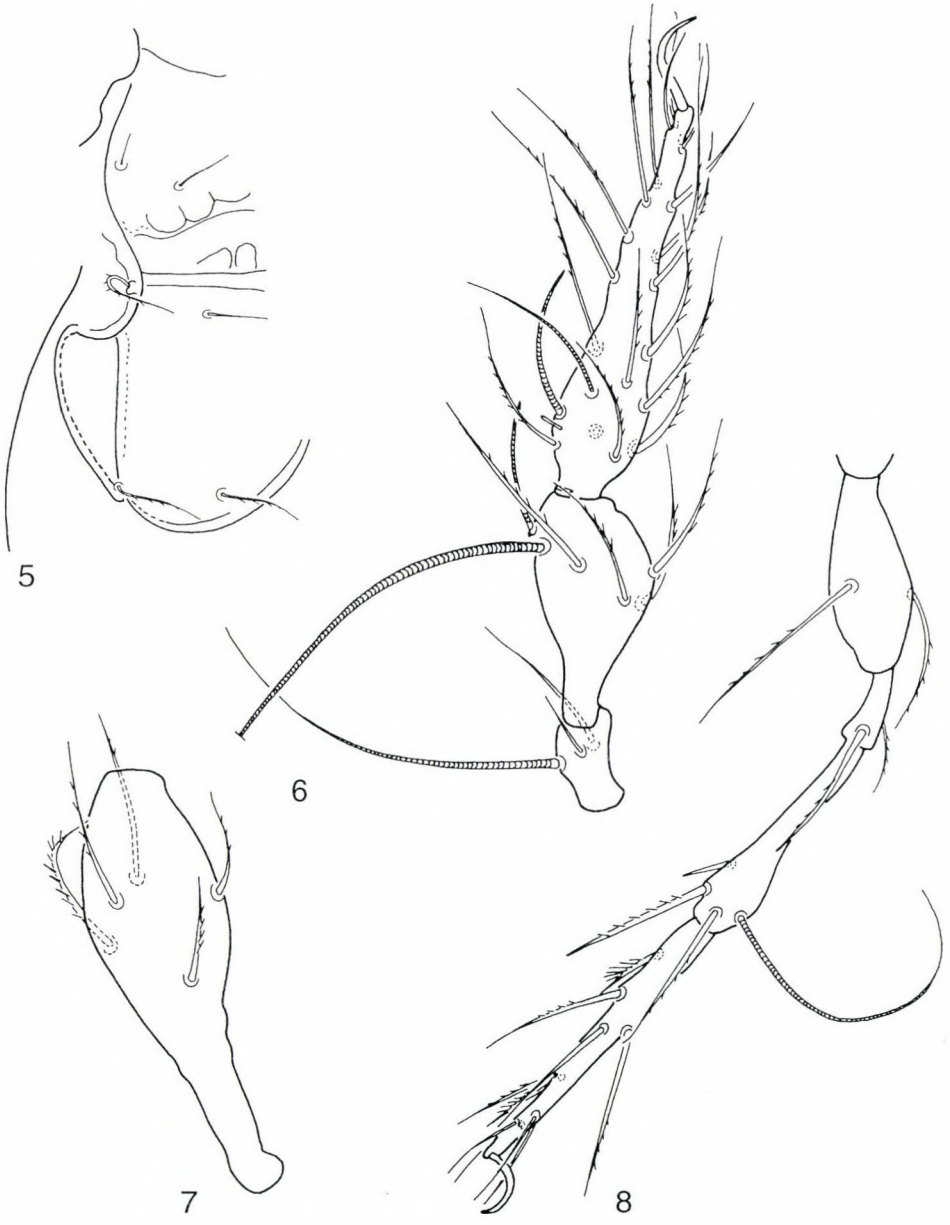

Figs 5–8. *Arcoppia (Dysarcoppia) mexicana* sp. n. 5: lateral part of epimera III and IV, 6 = genu, tibia and tarsus of leg I, 7 = femur of leg I, 8 = leg IV

the prodorsum also unique in the genus *Arcoppia* HAMMER, 1979 and this combination of characters was unknown in this genus.

Etymology: Named after the country of origin.

Berniniella (Canaloppia) subgen. n.

Diagnosis: Family Oppiidae GRANDJEAN, 1951, subfamily Oppiellinae SENICZAK, 1975. Rostral region with one pair of large apophyses bearing the rostral setae and a long median hollow connecting with these apopyses. Sensillus long, pectinate, bent inwards. True crista absent.

Other features are the same as in the nominate subgenus.

Type species: *Berniniella (Canaloppia) borhidii* sp. n.

Remarks: The species of *Berniniella* described earlier form a quite homogeneous taxon (see SUBIAS & BALOGH 1989). From this group a Mexican species was already known [*Berniniella tequila* (MAHUNKA, 1983)]. The sensillus and the prodorsal sculpture of the new species are so distinct that it should be treated as a subgenus.

Etymology: Named after the characteristic prodorsal sculpture.

Berniniella (Canaloppia) borhidii sp. n.
(Figs 9–16)

Measurements. – Length of body: 252–258 μm, width of body: 137–143 μm.

Prodorsum: Rostrum tripartite, rostral apex aproximately pointed, longer than the lateral teeth. Rostral incisions very deep and broad, the three parts well separated. Costulae conspicuous and uniquely shaped. Behind the rostrum one pair of apophyses is present, their apex bearing the rostral setae (Fig. 10). From innner margin of these structures a pair of laths run to the basal part of the prodorsum, between them is a longitudinal hollow. In the basal region a pair of typical, horn-shaped, well sclerotised costula present, which are tightly connected to the dorsosejugal margin of the notogaster. A pair of thinner, longitudinal laths run laterally, without connection of the basal ones. Some rounded sigillae are also present in the lateral part of the prodorsum. Bothridia large, also well sclerotised, each with a relatively small, nearly triangular apophysis. Two pairs of sigillae present in the interbothridial region directed backwards on their posterior margin. Alongside porose areas observable. Prodorsal setae, except the lamellar ones, strong, setiform, well ciliate. No essential difference exists among them. Sensillus long, bent inwards (Fig. 9), pectinate, its peduncle slightly incrasate, but without typical clavate head, with 8 long branches.

Notogaster: Rounded. Median part of the dorsosejugal region elongated anteriorly and deeply penetrates into the interbothridial region (Fig. 9). No cristae observable, but a pair of weak longitudinal thickenings present medially. Ten pairs of notogastral setae present, setae c_2 of the same size and only slightly shorter than the remaining others, all setae simple, smooth. Setae *lm* arising clearly anterior to setae *la*.

Lateral part of podosoma: Acetabula I-IV normal, lying at the same level (Fig. 12) Exobothridial and acetabular regions well sclerotised, partly granulated. Pedotecta I very small, pedotecta

II-III reduced, discidium short, with protuberances. Exobothridial setae each arising from an apophysis, alveoli of the secomd reduced pair of exobothridial setae conspicuous.

Ventral parts of the body: Epimeral borders and apodema normally developed except the longitudinal sternal border between *bo.* 2 and *bo. sej.*, while other parts are reduced. Epimeral borders *bo. sej.* with a pair of longitudinal crests medially. Epimera III and IV normal in shape, with serrated posterior border (Fig. 11). Epimeral setal formula: 3 – 1 – 3 – 3. Setae *1c* located laterally,

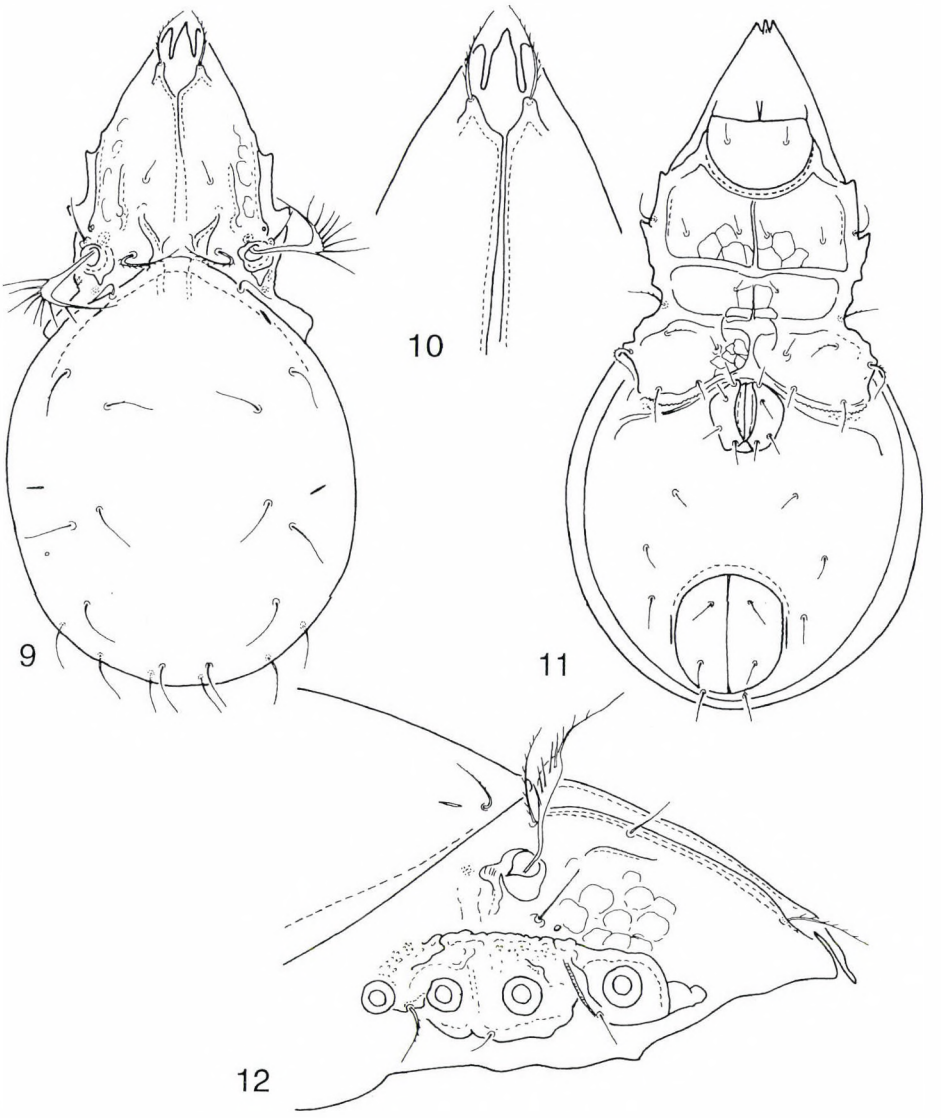

Figs 9–12. *Berniniella (Canaloppia) borhidii* sp. n. 9: body in dorsal view, 10 = rostrum, 11 = body in ventral view, 12: lateral part of podosoma

on the margin of pedotecta I. Setae *4c* arises on pedotecta IV. Epimeral setae of normal size, setae *1c, 3c, 4b* and *4b* well ciliated, all others nearly smooth.

Genital opening much smaller than anal one. Anogenital setal formula: 4 – 1 – 2 – 3. Position of the aggenital setae normal, setae ad_1 in postanal position. Setae in this region mostly smooth.

Infracapitulum, chelicera and palps normal.

Legs: Form and setation of leg I and IV as shown on figures 13–16.

Material examined: Holotype: México: Hidalgo: near Pachuca. Cultived field "La Estanzuela", 25.X.1997. leg. J. PALACIOS-VARGAS. 3 paratypes from the same sample. Holotype (1596–HO-98) and 1 paratype (1596–PO-98) (with identification numbers of the specimens in the Collection of Arachnida) deposited in the Hungarian Natural History Museum, Budapest, 1 paratype in the Laboratorio de Ecologia y Sistemática de Microartrópodos, Depto. Biologia, Fac. Ciencias, UNAM, México and 1 paratype in the Muséum d'Histoire naturelle, Geneve.

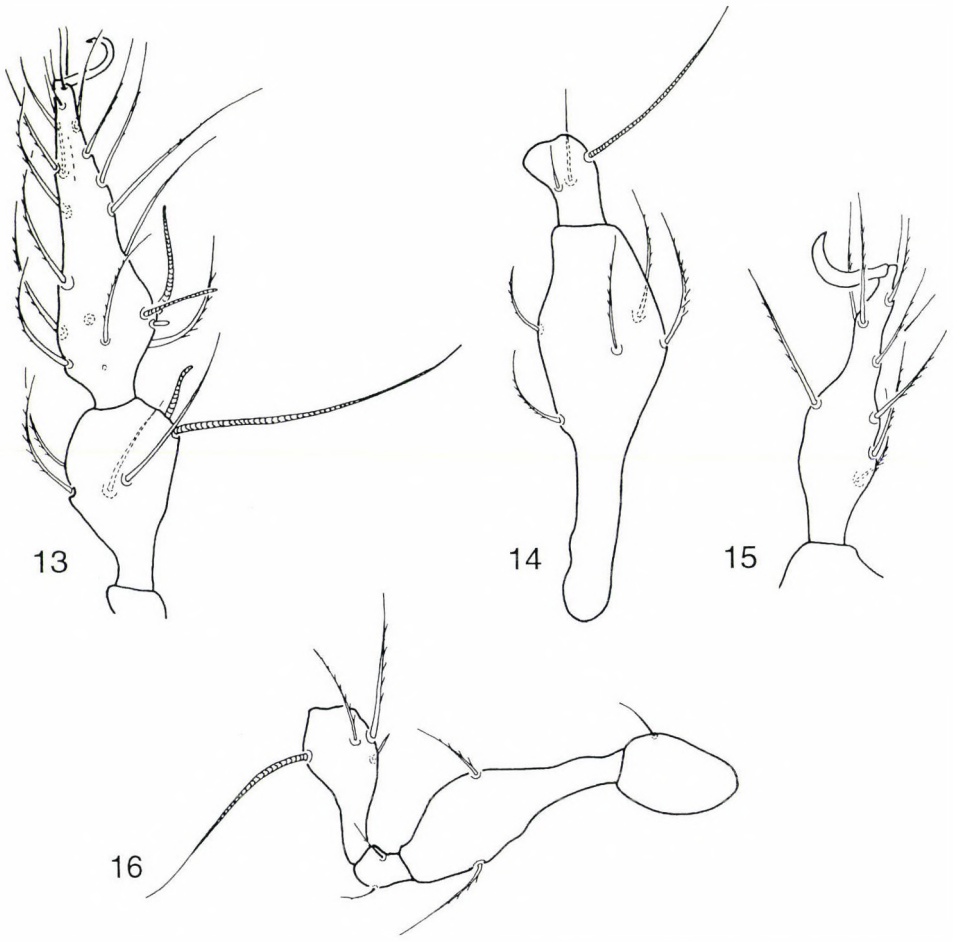

Figs 13–16. *Berniniella (Canaloppia) borhidii* sp. n. 13: tibia and tarsus of leg I, 14 = femur and genu of leg I, 15: tarsus of leg IV, 16 = trochanter, femur genu and tibia of leg IV

Remarks: The new species is well distinguishable from all related taxa by the unique structure, longitudinal hollow in the rostral region of the prodorsum.

Etymology: We dedicate the new species to our friend Dr A. BORHIDI, the renown botanist, and the head of our project.

Microppia minus (PAOLI, 1908)

The only hereto known locality of this species from Mexico is given by MORENO (1985). The specimens found in our study are identical with the European nominate specimens.

Oppiella nova (OUDEMANS, 1902)

Also according to PALACIOS-VARGAS (1994), this species is already recorded in Mexico. The examined specimens are well sclerotised and strongly haired. They match the European nominate type.

Pararamusella gen. n.

Diagnosis: Family Oppiidae GRANDJEAN, 1951, subfamily Oppiellinae SENICZAK, 1975. Rostrum rounded. Prodorsal surface without costulae, a fine lamellar line and three pairs of interbothridial sigillae. Sensillus fusiform, ciliate dorsally and ventrally as well. Notogaster without crista, nine pairs of setae and one pair of alveoli (for setae c_2) present. Exobothridial surface well sclerotised, covered by granules. A characteristic sclerotised plate present in front of acetabula I. Position of the acetabula of legs characteristic, acetabula IV removed posteriorly, far from acetabula III. Discidium long, reaching acetabula IV. In the sternal region there is a pronounced minitectum. Epimer I-II narrow, epimer III and IV very large, their posterior borders directed posteriorly to acetabula IV.

Type species: *Pararamusella disiuncta* sp. n.

Remarks: The new genus is undoubtly related to the *Ramusella* HAMMER, 1962 group. In other genera and subgenera the position of the acetabula and, in connection with it, the structure of podosoma and the coxisternal region is normal. In the new genus as a consequence of the more backward position of leg IV. The shape of the coxisternal region changed as given in the diagnosis. The special plate in front of acetabulum I is also an important feature, as is the presence

of a pronounced minitectum in the sternal region. This is such a difference from the known related taxa that separation at the generic level is justified.

Etymology: The name indicates the close relationship with *Ramusella* HAMMER, 1962.

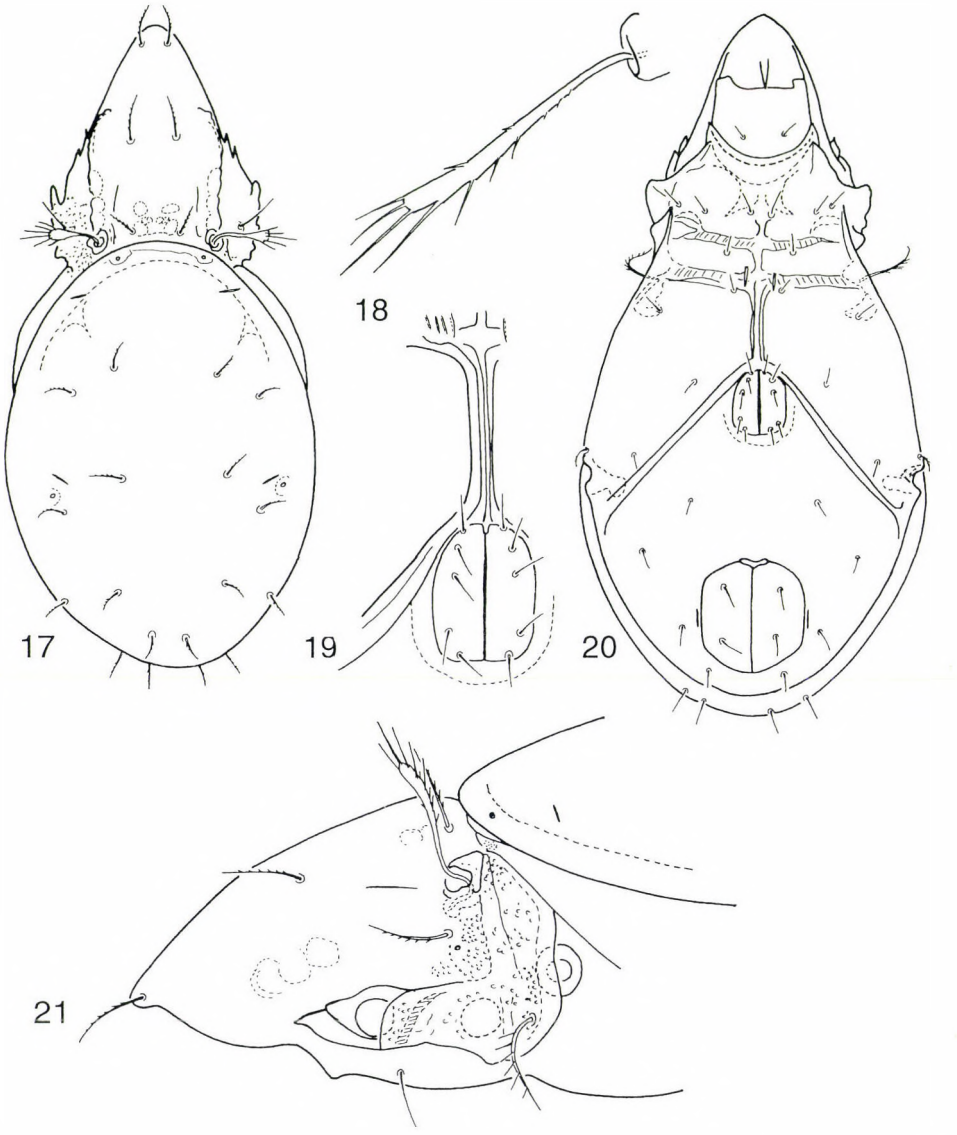

Figs 17–21. *Pararamusella disjuncta* gen. n., sp. n. 17: body in dorsal view, 18 = sensillus, 19 = median part of the coxisternal region and genital plates, 20 = body in ventral view, 21 = lateral part of podosoma

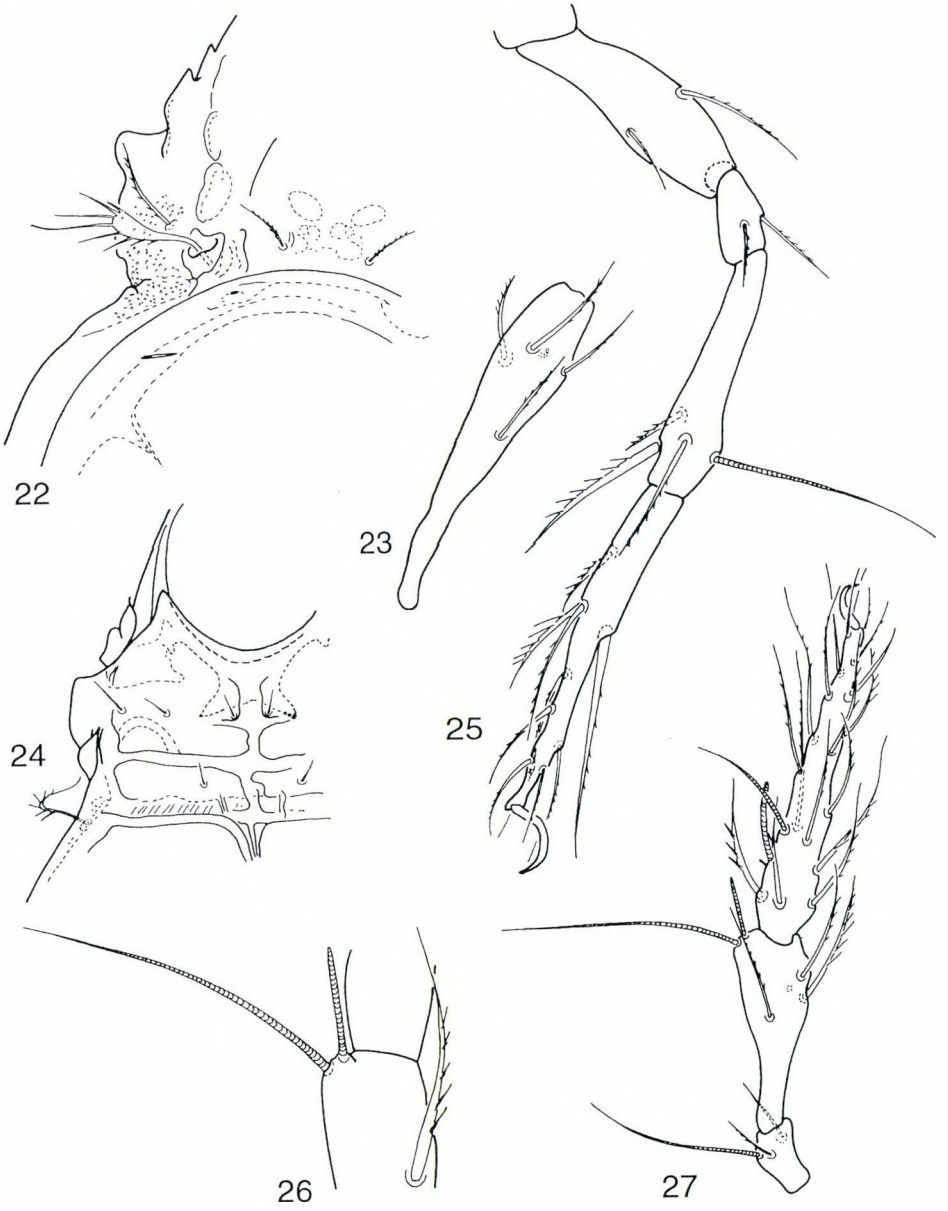

Figs 22–27. *Pararamusella disjuncta* gen. n., sp. n. 22: lateral part of prodorsum 23 = femur of leg I, 24 = anterior part of the coxisternal region, 25 = leg IV, 26 = solenidia of tibia I, 27 = genu, tibia and tarsus of leg I

Pararamusella disjuncta sp. n.
(Figs 17–27)

Measurements. – Length of body: 432–488 μm, width of body: 213–236 μm.

Prodorsum: Rostrum widely rounded. Prodorsal surface with a pair of short lamellar lines. Three pairs of interlamellar and some lateral sigillae present (Fig. 22). Bothridia relatively small, nearly oval with large posterior apophysis. Rostral setae arise far apart on the prodorsal surface. All four pairs of prodorsal setae setiform, well ciliated, no great difference among them (Fig. 21). Sensillus (Fig. 18), comparatively short with small head and radiate branches. A pair of porose areas present in the sejugal region, behind the bothridia.

Notogaster: Well elongated. Median part of the dorsosejugal suture slightly arched (Fig. 17). Nine pairs of notogastral setae present, setae c_2 represent only by their alveoli. All others short, but setiform, ciliated. Setae *la* arising clearly in front of *lm*.

Lateral part of podosoma: In front of acetabula I is a double, leaf-shaped, well sclerotised plate (Fig. 21). Acetabula IV located far posterior from acetabula III; distance between acetabula III and IV four times longer than the distance between acetabula II and III (Fig. 20). Exobothridial region and region between acetabula II and III well granulated. Pedotecta I large, pedotecta II–III missing, discidia very long, flat, reaching acetabula IV.

Ventral parts of the body: All epimeral borders and apodema well developed, except the anterior part of the sternal apodeme and borders. Epimera III and IV very large, apodema IV directed posterior to acetabula IV, straight, arched only near acetabula IV. Along the sternal apodeme a well developed tectum present (Fig. 19). Some short, longitudinal ridges also present on the sejugal borders (Fig. 20). Setae *1c* arise far medially from pedotecta I. Setae *4c* arise on pedotecta IV. Epimeral setae of normal size, setae *1c, 3c, 4b* and *4b* well ciliated, all others nearly smooth. Setae *3c* with very long cilia, some short ones visible on setae *4b* and *4c*. Epimeral setal formula: 3 – 1 – 3 – 3.

Genital opening much smaller than anal one. Anogenital setal formula: 5 – 1 – 2 – 3. Position of aggenital setae normal. Adanal setae ad_1 located posteriorly. Setae in the anogenital region smooth.

Infracapitulum, chelicera and palps normal.

Legs: All conspicuously long. Shape of leg I and IV shown on figures 23, 25–27.

Material examined: Holotype: México: Hidalgo: near Pachua. Cultivated field "La Estanzuela", 25.X.1997. leg. J. PALACIOS-VARGAS. 9 paratypes from the same sample. Holotype (1595–HO-98) and 5 paratypes (1595–PO-98) (with identification numbers of the specimens in the Collection of Arachnida) deposited in the Hungarian Natural History Museum, Budapest, 3 paratypes in the Laboratorio de Ecologia y Sistemática de Microartrópodos, Depto. Biologia, Fac. Ciencias, UNAM, México and 1 paratype in the Muséum d'Histoire naturelle, Geneve.

Remarks: The new species is well characterised by the long distance between acetabula III–IV.

Etymology: The name relates to the large distance between acetabula III and acetabula IV.

REFERENCES

BALOGH, J. (1983) A partial revision of the Oppiidae Grandjean, 1954 (Acari: Oribatei). *Acta zool. hung.* **29**: 1–79.

BEHAN-PELLETIER, V. M. (1984) Ceratozetes (Acari: Ceratozetidae) of Canada and Alaska. *Can. ent.* **116**: 1449–1517.

BORHIDI, A., MAHUNKA, S. & PALACIOS-VARGAS, J. G. (1996) Report on the first year activity carried out in the framework of Hungarian-Mexican soil zoological co-operation: "Diversity of the fauna of Mexico" 1995. *Folia ent. hung.* **57**: 79–85.

FRANKLIN, E. & WOAS, S. (1992) Some oribatid mites of the family Oppiidae (Acari, Oribatei) from Amazonia. *Andrias* **9**: 5–56.

MAHUNKA, S. (1983) Neue und interesante milben aus dem genfer Museum XLV. Oribatida Americana 6: Mexico II (Acari). *Revue suisse Zool.* **90**: 269–298.

MAHUNKA, S. (1996*a*) Oribatids from Sarawak I. (Acari: Oribatida). New and interesting mites from the Geneva Museum LXXVIII. *Revue suisse Zool.* **103**: 259–282.

MAHUNKA, S. (1996*b*) Oribatid mites (Acari: Oribatida) from Madagascar. II. Description of six species. *Folia ent. hung.* **57**: 109–123.

MORENO, J. A. (1985) Análisis de la variación estacional de los ácaros del suelo en la comunidad de bosque de Pinus hartwegii Lind. del Volcán Popocatépetl en el Estado de México. Tesis. Escuela Nacional de Ciencias Biológicas, Instituto Politécnico Nacional, México, D. F. 149 pp.

NORTON, R. A. (1982) Arborichthonius n. gen., an unusual enarthonote soil mite (Acarina: Oribatei) from Ontario. *Proc. Ent. Soc. Wash.* **84**: 85–96.

PALACIOS-VARGAS, J. G. (1994) Los acaros oribatidos de México. *An. Inst. Biol. UNAM, Mexico, Ser. Zool.* **65**: 19–32.

SUBIAS, L. S. & P. BALOGH (1989) Identification keys to the genera of Oppiidae Grandjean, 1951 (Acari: Oribatei). *Acta zool. hung.* **35**: 355–412.

SUBIAS, L. S., RODRIGUEZ, P. & M. E. MINGUEZ (1987) Los Oppiidae (Acari, Oribatida) de los sabinares (Juniperus thurifera) de Espana, V. Berniniella Balogh, 1983. *Cuad. Invest. Biol.* **10**: 35–50.

WOAS, S. (1986) Beitrag zur Revision der Oppioidea sensu Balogh, 1972 (Acari, oribatei). *Andrias* **5**: 21–224.

Received 26th February, 1998, accepted 10th November, 1998, published 30th December, 1998

Acta Zoologica Academiae Scientiarum Hungaricae 44 (4), pp. 297–310, 1998

NIDOMYIINI, A NEW TRIBE, GENUS AND SPECIES OF BORBOROPSIDAE (DIPTERA), WITH THE REDEFINITION OF THE FAMILY*

L. PAPP

Department of Zoology, Hungarian Natural History Museum
H–1088 Budapest, Baross u. 13, Hungary

A new species, *Nidomyia cana* sp. n. is described from Hungary as the type-species of *Nidomyia* gen. nov. The genus *Borboropsis* CZERNY, 1902 is re-described with notes, based mainly on the genitalia of *B. puberula* (ZETTERSTEDT, 1838). A redefinition of the family is given with a key for tribes and genera including Nidomyiini, new tribe. With 21 original figures.

Key words: Borboropsidae, *Nidomyia*, new species, genus and tribe, taxonomy, bird-nest

Borboropsis CZERNY, 1902 is a genus of Holarctic heleomyzoids: one Nearctic species (*B. steyskali* MATHIS, 1973) and one Palaearctic species *B. puberula* (ZETTERSTEDT, 1838), the type-species of the genus, have been described hitherto. *Borboropsis* was the only genus in the family Borboropsidae (or in other works, Borboropsinae of the family Heleomyzidae).

In the course of studies for a contribution to the Manual of Palaearctic Diptera, all unnamed heleomyzid material in the HNHM was reviewed in the last days of 1996. I soon realized that there were five (mostly defected) specimens of a peculiar species (collected in nests of raptorial birds at Bugac, Central Hungary), which was relegated to a new genus. In the spring of 1997, my young friends, MIHÁLY FÖLDVÁRI and PÉTER PAULOVICS collected 17 other specimens, far better preserved, in other nests of raptorial birds near Szeged (southern Hungary). After some time-consuming studies I propose that this new genus belongs to the family Borboropsidae, formerly not recorded from Hungary.

The type-specimens of the species described below are deposited in the collection of the Department of Zoology, Hungarian Natural History Museum, Budapest (HNHM).

Below after the description of the new genus and species, the genus *Borboropsis* CZERNY, 1902 is also re-described with notes, based mainly on the genitalia of *B. puberula* (ZETTERSTEDT, 1838). A redefinition of the family is given with a key for tribes and genera including Nidomyiini, a new tribe.

* This paper is regarded as one of the first results in the project "Large blank spots in the Diptera fauna of Hungary".

Nidomyia gen. nov.
(Figs 1–13)

Type-species: *N. cana* sp. n.

Gender: feminine.

Diagnosis: face strongly concave as in *Borboropsis* (Fig. 1); other characteristics shared with *Borboropsis*: arista thickened at base, frons with short scattered setae; flagellomere rounded; 2 pairs of *ors*, subequal (anterior pair slightly shorter) lateroclinate (as in *Borboropsis*), or anterior pair re- and slightly lateroclinate; *oc* very large, *vte, vti* all long; postocellars (postverticals) small and crossing; ocellars are just on the triangle formed by ocelli (similarly to *Borboropsis).*

Arista bare (in *Borboropsis* with short cilia); 1 pair of very long vibrissae, peristomal hairs comparatively short (only the first one longer) in 1 row, 1 genal row of bristles. Palpi comparatively long and thin.

Thoracic chaetotaxy similar to that of *Borboropsis*, no prosternals, 1 *h,* 2 *np,* 1 *prsut,* 2 + 3 *dc,* 1 *postalar sa, 1 posterior ia,* 1 *prsc ac* (medium long), apical and lateral *sc* pairs nearly evenly long. Acrostichal microchaetae comparatively large but shorter than in *Borboropsis*, in c. 3 unarranged rows. One long and 2 shorter pairs of katepisternals (sternopleurals), posterior anepisternals: 1 long, 2 shorter pairs (Fig. 1).

Tibiae with dorsal preapicals minute or even indiscernible on fore and mid tibiae (as in *Borboropsis*); mid tibia with only 1 strong ventroapical seta.

Subcosta of wing close to R_1 (as in *Borboropsis*), costal conjointment indistinct; subcostal break and humeral thinning similar to those in *Borboropsis.*

Abdomen: Male 5th segment normal, 5th sternite short and broad. Male postabdomen: sternite 6 placed leftside, hardly or not at all seen in dorsal view (Fig. 2), left 6th spiracle apparently in tergite 6 (right to the sagittal line), right spiracle 6 in membrane (Fig. 4), left spr7 in the sternite; sternite 7 rather long, placed leftside, completely separated from sternite 8; there is a small thin sclerite on the dorsal wall of the inner genital vault, which is possibly tergite 7 (Fig. 4), "pressed" mesally by tergite 6, which is elongated mesally; both tergite and sternite 6 thin pointed at their ventral end, those apices crossing over the sagittal line; sternite 8 extremely large, in dorsal position (Fig. 2), free from sternite 7; no trace of T8.

Male genitalia: epandrium (Figs 3–4) rather large semiglobular, shiny black with short setae only; cerci very small with short bristles, those on its apex not much longer; surstyli (Figs 3–4) free, very large, somewhat tapering towards apex but rounded apically with short and pointed setae on both surfaces; no editum, characteristic for the heleomyzids. Subepandrial sclerite forms a second vault over the genitalia with numerus rather long bristles (Fig. 4). Phallus (aedea-

gus, Figs 6, 7) short, fully asymmetrical with very large basiphallus; a comparatively large epiphallus present; parameres (Figs 6–8) with narrow base and ventrally with 4 strong setae; both aedeagal apodeme and ejaculatory apodeme rod-like (Figs 7–8); gonopods long (Fig. 6) asymmetrical (their armature, too) with

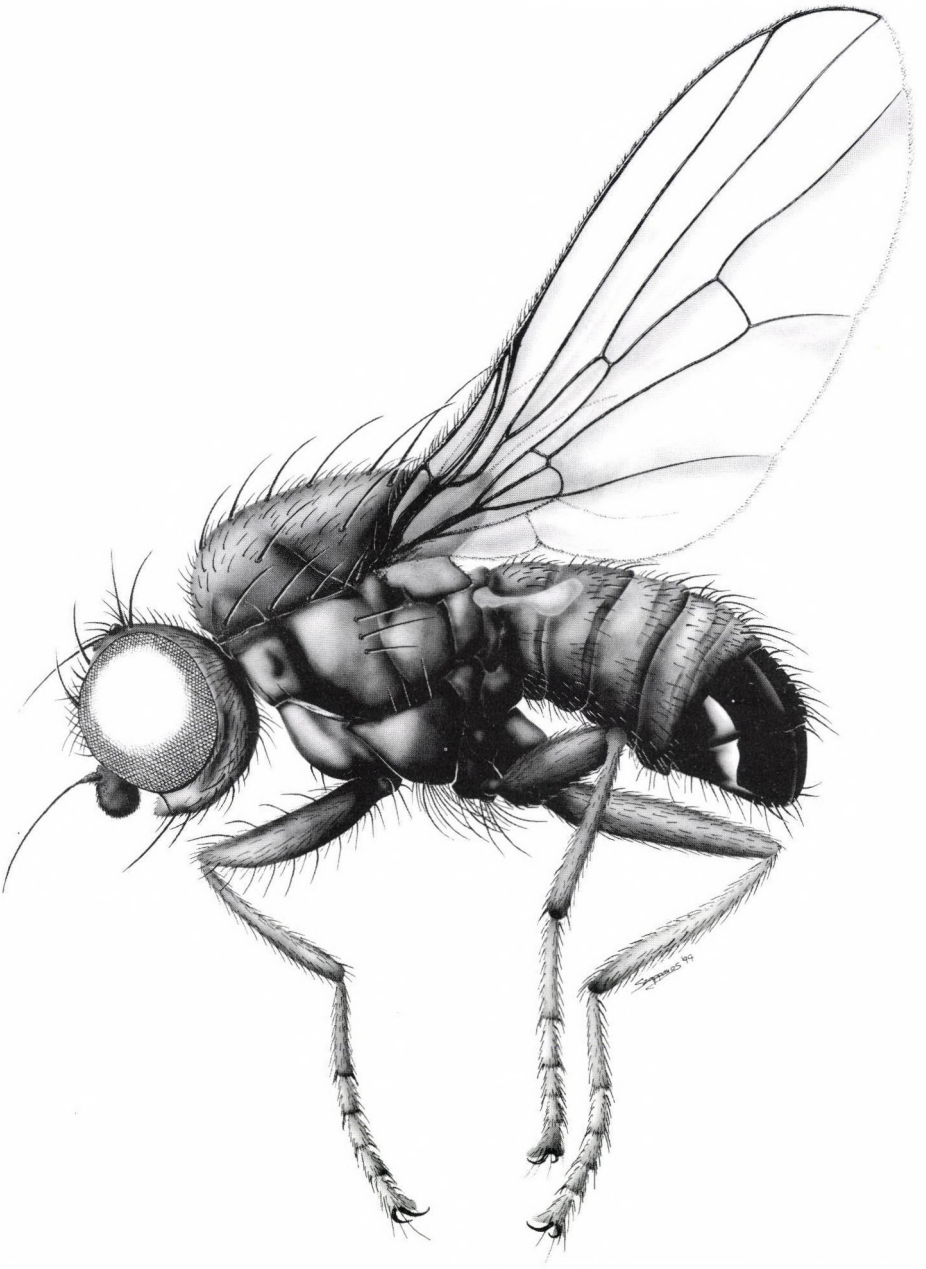

Fig. 1. *Nidomyia cana* sp. n., paratype male, habitus in lateral view

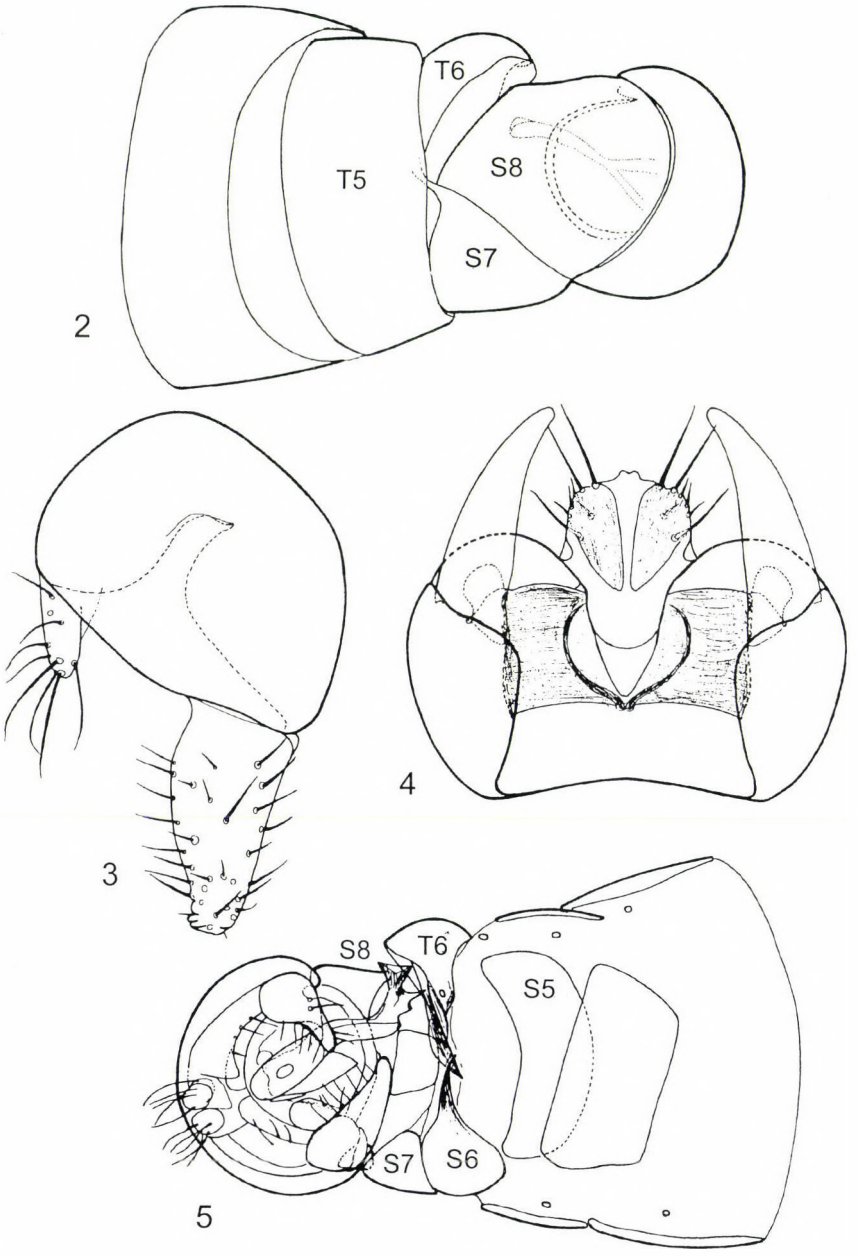

Figs 2–5. *Nidomyia cana* sp. n., male abdomen and genitalia: 2 = postabdomen, dorsal view; 3–4 = epandrium, cercus and surstylus: 3 = lateral view (right face), 4 = ventral view; 5 = postabdomen, ventral view. Scales: 0.2 mm for all

free caudal dorsal ends (not connecting there to any other parts by sclerotized connection) and with at least 3 ventral setae; hypandrium short and softly connected to the epandrium (Fig. 4).

Female abdominal tergites e.g. tergite 5 laterally with peg-like, short thick blunt pricks, instead of long bristles; tergite and sternite 6 otherwise normal; tergites and sternite 7 short with numerous long bristles (3 pairs on tergite), 7th spiracles in the tergite; tergite 8 not divided but small, sternite 8 minute in two parts. Epiproct and hypoproct very small, former one with a pair of long bristles apically. Female cerci (Figs 10–11) extremely small, only slightly overrunning apices of epiproct and hypoproct. Three globular spermathecae (2+1; Figs 12–13), ducts sclerotized on a short section, separate duct of the double spermathecae not seen from outside.

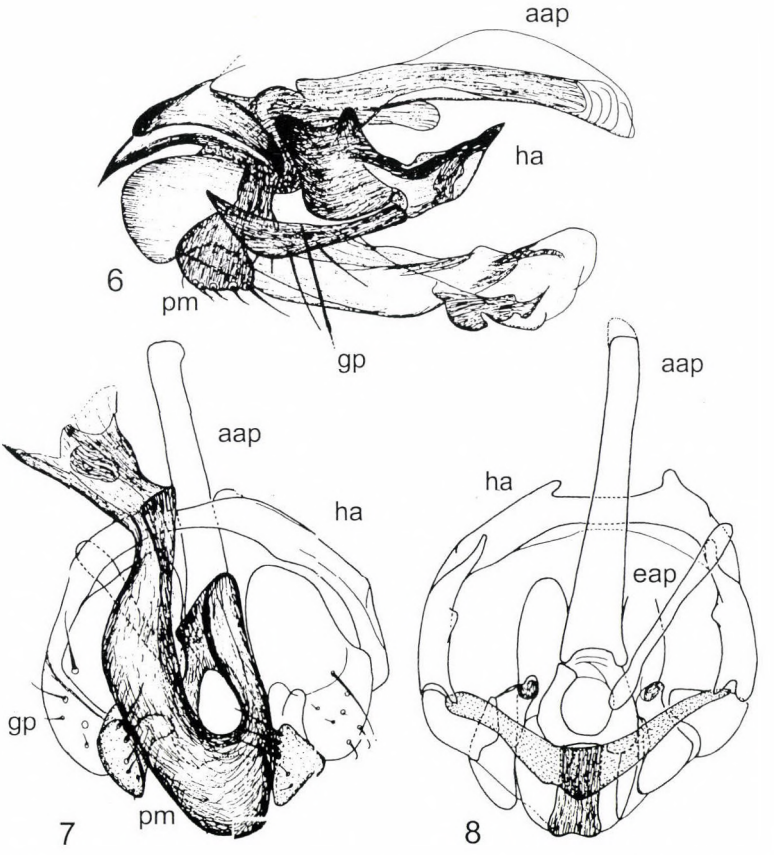

Figs 6–8. *Nidomyia cana* sp. n., male paratype, inner genitalia. 6 = lateral view, 7 = ventral view (epiphallus fully covered and so not depicted here); 8 = dorsal view (only basiphallus depicted here) (aap: aedeagal apodeme, eap: ejaculatory apodeme, gp: gonopod, ha: hypandrium, pm: paramere). Scale: 0.2 mm for all

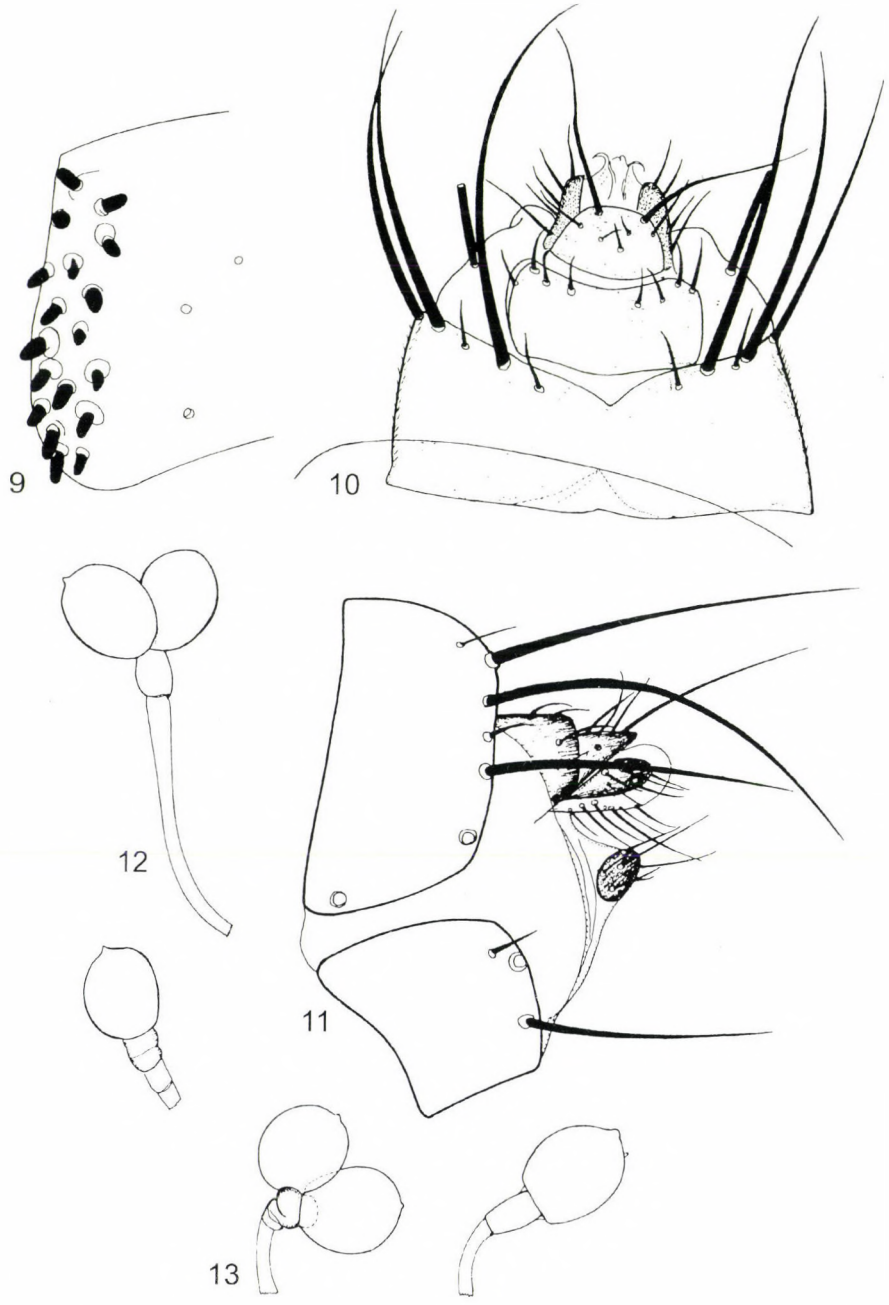

Figs 9–13. *Nidomyia cana* sp. n., paratype females, abdomen and genitalia. 9 = lateral part of tergite 5; 10–11 = postabdomen: 10 = dorsal view, 11 = extended, in lateral view; 12 and 13 = spermathecae of two specimens. Scales: 0.2 mm

Nidomyia cana sp. n.
(Figs 1–13)

Measurements in mm: body length 2.42 (holotype), 2.30–2.50 (paratype males), 2.50–3.15 (paratype females), length of wing 2.40 (holotype), 2.40–2.65 (paratype males), 2.58–3.17 (paratype females), width of wing 0.95 (holotype), 0.95–1.12 (paratype males), 1.05–1.23 (paratype females).

Head light grey but frons anteriorly as well as gena and face diffuse dirty yellow. Longitudinal axis of eye/genal width below eye: 0.64 mm/0.13 mm. Flagellomere reddish yellow basally on medial surface; pedicel and scape short, pedicel with a long thin dorsal apical bristle. Anterior *ors* thinner and nearly as long as length of posterior one. No facial carina but face concave. Peristomals medium long in one row, one row of upcurving genal bristles above. Palpi comparatively long and thin, reddish yellow with 4 ventral bristles. Proboscis short. Arista bare, shorter than head, its base much thickened.

Thorax light grey, covered with thick microtomentum, abdomen darker, male postabdomen shiny black. One propleural just above fore coxa plus 1 short bristle more caudally; 1 long posterior and 2 more anterior shorter pairs of katepisternals (Fig. 1).

Wings light greyish, almost clear, costal and other veins yellowish. Costal spinulae very small, hardly discernible but definitely no such spinulae in *Borboropsis*. Terminal section of vein M 0.89 mm, intercrossvein section 0.425 mm (male). Calyptral cilia white. Halteres pale yellow.

Legs mainly grey, knees and tarsi greyish yellow. Dorsal preapicals on tibiae indiscernible.

Abdomen darker grey than mesonotum, preabdominal spiracles in membrane (incl 5th pair of male); male postabdomen bright black, i.e., sternites 7 and 8 shiny black.

Male genitalia: epandrium (Figs 3–4) rather large semiglobular, shiny black with short setae only; cerci very small with short bristles, those on its apex not much longer; surstyli (Figs 3–4) free, very large, somewhat tapering towards apex but rounded apically with short and pointed setae on both surfaces; no editum, characteristic for the heleomyzids. Subepandrial sclerite rather large (Figs 3–4, 7); there is a short but very wide plate over the epiphallus (reaching the gonopods in dorsal view) which may be called as metaphallic plate, and which may be a derivative of subepandrial sclerite. Phallus (aedeagus, Figs 6, 7) short, fully asymmetrical with very large basiphallus; a comparatively large epiphallus present; parameres (Fig. 6) with narrow base and ventrally with 4 strong setae; aedeagal apodeme comparatively long rod-like; a narrow rod-like ejaculatory apodeme present (Figx 7–8); gonopods long (Fig. 6) asymmetrical (their armature, too) with free caudal dorsal ends (not connecting here to any other parts by sclerotized connection) and with at least 3 ventral setae; hypandrium short and softly connected to the epandrium (Fig. 8).

Female abdominal tergites 3 to 6 laterally with peg-like, short thick blunt pricks (Fig. 9), instead of long bristles; tergite and sternite 6 otherwise normal, sternite 6 broad, almost reaching margins of tergite 6 (preabdominal sternites narrower); tergites and sternite 7 short with numerous long bristles (3 pairs on tergite), 7th spiracles in the tergite; tergite 8 not divided but small, sternite 8 minute in two parts. Epiproct and hypoproct very small, former one with a pair of long bristles apically. Female cerci (Figs 10–11) extremely small, only slightly overrunning apices of epiproct and hypoproct. Integument in postabdomen strong enough to bear so large and thick setae as given in Fig. 10. Three spermathecae (2+1; Figs 12–13) globular with a minute tit-like dorsal central wart, ducts sclerotized on a short section, separate duct of the double spermathecae not seen from outside.

Holotype, male (HNHM) – Hungary: Kiszombor, Maros-part – héjafészek fehérnyáron [goshawk nest on white poplar], 10–11 m – 1997.VI.10., leg. FÖLDVÁRI & PAULOVICS (together with 3 males + 1 female of *Carnus hemapterus*).

Paratypes (all HNHM, double-mounted): 8 males + 8 females (one in copula): Szeged, Szőreg, Budzsáki-erdő – ragadozómadár fészek tölgyfán [raptor's nest on oak], 7–8 m – 1997. VI. 10., leg. FÖLDVÁRI & PAULOVICS (together with a male of *Gymnochiromyia (?) inermis* COLLIN, 1933). 2 males + 3 females: Bugac, Bugacpusztaháza, leg. J. RUDNER, 1990: 1 male + 1 female: 8

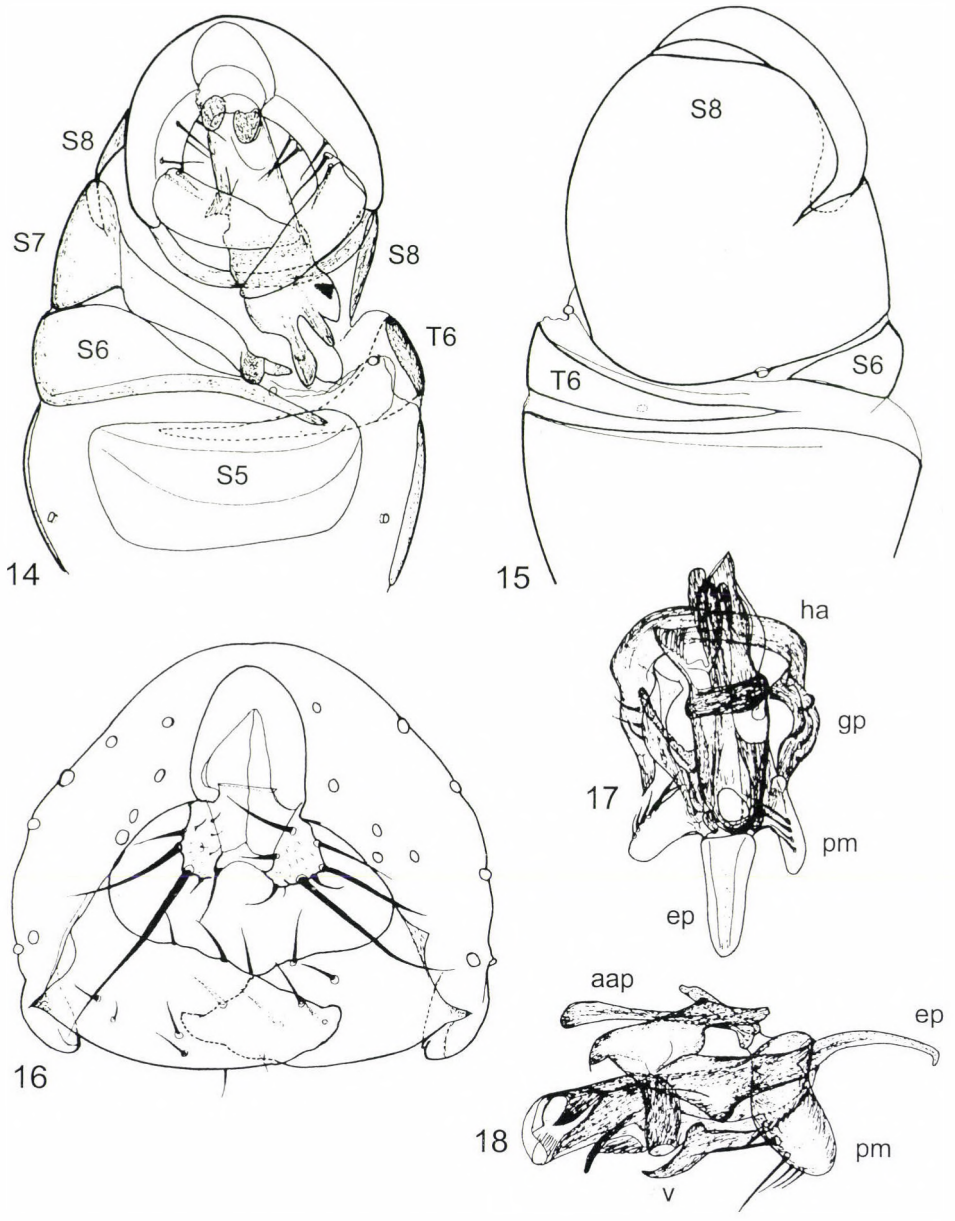

Figs 14–18. *Borboropsis puberula* (ZETTERSTEDT), male. 14 = postabdomen: 14 = ventral view, inner genitalia not drawn (all setae omitted, except on subepandrial sclerite; vestige of tergite 7 in black, covered by phallus in this view), 15 = dorsal view; 16 = epandrium, cerci and surstyli in caudal view (epandrial setae omitted); 17–18 = inner genitalia: 17 = lateral view, 18= ventral view (aap: aedeagal apodeme, eap: ejaculatory apodeme, ep: epiphallus, gp: gonopod, ha: hypandrium, pm: paramere, v: ventral sclerite of phallus)

May, *Populus alba*, 8 m, ex nido *B. buteo*; 1 male + 1 female: ibid., 24 May; 1 female: ibid., 5 June, *Populus canadensis*, ex nido *Accipiter gentilis*.

Remark on habits of *N. cana*. The structure of the female abdomen clearly refers to a peculiar way of life. The females may probably be hidden in the plumage of the raptorial birds. The wings of the first captured five specimens were defected ("frayed"), which I thought to be damages during their capturing. Contrarily, some of the specimens collected in 1997 with much care, had wings damaged in the same way. I suppose, this is again a consequence of their movement among the feathers. If these flies are really specialized to live in raptorial bird nests, they have difficulties in finding a "new" nest, and so probably change nests attached to the birds. The structure of the female postabdomen suggests a macrooviparous, or even larviparous habit (the abdomen of three females, which were dissected, do not contain any eggs or else). The mouth-parts of the adults are of a simple sucking type, i.e., they show no signs of any adaptation of blood-sucking etc. (there are no piercing parts in it). In any case, further observations on the habits of *N. cana* are necessary.

Borboropsis CZERNY, 1902
(Figs 14–21)

CZERNY 1902: Wien. ent. Z. 21: 256.
Type-species: *Anthomyza fulviceps* STROBL, 1898: 269 (mon.).
MATHIS 1973: 373, 376.

Small, body length 2–3 mm. Two pairs of lateroclinate fronto-orbitals. Face strongly concave. Genal bristles comparatively weak upcurved, in one row. Interfrontals unarranged. No definite vibrissal angle but 1 pair of very long crossing vibrissae present. Mouth opening small. Palpi small but not thin. Arista with short or longer cilia.

Thoracic pits present dorsally between pronotum and mesonotum. Mesonotal microchaetae very strong. Dorsocentrals comparatively weak, presutural *dc*-s not distinct from the microchaetae, 2 longer postsutural pairs. Prescutellar pair of *ac* very long. Anepisternum with 1 long and several shorter bristles. Prosternum bare. One proepisternal, 1 strong katepisternal bristle only.

Males with tergite 6 short and not elongated mesally (contrarily to *Nidomyia*); sternite 6 broader and a good part of it arched dorsally; both spiracles 6 in membrane (not far from each other): right one rightside, medially to the margin of tergite 6, left one in the membraneous vault of genitalia below sternite 6 (Fig. 15); a questionable 7th spiracle found dorsally on edge of sternite 7; sternite 7 overrunning sagittal line from left to right; sternites 7 and 8 mostly fused (Fig. 15); vestige of the 7th tergite minute but present; no vestige of 8th tergite detected. Subependrial sclerite large with several long setae, form a second genital vault under epandrium (Fig. 14).

Female postabdomen cylindrical-conical, convex even at rest (Fig. 19). Tergite 8 and sternite 8 nearly fused into a tube, spiracle 7 in the tergite at anterolateral margin.

Eggs extremely large (see below).

Borboropsis puberula (ZETTERSTEDT, 1838) (Figs 14–21)

Anthophilina puberula ZETTERSTEDT, 1838: 785; ZETTERSTEDT 1848: 2697.
Anthomyza fulviceps STROBL, 1898: 34(1897): 269.
Trixoscelis puberula (ZETTERSTEDT): CZERNY 1924: 123.
Borboropsis fulviceps (STROBL): CZERNY 1924: 21–22, GORODKOV 1970: 310, MATHIS 1973: 373, 376 and other authors.
Borboropsis puberula (ZETTERSTEDT): HACKMAN & ANDERSSON 1969: 269, PAPP 1981: 39, GORODKOV 1984: 18.

Material studied (all deposited in HNHM): Finland, leg. MIHÁLYI F., 1967: 4 males, 3 females: NL68°, Pallastunturi, Pyhäjoki – 27., 29. VII.; 1 female: ibid., meat trap, 28.VII.; 4 male: ibid., but without "Pyhäjoki"; 1 male: NL69°, Kilpisjärvi, 28. VII. Austria, leg. Zs. BAJZA and L. PAPP, 1974: 1 female: Obergurgl Untergurgl között [between], Pirchhüttenberg – *Larix* erdő

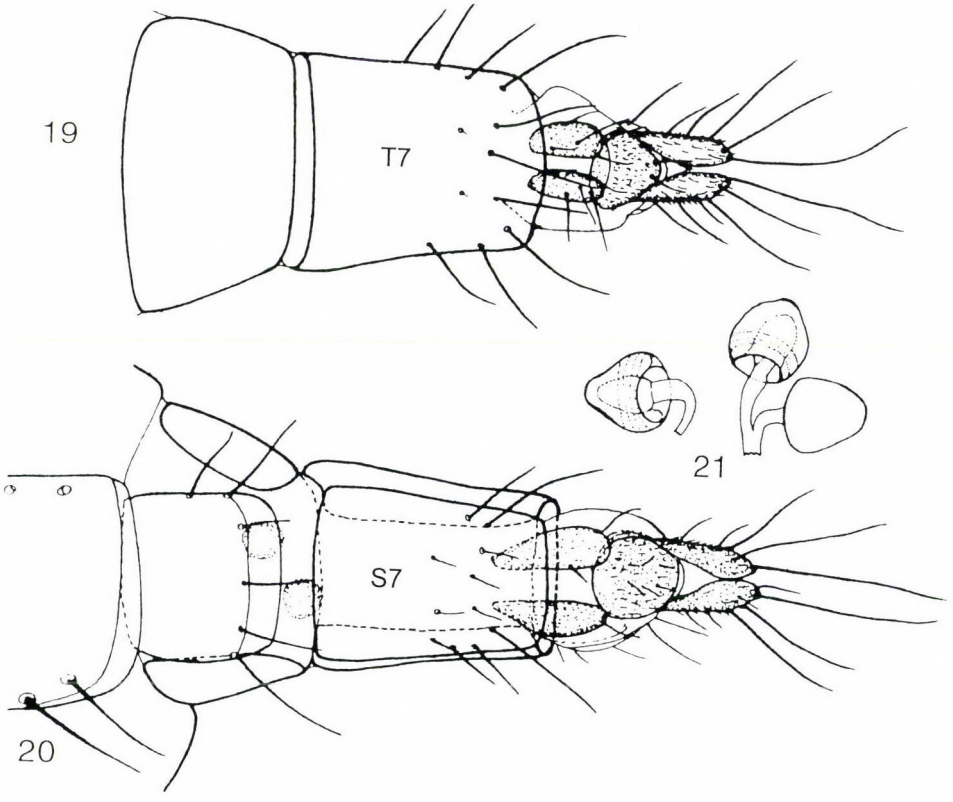

Figs 19–21. *Borboropsis puberula* (ZETTERSTEDT), female. 19–20 = postabdomen: 19 = dorsal view, 20 = ventral view (lateral margins of T7 covered by S7); 21 = spermathecae (scale bars: 0.2 mm)

[forest], 23. VII.; 1 female: Pillersee, 1777 m, fenyőerdő [fir forest], 24. VII. Slovakia: 1 male: Tátralomnic, patak mellett [Tatranska Lomnica, beside a creek], 900 m, 1963. VIII.4., leg. MIHÁLYI F. North Korea, leg. S. HORVATOVICH et J. PAPP, 1971: Prov. Ryang-gang, Plateau Chann-Pay, Samzi-yan, 1500 m, 24. Aug. – No. 195; 1 female: ibid., 1700 m, 27.Aug., No. 206; 1 male: Prov. South Pyongan, Sa-gam – No. 165, 12.VIII. New to Korea.

Dorsal preapical bristle indistinct also on hind tibia, no costal spines.

Male preabdominal sternites comparatively narrow, sternite 5 slightly asymmetrical (Fig. 14), sternite 6 mostly ventral (lateral apex reaching sagittal line dorsally; sternite 7 and 8 partly fused (Fig. 15), sternite 8 extremely large and fully dorsal; no remnant of tergite 8 was detected; epandrium not large and short, cerci comparatively very small with long bristles. Surstyli (Fig. 16) large tapering but not pointed at apex with rather short bristles. Subepandrial sclerite large – forming a second vault over the genitalia – and as broad as half of epandrium. Inner genitalia fully asymmetrical with an extremely large epiphallus (Figs 17–18), phallus short, fully asymmetrical, a distinct, well sclerotized and partly detached ventral sclerite of the phallus present (Fig. 17); parameres very large with several strong setae (Fig. 18); aedeagal apodeme comparatively short, rod-like, lying parallel with phallus when at rest; ejaculatory apodeme short rod-like but distinct; hypandrium short (Fig. 17), ventrally fused with gonopods; gonopods somewhat asymmetrical with strong ventral setae.

Female postabdomen convex even at rest, though telescopized (also segment 6). Segment 6 comparatively short, tergite 6 only 2/3 of the length of 5th. Tergite and sternite 7 forming a long tube though they are not fused. Both tergite and sternite 8 in two parts, all those 4 sclerites very small. Epiproct small with a pair of short apical setae (Fig. 19), hypoproct as small as epiproct (Fig. 20). Cerci not fused, much longer than in *Nidomyia*, with very long bristles. Three (2+1) spermathecae (Fig. 21), pear-shaped, duct short. Eggs extremely large, 0.43 mm long and 0.17 mm broad from a female collected in Austria.

The figure of the male genitalia, which was published by HACKMAN and ANDERSSON (1969), was obviously made of a male of *B. puberula*. However, the epiphallus is not drawn on it, connections of the genital parts are not seen but gonopods with their strong setae are depicted. GRIFFITHS' (1972) figure (fig. 110) is so much distorted that connections of genital parts or even some genital parts are not recognizable the gonopods are simply abandoned.

A Holarctic species, reported also from Alaska, Canada (MATHIS 1973) and the Russian Far East (GORODKOV 1984); in Europe from Sweden, Finland, Great Britain and Austria (GORODKOV 1984) and also from Slovakia (PAPP 1981); in the collection of the HNHM there are specimens also from North Korea.

The characters of the new genus seem so peculiar that also a new tribe is set up for it. The differences from Borboropsini are summarized in the key below. The characters evaluated at the tribal level come first; they are selected in view of the considerations, which characters are used in separating subfamilies/families or tribes in the superfamily Heleomyzoidea.

KEY TO THE TRIBES AND GENERA OF BORBOROPSIDAE

1 (2) Thoracic pits present dorsally between pronotum and mesonotum. Presutural dorsocentrals not separable from the extremely long microchaetae. Male 7th and 8th sternites mostly fused (Fig. 15). Female postabdomen cylindrical-conical, convex even at rest (Fig. 19), though telescopized, tergite and sternite 7 forming a long tube (BORBOROPSINI) – Male epiphallus extremely long. Arista with short cilia. Lateral parts of female tergites without peg-like prickles, the double spermathecae (Fig. 21) with distinct separate ducts (Holarctic) *Borboropsis* CZERNY, 1902

2 spp., *B. puberula* (ZETTERSTEDT, 1838) is with a Holarctic distribution. The relegation of a second species, *Borboropsis steyskali* MATHIS, 1973, to the genus needs corroboration.

2 (1) Thoracic pits less distinct. Dorsocentrals in 2+3 pairs, mesonotal microchaetae shorter than in *Borboropsis*. Male 7th and 8th sternites completely separated (Fig. 2). Female postabdomen extremely short, definitely concave when at rest (NIDOMYIINI new tribe). – Male epiphallus strong but not extremely long (Fig. 6). Arista bare. Lateral parts of female tergites with strong peg-like prickles, the double spermathecae (Figs 12–13) without separate ducts seen from outside (Hungary) **Nidomyia** gen. n.

One species, *N. cana* L. PAPP is described here from nests of raptorial birds in South Central Hungary.

After the description of this new genus and tribe, it is necessary to re-define the family Borboropsidae (or subfamily Borboropsinae), as follow.

Face strongly concave (Fig. 1). Two pairs of strong fronto-orbitals: lateroclinate, or anterior pair re- and slightly lateroclinate; *oc* very large, *vte, vti* all long; postocellars (postverticals) small and crossing; ocellars are just on the triangle formed by ocelli. Arista bare or with short cilia only.

2 + 3 pairs of dorsocentrals or only 2 postsutural pairs detectable in the strong mesonotal microchaetae. Anepisternum with 1 to 3 long and several shorter bristles. Prosternum bare.

Tibiae with dorsal preapicals indiscernible on fore and mid tibiae; mid tibia with only 1 strong ventroapical seta. Costal vein without strong spiniform setae, bM-Cu basal crossvein present, anal vein A_2 long extending to the wing margin, also an axial vein-fold discernible.

Male tergite 7 almost completely reduced (only a vestige present), postabdomen with small or very small cerci, which bear long bristles. Surstyli large and

free, no trace of an "editum" or "second telomere". Phallus short, extremely asymmetrical but rigid with strongly sclerotized sclerites. Phallophore bearing large epiphallus (Figs 6, 16). Aedeagal apodeme comparatively short, rod-like, c. parallel with aedeagus when at rest. A medium-long but distinct rod-like ejaculatory apodeme present. Parameres (postgonites") large with strong setae. Gonopods are distinct or even large sclerites with long setae. Hypandrium short, ventrally fused with gonopods. Subependrial sclerite large and setose, forming a second genital vault under epandrium (hindgut running between the two vaults). Male sternite 7 and sternite 8 large to extremely large in dorsal position (completely separated: *Nidomyia*, or mostly fused: *Borboropsis*). I was unable to detect any trace of male tergite 8; vestige of tergite 7 was found in both tribes, however, I do not regard its presence as very important in the analysis of phylogenetic relationships among heleomyzoids.

The female postabdomen is extremely different in the two tribes, so presently no character is to be evaluated of this taxonomic level. Three (2+1) small spermathecae (Figs 12–13, 21).

* * *

Acknowledgement – I would like to thank Dr ALBERT SZAPPANOS (Kecskemét, Hungary) for the habitus figure and to MIHÁLY FÖLDVÁRI and PÉTER PAULOVICS (Department of Ecology, József Attila University, Szeged) for their efforts to collect adults of *N. cana*.

REFERENCES

CZERNY, L. (1902) Bemerkungen zu den Arten der Gattung Anthomyza Fll. und Ischnomyia Loew. *Wien. ent. Z.* **21**(10): 249–256.

CZERNY, L. (1903) Bemerkungen zu den Arten der Gattung Geomyza Fll. *Wien. ent. Z.* **22**: 123–127.

CZERNY, L. (1924) Monographie der Helomyziden. *Abh. zool.-bot. Ges. Wien* **15**(1): 1–166.

GILL, G. D. (1962) The heleomyzid flies of America North of Mexico (Diptera: Heleomyzidae). *Proc. U.S. natn. Mus.* **113**(3465): 495–603.

GILL, G. D. & PETERSON, B. V. (1987) Chapter 89. Heleomyzidae. Vol. 2, pages 973–980, *in* MCALPINE, J. F. et al. (eds): *Manual of Nearctic Diptera*. Research Branch, Agriculture Canada, Ottawa. Agric. Can. Monograph No. 28, vi + 675–1332 pp.

GORODKOV, K. B. (1970) 80. Sem. Helomyzidae (Heleomyzidae). *In*: STACKELBERG, A. A. and NARTSHUK, E. P. (eds): *Opredelitel' nasekomykh evropejskoj chasti SSSR*. **5**(2): 306–325. [In Russian]

GORODKOV, K. B. (1984) Family Heleomyzidae (Helomyzidae). Vol. 10, pages 15–45, *in* SOÓS, Á. and PAPP, L. (eds): *Catalogue of Palaearctic Diptera*. Akadémiai Kiadó, Budapest, 402 pp.

GRIFFITHS, G. C. D. (1972) *The phylogenetic classification of Diptera Cyclorrhapha with special reference to the structure of the male postabdomen*. Series Entomologica, Vol. 8, Junk, The Hague, 340 pp.

HACKMAN, W. & ANDERSSON, H. (1969) Trixoscelis puberula (Zetterstedt), a heleomyzid fly (Diptera). *Notul. ent.* **49**: 269–270.

MATHIS, W. N. (1973) A review of the genus Borboropsis (Diptera: Heleomyzidae). *Pan-Pacif. Entomologist* **49**(4): 373–377.

PAPP, L. (1981) 54. család: Heleomyzidae – Tüskésszárnyú legyek. In: *Magyarország Állatvilága, Fauna Hungariae*, **15**(5): 1–77. Akadémiai Kiadó, Budapest.

STROBL, G. (1898) Die Dipteren von Steiermark, IV. Theil. *Mitt. naturw. Ver. Steierm.* **34**(1897): 192–298.

ZETTERSTEDT, J. W. (1838) *Insecta Lapponica*. Lipsiae, 1139 pp.

ZETTERSTEDT, J. W. (1848) *Diptera Scandinavica*. Lund, 7: 2581–2934 pp.

Received 10th August, 1998, accepted 25th September, 1998, published 30th December, 1998

Acta Zoologica Academiae Scientiarum Hungaricae 44 (4), pp. 311–327, 1998

SEVEN NEW SPECIES OF NOCTUIDAE (LEPIDOPTERA) FROM ASIA

GYULAI, P.[1] and L. RONKAY[2]

[1]*H-3530 Miskolc, Mélyvölgy u. 13/A, Hungary*
[2]*Department of Zoology, Hungarian Natural History Museum*
H-1088 Budapest, Baross u. 13, Hungary
E-mail: ronkay@zoo.zoo.nhmus.hu

Description of seven new Noctuidae species, *Discestra rosea* sp. n. (China, Tibet), *Hada fraterna* sp. n. (China, Tibet), *Lacanobia w-latinoides* sp. n. (Uzbekistan), *L. kirghisa* sp. n. (Kirghisia), *L. altyntaghi* (China, Altyn-Tagh), *Estagrotis roseosericea* sp. n. (China, Kuku-Noor) and *Amphipoea cuneata* sp. n. (Kirghisia) are given. With 33 figures.

Key words: Noctuidae, new species, Turkestan, China

INTRODUCTION

Present paper is the third contribution of the series dealing with the new taxa preserved in large private collections in Hungary and/or discovered by Hungarian lepidopterological expeditions (the second part was published by RONKAY & GYULAI (1997)), containing the descriptions of species discovered recently in Turkestan (Uzbekistan, Kirghisia) and in China.

The holotypes, deposited in coll. P. GYULAI (Miskolc, Hungary) are available for studies through the Hungarian Natural History Museum, Budapest.

Discestra rosea sp. n.
(Figs 1–2, 24)

Holotype: male, East Tibet, Quamdo, 3200 m, 14.06.1996, leg. W. FICKLER, Slide No. 722 GYULAI (coll. P. GYULAI).

Diagnosis: The new species has a very characteristic appearance, differing strongly from all known taxa of *Discestra* HAMPSON, 1905, by its pink ground colour of the forewings and the cilia; the pubescence of the body and of the legs is also pinkish. The pink colour appears in a few occasions in the less allied members of the genus-group, distributed only in the southern basin of the Mediterranean region, e.g. *Discestra pugnax atlantis* (SCHWINGENSCHUSS, 1955), and *Cardepia deserticola mauritanica* (ROTHSCHILD, 1920) and also in *Conisa-*

nia HAMPSON, 1905, species (e.g. *C. roseipicta* DRAUDT, 1950), but, in other respects, these species are (rather) strongly dissimilar.

The male genitalia of the new species differ from those of the species of the *D. marmorosa – D. pugnax* species-group by the presence of the serrated subbasal plate of the vesica, the less acute uncus and the longer, subapically broader

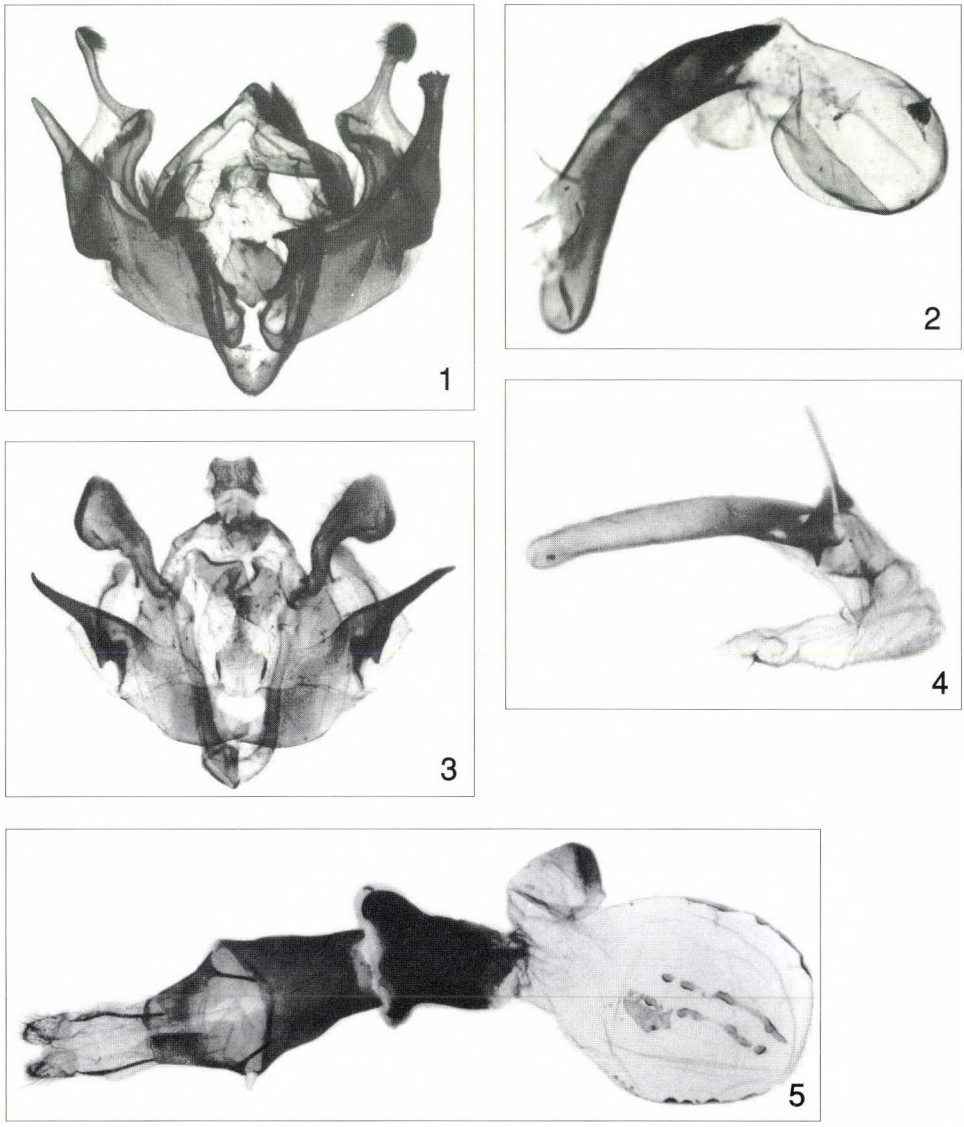

Figs 1–5. Genitalia figures. 1–2 = *Discestra rosea* sp. n., holotype; 3–5 = *Hada fraterna* sp. n., 3-4 = holotype; 5 = paratype

valva, from the taxa of the *D. furca* species-group by the essentially shorter, broader (globular-elliptical, not tubular) diverticulum of the vesica, the lanceolate uncus, the larger, broader but less high fultura inferior, etc.

Description: wingspan 33.5 mm, length of forewing 16 mm. Head, thorax, palpi and legs dark pinkish, mixed with black-tipped pink hairs. Antennae filiform, blackish with pinkish base. Forewing elongated, triangular with apex pointed, ground colour dark pinkish, irrorated sparsely with black scales, especially along costal margin, forming some black patches. Wing pattern less conspicuous, crosslines and stigmata obsolescent, often hardly visible. Transverse lines sinuous, pinkish, paler than ground colour, basal and antemedial defined by reddish brown scales on both sides, postmedian only at inner side. Orbicular and a part of reniform paler pinkish, lightest elements of forewing, lower part of reniform darker, filled partly with blackish; inner part of cell forming conspicuous, reddish brown field between orbicular and reniform stigmata. Subterminal line fine, wavy, pale pinkish, marked with three dark arrowheads; cilia dark pinkish with two fine black lines. Hindwing pale brown, with faint pinkish suffusion, marginal area somewhat darker. Discal spot brown, rather strong, cilia pink. Underside of wings pinkish brown, costal part of forewing and veins of hindwing covered with blackish scales. Discal spots brown, well visible; traces of transverse lines also recognizable as fine brown stripes, cilia like on the upper side.

Male genitalia (Figs 1–2): uncus medium long, lanceolate, with pointed tip, tegumen broad, low, penicular lobes elongated, densely hairy. Fultura inferior asymmetrical, shield-like, with short, pointed apical process, vinculum short, strong, V-shaped. Valvae elongated, arcuate, broad at base, distally tapering, cucullus small, rounded, sitting on narrow, long neck, subapical costal lobe triangular, with rounded, inflated prominence. Sacculi asymmetrical, left clavus rounded, wrinkled, right clavus much larger, flattened, claw-like, finely serrate. Saccular extensions large, long, horn-shaped, somewhat shorter, acute on left side, broader, longer on right side, with crater-like, strongly serrated apical part. Aedeagus cylindrical, arcuated, carina with short ventral and long, acute, dorsal plate. Vesica tubular, recurved ventro-laterally, basal part with small, dentated dorso-lateral bar and large, inflated, diverticulum armed with small, acute, bulbed cornutus. Distal tube of vesica membranous, rather short.

Female unknown.

Bionomics and distribution: Known only from the type-locality, East Tibet.

Etymology: the species name refers to the pinkish colouration of the forewing.

Hada fraterna sp. n.
(Figs 3–5, 25)

Holotype: male, "East-Tibet, Taba, 3.900 m, 18.06.1996, leg. Willi Fickler", "Dr. P. Gyulai, HUNGARY" (yellow label); coll. P. GYULAI, Slide No. 5946 RONKAY.

Paratype: female, with the same data as the holotype, coll. G. RONKAY (Budapest). Slide No. 5942 RONKAY (female).

Diagnosis: The new species is the third, most ancient member of the *Hada bryoptera* (PÜNGELER, 1900) – *H. honeyi* PLANTE, 1982 species-group, displaying a rather simple male genitalia compared with those of the other two species. *H. fraterna* differs from the related species by its larger size, broader, darker blackish grey forewings without greenish but with fine, pale bluish-grey

irroration, somewhat more distinct noctuid pattern and by the configuration of the genitalia, displaying very conspicuous differences in both sexes. The male genitalia of the new species (Figs 3–4) differs from those of the allied species (see PLANTE 1982, figs 13, 14) by the broad, short uncus, much broader, sclerotized, rounded cucullus without double pollex but with narrow neck, simple-peaked saccular extension having a twice folded, sclerotized basal appendix. The aedeagus of *H. fraterna* is considerably longer than those of the related taxa, the carina is armed with strong, long processi, the vesica has a very long, fine, acute subbasal cornutus and a small terminal cornuti field consisting of tiny spiculi. The female genitalia of *H. fraterna* and *H. honeyi* (Figs 5–6) have the same ground plan but the ostium bursae of the new species is larger, broader, more trapezoidal, without convex caudal plate, ostium and ductus bursae not fused but separated by a membranous neck, ductus bursae shorter but much broader, with rounded lateral lobes at caudal edge, cervix bursae less conical, with apex rounded, its sclerotization weaker, less extensive.

Description: wingspan 43–44 mm, length of forewing 20–21 mm. Head and thorax blackish grey, frons and collar mixed with some whitish and yellowish hairs. Palpi short, slightly arcuate, antennae of male finely ciliate, those of female filiform. Abdomen paler, ochreous grey, dorsal crest strong, dark, legs dark brownish with long blackish grey fringes on tibiae and fine ochreous rings on tarsi. Forewing elongated with apex acute, outer margin finely crenulate. Ground colour dark blackish grey with some plumbeous-bluish shining and with variably strong pale bluish-grey irroration. Wing pattern rather diffuse, subbasal, ante- and postmedial crosslines double, sinuous, darker blackish grey, filled and/or defined by pale whitish- or bluish grey; medial line a diffuse, blackish stripe. Subterminal obsolescent, represented by indistinct blackish spots, marked with lighter greyish and a few ochreous scales. Orbicular and reniform stigmata relatively sharply defined, former small, rounded, latter more or less lunulate, both encircled with whitish grey, filled with blackish and a few whitish. Terminal line a row of black(ish) triangles, cilia white(ish), chequered with blackish grey. Hindwing ochreous, suffused strongly with brownish grey. Transverse line diffuse, somewhat darker, discal spot hardly visible or absent. Terminal line dark grey-brown, cilia ochreous, finely marked with pale grey. Underside of wings pale ochreous-whitish, forewing suffused strongly, hindwing irrorated sparsely with dark grey. Traces of discal spots present on both wings, transverse lines dark, broad but diffuse, inner area of hindwing with a characteristic, broad, diffuse, oblique dark shadow.

Male genitalia (Figs 3–4): uncus short, broad, spatulate, apex with slight medial incision. Tegumen very low, narrow, penicular lobes small, finely setose. Fultura inferior large, subdeltoidal with high apex, fultura superior consisting of rather strong, flattened, broad plates; vinculum short but strong, U-shaped. Valva relatively short, broad, constricted below cucullus forming narrow neck; ventral margin with pointed triangular, membranous medial lobe. Cucullus big, rounded, with apex finely pointed; corona missing, substituted by sclerotized marginal crest. Sacculus long, partly membranous, clavus a small, more or less rounded lobe continued in scarcely setose field, distal end of sacculus projected into very long, heavily sclerotized, acute extension, having sclerotized, twice folded basal plate ventrally. Harpe reduced to its long, curved, flattened basal plate, ampulla absent, pulvillus small, globular, densely setose. Aedeagus long, cylindrical, carina with two sclerotized bars, dorso-lateral bar terminated in nail-shaped cornutus, ventro-lateral plate armed with long, wedge-shaped, finely bifurcated thorn. Vesica membranous, broadly tubular, everted forward, recurved laterally, with a tubular, narrow subbasal diverticulum terminated in very long, slender, acute cornutus and with small terminal spinulose field consisting of a few small, fine spiculi.

Female genitalia (Fig. 5): ovipositor medium-long, conical, relatively weak, gonapophyses short. Ostium bursae large, trapezoidal, heavily sclerotized, flattened, ductus bursae rather long, flattened, sclerotized, posterior third dilated, laterally rounded, anterior end scobinate. Cervix bursae small, elongated-elliptical, slightly folded, apically sclerotized, corpus bursae ovoid, membranous, with four narrow, more or less continuous signum-stripes consisting of stronger signum-patches.

Bionomics and distribution: The area of the species-group is restricted to the Tibetan plateau and the southern Himalayan region, showing an allopatric distribution pattern: *H. bryoptera* occurs in the Kuku-Noor region, *H. fraterna* at the south-eastern part of the plateau while *H. honeyi* is recorded from different parts of the Nepal Himalaya.

Etymology: The specific name refers to the dark, blackish colouration of the species.

Lacanobia (Lacanobia) w-latinoides sp. n.
(Figs 7–10, 23B, 26–27)

Holotype: male, Uzbekistan, W-Thien-Shan region, Tashkent distr., Chimgan, 28.06.-10.07.1993, leg. VODYANOV, slide No. 739 GYULAI; coll. P. GYULAI.

Paratypes: 1 male, 2 females, Uzbekistan, Chatkal Mts, 60 km SE of Tashkent, Krasnogorsk, 1200 m, 31.05.1994, leg. LUKHTANOV; 1 male and 1 female in coll. P. GYULAI, 1 male in coll. G. RONKAY.

Slide Nos 656 GYULAI (males), 655 GYULAI (female).

Diagnosis: The new species is a sympatric sibling of *Lacanobia (Lacanobia) w-latinum* (HUFNAGEL, 1766). The two species are highly similar externally, while the genitalia of both sexes are easily distinguishable for the first look. Comparing the external appearance of the two related taxa, there are several small but recognizable differences in the antennae, the collar and the shape, colouration and pattern of the forewings. The new species has ochreous (males) or reddish (females) collar with a few greyish hairs but not grey as in case of *L. w-latinum* and the black stripe of the collar is sharper, the antennae are not uniformly brownish but chequered with grey and blackish and the thorax is also mixed with reddish hairs. The forewings of *L. w-latinoides* are more elongated, narrower, with more intense reddish-brown irroration, the orbicular and reniform stigmata are essentially lighter reddish, the latter and the claviform are larger than in *L. w-latinum*; the antemedial line is more diffuse, more straight, etc.

Some of the differences are shown by the annexed quick drawing (Fig. 23); the new species is recognizable by them without checking the genitalia but only the dissection of the specimens can serve as a basis of the sure identification

The male genitalia of the new species (Figs 7–9) are very characteristic, differing from those of *L. w-latinum* (Figs 11–12) mostly by the shape of the valva, dilated subapically below cucullus, the cucullus is much shorter, broader, more or

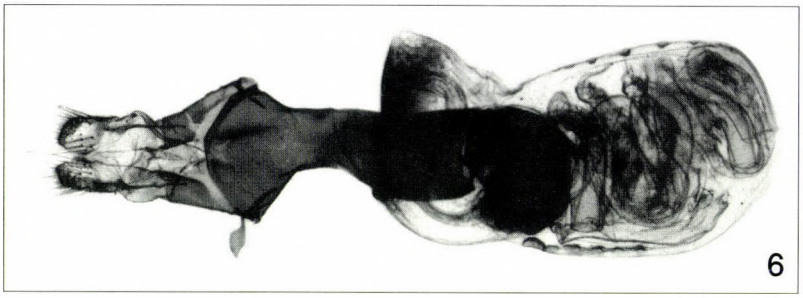

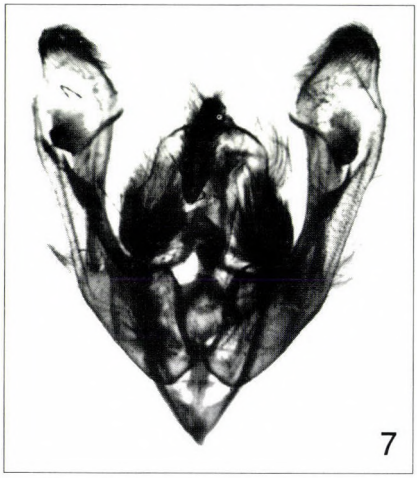

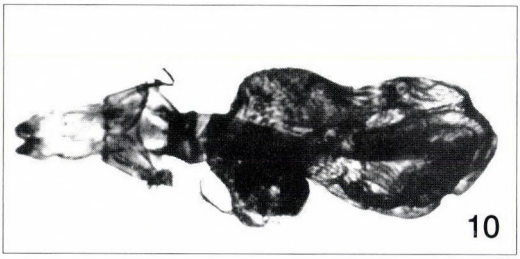

Figs 6–10. Genitalia figures. 6 = *Hada honeyi* PLANTE, Nepal; 7–10 = *Lacanobia w-latinoides* sp. n., 7–8 = holotype, 9 = paratype male, 10 = paratype female

less trapezoidal, without narrow neck, the corona is smaller, the sclerotized costal lobe is larger, its extension more acute, originating from the proximal part of the plate (its shape resembling more to that of *L. (Diataraxia) aliena* (HÜBNER, 1807) than to that of *L. w-latinum*), the apical sclerotization of the fultura inferior is more acute, triangular. The aedeagus of *L. w-latinoides* is broader, more robust, the digitiform subbasal diverticulum is shorter but broader. In the female genitalia the differences can be found in the shape of the lamella antevaginalis, the ostium and the ductus bursae. The lamella antevaginalis of the new species is weaker, smaller, its incision broader, lyriform, the ostium bursae is smaller, trapezoidal, the ductus bursae is broader but shorter, less sclerotized.

Description: wingspan 35–37 mm (males), 38–38.5 mm (females), length of forewing 19–19.5 mm. Pubescence of head whitish mixed with black, collar ochreous with some reddish (males) or grey with reddish (females), its black line fine but well visible. Thorax reddish brown, medial part greyish, some hairs with white-black tips. Antennae fine, filiform, chequered with pale grey and black. Forewing elongated, rather narrow, with apex pointed, ground colour light reddish brown, irrorated with brown and a few blackish, basal area and inner part of the marginal field suffused with pale ashy grey. Dark streak of submedian fold long, blackish, defined with reddish scales. Antemedial line slightly sinuous, finely arcuate, double, dark brown filled with whitish grey, marked with some reddish. Medial line an indistinct, dark brownish shadow, postmedial line arcuate, serrated, upper part reddish, lower half blackish, defined with white scales. Orbicular small, more or less rounded, reniform elliptical, narrow, both stigmata incompletely encircled with blackish, filled partly with ochreous and red scales. Claviform big, reddish brown with blackish outline. Subterminal whitish, sinuous, defined with brown, reddish brown and black scales and some black arrowheads at inner side. Terminal line interrupted, fine, whitish marked with blackish and a row of small, black arrowheads. Cilia dark brown, striolate with paler brown and whitish. Hindwing pale ochreous, suffused with light brown, veins and marginal area covered with darker brown; discal spot and transverse line obsolete. Cilia whitish with an interrupted, fine brown stripe. Underside of forewing pale grey-brown with reddish suffusion, especially at fore angle of marginal field. Hindwing whitish with scarce brownish irroration, stronger at costal margin. Discal spot brown, diffuse but well visible, transverse line very fine, obscure, brownish; cilia as on upperside.

Male genitalia (Figs 7–9): uncus long, slender, pointed, tegumen low, small, penicular lobes well-developed. Fultura inferior subdeltoidal with triangular apical process having sclerotized ribbon along its base; vinculum strong, V-shaped, relatively short. Valva elongated, slender at basal half, dilated subapically, costal margin with small, rounded subapical lobe. Cucullus without narrow neck, short, broad, trapezoidal, with apex rounded; corona rather weak. Sacculus short, sclerotized, clavi asymmetrical, larger at right side. Harpe represented by long, bar-shaped plate, costal extension well-developed, its acute process originating proximally. Aedeagus strong, curved, carina with strong dorsal plate. Vesica everted ventro-laterally, its basal tube spacious, having long, tubular diverticulum armed with fine, bulbed cornutus and small but broad, membranous subbasal diverticulum. Distal tube of vesica narrow, armed with long, narrow sclerotized plate, terminal part with digitiform, small diverticulum.

Female genitalia (Fig. 10): ovipositor weakly sclerotized, medium-long, conical, gonapophyses short. Lamella antevaginalis rounded-arcuate, its incision deep, lyriform. Ostium bursae broad but short, quadrangular, sclerotized, ductus bursae short, flattened, proximally tapering, granulosely sclerotized, joined to bursa with arcuate plate continuing in sclerotized, short crests. Cervix bursae folded, its apical part more or less rounded.

Bionomics and distribution: The careful checking of a vast material of *L. w-latinum* from various parts of Central Asia resulted in the finding of the four

known specimens of the new species; all from the western edge of the Tien Shan massif, the Chatkal Mts, Uzbekistan, supposedly restricted to this area. The new species occurs sympatrically with *L. w-latinum* in the moderately high elevations but appears as a rarity while *L. w-latinum* is commonly found during the same period.

Etymology: the specific name refers to the similarity of the new species with *L. w-latinum*.

Lacanobia (Dianobia) altyntaghi sp. n.
(Figs 13–15, 27–29)

Holotype: male, "China, Altun Shan Mts, Quecho, 28.07. 1996, leg. KOPP-NYKL.", Slide No. 800 GYULAI (coll. P. GYULAI).

Paratypes: 1 male and 2 females with the same data as the holotypes, a further male from the same locality, 21.07.1996 (1 male, 2 females in coll. P. GYULAI; 1 male in coll. G. RONKAY).

Slide No. 841 GYULAI (female).

Diagnosis: The new species has no close relative, the only similar species within the genus is *Lacanobia (Diataraxia) blenna* (HÜBNER, 1824), they are easily separable by their strongly different genitalia. *L. altyntaghi* differs externally from *L. blenna* by its essentially darker hindwings and darker brownish forewings with sharply defined, whitish-greyish orbicular and reniform stigmata.

The configuration of the male genitalia of the new species resemble mostly to those of *L. (Dianobia) mongolica* BEHOUNEK, 1992*, but *L. altyntaghi* has thicker uncus, their valval processi asymmetrical, shorter on left side, smaller and shorter than those of *L. mongolica*. The cucullus of the new species is longer, its base more angular, the clavi are longer, the vesica has no cornutus on subbasal diverticulum and the bundle of spinules is shorter. The female genitalia of the new species resemble also to those of *L. mongolica* but with smaller, shorter ostium and ductus bursae and shorter, more rounded corpus bursae.

Description: wingspan 27.5 mm (males), 29.5–31.0 mm (females), length of forewing 15.0–15.2 mm (males), 16.5–17.5 mm (females). Head and thorax pale hazel brown, mixed with whitish and a few blackish, especially on frons. Antennae filiform in both sexes, those of male slightly thicker with short, fine setae; axis white but brown on underside. Forewing narrow, elongated with apex pointed, ground colour greyish hazel brown, irrorated strongly with whitish, dark brown and a few orange scales. Wing pattern contrasty, ante- and postmedial crosslines sinuous, double, dark greyish brown filled with whitish, defined with some black scales at inner side; medial line indis-

* The monographic work of BEHOUNEK (1992) on the genus *Lacanobia* BILLBERG, 1820 gives a good survey about the largest part of the former *Mamestra* (s. l.) species, including the excellent illustrations of the genitalia of both sexes. The newly discovered three Palaearctic species of the genus are described below. The genitalia of the formerly known species are illustrated for comparison only in a few cases when it was necessary to show additional details, otherwise the drawings of BEHOUNEK are considered as appropriate references.

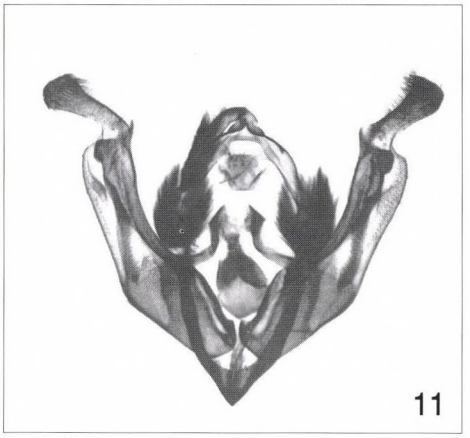

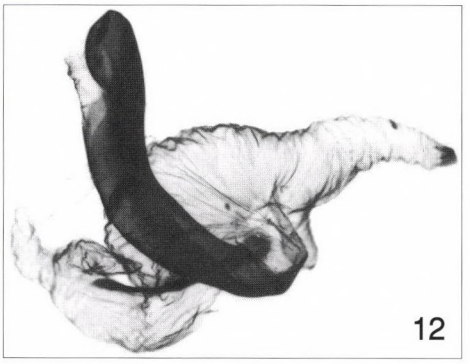

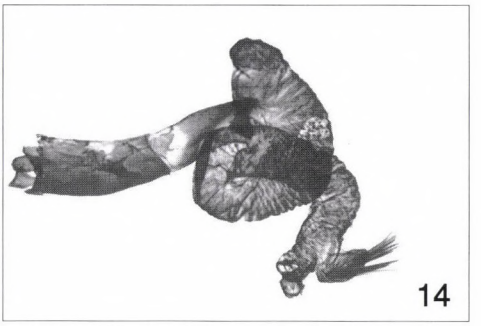

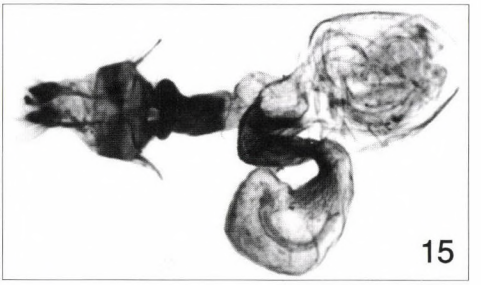

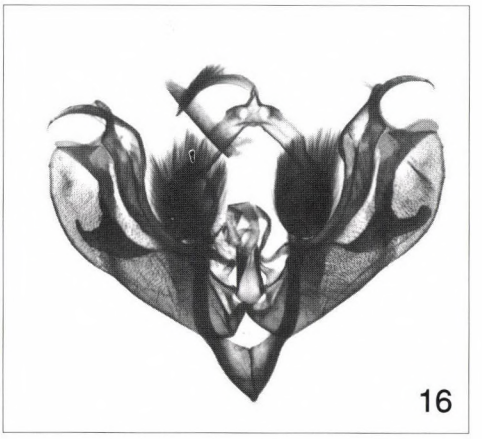

Figs 11–16. Genitalia figures. 11–12 = *Lacanobia w-latinum* (HUFNAGEL), Hungary; 13–15 = *Lacanobia altyntaghi* sp. n., 13–14 = holotype, 15 = paratype; 16 = *L. kirghisa* sp. n., paratype

tinct brownish shadow. Orbicular and reniform stigmata incompletely encircled with blackish brown, filled partly with whitish and ground colour. Orbicular small, rounded or slightly flattened, reniform narrow, more or less quadrangular; with large, dark brownish patch between reniform and postmedial line. Claviform stigma rather short, dark brown, encircled partly with blackish. Subterminal more or less continuous, clear white, strongly sinuous, defined by small brownish and blackish dots, W-mark less conspicuous. Terminal line fine blackish brown, followed by row of black spots, cilia ochreous brown, striolate with whitish and dark brown. Hindwing pale ochreous, irrorated with brown, veins and broad marginal area covered with dark brown; with small white spot at inner angle. Traces of discal spot and transverse line present but pale, often hardly visible. Terminal line blackish brown, cilia ochreous with pale brown inner stripe. Underside of wings whitish, forewing strongly, hindwing less intensely suffused with pale brown. Discal spots and transverse lines present, stronger than on upperside.

Male genitalia (Figs 13–14): uncus slender, moderately long, tegumen small, low, penicular lobes large, rounded, densely hairy. Fultura inferior ovoid, vinculum short, strong, V-shaped. Valva arcuate, relatively narrow with parallel margins, cucullus narrow, acute, claw-like, corona reduced. Sacculus rather long, clavi long, bar-like, distal extensions of sacculi slightly asymmetrical, strong, broadly triangular with rounded apices. Valval processi asymmetric, all shorter, weaker on left valva. Basal plate of harpe fused partly with saccular extension, distal process small, more or less rounded. Costal extension ("digitus") long, acute, thorn-like. Aedeagus cylindrical, arcuate, dorsal plate of carina strong, lateral plate rounded, covered with fine teeth. Basal part of vesica spacious, subbasal diverticulum broadly conical with rounded tip, without cornutus, distal half narrowly tubular, terminal diverticulum small, semiglobular, bearing a bundle of short, fine spinules.

Female genitalia (Fig. 15): ovipositor conical, weak, gonapophyses rather short. Lamella antevaginalis strong, rounded triangular, its incision deep, narrow, with relatively weak medial lamina. Ostium bursae heavily sclerotized, trapezoidal with stronger postero-lateral margins. Ductus bursae short, broad, flattened, proximal part membranous. Cervix bursae long, basal part tubular, distally strongly dilated, basal and medial parts with strongly sclerotized crests; corpus bursae rounded-elliptical, with long, weak signum-stripes.

Bionomics and distribution: The new species is known only from one locality of the Altun Shan (= Altyn Tagh) Mts, NW China, where it is probably not rare.

Etymology: the specific name refers to the type locality of the species.

Lacanobia (Dianobia) kirghisa sp. n.
(Figs 16–18, 30–31)

Holotype: male, "KIRGISIA, Chon-Kemin river, 1800 m, 01–08.06.1994, leg. Toropov, Dr. P. Gyulai, HUNGARY" (coll. P. GYULAI).

Paratypes: 16 males, 4 females, with the same data. A part of the paratypes is deposited in coll. G. RONKAY (2 males) and the HNHM Budapest (1 male), the other paratypes are in coll. P. GYULAI.

Slide Nos: 679, 708, 762 GYULAI, 5928 RONKAY (males); 764 GYULAI (female).

Diagnosis: The new species is allied to *L. (Dianobia) thalassina* (HUFNAGEL, 1766), *L. (D.) contrastata* (BRYK, 1942) and *L. (D.) suasa* ([DENIS et SCHIFFERMÜLLER], 1775). Comparing the genital organs, the male genitalia of *L. kirghisa* is close to those of *L. thalassina* while the female genitalia of the new species resemble mostly to *L. contrastata*. The typical specimens of the new species differ externally from *L. thalassina* and *L. suasa* by its broader, more

triangular forewings, darker ground colour, strongly reduced (often completely missing) pinkish suffusion, broader, clear white subterminal line, more serrated ante- and postmedial crosslines, stronger greyish suffusion of inner half of marginal area. The strong, whitish subterminal line is very characteristic to the new species, it is easily recognizable even on the unicolorous, black specimens.

The male genitalia of the new species differ very strongly from those of *L. suasa*, displaying close affinities with *L. thalassina*. Comparing with this latter species, *L. kirghisa* has narrower, more arcuate costal extension ("digitus"), narrower, apically tapering distal process of harpe, narrower valva, broader basal and medial parts of the vesica are broader, the subbasal diverticula are somewhat larger. The major difference between *L. kirghisa* and *L. mongolica* lies in the shape and size of the distal process of the harpe which is essentially larger, broader in case of the new species.

The female genitalia of *L. kirghisa* differ from those of *L. thalassina*, *L. contrastata* and *L. mongolica* by their broader ostium, narrower ductus bursae and longer, more sclerotized cervix bursae.

Description: wingspan 33–38 mm (males), 35–37.5 mm (females), length of forewing 14.5–18 mm (males), 17–18 mm (females). Head and thorax chocolate brown, mixed with more or less white tipped individual hairs; antennae filiform, dark brown. Ground colour of forewings most often chocolate brown, sometimes dark brown or black, irrorated with white. Costal margin, suborbicular patch and inner half of marginal area suffused with whitish grey, an area between reniform stigma and subteminal line covered with reddish brown. Elements of pattern rather diffuse, except conspicuous, clear white, dentated subterminal line. Ante- and postmedian lines double, sinuous, blackish brown defined with some whitish, orbicular and reniform stigmata encircled partly with blackish and whitish lines, filled partly with plumbeous grey (in some cases also with reddish brown); claviform short, its outline fine, blackish, continued in dark blackish-brownish stripe connecting ante- and postmedian crosslines. Terminal line row of black triangles, cilia dark brown, striolate with whitish and blackish. Hindwing almost unicolorous dark brown, a little lighter shade at base, discal spot obsolescent. Marginal suffusion broad, dark, cilia white with dark medial line, especially in females. Underside of wings pinkish-whitish, forewing strongly, hindwing less intensely irrorated with brown, trace of reniform spot pale but visible on forewing, discal spot of hindwing sharper, rounded; cilia like on the upper side.

Male genitalia (Figs 16–17): uncus slender, rather short, tegumen narrow, low, penicular lobes elongated, densely hairy. Fultura inferior relatively small, pentagonal, vinculum short, strong, V-shaped. Valva arcuate, relatively narrow, distally slightly dilated, cucullus narrow, acute, clawlike; corona reduced. Sacculus medium long, clavi short, digitiform, distal extensions of sacculi symmetrical, broad-based with narrow, curved, apically rounded processi. Valvae symmetrical, basal plate of harpe fused partly with saccular extension, distal process of harpe large, broad, apically tapering, its tip rounded. Costal extension ("digitus") narrow, medium long, pointed. Aedeagus cylindrical, slightly sinuous, dorsal plate of carina strong, lateral plate finely dentated. Vesica tubular, basal third broad, armed with small but broad, bulbed cornutus and with small, semiglobular subbasal diverticulum, medial and terminal parts narrower, latter with small diverticulum bearing a bundle of spinules.

Female genitalia (Fig. 18): ovipositor conical, weak, gonapophyses rather short. Ostium bursae broadly trapezoidal with rounded caudal edge and with sclerotized crests on ventral surface. Ductus bursae medium-long, narrow, with stronger margins. Cervix bursae long, proximal part long, tubular, with strongly sclerotized ribs, distal part strongly dilated, rounded. Corpus bursae elongated, sacculiform, with long, weak signum-stripes.

Bionomics and distribution: *L. (D.) kirghisa* sp. n. was found only in one locality, where it was not rare. Flight period relatively early, respecting the elevation of the locality. The new species must be very local, because thousands of the allied *Lacanobia (Dianobia)* species were collected in Kirghisia in the last ten years but no other population of the n. sp. have been found yet.

Etymology: The new species is known only from Kirghisia.

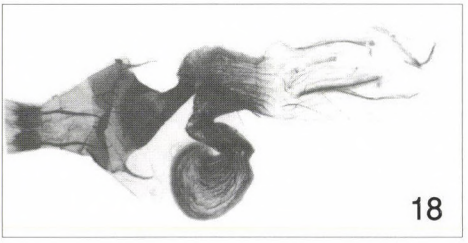

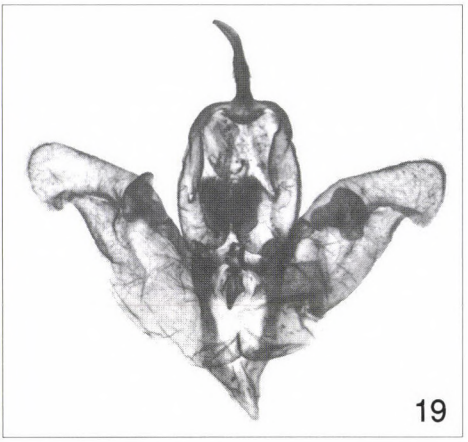

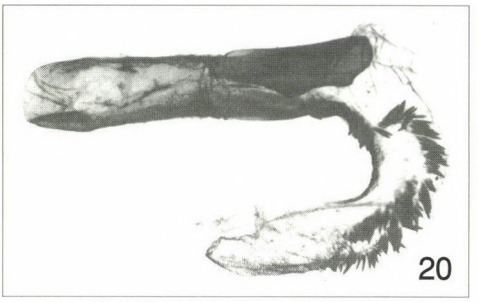

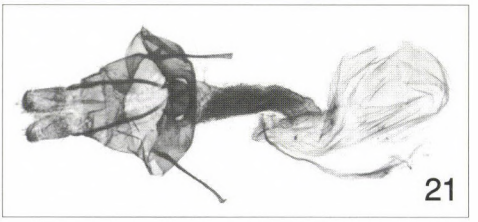

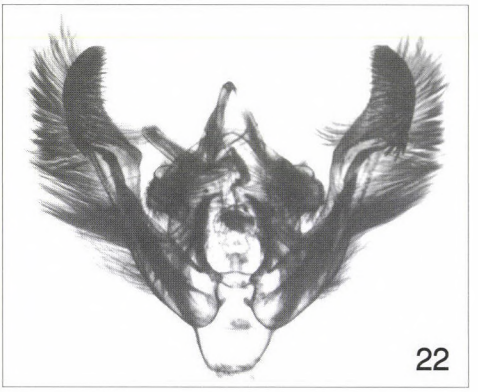

Figs 17–22. Genitalia figures. 17–18 = *L. kirghisa* sp. n., 17 = paratype male, 18 = paratype female; 19–21 = *Estagrotis roseosericea* sp. n., 19–20 = holotype, 21 = paratype; 22 = *Amphipoea cuneata* sp. n., holotype

Estagrotis roseosericea sp. n.
(Figs 19–21, 32)

Holotype: male, "China – Quinghai, Chaka, 3300–4600 m., 6–12. 7. 1991, leg. PAULUS", Slide No. 733 GYULAI; coll. P. GYULAI (Miskolc, Hungary).

Paratype: female, with the same data as the holotype (coll. M. HREBLAY, Érd).
Slide No. 10464 HREBLAY (female).

Diagnosis: The new species resembles externally to *Himalistra eriophora eriophora* (PÜNGELER, 1901), *Estagrotis plantei* HACKER et RONKAY, 1992 and *E. gemina* HREBLAY et RONKAY, 1995. The externally most similar species is, surprisingly, *H. eriophora*, but the new species has shorter, more homogenous forewing, very fine, whitish terminal line, darker hindwing and the characteristic, U-shaped blackish line between the orbicular and reniform stigmata, in addition to the strongly different male genitalia.

The new species differs from its congeners by its narrower, shorter forewings with generally lighter, more homogenous ground colour and less distinct dark pattern, including the very fine, weak, not wavy subterminal and the almost complete lack of the transverse lines on both surfaces. The distinctive features of the male genitalia, compared with *E. plantei*, are the larger, shorter but broader, rounded harpe, the more curved apical third of valva, the smaller, triangular "ampulla" and the more elongated, narrower distal part of the vesica armed with a larger amount of short spiculi. The second related species of the genus, *E. canescens* HACKER, 1992 has more elongated valvae with narrower, not bird-head-like cucullus, smaller harpe, shorter vesica with different armature of cornuti. The female genitalia are very close to those of *E. canescens*, but the ductus bursae is somewhat shorter with weaker sclerotization and the ostium bursae is slightly higher, more rounded. The female genitalia are similar in type also to those of *E. plantei* but the ductus bursae is narrower, significantly longer and the ostium bursae is narrower, more rounded and of *E. gemina* but the anterior edges of lamina antevaginalis are rounded, not angled, in addition, the ductus bursae is longer and the ostium bursae is more rounded.

Description: wingspan 30–31 mm, length of forewing 15–15.5 mm. Head and thorax uniformly pale pinkish brown, palpi with a few darker greyish hairs laterally. Antennae very fine, filiform, pale brown, each segment striolate with grey whitish. Forewing elongated, rather short, with apex pointed, outer margin arcuate. Ground colour shining pinkish brown, irrorated with pale greyish, wing pattern obsolescent except fine, long, black streak of submedian fold. Ante- and postmedian crosslines hardly visible, double, sinuous, defined by a few brownish and reddish scales and paler filling, medial line pale, narrow, brownish; subterminal interrupted, indistinct, consisting of tiny whitish dots. Orbicular and reniform stigmata present but indistinct, former oblique, more or less flattened, latter narrow, elliptical, their outlines generally pale except facing intracellular parts, which may form fine, blackish V; claviform deleted. Terminal line pale ochreous brown, cilia darker ochreous-brownish, with two fine brown stripes. Hindwing unicolorous, pale, shining ochreous-brown, veins somewhat darker, discal spot represented by fine grey arch; cilia pinkish.

Underside of wings bright, homogenous, pale pinkish brown, veins covered partly with brown scales, transverse lines absent or very pale, diffuse, discal spot of forewing obsolete, that of hindwing much stronger, lunulate.

Male genitalia (Figs 19–20): uncus short, slender, weak, tegumen high, narrow, rather strong, penicular lobes large, rounded, covered densely with short, spiculiform setae, especially on inner surfaces. Fultura inferior small, deltoidal, with acute medio-apical processus, vinculum short, V-shaped. Valva relatively short, broad, apical third curved, cucullus bird-head-shaped with short pollex-like crest; corona reduced to a few hairy setae. Sacculus short, clavus small, rounded triangular lobe. Harpe large, flattened, ear-shaped with rounded tip, "ampulla" represented by small, triangular prominence. Aedeagus short, carina with shorter dorso-lateral and a considerably longer, stronger ventro-lateral plate. Vesica tubular, everted forward, then recurved laterally. Basal curve with long field of small but rather strong cornuti extending into medial third of vesica, running parallel with shorter field of spinules; terminal part of vesica covered with fine, minute, hair-like spiculi.

Female genitalia (Fig. 21): ovipositor medium-long, strong, posterior papillae anales covered apically with short setae, gonapophyses long, strong, rather slender. Lamina antevaginalis broad with more or less rounded lateral edges. Ostium bursae rounded, sclerotized, ventral surface covered with minute granuli. Ductus bursae tubular, flattened, almost as long as ovipositor, anterior third slightly curved, both surfaces with granulosely sclerotized plates and gelatinous parts. Cervix bursae rather long, conical, wrinkled, corpus bursae ovoid-elliptical, hyaline.

Bionomics and distribution: *E. roseosericea* sp. n. is the northermost known member of the genus. The holotype male and the paratype female were collected in the Quinghai (= Kuku Noor) region; the female specimen of the *Estagrotis* species recorded from the Nan-Shan Mts (HACKER & RONKAY 1992) represents most probably another example of the species. As we had no opportunity to study the specimen in detail, it is not designated as paratype.

It is worth to mention that the two specimens of the new species were collected very late in the year, at the beginning of July, while the flight period of the other members of the genus extends regularly from the mid-autumn until the late spring.

Amphipoea cuneata sp. n.
(Figs 22, 33)

Holotype: male, "KIRGISIA, 1800 m, Chon – Kemin river, 15–20.07.1993, leg.: Toropov, Dr. P. Gyulai, HUNGARY", Slide No. 731 GYULAI (coll. GYULAI).

Diagnosis: The new species externally resembles to the medium-sized, red-brownish *Amphipoea* BILLBERG, 1820 species, mostly to *A. crinanensis* (BURROWS, 1908), *A. asiatica* (BURROWS, 1911), less to *A. distincta* (WARREN, 1911) and *A. oculea* (LINNAEUS, 1761), respectively; but easily distinguishable by the features of the male genitalia. The spine-like, simple harpe displays the closer relationship with *A. chovdica* GYULAI, 1989, and an undescribed species found in Siberia (GYULAI & RONKAY, 1994; figs 4, 7, 12). The new species is easily separable from the other taxa by its significantly narrower, longer valva

and cucullus and the weaker, more slender uncus. The species of the *crinanensis-asiatica* species-group have narrower, higher cucullus, broader valva, shorter, thicker, less spine-like harpe and shorter, stronger, more sclerotized clavus, while the harpe of *oculea* is bifid (one of the two arms is rather long, broad).

Description: wingspan 32 mm, length of forewing 15 mm. Head and thorax vivid red-brown mixed with ochreous, collar paler, with dark subapical line. Antenna of male shortly serrate and ciliate. Prothoracic tuft dark brown with violaceous tip, metathoracic tuft broad, red-brownish with brown tip. Abdomen paler, ochreous, dorsal crest fine, red-brownish. Forewing elongated with apex acute, outer margin slightly concave below apex. Ground colour red-brown with fine pinkish-violaceous shade, basal area and inner part of medial field irrorated with yellowish. Ante- and postmedial lines broad, double, sinuous, darker brown, medial line narrow, diffuse, greyish brown stripe; subterminal obsolescent, represented by indistinct, waved, brownish shadow. Orbicular small, round, yellow, reniform large, consisting of white and ochreous-whitish spots and fine brownish markings; claviform an indistinct yellowish patch. Terminal line fine, continuous, dark red-brown, cilia as ground colour. Hindwing whitish-ochreous, irrorated with dark brown, veins somewhat darker; marginal suffusion rather strong. Transverse line diffuse, brown, discal spot pale, shadow-like. Terminal line grey-brown, cilia pinkish brown. Underside of wings shining, pale ochreous, costal areas irrorated with pinkish brown, inner part of forewing suffused with greyish-brown. Traces of discal spots present on both wings as minute dots, transverse lines also diffuse but somewhat stronger, more or less continuous.

Male genitalia (Fig. 22): uncus long, slender, relatively weak, tegumen broad, rather low, penicular lobes well-developed. Fultura inferior subdeltoidal, apical third slightly dilated, medially incised, vinculum strong, rather short, U-shaped. Valva elongated, narrow, costal part angled at distal third. Cucullus high, narrow; with apex finely pointed, corona strong but short, crista well-developed, covering major part of cucullus. Sacculus long, narrow, sclerotized, clavus long, wedge-shaped, finely arcuate. Harpe very characteristic, croissant-shaped, not furcated, terminated in single, acute tip. Aedeagus long, cylindrical, slightly arcuate, carina with stronger, bar-like ventral extension. Vesica elliptical, membranous, armed with relatively small subbasal field of cornuti consisting of fine, acute spinules; ductus ejaculatorius projected ventro-laterally.

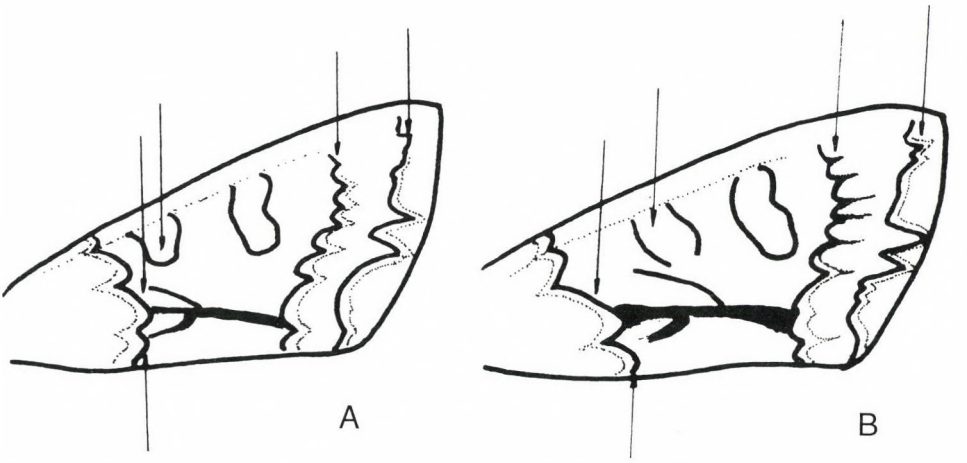

Fig. 23. The forewing pattern of *Lacanobia w-latinum* (HUFNAGEL) and *L. w-latinoides* sp. n., with the sketch of the differences between the two taxa. A = *Lacanobia w-latinum*, B = *L. w-latinoides*

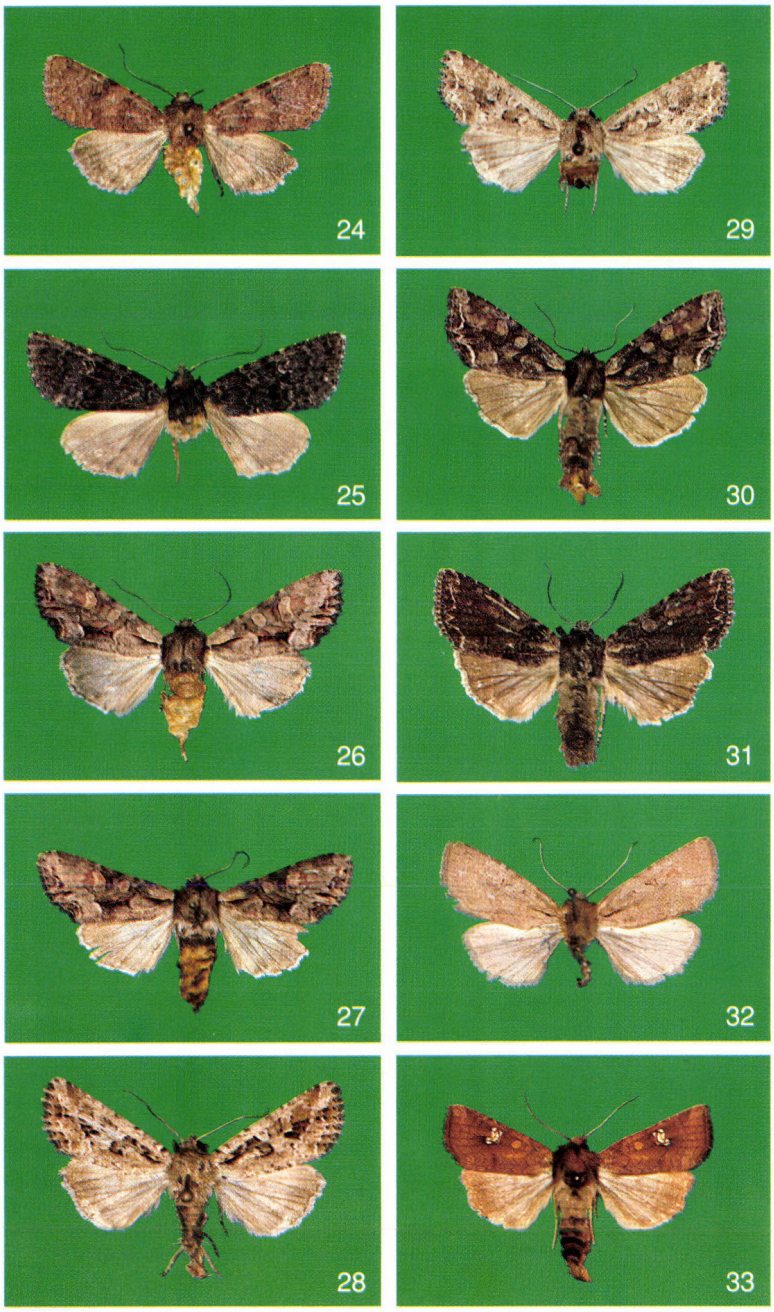

Figs 24–33. 24 = *Discestra rosea* sp. n., holotype; 25 = *Hada fraterna* sp. n., holotype; 26–27 = *Lacanobia w-latinoides* sp. n., 26 = holotype, 27 = paratype, female; 28–29 = *L. altyntaghi* sp. n., 28 = holotype, 29 = paratype, female; 30–31 = *L. kirghisa* sp. n., 30 = holotype, 31 = paratype, male; 32 = *Estagrotis roseosericea* sp. n., holotype; 33 = *Amphipoea cuneata* sp. n., holotype

Bionomics and distribution: The new species occurs sympatrically with two other congeners, *A. asiatica* and *A. fucosa* (FREYER, 1830), respectively, the former species was very common in the same habitat while the latter was also frequent. *A. cuneata* sp. n. is supposedly a rarity, according to its representation in the vast material originating from various parts of Kirghisia (more than 85.000 specimens of Noctuidae were collected and checked).

* * *

Acknowledgements – The authors are indebted to Mr. G. BEHOUNEK (Deisenhofen), Mr. M. HONEY (London), Dr. M. HREBLAY (Érd, Hungary) and Prof. Dr. Z. VARGA (Debrecen) for their kind help; to Mr. P. KOZMA (Debrecen) and Mr A. KUN (Budakeszi) for the photographs.

The research was supported by the Hungarian Scientific Research Fund (OTKA, No. 16465).

REFERENCES

BEHOUNEK, G. (1992) Die holarktischen Arten der Gattung Lacanobia Billberg, 1820 (Lepidoptera: Noctuidae, Hadeninae). *Esperiana* **3**: 33–65.

DRAUDT, M. (1935) Die Palaearktischen eulenartigen Nachtfalter. In: SEITZ, A.: *Die Gross-Schmetterlinge der Erde, 3, Suppl.* Alfred Kernen Verlag, Stuttgart, 332 pp.

DRAUDT, M. (1950) Beiträge zur Kenntnis der Agrotiden-Fauna Chinas. Aus den ausbeuten Dr. H. Höne's (Beitrag zur Fauna Sinica). *Mitt. münchn. ent. Ges.* **40**: 1–174.

GYULAI, P. & RONKAY, L. (1994) A new Amphipoea Billberg, 1820 species from West Siberia (Lepidoptera, Noctuidae). *Annls hist.-nat. Mus. natn. hung.* **86**: 45–51.

HACKER, H. (1990) Die Noctuidae Vorderasiens (Lepidoptera). – *Neue ent. Nachr.* **27**: 1–707.

HACKER, H. & RONKAY, L. (1992) Beschreibungen neuer Taxa der Spätherbst – Noctuidae – Fauna Zentralasiens und des Himalayaraumes (Cuculliinae sensu Hampson) (Lepidoptera). *Esperiana* **3**: 193–221.

HAMPSON, G. F. (1905) *Catalogue of the Lepidoptera Phalaenae in the British Museum.* Vol. 5, London, Taylor & Francis, 634 pp.

HREBLAY, M. & RONKAY, L. (1995) On the taxonomy of the genera Himalistra Hacker et Ronkay, 1993, and Estagrotis Nye, 1975 (Lepidoptera, Noctuidae). *Acta zool. hung.* **41**(3): 235–250.

PLANTE, J. (1982) Quatre especes nouvelles de Noctuidae Hadeninae de l'Himalaya [Lep.]. *Bull. soc. ent. franc.* **87**: 286–292.

RONKAY, L. & GYULAI, P. (1997) Six new species of Noctuidae (Lepidoptera) from Asia. *Acta zool. hung.* **43**(2): 133–147.

VARGA, Z. & RONKAY, L. (1991) Taxonomic studies on the Palaearctic Noctuidae (Lep.) I. New taxa from Asia. *Acta zool. hung.* **37**(3–4): 263–312.

Received 31th March, 1998, accepted 7th September, 1998, published 30th December, 1998

Acta Zoologica Academiae Scientiarum Hungaricae 44 (4), pp. 329–339, 1998

FOUR NEW SPECIES OF NOCTUIDAE (LEPIDOPTERA) FROM CENTRAL AND INNER ASIA

P. GYULAI[1] and Z. VARGA[2]

[1]*Mélyvölgy u. 13b, H-3530 Miskolc, Hungary*
[2]*Department of Zoology and Evolution*
Kossuth Lajos University, H-4010 Debrecen, Hungary

New species of Noctuidae *Hadula nekrasovi* sp. n. (Tadjikistan), *Cardiestra halolimna* sp. n. (Kazakhstan), *Conisania oxyptera* sp. n. (Kyrgyzstan) and *Bryopolia bryoxenoides* sp. n. (Kyrgyzstan) are described. With 20 figures.

Key words: Noctuidae, new species, Central and Inner Asia

INTRODUCTION

During recent years very significant materials of Noctuidae have been collected in different parts of the former Soviet Central Asia. A considerable part of this valuable material is preserved in the collection of P. GYULAI. The holotypes of the new taxa described here are deposited in the Department of Zoology of the Hungarian Natural History Museum, Budapest, but paratypes have been distributed among other important public and private collections.

Abbreviations: HNHM: Hungarian Natural History Museum, Budapest; ZIUD, ZV: Zoological Institute, L. Kossuth University, Debrecen, coll. Z. VARGA; BH: coll. B. HERCZIG, Tata; PGy: coll. of Peter GYULAI, Miskolc; GyF: coll. Gy. FÁBIÁN, Budapest; HH: coll. H. HACKER, Staffelstein; coll. A. V. NEKRASOV, Moscow, Russia; GR: coll. G. RONKAY, Budapest.

DESCRIPTIONS OF THE NEW SPECIES

Hadula nekrasovi GYULAI, HACKER et VARGA (Figs 14–15)

Holotype: male, Tadjikistan, Turkestan Mts, Shakhristan, Kushikat pass, 2000 m, 05–08.06.1994, leg. Lukhtanov, coll. GYULAI (Miskolc, Hungary), deposited in HNHM.

Paratypes: female with the same data as the holotype (coll. GR), 6 males and 2 females: W. Pamir, Kishl. Barvoz, 2800 m, 09.06.1984, leg Zaprjagaev (coll. HH and VN).

Slides: 677 (GYULAI), male, holotype, 10393 (HACKER), male, paratype and 10394 (HACKER), female, paratype.

Diagnosis: One of the largest species of the genus, with elongate shape of forewing, light whitish-grey colouration and obsolescent marking. Externally, it is quite dissimilar to all other species of the genus. In some characters (size, shape of wings, reduced markings, etc.), it seems to be somewhat similar to the smaller, pale-coloured species of the genus *Ctenoceratoda* VARGA, 1992 ("*turpis*-group"), but strikingly differs by the not pectinated male antenna and shorter antenna in general. The male genitalia are very typical to *Hadula* (Figs 1–4), with strongly expressed secondary asymmetry (i. e. dyssymmetry) in the ventral extension of sacculus and also with specialized shape of vesica (base of ductus ejaculatorius allocated near to the carina, only single elongate diverticulum with short, pointed cornutus), which seems to be rather constant within the whole genus. The genital capsula is most similar to *H. insolita* STAUDINGER, 1889, but the whole structure is more robust, juxta less dyssymmetrical, cucullus broader, the clavi are more dyssymmetrical, the left processus of sacculus is more elongate and falcate, much more dentate. The female genitalia are with conspicuously elongate, "ductus-like" appendix bursae (Fig. 11).

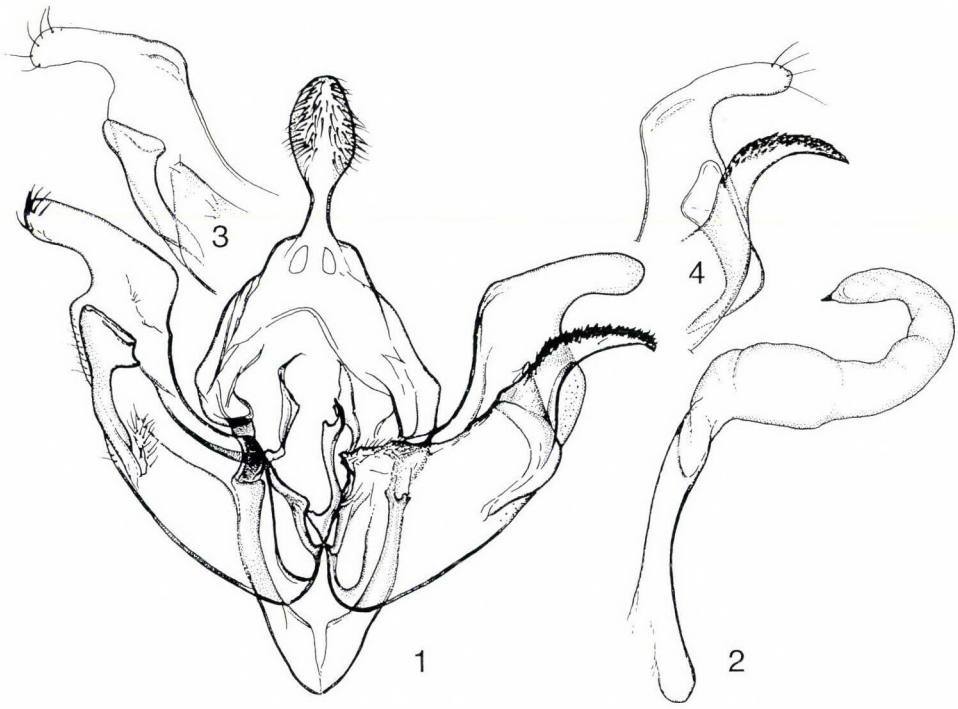

Figs 1–4. 1–2. *Hadula nekrasovi* sp. n., male, genital capsula and vesica everted, slide (GYULAI): 677 (Kyrgyzstan, holotype); 3–4. details of valvae, slide (HACKER): 10393 (Tadjikistan, paratype)

The new species should be placed between the *H. insolita* STAUDINGER, 1889 – *anthracina* HACKER, 1997 and the *Hadula sabulorum* (ALPHÉRAKY, 1882) – *pulverata* (BANG-HAAS, 1907) – *segnis* (PÜNGELER, 1906) – *leucheima* BOURSIN, 1963 species-groups, respectively.

Description – Forewing length, male: 18.5–19.5 and female: 19–20 mm, wingspan, male: 39–41 and female: 38–42 mm. Antennae filiform, densely ciliate (male) or scarcely and very shortly ciliate (female). Head and thorax pale ochreous grey (female paler), covered by whitish-greyish hairs, sometimes irrorated with blackish-brownish ones. Abdomen pale grey, shiny, with pale grey and ochreous-yellowish scales and longer whitish-yellowish hairs, mostly at end of abdomen. Forewing elongate, apex acute, pale ochreous grey, irrorated with whitish and darker, blackish-brown scales. Double ante- and postmedian lines, median shadow and inner, semilunular part of reniform spot marked with darker scales. Orbicular spot obsolescent, unicolorous, only its inner part marked with some few whitish scales. Reniform spot semilunular, more expressed in the male, inner part more marked, outer margin obsolescent. Antemedian line slightly waved, broader than postmedian, marked by blackish and yellowish-brown scales. Postmedian line regular, acutely crenulate, slightly shaded. Median shadow broad, weakly crenulate, sharply broken. Submarginal line obsolescent, only marked by some whitish or (at margin) brownish scales. Fringes pale yellowish basally, dark brown medially, tips of scales pale brownish yellow. Veins obsolescent. Hindwing pale grey with yellowish shine; lighter medially, with broad brownish-grey stripe marginally. Discal lunule well-marked, postmedian waved, well-marked, separated from marginal field by lighter zone. Veins marked by dark brownish scales. Fringes pale yellow, irrorated with a few dark brown scales. Underside of wings shiny whitish-grey. Medial part light, whitish (especially in female). Only postmedian line well-marked on both wings, crenulate, on forewing broad, on hindwing narrow. Discal lunules well-marked. Marginal field whitish-grey. Fringes on forewing yellowish basally, with brown tips, on hindwing pale yellow. Sexes similar.

Remarks: specimens from the Pamir area are slightly more ochreous, but without significant distinctive characters.

Male genitalia: Genital capsula strongly sclerotized, relatively large, with strongly expressed dyssymmetrization of valvae (Fig. 1). Uncus relatively short, broad, spatulate; tegumen high with only small lobes of peniculi; juxta narrow, dyssymmetrically curved, S-shaped, basal part trigonically extended, apically bifid. Clavus dyssymmetrical, on right valva only finely dentate, left one strongly sclerotized, acute with strong setae; ventral processus of sacculus on right side relatively short, acute, moderately sclerotized, apically covered by setae; left one very strongly sclerotized, extended and curved, dorsally strongly dentate; harpe also dyssymmetrical, right harpe stronger and more curved, left harpe weaker and smaller, but strongly curved; cucullus small, narrow; corona reduced; aedeagus relatively small; vesica typical of *Hadula*, with ductus ejaculatorius near to carina, with very long, recurved diverticulum terminated in small, fine, pointed cornutus (Fig. 2).

Remarks: the genitalia of specimens from the W Pamir Mts are very similar, the dyssymmetrization of valvae is slightly more expressed, but it is within the range of variation of the species (Figs 3–4).

Female genitalia – Typical of *Hadula*. Papillae anales weakly sclerotized, distal end rounded off; distal apophyses very thin and nearly straight; proximal apophyses short, medially curved; ostium and ductus bursae strongly sclerotized, ductus bursae very short, shield-like, continued in very elongate and heavily sclerotized appendix bursae ("false" ductus) which is longitudinally strongly ribbed; corpus bursae large, globular with two large and three smaller signa (Fig. 11).

Taxonomic remarks – *Hadula nekrasovi* sp. n. seems to be quite isolated from other species and species-groups of the genus. In the male genitalia, most characters (strongly dyssymmetrical juxta, small, narrow cucullus, long, laterally curved and extended left-side extension of sacculus) are in common with *H. in-*

solita, *H. anthracina* and with one undescribed species from this group. The shorter, more elliptical shape of uncus, the smaller lobes of peniculi and also the elongate, curved, acute and dorsally dentate shape of the left-side ventral extension of sacculus also display similarity to the taxonomically difficult species of the *Hadula sabulorum-pulverata-segnis-leucheima* group, which consists of numerous, very similar, but in contrast to *H. nekrasovi*, mostly lowland-inhabiting species. Taxonomically, the new species should be placed between these two species-groups, but closer to the former one.

The female genitalia are also very remarkable, because the ductus seminalis is attached near to the proximal end of the very short, shield-shaped ductus bursae. Thus, the very elongate, sclerotized and longitudinally strongly ribbed appendix bursae makes the impression of a very elongate proximal sector of the ductus bursae, which appearance is, of course, anatomically false. This very curious position of the ductus seminalis is obviously correlated to the similarly peculiar position of the ductus ejaculatorius near to the carina. Essentially the same characters are also typical for the genitalia of *Discestra* and *Cardiestra* species. They can be regarded as a set of highly correlative synapomorphies of the monophyletic group of genera: *Hadula*, *Discestra*, *Cardiestra*, *Thargelia* and *Odontelia* (see VARGA & RONKAY 1991).

Distribution – The new species is known only from the type locality (Tadjikistan, Turkestan Mts) and from the Western Pamir, but it probably has a larger distribution in the high mountains of adjacent parts of Central Asia. It seems to be an early flying species, because all specimens were collected in the first decade of June in fairly high altitudes (2000–2800 m). It seems to be quite typical that members of the *H. insolita* group inhabit cold, continental, high-mountain semi-deserts in Central Asia, while members of the *sabulorum-pulverata-segnis-leucheima* group populate mostly lowland deserts and semi-deserts from Western and Central Asia to Northern Africa.

Etymology – The new species is dedicated to the honoured amateur entomologist, Prof. Ing. A. V. NEKRASOV (Moscow).

Cardiestra halolimna sp. n.
(Figs 16–17)

Holotype: male, W Kazakhstan, Batkul lake, 15–31.07.1994, leg. MIATLEVSKI, coll. P. GYULAI (Miskolc), deposited in HNHM.

Paratypes: 32 males and 25 females with the same data, colls HNHM, GyF, PGy, BH, GR and ZIUD-ZV; 5 males and 4 females: W Kazakhstan, Sajkyn, 20–31.07.1995, leg. MIATLEVSKI, coll. PGy.

Slides: 7026 (VARGA) male, 810 (GYULAI) female, paratypes.

Diagnosis: relatively small and well-marked species of the genus. Differs from all other *Cardiestra* species by its irrorated brownish-ochreous colouration, well-marked maculation and transversal lines of the forewing and by dark ochreous-brown hindwing. Male genitalia with characters typical for the genus, costal margin of valva with peculiar hump-like edge. Close to *C. vaciva* PÜNGELER, which species is, however, paler and poorly marked.

Description: Forewing length, male: 13–13.5 mm and female: 15.5–16.5 mm; wingspan 26–27 mm (males) and 31–33 mm (females).

Male: Antenna dark brown with fine white brushes of ciliae, head and thorax light ochreous brown, irrorated with whitish and black-tipped hairs. Abdomed slightly lighter ochreous brown. Forewing ochreous hazel brown with darker brown or greyish-brown irroration. Costa with small black patches. Orbicular and reniform spots whitish ochreous, finely encircled by black scales. Claviform spot dark hazel brown, marked with black scales. Ante- and postmedian lines double, finely dentate, filled with lighter scales. Median shade only slightly darker than ground-colour. Subterminal line waved, at inner side blackish arrowheads. Cilia ochreous brown basally, then whitish. Hindwing light brownish with darker fuscous terminal stripe, lighter basally with darker postdiscal line and cellular lunule. Cilia whitish. Underside of wings whitish or whitish brown with darker brown postmedian line, reniform spot and cellular lunule marked with dark brown scales.

Female: Larger and more robust than male, antenna filiform, dark brown with whitish segmental rings, forewing often with whitish irroration, dark arrowheads more marked.

Male genitalia: Uncus spatulate, broad; tegumen high with well-developed penicular lobes; juxta shield-like with dorsal sclerotized crest, covered by short spinulae; valva broad, costa with hump-like protuberance; processus of sacculus short, weakly sclerotized, only slightly dyssymmetrical; harpe typical for the genus, plate-like; cucullus with broad "neck" and with rounded corona

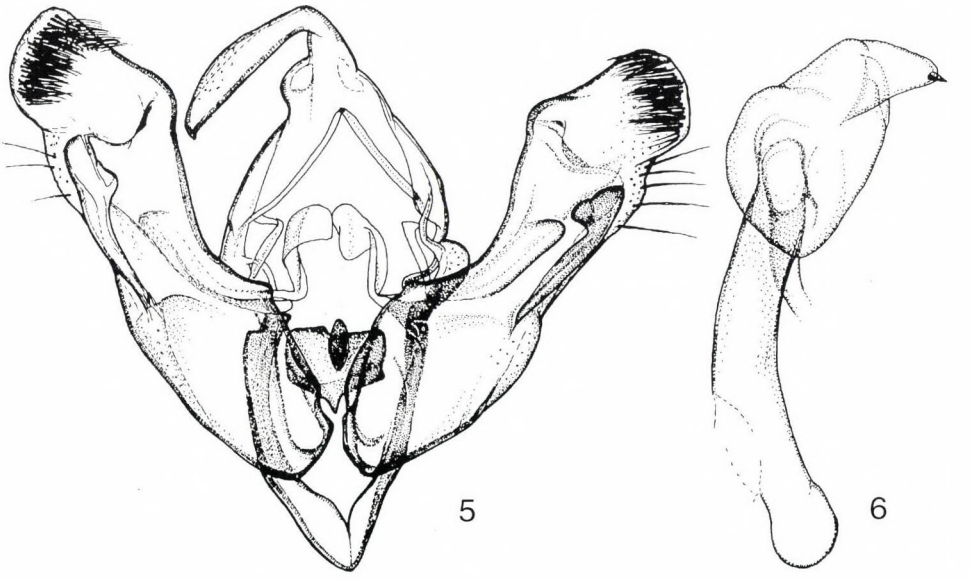

Figs 5–6. *Cardiestra halolimna* sp. n., male, genital capsula and vesica everted, slide (VARGA): 7026 (Kazakhstan, paratype)

(Fig. 5). Aedeagus thin, slightly curved, vesica simple, short, globular, with long, arched diverticulum and with fine, acute cornutus; ductus ejaculatorius close to carina (Fig. 6).

Female genitalia: Papillae anales elliptical; distal apophyses extremely thin; proximal apophyses relatively thin and long, medially only slightly curved. Ductus bursae short, moderately sclerotized, continuing in rather long and broad, moderately sclerotized and longitudinally ribbed appendix bursae ("false ductus"); corpus bursae globular with two signa (Fig. 12).

Bionomy and distribution: The new species is known only from W Kazakhstan where it is locally frequent at low altitudes. Its habitats are salty semi-deserts near semistatic saline lakes.

Etymology: the name refers to the habitat, near "saline lakes" (Greek).

Conisania oxyptera sp. n.
(Fig. 18)

Holotype: male, Kyrgyzstan, Alai Mts, Tshak, 2700 m, 39°37'N, 72°00'E, 16–17.07.1993, leg. V. & A. LUKHTANOV, coll. P. GYULAI, deposited in HNHM. Slide: 636 (GYULAI).

Paratypes: one female with the same data as the holotype; one female, Kyrgyzstan, Alai Mts, 10 km N from Darai Kurgan, Tengisbai pass, 3500 m, 11–25.07.1995, one male and two females from Tadjikistan, Turkestan Mts, Shakhristan pass, Khushikat, 3100 m, 26–28.07.1994. leg. LUKHTANOV; one female, Tadjikistan, Turkestan Mts, Zeravshan, 07. 1995, leg. VODANOV; one female, Tadjikistan, Peter I. Chain, Chasor Tshazma, 2100 m, 24.07.1976, leg. YU. L. SHCHETKIN (coll. PGy, GR and ZIUD-ZV). Slide: 6107 (RONKAY), female.

Diagnosis: Forewing acute apically, concolorous with very obsolescent markings and – in contrast to the nearest species *C. xanthothrix* BOURSIN – nearly without any yellowish scales. The male genitalia (Fig. 7) are clearly distinct from those of *C. xanthothrix* (Fig. 8) in the generally stronger sclerotisation of

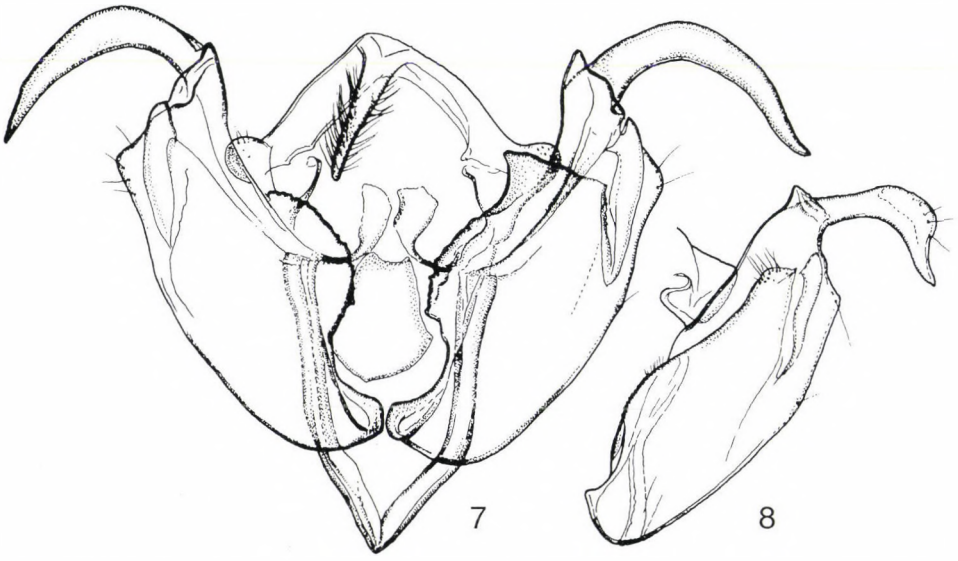

Figs 7–8. 7. *Conisania oxyptera* sp. n., male, genital capsula, slide (GYULAI): 636 (Kyrgyzstan, holotype); 8. *C. xanthotrix* BOURSIN, valva, slide (VARGA): 4728 (Afghanistan)

the genital capsula, by the slightly asymmetrical, more elongate, horn-like tip (modified cucullus with completely reduced corona) and the more developed costal extension of valvae, less numerous but thicker fasciculate cornuti and shorter basal cornutus on the vesica.

Description – Wingspan: 31 mm (holotype male), 30.2 mm (paratype male), 28–32.5 mm (paratype females), length of the forewing 16 mm (holotype, male), 15 mm (paratype male), 14.8 – 16.5 mm (paratype females). Antenna filiform, densely ciliate (male) or scarcely covered with fine, short hairs (female). Head and thorax grey (female slightly lighter), covered by dark brownish hairs with whitish-yellow basis and white tip, irrorated with whitish hairs with darker tip. Female more unicolorous. Abdomen covered by slightly shiny yellowish-brown scales and brownish hairs with white tip. Wings slightly shiny brownish-grey. Forewing covered by yellowish scales with darker brownish-grey tip. All markings obsolescent, maculation only very indistinctly marked by darker scales between orbicular and reniform and basally from orbicular. Ante- and postmedian very indistinctly marked by darker scales. Median field slightly darker (in males more suffused). Hindwing nearly unicolourous. Fringes on forewing yellow basally, dark brown medially with yellowish-brown tip, on hindwing slightly paler. Underside of forewing unicolorous brownish-grey, hindwing similar with slightly darker marginal field. Sexes similar.

Male genitalia: Uncus relatively short, straight; tegumen broad with small, elliptical lobes of peniculi; juxta broad, shield-shaped; clavus dyssymmetrical: on right side strongly dentate with only short dorsal extension of sacculus; on left side with more expressed triangular extension; harpe nearly symmetrical; right valva with smaller, left valva with stronger dorsal costal extension; cucullus dyssymmetrical, sickle-shaped, stronger on the left side (Fig. 7). Aedeagus strong, carina strongly sclerotized; vesica with short and strong basal cornutus and with relatively thick fasciculate cornuti.

Female genitalia: Papillae anales broad, quadrangular, terminally obtuse, densely covered by long and thin setae; distal apophyses strong, straight; ostium bursae strongly sclerotized bilaterally, ductus bursae of medium length, slightly curved; moderately sclerotized, broader proximally and rugulose longitudinally; corpus bursae elliptical with two signa; appendix bursae strongly sclerotized, acute apically (Fig. 13).

Taxonomic relationships of the new species – The new species is characterized by its more acute forewing shape and unicolorous colouration with very obsolescent markings and less yellowish component of the scales. Closely related to *C. xanthothrix* BOURSIN, occurring in the Pamir area (Afghanistan and Tadjikistan) and in the Hindukush Mts. It appears to be the western, allopatric sister species of *C. xanthothrix*.

Distribution – The new species seems to have a more northwestern distribution than that of *C. xanthothrix*. Their ranges probably do not overlap.

Etymology: acutely winged (Greek).

Bryopolia bryoxenoides sp. n.
(Fig. 20)

Holotype, male, Kyrgyzstan, Za-Alajsky hrebet, Aram-kungei, 3200 m, 10–26.07.1994, leg. TITOV, coll. P. GYULAI, deposited in HNHM. Slide 688 (GYULAI).

Diagnosis: The new species mostly resembles *Bryopolia chrysospora* BOURSIN, 1954 but displays numerous essential differences. The new species is smaller, the fields of forewing are darker, more homogenously coloured, filling of reniform and orbicular spots are also more homogenous, orbicular relatively bigger, medial line much more oblique; the differences in male genitalia are quite conspicuous (Figs 9–10). Some pinkish specimens of *B. ronkayorum* HACKER, 1996, also show some external similarity to the new species, but *B. ronkayorum* has much narrower, more pointed wing form and, according to the structure of male genitalia, belongs to a completely other species-group (*B. monotona* VARGA et RONKAY – *B. thomasi* HACKER, VARGA et RONKAY, 1990).

Description – Male: Wingspan 29.5 mm, forewing length 17 mm. Antenna filiform, ciliate. Head and thorax ochreous grey, without pinkish hairs. Abdomen greyish-brown, dorsal crest light, ochreous grey. Forewing elongate, outer margin arcuate. Ground colour ochreous grey, more or less covered with pinkish, pinkish-brown and brown scales. Marginal area and medial field densely covered with dark scales. Transversal lines strongly sinuose, brownish, partly doubled, filled with greyish-brown scales, darkest at fore margin. Orbicular spot large, quadrangular, very oblique; reniform spot slightly larger, quadrangular. Both spots encircled with brown scales, mostly marginally, and filled with pinkish and pinkish-brownish scales. Claviform spot small, narrow, greyish-brown, obsolescent. Subterminal line interrupted, sinuous, pinkish with three weakly marked black arrowhead spots. Terminal line sinuous, blackish, almost continuous, interrupted by some pinkish scales

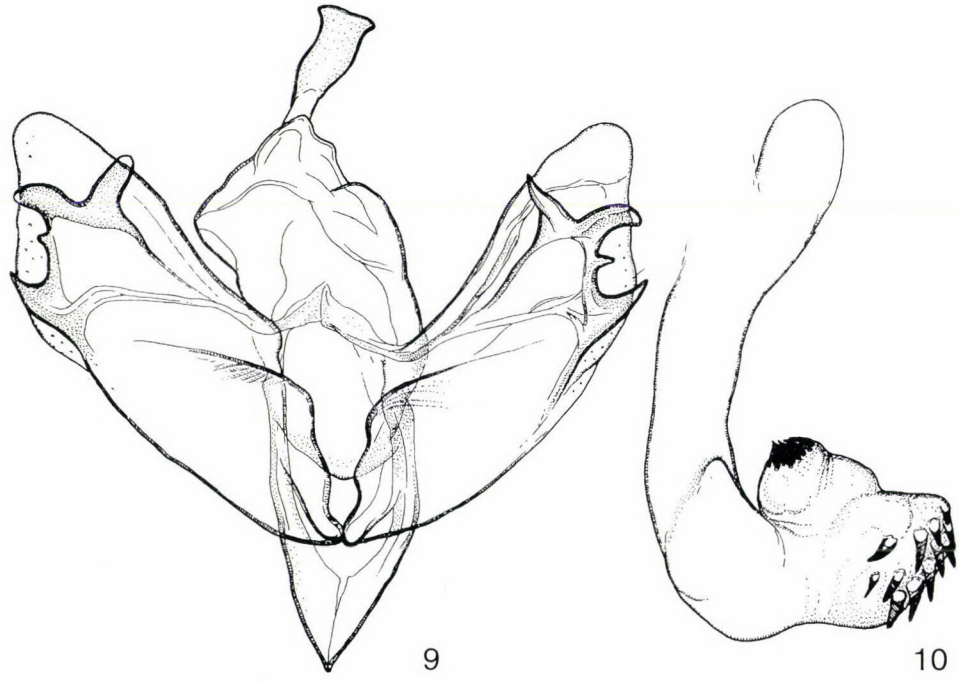

Figs 9–10. *Bryopolia bryoxenoides* sp. n., male, genital capsula and vesica everted, slide (GYULAI): 688

only. Cilia pinkish, with greyish-brown stripe. Hindwing ochreous, densely covered by brown scales. Veins and cellular lunule darker, marginal part with darker suffusion. Cilia ochreous with brown stripe. Underside of forewing ochreous, densely covered with brownish-grey scales, almost unicolorous, only marginal field slightly lighter, with more light ochreous and white scales. Shadows of subterminal line, orbicular and reniform spots visible only, but obsolescent. Hindwing lighter, whitish ochraceous, slightly suffused with brown. Cilia ochreous.

Female unknown.

Male genitalia: Uncus broad, straight, slightly spatulate; tegumen high, penicular lobes reduced; valva broad with reduced cucullus and corona, and with typical trifid extension: digiti of extension relatively short, claw-like, curved, with an additional, very short fourth digitus between the laterally oriented ones (Fig. 9). Aedeagus nearly straight, broad, carina moderately sclerotized; vesica with two groups of claw-like, relatively short but strong cornuti connected to two large, semiglobular diverticula (Fig. 10).

Taxonomic relationships: The similarity of the new species to the species of the genus *Bryoxena* VARGA et RONKAY, 1990 is only superficial. It is a true

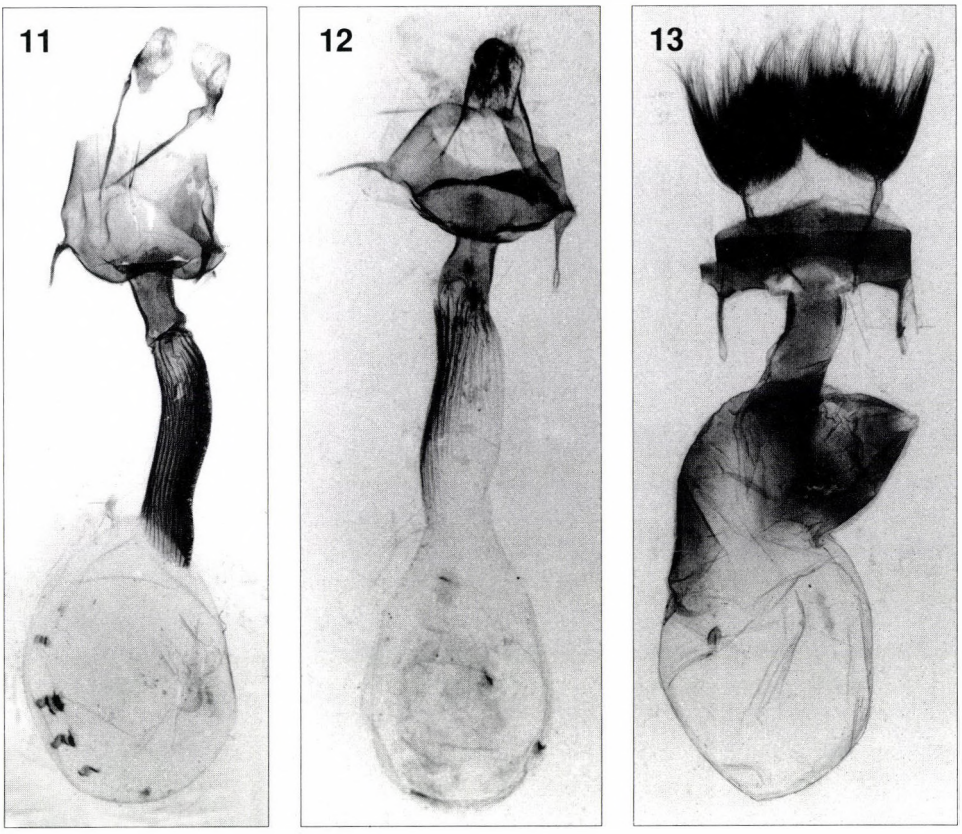

Figs 11–13. 11 = *Hadula nekrasovi* sp. n., female genitalia, slide (HACKER): 10394 (Tadjikistan, paratype); 12 = *Cardiestra halolimna* sp. n., female genitalia, slide 810 (GYULAI); 13 = *Conisania oxyptera* sp. n., female genitalia, slide 6107 (RONKAY)

Figs 14–20. 14–15 = *Hadula nekrasovi* sp. n. male and female, paratypes; 16–17 = *Cardiestra halolimna* sp. n. male, holotype and female, paratype; 18 = *Conisania oxyptera* sp. n., male, holotype; 19 = *Conisania xanthotrix* BOURSIN, male; 20 = *Bryopolia bryoxenoides* sp. n., male, holotype

Bryopolia BOURSIN, 1954 of small size; it is one of smallest species of the entire genus. It should be placed between *Bryopolia chamaeleon* (ALPHÉRAKY, 1887) and *Bryopolia chrysospora* BOURSIN, 1954. The many specific characters of the genitalia practically exclude that it could be only an aberrant specimen.

Geographical distribution – The only known specimen was found in the Transalai range, in fairly high elevation (3200 m). This place, "Aram-kungei" is, however, a well-known, classical locality in the lepidopterological literature, but the new species remained undiscovered until now. Thus, the new species must be rare, probably with spot-like distribution at higher altitudes.

Etymology: similar to *Bryoxena.*

* * *

Acknowledgements – The authors would like to express their sincere thanks to Dipl. Ing. H. HACKER and Dr L. RONKAY for their many-sided support of our efforts, for studies on comparative materials, helpful suggestions and comments. We also appreciate the valuable technical assistance of Mr P. KOZMA.

The surveys were supported by Hungarian Research Fund (OTKA, grant no T16465).

REFERENCES

BOURSIN, CH. (1960) Nouvelles "Trifinae" d'Afghanistan de l'expedition Klapperich (3rd note) (Lep. Noctuidae) (Diagnoses préliminaires). *Bull. mens. Soc. linn. Lyon* **29**: 136–152.

BOURSIN, CH. (1963*a*) Eine neue Hadula aus Zentralasien. Beiträge zur Kenntnis der "Noctuidae-Trifinae" 132. *Zschr. wien. ent. Ges.* **48**: 43–45.

BOURSIN, CH. (1963*b*) Eine neue palaearktische Gattung der Unterfamile Hadeninae. Beiträge zur Kenntnis der "Noctuidae-Trifinae" 133. *Zschr. wien. ent. Ges.* **48**: 86–88.

BOURSIN, CH. (1966) Eine neue Conisania aus Sining nebst Synonymie-Notizen. Beiträge zur Kenntnis der "Noctuidae-Trifinae" 154. *Zschr. wien. ent. Ges.* **51**: 154–159.

VARGA, Z. (1973) Neue Noctuiden von Zentralasien aus der Zoologischen Staatssammlung München und aus dem Naturwissenschaftlichen Museum Budapest. *Mitt. münchn. ent. Ges.* **63**: 194–222.

VARGA, Z. (1974) Ergebnisse der zoologischen Forschungen von Dr. Z. Kaszab in der Mongolei, Nr. 335. Noctuidae: Hadeninae (Lep.) *Annals hist.-nat. Mus. natn. hung.* **66**: 289–322.

VARGA, Z. & RONKAY, L. (1991) Taxonomic studies on the genera Sideridis Hübner, Saragossa Staudinger and Conisania Hampson (Lep.: Noctuidae, Hadeninae) *Acta zool. hung.* **37**: 145–172.

VARGA, Z., RONKAY, L. & HACKER, H. (1990) Revision of the genus Bryopolia Boursin, 1954 (Lepidoptera, Noctuidae). *Esperiana (Schwanfeld)* **1**: 427–469.

Received 25th May, 1998, accepted 7th September, 1998, published 30th December, 1998

Acta Zoologica Academiae Scientiarum Hungaricae 44 (4), pp. 341–372, 1998

SIBLING SPECIES AND SPECIES-GROUPS IN THE GENUS CHERSOTIS BOISDUVAL, 1840 (LEPIDOPTERA, NOCTUIDAE: NOCTUINAE) WITH DESCRIPTION OF TWO NEW SPECIES

Z. VARGA

Department of Zoology and Evolution, Kossuth Lajos University
H-4010 Debrecen, Hungary, E-mail: zvarga@tigris.klte.hu

Pairs or groups of closely related species are a general phenomenon in the genus *Chersotis* BOISDUVAL, 1840. A phylogenetic and biogeographic analysis is presented, with descriptions of two new species: *Chersotis petermarci* sp. n. which is the sibling species of *Ch. vicina* CORTI, 1930, and *Chersotis shandur* sp. n. which belongs to the *Ch. juvenis* species-group. Species-groups in *Chersotis*, their significant morphological characters and phylogenetic relationships are considered. With 66 figures.

Key words: genus *Chersotis*, sibling species, species-groups, allopatric speciation

INTRODUCTION

During the last two decades several new species of the genus *Chersotis* BOISDUVAL, 1840 have been described and some species-groups have also been revised (DUFAY 1981, 1984, 1986, DUFAY & VARGA 1995, HACKER & VARGA 1990, MIKKOLA *et al.* 1987, VARGA 1986, 1997, VARGA & RONKAY 1996). This genus is rich in species. POOLE (1989) has listed 51 species and numerous infraspecific taxa; some of them (see check-list) were erroneously synonymised. Further species are here considered to belong to genera other than *Chersotis*. Most of the *Chersotis* species have a Palaearctic distribution, the majority them inhabits dry, rocky habitats in the Mediterranean and West- and Central Asiatic mountains. A smaller number of species is confined to the Himalayas and to the boundary area between the Palaearctic and Indo-Malaysian region, respectively, and only a single species is recorded from North America. The distribution of the genus in the Afrotropical region is not yet clarified, although it is very probable that some species occur in the Ethiopian highlands. Certain authors tried also to subdivide this genus, because it is obvious that it consists of several groups of more closely related species (FIBIGER 1997, FIBIGER & HACKER 1990, HACKER & VARGA 1990, MIKKOLA *et al.* 1987). This subdivision was based in most cases, however, only on short morphological diagnoses and unfortunately, without any phylogenetic considerations (BECK 1992, 1996). Thus, we cannot accept the newly erected genera of the last author. Because the characters of the genita-

lia include numerous derived ones which proved to be synapomorphic with certain other genera of Noctuinae (e.g. the strongly sclerotized, dentate clavus and the short, conical medial diverticulum of vesica, see also in some *Rhyacia* and *Epipsilia* species) or only seem to be a consequence of a convergent reduction of certain structures (e.g. the absence of cucullus and corona, typical for numerous Noctuini genera), the phylogenetic analysis of this genus can be carried out only including several other noctuine genera. Hence, this paper can only be regarded as a preliminary study of the phylogenetic analysis of the genera, mentioned above, outlining the groups of species only within the traditional frames of the genus *Chersotis*.

Abbreviations: HNHM: Hungarian Natural History Museum (Budapest), FMNH: Finnish Museum of Natural History, University of Helsinki (Helsinki), ZFMK: Zoologisches Forschungsinstitut und Museum Alexander Koenig (Bonn), ZIKU: Zoological Institute of the Kossuth Lajos University (Debrecen), ZMUL: Zoological Museum of the University Lomonosov (Moscow), ZSM: Zoologische Staatssammlung (München)

DESCRIPTIONS OF THE NEW SPECIES

Chersotis petermarci sp. n.
(Figs 51–53)

Holotype: male, "USSR, ÜBSSR, W Tien-Shan, Mts Chimgan, 800–2000 m, 69°58'E 41°32'N, 18–25.07.1990. leg Gyulai & Hreblay", coll. P. GYULAI (Miskolc).*

Paratypes: 42 males and 14 females with the same data, in coll. HNHM, GYULAI, HREBLAY (Érd), G. RONKAY (Budapest), VARGA (ZIKU); 9 males and 6 females, Samarkandsk. obl., urotshishtshe Amankutan (Cyrillian letters), 1938.VI.23, coll. ZMUL, one male with the same data, coll. VARGA (ZIKU), one male, Zeravshan, coll. HÖNE, coll. ZMFK. Slides: males, Hö 557 (BOURSIN**, everted by VARGA), 3385, 3386***, 5819, 5981, 5982 (VARGA); 2809 (HREBLAY); females, 6427, 6812 (VARGA).

Diagnosis: This small, short-winged species is closely related to *Chersotis vicina* CORTI, 1930, but it seems to be generally smaller and darker, the black arrowheads on forewings are obsolescent or missing and the postmedian line is more distinctly marked, forming a right angle with the posterior margin of the forewing. Genitalia of both sexes are clearly differentiated from *Ch. vicina*. The distinctive characters are as follows: in males the S-shaped double coiling of

* Type materials, preserved in private collections of GY. FÁBIÁN, P. GYULAI, M. HREBLAY and G. RONKAY, are accessible through the Department of Zoology of the Hungarian Natural History Museum, Budapest.

** This specimen was identified as *Chersotis vicina* CORTI by BOURSIN.

*** The genitalia of this specimen were figured by VARGA (1990) as *Chersotis vicina* CORTI.

vesica, the shape of the large medial cornutus and the subbasal fasciculate cornuti; in females the very long and curved ductus bursae (Figs 4–7, 13–16, 19–20).

Description. Male: Wingspan 27–32 mm, forewing length 13–15 mm. Antenna filiform with very short ciliation. Head and thorax medium grey with blackish irroration and with ochreous hairs, mostly on collar. Abdomen lighter grey with ochreous shine. Forewing medium grey, darker terminally, with blackish irroration and ochreous shine. Maculation regular, spots marked with fine light ochreous grey margin. Between the orbicular and reniform spots, orbicular and antemedian line, and reniform and postmedian line black intermaculation. At base of claviform a black spot, between end of claviform and postmedian line indistinct blackish longitudinal shadow. Ante- and postmedian lines double, filled with light ochreous grey scales. Lower part of postmedian line nearly straight and forms right angle with posterior margin of forewing. Subterminal line slightly waved, light ochreous grey, arrowheads very indistinctly marked or missing. Cilia unicolorous brownish grey, basally with lighter ochreous line. Hindwings greyish white with brownish grey veins and slightly darker terminal shadow. Underside nearly unicolorous whitish grey, only costal part of postmedian more distinctly marked.

Female: Wingspan 26–28 mm, forewing length 12–13.5 mm, generally similar to male, but ground colour and terminal shadow of hindwing slightly darker, underside more suffused with dark scales.

Male genitalia (Figs 4–7, 13–16): Uncus strong, falcate; valva elliptical, cucullus and corona reduced; clavus small, harpe strong, acute, slightly arcuate; aedeagus with huge coecum, vesica very long and broad, having S-shaped double coiling, densely covered with fine and short, thorn-like protuberances, medially forming a zigzag-like bundle, with huge, terminally obtuse medial cornutus and with falcate bundle of short, strongly sclerotized conical cornuti.

Female genitalia (Figs 19–20): Papillae anales short, weakly sclerotized, with thin setae; anthrum with broad, U-shaped incision, ductus bursae very long, proximal part rugulose longitudinally, recurved distally, granulose and roughly ribbed, appendix bursae elliptical, corpus bursae huge, without signa.

Taxonomic relationships: *Chersotis petermarci* is the allopatric sister species of *Chersotis vicina* CORTI. The external differences between them are rather small. Only the straighter postmedian line and the obsolescence or lack of the arrowheads are the distinguishing features. The genitalia of both sexes clearly demonstrate that they are separate species. The shorter and simply recurved vesica of *Ch. vicina* clearly corresponds to the relatively short and straight ductus bursae (Figs 8–12, 17–18). The smaller size of the granulose and longitudinally roughly ribbed part of the ductus bursae closely corresponds to the smaller size of the obtuse cornutus. In contrast to the clearly differentiated, sophisticated "lock-and-key" features of the vesica and the bursa, the male clasping apparatus displays practically no differential features (Figs 1–3 vs. 4–6). This is the reason why the old specimens, collected in the Samarkand area and in the Zeravshan Mts, were formerly not recognised as representatives of a species distinct from *Ch. vicina*.

Bionomy and distribution: The new species was collected in a long series in medium high elevations of the western Tien-Shan Mts in Uzbekistan. I could also study a series of specimens collected by the late V. TSVETAEV near Samarkand (ZMUL) and one male from the Zeravshan Mts in the collection HÖNE (ZFMK)

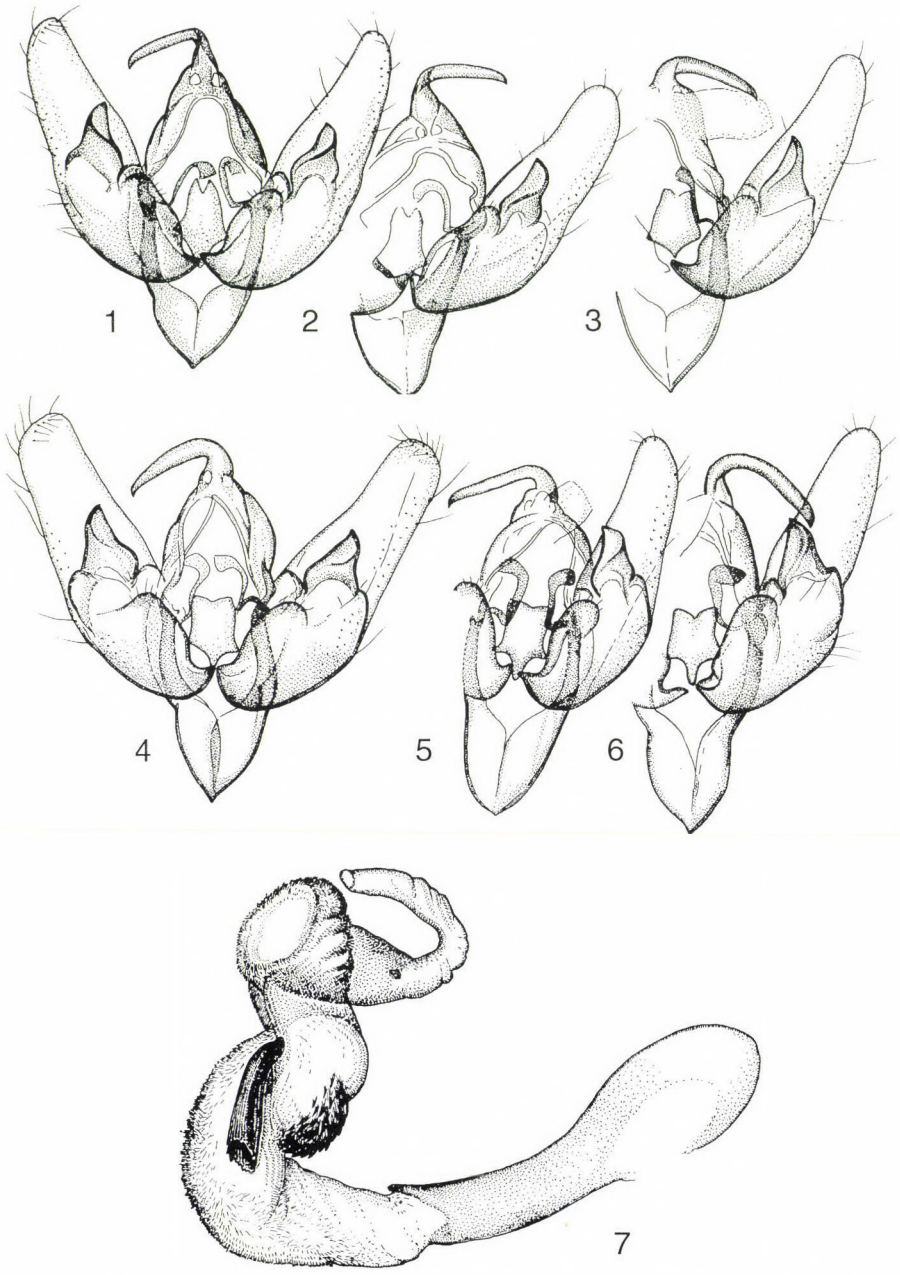

Figs 1–7. 1–3. *Chersotis vicina* CORTI, male genital capsulae, slides (VARGA): 6841 (Issyk-kul, paratype), 6805 (Kyrgyzstan), 6972 (Kyrgyzstan); 4–6. *Chersotis petermarci* sp. n., male genital capsulae, slides (VARGA): 6819, 5982 (Uzbekistan, paratypes), 3386 (Zeravshan, paratype); 7. *Chersotis petermarci* sp. n., male, vesica everted, slide 6819 (VARGA)

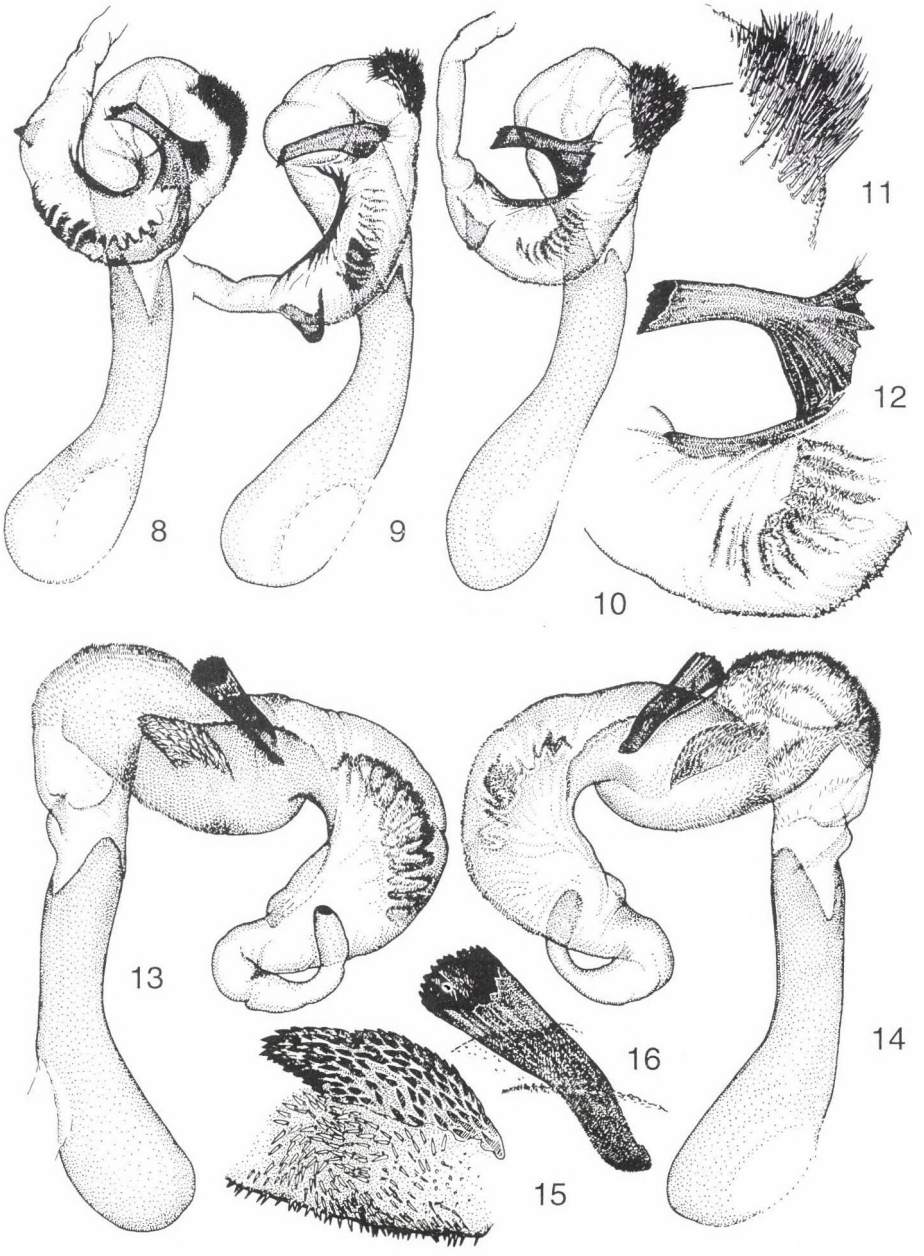

Figs 8–16. 8–10. *Chersotis vicina* CORTI, males, vesicae everted, slides (VARGA): 6841, 6306 (Issyk-kul, paratypes), 6372 (Aksu, paratype); 11–12. details of the slide 6372; 13–14. *Chersotis petermarci* sp. n., males, vesicae everted, slides (VARGA): 6819, 5982 (Uzbekistan, paratypes); 15–16. details of the slide 5982

which were identified as *Ch. vicina* CORTI. Specimens of the "true" *Ch. vicina* CORTI are known from numerous localities of Kazakhstan, Kyrgyzstan (several localities near the lake Issyk-Kul) and Chinese Turkestan (Aksu), thus it seems to be a more eastern species. Both species appear, however, to be confined to the Tien-Shan mountain system. All known specimens of both species were collected in summer. The type series of *Ch. petermarci*, collected in the second half of July, consists mostly of more or less worn specimens. Most of the females had small, contracted abdomina containing hardly any eggs and no well-developed fat bodies. Relatively fresh specimens were collected by TSVETAEV at the end of June. In the late summer of 1995, in Kazakhstan we could collect only specimens of *Ch. leucostola* VARGA et RONKAY and *Ch. calorica* CORTI. Hence I think that *Ch. vicina* and *Ch. petermarci* do not aestivate, in contrast to *Ch. capnistis*, *Ch. leucostola* and also several other species of the genus *Chersotis* (VARGA & RONKAY 1996).

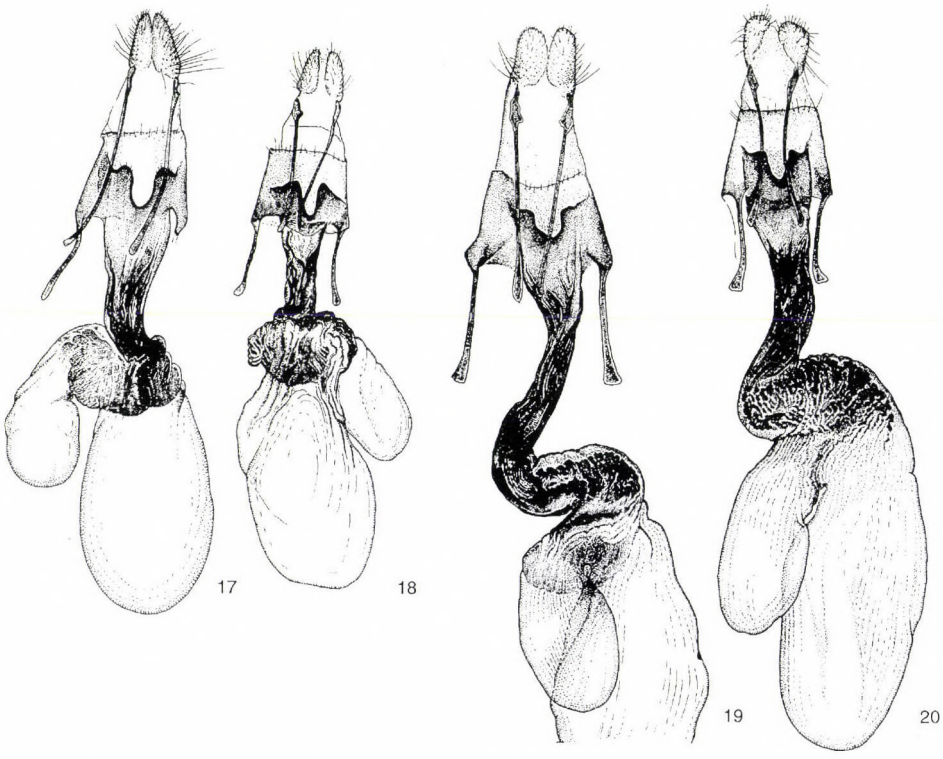

Figs 17–20. 17–18. *Chersotis vicina* CORTI, female genitalia, slides (VARGA): 6826 (Kyrgyzstan), 6373 (Issyk-kul, paratype); 19–20. *Chersotis petermarci* sp. n., female genitalia, slides (VARGA): 6812, 6427 (Uzbekistan, paratypes)

Etymology: The name *petermarci* is combined from the given names of the collectors of the new species: PETER GYULAI and MÁRTON (= Marci) HREBLAY.

Chersotis shandur sp. n.
(Figs 59–60)

Holotype, male: Pakistan, Hindukush Mts, Shandur pass, 3750 m, 72°38'E, 46°07'N, 30.08.1997. leg. GY. FÁBIÁN & G. RONKAY, coll. G. RONKAY (Budapest)

Paratypes: 2 females with the same data, coll. GY. FÁBIÁN (Budapest) and P. GYULAI (Miskolc).

Slides: male, 5997 (L. RONKAY), female, 5998 (L. RONKAY)

Diagnosis: The new species is closely related to *Chersotis kouros* VARGA et RONKAY, 1996 and *Ch. calorica* CORTI, 1930, but it is duller, darker; the markings are more obsolescent than in *Ch. kouros*, the forewing is less shiny and more densely irrorated with blackish-brown scales than in *Ch. calorica*, the black arrowheads on forewing are obsolescent or missing.

The genitalia of both sexes are clearly differentiated from the related species. The male genital capsula is generally similar to that of the related species, but the valva and the harpe are more elongate, juxta ventrally with long extension, vesica proximally hollowed, with huge, sinuously curved cornutus. In the female genitalia, the ductus bursae has large lateral pocket and hollowed proximal part (Figs 21–23 and 34: *Ch. shandur*, Figs 24–27 and 37: *Ch. calorica*, Figs 30, 32–33 and 36: *Ch. kouros*, Figs 28–29, 31 and 35: *Ch. juvenis*).

Description. Male: Wingspan: 34 mm, forewing length: 14.5 mm. Antenna filiform with short ciliation. Head and thorax greyish brown with blackish brown scales on vertex, collar and tegulae, abdomen lighter grey with ochreous shine. Forewing greyish brown, with blackish-brown irroration and ochreous shine. Longitudinal veins marked with light ochreous-grey scales. Maculation regular, spots marked with fine light ochreous grey annuli and with blackish-brown intermaculation between orbicular and reniform spots, orbicular and antemedian line, and reniform and postmedian line. At base of claviform black spot, between end of claviform and postmedian line indistinct blackish-brown suffusion. Ante- and postmedian lines doubled, marked with blackish-brown spot at costa, filled with light ochreous grey scales. Arrowheads very indistinctly marked or missing. Cilia unicolorous brownish grey, basally with lighter ochreous line. Hindwings light greyish-brown with brownish grey veins and slightly darker terminal shadow. Underside: forewing nearly concolorous light grey, shiny; postmedian line darker greyish brown; hindwing whitish ochreous, shiny.

Female: Wingspan 36 mm, forewing length 15.5 mm, generally similar to male, but forewing with stronger blackish-brown irroration, less shiny; ground colour and terminal shadow of hindwing slightly darker, underside more suffused with dark scales.

Male genitalia: Uncus strong, falcate; valva elongate, especially distally, with nearly parallel margins, cucullus and corona reduced; clavus very small, flattened; harpe strong, elongate and acute, slightly arcuate; juxta pentagonal, broad, ventrally with long extension; aedeagus only slightly arcuate with huge coecum, vesica recurved, hollowed proximally, with very strong longitudinal sclerotization and with strong, elongate and sinuously curved cornutus, attached to segmented sclerotized basal plate (Figs 21–23).

Female genitalia: Papillae anales short, weakly sclerotized, with thin setae; anthrum with broad, U-shaped incision, ductus bursae long, with large lateral pocket medially, proximal part rugulose and granulose, hollowed; appendix bursae relatively small, globular, corpus bursae large, elongate, without signa (Fig. 34).

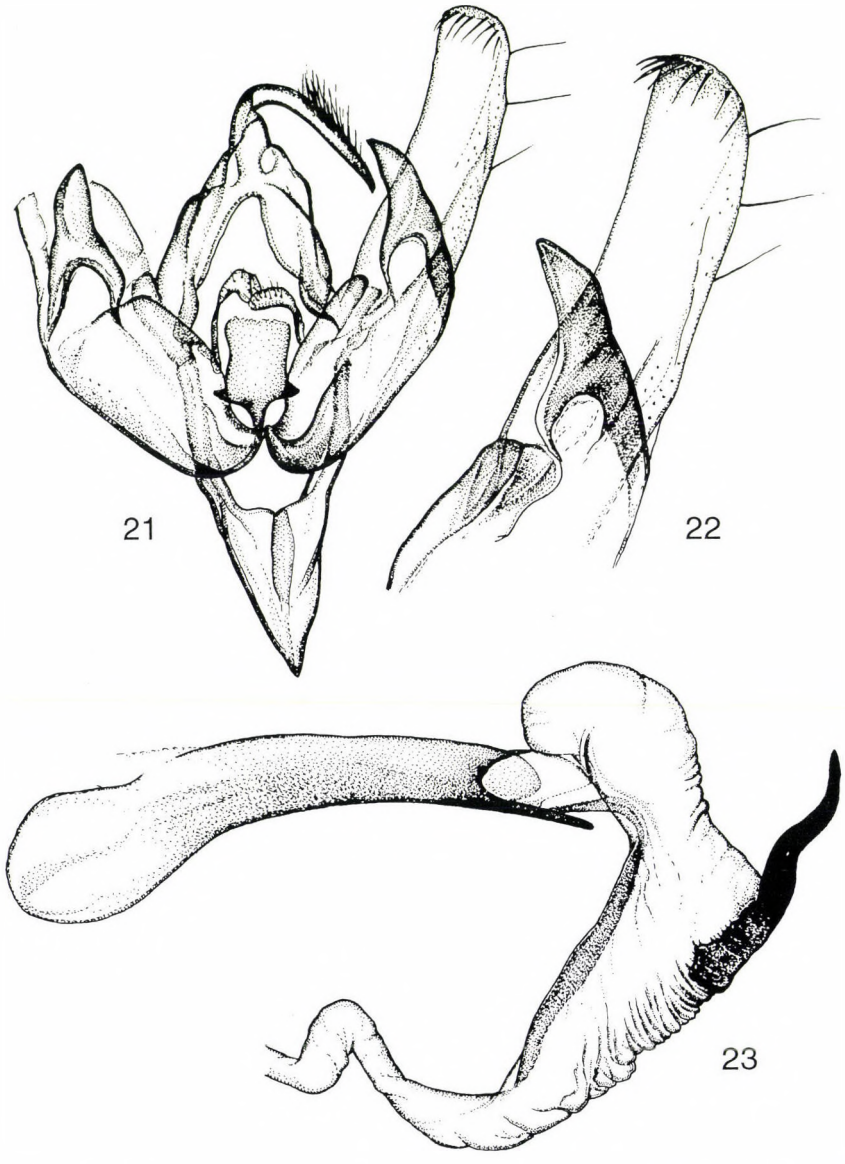

Figs 21–23. 21. *Chersotis shandur* sp. n., male genital capsula, slide (RONKAY): 5997 (Pakistan, holotype); 22. detail of the slide 5997; 23. *Chersotis shandur* sp. n., male, vesica everted, slide (RONKAY): 5997 (Pakistan, holotype)

Taxonomic relationships: *Chersotis shandur* belongs to the *Chersotis juvenis-kouros-calorica* species-group. Externally, it is the most similar to *Chersotis calorica*, it superficially seems like a duller and darker specimen of this species. The male genital capsula displays all the basic features of this species-group (see below). It proved also quite typical for this species-group (see also: *Ch. vicina – petermarci* species-pair) that the differentiation in the genital capsula is rather weak, but a very evident differentiation of the vesica and the cornuti can be observed. All species are characterized by large, elliptical proximal diverticulum, by the rather strong, recurving longitudinal sclerotisation of the vesica and by strong, claw-like medial cornutus. The westernmost species, *Ch. juvenis* shows the simplest vesica and cornutus structure. *Ch. kouros* is characterized by very distinct, hollowed proximal part and narrower distal part of the vesica, in ad-

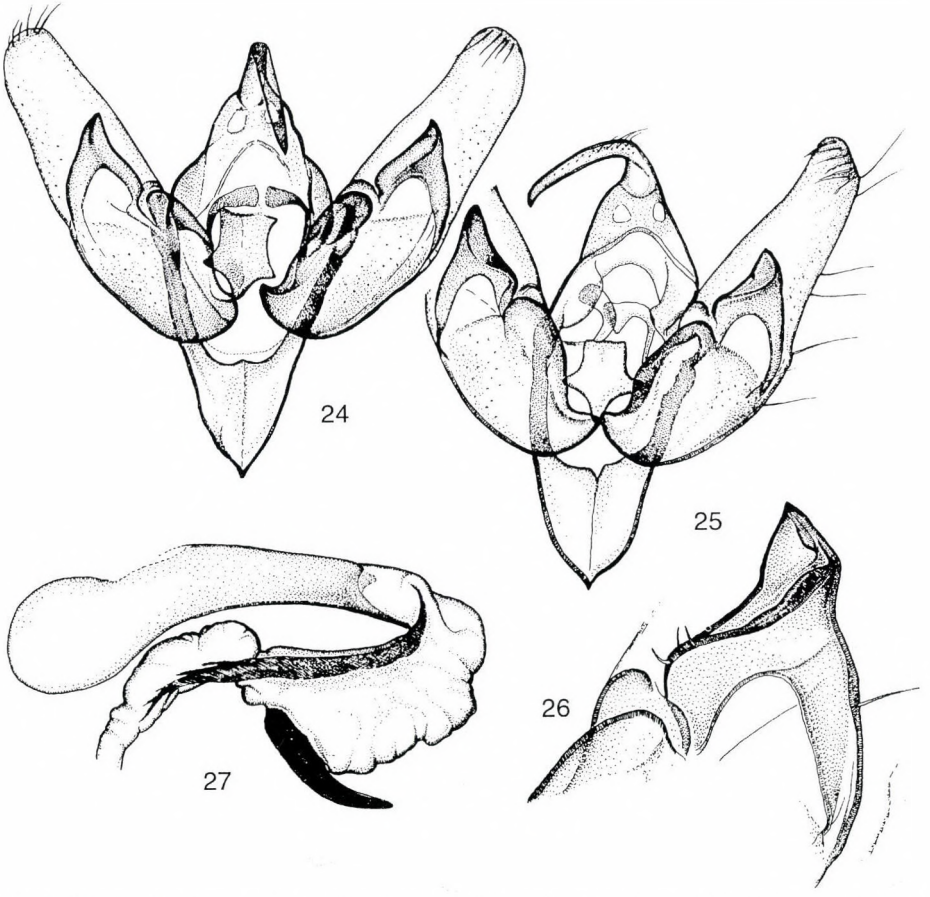

Figs 24–27. 24–25. *Chersotis calorica* CORTI, male, genital capsulae, slides (VARGA, BOURSIN): 7023 (Kazakhstan), MM34 (Aksu); 26. detail of the slide MM34; 27. *Chersotis calorica* CORTI, male, vesica everted, slide (VARGA) 7023 (Kazakhstan)

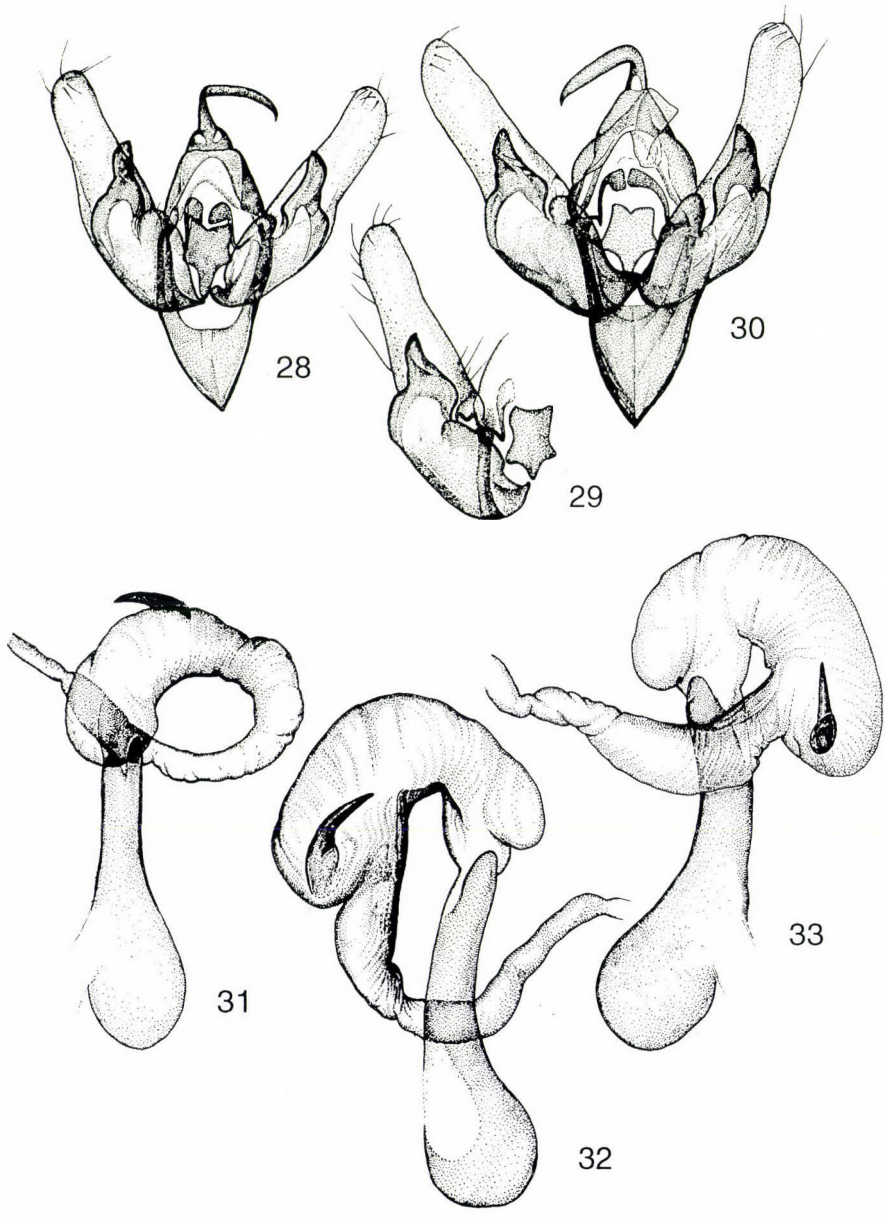

Figs 28–33. 28–29. *Chersotis juvenis* STAUDINGER, male, genital capsula & valva, slides (VARGA): 5587, 6769 (Turkey); 30. *Chersotis kouros* VARGA et RONKAY, male, genital capsula, slide (VARGA): 6525 (Turkmenistan, paratype); 31. *Chersotis juvenis* STAUDINGER, male, vesica everted, slide (VARGA): 5587 (Turkey); 32–33. *Chersotis kouros* VARGA et RONKAY, male, vesicae everted, slide (VARGA): 6525, 6582 (Turkmenistan, paratypes)

dition the cornutus has a shape and orientation different than in *juvenis*. *Ch. calorica* has similarly subdivided, but shorter vesica and broader, claw-like cornutus than *Ch. kouros*. The last character seems to show some geographical variability (figured in VARGA 1990). *Ch. electrographa* is the most differentiated species of this group, because it has highly specialized, shortened form of valva with only partially reduced corona and it has medially (not proximally) hollowed form of the huge vesica with strong, claw-like cornutus and with a small, pocket-like subterminal diverticulum. The female genitalia are similarly differentiated, with evident "lock-and-key" structures in the ductus bursae. The size and orientation of the medial pockets of ductus and its hollowed, rugulose proximal part

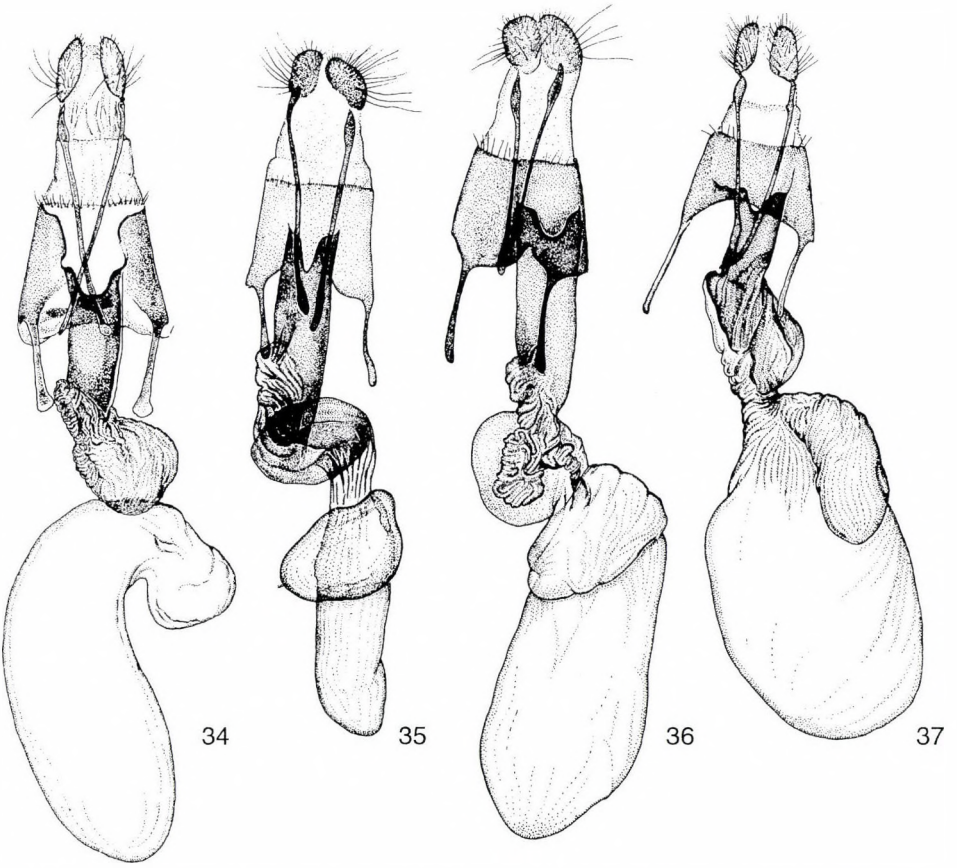

Fig. 34–37. 34. *Chersotis shandur* sp. n., female genitalia, slide (RONKAY): 5998 (Pakistan, paratype); 35. *Chersotis juvenis* STAUDINGER, female genitalia, slide (VARGA): 6370 (Turkey); 36. *Chersotis kouros* VARGA et RONKAY, female genitalia, slide (VARGA): 6489 (Turkmenistan, paratype); 37. *Chersotis calorica* CORTI, female genitalia, slide (VARGA): 6369 (Dzharkent, paratype)

clearly corresponds to the orientation and size of cornutus. The incision of the anthrum is narrow, V-shaped in *Ch. juvenis*, broad, not deep and U-shaped in *Ch. kouros*, similarly not deep, but more V-shaped in *Ch. calorica*, while deep and broadly U-shaped in the new species. *Ch. shandur* sp. n. lies morphologically and also geographically between *Ch. kouros* and *Ch. calorica*, but it seems to be differentiated and also geographically quite isolated from both relatives. Based on the morphological considerations, it appears to be the sister species of *Ch. calorica*.

Bionomy and distribution: The three known specimens of the new species were collected at the Shandur Pass, which separates the easternmost part of the Hindukush range from the western slopes of the Karakoram Mts. This locality is quite remote from all other known localities, at which the closely related taxa have been collected. It seems to be a quite local and rare species, because it was not collected during many recent lepidopterological expeditions in this part of Pakistan. This fact is, however, not very surprising, because all species of this species-group are represented even in the largest collections mostly by single specimens (*Ch. calorica*, *Ch. electrographa*) or only short series (*Ch. juvenis*, *Ch. kouros*).

Etymology: Name refers to the type locality.

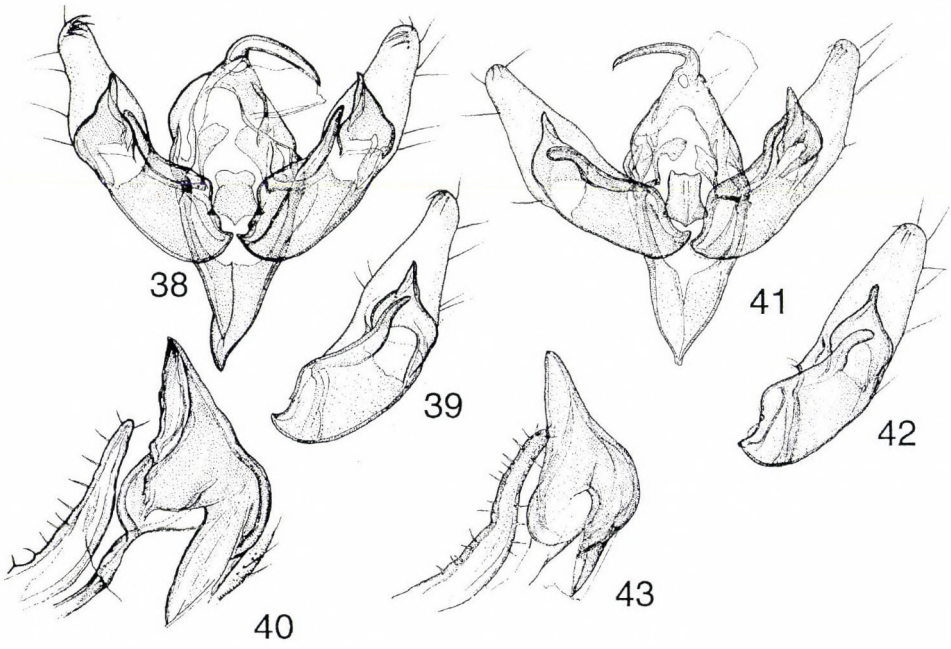

Figs 38–43. 38–40. *Chersotis semna* PÜNGELER, males, genital capsula & valva, slides (VARGA): 2560, 4264 (Iran); 40. details of the slide 2560; 41–42. *Chersotis pachnosa* VARGA, males, genital capsula & valva, slides (VARGA): 4823, 4802 (Afghanistan, paratypes), 43. detail of the slide 4823

SIBLING SPECIES, SPECIES-GROUPS, SUBGENERA AND PHYLOGENETIC RELATIONSHIPS IN CHERSOTIS BOISDUVAL

CHECKLIST ARRANGED ACCORDING TO SPECIES-GROUPS OF THE GENUS CHERSOTIS*

Type species of the genus: *Noctua rectangula* [DENIS et SCHIFFERMÜLLER], 1775 by subsequent designation by DUPONCHEL (1843, in D'ORBIGNY, *Dict. Universal Hist. Nat.* **3**: 471).

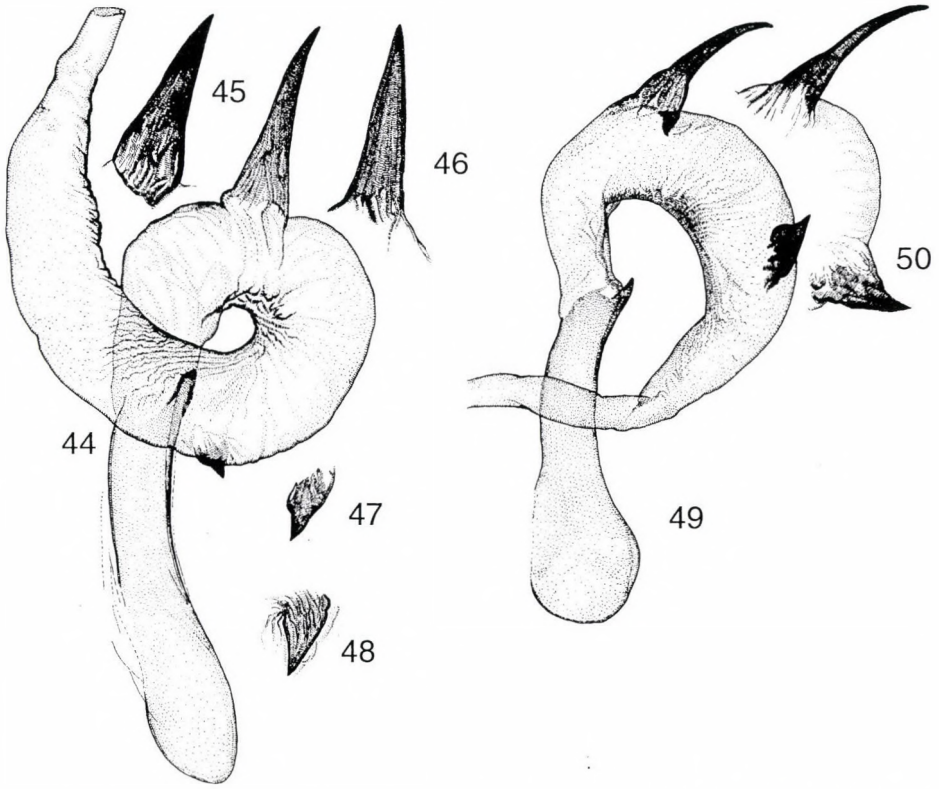

Fig. 44–50. 44. *Chersotis semna* PÜNGELER, male, vesica everted, slide (VARGA): 2560 (Iran); 45–48. cornuti, slides (VARGA): 4264 (Iran), 3771 (Armenia); 49. *Chersotis pachnosa* VARGA, male, vesica everted, slide (VARGA): 4823; 50. cornuti, slide (VARGA): 5422 (Afghanistan, paratypes)

* European species of *Chersotis* were recently grouped by BECK (1996) and FIBIGER (1997), but without considering the species outside of Europe and their phylogenetic relations.

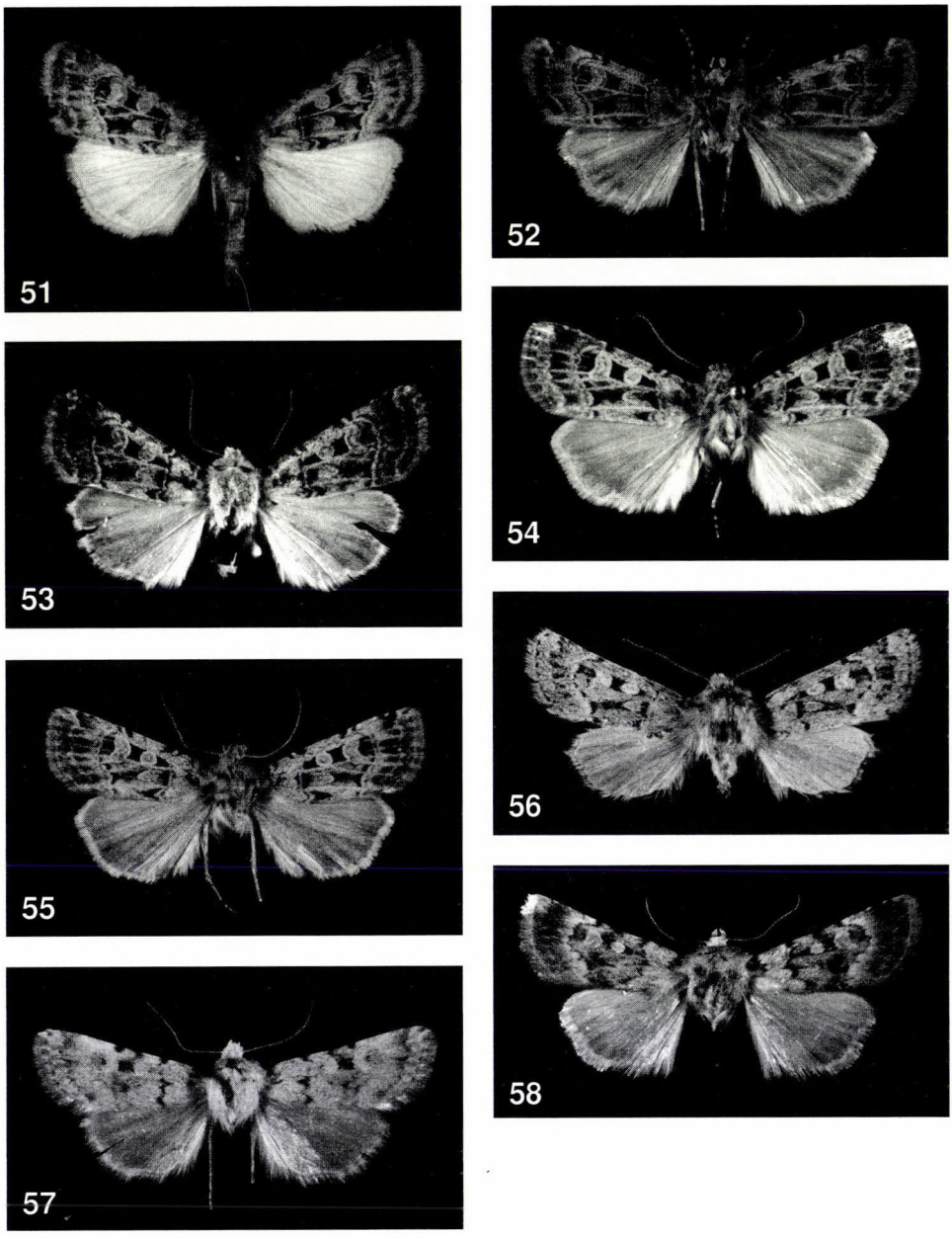

Figs 51–58. 51. *Chersotis petermarci* sp. n., male, Uzbekistan, holotype; 52. Ch. petermarci sp. n., male, Samarkand, paratype; 53. *Ch. petermarci* sp. n., female, Uzbekistan, paratype; 54. *Ch. vicina* CORTI, male, Issyk-kul, paratype, 55. *Ch. vicina* CORTI, male, Kyrgyzstan; 56. *Ch. nekrasovi* VARGA, male, Tadjikistan, holotype; 57. *Ch. antigrapha* BOURSIN, male, Afghanistan, paratype; 58. *Ch. binaloudi* BRANDT, male, Iran, paratype

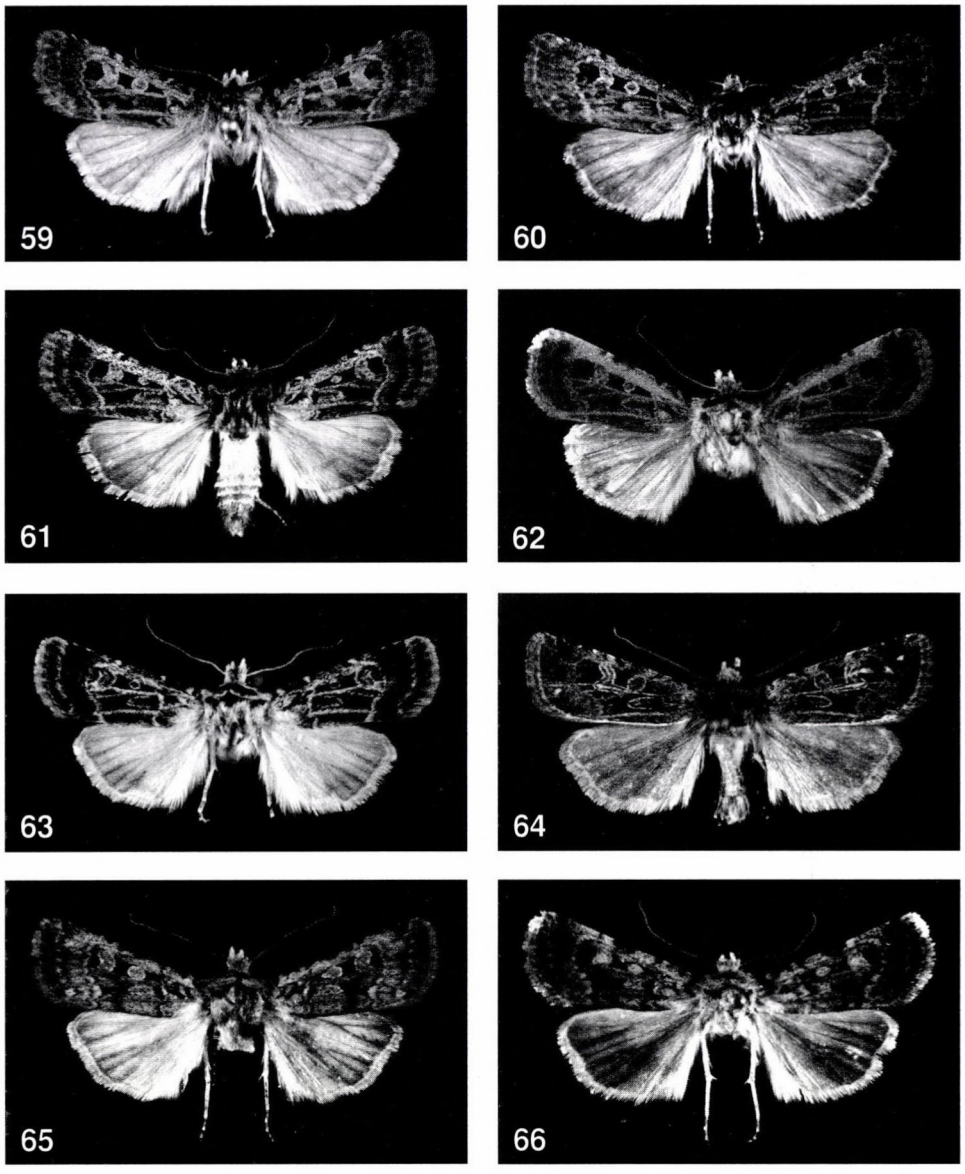

Figs 59–66. 59. *Chersotis shandur* sp. n., male, Pakistan, holotype; 60. *Ch. shandur* sp. n., female, Pakistan, paratype; 61. *Ch. kouros* VARGA et RONKAY, female, Turkmenistan, paratype; 62. *Ch. calorica* CORTI, female, Kazakhstan; 63. *Ch. juvenis* STAUDINGER, female, Turkey; 64. *Ch. herczigi* VARGA, male, Pakistan, paratype; 65. *Ch. leucostola* VARGA et RONKAY, female, Kazakhstan; 66. *Ch. nitens* BRANDT, female, Turkmenistan

1. species-group: "rectangula-group":

Chersotis rectangula ([DENIS et SCHIFFERMÜLLER], 1775)
Chersotis andereggii (BOISDUVAL, [1837] 1837)
Chersotis acutangula (STAUDINGER, 1892)
Chersotis juncta (GROTE, 1878)
Revision: MIKKOLA *et al.* (1987)

Important genital characters. Male genitalia: Uncus relatively long, basally arcuate, distally acute; clavus strongly sclerotized and densely covered by short, triangular spinules; dorsal costa of valva with broad, triangular, weakly sclerotized lobe; harpe thick, relatively short, straight; juxta broad, shield-like; aedeagus relatively short with huge, globular coecum, only slightly curved; carina thorn-like, acute; basal cornutus reduced, vesica fully recurved, with short, conical medial diverticulum. Female genitalia: Anthrum with large triangular plate; incision on the 8th sternite weakly expressed; ductus bursae relatively short, distal part broad, elliptical, dorsally with unsclerotized, folded pouch (corresponding to basal diverticulum of vesica); proximal part narrow, rugulose, with sclerotized pouch (corresponding to the medial, conical sclerotized diverticulum of vesica); appendix bursae short, recurved, rugulose; corpus bursae long, saccate, without signa.

2. species-group: "sordescens-group":

Chersotis sordescens (STAUDINGER, [1900] 1899)
Chersotis firdusii SCHWINGENSCHUSS, 1937
Chersotis herczigi VARGA, 1997
Taxonomic relationships: VARGA (1997)

Important genital characters. Male genitalia: Uncus of medium length, strong, basally slightly curved; clavus very strong, elongate, heavily sclerotized and densely covered by short, acute, triangular spinules; dorsal costa of valvae with only weakly expressed lobe, without sclerotized angle; harpe strong, elongate, apically curved; aedeagus relatively short with huge, globular coecum, carina thorn-like, acute; basal cornutus reduced, vesica recurved with short, conical medial diverticulum. Female genitalia: Anthrum strongly sclerotized, with narrow incision; ductus bursae strongly sclerotized; appendix bursae short, recurved; corpus bursae only moderately elongate, without signa.

3. species-group: "ocellina-group"

Chersotis ocellina ([DENIS et SCHIFFERMÜLLER], 1775)
Chersotis alpestris (BOISDUVAL, [1837] 1834)
Chersotis oreina DUFAY, 1984
Chersotis transiens (STAUDINGER 1986)
(= *Chersotis altajensis* RÉZBÁNYAI-RESER, 1997 **syn. nov.**)

Chersotis stridula (HAMPSON, 1903) **bona sp., stat. rev.**

? *Chersotis cortifera* RÉZBÁNYAI-RESER, 1997 (= "*vissifera*" CORTI i. l.*)

Taxonomic relationships: DUFAY (1984).

Important genital characters. Male genitalia: Uncus relatively short, straight; clavus moderately elongate, digitiform, not dentate; dorsal costa of valva with acute, sclerotized angle; harpe moderately elongate, slightly curved, obtuse with specialized, teat-like tip; aedeagus relatively long, arched; carina acute, thorn-like; basal cornutus, near carina, thorn-like, often shortly dentate; medial cornutus reduced to a short, weakly sclerotized, conical diverticulum. – Female genitalia: Anthrum strongly sclerotized, shield-like with narrow V-shaped or broad, U-shaped incision; ductus bursae strongly sclerotized, granulose and ribbed longitudinally, with large, sclerotized left-hand pocket proximally (corresponding to cornutus of vesica), appendix bursae short, recurved, rugulose; corpus bursae elliptical with four longitudinal signa.

4. species-group: "capnistis-group"

Chersotis capnistis (LEDERER, 1871)
Chersotis leucostola VARGA et RONKAY, 1996
Chersotis nitens BRANDT, 1941
Chersotis metagrapha VARGA, 1975
Chersotis sterilis (BRANDT, 1938)
Chersotis ronkayorum FIBIGER, HACKER et VARGA, 1992

Taxonomic relationships: VARGA et RONKAY (1996)

Important genital characters. Male genitalia: Uncus moderately long, arcuate; clavus digitiform, slightly arcuate, not dentate; dorsal costa of valva without sclerotized angle, harpe thick, basally broad, acute, on the inner side often with dentate crest; carina obtuse, vesica recurved with two strong, basal and medial, cornuti. Female genitalia: Anthrum with very broad, U-shaped incision; ductus

* RÉZBÁNYAI-RESER (1997) studied the type material of this "*in litteris*" new species, belonging to the CORTI collection (Natural History Museum Basel, Switzerland). He noticed that the specimens labelled by CORTI as "*vissifera*" represented an undescribed species which was renamed by him: *Ch. cortifera* sp. n. Because this material was lent to Dr. RÉZBÁNYAI-RESER, I could not study the type material of *Ch. vissifera* CORTI i. l. The drawings, however, prepared and sent to me by Dr. RÉZBÁNYAI-RESER, which were recently (1997, Ent. Ber. Luzern) also published, could not convince me, that the differences, which were found by him in the female genitalia only, are sufficient to separate this taxon as a species. The differences of cornuti, figured by him, are clearly insufficient, because the shape and dentition of cornuti show a considerable range of variation. In addition, he obviously changed the aedeagi of *Ch. transiens* and *stridula* (loc. cit. : Abb. 8) which fact, unfortunately, resulted in the completely erroneous description of *Ch. altajensis* "n. sp." which could be an insignificant local variation of *Ch. transiens* only. NB. : the type locality of *Ch. transiens* is: "Jedirin-Gol" which belongs to Mongolia, which fact was also obviously overlooked by Dr. RÉZBÁNYAI-RESER.

bursae long, straight, strongly sclerotized, folded longitudinally with two sclerotized pockets (corresponding to the basal und medial cornuti of vesica); bursa bifid (like *Dichagyris*!), appendix bursae broad, elongate and slightly arcuate but not recurved; corpus bursae long, saccate.

5. species-group: "multangula-group"

Chersotis multangula (HÜBNER, [1803])
Chersotis andreae DUFAY, 1973
Chersotis semna (PÜNGELER, 1906)
Chersotis pachnosa VARGA, 1975

Taxonomic relationships: VARGA (1975), HACKER & VARGA (1990).

Important genital characters. Male genitalia: Uncus strong, arcuate; clavus digitiform, slightly arcuate, not dentate; dorsal costa of valva without any sclerotized angle, harpe thick, basally broad, without dentate crest; aedeagus long, only slightly curved; carina obtuse, in some species strongly sclerotized or with dentate sclerotization; vesica recurved with two strong, basal and medial, cornuti; medial cornutus often very large. Female genitalia: Anthrum with very broad, U-shaped incision; ductus bursae long, straight, strongly sclerotized, with two sclerotized pockets (corresponding to basal und medial cornuti of the vesica); bursa bifid (like *Dichagyris* LEDERER, 1857!), appendix bursae long and broad, slightly arcuate but not recurved; corpus bursae long, saccate, with spot-like signa.

Because the male genitalia of *Ch. pachnosa* with everted vesica are not figured in the original description, this omission remedied here (Figs 38–50).

6. species-group: "griseivena-group"

Chersotis griseivena (HAMPSON, 1894)
Chersotis harutai RONKAY et VARGA, 1998
Chersotis vargai HACKER, 1992

Taxonomic relationships: HACKER (1990), HREBLAY & RONKAY (1998).

Important genital characters. Male genitalia: Uncus strong, basally curved; clavus digitiform, slightly arcuate, not dentate; dorsal costa of valva without any sclerotized angle, harpe strong, basally broad, curved and apically pointed; aedeagus relatively short, with large, globular coecum, carina strongly sclerotized; vesica recurved, with one huge medial cornutus. Female genitalia: Anthrum with broad, U-shaped incision; ductus bursae long, straight, strongly sclerotized, distally with sclerotized pocket (corresponding to large medial cornutus of vesica); appendix bursae long and broad, slightly arcuate but not recurved; corpus bursae long, saccate.

7. species-group: "juvenis-group"

Chersotis juvenis (STAUDINGER, 1901)

Chersotis kouros VARGA et RONKAY, 1996
Chersotis shandur sp. n.
Chersotis calorica (CORTI, 1930)
Chersotis electrographa VARGA, 1990
Taxonomic relationships: VARGA (1990), VARGA & RONKAY (1996)

Important genital characters. Male genitalia: Uncus strong, basally curved; clavus very short, semiglobular or short digitiform; costa of valva without any sclerotized angle; harpe thick and short, slightly curved, acute; aedeagus short, slightly curved, with huge coecum; carina acute, strongly sclerotized; vesica long, recurved, with huge medial cornutus, proximal part hollowed, distal part narrower. Female genitalia: Anthrum strongly sclerotized with U-shaped incision; ductus bursae long, folded and with rugulose lateral pocket (lock-and-key with the huge cornutus), appendix bursae recurved and rugulose; corpus bursae elliptical, without signa. While the first four species have very similar genitalia, *Ch. electrographa* shows a mixture of specialized (shortened valva) and plesiomorphic (form of clavus, not fully reduced corona) characters.

8. species-group: "vicina-group"

Chersotis vicina (CORTI, 1930)
Chersotis petermarci sp. n.
Taxonomic relationships: see the description of *Ch. petermarci.*

Important genital characters. Male genitalia: Uncus strong, basally curved; clavus very short, semiglobular; dorsal costa of valva without any sclerotized angle; harpe thick and short, acute; the whole genital capsula in general similar to those of members of the former species-group; aedeagus short, slightly curved, with huge coecum; carina acute, strongly sclerotized; vesica long, recurved or S-like, its surface covered with tiny spinules; with huge, obtuse medial cornutus and with claw-like field of short, pyramid-like cornuti. Female genitalia: Anthrum strongly sclerotized with narrow, V-shaped incision; ductus bursae long, folded; distally with rugulose lateral pocket (lock-and-key structure with huge cornutus), appendix bursae recurved and rugulose; corpus bursae elliptical, without signa.

9. species-group: "binaloudi-group"

Chersotis antigrapha BOURSIN, 1961
Chersotis binaloudi BRANDT, 1941
Chersotis deplanata (EVERSMANN, 1843)

Important genital characters. Male genitalia: Uncus strong, basally curved; clavus very short, semiglobular; dorsal costa of valva without any sclerotized angle; harpe thick and short; aedeagus short, slightly curved, with huge coecum; carina acute, strongly sclerotized; vesica very long, fully recurved with a very

long, acute, spine-like cornutus. Female genitalia: Anthrum strongly sclerotized with broad, U-shaped incision; ductus bursae long, folded, relatively weakly sclerotized; distally with rugulose lateral pocket (lock-and-key structure with huge cornutus), appendix bursae broad, recurved; corpus bursae elliptical, without signa. The first described species of this group, *Chersotis deplanata* (EVERSMANN) shows several autapomorphic features, thus it seems to be more remote from other species. *Ch. antigrapha* and *binaloudi* surely form a pair of sister species.

10. species-group: "hahni-group"

Chersotis hahni (CHRISTOPH, 1885)
Chersotis curvispina BOURSIN, 1961
Chersotis zukowskyi (DRAUDT, 1936)
(= *Chersotis hellenica* BOURSIN, 1961)
Taxonomic relationships: VARGA (1990).

Important genital characters. Male genitalia: Uncus relatively short, strong; clavus short, digitiform; dorsal costa of valva without any sclerotized angle; distal end of valva obtuse, with short, digitus-like processus; harpe thick, strong; aedeagus straight, long; carina strongly sclerotized; vesica recurved with very long, huge medial cornutus. Female genitalia: Anthrum strongly sclerotized with narrow, V-shaped incision; ductus bursae short, relatively weakly sclerotized; with a rugulose lateral pocket distally (lock-and-key structure with huge cornutus), appendix bursae long, tubular; corpus bursae elongate and saccate, without signa.

11. species-group: "obnubila-group"

Chersotis obnubila (CORTI, 1926)
Chersotis ebertorum KOÇAK, 1980
(= *Ch. maraschi* CORTI et DRAUDT, 1933)
Taxonomic relationships: KOÇAK (1980), VARGA & RONKAY (1996)

Important genital characters. Male genitalia: Uncus relatively thin, basally curved; clavus very short, digitiform; valva elliptical, elongate; harpe short, with club-like tip; aedeagus very long and thin, carina rather specialized, strongly sclerotized, boat-hook-shaped; vesica recurved, pyramid-like medial diverticulum transformed into huge, straight, moderately sclerotized cornutus. Female genitalia: Anthrum strongly sclerotized with narrow, V-shaped incision; ductus bursae long, folded; distally with rugulose lateral pocket (lock-and-key structure with the huge cornutus), appendix bursae recurved and rugulose; corpus bursae elongate, without signa.

12. species-group: "sjuntensis-group"

Chersotis sjuntensis (KUSNETZOV, 1958)

Taxonomic relationships: VARGA & RONKAY (1996)

Only a single, very peculiar species, with several, probably autapomorphic characters.

Important genital characters. Male genitalia: Uncus strong, basally curved, clavus relatively short and unspecialized; valva very elongate; harpe huge, thick; aedeagus long, carina thin, but strongly sclerotized, needle-shaped; vesica with acute basal diverticulum, helicoid curving and densely covered by minute setae; pyramid-like medial diverticulum transformed into huge, straight, strongly sclerotized, spatula-formed cornutus. Female genitalia: Anthrum strongly sclerotized with narrow, V-shaped incision; ductus bursae long, folded; distally with rugulose lateral pocket (lock-and-key with the huge cornutus), appendix bursae recurved and rugulose; bursa without signa.

13. species-group: "elegans-group"

Chersotis elegans (EVERSMANN, 1837)

Chersotis kacem (LE CERF, 1933)

Chersotis eberti DUFAY et VARGA, 1995

Chersotis anatolica (DRAUDT, 1936)

Chersotis larixia (GUENÉE, 1852)

Taxonomic relationships: DUFAY (1981, 1986), DUFAY & VARGA (1995), VARGA (1986).

Important genital characters. Male genitalia: Clavus very short, digitiform; valva elliptical, elongate; harpe strong, straight, obtuse; aedeagus very long, with huge coecum, carina triangular, strongly sclerotized; vesica recurved, with huge, claw-like cornutus; its surface densely covered with tiny, spinule-like structures. Female genitalia: Anthrum strongly sclerotized with typical U- or V-shaped incision; ductus bursae long, ribbed and folded longitudinally; with large rugulose lateral pocket distally (lock-and-key structure with huge cornutus), appendix bursae rugulose, with very special structures (see DUFAY & VARGA 1995); corpus bursae large, elliptical, without signa.

Chersotis larixia is relatively remote from all other taxa of the species-group. Thus, it was placed by FIBIGER (1997) to its own, monotypic species-group. The male genitalia show several rather specialized, autapomorphic features, the female genitalia, however, clearly indicate that this species is closely related to the other species of this group.

14. species-group: "fimbriola-group"

Chersotis rungsi BOURSIN, 1944

Chersotis stenographa VARGA, 1979

Chersotis cuprea ([DENIS et SCHIFFERMÜLLER], 1775)
Chersotis gratissima (CORTI,1932)
Chersotis nekrasovi VARGA, 1997
Chersotis friedeli PINKER, [1972] 1974*
Chersotis fimbriola (ESPER, [1803])
Chersotis laeta (REBEL, 1904)
Taxonomic relationships: HACKER & VARGA (1990)

This species-group is a complex of several species-pairs and groups of more closely related species. It will be treated here as a species-group without a more detailed analysis, because it was already revised by HACKER and VARGA (1990).

Important genital characters. Male genitalia: Clavus variable, often digitiform, straight (*fimbriola* and *laeta*) or curved (*cuprea*), in other species long and acute (*rungsi*, *gratissima*, *friedeli*), in two species short, displaying the short digitiform (plesiomorphic) structure (*stenographa*, *nekrasovi*); valva elliptical, distally often elongate; harpe strong, arcuate, obtuse and often distally spatulate (e.g. *gratissima*, *nekrasovi*, *friedeli*); aedeagus arcuate, moderately long with huge coecum, carina triangular, strongly sclerotized; vesica recurved, in most species with a row or field of huge cornuti (*cuprea*, *rungsi*, *stenographa*, *gratissima*) or with bundle of fine, spicule-like cornuti (*nekrasovi*, *fimbriola*, *laeta*), in one single species cornuti reduced (*friedeli*). Female genitalia: Anthrum strongly sclerotized with broad U-shaped incision; ductus bursae short, broad, proximal part widened, finely granulose; appendix bursae recurved, rugulose, bursa with longitudinal signa.

15. species-group: Chersotis illauta (DRAUDT, 1936)

Chersotis illauta (DRAUDT, 1936)
Taxonomic relationships: HACKER & VARGA (1990)

Important genital characters. Male genitalia: clavus long, arcuate and acute, valva elliptical, distally elongate; harpe short, broad, apically rounded; aedeagus moderately long, arcuate, carina triangular, strongly sclerotized; vesica long, tubular, with S-like curving, with only a single basal cornutus (like *Dichagyris* LEDERER, 1857). Female genitalia: Anthrum with only a weak incision, bursa bisaccate (like *Dichagyris*-species), appendix bursae elongate.

HACKER and VARGA (1990) included this species in the *fimbriola*-group. It seems to be, however, more remote from this group. The structure of the vesica with the single large, subbasal cornutus proved to be unique within the genus.

* The supposed synonymy (HACKER & VARGA 1990) of *Chersotis friedeli* PINKER with *Lycophorus villosus* (ALPHERAKY, 1887) is erroneous; latter species is closely related to the genus *Agrotis* (type studied by RONKAY & VARGA, ZIN, St. Petersburg)

Probably this character may be an evidence for *Chersotis* and related genera belonging to the Agrotini and not to Noctuini (as opposed to the opinion of LAFONTAINE & POOLE 1993).

16. species-group: "glebosa-group"

Chersotis glebosa (STAUDINGER, 1900)

Taxonomic relationships: a fairly isolated species, with some autapomorphic characters in the male genitalia.

Important genital characters. Male genitalia: Uncus strong, moderately long, clavus short, rounded; valva elliptical, distally slightly elongate; harpe short, broad, apically acute; aedeagus short, slightly curved, with huge coecum; carina acute, strongly sclerotized, with needle-like longitudinal processus which is unique not only for this genus, but for Noctuinae in general; vesica very long, recurved, without cornutus. Female genitalia: Anthrum with weak incision only, ductus bursae with peculiar lateral pocket corresponding to the large longitudinal processus of carina.

17. species-group: "sarhada-group"

Chersotis sarhada BRANDT, 1941

Chersotis delear BOURSIN, 1970

Taxonomic relationships: BOURSIN (1970)

Important genital characters. Male genitalia: Uncus long, strong, arcuate, clavus very short, semiglobular; ventral saccular process thick, strongly sclerotized (autapomorphic character for this species pair!); valva elliptical, relatively short and narrow; harpe basally broad, curved in right angle, apically pointed; juxta very broad, pentagonal, with two acute edges dorsally; aedeagus relatively long, arcuate, with large, semiglobular coecum, carina triangular or with dentate processus, strongly sclerotized; vesica long, fully recurved, with short, conical diverticulum medially and short and acute bulbed cornutus. Female genitalia: Anthrum with broad, V-shaped incision; ductus bursae very broad, relatively short, very strongly sclerotized; corpus bursae elliptical, large; with numerous (9–10) spot-like signa; appendix bursae short, conical, rugulose.

18. species-group: "margaritacea-group" (= subg. Margasotis BECK, ***nom. nud.)***

Chersotis margaritacea (DE VILLERS, 1789)

Chersotis cyrnaea (SPULER, 1907)

Taxonomic relationships: BECK (1991), FIBIGER (1993)

Important genital characters. Male genitalia: Uncus relatively long, basally curved; clavus long, moderately sclerotized; harpe strong, elongate and laterally curved; juxta broad, shield-like; aedeagus strong, straight; vesica curved, rela-

tively simple, with semilunar basal diverticulum, without cornuti. Female genitalia: Anthrum only moderately sclerotized with very broad U-shaped incision; ductus bursae short, broad, slightly curved medially; appendix bursae curved laterally, rugulose, bursa with four stripes of signa.

19. Species-group: "anachoreta-group" (subg. or genus Cyrebia GUENÉE, 1852)

Chersotis anachoreta (HERRICH-SCHAEFFER, 1851)
Chersotis luperinoides (GUENÉE, 1852)
Taxonomic relationships: FIBIGER (1997)

Important genital characters. Male genitalia: Uncus short, thick; clavus short, elliptical, moderately sclerotized; dorsal costa of valva medially convex; harpe strongly sclerotized; aedeagus short, thick; vesica recurved, hollowed basally, cornuti reduced. Female genitalia: Ductus bursae broad, antrum finely dentate only; appendix bursae broad and short, corpus semiglobular, without signa.

PHYLOGENETIC REMARKS ON THE SPECIES-GROUPS OF CHERSOTIS

The species of the genus *Chersotis* display numerous derived characters. Most of them are typical, unfortunately, only for a limited number of species. Other ones are present, however, also in those species, which recently have been relegated to other genera. Some of these characters proved to be true synapomorphies, while other ones seem to be only convergent reductions of certain structures. The type species of the genus, *Ch. rectangula* belongs to those species which display a relatively great number of derived characters of both types. In the present paper we could not reach all the taxonomic consequences which follow from this peculiar situation, only some of the possible solutions are proposed.

The best synapomorphic character, on which the genus *Chersotis* can be based, seems to be the U- or V-like incision of the strongly sclerotized anthrum in the females, being present in most of *Chersotis* species. This character I could not observe in this typical form in any other Noctuinae species. Other characters, however, which are widely used by the different authors for taxonomic characterization of the genus *Chersotis*, seem to be phylogenetically misleading or not valuable. We have to point out here two often-mentioned characters.

Some authors (FIBIGER 1990, 1993, LAFONTAINE 1991, LAFONTAINE & POOLE 1993) ascribe great taxonomic significance to the strongly sclerotized ductus bursae of the females, which is used for the basic dichotomy of Noctuinae (Noctuini vs. Agrotini). It is correctly pointed out that in a monophyletic group of genera (e. g. *Xestia* s. l. and related genera, *Eugraphe*, *Eugnorisma*, *Noctua*,

Spaelotis etc.) the strong sclerotisation originates from two main parts which are subdivided by a membranous zone. However, the genus *Chersotis*, and of course also the closely related genera *Rhyacia* and *Epipsilia*, do not have this subdivision of the ductus, which is also often not heavily sclerotized, and consequently, they cannot belong to this phylogenetic unit. It is obvious that in this genus (and genera, respectively) the plesiomorphic state of this character is a membranous, but usually longitudinally folded, rugulose or granulose ductus, approximately in the same form which can be observed in many species of *Dichagyris*. The "core areas" of the heavier sclerotization and the often well-developed lateral pockets evidently have been evolved under the constraints of heavily sclerotized cornuti of vesica, corresponding the species-specific "lock-and-key" structures in female and male genitalia (MIKKOLA *et al.* 1987).

The reduction of cucullus and corona which is often evaluated as a synapomorphy of a major evolutionary lineage within Noctuinae (NB: it was regarded as a distinctive character for both major subgroups of Noctuinae by KOZHANTSCHIKOV 1937 and also phylogenetically interpreted by LAFONTAINE & POOLE 1993) occurs convergently in numerous Noctuidae groups which are surely phylogenetically not closely related. I think it is true also for the Noctuinae. On the other hand, the strongly modified clavus (which is often mentioned as "dorsal processus of the sacculus"), is developed also in such species in similar form which are actually relegated as *Rhyacia* (e.g. *Rh. diplogramma* HAMPSON, 1903, *Rh. oromys* VARGA, 1990) and *Epipsilia*. The rounded, not strongly sclerotized costal lobe on the dorsal margin of the valva was regarded by MIKKOLA *et al.* (1987) as a synapomorphy of the *Chersotis rectangula*-group. In reality, this character occurs in weakly expressed form also in the species of the *Ch. sordescens*-group which surely forms the sister-group of the *rectangula*-group (see thorny dorsal processus of sacculus, thorny form of carina, completely recurved vesica without cornutus; short, conical diverticulum in medial position etc.). This character, as a strongly sclerotized angular lobe, can be also observed in a more expressed form in some other species-groups of *Chersotis* (see *Chersotis ocellina*-group) and in fact in most "*Rhyacia*" species mentioned below which have the hook-like structure of the carina.

The thorn-like, strongly sclerotized form of carina occurs in some *Rhyacia* (e.g. *Rh. hampsoni* BANG-HAAS, 1910, *Rh. electra* STAUDINGER, 1888) species, and the hook- or thorn-like structures, which can be derived from it, are to be found in numerous *Rhyacia* species as well (*Rh. similis* STAUDINGER, 1881, *nyctimerina* STAUDINGER, 1888, *nyctimerides* BANG-HAAS, 1922, *subdecora* STAUDINGER, 1888, *oxytheca* BOURSIN, 1957, *evartianae* VARGA, 1990, *gabori* VARGA, 1997, *diplogramma* HAMPSON, 1903, *oromys* VARGA 1990, *junonia* STAUDINGER, 1881, *oreas* PÜNGELER, 1904, *karakoreas* HACKER et VARGA, 1991, *peksi* HACKER et VARGA, 1991, *mirabilis* BOURSIN, 1954, *"Standfuss-*

rhyacia" chimaera HACKER et VARGA, 1991 **stat. rev.***). It seems to be very important that also the short, conical medial diverticulum of the vesica (with or without a short, spine-like or conical cornutus) occurs also in all of the *Rhyacia* species mentioned above.

Based on the genital characters mentioned above, we can draw the following conclusions on the phylogenetic relations of the species-groups within the genus:

- *The phylogenetic relationships of the species-groups 1, 2 and 3:* The *rectangula*-group (1) and *ocellina*-group (3) was already regarded by MIKKOLA *et al.* (1987) as closely related. I can support here this view with the reservation, that the *sordescens*-group (2) should be the true sister-group of the *rectangula*-group (1). Thus, (1 + 2) can be evaluated as sister-group of (3). The assumed sister-group of this [(1+2) + 3] monophylum is probably the group of the "*Rhyacia*" species mentioned above, however, which has been relegated until now to the genus *Rhyacia*. Consequently, the latter large and rather heterogenous genus probably must be subdivided. This procedure, however, cannot be done without a detailed revision of all species, recently relegated as *Rhyacia* and *Epipsilia*. As a consequence of this situation, I cannot try here to solve all the phylogenetic and nomenclatorical questions connected to the probably monophyletic generic complex *Chersotis*, *Rhyacia* and *Epipsilia*.
- A similar situation can be observed in the species-groups 4, 5 and 6. Based on numerous synapomorphies (digitiform costal process of valva; short, basally thick, apically pointed harpe; recurved vesica with two large cornuti etc.), the *capnistis*-group (4) and the *semna*-group (5) proved to be the sister-groups. Thus, the much more heterogeneous *multangula*-group (6) can probably regarded as sister-group of the antecedents (4 + 5).
- The species-groups 7–12 form the next, more complicated, assumed monophyletic unit within the genus. Their phylogenetic relationships are difficult to clarify because of presence of a great number of very peculiar autapomorphic characters, in some cases typical for whole species-groups or pairs of sibling species (e.g. the very long, needle-like medial cornutus of the *antigrapha*-group; the transformation of the pyramid-like medial diverticulum into a huge, straight, moderately sclerotized cornutus in the *obnubila*-group, or the large, semilunar, obtuse medial cornutus and other specializations of vesica in the *vicina*-group, the peculiar, distally obtuse form of valva in the *Ch.*

* This "genus" was erroneously considered in the original description as transitional between *Rhyacia* and *Standfussiana*. These genera are, however, not closely related to each other, and the species *Rhyacia chimaera* (stat. rev.) is a *Rhyacia* belonging to the species group, related to *Rh. junonia* STAUDINGER.

hahni-group etc.), in others, however, being present only in single species (e. g. the very curious surface structure of the vesica and the huge, spade-like cornutus of *Ch. sjuntensis*). Here, a phylogenetically older radiation into species-groups and a much more recent speciation leading to very closely related sibling pairs of species seem to be very probable.

- The "*elegans*"-group has been treated by DUFAY & VARGA (1995). Here a recent speciation due to marginal splitting (*Ch. elegans* vs. *Ch. kacem* and *eberti*), leading to allopatric siblings, seem to be very probable. *Ch. anatolica* which is largely sympatric with *Ch. elegans* can be regarded as a result of an earlier wave of speciation, while *Ch. larixia* is surely the mostly separated species within this group.
- The next larger group of the genus is formed by the species of the "*fimbriola*-group", analysed elsewhere (HACKER & VARGA 1990). The supposed sister-group relations are only slightly changed by the description of *Ch. nekrasovi* VARGA, 1997, which proved to be the sister species of *Ch. gratissima* CORTI.

CONCLUSIONS ON THE POSSIBLE MODES AND MECHANISMS OF SPECIATION IN CHERSOTIS

The genus *Chersotis* is rich in groups or pairs of very closely related species. Here only those species-pairs (or in few cases "triplets" of species) are analysed which are very closely related, thus they can be regarded as "sibling species" which may have originated very recently. Most of them show greatly allopatric range of distribution, in some cases with insignificant overlap (Table 2), and only relatively few pairs of species show greatly overlapping ranges of distribution (Table 3). Because in all cases of partial overlap of distributions at least one of the overlapping species has (in some cases both have) a fairly large range (e.g. extant species: *Ch. capnistis*, *Ch. semna*, *Ch. juvenis*, *Ch. sarhada*, extant pairs of species: *Chersotis rectangula* and *Ch. andereggii*, *Ch. firdusii* and *Ch. sordescens*, *Ch. elegans* and *Ch. anatolica*, *Ch. fimbriola* and *Ch. laeta*), it seems to be very probably that all these cases are secondary overlaps, subsequent to a previous allopatric type of speciation.

The geographical extension of the allopatric areas may be quite different. The completely allopatric *Chersotis andereggii* and *Ch. juncta*, *Ch. capnistis* and *Ch. leucostola*, *Ch. sarhada* and *Ch. delear* have relatively extended ranges, while in numerous cases the large area of an extant species is combined with the peripherically isolated area of some strictly endemic species, obviously originated by marginal splitting: *Chersotis firdusii* vs. *Ch. herczigi*; *Ch. semna* vs. *Ch. pachnosa*; *Ch. ebertorum* vs. *Ch. obnubila*, *Ch. elegans* vs. *Ch. kacem* and *Ch.*

Table 1. Species excluded from the genus *Chersotis* BOISDUVAL (compared with the check-list of POOLE (1989))

Name of species	Suggested genus (with references)
albifurca (ERSHOV, 1877)	*Eugraphe* HÜBNER, [1821] (HACKER, 1996)
bonza (PÜNGELER, 1899)	*Xestia* HÜBNER, [1818]
melancholica (LEDERER, 1853)	*Pseudohermonassa* VARGA et RONKAY, 1989
monogramma (HAMPSON, 1903)	*Protexarnis* (HACKER, 1996)
ononensis (BREMER, 1861)	*Pseudohermonassa* VARGA et RONKAY, 1989
poliogramma (HAMPSON, 1903)	*Dichagyris* LEDERER, 1857
Species, erroneously synonymised by POOLE (1989)	
Proposed synonymy by POOLE	Revised status
Agrotis rectangula var. *acutangula* STAUDINGER = *Chersotis andereggii* (BOISDUVAL)	*Ch. acutangula* (STAUDINGER), **bona sp.**, see also MIKKOLA *et al.* (1987)
Rhyacia elegans subsp. *anatolica* DRAUDT	*Chersotis anatolica* (DRAUDT), **bona sp.**, see also VARGA (1986), DUFAY & VARGA (1995)
Agrotis cyrnea SPULER = *Chersotis margaritacea* (DE VILLERS)	*Ch. cyrnea* (SPULER), **bona sp.**, see also FIBIGER (1993, 1997)
Chersotis elegantula BOURSIN = *Ch. elegans* (EVERSMANN)	*Chersotis elegantula* BOURSIN = *Ch. anatolica* (DRAUDT), see also VARGA (1986), DUFAY & VARGA (1995)
Agrotis fimbriola var. *laeta* REBEL = *Ch. fimbriola* (ESPER), subsp.	*Chersotis laeta* (REBEL), bona sp. see also CORTI & DRAUDT (1933), HACKER & VARGA (1990), FIBIGER (1997)
Caradrina (Chersotis) sjuntensis KUSNETZOV = *Chersotis sordescens* (STAUDINGER)	*Chersotis sjuntensis* (KUSNETZOV), **bona sp.** see also VARGA & RONKAY (1996)
Episilia stridula HAMPSON = *Chersotis transiens* (STAUDINGER)	*Chersotis stridula* (HAMPSON), **bona sp.**
Species incertae sedis	
secreta (CORTI et DRAUDT, 1933)	
tragica (CORTI et DRAUDT, 1933)	
geochroa BOURSIN	

eberti; *Ch. juvenis* vs. *Ch. kouros*, *Ch. calorica* and *Ch. shandur*. In the cases of *Chersotis fimbriola* and *Ch. fimbriola raddei* we can observe probably this type of speciation "*in statu nascendi*". It seems also quite typical that in some cases both members of an allopatric pair are strictly localised endemic species, e.g.: *Chersotis ronkayorum* and *Ch. sterilis*, *Ch. nitens* and *Ch. metagrapha*, *Ch. petermarci* and *Ch. vicina*, *Ch. binaloudi* and *Ch. antigrapha*, *Ch. rungsi* and *Ch. stenographa*, *Ch. gratissima* and *Ch. nekrasovi*.

Table 2. Allopatric pairs of species (only exceptionally with a partial overlap)

western species	eastern species
Ch. andereggii BOISDUVAL: N Europe, Alps, Balkans, Asia Minor, Caucasus, Transcaucasus, Iran, Mts of Southern Siberia	*Ch. juncta* GROTE: Eastern Siberia, Beringia, North America
Ch. firdusii SCHWINGENSCHUSS: Elburs, Hindukush, Hissar and Darwaz range	*Ch. sordescens* STAUDINGER: Tien-Shan range, Hindukush, Hissar and Darwaz range *Ch. herczigi* VARGA: W Himalaya Mts in Pakistan
Ch. ronkayorum FIBIGER, HACKER et VARGA: Asia Minor	*Chersotis sterilis* BRANDT: Zaghros Mts
Ch. nitens BRANDT: Kopet-Dagh, Khorassan	*Ch. metagrapha*: Afghanistan, Hindukush Mts, Badakhshan
Ch. capnistis LEDERER: S-Russia, Caucasus and Transcaucasus, Asia Minor, S-Balkans	*Ch. leucostola* VARGA et RONKAY: Tien-Shan Mts
Ch. semna PÜNGELER: Asia Minor, Transcaucasus, Elburs, Khorassan and Kopet-Dagh	*Ch. pachnosa*: Afghanistan, Badakhshan
Ch. juvenis STAUDINGER: Asia Minor, Transcaucasus, Elburs Mts, Zaghros Mts.	*Ch. kouros* VARGA et RONKAY: Kopet-Dagh Mts *Ch. shandur* sp. n. : Pakistan, Karakoram Mts *Ch. calorica* CORTI: N and E Tien-Shan Mts
Ch. petermarci VARGA: Zeravshan Mts, W Tien-Shan Mts	*Ch. vicina* CORTI: N and E Tien-Shan Mts
Ch. binaloudi BRANDT: Khorassan Mts	*Ch. antigrapha* BOURSIN: Hindukush Mts
Ch. ebertorum KOÇAK: Asia Minor, Transcaucasus, Libanon Mts, Elburs Mts	*Ch. obnubila* CORTI: Kopet-Dagh Mts
Ch. kacem LE CERF: Atlas Mts *Ch. elegans* EVERSMANN: Iberian Mts, Pyrenées, Alps, Balkans, Asia Minor, Transcaucasus, S Russia, W Tien-Shan and W Altai Mts	*Ch. eberti* DUFAY et VARGA: Elburs Mts, Zaghros Mts
Ch. sarhada BRANDT: Asia Minor, Transcaucasus, Elburs and Kopet-Dagh Mts	*Ch. delear* BOURSIN: Hindukush, Hissar and Darwaz Mts
Ch. rungsi BOURSIN: Atlas Mts	*Ch. stenographa* VARGA: Asia Minor, Transcaucasus
Ch. gratissima CORTI: Asia Minor, Transcaucasus, Elburs Mts	*Ch. nekrasovi* VARGA: Pamir Mts

The restricted areas of such sister-species completely fulfill the criteria of the "areas of endemism" (HAROLD & MOOR 1994), thus they can be regarded as highly valuable pairs of monophyletic species for phylogenetic-biogeographical studies. The existence of few, phylogenetically quite isolated species (e.g. *Ch. sjuntensis*, *Ch. glebosa*, *Ch. illauta*) however, indicate that probably also an older wave of speciation had taken place in this genus, from which most of the species

Table 3. Mostly sympatric pairs and groups of species

Ch. rectangula ([DENIS et SCHIFFERMÜLLER]): Central and Southern Europe, Caucasus, Asia Minor	*Ch. andereggii* BOISDUVAL: N Europe, Alps, Balkans, Asia Minor, Caucasus, Transcaucasus, Iran, Mts of Southern Siberia *Ch. acutangula* STAUDINGER: Transalai and Hindukush Mts
Ch. hahni CHRISTOPH: Transcaucasia, Elburs, Kopet-Dagh Mts	*Ch. curvispina* BOURSIN: Kopet-Dagh Mts, Hindukush Mts
Ch. elegans EVERSMANN: Iberian Mts, Pyrenées Alps, Balkans, Asia Minor, Caucasus, Transcaucasus, S Russia, W Tien-Shan and W Altai Mts *Ch. eberti* DUFAY et VARGA: Elburs Mts, Zaghros Mts	*Ch. anatolica* DRAUDT*: Iberian Mts, Pyrenées, Alps, Central Appenines, Balkans, Asia Minor, Caucasus, Transcaucasia, S Russia, Kopet-Dagh, W Tien-Shan Mts
Ch. fimbriola ESPER: Atlas, Iberian Mts, Pyrenées, Sicily, W Alps, Pannonian basin, Balkans Asia Minor, Crymaea, Transaucasus, Zaghros, Elburs Mts, Kopet-Dagh Mts	*Ch. laeta* REBEL: Balkans, W coastal area of Black Sea, Asia Minor, Caucasus, Transcaucasus, Elburs Mts

* These species are not true sibling species, because they are strongly differentiated from each other (see: DUFAY & VARGA 1995).

became extinct. This hypothesis is strongly supported by those cases in which the species-groups consist of a more isolated species, which can be regarded as the "outgroup" of the all other members of the group, e.g. *Chersotis electrographa* for the *Ch. juvenis-kouros-calorica-shandur* group, or *Ch. larixia* for the *Ch. elegans-kacem-eberti-anatolica* group.

Summarizing all these cases analysed here, they seem strongly in support of the primarily allopatric mode of speciation in the genus *Chersotis*.

ADDENDA AND CORRIGENDA TO FORMER PUBLICATIONS

In the publication: New and revised species of Noctuinae (VARGA, Z. & RONKAY, L. 1996, *Esperiana* **5**) some figures mixed up. Aedeagi of *Ch. obnubila* CORTI: Figs 68, 69 and 71; those of *Ch. ebertorum* KOÇAK: Figs 70, 72, 73. The figures 1–8 and 9–16, respectively, on the photoplates were also mixed up.

* * *

Acknowledgements – The author would like to express his sincere gratitude to the late Mr E. DE BROS, to Mrs E. VARTIAN, Mr G. EBERT, Mr GY. FÁBIÁN, Dr B. HERCZIG, Dr M. HREBLAY, Dr P. GYULAI, Dr K. MIKKOLA, Prof. Dr C. M. NAUMANN, Mr G. RONKAY, Dr L. RONKAY and Dr A.

SVIRIDOV for loan of valuable comparative material, including types, for helpful suggestions and criticism. The valuable technical assistance of Mr. P. KOZMA is highly appreciated.

This survey was supported by OTKA (grant number T16465).

REFERENCES

BECK, H. (1992) Taxonomische Änderungen bei den Noctuinae, Cuculliinae and Plusiinae. *Atalanta* **22**: 175–232.

BECK, H. (1996) Systematische Liste der Noctuidae Europas (Lepidoptera: Noctuidae). *Neue ent. Nachrichten* **36**: 1–122.

BOURSIN, Ch. (1961) Eine neue Chersotis aus Griechenland. *Zschr. wiener ent. Ges.* **46**: 137.

CORTI, A. (1926) Studien über die Subfamilie der Agrotinae. IX. Drei neue palaearktische Agrotinae: A. glabripennis sp. n., Lycoph. strenua sp. n. und Epips. obnubila sp. n. *Soc. ent.* **41**: 14–16.

CORTI, A. (1930) Studien über die Subfamilie der Agrotinae. XXIII. A. multangula und deren Formen; A. vicina sp. n., guberlae sp. n., calorica sp. n. und einige verwandte Arten. *Mitt. münch. ent. Ges.* **20**: 1–20.

CORTI, A. & DRAUDT, M. (1933) *Agrotinae*. In: Seitz, A. : *Die Großschmetterlinge der Erde*, 3. *Die palaearktischen eulenartigen Nachtfalter*, Suppl., Alfred Kernen Verlag, Stuttgart, pp. 22–95.

DUFAY, CL. (1973) Description d'un nouveau Chersotis B. Atlanto-Mediterranéen (Lepidoptera: Noctuidae, Noctuinae). *Entomops* **4**(30): 177–184.

DUFAY, CL. (1981) Chersotis grammiptera (Rambur [1839]) bona sp. en France et en Espagne (Lep.: Noctuidae, Noctuinae). *Alexanor* **12**(3): 103–117.

DUFAY, CL. (1984) Chersotis oreina sp. n., noctuelle méconnue des montagnes de l'Europe occidentale. *Nota lepid.* **7**: 8–20.

DUFAY, CL. (1986) Révision de la nomenclature de deux Chersotis Boisduval, distinguées récemment (Noctuidae, Noctuinae). *Nota lepid.* **9**(1–2): 51–54

DUFAY, CL. & VARGA, Z. (1995) A new Noctuid species from Iran: Chersotis eberti sp. n. (Lepidoptera: Noctuidae). *Acta zool. hung.* **41**(1): 35–45.

FIBIGER, M. (1993) *Noctuinae* II, In: *Noctuidae Europeae* vol. 2. Entomological Press, Sorø, pp. 41–70.

FIBIGER, M. (1997) *Noctuinae* III, In: *Noctuidae Europeae* vol. 3. Entomological Press, Sorø, pp. 141–150.

FIBIGER, M. & HACKER, H. (1991) Systematic list of the Noctuidae of Europe (Lepidoptera). *Esperiana* **2**: 1–109.

HACKER, H. (1990) Die Noctuidae Vorderasiens (Lepidoptera). *Neue ent. Nachrichten* **27**: 1–739.

HACKER, H. (1992) Ergänzungen zu "Die Noctuidae Vorderasiens" und neuere Forschungs-ergebnisse zur Fauna der Türkei. *Esperiana* **3**: 409–446.

HACKER, H. & VARGA, Z. (1990) Die Gattung Chersotis Boisduval, 1840. I. Die fimbriola (Esper, [1803])/ laeta (Rebel, 1904)-Gruppe. *Spixiana* **13**: 277–327.

HAROLD, A. S. & MOOR, R. D. (1994) Areas of Endemism: definition and recognition criteria. *Syst. Biol.* **43**(2): 261–266.

HREBLAY, M. & RONKAY, L. (1998) Noctuidae. In: HARUTA, T. (ed.): *Moths of Nepal*, Part 5. *Tinea* **14**: 117–310.

KOÇAK, A. Ö. (1980) On the nomenclature of some genus and species group names of Lepidoptera. *Nota lepid.* **2**: 139–146.

KOZHANCHIKOV, I. V. (1937) *Sovki (Agrotinae).* Fauna SSSR, XIII (3), Moscow-Leningrad. [in Russian]

LAFONTAINE, D. J. (1987) Noctuoidea, Noctuidae (part Euxoa). *The Moths of America North of Mexico.* Fasc. 27. 2. Washington, pp. 237.

LAFONTAINE, D. J. & POOLE, R. W. (1993) Noctuoidea, Noctuidae (part Plusiinae). *The Moths of America North of Mexico.* Fasc. 25. 1. Washington, pp. 182.

MIKKOLA, K., LAFONTAINE, D. J. & GROTENFELDT, P. (1987) A revision of the Holarctic Chersotis andereggi-complex (Lepidoptera: Noctuidae). *Nota lepid.* **10**: 140–157.

POOLE, R. W. (1989) *Lepidopterorum Catalogus* (New Series) Noctuidae I-III. Fasc. 118. Brill, Leiden, Kobenhavn, Köln.

RÉZBÁNYAI-RESER, L. (1997) Chersotis-Studien 1. – Revision der transiens-stridula-Gruppe (Süd-Ural und Mittelasien) mit der Beschreibung von sp. n. cortifera und altajensis sowie ssp. n. uralica (Lepidoptera, Noctuidae) *Ent. Ber. Luzern* **38**: 155–170.

VARGA, Z. (1979) Neue Noctuiden aus der Sammlung Vartian (Wien) II. (Lepidoptera, Noctuidae). *Zschr. Arbeitsgem. österr. Ent.* **31**(1/2): 1–12.

VARGA, Z. (1990) New species of Noctuidae from Afghanistan and adjacent territories. I. The genera Euxoa Hübner, [1821] 1816, Dichagyris Lederer, 1857, Rhyacia Hübner, [1821] 1816 and Chersotis Boisduval, 1840 (Lepidoptera: Noctuidae, Noctuinae). *Esperiana* **1**: 167–198.

VARGA, Z. (1997) New species and subspecies of Dichagyris, Chersotis and Rhyacia (Lepidoptera, Noctuidae) from Central Asia. *Acta zool. hung.* **42**(3): 195–230.

VARGA, Z. & RONKAY, L. (1996) New and revised taxa of the genera Chersotis Boisduval, 1840 and Dichagyris Lederer, 1857 from Central Asia (Lepidoptera: Noctuidae, Noctuinae). *Esperiana* **4**: 103–132.

Received 25th May, 1998, accepted 7th September, 1998, published 30th December, 1998

ACTA ZOOLOGICA
ACADEMIAE SCIENTIARUM HUNGARICAE

An international journal of animal taxonomy and ecology

Instruction to authors

Submission of a paper implies that it has not been published previously, that is not under consideration for publication elsewhere, and that if accepted for the Acta Zoologica Hungarica, the authors will transfer copyright to the Hungarian Academy of Sciences/the Hungarian Natural History Museum as is customary. Articles and illustrations become the property of the HAS/HNHM.

Papers must be in English with British spelling, and be original contributions in the field of animal taxonomy, systematics, zoogeography and ecology. All manuscripts must be submitted to one of the editors (editor, assistant editor).

Entire manuscripts must be submitted on IBM compatible floppy disk and in duplicate printed copies and the author should retain a copy. In the case of multiple authors, the corresponding author should be indicated. Series of numbered papers will not be considered.

Manuscripts must be printed with double spacing (including the reference list), and with wide margins (30–35 mm) on the left side of the paper only. Authors are requested to keep their communications as concise as possible. Footnotes should be avoided or minimized, and italics should not be used for emphasis. A running head of not more than 30 letters should be supplied.

The manuscript should contain the following information:

Title should be followed by the name and full address of the author(s). Where possible, the fax and/or e-mail number of the corresponding author should be supplied with the manuscript, for use by the publisher.

Abstract should be a brief summary of the contents and conclusions of the paper, and should not be longer than 200 words and should not contain references.

Key words should not be more than five (exceptionally 6) key word entries.

Introduction should contain a brief survey of the relevant literature and the reasons for doing the work.

Materials and Methods supply sufficient information to permit repetition of the experimental or field work. The technical description of methods should be given only when such methods are new.

Results should be presented concisely. Only in exceptional cases will it be permissible to present the same set of results in both table and a figure. The results section should not be used for discussion.

Discussion should be separate from the results section and should deal with the significance of the results and their relationship to the object of the work (and, this is the place of the identification key in taxonomic revisions).

Acknowledgements (at most in 10 lines).

References. In principle the Harvard system is to be followed. References should be detailed in the following order: authors' names and initials, date of publication (in parentheses), the title of the article, the name of the journal as abbreviated in the World List of Scientific Periodicals (4th edn 1963), the volume, and the first and last pages of the article, e.g.

NORRBOM, A. L. and KIM, K. C. (1985) Taxonomy and phylogenetic relationships of Copromyza Fallén (s.s.) (Diptera: Sphaeroceridae). *Ann. Entomol. Soc. Am.* **78**: 331–347.

For books the author's names, date of publication, title, edition, page reference, publisher's name and the place of publication should be given, e.g.

HINTON, H. E. (1981) *Biology of insect eggs*, vol. 2. Pergamon Press, New York.

or

MCALPINE, J. F. (1981) Morphology and terminology, adults, pp. 9–63. *In* MCALPINE *et al.* (eds) *Manual of Nearctic Diptera*, vol. 1. Agriculture Canada, Ottawa.

In the text references should be given as MARSHALL (1992) or (MARSHALL 1992). When a citation includes more than two authors, e.g. GREY, BLACK and WHITE, the paper should be referred to in the text as GREY *et al.*, provided that this not ambiguous. If papers by the same author(s) in the same year are cited, they should be distinguished by the letters, *a, b, c,* etc., e.g. MARSHALL (1992*a*).

References to papers "in press" must mean that the article has been accepted for publication. References to "personal communications" and unpublished work are permitted in the text only: references to papers in preparation or submitted are not permissible.

All necessary **illustrations** should accompany the manuscript, but should not be inserted in the text. All photographs, graphs and diagrams should be numbered consecutively in Arabic numerals in the order in which they are referred to in the text. Glossy photographs or positive prints should be sent unmounted wherever possible and should be kept to a minimum. Figures should be of good quality. Explanation of lettering and symbols should be given in the figure caption and only exceptionally in the figures. Lettering and symbols to appear on the illustration should be of sufficient size to allow for considerable reduction where necessary (usually proper for a 50% reduction in size). Scales must be indicated on micrographs, not by magnifications in the legends. Figure size must not exceed 24×30 cm. On the back of each illustration should be indicated the author's name, the figure number (in Arabic numerals), and the top of the illustration, where this is not clear. Halftones should be included only when they are essential. Details and quotation of publication of colour plates should be made to the editors. The following symbols should be used on line drawing: ● ■ ○ ❑ ▲ ◆ ♦ etc.

Legends to figures should be typed on a separate sheet. They should give sufficient data to make the illustration comprehensible without reference to the text.

Tables and appendices should be constructed so as to be intelligible without reference to the text, numbered in Arabic numerals and typed on separate sheets. Every table should be provided with an explanatory caption and each column should carry an appropriate heading. Units of measure should always be indicated clearly (metric units are preferred). All tables and figures must be referred to in the text.

Only standard **abbreviations** should be used. Arbitrary abbreviations and jargon will not be accepted.

The Latin names should be given for all species used in the investigation, although taxonomic affiliation and authority need not be provided in the title.

Page proofs will be sent to the author (or the first-mentioned author in a paper of multiple authorship) for checking. Corrections to the proofs must be restricted to printers' errors. Any substantial alterations other than these may be charged to the author. Authors are particularly requested to return their corrected proofs as quickly as possible in order to facilitate rapid publication. Please note that authors are urged to check their proofs carefully before return, since late corrections cannot be guaranteed for inclusion in the printed journal.

Fifty reprints free of charge will be sent to the first author; extra copies of the issue (at a specially reduced rate) can be ordered on the form which will accompany the proofs. These should be returned to: The Editorial Office of the Acta Zoologica, Hungarian Natural History Museum, Budapest, Baross u. 13, H–1088, Hungary

The **page charge** required from authors outside Hungary is USD 15 per printed page. In exceptional cases, the page charge may be waived. Please contact the editor in before submitting a paper if you ask for a waiver. Authors of papers exceeding 16 printed pages are asked to pay USD 40 (or HUF equivalent) for each such page, i.e. all costs of publication (irrespective of their nationality).

FOR FURTHER INFORMATION PLEASE CONTACT US
The Editorial Office of the Acta Zoologica
H–1088 Budapest, Baross u. 13, Hungary
Fax: (36–1) 3171669
http://actazool.nhmus.hu/
E-mail: perego@zoo.zoo.nhmus.hu

SUBSCRIPTION INFORMATION

Orders should be addressed to

Editorial Office of the Acta Zoologica
Hungarian Natural History Museum
H–1088 Budapest, Baross u. 13, Hungary
Fax: (36–1) 3171669
E-mail: perego@zoo.zoo.nhmus.hu

Typeset: Pars Ltd., Budapest.
Printed by mondAt Ltd., Hungary

CONTENTS

HU ISSN 1217–8837